GEOPHYSICAL AND HYDROCHEMICAL INVESTIGATIONS OF ABEOKUTA AND IKORODU AREAS OF SOUTHWESTERN NIGERIA

BY

MOROOF OLASUNBO, OLORUNTOLA

B.Sc. Geology (Ago-Iwoye), M.Sc. Hydrogeology/Engineering Geology (Ibadan)

A Thesis in the Department of Geology,

Submitted to the Faculty of Science

in partial fulfilment of the requirements for the Degree of

DOCTOR OF PHILOSOPHY

of the

UNIVERSITY OF IBADAN

JUNE 2012

ABSTRACT

Most studies on groundwater in Nigeria have always been limited to either their occurrence or chemistry, with insufficient attention on potential, chemical character and evolution. This study therefore was designed to evaluate groundwater in Abeokuta (Basement Complex) and Ikorodu (Sedimentary) areas with the aim of highlighting groundwater potential, chemical characteristics and provenance in the two geologically contrasting terrains.

A total of 125 Vertical Electrical Soundings (VES) in Abeokuta (75) and Ikorodu (50) areas were carried out using Schlumberger array. The field data were curve-matched and computer iterated. Fifty groundwater samples were collected from shallow hand-dug wells in Abeokuta area while 50 groundwater samples were collected from shallow wells (16) and borehole (34) from Ikorodu area and analysed using the Inductively Coupled Plasma Optical Emission Spectrometry and Ion Chromatography. Stable isotopes (^{18}O and ^{2}H) of 10 water samples from each geological terrain were determined using the Optima Dual-Inlet Mass spectrometer. Data were analysed using linear regression.

Three to five sub-surface geoelectric layers were identified in Abeokuta area. The layer resistivities (Ωm) from top to bottom ranged from 24 - 6428, 9 - 2250, 13 - 11563, 65 - 6655 and 400 - 9095 while the thicknesses (m) were 0.4 - 2.5, 0.6 - 30.0, 1.5 - ∞, 3.4 - ∞ and the undeterminable thicknesses respectively. The bedrock reflection coefficients vary from 0.4 - 1.0 delineating confined, unconfined and weathered/fractured basement aquifers. Areas with confined and weathered/fractured basement aquifers have high groundwater potential. In Ikorodu, three to six sub-surface layers of alternating sequences of clay, sandy-clay, ferruginised sands and sands were identified. The resistivities (Ωm) of these layers are 11.2 - 588.6, 3.3 - 3787.7, 7.4 - 7789.4, 5.7 - 3592, 27.8 - 5785.1 and 9.8 - 822.9 while the thicknesses in metres were 0.5 - 4.4, 0.8 - 60.1, 1.5 - 101.9, 6.6 – 154.1, 35.5 – 112.4 and undetermined respectively. Areas delineated as confined and unconfined aquifers in Ikorodu have high groundwater potential. In Abeokuta, $Ca(Na)_2(HCO_3)_2(Cl)_2$ and $NaHCO_3(Cl)$ water types predominate in locations underlain by gneisses and granites respectively, whereas in Ikorodu, the water types were predominantly $NaHCO_3(Cl)$ and NaCl (lagoon area) and $Ca(Na)_2(HCO_3)_2$ (inland) area. These reflected influence of silicate weathering and ion exchange in Abeokuta while dissolution of calcite and dolomite, silicate weathering and ion exchange controlled the chemistry in Ikorodu area. The ∂^2H, $\partial^{18}O$ and the deuterium excess respectively vary from -7.6 to -11.1 ‰, -2.3 to -2.7 ‰, 9.6 to 11.4 in Abeokuta and -14.2 to -18.5 ‰, -2.5 to -3.3 ‰ and 5.6 to 7.8 in Ikorodu. In Abeokuta, relationship between ^{18}O and ^{2}H ($\partial^2H = 7.6\,\partial^{18}O + 9.3$) indicates recharge dominated by precipitation formed by Rayleigh process with little or no influence of evaporation, while in Ikorodu area, the relationship ($\partial^2H = 5.8\,\partial^{18}O + 0.8$) shows isotopic exchange between groundwater and aquifers.

High groundwater potentials were associated with confined and weathered/fractured basement aquifers, with $Ca(Na)_2(HCO_3)_2(Cl)_2$, $NaHCO_3(Cl)$, NaCl and $Ca(Na)_2(HCO_3)_2$ water types. Provenance indicated recharge by precipitation and isotopic exchange between groundwater and aquifer materials.

Word count =500

Keywords: Geophysical, Aquifers, Geochemical, Groundwater, Hydrochemical facies

ACKNOWLEDGEMENTS

I am eternally grateful to my supervisor Prof. G. O. Adeyemi for his fatherly role, love, guidance, support and understanding throughout the duration of the programme. I will forever be thankful for all his efforts and immeasurable inputs to my progress since my undergraduate days. May the almighty God continue to guide him and all his entire family.

I am greatly indebted to all members of staff of the Department of Geology, University of Ibadan, specifically Prof. A. A. Elueze, Prof. A. I. Olayinka, Prof. A. F. Abimbola, Prof. M. N. Tijani, Dr. I. M. Akaegbobi, Dr. A.T. Bolarinwa, Dr. O.A. Okunlola, Dr. O. A. Ehinola, , Dr. M. Nton, Dr. O. A. Boboye, Dr. A. S. Olatunji, and Dr. O. C. Adeigbe for their useful criticisms, suggestions and advice at one time or the other. I equally want to appreciate other lecturers in the Department like Dr. M. A. Oladunjoye, Dr. O. O. Osinowo, Dr. I. A. Oyediran and Mr. M. A. Adeleye. I am grateful to all the other members of academic and non-academic staff in the Department for their individual and collective contribution to the successful completion of this programme. I will like to appreciate Mrs. S. Bamidele for the courtesies she extended to me as well as other students. The assistance rendered by Mr. Jelili is greatly appreciated. The concern, support, criticism, suggestions and advice of Dr. A. S. Olatunji, at all times during this programme is also highly appreciated. I am indeed very grateful for his brotherly love always. May the almighty God continue to bless him and his household.

I am greatly indebted to Olabisi Onabanjo University, Ago-Iwoye (OOU), for offering me a job after my first degree. Without the job, it would have been difficult, if not impossible, for me to run any postgraduate programme. May the almighty Allah continue to bless Prof. G. O Adeyemi, who as the then Head of Department, recommended me to the management and Professor 'Layi Ogunkoya (the Acting Vice-Chancellor) who approved the job offer. I am grateful to Prof. Afolabi Soyode who as the then Vice-Chancellor, granted financial assistance for this work.

The concern, advice and constant pressure from Prof. S. S. Dada immensely contributed to the success of this work. I am thankful for the progress I made under his

guidance and his contribution towards my progress. I am grateful to all those that assisted me one way or the other during the field work especially Dr. O. Bayewu, Messrs Tayo Folorunso, I. Omotayo, G. Akintola and Adegoke, B. I appreciate other people in OOU both academic and non-academic staff members especially Prof. O. O. Kehinde-Phillips, Messers G. O. Mosuro, S. O. Ariyo and Dr. P. Ikhane for all their suggestions and encouragement.

The successful completion of this work was greatly aided by the employment opportunity I was offered by the Department of Geosciences, University of Lagos. I am very thankful for the rare privilege of working in such a stable environment. The support and encouragement given by my bosses (Prof. O. B Familoni, Prof. E. A, Ayolabi and Prof. S. B. Olobaniyi) are highly appreciated. May the almighty God continue to bless and protect them and their household.

I am very grateful to my wife, Mrs. Oluwaseyi, Oloruntola without whom the completion of the programme would have been impossible. I am very grateful to her and I commend her immeasurable perseverance, understanding, superb encouragement, positive criticism and moral support throughout this programme. I will also like to acknowledge the sacrifice made by my children, Mumin, Moshood and Mutiu to the successful completion of the programme. I am thankful to my parents; Alhaji M. O. Oloruntola and Mrs W. Oloruntola for their determination and courage to support me and my other siblings.

I am very grateful to all my friends and family members that have directly or otherwise contributed to the success of this programme and/or any other programme that I have done in the past. I thank them all, Allah will reward them abundantly.

Glory be to Almighty Allah the most gracious and the most merciful for protecting me and my family, sustaining us and ensuring the successful completion of this work.

CERTIFICATION

I certify that this work was carried out by Mr. M.O. Oloruntola in the Department of Geology, University of Ibadan

…… ……

Supervisor

G. O. Adeyemi,

B. Sc., M.Sc., Ph.D. (Ife)

Professor, Department of Geology,

University of Ibadan, Nigeria

DEDICATION

This thesis is dedicated to the Almighty God, all the people that have taught me one thing or the other to date and to my understanding and supportive wife, Oluwaseyi as well as my sons: Mumin; Moshood; and Mutiu.

TABLE OF CONTENTS

LIST OF TABLES

LIST OF FIGURES

CHAPTER ONE

INTRODUCTION

1.1 General Statement

Evaluation of groundwater resources of Nigeria started as early as 1928, when data on groundwater resources were incorporated as sections of geological mapping report by the Geological Survey of Nigeria (Offodile 2002). The earliest published results of regional hydro-geological studies were prepared by Raeburn and Jones (1934). In the last few decades, more detailed appraisal of groundwater resources has received tremendous attention from geoscientists, especially in the southwestern part of Nigeria. Various studies (Olayinka et al, 1999; Olorunfemi et al., 1999; Abimbola et al., 1999; Ehinola, 2002 and Tijani et al, 2005) have highlighted a number of reasons why groundwater appraisals have occupied the front burner of geological discourse in the last few decades. Some of the reasons identified include growing urban population, epileptic or unavailable municipal water supply, contamination and pollution problems. In addition to the contributions of these works, qualitative and quantitative data on groundwater occurrence and quality, invaluable to future groundwater development, policy formulation and environmental auditing are only available for few areas and in most cases, these are inadequate.

The evaluation of groundwater resources, especially in the different parts of southwestern Nigeria has focused on different aspects of groundwater studies. These include geophysical studies (Olayinka, 1990; Dan-Hassan and Adekile, 1991; Olorunfemi et al., 1999, Oladapo et al, 2004; Ako et al., 2005), hydrogeochemical (Tijani, 1994; Ehinola 2002; Abimbola et al., 2002; Elueze et al., 2004 and Tijani et al., 2005). A few studies have employed some environmental isotopes in groundwater assessment, especially in northern part of Nigeria (Onugba et al, 1989; Adelana and Olasehinde 2001; Tijani and Abimbola, 2003 and Onugba and Eduvie, 2005)

These studies and many others have contributed tremendously to the development and management of groundwater resources. However, except for a few, these studies are restricted mainly to major anions and cations and the use of analytical equipment with low precision. The significance of evaluating groundwater chemistry using only major cations and anions becomes important, when many ailments and diseases such as alzheimer, hypertension, cancer

(WHO, 2006) that have been associated with the occurrence of trace elements and heavy metals in groundwater above a threshold value are considered. The importance of high precision equipment is better appreciated when the difficulties associated with reproducibility of analytical results of the same geological materials are considered. This is best exemplified by clearly different results of the study of heavy metals and implication on health in Ago-Iwoye using Atomic Absorption Spectrophotometer (Kehinde-Phillips et al, 2005) and a similar study on groundwater collected from the same wells and at the same period of the year, using Inductively Coupled Plasma Optical Emission Spectrophotometer (Adebanjo, 2008).

Furthermore, as noted by Okagbue (1998), a complete appraisal of groundwater will involve an integration of geophysical and hydro-geochemical studies. Majority of the studies had appraised only aspects of groundwater except for a few (e.g Olayinka et al, 1999). Today, environmental isotopes are routinely employed to complement geochemistry and physical hydrogeology in the investigation on groundwater provenance, its renewability and the subsurface processes affecting its quality.

Geological, geophysical and hydro-geochemical studies complemented with environmental isotopes were integrated to appraise the groundwater occurrence and chemistry in Abeokuta (Fig. 1.1) and Ikorodu (Fig. 1.2) areas of southwestern Nigeria. These two ancient communities have in recent times suddenly witnessed population explosion despite the inefficient (in Abeokuta) or total absence (in Ikorodu) of municipal water supply. A number of studies (Abimbola et al, 1999; Olatunji et al, 2005; Ako et al, 2005 and Olatunji, 2006) mostly limited to aspects of groundwater occurrences and chemistry, have been undertaken in these localities. Therefore, this study will ultimately, provide unique qualitative integrated assessment of groundwater potential and character in these two contrasting geological terrains.

The city of Abeokuta and its environs have expanded over the last few years, from the central part spreading in all directions such that areas that were hitherto rural communities have developed into big towns. In addition, population explosion in recent years has seriously affected the efficiency of municipal water supply in areas covered by municipal water supply, such that the search for potable water has become a common challenge for the people of the town. Most of the inhabitants who are mostly artisans with the few employed populations (mainly civil servants), rely on the construction of shallow hand dug wells to solve their water

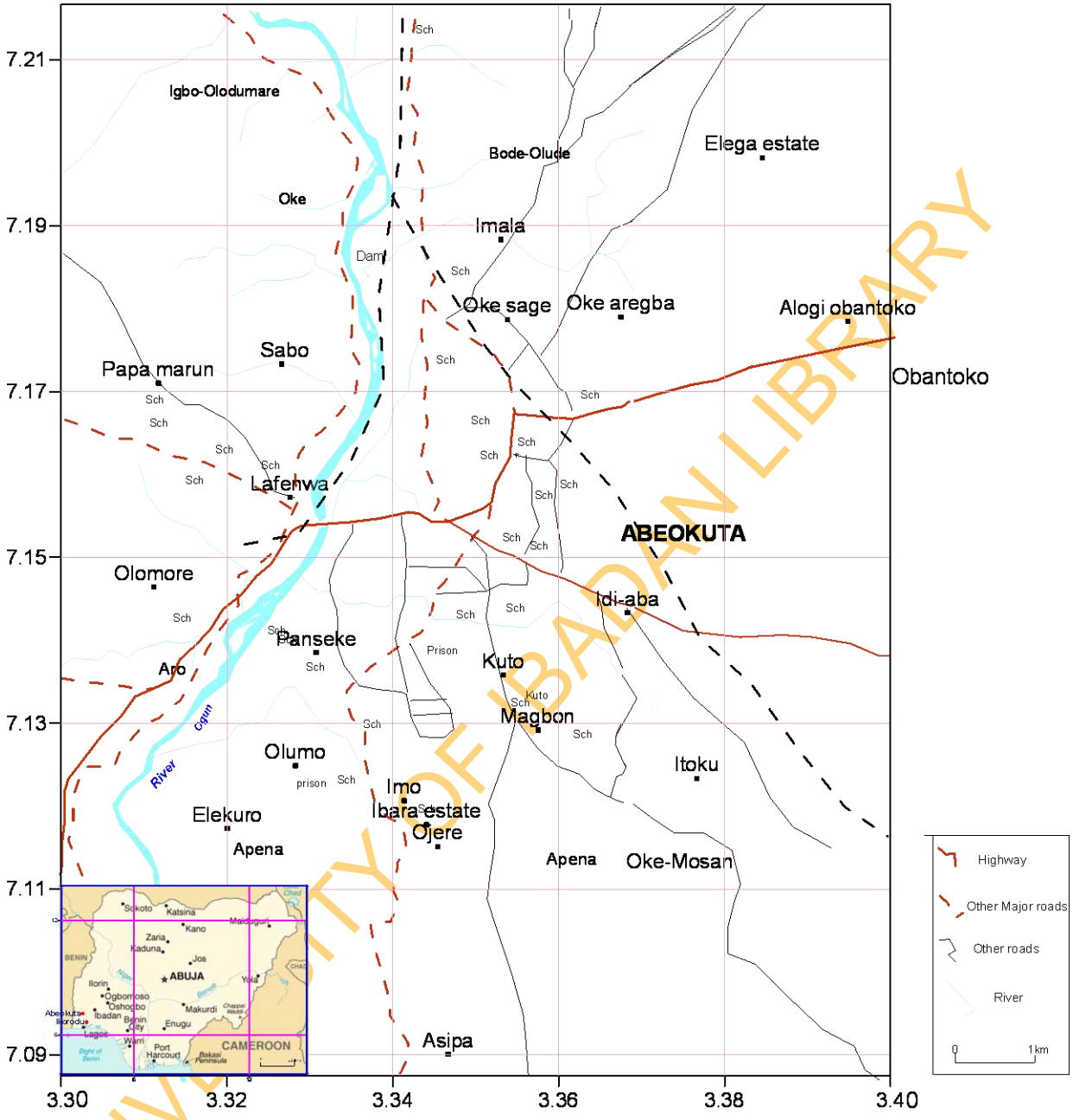

Fig 1.1: Location Map of Abeokuta area (Inset: map of Nigeria showing Abeokuta).

Fig 1.2: Location map of Ikorodu (Inset: map of Nigeria showing Ikorodu).

supply need, due to the unaffordable cost of drilling boreholes. These wells are generally shallow, due to the rocky terrain of most parts of the township. A substantial number of the wells are not lined while some of the wells are sited close to tombs, refuse dumps and sewage.

Most parts of Abeokuta are underlain mainly by crystalline Basement Complex rocks described as Older Granites (Rahaman, 1988) consisting of rocks such as hornblende-biotite gneiss, porpyroblastic gneiss, granite, porphyritic granite and pegmatitic intrusions. These rocks in their unaltered form have poor hydrogeological properties; hence groundwater occurrence in this area is erratic, localized and discrete. This type of environment usually has poor groundwater potential and groundwater is extracted through shallow hand-dug wells, which are easily susceptible to pollution. Localized concentration of heavy metals in weathered bedrock may release some of the ions and metals into groundwater beyond the threshold level, above which the groundwater becomes unsuitable for domestic purposes.

Ikorodu and its environs on the other hand, have existed for long with inadequate municipal water supply with less than 5% of the inhabitants currently having access to municipal water supply. In addition to this scenario, there has been a progressive population explosion in the communities, coupled with the emergence of many large scale industries in recent years (last five years), due to unavailability of land in 'main' Lagos. These have led to the sudden emergence of wells and boreholes in every part of the town. Many problems have been reported ranging from poor water quality (especially around the lagoon and swampy parts) (Olatunji et al, 2005) to unsuccessful wells and boreholes. Other notable problems reported in areas with similar geography and geology include rapidly changing facies, occurrence of thick clay layer and intrusion of saline water in some coastal communities (Ako et al, 2005). Ikorodu and its environs are within the Dahomey basin, underlain by the Recent Alluvial and the Coastal Plain sands.

Evaluation of groundwater occurrence and quality using the combination of geological, geophysical and hydrogeochemical data complemented with isotopes in these areas will provide invaluable information on the baseline conditions and assess the groundwater quality. These will provide a global view of groundwater situations, baseline data for future groundwater exploration and development and may be useful for policy formulation.

In addition, it will provide an opportunity for a complete comparative study of the groundwater conditions in the two contrasting geological terrains, allowing the possibility of highlighting the influence of geology on the occurrence, quality and isotopic signature of groundwater. Successful integration of these studies will provide reliable medium-scaled

detailed high precision hydrogeological information upon which future groundwater development and groundwater management policies can be implemented for these areas and similar localities.

1.2 Objectives of the Study

The hydro-geological appraisal of the study areas (Abeokuta and Ikorodu) was aimed at achieving the following objectives:

1. Hydro-geophysical delineation of the subsurface layers to evaluate the groundwater potential of the areas;
2. Hydrochemical evaluation of the groundwater, production of hydrochemical (isocones) maps as well as the evaluation of the geochemical processes and mechanism controlling groundwater chemistry in the areas;
3. Determination of the influence of geology, if any, on the groundwater chemistry in the study areas;
4. Determination of isotopic signatures of groundwater as well as groundwater origin, source of recharge; and
5. Ultimately, integration of hydro-chemical, hydro-geophysical and isotopic data in order to characterize the groundwater resources of the two different geological terrains.

1.3 Description of the Study Locations

Abeokuta area (Fig 1.1), lies between latitudes 7.09^0 N and 7.23^0 N by longitudes 3.30^0 E and 3.40^0 E, covering an area of 151.2 km^2. Notable settlements within the area include Lafenwa, Kuto, Ita-Elega, Sabo and Igbo-Olodumare.

Ikorodu (Fig 1.2), lies between latitudes 6. 53^0 N and 6.69^0 N by longitudes 3.44^0 E and 3.67^0 E, covering an area of 419.9 km^2. Some of the settlements in the area include Ipakodo, Baiyeku, Imota, Isiwu town, Igbalu town, Ijede, Agura, Igbokuta, Oke-Agbo town and Oke-Olokun town. The area is located within the sedimentary basin of south-western Nigeria.

Ikorodu is bounded in the east by Epe town, in the south by the Lagos lagoon, the north by Sagamu and in the west by Majidun and its environs. The proximity of Ikorodu (about 30 km) to central Lagos (Ikeja) has recently led to the massive influx of people and industry to the area due to the availability of relatively cheap land and labour.

1.4 Climate and Vegetation

The study areas fall within the tropical rain forest belt. The climate is characterized by alternate wet and dry seasons. There is seasonal shift in the wind pattern with a fairly seasonal and diurnal variation in temperature, dependending on the two prevailing air masses blowing over the country at different times of the year (Ojo, 1977). Precipitation in the study area is usually in the form of rainfall. The amount of rainfall ranges between 750 mm and 1000 mm in the rainy season (March & October) and 250 mm & 500 mm in the dry season between November & March (Akanni, 1992). However, the amount of rainfall recorded during the August break is usually lower than the annual average due to the little dry season commonly experienced in August in southwestern part of the country (Akanni, 1992).

Temperature ranges from a mean maximum of 32˚C in February to a mean minimum of about 21˚C in June, August and September with high relative humidity throughout the year at above 80%.

Many parts of Ikorodu have been developed with few areas still having derived vegetation represented mostly by tree crops and bushes that have grown around them over the years. The dominant vegetation in the area is the mangrove forest made up of mangrove plants of different species such as Mahogany (Odumosu, 1999). Abeokuta on the other hand, is characterized by derived savanna vegetation resulting from the effect of bush burning, high rural population densities, shifting cultivation, other farming activities and urbanization. However, some areas still have isolated stands of few forest-emergent trees, which represent the remnants of the original forest.

1.5 Topography

Abeokuta area is characterized by an undulating topography with elevation ranging from 100 m to 400 m above sea level. In the area, the older granite masses and in some cases, the migmatite and gneiss form rugged topography with inselbergs which are bare domes. The area has low relief around the River Ogun and relatively high relief in the north-eastern and north western parts. The slope gradient varies from one point to the other thereby creating an uneven topography.

Ikorodu area is characterized by considerable variation in topography. Some parts of Ikorodu are characterized by steep gradients which are completely absent in the Lagos and Badagry areas (Reuben, 1970). The topography of the lagoon side varies from areas where the land rises very gently from the edge of the water to areas with markedly steep rise in relief around the lagoon such as Ijede. Many parts of the landward areas north of the town have

elevation of over 50 m above sea level while most other areas have a relatively flat topography with elevation of less than 25 m above sea level.

1.6 Drainage

The drainage pattern of Abeokuta area is basically dendritic. The main water course in the area is River Ogun, which flows from the northern part southward (Fig.1.1a). The river and its many tributaries form a dendritic flow pattern in the area. Another notable water course in the area is River Olomore that flows from the east of the study area and empties into the main River Ogun.

Ikorodu is located at the upland areas of Lagos State hence; the area is drained through the slopes, several rivers (Odumosu, 1999) and canals that flow into the lagoon. One of the main physical characteristics of this region is its poor drainage. With the exception of such major rivers as Ogun, Osun and Shasha which flow directly into the lagoon, the numerous short streams draining this region get lost in the fresh water swamps north of the lagoon where they wander about a system of creeks (Reuben, 1970).

CHAPTER TWO

LITERATURE REVIEW

2.1 Review of Previous Studies on Groundwater Occurrence and Chemistry

Studies on groundwater occurrence and quality have been carried out in different parts of southwestern Nigeria in particular and the entire country in general for many decades. The studies have covered both sedimentary and the Basement Complex terrains. However, only a few of these studies have been done in the sedimentary areas when compared with Basement Complex environment. This may not be unconnected with the unpredictable nature of the aquifers in areas underlain by crystalline rocks and the shallow nature of wells in such areas.

Studies have shown that the electrical resistivity of fractured basement rocks is often less than 1,500 Ohm-m (David, 1988; Hazell et al., 1992) but can be as high as 3,000 ohm-m (White et al., 1988) while bedrock resistivity exceeding 3,000 ohm-m can therefore, be thought as representing fresh bedrock, containing little or no water (Olayinka,1996).

Olayinka and Olorunfemi (1992) employed Wenner Vertical Electrical Soundings in Okene area to locate productive borehole. The computer-assisted sounding interpretation showed good agreement with results of subsequent drilling. Contrary to Jones (1985) who suggested that basement aquifers should be fairly uniform, the study agrees with Chilton and Smith-Carington (1984) that large local variations in the basement aquifers exist due to variation in mineralogy and rock structures. It further noted that bedrock resistivity less than 1,000 ohm-m may be indicative of the presence of fractures, hence constituting good groundwater resource.

However, Olayinka (1996) demonstrated that the major factor determining the slope of the terminal segment of a vertical electrical sounding (VES) curve is not the absolute value of the bedrock resistivity but rather, it is the resistivity contrast at the weathered zone-bedrock interface. Steep rising terminal branch on a sounding curve, contrary to the hitherto assumption, is not necessarily indicative of a fresh bedrock (Olayinka, 1996). However, the reflection coefficient at the bedrock rock interface was recommended as one of the geo-electrical characteristics in the evaluation of sounding results for the selection of borehole sites since it remains invariant for the different equivalent geoelectric models over a layered earth model (Olayinka, 1996).

Olayinka et al (1999) combined geophysical method with hydrogeochemical data to study shallow groundwater occurrence and chemistry in Ibadan, southwestern Nigeria. The

study identified five different water types, namely: (Na-Cl, Na-Ca-Cl and Na- Ca-Mg-Cl); (Ca-(Mg)-Na- HCO_3-Cl, Na-Ca- HCO_3-Cl and Ca- HCO_3-Cl); (Ca-(Mg)-Na-HCO_3 and Ca-Na-HCO_3),(Ca-Na-Cl-(SO_4)- HCO_3); and Ca-(Mg)-Na-SO_4- HCO_3. The different water types were attributed to the weathering of diverse rock types in the study area.

The evaluation of groundwater potentials of Akure Metropolis by Olorunfemi et al (1999) using Vertical Electrical Sounding technique, complemented with hydrological data revealed the presence of five types of aquifer in the area. These are: the weathered layer aquifers; weathered/fractured (unconfined) aquifer or partly weathered aquifer; weathered/fractured (confined) aquifer; weathered/ fractured (unconfined)/fractured (confined) aquifer; and fractured (confined) aquifer. As observed in the study, the nature of the overlying weathered layer, irrespective of the thickness of underlying fractured column, to a large extent determines the yield of borehole, with area overlain by clay (resistivities of <100 ohm-m) having low yield.

The study of groundwater and its occurrence in the coastal plain sands and alluvial deposits of parts of Lagos state by Ako et al (2005) revealed abrupt change in facie from sands to clay. The lithology of the area inferred from both geophysical survey and lithologic logs revealed a subsurface that consists mainly of a topsoil essentially laterite and layers of clay/sands (fine-medium-coarse), with occasional presence of highly resistive layer. The study identified problems preventing intuitive sinking of boreholes in coastal plain sands and alluvial deposits to include the presence of relatively thick clay layer in some localities and saline water in other places.

Abimbola et al (1999) studied some aspects of groundwater quality in parts of Abeokuta and its environs and noted that in the study area, the dominant ions in the groundwater are Ca^{2+} and HCO_3^-, hence characterizing the water type as mainly Ca- HCO_3 type with low TDS. This water type was reported to be the typical water type of the Nigerian Basement Complex.

The study of quality of groundwater around Oke-Agbe Akoko area of southwestern Nigeria by Olatunji et al (2001) revealed the occurrence of two broad groups of dominant water types namely; (Ca-Mg-(Na)-HCO_3 and Na-(K)-HCO_3) and (Ca-Mg-(Na)-Cl and Na-(K)-Cl) water types. The chemical characteristics of groundwater in this area were found within the recommended guidelines of World Health Organization (WHO, 1993) and Standard Organization of Nigeria (SON) standards for potable water except locations where nitrate concentrations were above the limit for potable water.

Tijani and Ayodeji (2001) assessed the chemistry of surface and groundwater in Ewekoro, Imashayi, Iboro and Isaga in parts of southwestern Nigeria. The study revealed that

the groundwater has higher temperature than surface water due to geothermal gradient that averages 65^0C/km (Idowu et al, 1999). The study further revealed that deep wells of Ewekoro Formation show similar trend with those of Abeokuta Group, implying that both wells may be tapping water from the same aquifer (the Cretaceous sediments of Abeokuta). In order of occurrence, Na (K)-Cl-(SO_4), Ca- (Mg)-Na-(K)SO_4 and Ca (Mg)-Na(K)HCO_3 water types were identified in the areas. Alkaline water; the dominant water type is noted to have its source from the arkosic sediments of the Abeokuta Group. The study further noted that surface water is of this category suggesting that the surface water flows over superficial deposits or soil cover that is rich in sodium and potassium. The overall hydrochemical characteristics of the samples were suggested to be partly affected by mixing of diverse water types, chemical ionic inputs from precipitation, chemical weathering, dissolutions of parent rocks and cation (base) exchange.

The influence of bedrock on the hydrogeochemical characteristics of groundwater in the Northern part of Ibadan metropolis was studied by Abimbola et al (2002). The study revealed that the chemical composition of the groundwater, especially those from weathered zone (hand dug wells) depends on the chemical weathering of the underlying bedrocks.

Ehinola (2002) found shallow groundwater from Oyo and Awe town to be slightly acidic to neutral with fairly high Total Dissolved Solids (TDS), moderate hardness with Na^+ and HCO_3^- being the dominant water type.

In order to evaluate the impact of dumpsite of Orita Aperin, Ibadan, southwestern Nigeria on hydrochemical characteristics of surface and shallow groundwater around the dumpsite, Tijani et al (2002) studied the character of the groundwater in both wet and dry seasons. The considerable influence of the leachates on the shallow groundwater was reflected in the high TDS (>1000-5568 mg/l). In addition, the effect of leachates and dilution during the wet season in the study area resulted in different water types for the wet season (Ca-Na-HCO_3) and Ca-Na-SO_4-Cl for the dry season.

The hydrogeochemical characteristics of surface water and groundwater in Ibokun, Ilesha area, southwestern Nigeria was investigated by Elueze et al (2004). The study identified four predominant water types, which include Ca-(Mg)-Na- HCO_3, Ca-Na-Cl-(SO_4) - HCO_3, Ca-(Mg)-HCO_3 and Na-(K)-Cl- SO_4. The diverse water types reflect the contribution of diversity of rock types and consequently, the product of weathering.

The influence of seawater on water quality in metropolitan Lagos was investigated by Tijani et al (2005). The study revealed the order of abundance of cations in surface waters as $Na^+>K^+>Mg^{2+}>Ca^{2+}$ and $Na^+>K^+>Ca^{2+}>Mg^{2+}$ for shallow and deep wells respectively. The anions are in the order of $Cl^->HCO_3^->SO_4^{2-}>NO_3^-$ for both surface and deep water samples

while they are HCO_3^->Cl^->SO_4^{2-}>NO_3^- for shallow wells. Comparatively, deep-wells have lower TDS, EC, total hardness than shallow wells, which in turn have lower values than surface water samples. Despite the glaring differences in TDS of the media, the study revealed that there is a common recharge source for the three different media. The surface water in the area was inferred to be dominated by Na-(SO_4)-Cl while the groundwater samples are dominated by Na-Ca-(SO_4)-HCO_3 facie. Using the salinity ratio, the study revealed that the surface water is largely affected by in-flow of saline water from the sea while the deep groundwater is not affected by seawater contamination, unlike shallow hand-dug wells where seawater influence had contributed to the overall TDS. Thus the seawater influence is more or less related to mixing of saline water from the sea with the shallow groundwater system through base-flow seepage or infiltration rather than through pump-induced upward seawater intrusion from greater depths.

Onugba et al (1989) studied the hydrochemical and isotopic characteristics of groundwater in parts of Gongola, Northern Nigeria. The study revealed that the values of Oxygen 18 ($\delta\ ^{18}O\%$+0.1SMOW) vary from -4.52 to -2.64 (groundwater) to -2.10 to 0.58 (rivers) and -4.55 to -3.89 (rain) and suggested that groundwater is recharged by rain with little or no evaporation.

A study by Xong et al (1999) revealed that only the groundwater formed by Rayleigh's process under an equilibrium condition has similar slope of regression to that of Meteoric Water Line (MWL). The study further noted that the slope of regression will tend towards 8 and deuterium excess will be about 10 if the recharge is dominated by precipitation formed through Rayleigh process under an equilibrium condition. However, precipitation was attributed to the effect of enrichment by evaporation where the slope and deuterium excess deviate from 8 and 10 respectively. Similarly, Tijani and Abimbola (2003) observed that the groundwater in Oke-Ogun area plotted along the Global Meteoric Water Line (GMWL) defined by $\delta^2H = 8\delta^{18}O + 10$ suggesting recharge of the aquifer by recent precipitation with little or no imprint of kinetic evaporation.

Few studies (for example Kehinde-Phillips et al, 2005), most especially in Nigeria have shown that although the heavy metals and other trace elements occur in minute quantities in groundwater, they can result in serious health effects. However, studies (Iwami et al., 1994; Takeda, 2003) in other parts of the world have indicated that excessive ingestion of heavy metals and trace elements may affect human health.

Kehinde-Phillips et al (2005) showed the relevance of heavy metals in evaluation of potability of groundwater. The study carried out using Atomic Absorption Spectrophotometry

(AAS) analytical method related elevated concentration of As (nd-3.12 mg/l) and Cd (nd-3.45 mg/l) in groundwater in Ago-Iwoye area to health disorders on respiratory, gastro-intestinal cardiovascular and nervous system in human. However, a similar study in the area using Inductively Coupled Plasma-Optical Emission Spectrophotometry (ICP-OES) method showed that these metals are below detection limits in the study area. The differences observed in the two studies may be largely due to higher precision and accuracy of the ICP-OES method compared to the AAS.

Takeda (2003) using evidence from occupational exposure indicates that manganese can affect the neurological function. Miners and welders exposed through airborne contamination for long periods have developed neurological disorders such as Parkinson's disease. Similarly, Foster (1992) established some links between exposure to manganese and a form of motor neuron disease found in the Pacific region, known as Guamian amyotrophic lateral sclerosis. Iwami et al. (1994) found correlations between the concentrations of manganese in food and the prevalence of motor neuron disease in the Kii Peninsula of Japan. Furthermore, Cawte et al. (1987) reported neurological symptoms in manganese ore miners from Australia. Occupational exposure to manganese has similarly been linked to liver, kidney and lung damage.

The studies reviewed above have contributed immensely to groundwater development and management. However, most of them (such as Onugba et al, 1989; Olayinka, 1990; Dan-Hassan and Adekile, 1991; Olayinka, 1996; Olayinka et al, 1999; Olorunfemi et al, 1999, Ehinola 2002; Abimbola et al 2002; Tijani 1994; Oladapo et al, 2004; Elueze et al 2004 and Ako et al, 2005) have evaluated only limited aspects of hydrogeology. Therefore, this research appraised geophysical, hydrogeochemical and isotopic characteristics of groundwater resource in the study areas. In addition, a comparative study of the hydrogeology of the two geologically different terrains was done to complement the available information in this area. Ultimately, it would provide comphrensive information on the chemical characters, hydrochemical maps and isotopes characters of groundwater in the two different geological terrains.

2.2 Fundamentals of Isotope Geochemistry

Isotopes are atoms of the same element that have different numbers of neutrons. Various Isotopes have different masses due to differences in the number of neutrons among the various isotopes of an element. Isotope names are usually pronounced with the element name first, as in "oxygen-18" instead of "18-oxygen.

Isotopes integrate small-scale variability to give an effective indication of catchment-scale processes (McDonnell and Kendall, 1992; Buttle, 1994), hence they have been found

useful in providing new insights into hydrologic processes in small catchment areas. In the last few years, environmental isotopes have contributed immensely to studies and investigations in hydrogeology, complementing physical and chemical hydrogeology. Many hydrogeological studies use the stable isotopes of water molecule to determine groundwater quality, origin, recharge mechanism and rock-water interaction.

In particular, ^{18}O, ^{2}H, and ^{3}H are integral parts of natural water molecules that fall as rain or snow (meteoric water) each year over a watershed and, consequently, are ideal tracers of water. This long-term wide-spread application of these natural tracers allow hydrologists to study runoff generation on scales ranging from macro-pores to hill-slopes to first- and higher-order streams (Sklash, 1990).

The science of stable isotope geochemistry is based on the fact that isotopes of the same element have slightly different thermodynamic and physical properties (Urey, 1947). Hence, their behaviour in chemical and physical reactions is slightly different. When isotopes, or compounds which contain them, participate in chemical reactions or undergo a change of state, they become separated or fractionated. The resulting changes in relative isotopic abundances are often measurable and provide important insights into many geochemical and hydro-geochemical processes.

Environmental isotopes are natural and anthropogenic isotopes whose wide distribution in the hydrosphere can assist in the solution of hydrogeochemical problems. As highlighted by Kendall and Caldwell (1998), typical uses of environmental isotopes in hydrology include:

I. identification of mechanisms responsible for stream flow generation;
II. testing flow path and water-budget models developed using hydrometric data;
III. characterization of flow paths that water follows from the time precipitation hit the ground until discharge at the stream;
IV. determination of weathering reactions that mobilize solutes along flow paths;
V. determination of the role of atmospheric deposition in controlling water chemistry;
VI. identification of the sources of solutes in contaminated systems; and
VII. assessment of biologic cycling of nutrients within an ecosystem.

Kendall and Caldwell (1998) stated that environmental isotopes can be used as tracers of waters and solutes in catchments because:

a. Waters recharged at different times, in different locations, or that follow different flow paths are often isotopically distinct; in other words, they have distinctive "fingerprints";

b. Unlike most chemical tracers, environmental isotopes are relatively conservative in reactions with catchment materials. This is especially true of oxygen and hydrogen isotopes in water. Meteoric waters retain their distinctive fingerprints until they mix with waters of different compositions or, in the case of isotopes of dissolved species, there are reactions with minerals or other fluids;

c. Solutes in catchment waters that are derived from atmospheric sources are commonly isotopically distinct from solutes derived from geologic and biologic sources within the catchment;

d. Both biological cycling of solutes and water/rock reactions often change isotopic ratios of the solutes in predictable and recognizable directions; these interactions often can be reconstructed from the isotopic compositions; and

e. If water from an isotopically distinctive source (e.g., rain with an unusual isotopic composition) is found along a flow path, it provides proof for a hydrologic connection, despite any hydraulic measurements or models to the contrary.

Stable isotope abundances are therefore measured as differences in the isotope ratios of two substances because it is analytically difficult to determine the rather restricted variations which occur in the absolute concentrations of a given isotope. Correspondingly, stable isotope data are reported as the δ, or del notation, in terms of its deviation, in parts per thousand (‰, or per mille), from the same ratio in an internationally accepted standard.

Stable isotope compositions of low-mass (light) elements such as oxygen, hydrogen, carbon, nitrogen, and sulphur are normally reported as δ values in units of parts per thousand (denoted as ‰ or permil, or per mil, or per mille -- or even recently, per mill) relative to a standard of known composition. δ value is given as:

$$\delta\ (in\ ‰) = \left[\frac{R_x}{R_s} - 1\right] \times 1000 \quad \ldots\ldots\ldots\ldots\ldots\ldots\ldots\ldots\ldots\ldots\ldots\ldots\ldots\ldots\ldots\ (2.1)$$

where R denotes the ratio of the heavy to light isotope (e.g., $^{34}S/^{32}S$), and R_x and R_s are the ratios in the sample and standard, respectively.

A positive δ value means that the isotopic ratio of the sample is higher than that of the standard; a negative δ value means that the isotopic ratio of the sample is lower than that of the standard. For example, a $\delta\ ^{15}N$ value of +30‰ means that the $^{15}N/^{14}N$ of the sample is 30 parts-per-thousand or 3% higher than the $^{15}N/^{14}N$ of the standard.

There are several commonly used ways for making comparisons between the δ values of two materials. The first two are preferred because of their clarity while the fourth should be avoided:

I. High vs. low values;

II. more/less positive vs. more/less negative (e.g., -10 ‰ is more positive than -20 ‰);

III. Heavier vs. lighter (the "heavy" material is the one with the higher δ value); and

IV. Enriched vs. depleted (stating what isotope is in short supply, e.g., a material is enriched in ^{18}O or ^{16}O relative to some other material, and that the enrichment or depletion is a result of some reaction or process). For example, to say that "one sample is enriched in ^{34}S relative to another because of sulphate reduction" is proper.

2.2.1 Standards

The isotopic compositions of materials analyzed in mass spectrometers are usually reported relative to some international reference standards. Samples are either analyzed at the same time as this reference standard or with some internal laboratory standards that have been calibrated relative to the international standard. Alternatively, the absolute ratios of isotopes can be reported. Small quantities of these reference standards are available for calibration purposes from both the National Institute of Standards and Technology (NIST) in the USA and the International Atomic Energy Agency (IAEA) in Vienna (Kendall and Caldwell, 1998).

Various isotope standards are used for reporting light stable-isotopic compositions (Table 2.1). The δ values of each of the standards have been defined as 0 ‰. δ D and δ ^{18}O values are normally reported relative to the SMOW standard (Standard Mean Ocean Water; Craig, 1961) or the equivalent VSMOW (Vienna-SMOW) standard. δ ^{13}C values are reported relative to either the PDB (Pee Dee Belemnite) or the equivalent VPDB (Vienna-PDB) standard. δ ^{18}O values of low-temperature carbonates are commonly reported relative to PDB or VPDB. VSMOW and VPDB are virtually identical to the SMOW and PDB standards. Use of VSMOW and VPDB is supposed to imply that the measurements were calibrated according to IAEA guidelines for expression of δ values relative to available reference materials on normalized per millle scales (Kendall and Caldwell, 1998 citing Coplen, 1994; 1995; 1996).

Radioisotopes are reported as absolute concentrations or ratios. Tritium (^{3}H) values are typically reported as absolute concentrations, called Tritium Units (TU) where one TU corresponds to 1 tritium atom per 10^{18} hydrogen atoms. Tritium values may similarly be expressed in terms of activity (pico-Curies/liter, pCi/L) or decay (disintegrations per minute/liter, dpm/L), where 1 TU = 3.2 pCi/L = 7.2 dpm/L. ^{14}C contents are typically expressed as percentages of modern carbon (pmc) and are referenced to an international standard known as "modern carbon"(Kendall and Caldwell, 1998).

2.2.2 Dependencies of Isotopic Composition

The isotopic signatures as encountered in precipitation depend on temperature, deficit of moisture in the air as well as the isotope ratio of the water vapour source.

Table 2.1: Abundance ratios and reference standards for some environmental isotopes.

Isotope	Ratio measured	Reference Standard	Abundance ratio of standard
^{2}**H**	$^{2}H/^{1}H$	VSMOW	$1.5575 \cdot 10^{-4}$
^{3}**He**	$^{3}He/^{4}He$	atmospheric He	$1.3 \cdot 10^{-6}$
^{6}**Li**	$^{6}Li/^{7}Li$	L-SVEC	$8.32 \cdot 10^{-2}$
^{11}**B**	$^{11}B/^{10}B$	NBS 951	4.04362
^{13}**C**	$^{13}C/^{12}C$	VPDB	$1.1237 \cdot 10^{-2}$
^{15}**N**	$^{15}N/^{14}N$	atmospheric N_2	$3.677 \cdot 10^{-3}$
^{18}**O**	$^{18}O/^{16}O$	VSMOW, or	$2.0052 \cdot 10^{-3}$
		VPDB	$2.0672 \cdot 10^{-3}$
^{34}**S**	$^{34}S/^{32}S$	CDT	$4.5005 \cdot 10^{-2}$
^{37}**Cl**	$^{37}Cl/^{35}Cl$	SMOC	0.324
^{87}**Sr**	$^{87}Sr/^{86}Sr$	Absolute ratio, or various materials	

Kendall and Caldwell (1998)

When these parameters are taken into consideration, the isotopic signatures give information about:

a. the origin of vapour, precipitation, and groundwater; and
b. partly about the climatic conditions during recharge processes in the past.

Dependencies of the isotopic composition of a groundwater sample could be deduced based on these interrelations (Moser and Rauert, 1980).

The elevation effect

During the rise of humid air due to orographic obstacles and successive precipitation, the concentration of heavy isotopes in the precipitation decreases with elevation. The depletion is a result of the general decrease of the cloud temperatures with elevation.

For the elevation effect the depletion is -1 to -4 ‰ and -0.15 to -0.5 ‰ for $\delta\ ^{2}H$ and $\delta\ ^{18}O$ per 100 m rise respectively (Appelo and Postma, 2005). Elevation correction **(**likewise known as altitude or alpine effect) distinguishes groundwater recharged at high altitudes from those of low altitudes. It therefore turns out to be a useful tool in hydrogeological studies.

The continental effect

During the condensation of atmospheric vapour the liquid phase (i.e. rain droplets) gets isotopically enriched while the vapour phase gets isotopically depleted. However, the amount of vapour in a cloud is limited. As this process continues, the isotopic signature of the vapour, and consequently of the condensed water is continuously changing. This, invariably, leads to a situation in which both the precipitation and groundwater are found depleted with respect to heavy isotopes as the distance away from the coast increases.

The effect of precipitation rate

The effect of precipitation rate is otherwise known as “amount effect”, which shows the dependence of the isotopic composition on the amount of rainfall. Heavier rain effects or greater precipitation amounts result in more negative $\delta\ ^{2}H$ and $\delta\ ^{18}O$ values. As the amount of precipitation increases depletion in the rain can be observed. During a single precipitation event significant difference of the isotopic signature are found due to progressive condensation and variations of the intensity of rain.

The temperature effect

Temperature is the driving force in cooling and condensing atmospheric vapour and this result in global variations of the isotopic composition of rain (Appelo and Postma, 2005). The isotopic composition of precipitation depends on the temperature at which the oceanic water is evaporated into the air. Seasonal fluctuations of the isotopic composition in local precipitation are influenced by fluctuations of temperature. Rain during winter is isotopically lighter than rain during the summer. Since the climate in the past was significantly different from those of today, the isotopic signature of groundwater formed in the past would strongly differ from the isotopic signature of modern precipitation and modern groundwater.

In coastal areas, the relation between temperature and isotopes, $\delta^{18}O$ and $\delta^{2}H$ given by Dansgaard (1964) is

$$\delta^{18}O = 0.695t_c - 13.6\ ‰ \quad \ldots\ldots\ldots\ldots\ldots\ldots\ldots\ldots\ldots\ldots\ldots\ldots\ldots\ldots\ldots\ldots\ldots\ldots\ldots\ldots (2.2)$$

$$\delta^{2}H = 5.6t_c - 100\ ‰ \quad \ldots\ldots\ldots\ldots\ldots\ldots\ldots\ldots\ldots\ldots\ldots\ldots\ldots\ldots\ldots\ldots\ldots\ldots\ldots\ldots (2.3)$$

where t_c is the average yearly temperature in ^{o}C

Moreover, the dependence of isotopic fractionation on temperature and moisture causes an annual fluctuation (seasonal effect) and depletion with latitude (latitude effect). In arid and semi-arid zones with low moisture saturation and precipitation, an enrichment of the heavy isotopes in rain drops occurs while they are falling (evaporation effect). Due to evaporation, surface water like river or lake gets isotopically enriched.

2.2.3 Meteoric Water Line

Craig (1961) showed that the delta values of the stable isotopes in precipitation, rivers, and lakes measured worldwide fit along a straight line called the "Global Meteoric Water Line, (GMWL)" on a $\delta^{2}H$ - $\delta^{18}O$ plot. The line is characterised by the relationship:

$$\delta^{2}H = 8\delta^{18}O + 10\ (‰) \quad \ldots\ldots\ldots\ldots\ldots\ldots\ldots\ldots\ldots\ldots\ldots\ldots\ldots\ldots\ldots\ldots\ldots\ldots\ldots\ldots (2.4)$$

The global meteoric water line by Craig (1961) was later refined from more than a decade world-wide monitoring of the stable isotopic composition of precipitation by IAEA, Global Network of Isotopes in Precipitation – GNIP, reported in Rozanski, et al. (1993) to be:

$$\delta^{2}H = 8.13\delta^{18}O + 10.8\ (‰) \quad \ldots\ldots\ldots\ldots\ldots\ldots\ldots\ldots\ldots\ldots\ldots\ldots\ldots\ldots\ldots\ldots\ldots\ldots\ldots\ldots (2.5)$$

From equation (2.4), the gradient of the GMWL line is 8 and the intercept on the y-axis, “d”, is 10 ‰. As noted by Appelo and Postma (2005), the value of d was first used by Dansgaard (1964) to characterise the deuterium excess in global precipitation and is defined from equation (2.4) as:

$$d = \delta^{2}H - 8\delta^{18}O\ (‰) \ldots\ldots\ldots\ldots\ldots\ldots\ldots\ldots\ldots\ldots\ldots\ldots\ldots\ldots\ldots\ldots\ldots\ldots (2.6)$$

Changes in gradient of the straight line to values <8 are essentially caused by evaporation during precipitation

2.2.4 Stable Isotopes of Water Molecule (^{2}H, ^{18}O)

Basically, water is composed of hydrogen and oxygen, which occur with different isotopic combinations in its molecules. In nature hydrogen occurs as a mixture of ^{1}H and ^{2}H while oxygen is found as isotopes of ^{16}O, ^{17}O, ^{18}O. Ocean water contains two ^{18}O atoms for every thousand of ^{16}O (Table 2.1) but the ratio is different in fresh water. The ratio of $^{2}H/^{1}H$ in ocean water is 1.556 x 10^{-4}. ^{1}H, ^{2}H, ^{16}O, ^{18}O and ^{17}O do not engage in nuclear transformation hence, they are called stable isotopes (Appelo and Postma, 2005). In contrast, radioactive isotope like ^{3}H (tritium) will decay over time and are therefore used for dating.

The reference standard commonly adopted for oxygen and hydrogen stable isotopic variation in natural water is V-SMOW (Vienna Standard Mean Ocean Water). This is isotopically identical to SMOW (Gonfiantini, 1978; Gat and Gonfiantini, 1981).

The difference between ratio of isotopes in samples and the reference standard is expressed in the following relations:

$$\text{Delta } (\delta) = \left[\frac{R_{sample} - R_{standard}}{R_{standard}}\right] * 1000\ (per\ mill \text{ or } ‰) \ldots\ldots\ldots (2.7)$$

For Oxygen, the equation is

$$\delta = \left[\frac{{}^{18}O/{}^{16}O\ \ (Sample)}{{}^{18}O/{}^{16}O\ \ (SMOW)} - 1\right] * 1000\ (per\ mill \text{ or } ‰) \ldots\ldots\ldots\ldots (2.8)$$

while for hydrogen, it is

$$\delta = \left[\frac{{}^{2}H/\,{}^{1}H\ \ (Sample)}{{}^{2}H/\,{}^{1}H\ \ (SMOW)} - 1\right] * 1000\ (per\ mill \text{ or } ‰) \ldots\ldots\ldots\ldots (2.9)$$

The seawater standard has $\delta^{2}H$ and $\delta^{18}O$-values equal 0 ‰ while negative values characterize water isotopically depleted ("lighter") and positive values correspond to water samples isotopically enriched ("heavier") with respect to the standard. The measuring accuracy is 0.15 ‰ for $\delta^{18}O$ and 1 ‰ for delta $\delta^{2}H$ while details of the measuring technique are given in IAEA (1998).

2.2.5 Isotopic Fractionations

Isotopic fractionations are produced by two main phenomena; namely isotope exchange reactions and kinetic processes. Isotope exchange reactions can be viewed as a subset of kinetic

isotope reactions where the reactants and products remain in contact in a closed, well-mixed system such that back reactions can occur and chemical equilibrium can be established. Under such circumstances, isotopic equilibrium can be established.

Environmental isotopes of the same element can be partitioned or separated in a thermodynamic reaction due to differences in rates of reaction of the different molecular species. Isotopes of a given element fractionate during chemical and physical processes because the strengths of chemical bonds vary slightly with the mass of the isotope. In general, light isotope forms weaker bonds than a heavier isotope. This gives rise to the three types of isotope fractionation seen in natural systems:

1) Kinetic isotope effects, which arise because the lighter isotope reacts more rapidly than the heavier isotope;

2) Equilibrium isotope effects, which are controlled by the differing thermodynamic properties of each isotope; and

3) Vital or biological isotope effects, observed in certain organisms which produce mineral skeletons which are out of isotope equilibrium with the water formed.

Fractionation is a fundamental process common to stable isotopes of hydrogen, boron, carbon, oxygen, nitrogen, sulphur and chlorine and can occur under equilibrium or non-equilibrium (kinetic) conditions. Fractionation can occur as a result of molecular diffusion.

Formation waters

Reactions of interest to petroleum geologists tend to occur in aqueous media and include precipitation of mineral skeletons from marine waters and diagenetic reactions which may occur in a wide variety of water types from marine and meteoric to deep basal fluids. Accordingly, information can be obtained about the reactions by studying not only digenetic minerals, but waters from which they may have precipitated. In addition, isotopic study of waters in petroleum reservoirs can provide information about the continuity of different water types in reservoir and can assist in reservoir correlations and in identifying changes in water composition as the reservoir is produced.

Formation waters are derived from four basic sources, each of which is isotopically (and chemically) distinct (Fig. 2.1).

1) Meteoric water: Meteoric waters originate as rain and snow. Their δD and δ18O compositions vary systematically and define the meteoric water line (MWL), which is expressed as (Craig, 1961):

$$\delta d = \delta\, ^2H - 8\delta^{18}O\ (‰) \ldots\ldots\ldots\ldots\ldots\ldots\ldots\ldots\ldots\ldots\ldots\ldots\ldots\ldots 2.10$$

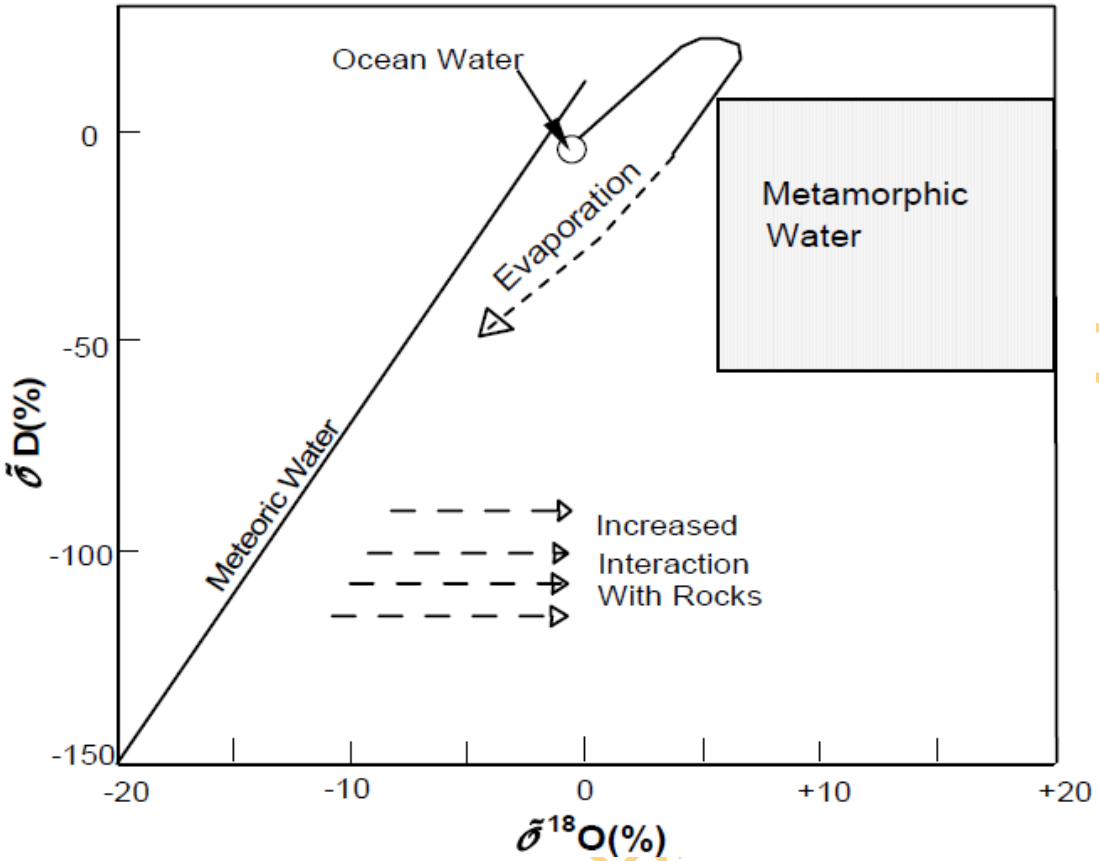

Fig. 2.1: Hydrogen and oxygen isotope compositions of the types of water which may contribute to formation waters (Knauth & Beeunas, 1986).

Water evaporated from the oceans is depleted in ^{18}O and ^{2}H compare to ocean water, becoming increasingly depleted as an increasing proportion of the water vapour condenses as rainfall (Rayleigh fractionation). Since on a global scale water vapour is transported from low to high latitudes and from ocean to continental interiors; the isotopic composition of meteoric water changes in a geographically predictable way. With paleogeographical insight, one can thus estimate the isotopic composition of palaeo-meteoric waters.

2) Ocean water: Standard mean ocean water (SMOW) has, by definition, $\delta^{18}O$ and $\delta\ ^{2}H = 0‰$ and most ocean waters fall close to this value. The oxygen isotope ratio of sea water is intimately linked with fractionation processes within the hydrological cycle. The cycle comprises evaporation, atmospheric vapour transport, precipitation and subsequent return of freshwater to the ocean (directly via precipitation and via runoff or iceberg melting). Long-term storage of freshwater in aquifers and ice sheets is important for sea water isotope ratios. Finally, the spatial distribution of oxygen isotopes in the world oceans depends on processes of advection and mixing of water masses from different source regions with different isotopic signatures (Dansgaard, 1964; Gonfiantini, 1986).

3) Evaporation residues (bitterns): During the evaporation of seawater, the isotopic compositions of the residual brine define a hook on a plot of δD versus $\delta^{18}O$ (Fig. 2.1; Knauth & Beeunas, 1986). Depending on the degree of evaporation, these waters can be enriched or depleted in D and ^{18}O compared to seawater.

4) Metamorphic water: Metamorphic waters are defined here as waters which have been expelled into sediments from underlying basement rocks. They have variable isotopic ratios but are characterized by their high $\delta^{18}O$ values. Most formation waters have isotopic compositions which plot to the right of the MWL as shown in Fig. 2.1.

Waters within individual basins have isotopic compositions which often define restricted regions of the standard δD: $\delta^{18}O$ diagram. Nevertheless, a wide range of isotopic compositions occur in any one basin, and it is dangerous to assume a single composition for calculating precipitation temperatures from mineral oxygen isotope data. The chemical and isotopic composition of formation water is related to its origin.

2.2.6 Interpretation and Applications of Stable Isotopes

Common uses of environmental isotopes in catchment hydrology include water isotope hydrology, mixing, solute isotope biogeochemistry, isotopically labelled materials and stable isotopes in geochemical modelling. A few of the applications are briefly described below.

I. Water isotope hydrology

Isotope hydrology covers the application of the measurements of isotopes that form water molecules. These are the oxygen isotopes (oxygen-16, oxygen-17, and oxygen-18) and the hydrogen isotopes (protium, deuterium, and tritium). These isotopes are ideal tracers of water sources and movement because they are integral constituents of water molecules, not something that is dissolved in the water like other tracers that are commonly used in hydrology (e.g., dissolved species such as chloride). Water isotopes can sometimes be useful tracers of water flow paths, especially in groundwater systems where a source of water with a distinctive isotopic composition forms a "plume" in the subsurface.

II. Mixing

Isotopic compositions mix conservatively. In other words, the isotopic compositions of mixtures are intermediate between the compositions of the end-members. The compositions can be treated just like any other chemical constituent (e.g., chloride content) for making mixing calculations. For example, if two streams with known discharges (Q_1, Q_2) and known $\delta^{18}O$ values ($\delta^{18}O_1$, $\delta^{18}O_2$) merge and become well mixed, the $\delta^{18}O$ of the combined flow (Q_T) can be calculated from:

$$Q_T = Q_1 + Q_2 \quad \ldots\ldots\ldots\ldots\ldots\ldots\ldots\ldots\ldots\ldots\ldots\ldots\ldots\ldots (Eq.\ 2.11)$$

$$\delta^{18}O_T Q_T = \delta^{18}O_1 Q_1 + \delta^{18}O_2 Q_2 \quad \ldots\ldots\ldots\ldots\ldots\ldots (Eq.\ 2.12)$$

Mixing proportions of two waters with known $\delta^{18}O$ and δD values will fall along a tie line between the compositions of the end-members on a $\delta^{18}O$ vs. δD plot (Kendall and Caldwell, 1998). On many types of X-Y plots, mixtures of two end-members will not necessarily plot along lines but instead along hyperbolic curves as shown in Figure 2.2 (Kendall and Caldwell 1998). This is clearly exemplified by Faure (1986) using the example of $^{87}Sr/^{86}Sr$ ratios. The basic principle is that mixtures of two components that have different isotope ratios (e.g., $^{87}Sr/^{86}Sr$ or $^{15}N/^{14}N$) and different concentrations of the element in question (e.g., Sr or N) form hyperbolas when plotted on diagrams with coordinate of isotope ratios versus concentration. As the difference between the elemental concentrations of two components (end-members) approaches 0, the hyperbolas flatten to lines. The hyperbolas are concave or convex depending on whether the component with the higher isotope ratio has a higher or lower concentration than the other component. Mixing hyperbolas can be transformed into straight lines by plotting isotope ratios versus the inverse of concentration (1/C), as shown in Fig. 2.2b (Kendall and Caldwell 1998).

Graphical methods are commonly used for determining whether the data support an interpretation of mixing of two potential sources or fractionation of a single source. Implicit in such efforts is often the idea that mixing will produce a "line" connecting the compositions of the two proposed end-members whereas fractionation will produce a "curve." However, as shown in Fig 2.3a in Mariotti et al. (1988) cited in Kendall and Caldwell (1998) both mixing and fractionation (in this case, denitrification) can produce curves. Both relationships can look linear for small ranges of concentrations. However, the equations describing mixing and fractionation processes are different and under favorable conditions, the process responsible for the curve can be identified (Kendall and Caldwell 1998). This is because Rayleigh fractionations are exponential relations, and plotting δ values versus the natural log of concentration will produce a straight line Fig 2.3b.

2.3 Geology of Nigeria

The surface area of Nigeria is covered in nearly equal proportions by crystalline rocks and sedimentary rocks (Offodile, 2002; Ocan 2006). Around half of the surface area of Nigeria underlain by sedimentary rocks, has crystalline rocks buried beneath Cretaceous and younger sediments while the other half outcrops largely in the North-central, South-west (where this study was done) and in three smaller region from the North to the south along the eastern boundary between Nigeria and Cameroon.

The crystalline rocks are further divided into three (3) main groups, namely:

I. The Basement Complex;
II. The Younger Granites; and
III. The Tertiary-Recent Volcanics.

The sedimentary rocks occur in seven sedimentary basins. Many of these basins were formed by various tectonic forces during the Mesozoic era. The sedimentary basins include: Dahomey basin (part of the study area), Niger Delta basin, Anambra basin, Chad basin, Mid-Niger basin, Iullemeden basin and the Benue trough.

Detailed description of the geology of the study areas (basement complex areas and sedimentary basin are given in the subsections below.

2.3.1 Review of the Basement Complex of Nigeria

The Basement Complex of Southwestern Nigeria lies to the east of the West African craton in the region of the late Precambrian to early Palaeozoic orogenesis (Rahaman, 1976). Five major groups of rocks were identified in the basement complex terrain of Nigeria by

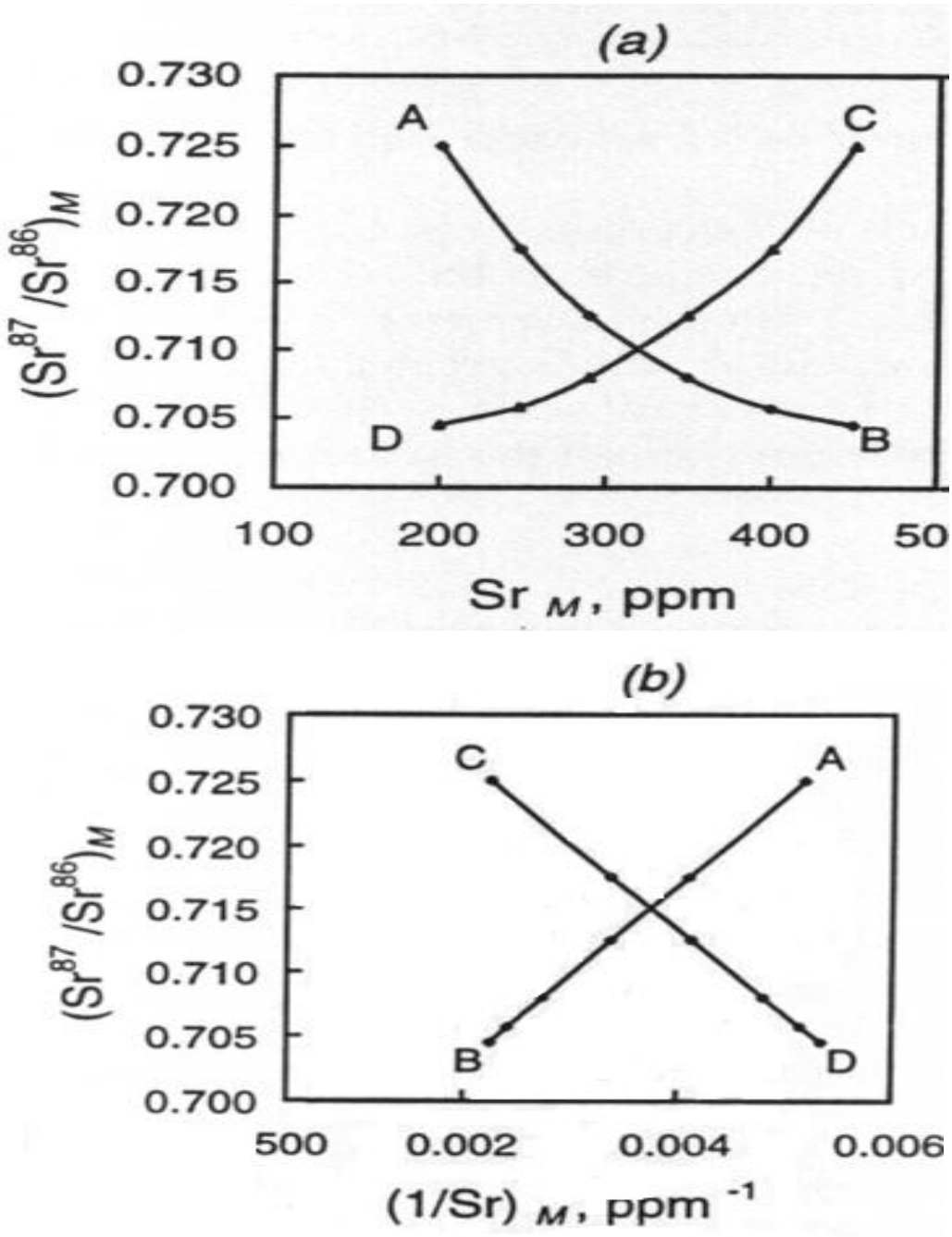

Fig.2.2 Hyperbola formed by mixing of components (water or minerals) A and b with different concentrations and Sr isotope ratio (Faure, 1986 modified by Kendall and Caldwell, 1998)

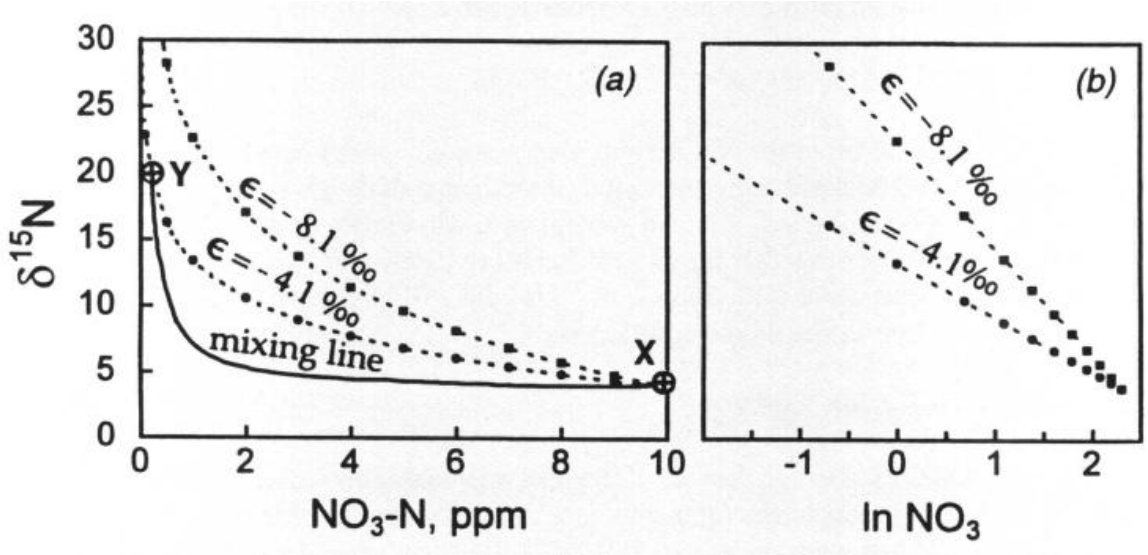

Fig. 2.3: (a) Theoretical evolution of the $\delta^{15}N$ and the nitrate-N concentration (solid line) of two waters X and Y during isotope fractionating process. (b) Plotting the natural log of the concentrations of a fractionation process for different enrichment (ε) value (Kendall and Caldwell (1998) citing Mariotti et al 1988).

Rahaman (1976). These are:

1. Migmatite-Gneiss-Quartzite Complex which comprises biotite hornblende gneisses, quartzites and quartz schist as well as small lenses of calc-silicate rocks;

2. Slightly migmatised to unmigmatised paraschist and metaigneous rocks which comprise pelitic schist, quartzites, amphibolites, talcose rocks, and metaconglomerates, marbles and calc-silicate rocks;

3. Charnokitic rocks;

4. Older Granites which vary in composition from granodiorite to true granites and potassic syenite; and

5. Unmetamorphosed dolerite dykes believed to be the youngest.

I. The migmatite -gneiss-quartzite Complex

The Migmatite-Gneiss-Quartzite Complex is the most widespread in the basement complex of Nigeria. It includes quartzites, calc-silicate rocks, biotite-hornblende schist and amphiboles (Rahaman, 1976)

Three petrological units characterize the Migmatite-gneiss complex. These are:

1. A grey foliated biotite and biotite hornblende quartzo-feldspathic rock of granodioritic to quartz dioritic composition, which is otherwise known as the grey gneiss or early gneiss (Rahaman, 1981). It is present in most outcrops and best seen in migmatites around Ibadan, Iseyin and Ikare.

2. Mafic to ultramafic component, which where present, often outcrops as discontinuous boudinaged lenses or concordant sheet of amphibolites with minor amount of biotite- rich ultramafic. In addition to amphibolites, the mafic to ultramafic component include biotite and biotite hornblende schist and are usually strongly foliated. Except where it constitutes the paleosome to the migmatite, it is present in grossly subordinate amount to the grey gneiss.

3. Granitic or felsic component is a varied group of rocks consisting essentially of pegmatite, aplite, quartz-oligoclase veins, fine grained granite gneiss, porphyroblastic gneiss.

The quartzites tend to form good topographic features, outcropping poorly in most places, however a few good outcrops occur around Ibadan. Rahaman (1976) noted that the quartzite contains at most eight minerals but usually three or four minerals, with greater than 90% quartz, with minor amount of muscovite, sillimanite, staurolite, garnet, haematite, graphite, tourmaline and zircon. Clino-pyroxene, tremolite, actinolite, epidote, calcite and sphene have been described (Rahaman, 1973) from Iseyin quartzite.

The calc-silicate rocks outcrop as low-lying bodies, continuing for a few meters, in the migmatitic gneiss of the Basement Complex.

II. Slightly migmatised to unmigmatised paraschist and metaigneous rocks

The slightly migmatised to unmigmatised paraschist and metaigneous rocks include rocks that have been previously described as newer or younger metasediments as well as the belts of low to medium grade pelitic schists and metaigneous rocks previously grouped with the "Older Metasediments" by Jones and Hockey (1964) and Burke and Dewey (1972).

The schist belt occupies generally N-S trending synformal troughs infolded into the migmatite-gneiss complex and which is best developed in the western part of the country. Seven main belts have so far been identified (Turner, 1983). The belts define the structural grain of the basement and are largely sediment dominated. The most important lithologies are pelites and quartzite. In some belts, chemical sediments are now present as marble or banded iron formation (BIF). Mafic to ultramafic rocks are present as amphibolites and ultramafites. Minor felsic to intermediate metavolcanic rocks and greywacke has been described. The schist belts are about the best-studied group of rocks in Nigeria (Russ 1957 and Truswell & Cope 1963) as a result of the known mineralization such as gold, BIF, marbles and manganese.

III. Charnockitic rocks

Charnokitic rocks represent important petrological units among the Precambrian Basement Complex rocks (Olarewaju, 2006). Texturally and compositionally the charnokitic rocks are of different varieties (Oyawoye, 1964, 1965; Cooray 1977; Rahaman, 1976 and Olarewaju 1999). The most important types are diorites and bauchite (Oyawoye, 1965). The bauchite is greenish in colour and petrographically is a fayalite- bearing quartz monzonite. Charnokitic rocks are associated mainly with the migmatite- gneisses and older granites (Rahaman, 1976). Gabbroic and dioritic rocks are more widely distributed and appear as small bodies and stocks.

Charnokite has three major modes of occurrence. Commonly it occurs in the core of an aureole of granitic rocks as well as along the margins of older granite bodies especially porphyritic biotite and biotite- hornblende granites. it similarly occurs as discrete individual bodies in the gneiss complex (Olarewaju, 2006). Charnokites, in general, outcrop as smooth widely distributed rounded boulders. They are composed of alkali feldspar, quartz, plagioclase, orthopyroxene, clinopyroxene, hornblende and biotite and accessory amounts of opaque ore such as apatite, and zircon and so on.

IV. Older granites

The term 'Older granites' was first used by Falconer (1911) to differentiate between the tin-bearing younger granite from other granites. Older granites vary in composition ranging from granites, granodiorites, adamalites, quartz monzonite, pegmatites and syenite, with granitic/granodioritic composition being the most common (Rahaman, 1976). Texturally, they vary from strongly foliated gneiss varieties to undeformed rocks.

The most abundant and the most typical member of the Older Granite suite is coarse porphyritic granite, which has been described by Oyawoye (1972). The porphyritic granites are typified by abundant large feldspar set in groundmass rich in biotite or hornblende. The colour of the feldspar may be white, pink, purple, yellowish brown or dark grey and may vary in size from 0.5cm in length as in Igarra area to about 10 cm in the Abeokuta granite. Rahaman (1988) described the following petrographic types: migmatitic granite gneiss, early pegmatite, aplites and vein quartz.

V. Unmetamorphosed dolerite dykes

Unmetamorphosed Dolerite Dykes occur as tabular unmetamorphosed bodies cross cutting the foliation in host rocks and are regarded as the youngest member of the Basement Complex. The dolerite dykes are generally black and fine grained and composed largely of augite and plagioclase of andesine-labradorite composition.

2.3.2 Dahomey Basin

Ikorodu area is underlain by the rocks of the Dahomey basin. Dahomey basin is an extensive sedimentary basin, extending from southwestern Ghana in the west to the western flank of the Niger - Delta. However, only the eastern end of the basin is within Nigeria. Here, it is bounded in the North by the Precambrian Basement Complex and by the gulf of Guinea to the south.

The sedimentary basin in southern Nigeria is partially divided into western and eastern portions by the 'Okitipupa Ridge' (Adegoke, 1969), a submarine basement ridge. The incompleteness of this separation is evidenced by the similarity of lithologic units bearing identical marine faunas in both parts of the basin.

The stratigraphy of the eastern Dahomey basin from surface as well as sub-surface data has been described by Jones and Hockey (1964), Billman (1976), Omatsola and Adegoke (1981) and Agagu (1985).

In order of succession, the stratigraphic sequence of the Dahomey basin from the bottom to the top consists of Abeokuta group, Ewekoro Formation, Akinbo shale, Oshosun Formation, Ilaro Formation, Ameki Formation and coastal plain sands and recent alluvium.

2.3.2.1 The Abeokuta Group

These are the oldest sediments lying uncomformably on the erosional surface of the Precambrian Basement. The Abeokuta Group consists of three distinct Formations— Ise, Afowo and Araromi (Omatsola & Adegoke, 1981).

The first major marine transgression in southwestern Nigeria occurred during the Maastrichtian when the sediments of the Abeokuta Group were deposited. The Group thickens towards the west and dips towards the east. Dahomey basin is about 600 ft thick in the type area and only 400 ft thick at the eastern edge (Agagu, 1985).

A . Ise Formation

In areas where Ise Formation overlies the basement such as Ise-2 borehole, the formation depicts a predrift sequence of continental sands, grits and siltstones. Commencing with a basal conglomerate directly overlying the basement; the upper sequences consist of coarse to medium-grained loose sands, sandstones and grits that are interbedded with kaolinitic clays. It has a known maximum thickness of about 1862 m (4,100 – 5,962 m interval).

B . Afowo Formation

Succeeding the Ise Formation is an alternation of brackish to marine sandstones and shales known as Afowo Formation (Omatsola & Adegoke, 1981). The beds are composed of coarse to medium-grained sandstones with variable, but thick interbedded shales, siltstones and clay, with the shale component increasing progressively from the bottom to the top. The lower sequence is transitional with mixed brackish to marginal horizons. This alternates with well-sorted sub-rounded, clean but loose fluviatile sands, indicating a littoral or estuarine near–shore environment of deposition in which water level fluctuated fairly rapidly. Intense pyritisation of clayey horizons are common. Thicknesses vary from 1,430 m in Afowo – 1, 2,300 m, 2,033 m and 1,100 m in Bodashe – 1, Ileppaw – 1 and Ojo – 1 boreholes. The Formation age is Maastrichtian, containing marine foraminifera and ammonites.

c. Araromi Formation

The formation was first described by Reyment (1965) as “Araromi Shale’’. It is composed of fine to medium-grained sand at the base, overlain by shale and siltstone with their interbedded limestones and marls at the Araromi – 1 borehole to the east on Okitipupa ridge, where lignitic

bands are common. The shales are light to gray black and are essentially marine rich in organic content. Offshore Badagry, the Afowo and Araromi sequences have together recorded very high TOC, HI and average maturity with hydrocarbon potentials in the Aje wells. The age is now regarded as Upper Maastrichtian, being rich in planktonic foraminifera, ostracods, pollens and spores. Tar sand bearing sections abound in this formation.

2.3.2.2 Ewekoro Formation

The Ewekoro Formation was deposited during the Paleocene in the western part of the basin. The formation lies conformably on the Maastrichitian Abeokuta and Nsukka, and with Akinbo Formation. It constitutes the lateral equivalent of Imo formation in the eastern part of the basin. The type section of Ewekoro Formation is the limestone exposed in the quarry at Ewekoro. The thickness of the Formation at the type section is about 112.5 m. The limestone has been sub-divided into three units by Adegoke (1970). Ogbe (1970) proposed a fourth unit. The units are listed below in stratigraphic order:

1. Sandy Biomicrosparite (bottom);
2. Shelly Biomicrite;
3. Algal Biosparite; and
4. Red Phosphatic Biomicrate (top).

The Ewekoro formation is well described in literature due to its importance in the production of cement. It contains abundant foraminifera, ostracods, coralline algae, gastropods, pelecypods, echinoids in the limestones–shale assemblage. The base of the Ewekoro Formation is approximately defined by an increasing proportion of sandstone and siltstone towards the top of the Araromi Formation.

The fauna in the Ewekoro Formation include the foraminifera, ostracodes and other invertebrate fossils.

2.3.2.3 Akinbo Formation

The shale overlying the Ewekoro limestone was accorded formational status named Akinbo Formation by Ogbe (1970), with the type section at the Ewekoro quarry. It comprises shale, glauconitic rock band, gritty sand to pure grey with little clay. Lenses of limestone from the underlying Ewekoro Formation grades into the Akinbo Formation, close to the basal shale – rich sequence. The age straddles from Palaeocene to Eocene. The Formation is the lateral equivalent of the Imo Formation in southwestern Nigeria (Adegoke, 1969 and Fayose, 1970).

The shale is characteristically laminated with an intermediate band of glauconitic rock. It is very richly fossiliferous containing poorly preserved molluscs (microforms) occurring as ferruginous casts, except around the limestone bands and lenses. Upwards the shale loses its lamination, becomes more arenaceous and passes gradationally into massive mud.

2.3.2.4 Oshosun Formation

Overlying the Akinbo Formation is the Oshosun Formation. It is a sequence of laminated pale greenish – grey phosphatic light grey to purple-white clay with interbeds of sandstones. The Formation contains claystone underlain by argillaceous limestone of phosphatic and glauconitic materials in the lower parts. The formation is Eocene (Agagu, 1985).

Adegoke (1969) observed that the Oshosun fauna which include Molluscs, corals, crinoids, crustaceans, pelagic and planktonic foraminifera, fishes and sea snakes show that the formation was deposited in a predominantly marine environment and not in a lagoon swamped periodically by the Eocene sea, as suggested by Russ (1924).

2.3.2.5 Ilaro Formation

The sedimentation of the Oshosun Formation was followed by a regression which deposited the transitional to continental, dominantly sandy Ilaro Formation. The name Ilaro Formation was given by Jones and Hockey (1964) to a sequence of mainly coarse, sandy estuarine, deltaic and continental beds that display rapid lateral facies change. The Formation is predominantly Eocene in age.

The Ilaro Formation varies in thickness between 37 and about 60 m, the thickest section occurs at Hetin Scotta near the axis of the Togo - Dahomey western Nigeria basin. The top of Ilaro Formation is marked by a very thick grey-black shale sequence (Berggren, 1960).

2.3.2.6 The Coastal Plain Sands

The coastal plain sands are characterized by soft, very poorly sorted clayey sands, pebbly sand, sandy clay and rare thin lignite (Agagu, 1985). The coastal plain sands occur in the coastal area of Nigeria, especially in the western and mid western Nigeria. Coastal plain sands boundary is assumed to be at uneven surface underlain by variegated sandy clay of the Ilaro Formation (Jones and Hockey, 1964). Tattam (1943) described the extensive red earth and loose ill-sorted sands underlying the Eocene Bendel—Ameki group and named it coastal plain sands. The name is now well known in the stratigraphy of the Delta, and it has been retained in

the southwestern coastal sedimentary basin. The coastal plain sands do not contain fossils except for plant remains. The age is between Oligocene - Pleistocene.

2.3.2.7 Recent Sediments

The superficial deposits above the Coastal Plain Sands consist of littoral and lagoonal sediments of the coastal belt and the alluvial sediments of the major drainage systems around the coastal belt. There is a gradation from one into the other on the landward side near the mouths of the large rivers and the lagoons. The coastal belt sediments vary along the 180 km Atlantic coastline from about 8 km near the Republic of Benin border to 24 km towards the eastern end of Lagos lagoon.

The lithology of these littoral and lagoonal sediments consists of unconsolidated sands, clays and mud with varying proportions of vegetal matter while occasional beds of sandstone with ferruginous cement are encountered. Most of the shallow units of the boreholes are made up of thick beds of loose, coarse-grained, shelly sand alternating with variable thickness of dark mud, which sometimes consists almost entirely of partly carbonized organic matter (Jones and Hockey, 1964). Correlation at such shallow depths for sediments deposited under littoral and lagoonal conditions that reflect continuously shifting lagoon and sea beach patterns with concomitant varying sedimentation conditions is hardly possible.

2.4 Geology of Abeokuta Area and its Environs

The study area in Abeokuta is limited to section underlain mainly by crystalline Basement Complex rocks described as older granites (Rahaman, 1988). The area is mainly underlain by hornblende-biotite gneiss, porpyroblastic gneiss, granite, porphyritic granite and pegmatitic intrusions. The geology of the area is presented in Fig 2.4. The northeastern part of the area is underlain by porphyritic gneiss while the hornblende biotite gneiss is largely restricted to the southwestern part of the study area. Detailed description of the petrographic characteristics of the different rock types is discussed under results and discussions.

2.5 Geology of Ikorodu Area

The geological map of Lagos area was established using several boreholes drilled for various purposes (water supply, foundation engineering and hydrocarbon exploration including bitumen). The stratigraphic relationships of the boreholes and their electric logs from the earliest wells (Afowo of Mobil) to most recent (Aje wells of Folawiyo) on the western frontier

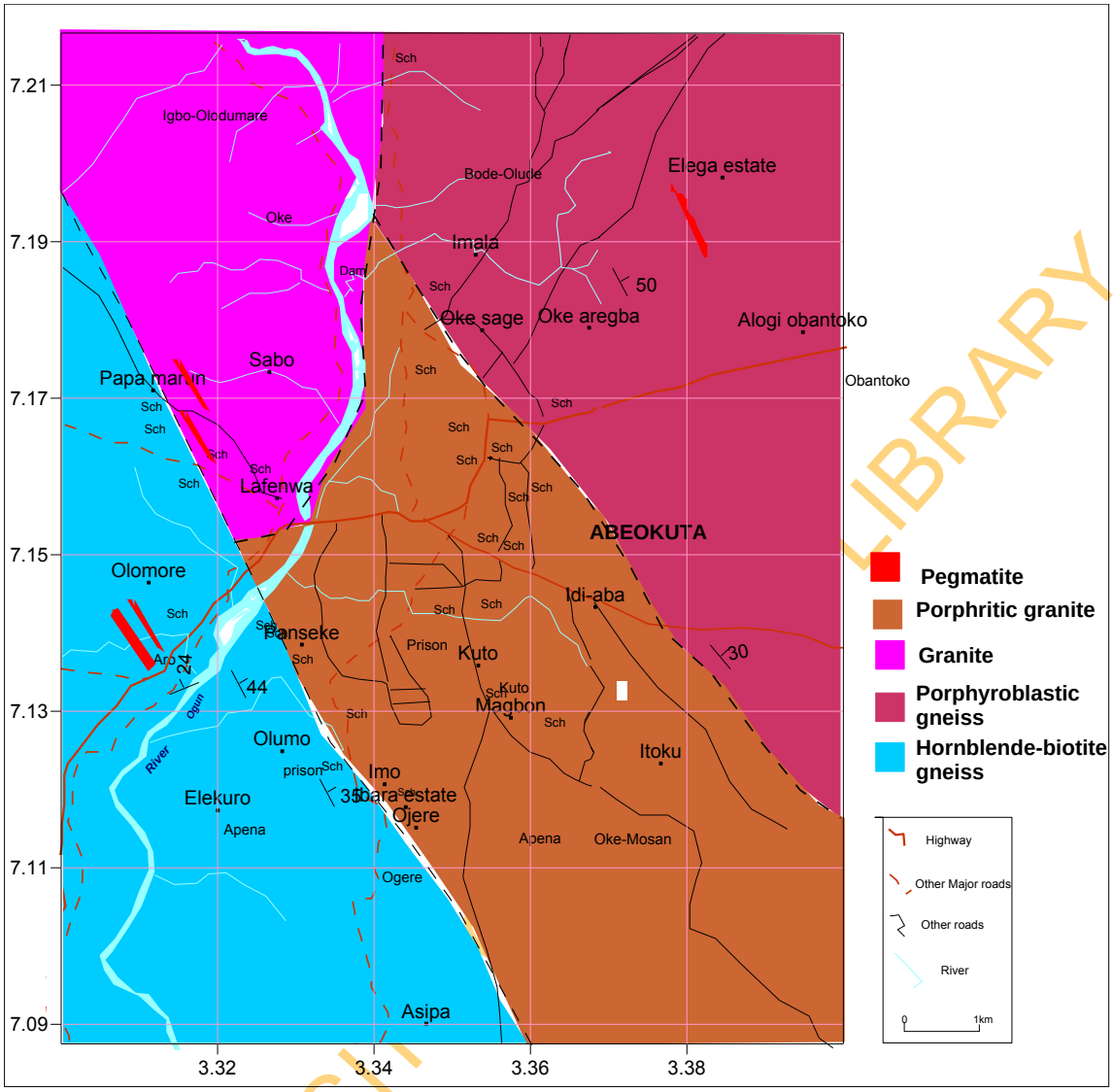

Fig. 2.4: Geological map of Abeokuta area.

with the Republic of Benin eastwards to Okitipupa Ridge (Ise Graben) was used in deciphering the geology of the area at depth (Olatunji 2006). Ikorodu area is located within the Dahomey basin adjacent to the Lagos lagoon. Most part of Lagos State, southwestern Nigeria (Fig 2.5), is underlain at the surface by the Quaternary Oligo–Pleistocene Coastal Plain sands and Recent littoral and lagoonal alluvial deposits. Borehole evidence indicates that the Cretaceous and Tertiary sediments underlie the Coastal Plain Sands with a general southward gentle dip and an apparent thickening seawards.

Borehole log of Ikorodu area (Fig 2.6) revealed that Ikorodu is underlain by thick lateritic clay, which can be as thick as 30 m in the landward areas and totally absent in some areas around the lagoon. The clay is underlain by sand, which in turn is underlain by thick clay horizon. This clay is underlain by another sandy layer overlying a very thick clay horizon which lies on a very thick shale.

Most of the boreholes in the landward area tapped groundwater from the second sandy horizon while groundwater is exploited through shallow hand-dug wells from sandy layer exposed on the surface around most parts of the areas close to the Lagos lagoon.

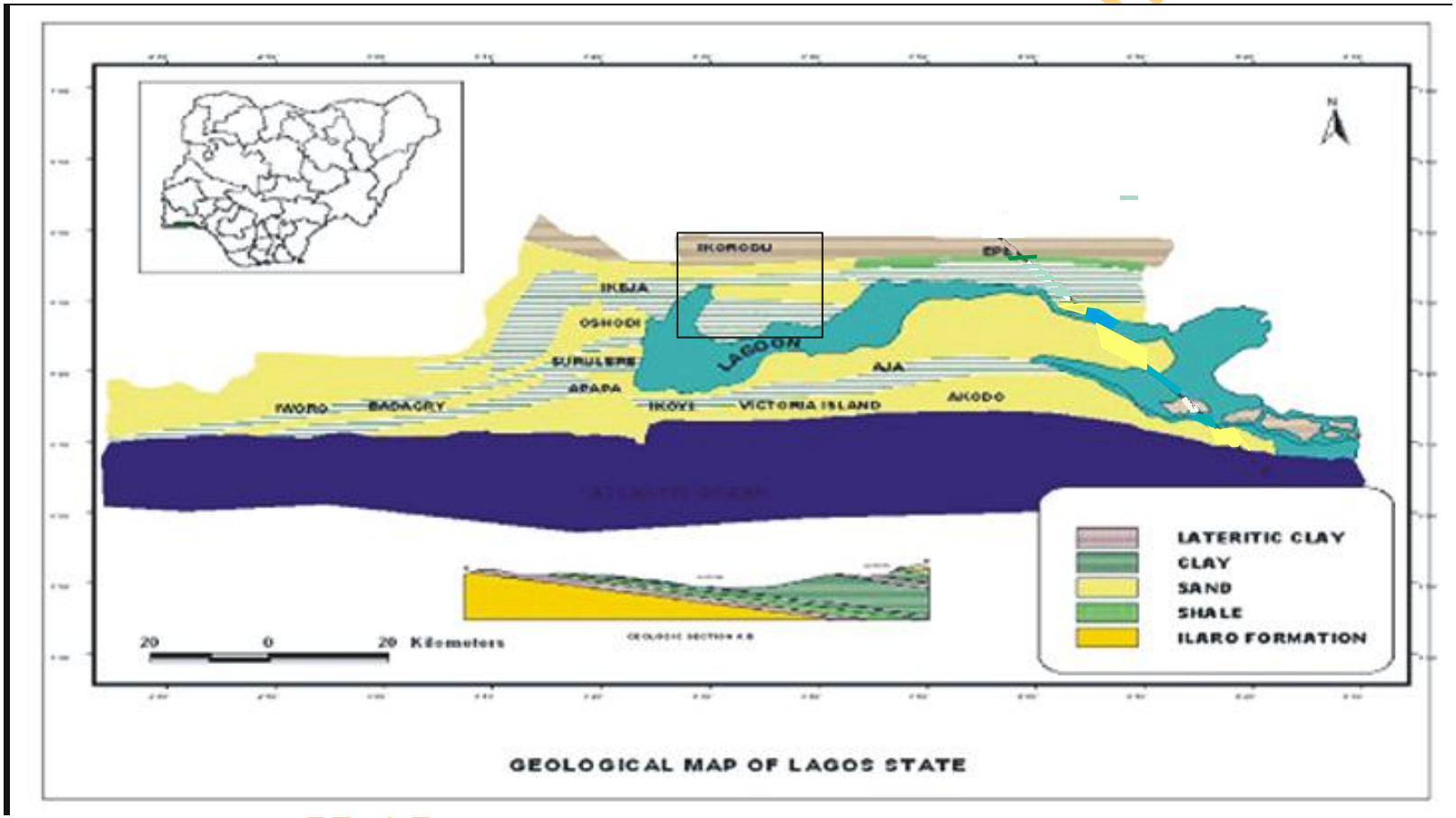

Fig. 2.5 Geological map of Lagos State (Olatunji, 2006)

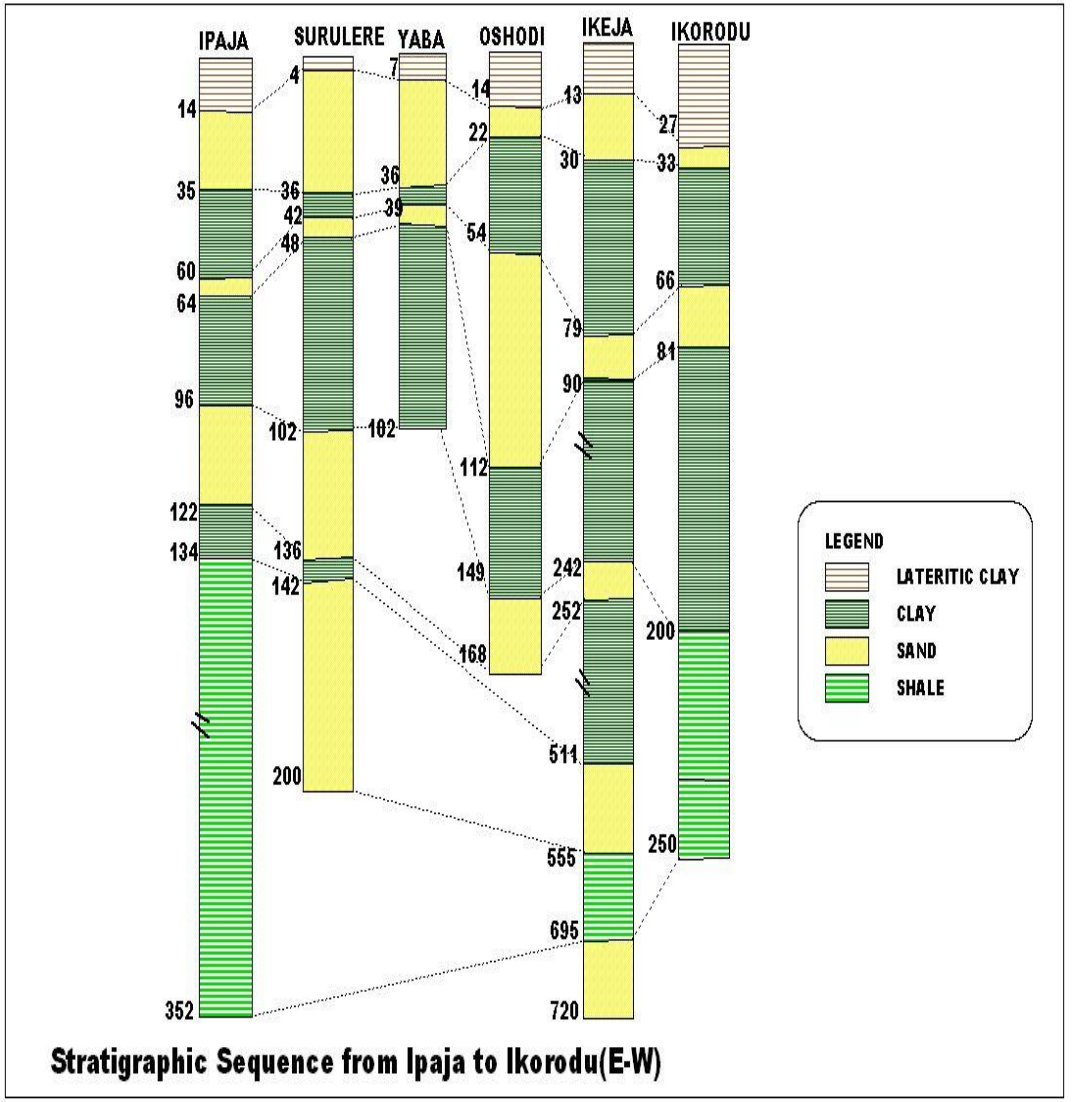

Fig. 2.6: Stratigraphic sequence (E-W) from Ipaja to Ikorodu (Olatunji, 2006)

CHAPTER THREE
METHODOLOGY

3.1 Field Works

The field works carried out during this study include geological field mapping, geophysical survey and groundwater sampling in the two areas. The procedure employed in carrying out the mapping, survey and sampling exercises as well as the instrumentation and analytical procedures for laboratory works are described in the following sections.

3.2 Geological Field Mapping

Geological field mapping was carried out by first studying the topographical map and dividing the map into eight grids for easy and even (as much as possible) coverage. The instruments used for the field exercise are Garmin 76 global positioning sysem (GPS), compass-clinometer, sample bag, field notebook, base map, protractor, pencils, hand lens, hammer, camera and chisel. The detailed field exercise entailed the following:

1. Observation and identification of rocks at outcrop location;
2. Capturing of the locations of coordinates of outcrops with the aid of a GPS, recording of measurements and observations on the map and in the field notebook; and
3. Collection and labelling of fresh samples and taking of photographs of important features such as foliation, faults, joints and intrusion.

Where outcrops are located, detailed observation was undertaken while walking around the outcrop. Notes and measurement were taken at the most appropriate parts of the outcrop, which give a fair representation of the outcrops. Information noted includes mineral composition, mode of occurrence and structures.

The various observations and measurements were then plotted on the base map. The data plotted on the map are the strikes and dips of foliations. Representative fresh samples were collected and labelled. Photographs of observed structures such as foliations, folds, veins were taken. Thin sections of samples were made for photomicrographs of the different rock types in the mapped area for petrological studies.

3.3 Geophysical Survey

The study was carried out with the aid of Syscal Junior Terrameter, measuring tapes, current and potential electrodes, hammers, compass/clinometer and Garmin Global Positioning System (GPS). In Abeokuta area, seventy five (75) Vertical Electrical Sounding (VES) stations were covered ensuring wide and systematic coverage of the study area depending on the

availability of space for spreading the electrodes such that AB/2=100 m (Fig. 3.1). Similarly, fifty (50) VES stations were occupied in Ikorodu area ensuring wide coverage of the area (Fig. 3.2), with AB/2 of between 250 and 500 m as dictated by availability of space for electrode spread. The practical difficulty of laying out long lengths of cables in these areas because of urban development in many parts is a problem that had to be overcome for the successful geophysical survey of the areas.

The Slumberger array was used at each of the VES points. At chosen points for VES soundings, an iron rod was driven into the ground to mark the base station. The Iron rod served as the midpoint from where MN/2 (potential electrode) and AB/2 (current electrode spacing) were measured in both directions. The electrodes were driven in on both side and the spacings given as AB/2. A straight line was maintained by the configuration of all the electrodes as shown in Fig 3.3.

The measurements were repeated and recorded with MN fixed at its initial distance while the current electrodes were progressively and symmetrically increased. When the resistance measure becomes too small, MN/2 was increased symmetrically. At all points, the criterion MN/2 < AB/5 was satisfied. The change in distance between the current electrodes increases the depth range at which current penetrates. The apparent resistivity (ρ) was then plotted against the corresponding half electrode spacing (AB/2) on a bi-logarithm paper.

3.3.1 Interpretation

The data of vertical electrical sounding (VES) are usually presented as a series of graphs expressing the variation of apparent resistivity with increasing electrode separation. These curves qualitatively represent the variation of the resistivity with depth and as such the curves may be qualitatively interpreted by inspection.

Several authors have introduced many methods of interpreting resistivity data obtained in the field. Such methods include numerical method of interpretation, interpretation by curve matching technique and interpretation by auxiliary point method (Zohdy, 1974).

Recently, however the calculation of the vertical electrical sounding (VES) curves of the Schlumberger type of horizontal stratified media was simplified and greatly accelerated through the use of convolution method.

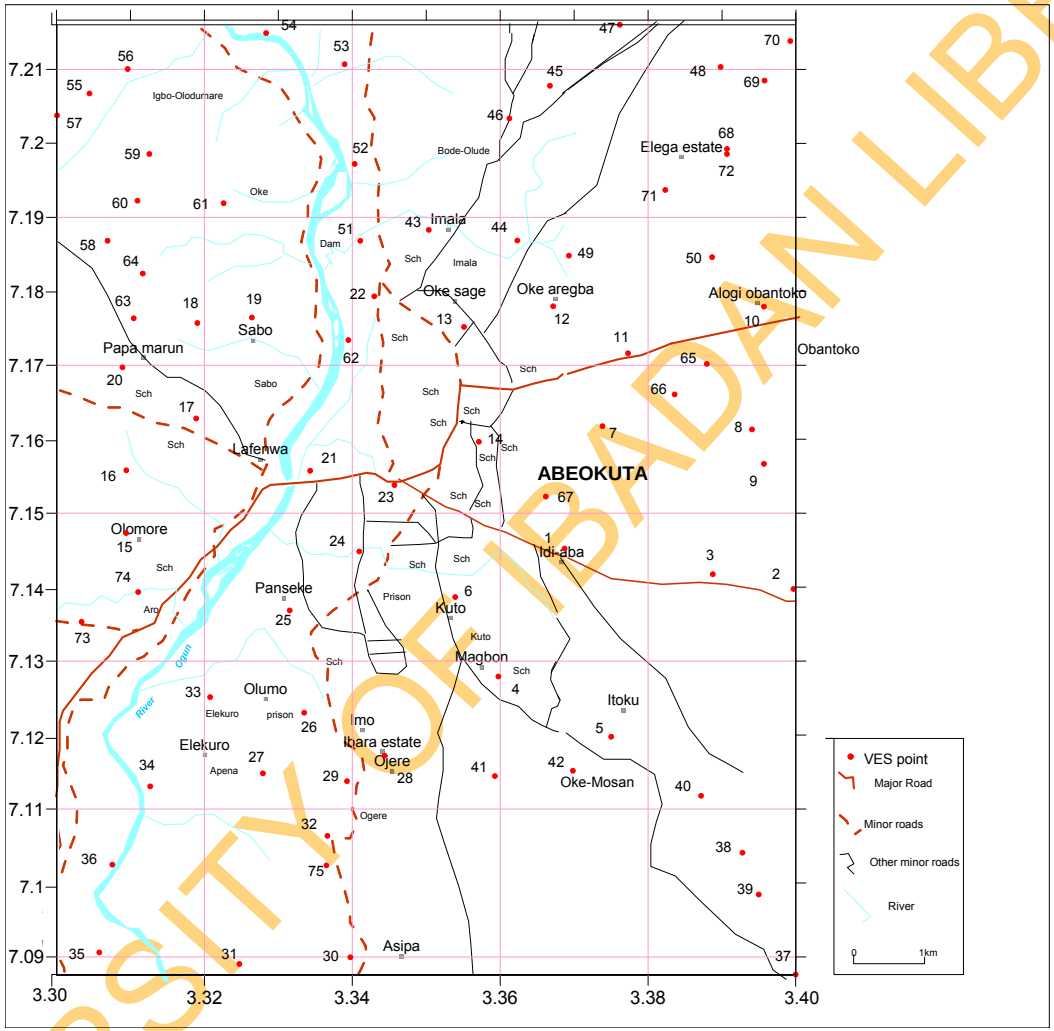

Fig. 3.1: Vertical Electrical Sounding (VES) points in Abeokuta Area.

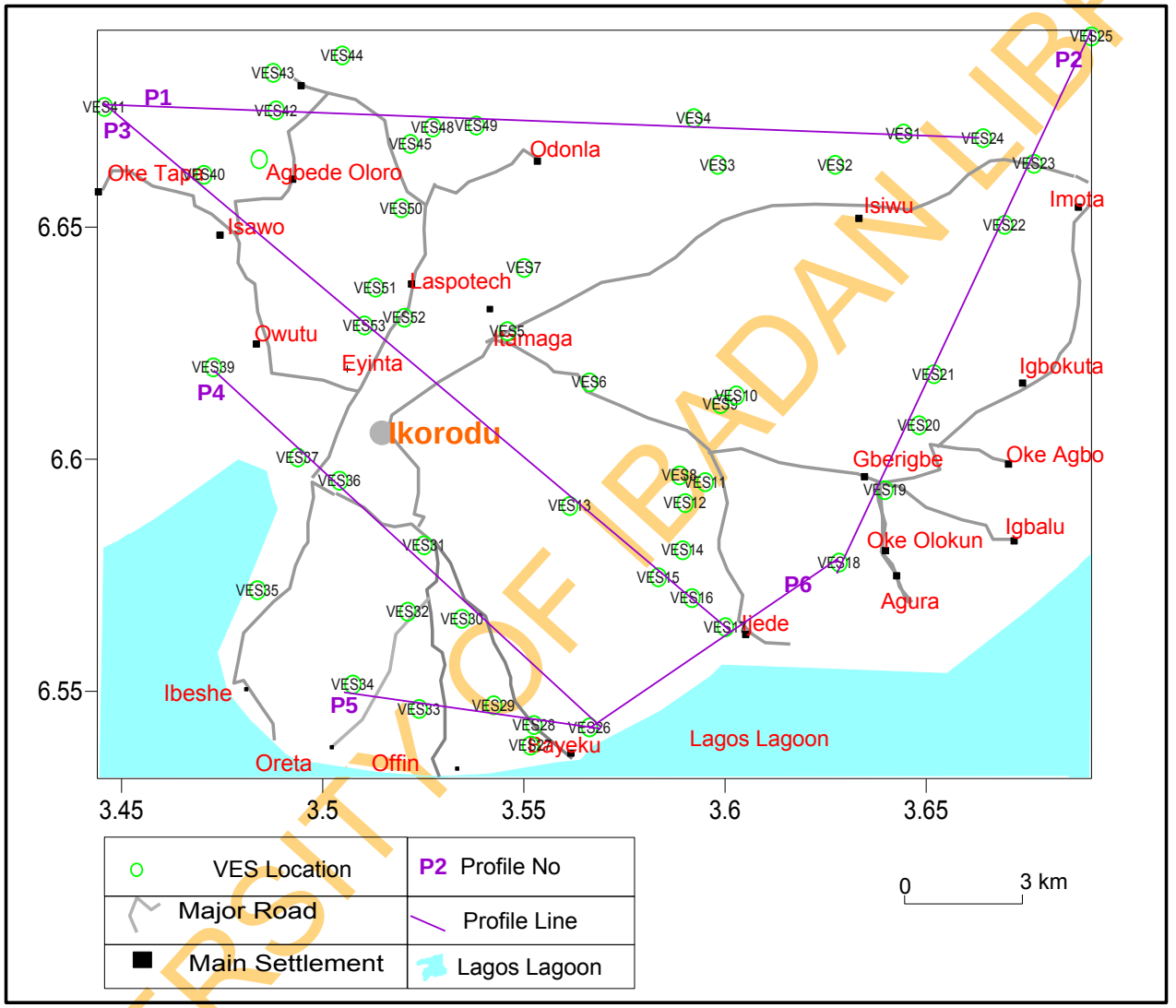

Fig. 3.2: Vertical Electrical Sounding (VES) points and Borehole locations in Ikorodu Area.

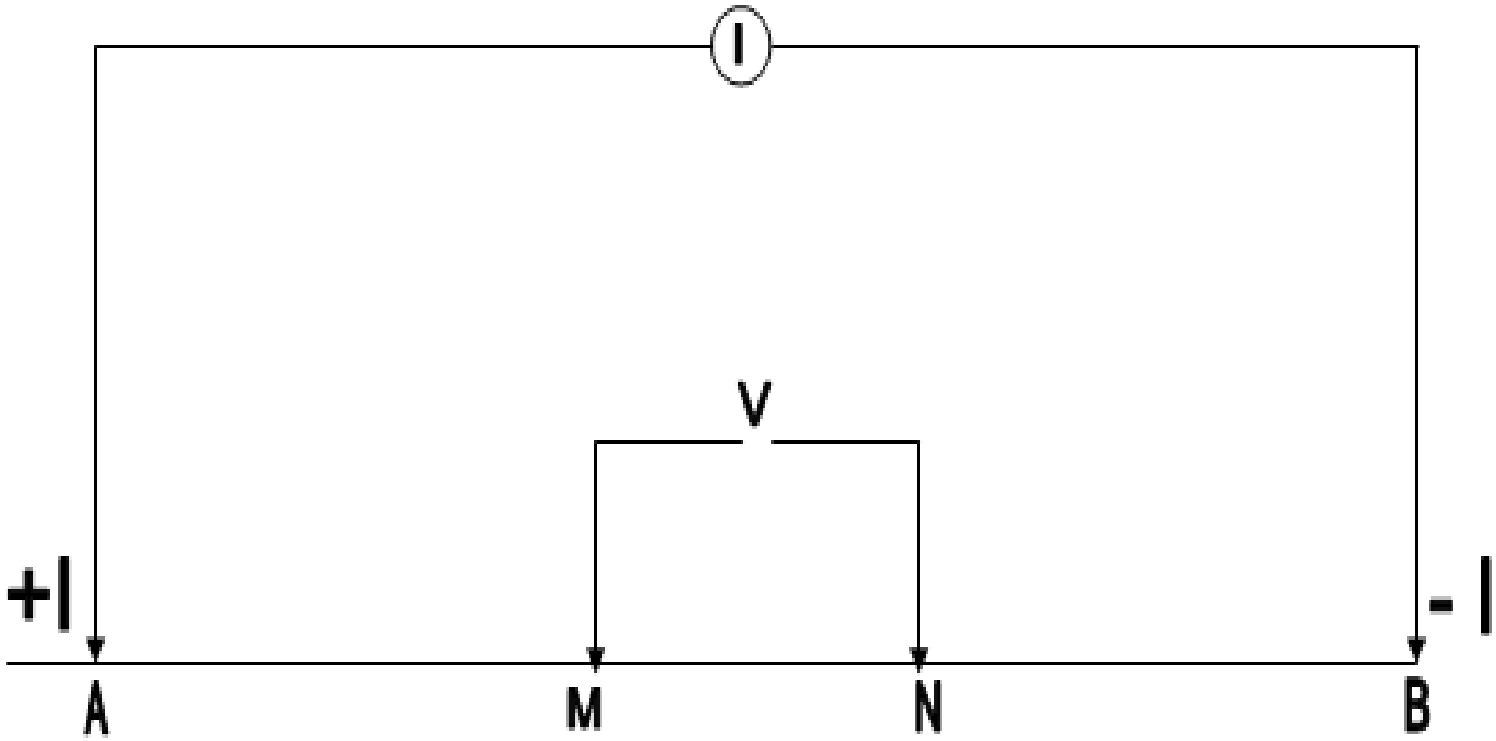

AB = Current Electrodes, MN = Potential Electrodes

Fig. 3.3: Generalized System Electrode Array.

3.3.2 Partial Curve Matching

This involves the comparison of field curves with standard curves. The standard curves are based on the relationship between the hypothetical curves of resistivity against depth (Telford et.al., 1976 and Dobrin, 1976). The partial curve matching technique uses two layer model curves and the corresponding auxiliary curves (Bhattacharya and Patra, 1968 cited in Bayowa et al, 2007).

Before interpretation is made with the master set of horizontal layer, it must be satisfied that the form of the sounding curve is sufficiently smooth and not distorted by sharp curves or discontinuities.

Different sets of curves are normally employed for this technique, and they are:

- Theoretical 2-Layer master curves;
- Auxiliary curves;
- Ascending type where $\rho2>\rho1$ or $\rho2/\rho1$ is greater than unity; and
- Descending type where, $\rho2<\rho1$ or $\rho2/\rho1$ is less than unity.

Furthermore, in conjunction with theoretical master curves, the four-auxiliary curves designed for use in more than two layer interpretations were used.

Partial curve matching enables field curves plotted on the logarithm transparent paper of the same model as the master curve to be compared with two layers theoretical curves.

The field curves were matched segment by segment starting from small electrode spacing. Matching starts from the left hand side of the profile towards the right hand side, then the profile is adjusted towards the left, right, up and down but always ensuring parallelism of coordinate axes until a best fit of the field curve against one of the theoretical curves is obtained.

Occasionally, the field curve may have to be matched between two of the master curves. The origin of coordinate of bi-logarithm transparent sheets containing the field curve corresponds to the resistivity and thickness of the first layer respectively. In addition, this yields the constant value corresponding to the resistivity contrast between this upper most layer and one that is directly underlying it. Resistivity of the second layer is calculated from the product of resistivity of the first layer and the constant value.

The computer generated model VES curves based on the starting model parameters were compared with the theoretical/field curves and where good fit was obtained between field/theoretical model curves, and the RESIST software-generated curves, the interpretation results (layer resistivities and thicknesses) were considered alright. Where a satisfactory fit was

not achieved, the starting model parameters (layer resistivities and thicknesses) were automatically adjusted and the whole procedure repeated.

3.3.3 Computer Iteration

Computer iteration was done by the use of the initial model extracted from the field data curve using the partial curve matching technique. The outcome of curve matching provided starting models for computer modelling which gives the final accepted geo-electric structures. The curve matching gets cumbersome where there are many layers, hence, the computer iteration makes the interpretation of such problems easier. The iteration process of a curve can be done between 1-30 times before achieving a perfect match, after which the computer displays the result of the iteration in form of curve and the layer parameters. However, it was largely ensured that the r.m.s error was not more than 5% in all the iterated curves. This method is the most efficient among the interpretation methods in terms of speed and accuracy.

3.4 Groundwater Sampling

Sampling was carried out in January 2007 in the study areas; Abeokuta and Ikorodu. Fifty water samples were randomly collected from hand-dug wells in Abeokuta area, ensuring as much as possible that samples were collected from areas underlain by different rock types. In Ikorodu Area, borehole water samples were collected mostly in the landward area because only borehole or Deep-wells are available in this area. In the area close to the Lagos lagoon groundwater samples were collected from the shallow hand-dug wells. The groundwater sampling points in the study areas are shown in Figs 3.4 & Fig. 3.5 respectively for Abeokuta and Ikorodu areas.

The coordinates of the locations were determined using GPS. The depth to water table and total depth of the wells were measured using an improvised device made up of measuring tape with a metal attached to the end of the tape. The measurements were done by lowering the heavy end of the measuring tape into the wells until it reachedthe water surface. The depth to this surface was read on the tape. The tape was then lowered further into the wells until it touched the bottom of the well.

The sampling bottles were rinsed twice with the water to be sampled before they were filled up. Two sets of samples were collected in 750 ml bottles in all locations in two areas. A set of the samples was acidified and labelled with a suffix A (e.g. 1A) to differentiate acidified samples from those that were not acidified.

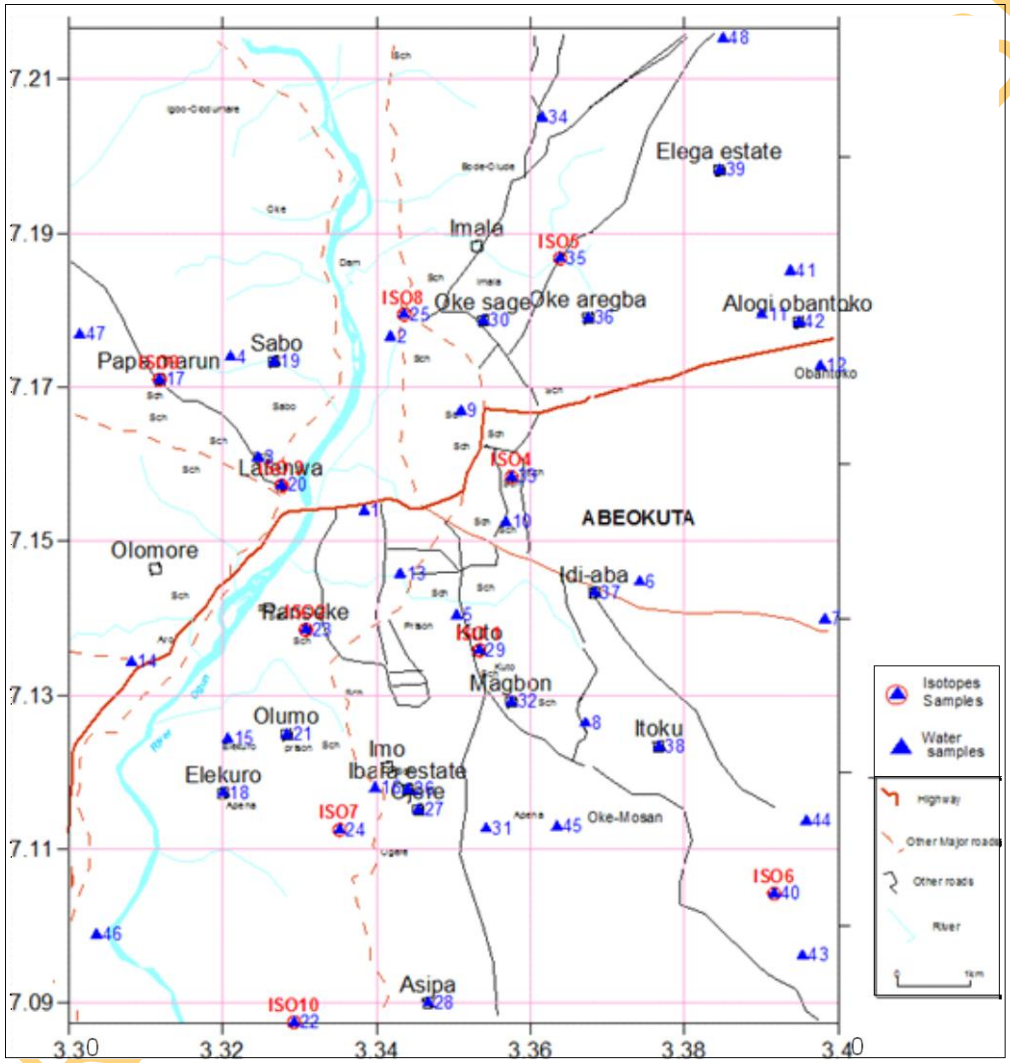

Fig. 3.4: Groundwater sampling points in Abeokuta area.

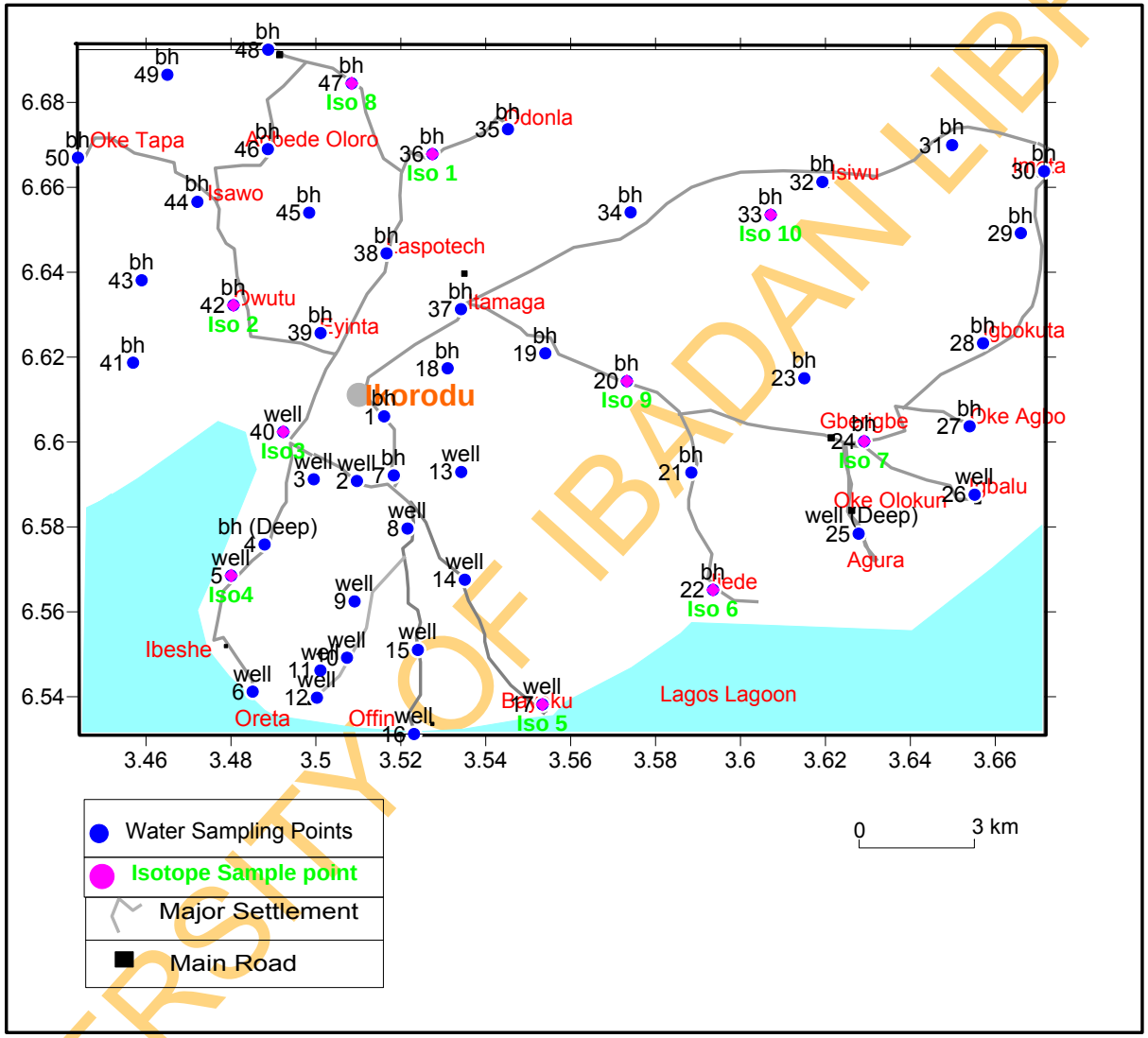

Fig. 3.5: Groundwater sampling points in Ikorodu area.

A third set of samples were collected from ten locations in the two areas into high-density polyethylene (HDPE) plastic bottles for analysis of groundwater isotopes (^{2}H and ^{18}O), ensuring the spread of the samples across the areas. Sensitive parameters like TDS, EC and pH were measured on the field using handheld digital meters. The meters were first rinsed with the samples before being used.

3.5 Laboratory Study

Thin sections of the rocks samples were cut at the Obafemi Awolowo University, Ile-ife and studied under petrological microscope at the Department of Earth Sciences, Olabisi Onabanjo University, Ago-Iwoye.

The geochemical analysis of the rock sample was carried out at the Acme Analytical Laboratories Ltd, Vancouver, Canada. Analysis of groundwater samples was carried out to determine the concentrations of the cations, including 36 other elements (heavy metals and some trace elements) as well as anions were determined at the Activation Laboratory (ACTLAB), Ontario, Canada. The isotope analyses (^{18}O and ^{2}H) were carried out at the Institute of Arctic and Alpine Research, Stable Isotope Laboratory, (SIL) INSTAAR, University of Colorado, Boulder, CO, USA. The analytical methods for the different analyses are described in the sections below.

3.5.1 Geochemical Analyses

Geochemical analysis of rock samples was carried out at Acme Analytical Laboratories Ltd, Vancouver, Canada, using the Inductively Coupled Plasma-Mass Spectrometry (ICP-MS) method to determine the elemental and major oxide content of the rock samples.

ICP-MS is a versatile, rapid and precise analytical technique, which provides high quality multi-element and isotopic analyses for samples in solution. It is capable of determining the concentrations of over 70 elements in a single analytical run. The detection limit for most elements in solution is in the sub-ppb range. For some elements, it may lie in the sub- ppt range.

In order to ensure proper analysis of the samples, digestion of the sample was carried out using the fusion method. The fusion method ensures that the whole sample is dissolved as all major oxides including SiO_2, rare earth elements (REE) and other high field strength elements are put into solution.

The fusion technique that employs a lithium metaborate/tetraborate flux was used. The resulting molten bead was rapidly digested in a weak nitric acid to produce a clear solution which was then analyzed using the ICP-MS.

The ICP-MS instrument employs argon plasma as the ionization source and a quadruple mass spectrometer to detect the ions produced. During analysis, the sample solution was nebulized into flowing argon gas and passed into inductively coupled plasma. The gas and nearly everything in it was atomized and ionized. The positive ions in the plasma were then focused down a quadruple mass spectrometer where they were separated according to mass, detected, multiplied and counted.

3.5.2 Groundwater Analyses

Water samples were analyzed using the Inductively Coupled Plasma Optical Emission Spectrometry (ICP-OES) for major cations and 36 other elements. The other elements are heavy metals, non-metals and trace elements constituents in all or some of the analysed groundwater in Abeokuta area include arsenic (As), barium (Ba), bismuth (Bi), cadmium (Cd), copper (Cu), cobalt (Co), iron (Fe), manganese (Mn), molybdenum (Mo), nickel (Ni), phosphorus (P), lead (Pb), antimony (Sb), sulphur (S), selenium (Se), silicon (Si), tin (Sn), strontium (Sr), tellurium (Te), titanium (Ti), thallium (Tl), uranium (U), vanadium (V), tungsten (W), yttrium (Y) zinc (Zn), beryllium (Be), silver (Ag), cerium (Ce), chromium (Cr) and lithium (Li). Ion Chromatography was used for determining the concentration of anions. These analyses were done at Activation Laboratories, Ontario, Canada. The stable isotopes were determined at the institute of arctic and alpine research, Stable Isotope Laboratory, (SIL) INSTAAR, University of Colorado, Boulder, CO, USA

3.5.2.1 Inductively Coupled Plasma Optical Emission Spectrometry (ICP-OES)

Most of the elements on the periodic table can be measured using ICP-OES. The major rock forming elements and some important trace elements can be determined simultaneously to sensitivities better than those of X-ray fluorescence.

The technique relies on placing the sample material into solution, which was done using fusion technique. The sample solution was then introduced into radio frequency excited plasma (~8000 ºK). Atoms within the sample are excited to the point that they emit wavelength-specific photons or light, which is characteristic of a particular element. The number of photons produced is directly related to the concentration of the element in the sample.

3.5.2.2 Ion Chromatography

In ion chromatography, a gas may be broken down into ions (electrically charged fragments) by passing it through a hydrogen flame, bombarding it with X-rays or radioactive material, or using adsorbent substances that exchange ions with the material being analyzed. The ion chromatography technique involves the vaporization of the sample by heating and the vaporized mixture is forced by an inert gas along a narrow, coiled tube packed with a material through which the components flow at different rates and are detected at the end of the tube.

3.5.3 Hydrogen Isotope Analysis

Water samples for hydrogen isotopic analyses are logged into the SIL sample database where pertinent information about each sample is recorded and each sample is assigned a sequential internal SIL Sample ID number. All samples were held in refrigerated storage until such time when 2 ml aliquots from each sample was pipetted into 5 ml glass auto sampler vials with septa caps for analysis. A Micromass SIRA Series II Dual Inlet mass spectrometer is dedicated to analyzing hydrogen isotopes in water, using a Gilson autosampler coupled to a uranium reduction system for 24 hours automated operation (Vaughn et al., 1998). The samples were arranged in the auto-sampler for the analysis of groups of seven, separated by one of 5 different, pre-calibrated internal laboratory standard waters, which are chosen with the expected isotopic range of the samples in mind (ranging from -3 ‰ to –430 ‰, relative to V-SMOW).

The autosampler automatically delivers 50 µl of water samples and standards to a two position, six-port Valco valve, which flushes, isolates and then injects a 5-microliter sample volume to the heated expansion chamber. The sample in water vapour form was subsequently expanded into glass chambers where the pressure bleeds to the mass spectrometer through a heated (600°C) uranium reduction furnace. The resulting hydrogen escapes from the uranium and was fed into the mass spectrometer where the gas was ionized, accelerated by a ~3 kv electric field. The resulting ion beams were then separated by a fixed magnet that surrounds the flight tube into their constituent masses, and currents were measured on collectors (faraday cups). Sample and reference gas were alternated to achieve statistically significant ratio counts. The ratio of the beam currents was then converted to a delta value using standard notation, and the results were logged by the controlling computer. Computer files with sample data were post processed, where QA/QC evaluations were performed. The samples were drift corrected for measured differences between water standards of known values. The “memory” in the instrument from residuals of the previous sample was accounted for, based on previous memory determinations from widely varying standards of known values were analyzed sequentially. In

addition, a second, isotopically different (>150‰) standard was analyzed in the same run as if it were a sample. The determined value was compared to its known value as a secondary quality assurance (QA)/quality control (QC) check on all performed corrections. The internal (SIL) laboratory water standards were calibrated annually against water standards obtained from the International Atomic Energy Agency (IAEA), V-SMOW, SLAP, and GISP.

Results were reported relative to V-SMOW in per mil (‰). Typical reproducibility between multiple standards in one set of samples is ±0.3‰ in δ D (±1 ‰ is quoted). Digital results of the analyses were retained on three different hard drives, as well as a paper copy, for future reference and QA/QC.

3.5.4 Oxygen Isotope Analysis

Water samples for oxygen isotopic nalyses were logged into SIL sample database awhere all pertinent information about each sample was recorded and each sample assigned a sequential internal SIL Sample ID number. The method of isotopic analysis is based on Epstein and Mayed (1953). All samples were held in refrigerated storage until such time when 2 ml aliquots from each sample were pipetted into 5 ml glass auto sampler vials with for analysis. Care was taken to minimize evaporation of samples or standards. The remaining 3 ml head space in the vials was filled with CO_2 using a Plexiglas enclosure that floods the manifolds, vials and surrounding area with pure CO_2. Vials were positioned carefully in a matching rack, just below the manifold itself. All areas were flushed for 2 minutes with CO_2 tank gas entering through the manifold, and along the sides of the chamber, venting on the ends. After 2 minutes, the manifold was gently lowered onto the vials as a group; engaging the 'O-ring' fitted vial ports into the vials.

The samples were then placed in a custom sealed chamber that accommodated the rack-manifolds of 18 samples or standards. Typically, a rack contains 14 samples and 4 standards. Each rack-manifold was placed along with others in an enclosed equilibration block, where the temperature was controlled at 25°C (± 0.1°C) and the point where equilibration fractionation factors are well known. Samples and standards were allowed to equilibrate for a minimum of 8 hours, at which time the CO_2 becomes isotopically representative of the oxygen 18 ratio in the sample or standard.

For the isotopic analysis of the head space CO_2, a micromass optima dual inlet mass spectrometer (Fig. 3.6) was used. The head space CO_2 of the sample or standard was expanded into the mass spectrometer, via the sample below. The CO_2 was fed into the mass spectrometer where the gas was ionized, accelerated by a ~3 kv electric field. The resulting ion beams were

then separated by a fixed magnet that surrounded the flight tube into their constituent masses (44, 45, and 46), and currents were measured on collectors (Faraday cups). Samples and reference gas were alternated to achieve statistically significant ratio counts. The ratio of the beam currents was then converted to a delta value using standard notation, and the results were logged by the controlling computer.

Computer files with sample data were post processed, where QA/QC evaluations were performed. The samples were drift- corrected for measured of differences between water standards of known values. In addition, a second, isotopically different (>150‰) standard was analyzed in the same run as if it were a sample. The determined value was compared to its known value as a secondary QA/QC check on all performed corrections. The internal laboratory water standards are calibrated annually against water standards obtained from the International Atomic Energy Agency (IAEA), V-SMOW, SLAP, and GISP. Standards are frequently exchanged and compared with other laboratories. Results are reported relative to V-SMOW in per mil (‰). Typical reproducibility between multiple standards in one set of samples is ± 0.06 ‰ in $\delta^{18}O$. Digital results of the analyses were retained on three different hard drives, as well as a paper copy, for future reference and QA/QC.

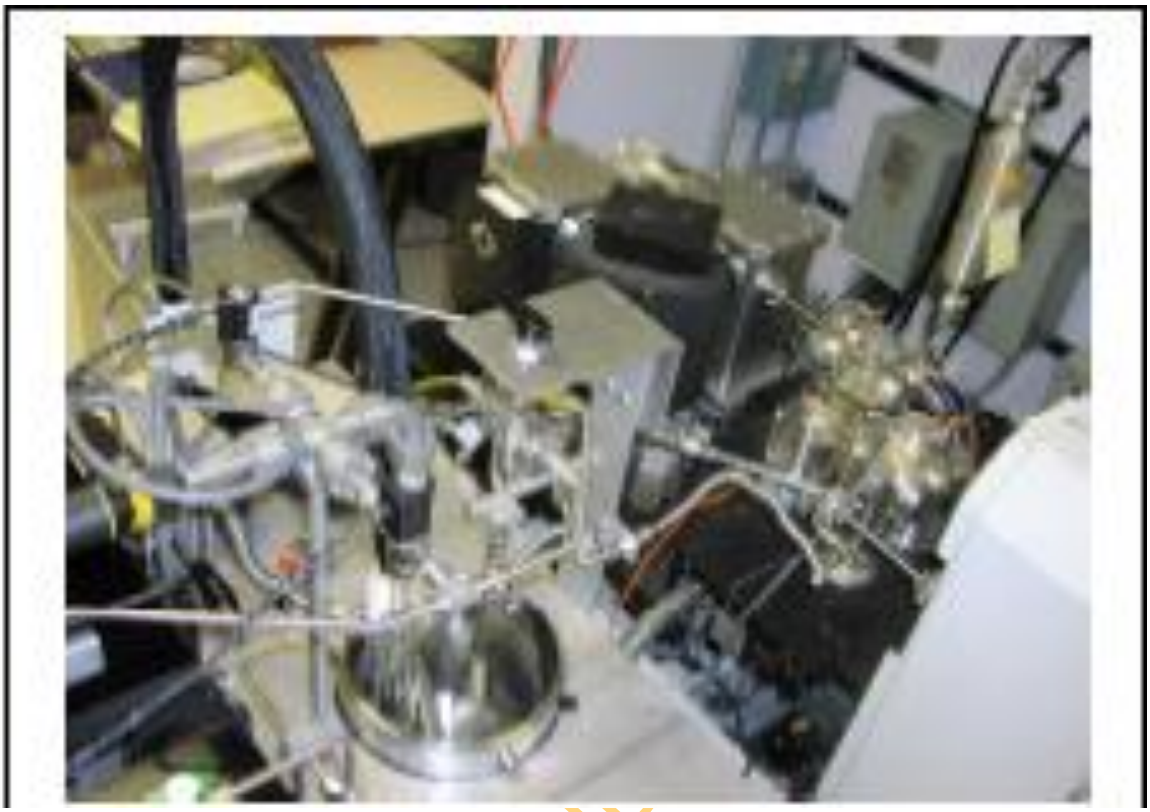

Fig.3.6: Optima dual-inlet mass spectrometer (Source: Stable Isotope Laboratory, INSTAAR)

CHAPTER FOUR

RESULTS AND DISCUSSIONS

4.1 General Statement

The field data acquired during vertical electrical soundings and geo-electric parameters obtained from the interpretation of the soundings are included in appendix I. Geochemical data from the study area are included as Apendix II while the VES curves of the study areas are attached as appendix III. Hydrochemical maps depicting the concentrations of the major constituents and some heavy metals/trace elements are attached as appendix IV. The petrographic characteristics of the rocks underlying Abeokuta area are discussed in the first section and the geochemical characteristic of the rocks is presented and discussed in the second section. Third section covers groundwater occurrence and potential in the study areas while the fouth section is on the geochemistry of groundwater including isotopic characteristics of groundwater in the study areas.

4.2 Petrographic Description of the Underlying Rocks in Abeokuta Area

Abeokuta area is underlain by hornblende biotite gneiss, porphyroblastic gneiss, granite and porphyritic granite. The granites occur mainly in the central part of the study area intruding the gneisses. The rocks are highly jointed and are mostly trending in the NW-SE direction (Fig.4.1). Pegmatite is a minor rock in the area, occuring largely as linear intrusion in few places in the underlying rocks. These intrusions trend in the NW-SE and NE-SW directions (Fig. 4.2).

The mineralogical and textural descriptions of the rocks in hand specimens and under photomicrographs are given in sections below.

4.2.1 Hornblende-Biotite Gneiss

The hornblende biotite gneiss (Fig 4.3) in Abeokuta area is strongly foliated occurring in the western and southwestern part of the study area. Hand specimen of the rock contains high percentage of hornblende, biotite, quartz and feldspar. In many areas, joints and veins on the rocks are discordant with the direction of foliation. The outcrops are intruded in a number of places by pegmatite. The occurrence of the xenoliths of gneisses (Fig. 4.4) in the granite in the study area clearly indicates that the gneisses are older than the granitic rocks in the area.

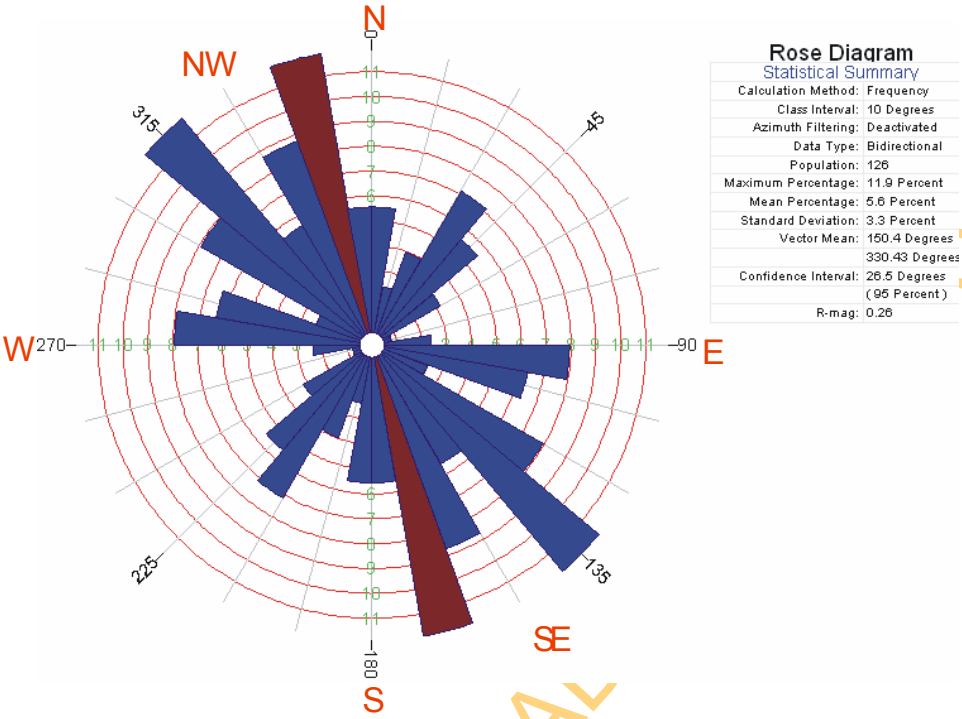

Fig 4.1: Rose diagram of joints in the rocks in Abeokuta area.

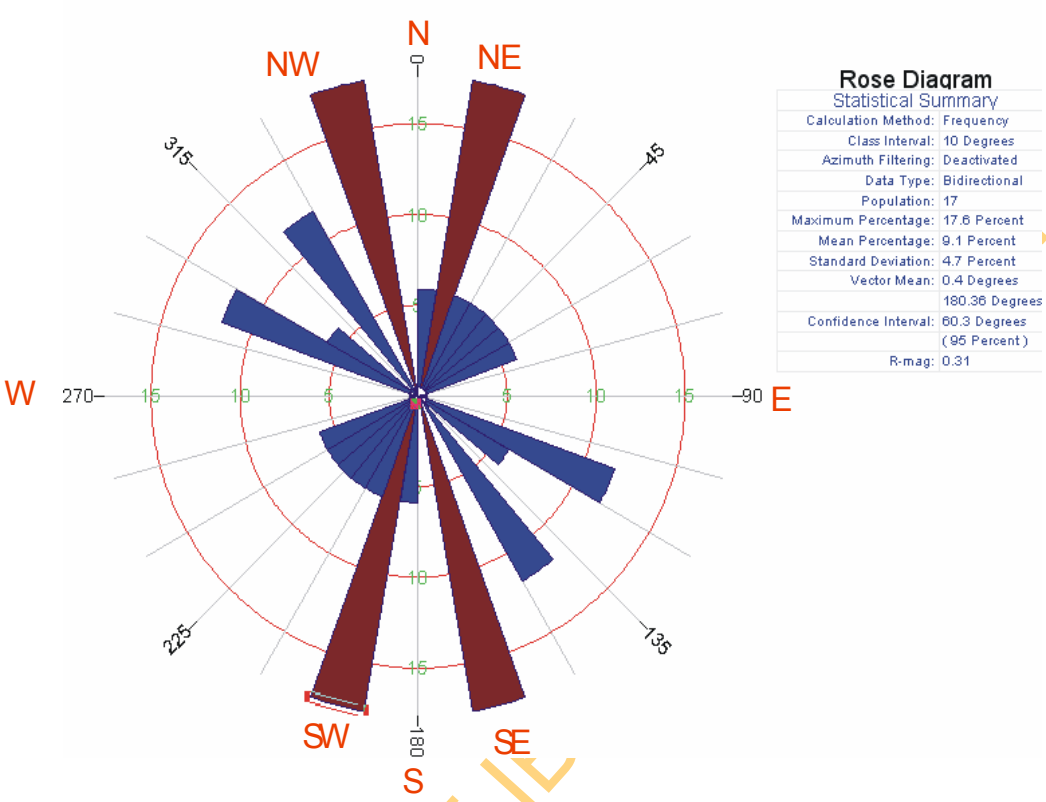

Fig 4.2: Rose diagram of pegmatite intrusions in Abeokuta area.

Fig. 4.3: Hornblende biotite gneiss in Abeokuta area

a 

b. 

Fig. 4.4a and b: Gneiss xenoliths in porphyritic granite in Abeokuta area

4.2.2 Porphyroblastic Gneiss

Porphyroblastic gneiss is characterized by preferred orientation of feldspar porphyroblasts within finer grained groundmass (Fig 4.5). The large feldspar crystals in the porphroblastic gneiss in the area are euhedral crystals, mostly rectangular in shape. The foliation dips towards the east with the outcrops being very massive and some very extensive in most areas. Porphyroblastic gneiss outcrops mainly in the northeastern part of the study area (Bode-Olude and North of Bode Olude).

4.2.3 Granite

Granite outcrops in Sabo, Oke and Lafenwa areas. The granite is intruded by pegmatite in a number of places, containing medium to coarse grains of quartz, biotite, alkali and plagioclase feldspars with granular texture. The granite is leucrocratic in colour with quartz, plagioclase feldspar and microcline being the dominant minerals. Biotite is present as minor constituents in the rock. Granite has pegmatitic intrusion in few locations and occurs in northwestern part of the area.

4.2.4 Porphyritic Granite

The porphyritic granite is part of the older granite rock recognized as the main phase of granitic-dioritic rocks by Jones and Hockey (1964). The porphyritic granite is typified by abundant feldspar megacryst haphazardly set in a finer ground mass rich in biotite (Fig 4.6). The colours of the feldspar are mostly dark grey. The feldspars are commonly 3 – 5cm long and often appear to be rectangular in outlines. The rock is leucocratic in colour and it underlies southeastern part of study area.

4.2.5 Pegmatite Intrusions

The pegmatite intrusions (Fig 4.7) are linear bodies of rocks that intruded into some of the main rocks (granites and the gneisses) underlying the area. They contain extremely coarse crystals of quartz, feldspar and muscovite. The intrusions are light grey in colour and trend mostly in both the NE-SW and NW-SE directions.

4.2.6 Petrological Characteristics of Rocks in Abeokuta

The results of the petrological studies of representative samples of the different rock types in Abeokuta area are presented below. Percentages of the minerals in the rock in thin section are presented in Table 4.1.

Fig. 4.5: Porphyroblastic gneiss in Abeokuta area.

Fig 4.6: Porphyritic granite in Abeokuta area.

Fig 4.7: Pegmatite intrusion in Abeokuta area.

Table 4.1: Mineralogical composition of rocks in Abeokuta

Minerals	Hornblende biotite gneiss	Porphroblastic gneiss	Granite	Porphyritic granite
Quartz	55	55	50	45
Biotite	15	22	7	10
Microcline	15	10	27	25
Plagioclase feldspar	5	5	10	10
Muscovite			3	5
Hornblende	6			
Others	4	8	3	5

4.2.6.1 Hornblende-biotite gneiss

Minerals observed under the microscope include biotite, hornblende, quartz and plagioclase feldspar (Fig. 4.8). The biotite is dark brown with high relief, and pleochroic, changing from light brown to dark brown when rotated. Perfect cleavage can be seen in many of the crystals. Biotite occurs as platy elongated mineral under plane polarized light (PPL). Hornblende is green to brown with strong pleochroism in shades of green, yellow and brown. Twinning is common. Plagioclase feldspar is distinguished from other feldspar types because of its characteristic polysynthetic twinning visible in the crystals. Plagioclase feldspar appears dark to light grey under cross nicol. It is colourless under PPL but shows first order of grey under cross nicols. Quartz is the dominant mineral in the rock (Table 4.1). Quartz is colourless using plane polarized light in most of the slides and display exceptionally yellowish colour when rotated. It has low relief using plane polarized light and weak birefringence. In order of abundance the minerals obsereved are quartz (55%), microcline (15%), plagioclase feldspar, (5%) biotite (15%) hornblende (6%) and other minerals (4%). The mineralogical composition, the characteristics of the outcrops and description of samples in hand specimen discussed in earlier section indicate that the rock is hornblende biotite gneiss.

4.2.6.2 Porphyroblastic gneiss

Minerals identified in the porphyroblastic gneiss under microscope (Fig 4.9) include quartz, biotite, plagioclase, microcline and muscovite. Quartz is the most abundant mineral in the thin-section with 55%. Other minerals include biotite (22%), microcline (10%) and plagioclase (5%). Based on the observed foliation on the field, the preffered alignment of porphyroblasts and the mineral composition, the rock is porphyroblastic gneiss.

4.2.6.3 Granite and porphyritic granite

As observed in the hand specimen, the crystals in the granite are almost equi-modal and haphazardly distributed. The minerals present in thin-section include quartz, feldspar and biotite. The most dominant minerals are quartz and feldspar. The photomicrograph of the granite sample is presented in Fig 4.10. The relative abundance of the minerals is as follow: quartz (50%), microcline (27%), plagioclase feldspar, (10%) biotite (7%), muscovite (3 %) and others (3%). The mineralogy as described in hand specimen and thin-section and the grain sizes indicate that the rock is granite.

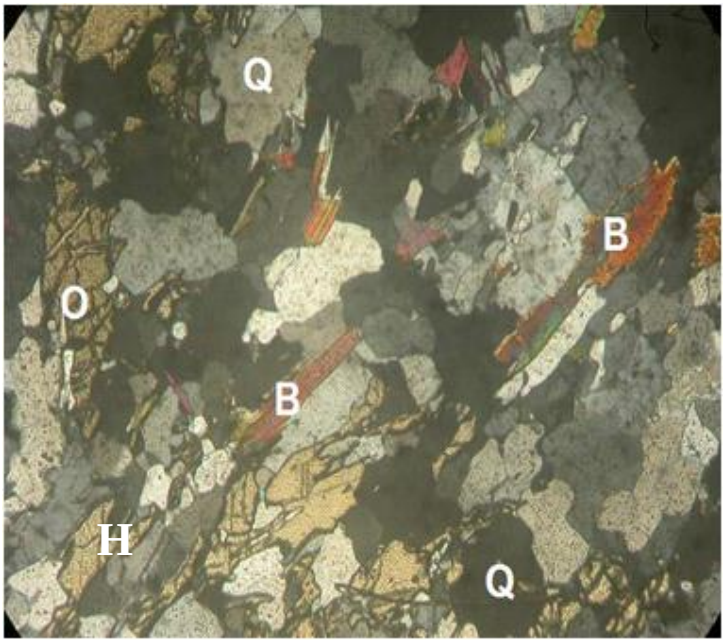

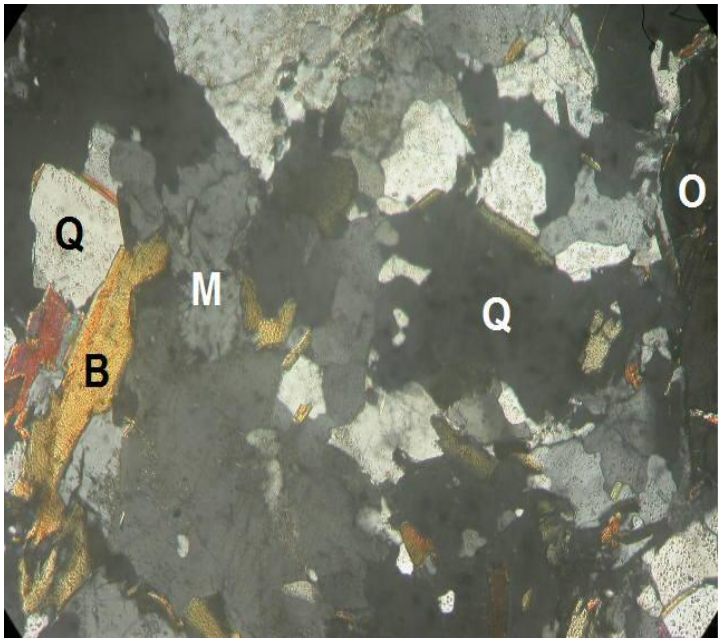

Fig. 4.8: Photomicrograph of hornblende-biotite gneiss in transmitted light showing hornblende and biotite.

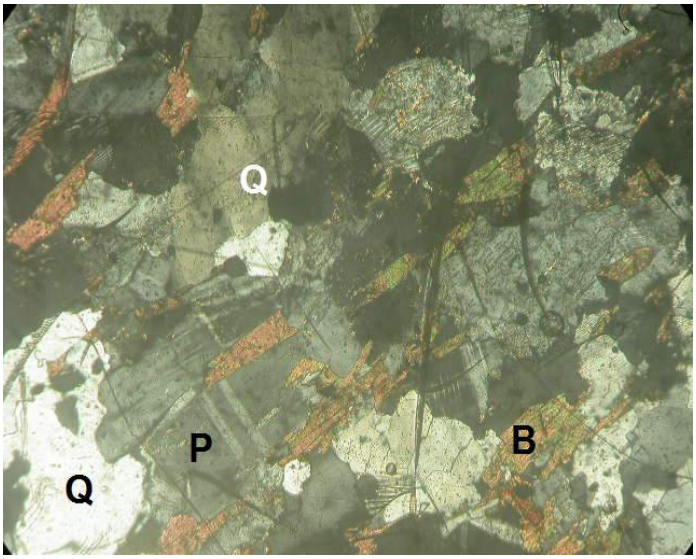

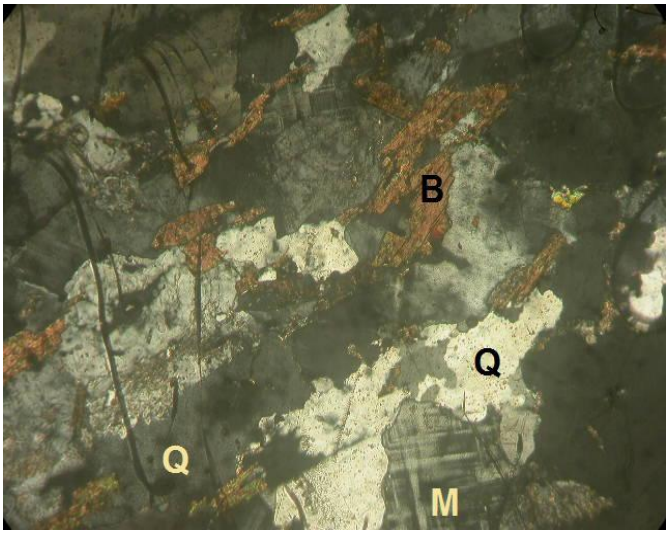

Fig. 4.9: Photomicrograph of porphyroblastic gneiss in transmitted light showing biotite aligned along a preferred direction.

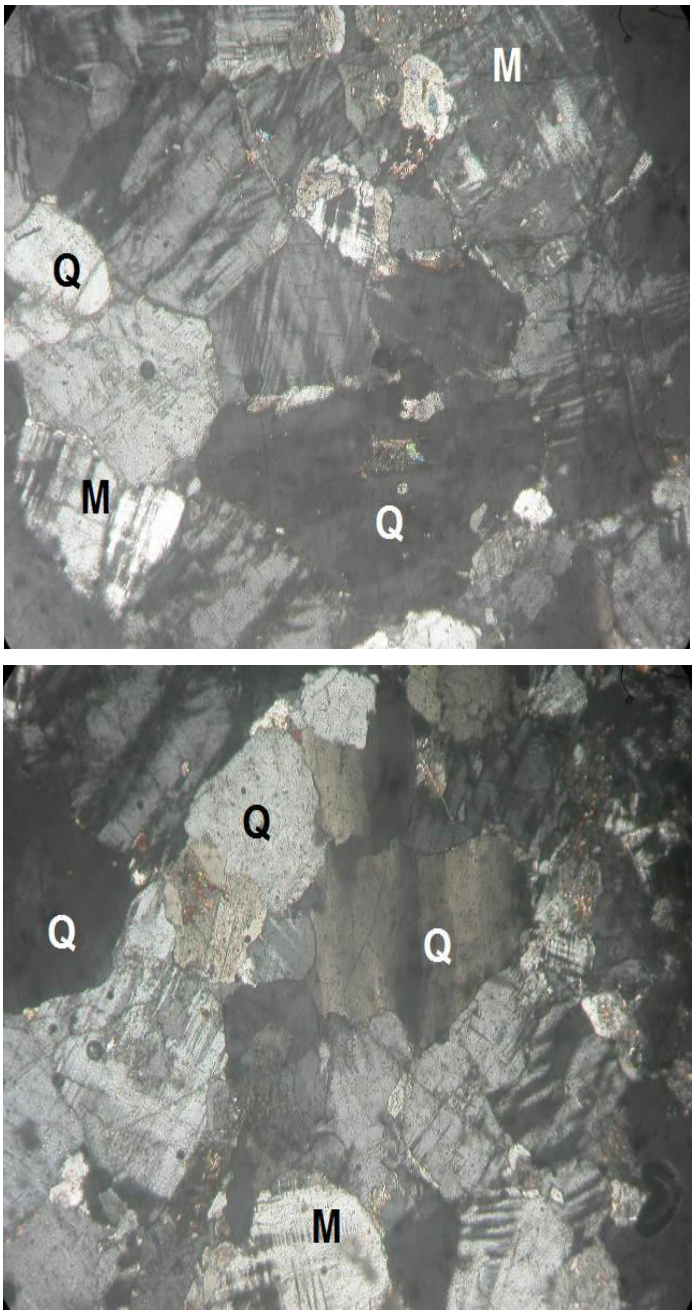

Fig. 4.10: Photomicrograph of granite in transmitted light showing microcline.

The photomicrograph of porphyritic granite (Fig 4.11) observed using microscope, revealed minerals that include quartz, microcline, plagioclase and biotite. The microcline feldspar is colourless under PPL and it displayed first order grey under cross nicols. It is characterized by cross-hatched twinning. Texturally, the microcline displays distinctively coarser crystal set in relatively finer matrix of quartz, biotite and other minerals. Quartz is is the most abundant mineral in the thin-section with 45 %. Other minerals include microcline (25%), plagioclase feldspar (10%) biotite (10%), muscovite (5%) and others (5%). The mineralogy as described in hand specimen and in thin-section as well as the grain sizes indicates that the rock is porphyritic granite.

4.2.7 Geochemistry of Rocks in Abeokuta Area

The results of the major oxides of representative rock samples and the trace metals/elements in ppm are presented Tables 4.2 and 4.3 respectively.

4.2.7.1 Major oxides and trace elements

The results of the major oxides in the underlying rocks in Abeokuta area are presented in Table 4.2. In almost all the rocks underlying the area, the relative abundance of the oxides is SiO_2>Al_2O_3>K_2O>Na_2O>CaO>MgO, except in hornblende-biotite gneiss. The relative percentages of the oxides reflect the similarities in the mineralogy of the various rock types. Silica and alumina are major constituents of all the rocks (aluminosilicate minerals) in the study area; however the relative percentage of the oxides of the alkalis and alkali earths (Fig 4.12) is proportionate to the types of minerals in the different rocks. Generally the order of abundance of all the alkali and alkali earth oxides is K_2O>Na_2O>CaO>MgO, with the exception of hornblende-biotite gneiss in which the relative abundance is CaO>MgO>Na_2O>K_2O. The higher CaO, MgO and FeO reflect the presence of hornblende [$Ca_2Na(Mg,Fe)_4(Al,Fe,Ti)_3Si_8O_{22}(O,OH)_2$], as an important constituent of the rock.

All the underlying rocks are mineralogically similar (Table 4.1) as they are all composed principally of quartz, feldspar and biotite (except hornblende biotite gneiss) that contain hornblende in addition to quartz, feldspar and biotite). The rocks are chemically alike as shown in Table 4.2 and Figure 4.12. High percentage of iron (5.22-8.86%) in the gneisses compared with the percentages in granites (0.24-4.02%) is largely due to the higher percentage of biotite that constitutes the mafic bands in the gneisses but is lower in the granitic rocks.

Table 4.2: Result of the major oxides of the rock samples in Abeokuta.

Analyte	Unit	MDL	Pegmatite	Porphyritic granite	Hornblende-biotite gneiss	Granite	Porphyroblastic gneiss
SiO_2	%	0.01	74.36	72.35	54.51	73.08	66.17
Al_2O_3	%	0.01	14.12	14.29	17.05	12.83	13.79
Fe_2O_3	%	0.04	0.24	1.58	8.86	4.02	5.22
MgO	%	0.01	0.03	0.22	2.47	0.67	1.07
CaO	%	0.01	0.10	1.07	12.55	2.90	2.32
Na_2O	%	0.01	1.39	3.00	0.95	3.10	2.70
K_2O	%	0.01	9.33	6.67	0.20	1.52	4.26
TiO_2	%	0.01	<0.01	0.12	2.17	0.75	1.11
P_2O_5	%	0.01	0.01	0.12	0.47	0.25	0.45
LOI	%	-5.1	0.40	0.40	0.40	0.70	2.60
Sum	%	0.01	99.96	99.83	99.69	99.82	99.70

Table 4.3: Summary of the result of the trace elements in the rock samples in Abeokuta

Elements	Range (ppm)	Elements	Range
Ni	Bdl – 29	Zr	7.2 – 532
Sc	Bdl – 42	Y	0.9 – 34.0
Ba	43 – 486	Mo	Bdl – 0.4
Be	Bdl – 4	Cu	1.5 – 13.2
Co	0.4 – 15.3	Rb	1.1 – 9.3
Cs	Bdl – 3.6	Zn	2- 107
Ga	13.5 – 24.5	Ni	0.6 – 5.4
Hf	0.4 – 14.4	As	Bdl -1.5
Nb	2.0 – 19.7	Cd	Bdl
Rb	3.8 – 306.3	Sb	Bdl – 0.2
Sn	Bdl – 3	Bi	Bdl
Sr	109.8 – 791.4	Ag	Bdl
Ta	0.1 – 1.4	Au	0.6 – 1.7
Th	1.3 – 84.5	Hg	Bdl
U	0.3 – 4.8	Tl	Bdl – 0.7
V	Bdl – 314	Se	Bdl
W	Bdl -0.8		

Bdl = Below detection limit

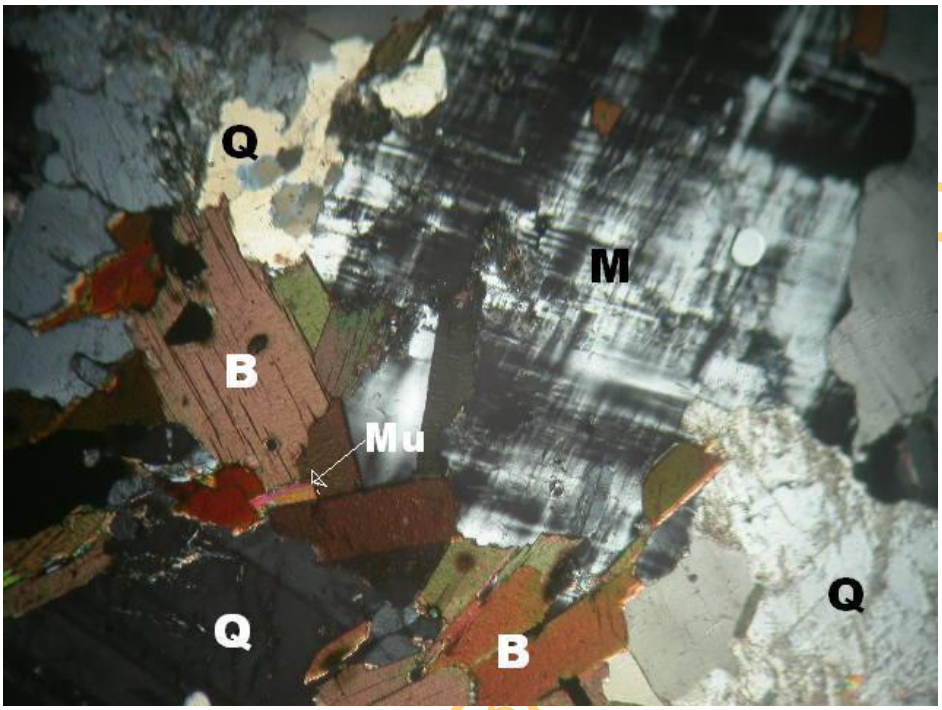

Fig. 4.11: Photomicrograph of porphyritic granite in transimitted light showing phenocryst of feldspar.

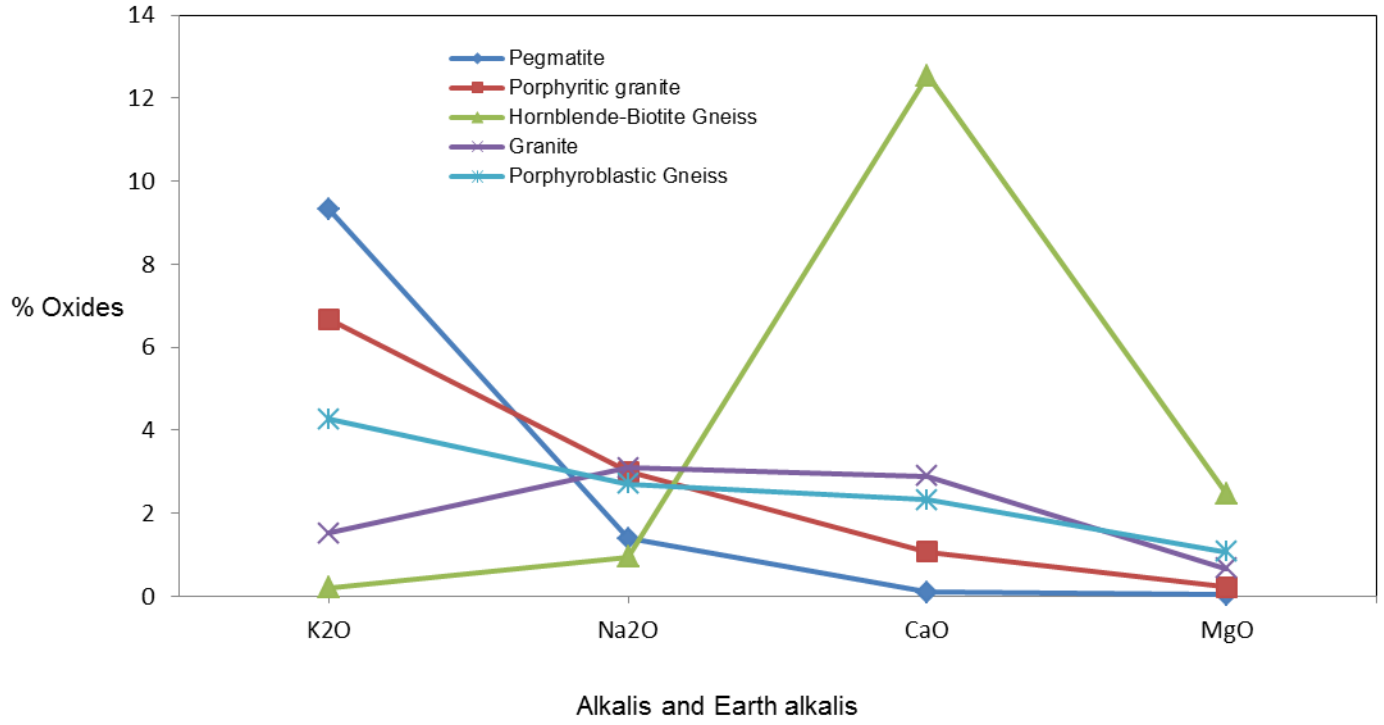

Fig 4.12: Relative abundance of the oxides of alkalis and alkali earths in rocks in Abeokuta area.

Most of the trace elements were detectable in ppm (Table 4.3) except for selenium (Se), mercury (Hg), silver (Ag), bismuth (Bi) and cadmium (Cd). Trace metals that are detectable in ppm in all the underlying bedrock include gold (0.6 -1.7 ppm), barium (43-486), strontium (109.8-791.4), thallium (1.3-84.5), thorium (1.3-84.5), uranium (0.3-4.8), copper (1.5-13.2), zinc (2-107), nickel (0.6-5.4), rubidium (3.8-306.3), zirconium (7.2-53.2) and yttrium (0.9-34.0). A few others, as shown in Table 4.3, are only present in some of the rocks while in others they are below detection limits. Several studies (WHO, 2006, Moskowitz et al., 1986; Monier-Williams, 1935) have shown that these elements, even in trace quantities in groundwater can have serious adverse effects on human health.

4.2.7.2 Classification of the Rocks

The plot of the ternary diagram of the relative abundance of Al_2O_3 and CaO to Fe_2O_3 (Fig 4.13) indicates that the underlying rocks in Abeokuta area contain more of the light coloured minerals (felsic) than the dark coloured minerals (mafic). Based on the total alkalis and the silica content of the rocks (Fig 4.14), all the rocks with the exception of hornblende-biotite gneiss, have silica content that is generally greater than 66%. Hence, they are essentially acidic rocks except for the hornblende-biotite gneiss (54.5%), which is has an intermediate composition.

4.3 Groundwater Occurrence and Potential

The characteristics of the subsurface, as inferred from the vertical electrical sounding results in the study areas, is discussed in this section. The geo-electric parameters are employed to identify the aquifer types to evaluate the groundwater potential of the study areas. The lineaments trace is used to complement geo-electric parameters of Abeokuta area in the assessment of groundwater potential.

4.3.1 Groundwater Occurrence in Abeokuta Area

Table 4.4 presents the summary of the geo-electric parameters of vertical electrical sounding in Abeokuta area. . In order to evaluate the influence of geology on the geo-electric parameters, the parameters based on the different rock types in the area are presented in Table 4.5. The reflection coefficient was used to characterize the nature of the bedrock in the study area. The reflection coefficients combined with the regolith resistivity and their thicknesses as well as lineament trace and other hydrogeological data were used to evaluate the groundwater potential of the area.

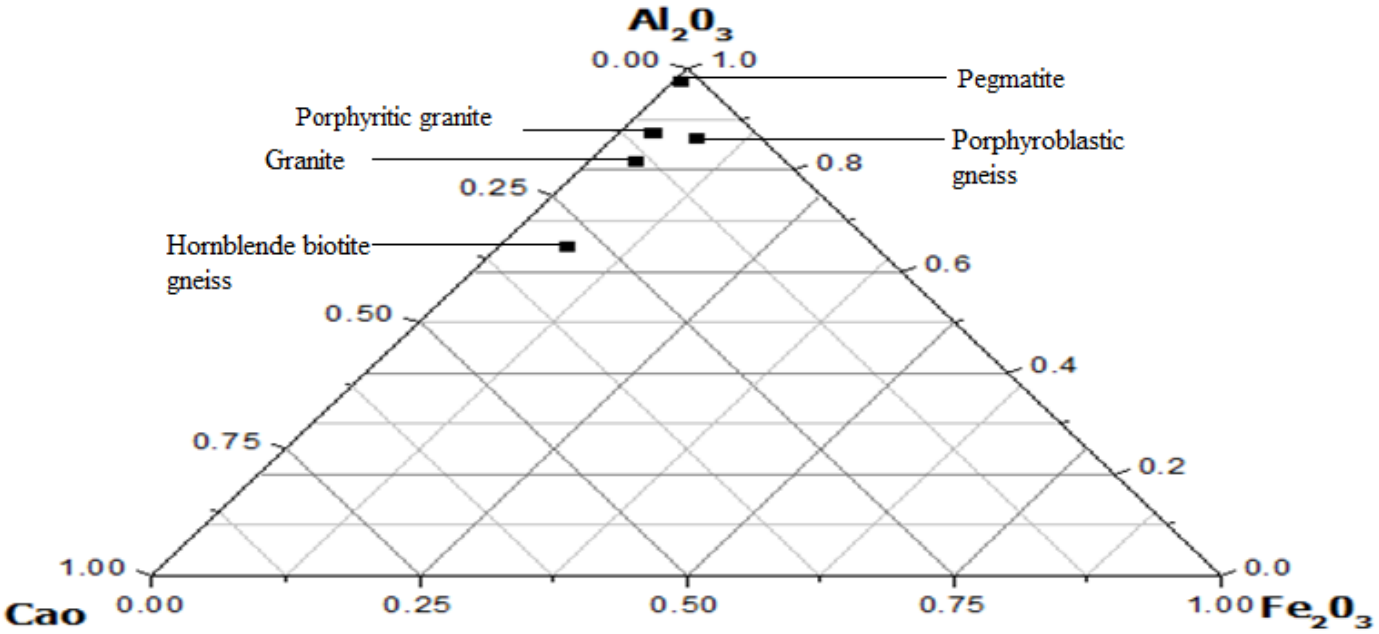

Fig 4.13: Plot of Al_2O_3, CaO, and Fe_2O_3 in the underlying rocks of Abeokuta

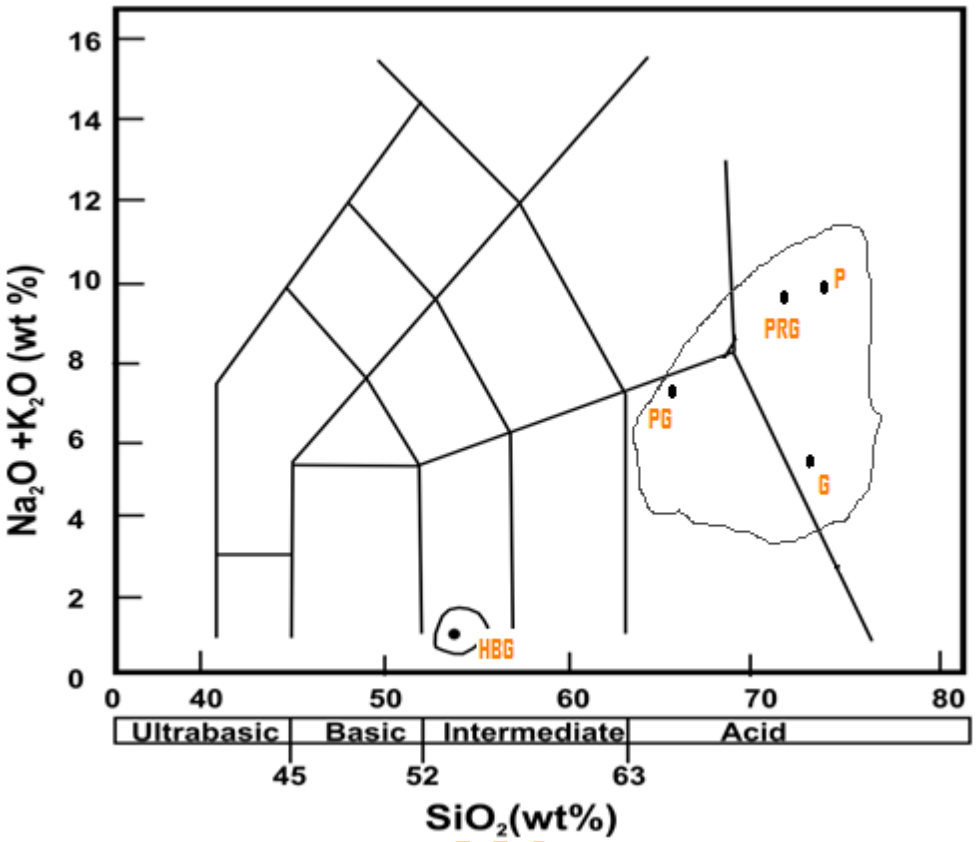

P: Pegmatite; **PRG**: Porphritic Granite; **PG** Porphyroblastic gneiss; **G**: granite **HBG**: Hornblende-biotite gneiss

Figure 4.14: Classification of rocks based on total alkalis and silica (Le Maitre et al 1989).

Table 4.4: Summary of the geo-electrical parameters in Abeokuta area.

Parameters	Resistivity (ohm-m)			Thickness in m		Depth to Basement	Reflection coefficient
	Topsoil	Regolith	Basement	Topsoil	Regolith		
Minimum	24.2	9.1	126.1	0.4	2.1	1.9	0.418
Maximum	6428.3	731.5	11563.1	2.5	41.1	55.4	0.996
Mean	830.795	116.81	2326.309	1.22	12.09	14.53	0.851
First quartile	159.9	29.2	598.9	0.9	6.5	7.3	0.756
Third quartile	1232.7	132.8	2660.4	1.5	15.9	18.4	0.961
Standard deviation	1130.81	136.21	2504.67	0.493	8.39	11.37	0.132
Coefficient of variation (%)	136	117	108	41	69	78	15

Table 4.5: Summary of the geophysical parameters of different rock types in Abeokuta

Rock types		Hornblende-biotite gneiss	Porphyroblastic gneiss	Granite	Porphyritic granite
No VES		17	23	15	20
Curve Types		H,HA,KH	H,HK,HKH,KH,A	H	H,HKH,KH,A
Top soil resistivity (ohm-m)	Range	24.2-2035.3	33.7-4095	311-6428	82.1-1233
	Mean± Standard deviation	460±540	943±1077	1866±1805	338±283
	coefficient of variation	117%	114%	97%	83%
Thickness of top soil (m)	Range	0.5-2.2	0.5-3.1	0.7-2.5	0.4-1.9
	Mean± Standard deviation	1.2±0.5	1.4±0.7	1.4±0.5	1.1±0.4
	coefficient of variation	41%	48%	33%	41%
Resistivity of the Regolith (ohm-m)	Range	11.9-212.4	14.8-518.6	22.2-368.2	9.1-731.5
	Mean± Standard deviation	72±63	119±124	91.2±92.5	167.5±196.9
	coefficient of variation	87%	104%	101%	117%
Thickness of Regolith (m)	Range	4.9-35.9	2.3-41.1	2.4-29.3	2.1-23.5
	Mean± Standard deviation	14.7±9.5	13.7±9.6	10.5±7.5	9.2±5.5
	coefficient of variation	65%	70%	71%	59%
Basement resistivity (Ohm-m)	Range	169-8816	126.1-9095	355-8319	400-11563
	Mean± Standard deviation	2397±24880	2272±2569	2318±2108	2533±2913
	coefficient of variation	103%	113%	91%	115%
Depth to geoelectric basement (m)	Range	2.2-39.8	1.9-55.4	3.5-31.2	3.6-46.6
	Mean± Standard deviation	15±10.3	17.8±13.4	12.0±7.8	13.8±11.6
	coefficient of variation	69%	75%	64%	84%
Reflection Coefficient	Range	0.640-0.988	0.548-0.991	0.635-0.995	0.418-0.996
	Mean± Standard deviation	0.895±0.108	0.827±0.139	0.881±0.107	0.824±0.151
	coefficient of variation	12%	17%	12%	18%
Nature of Regolith		Clay (53%), sandy clay (35%) and sands(12%)	Clay (63%),sandy clay (20%) and sands (17%)	Clay (71%), sandy clay (20%) and sands(9%)	Clay (42%), sands (29%) and sandy clay (29%)

Three geologic layers were identified in Abeokuta area. These layers include the topsoil, weathered layer, fractured basement and fresh basement. The sounding curves of Abeokuta area vary from 3 to 5 layers (in appendix III). Over 72% of the curves observed are of the H-type (Fig: 4.15a), while the KH (Fig: 4.15b), HKH (Fig: 4.15c) curve types constitute 14.7% and 5.3% correspondingly. Other curves observed in the area are HA (2.7%), A (2.7%) and HK (1.3%). The topsoil varies in lithology from clay through sandy clay, clayey sands, sands to gravelly lateritic soils.

The areas underlain by granite are characterized mainly by the H-type curve, while areas underlain by hornblende-biotite gneiss are typified by H, HA and KH-type curves. The porphyroblastic gneiss and porphyritic granite both have H, HKH, KH- type curves. Although, some curves were found more commonly on particular underlying rock types nevertheless, no particular curve-type can be used to characterize any of the underlying rocks.

The H curve has been identified by Olorunfemi and Olorunniwo (1985), Ajayi and Hassan (1990) and Olayinka and Olorunfemi (1992) as a common curve type in this type of geological terrain. The intermediate layer in the H-type curve is usually characterized by low resistivity made up of clayey or sandy clay and is often water-saturated. This layer has high porosity, low specific yield and low permeability (Jones, 1985). The KH type has succession that consists of topsoil, sandy/gravel underlain by clay overlying weathered/fractured basement. The HA type consists of the topsoil, clay and sand regolith overlying a weathered/fractured basement while the A type is common in areas where the bedrock is highly resistive, defined by a continuous increase in resistivity from the topsoil to the bedrock.

The resistivity of the topsoil varies from 24.2 to 6428.3 ohm-m with a mean of 830.8 ohm-m and a standard deviation of 1130.8 ohm-m, (showing a very high degree of dispersion) and a coefficient of variation of 173.8 %. The thickness of topsoil varies from 0.4 to 2.5 m, mostly less than 2 m with an average of 1.22±0.49 m. The coefficient of variation of the topsoil unlike the resistivity of the topsoil is relatively low at 40.5%. Nonetheless, this layer is of little or no significance as a hydrogeological unit because of its low degree of saturation (Olayinka and Olorunfemi, 1992).

The resistivity of the topsoil (Fig. 4.16) in most of the area (over 66%) varies from 100 to 1000 ohm-m. In about 25% of the area, the resistivity of the layer is greater than 1000 ohm-m. In this area, the topsoil is largely gravelly, made up of gravels washed from the hilly area.

The resistivity of the weathered regolith varies from 9.1 - 731.5 ohm-m and averages 116.8±136.2 ohm-m. It varies from areas underlain by one rock type to the other (Table 4.5 and Fig. 4.17). The areas underlain by hornblende-biotite gneiss and granite have low regolith

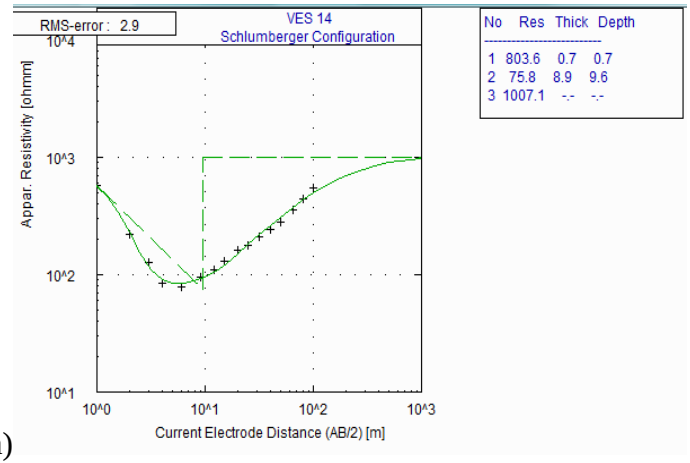

(a)

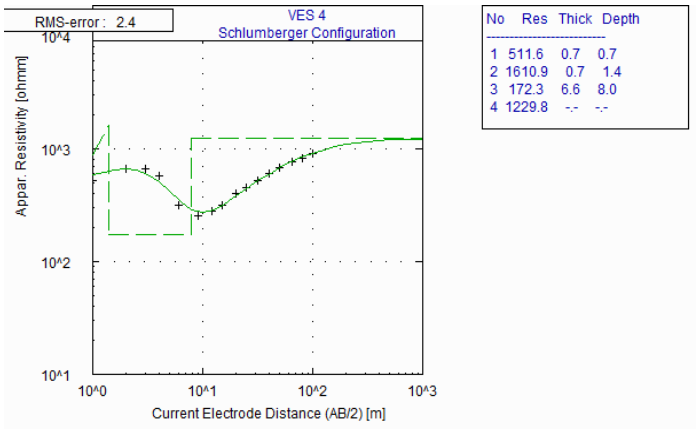

(b)

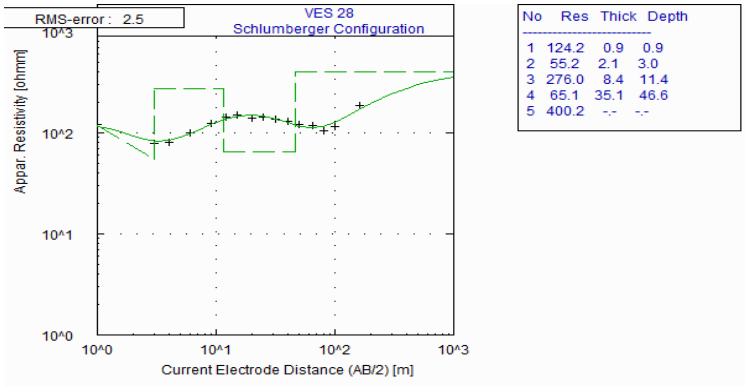

(c)

Fig 4.15 The major curve types in Abeokuta area (a. H- type , b. KH- type HKH –type)

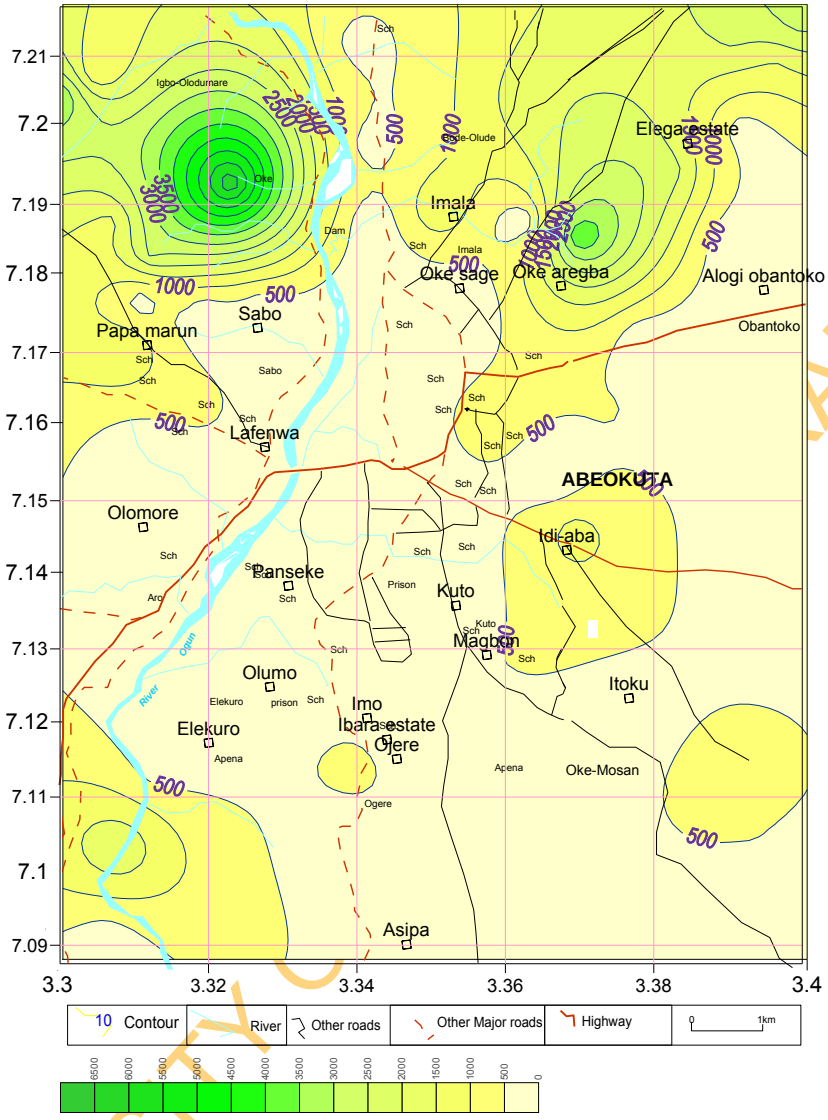

Fig 4.16: Variation of the resistivity of the top-soil in Abeokuta area.

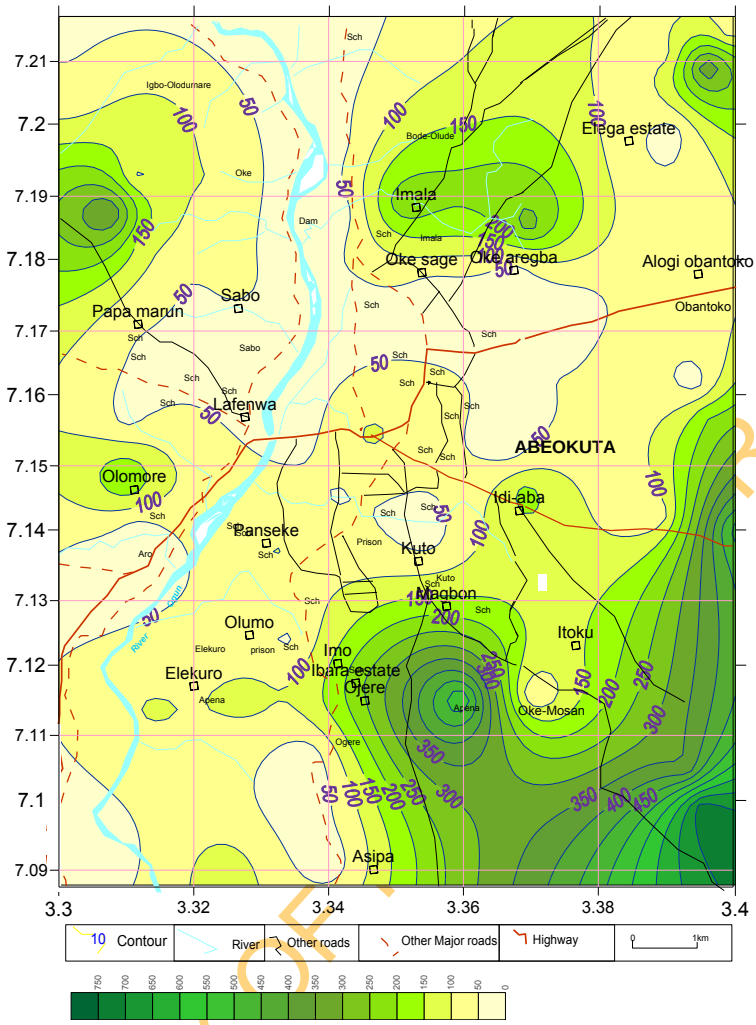

Fig 4.17: Map of the regolith resistivity in Abeokuta area

resistivity of 11.9 - 212.4 ohm-m and 22.2- 368.2 ohm-m respectively. The average resistivities of the regolith in these areas correspondingly are 72 ± 63 ohm-m and 91.2 ± 92.5 ohm-m.The areas underlain by porphyroblastic gneiss and porphyritic granite have resitivities of 14.8-518.6 ohm-m and 9.1-731.5 ohm-m respectively. In the areas underlain by hornblende biotite gneiss and porphyritic granite, the average resitivity of the regolith are 119 ± 124 ohm-m and 167.5 ± 196.9 ohm-m correspondingly. The gneisses have thicker overburden (greater depth to geoelectric basement) with an average of 17.8 ± 13.4 m for porphyroblastic gneiss and 15±10.3 m for hornblende-biotite gneiss compared to 12 ± 7.8 m and 13.8 ± 11.6m respectively for granite and porphyritic granite. Generally, as noticeable in Fig 4.18, there is an increase in overburden thickness away from either side of River Ogun, although there are other locations, especially those close to outcrops where the overburden thickness is thin despite being far away from River Ogun.

The resistivity of bedrock (Fig 4.19) in the area varies from 126 – 11,503 ohm-m, with an average of 2326 ± 2504 ohm-m, with a coefficient of variation of 108%. Olayinka (1996) has demonstrated that steeply rising terminal branch on a sounding curve and very high resistivity is not indicative of fresh bedrock. In place of resistivity of bedrock, Olayinka (1996) has shown the importance of reflection coefficients (K) at the bedrock interface in the identification of weathered/fractured bedrock due to its invariant for different geo-electric models over a layered earth. The reflection coefficients at the bedrock interface were employed in Abeokuta area to determine the nature of the bedrock from one point to the other. Comparatively, larger part of the area underlain by porphyroblastic gneiss has lower reflection coefficients than the areas underlain by other rock types (Fig 4.20), with average K of 0.827± 0.139 and a coefficient of variation of 17%. The reflection coefficients at the bedrock interface in area underlain by porphyroblastic gneiss vary from 0.548 to 0.991. Similarly, the porphyritic granite has K that varies between 0.418 and 0.996 with an average of 0.824 ± 0.151 with a coefficient of variation of 18%. The area underlain by porphyritic granite has lower reflection coefficient covering larger part compared to the other two main rocks. The similar nature of the reflection coefficient and the values of the coefficient of variation for these two rocks may be largely due to their similar mineralogy and grain size. The range of reflection coefficients for areas underlain by hornblende-biotite-gneiss and granite are 0.640 to 0.988 and 0.635 to 0.995 respectively. The average in the areas is 0.895 ± 0.108 and 0.881 ± 0.107 respectively. Similarly, the coefficients of variation in both areas are 12%.

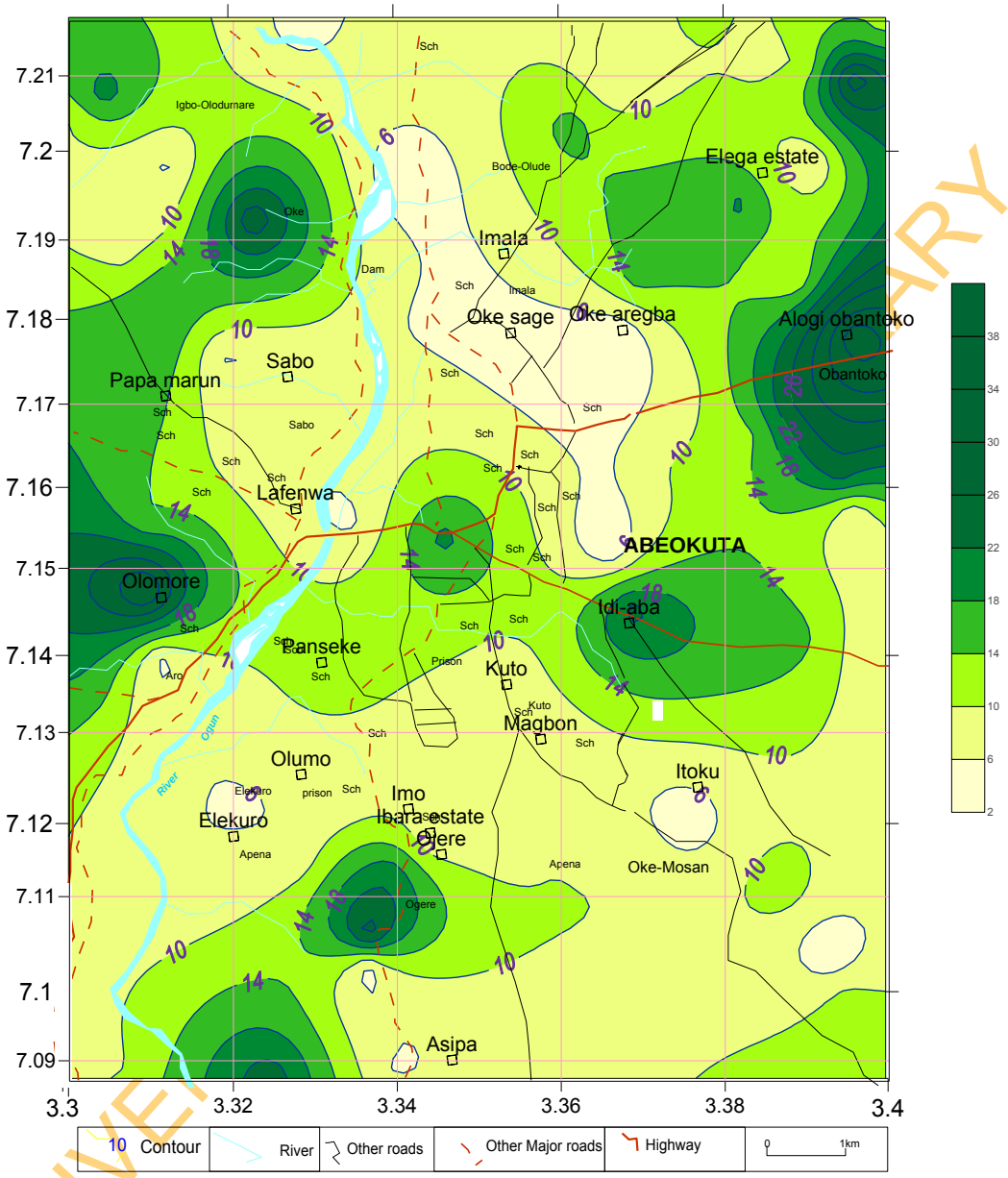

Fig 4.18: Isopach map of the regolith thickness in Abeokuta area.

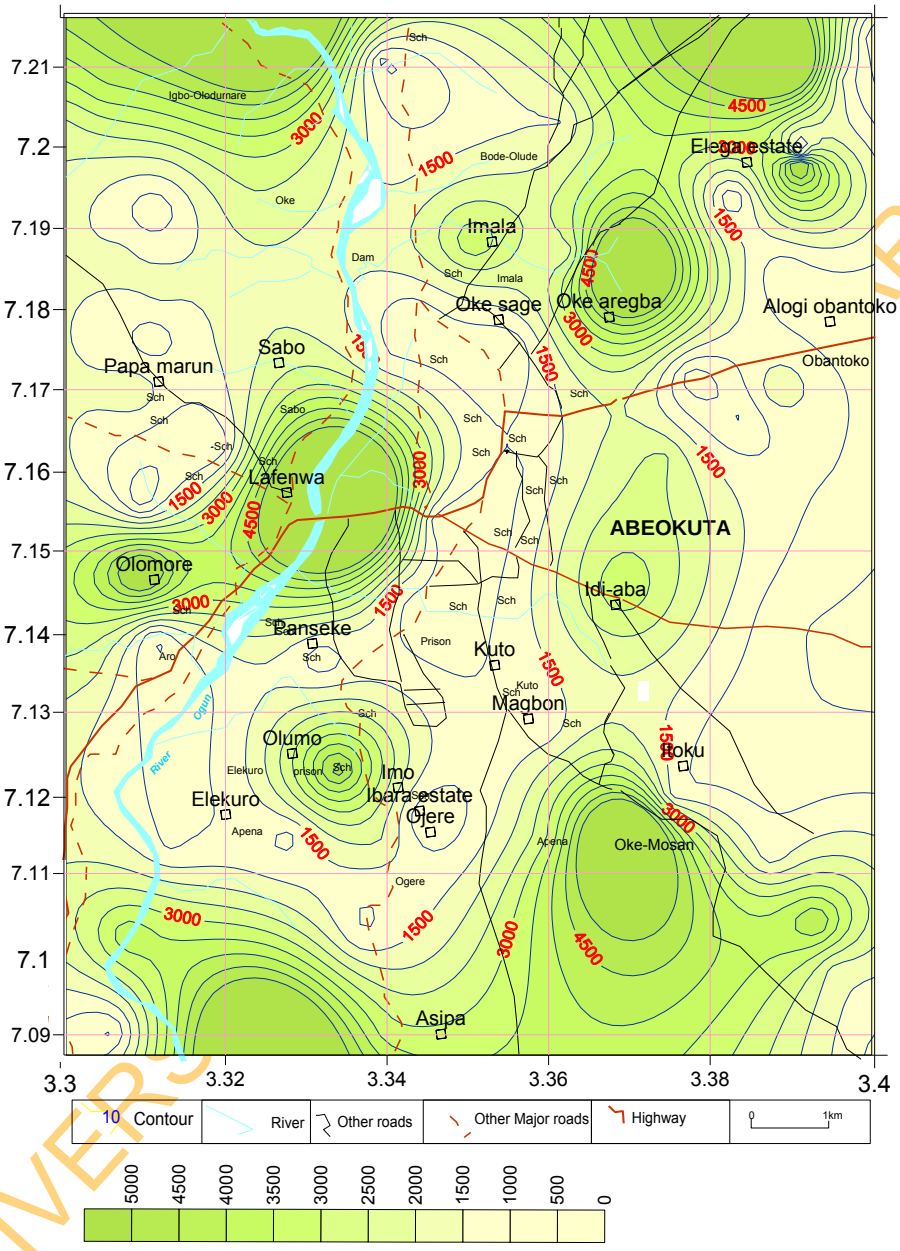

Fig 4.19: Contour map of the basement resistivity in Abeokuta area.

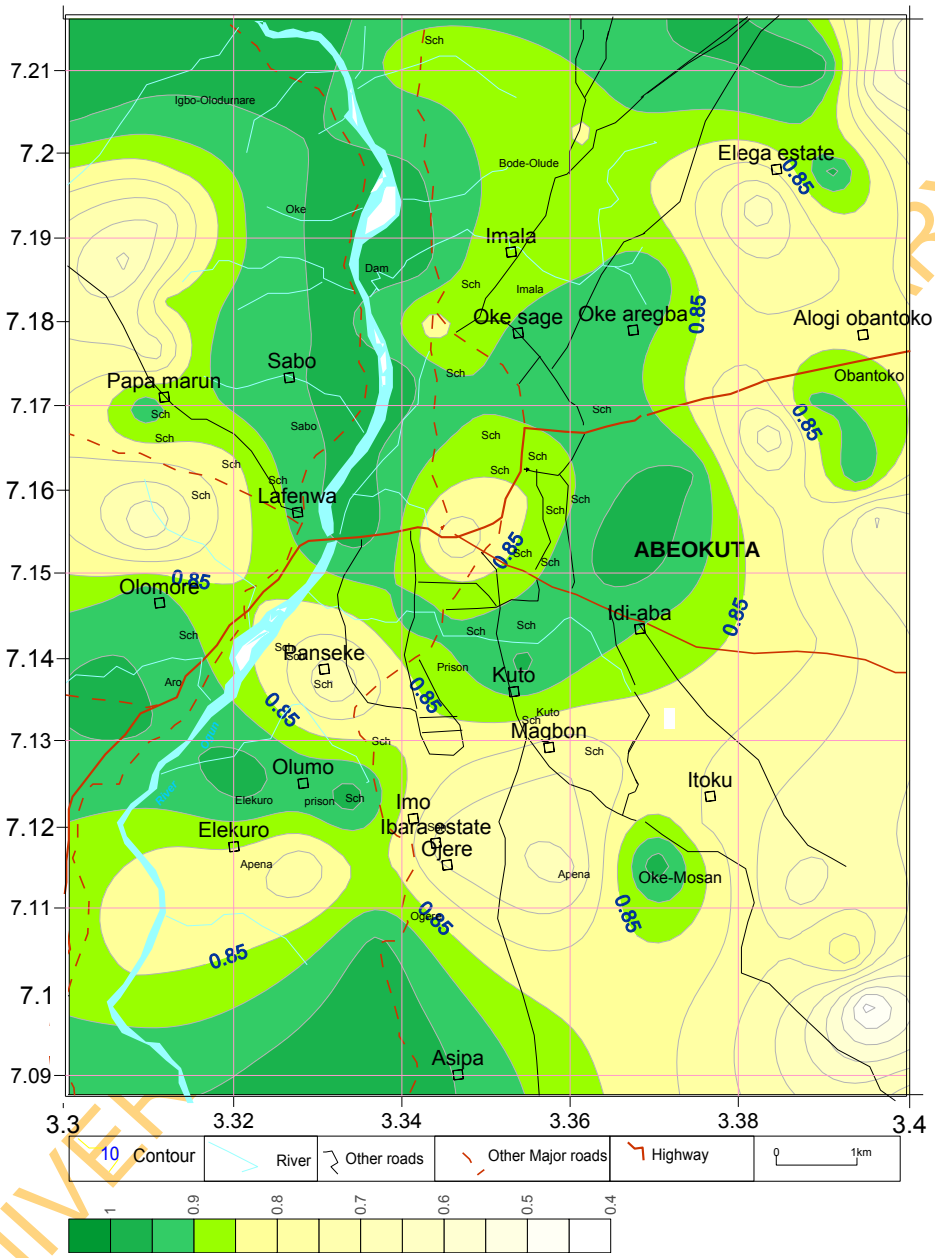

Fig 4.20: Reflection coefficient (K) in Abeokuta area.

The west-south and east-south views of the different horizons in Abeokuta are as shown in (Fig.4.21). The sandy regolith overlain by resistive topsoil occupies some section of the western part of the study area. The southern parts, especially southwestern area underlain by hornblende-biotite gneiss is mostly characterized by clayey topsoil overlying clayey regolith while in the southeastern area underlain by porphyritic granite, the succession is sandy to gravelly topsoil overlying largely sandy regoliths.

4.3.2 Lineament Frequency in Abeokuta Area

A Lineament is a linear topographic feature of regional extent. It may include valleys, rivers, streams controlled by faulting or jointing. Structural features associated with lineaments include fault zones, joint zones, fold axes. The lineament trace in Abeokuta area (Fig 4.22) was extracted from landsat imagery of the study area, to complement geo-electric parameters in the evaluation of the groundwater potential of Abeokuta area. The lineaments (Fig 4.23) are trending mostly in the NW-SE direction. The direction of most of the lineaments is similar to the foliation trend in the area. Other lineaments trend in NE-SW direction. The frequency of the lineament trace in an area of 1.08 sq km (Fig. 4.24) was determined and contoured to produce the lineament frequency map (Fig 4.25). The area underlain by porphyroblastic gneiss has higher lineament frequency than other parts of the study area.

4.3.3 Groundwater Potential of Abeokuta Area

The groundwater potential of any Basement Complex terrain is determined by complex inter-relationship between the geology, post emplacement history, weathering processes and depth and nature of the weathered layer, groundwater flow pattern, recharge and discharge processes (Olorunfemi et al, 1999).

In order to assess the groundwater potential of the area, the regolith resistivity map (Fig 4.17), the regolith thickness map (Fig 4.18) the reflection coefficient map (Fig 4.20) and the contour map of the lineament trace were all combined (super-imposed) to classify the area into:

a) High groundwater potential;
b) Medium groundwater potential; and
c) Low groundwater potential.

The groundwater potential of the area is defined by identifying areas with low reflection coefficient, high lineament frequency, high regolith resistivity (>100 ohm-m) and thick regolith.

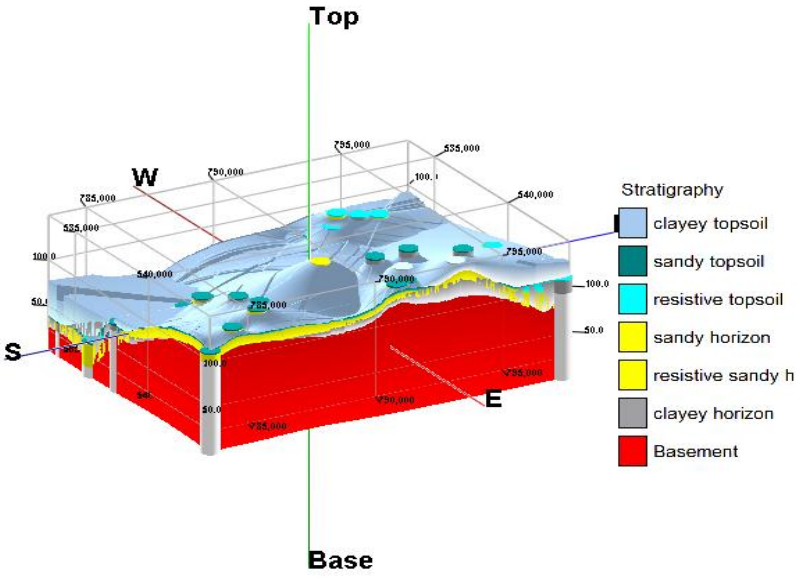

a

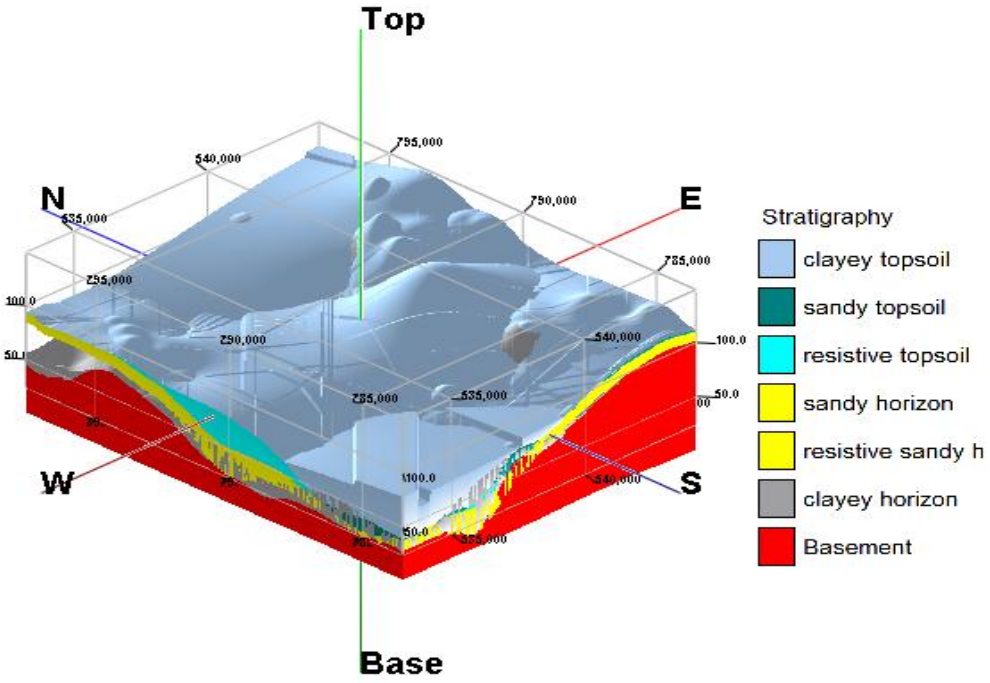

b

Fig.4.21: 3D model of the subsurface in Abeokuta area (a) E & S view (b) W & S view

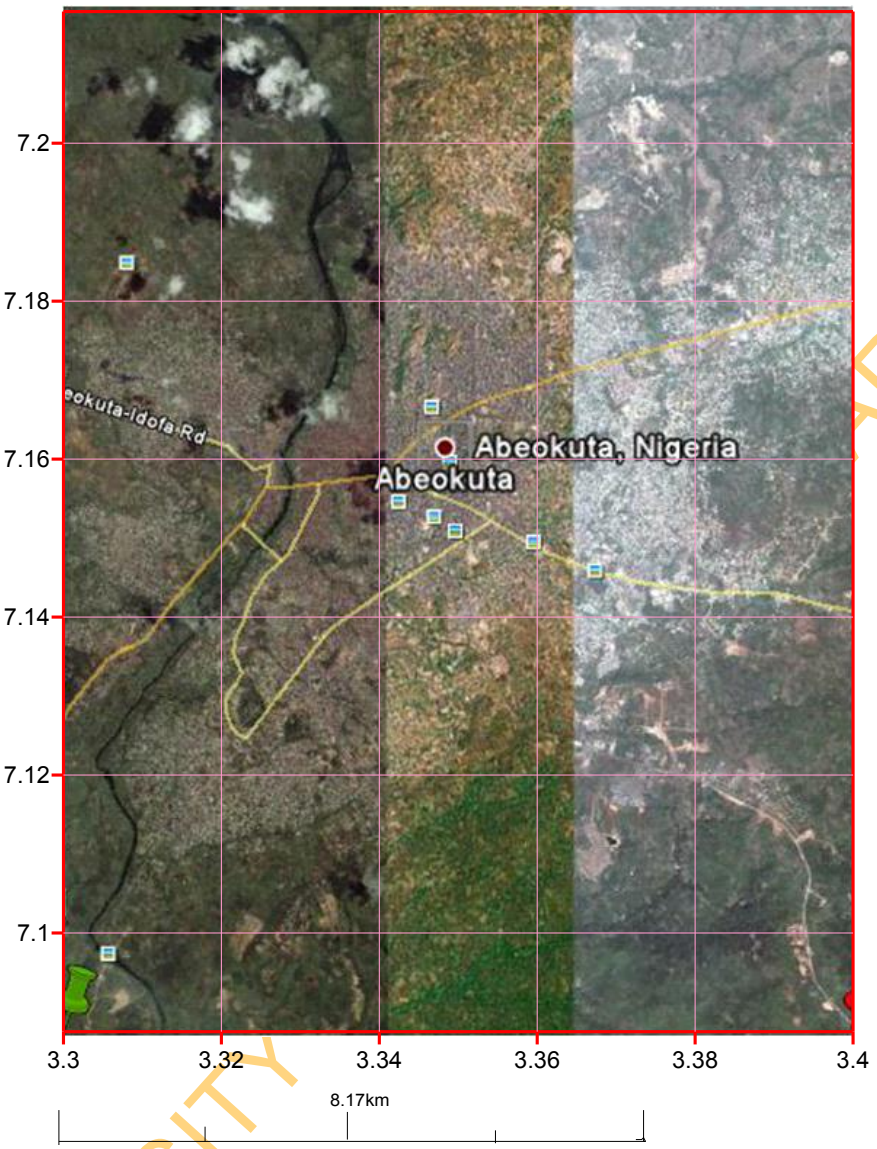

Fig.4.22: Landsat imagery of Abeokuta area.

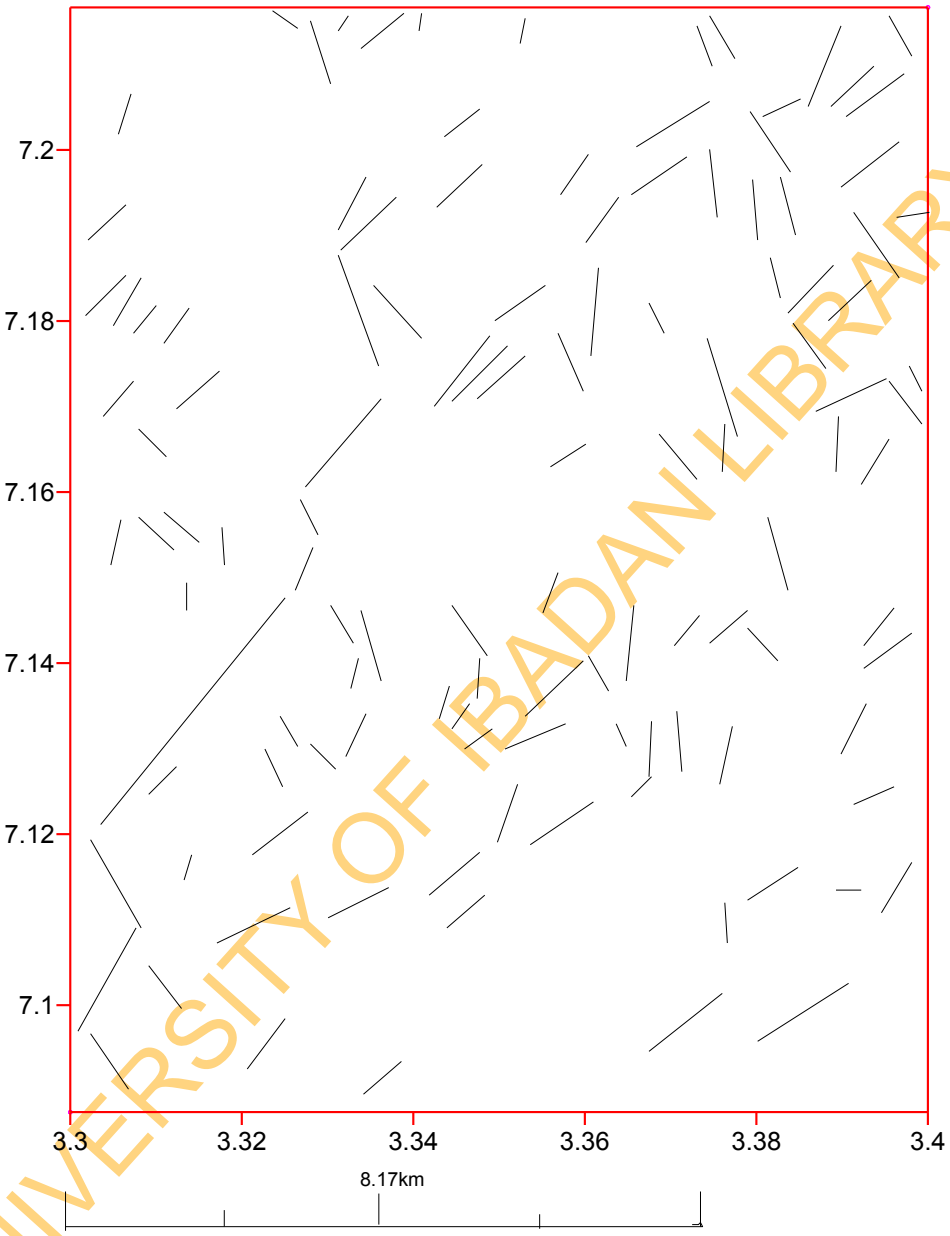

Fig.4.23: Lineament trace of Abeokuta area.

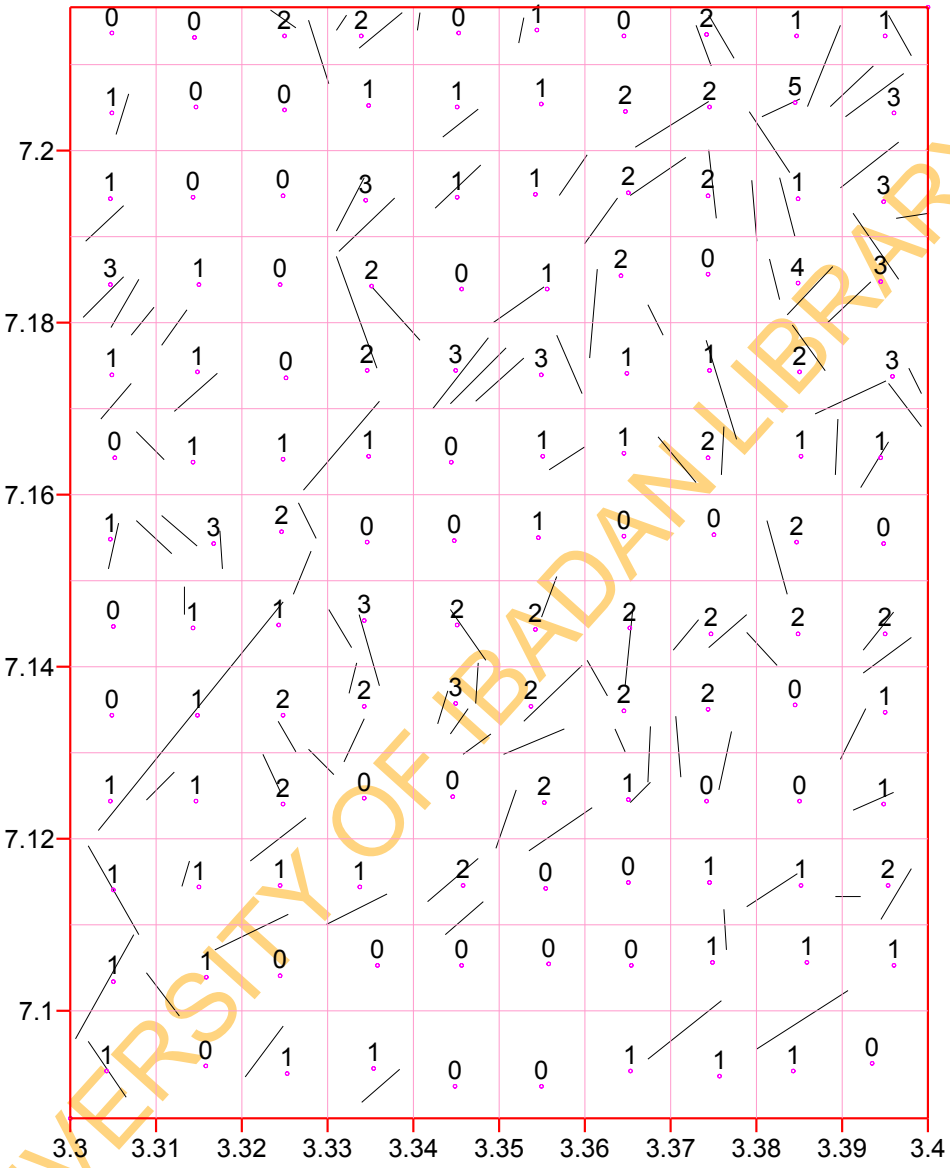

Fig.4.24: Frequency of lineament trace in Abeokuta area.

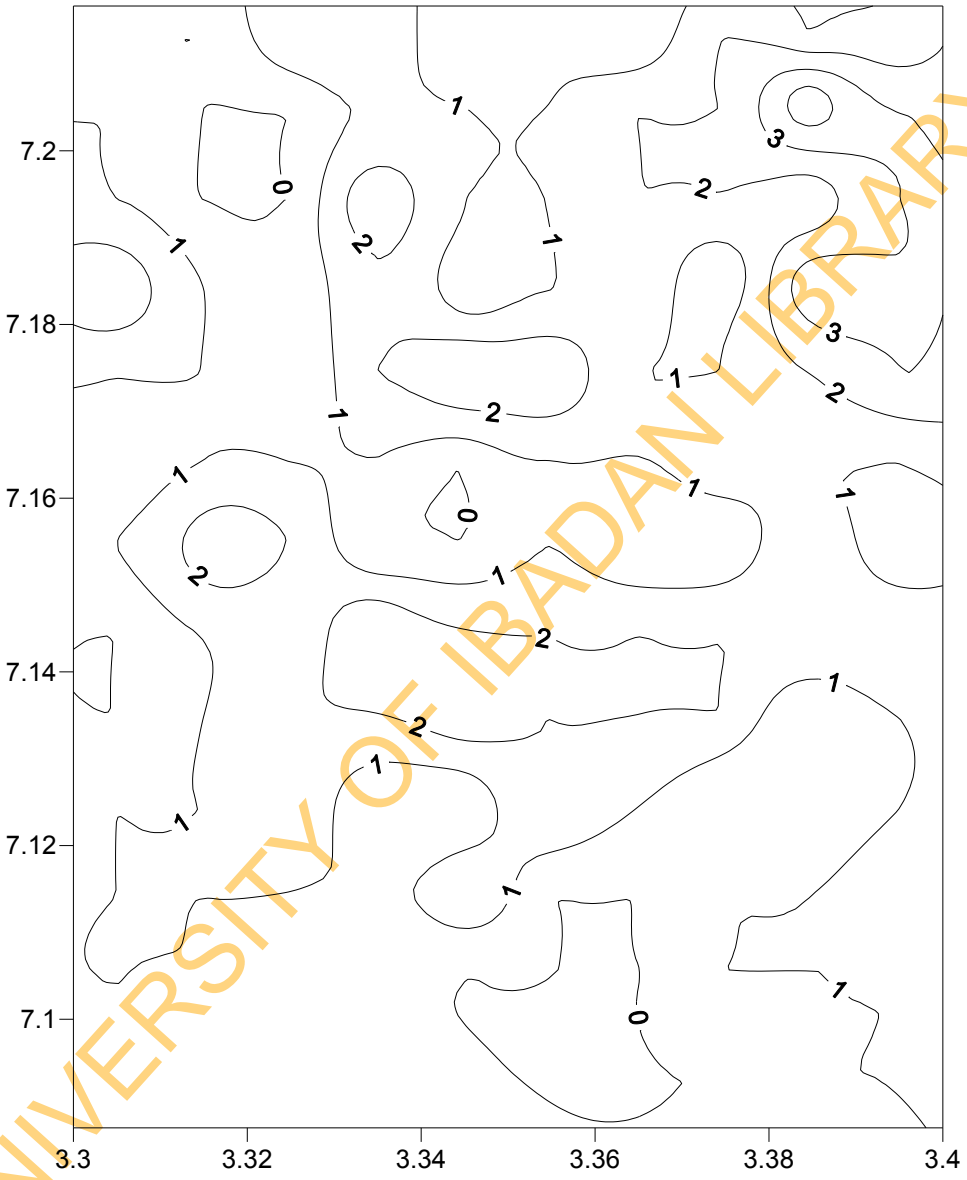

Fig.4.25: Contour map of lineament trace in Abeokuta area.

Where the reflection coefficients are low represent areas where the bedrock is weathered and fractured (Olayinka, 1996). Where the regolith resistivity is low (less than 100 Ohm-m), the regolith is essentially clay or clayey. Clay has high porosity, low specific yield and very low permeability (Jones, 1985 cited in Olayinka and Olorunfemi, 1992) and thus will not yield appreciable quantity of water to wells. Where the resistivity is high, the materials are usually essentially sandy and can serve as either an aquifer or an aquitard. For the regolith to supply an appreciable quantity of water to wells, the regolith must be sufficiently thick. The nature of weathered layer determines to a significant extent the yield of a borehole irrespective of the underlying fractured basement column, with area overlain by clay (resistivities <100 ohm-m), having low yield (Olorunfemi et al., 1999). Barker et. al (1992) observed that highest yielding boreholes in the basement complex of Zimbabwe are associated with weathered layer resistivities of between 100 and 600 ohm-m. A minimum thickness of 10 m was however recommended by White et al (1988) to ensure adequate yield to wells. Lineaments largely represent expression of linear structures in underlying rock on imagery. Commonly this may represent straight streams, rivers and

vegetation paths controlled by fractures in rocks. Areas with high lineament frequency are indicative of areas with higher fracture density. Adeyemi (1991) established positive relationship between lineaments lengths and well yield in parts of the Basement Complex of southwestern Nigeria.

A combination of these parameters with their maps super-imposed (Fig 4.26) was used to produce the groundwater potential map (Fig. 4.27) of the area.

High groundwater potential areas are defined by high regolith resistivity (100-730 Ohm-m), sufficiently thick regolith (> 10m), low reflection coefficient and high lineament frequency.

The medium groundwater potential areas are defined by either

I. Low reflection coefficient, high lineament frequency, combined with high regolith resistivity
II. High regolith resistivity and thick regolith thickness

The presence of combination of the parameters listed in I or II will provide fair to good groundwater yields in the wells.

Areas with low groundwater potential are classified by the presence of either

I. Low lineament frequency and low reflection coefficient or
II. High regolith resistivity and relatively thick regolith (greater than 6 m).

Areas where all the criteria listed above are absent will have poor groundwater potential. The groundwater flow direction (Fig 4.11) has an important role in the evaluation of the groundwater potential of an area, largely in this terrain recharge is usually direct, mostly through precipitation and in addition, groundwater flow from higher head to lower head may be impeded, due to the usually localised nature of the aquitard/aquifer and the basement relief (Fig. 4.28). As such the aquifer, especially in the high hill areas, may not be in hydraulic continuity with the entire area as obtainable in sedimentary areas.

Generally, less than 25% of the study area has high groundwater potential, restricted mostly to area underlain by porphyritic granite and porphyroblastic gneiss while over 50% of the area has poor groundwater potential. This invariably indicates the importance of detailed groundwater exploration in the study area for locating areas where successful boreholes can be drilled.

As noted in previous studies (e.g. Olorunfemi et al, 1999) the groundwater potential map (Fig 4.17) which displays the regional groundwater potential scenario in this area based on the criteria defined above is subject to local variations as a result of the well documented discontinuous nature of basement aquifers. However, the map provides a reliable guide of the groundwater potential of the area, especially as this has been shown to be related to the bedrock type.

4.4 Groundwater Occurrence in Ikorodu Area

The summary of the results of Vertical Electrical Soundings in Ikorodu is presented in Table 4.1b while the VES curves of the area are presented in the appendix. Six traverse lines were selected and the geo-electric logs of the VES along these profiles were correlated to highlight the extent of continuity of different layers and evaluate their hydrogeological significance in the study area.

The sounding curves obtained in Ikorodu area varies from the three-layer type-curves to six layer type-curves that include AK, AKH, HK, HKHK, HA, AKQ, KQQ, KHAK, HKHA, QH, K, and HK. The AK (Fig 4.29) and AKH curve types (Fig 4.30) together jointly constitute about 60% of the curve types and are mostly dominant in the landward area compared with the area around the Lagos lagoon. The many varieties of the curves obtained in this area are largely due to the rapid change in facies associated with this type of environment (Ako et al, 2005).

4.4.1 Lithological Profiles

Traverse lines were joined by connecting VES along different profile directions to correlate and evaluate the extent of continuity of each lithological horizon in the area. The

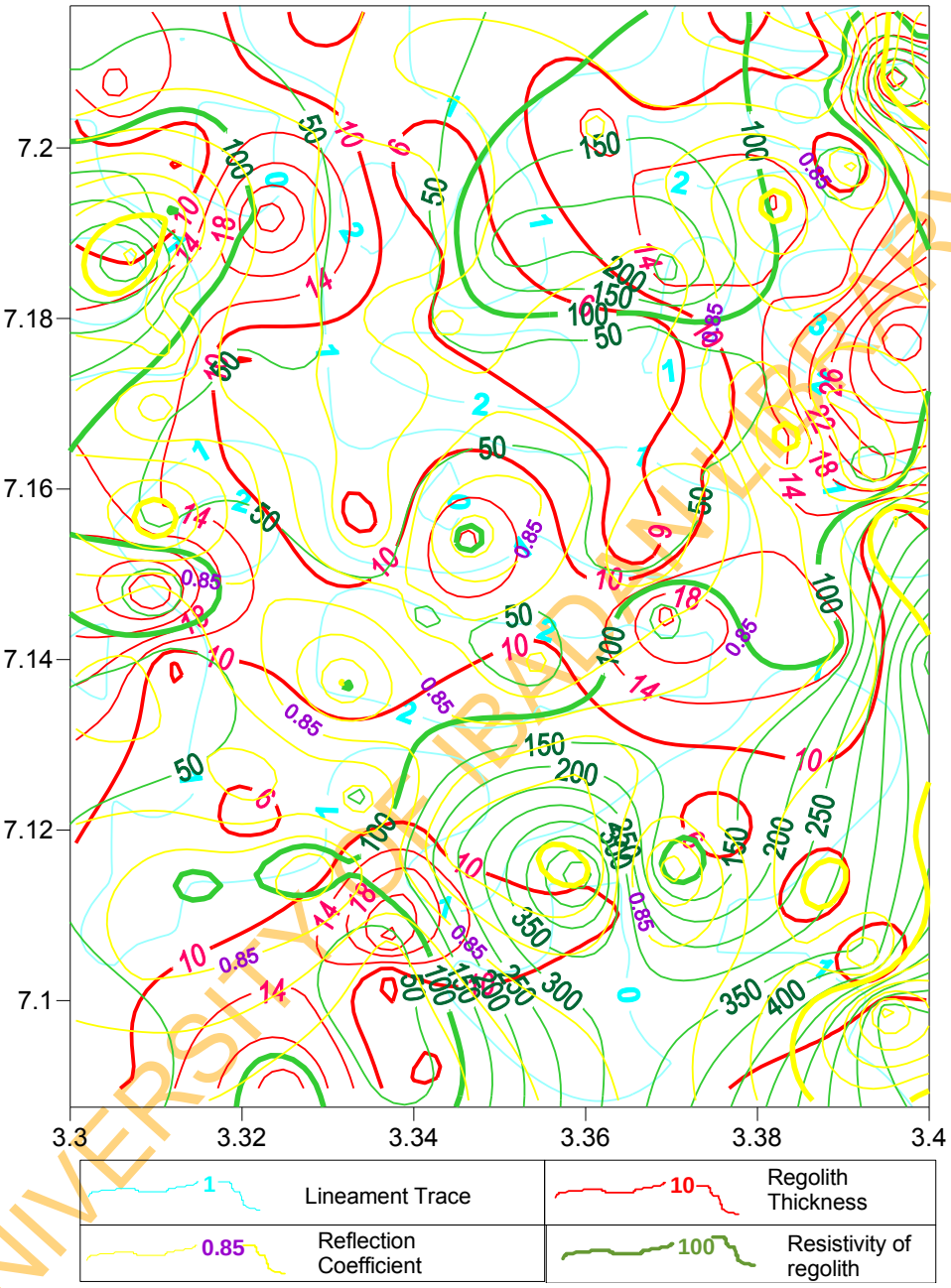

Fig.4.26: Combination of thickness and resistivity of regolith, lineament contour map and reflection coefficients.

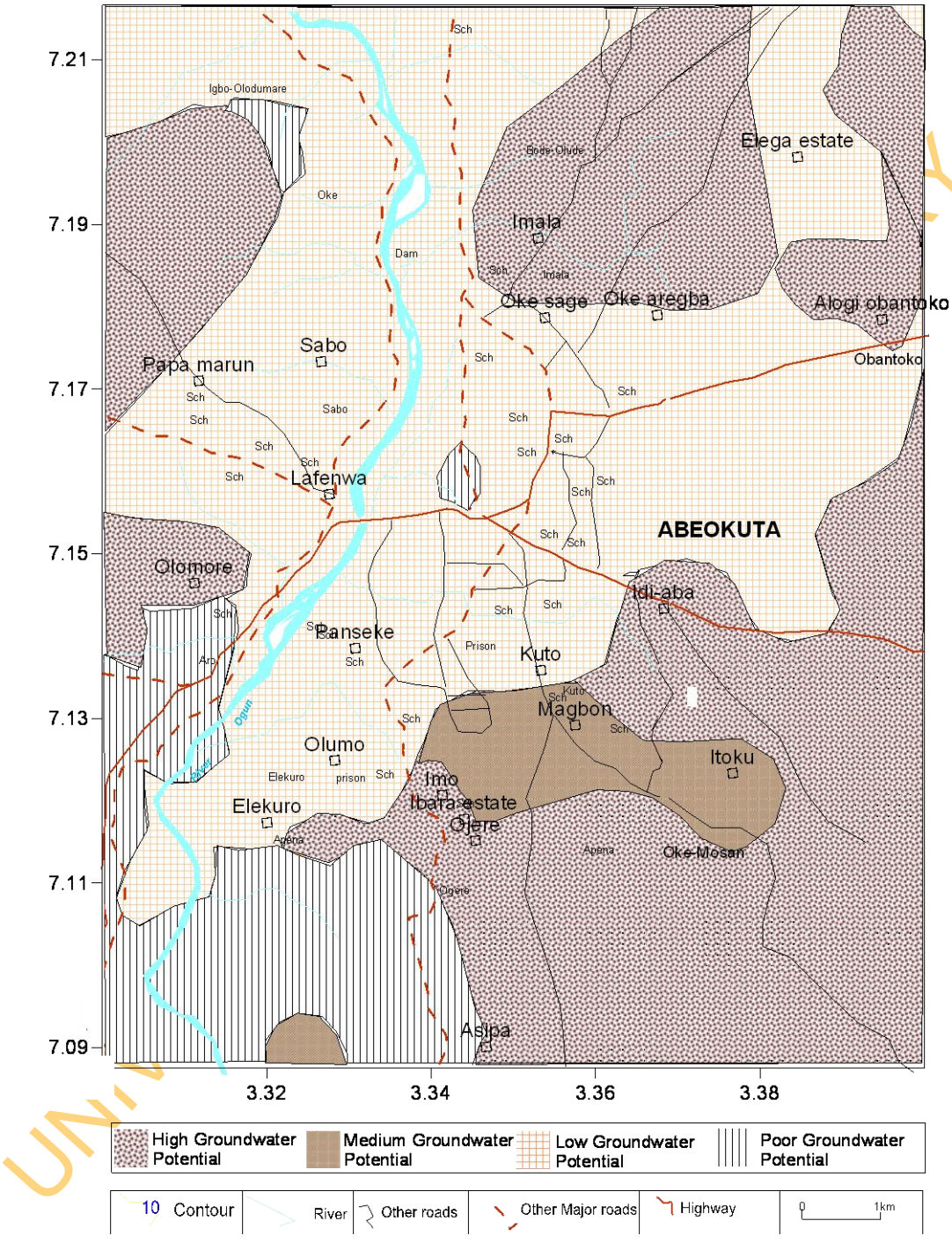

Fig.4.27: Groundwater potential map of Abeokuta area based on geophysical parameters.

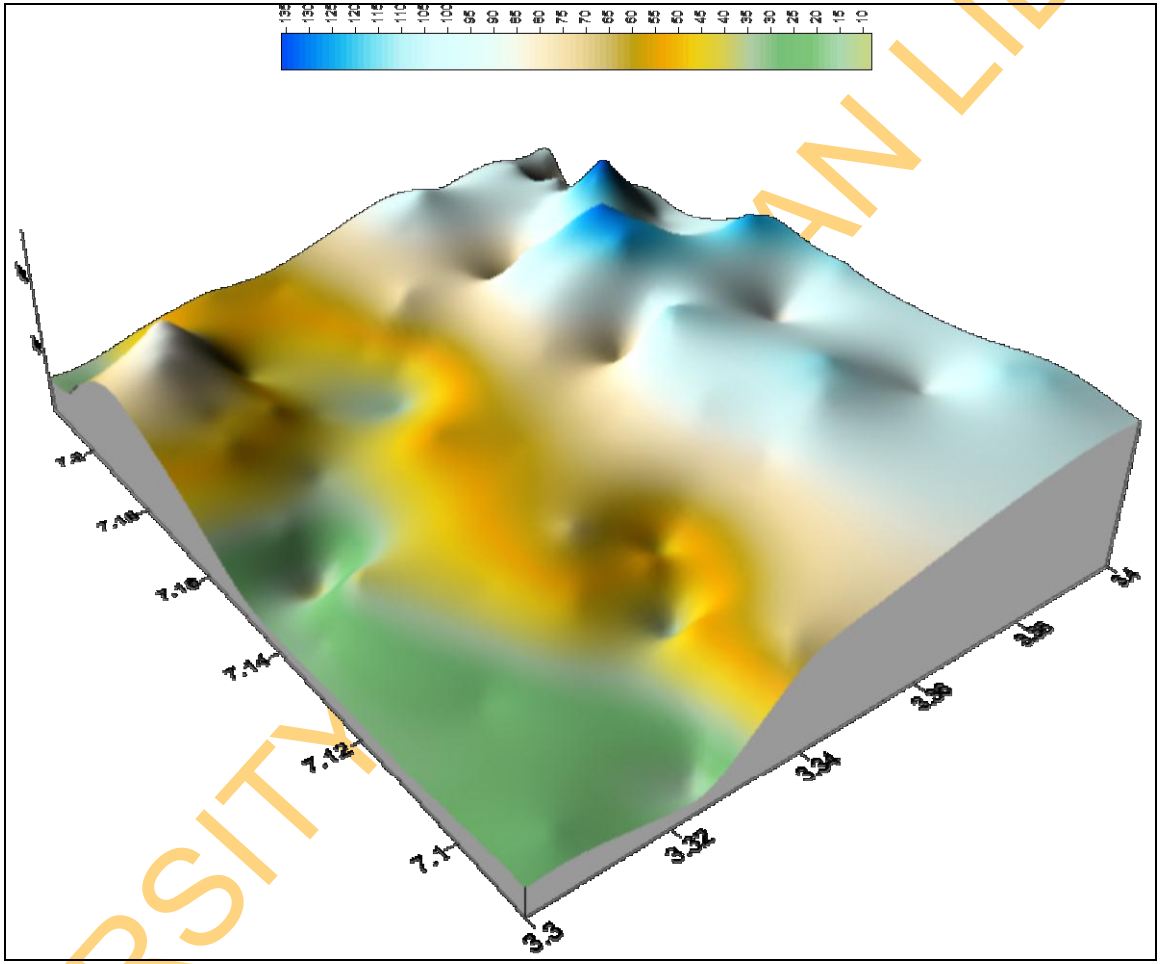

Fig. 4.28: Basement relief map of Abeokuta area.

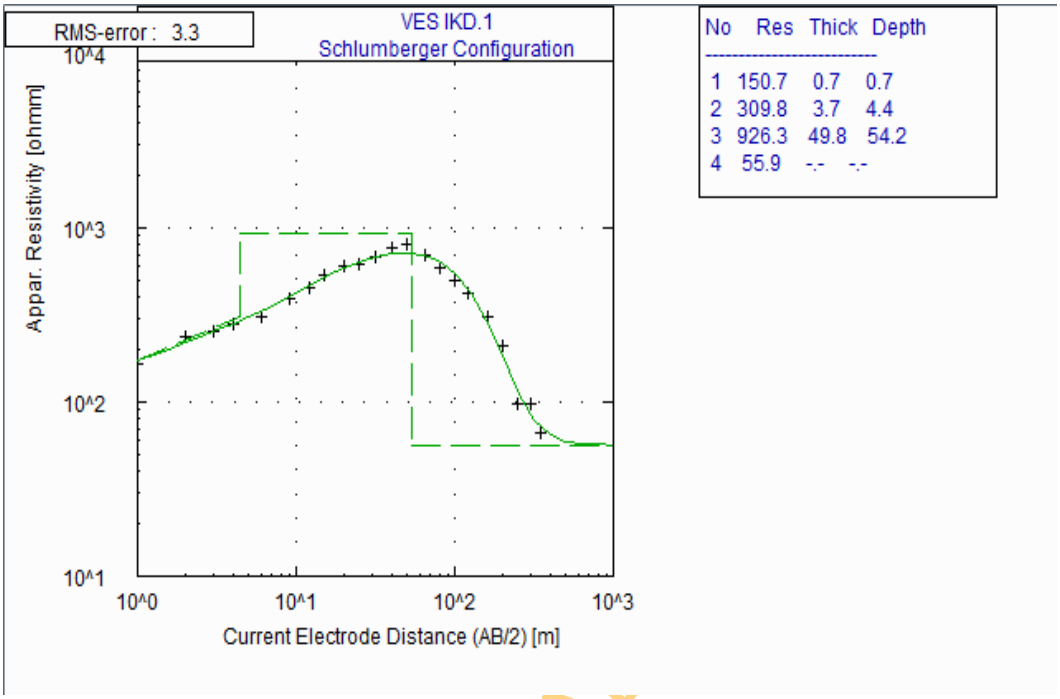

Fig 4.29: Typical AK curve-type in Ikorodu area.

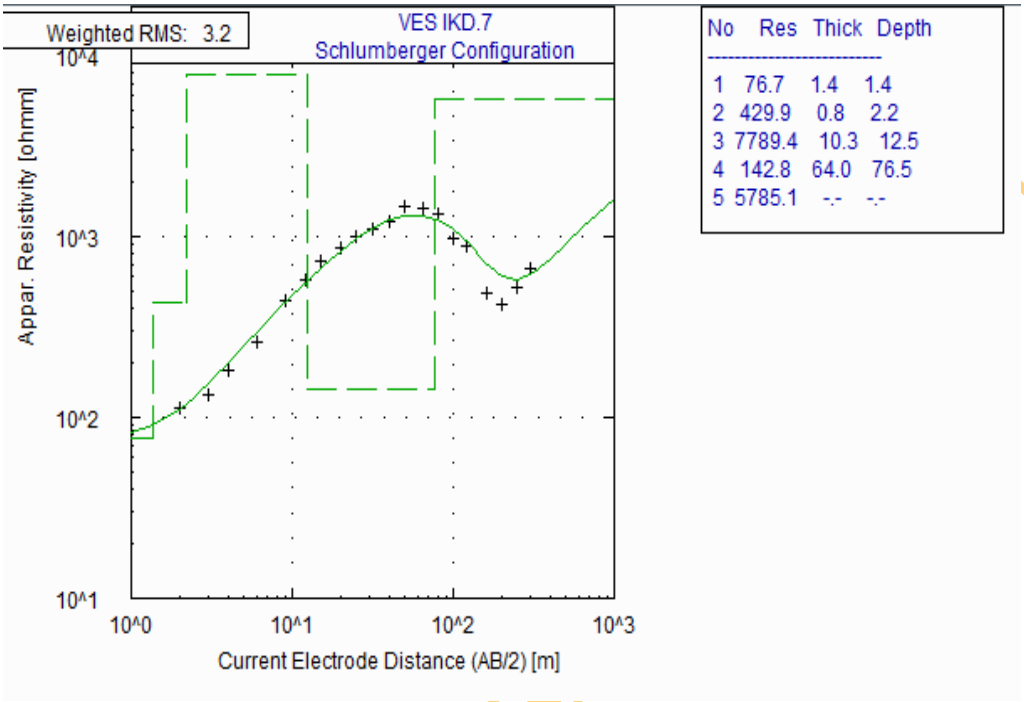

Fig 4.30: Typical KH curve-type in Ikorodu area.

sections were done with adequate consideration for the differences in elevation, in order to account for the effect of relief on the groundwater potential of the area.

4.4.1.1 Profile 1

Profile one consists of VES 41, VES 42, VES 48, VES 49, VES 4, VES 1 and VES 24 running from NW to NE of the area. The topography of the area is undulating (Fig. 4.31) with the highest points along the profile at VES 42 and VES 49. The first layer is characterized by clay in the western part and this grade gradually to sandy clay in the eastern area. The thickness of the horizon varies from 0.6-2 m and resistivity range of 28-150 ohm-m. However, the first layer in location 41 is sandy. Underlying the first layer is a highly resistive sandy layer (probably ferruginized) that grades gradually eastward to the sandy and clay horizon. The thickness of the resistive sand varies from 6.2 to 24.6 m. The sand which extends laterally from NW-NE varies in thickness from 3.3 m to 49 m. The sand is exposed at location of VES 41 to the ground surface but confined/semi confined in many places towards the north-eastern part of the area.

4.4.1.2 Profile 2

The profile (Fig. 4.32) covers NNE-SSW of Ikorodu area, including VES 25, VES23, VES 22, VES21, VES20, VES 19 and VES 18. The topography is gently sloping downward from VES 25 towards VES 18. The lithology along this profile is generally similar unlike some of the other profiles with rapid change in facie, similar to those described by Ako et al (2005) in some coastal areas of Lagos State southwestern Nigeria. The curves are mainly of AK-type (r1<r2<r3>r4), the commonest curve-type in Ikorodu area. The top layer ranges from sandy clay (117-181 ohm-m) to sand (394 ohm-m). While the sand is exposed at VES 25, it is semi-confined in VES18, VES 19 and VES 21 and confined in VES 23. Underlying the sand is highly resistive sand (1437-6941), probably ferruginized extending from VES 25 where it is very thick to VES 18 where it is relatively thin. Ako et al (2005) delineated the resistive sand horizon in part of coastal area of Lagos, southwestern Nigeria. Underlying the resistive sand is clay which grades intermittently to sandy clay with resistivity range of 22-143 ohm-m.

4.4.1.3 Profile 3

This profile (Fig 4.33) consists of VES 41, VES 40, VES 53, VES 13, VES 15, VES 16 and VES 17, covering NW-SE central section of the map. The curves are mostly of the K type (r1<r2>r3). The topography along the profile is undulating with the highest point around VES53.

The first layer is essentially clayey in the central section with resistivity between 22 and 93 ohm-m and thickness of 0.5-1.4 m. At the edges of the profile, the characteristics of the first layer vary from sand (363-499 ohm-m) to sandy clay (141-160 ohm-m). The highly resistive sand (1429-2809 ohm-m) extends laterally throughout almost the entire profile with a sharp contact around VES 17. Beneath the resistive sand (ferruginized sand) is a sandy horizon with resistivity of 275-416 ohm-m, covering the central area of the profile, and clay to sandy clay (30-115 ohm-m) at the flanks of the profile.

4.4.1.4 Profile 4

This covers VES 39, VES 37, VES36, VES31, VES30 AND VES26, traversing the western to the southern part towards the Lagos Lagoon (Fig 4.34). The first layer varies from clay (50-74 ohm-m) to sandy clay (140-144 ohm-m) and sand in the central area of the profile. The resistive sand occurs sporadically along the profile beneath the first layer and grades abruptly into sandy layer (454-754 ohm-m). The sand in the central area is semi confined and exposed towards the Lagos lagoon. Beneath this horizon is a clayey layer (22-75 ohm-m) with lenses of sandy clay around VES 36.

4.4.1.5 Profile 5

This is a profile of the area closest to the Lagos lagoon from west to east. It consists of VES33, VES29, VES28 and VES26, with a relatively flat relief (Fig.4.35). The curve types in the lagoon area is mainly the HK-type (r1>r2<r3>r4). The first layer, a sandy horizon has a resistivity of 219-700 ohm-m with a thickness of 1.3 m to 8.5 m. This layer is exposed to the surface almost entirely in the lagoon area and is linked to the confined upper sand in the landward area as shown in profiles 2, 4 and 6 Underlying this sand is a thick clay layer (8-71 ohm-m) which is thin in the central areas and thicker at the flanks of the area. Ako et al (2005) suggested that resistivity of 9 Ohm-m may be indicative of salt water intrusion in some parts of Lagos, southwestern Nigeria. However, as indicated by the low TDS of groundwater from shallow wells in the area (Table 4.8), the resistivity of 8 ohm-m does not in any way indicate saltwater intrusion in the study area. This may represent plastic clay. Below this layer is a very thick sand (322-778 ohm-m), which corresponds to the confined sand in the landward area. The sandy layer is underlain by clay (16-61 ohm-m) invariably sandwiching the lower sand in the area.

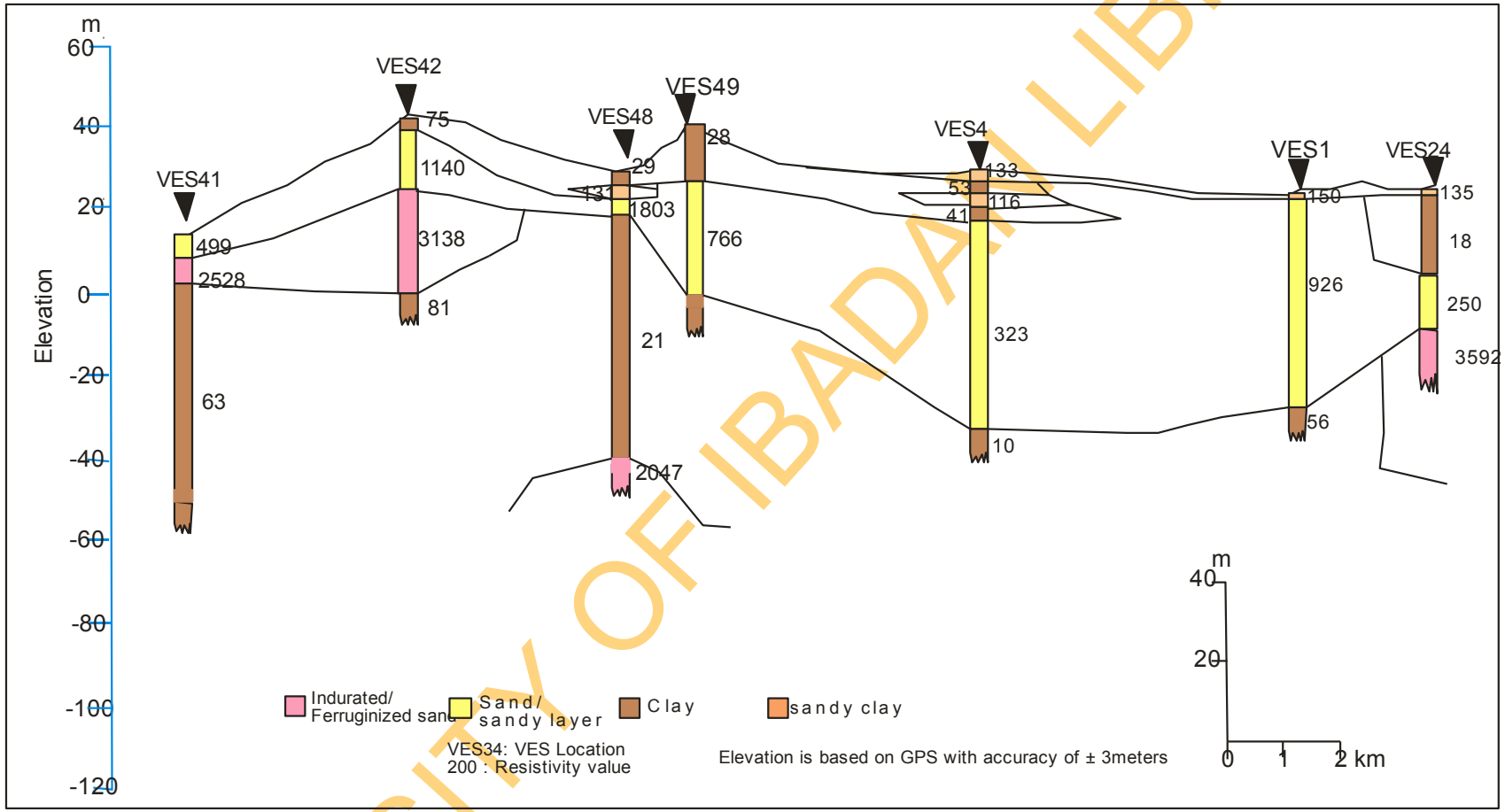

Fig.4.31 Geo-electric section of VES locations along profile 1 in Ikorodu area.

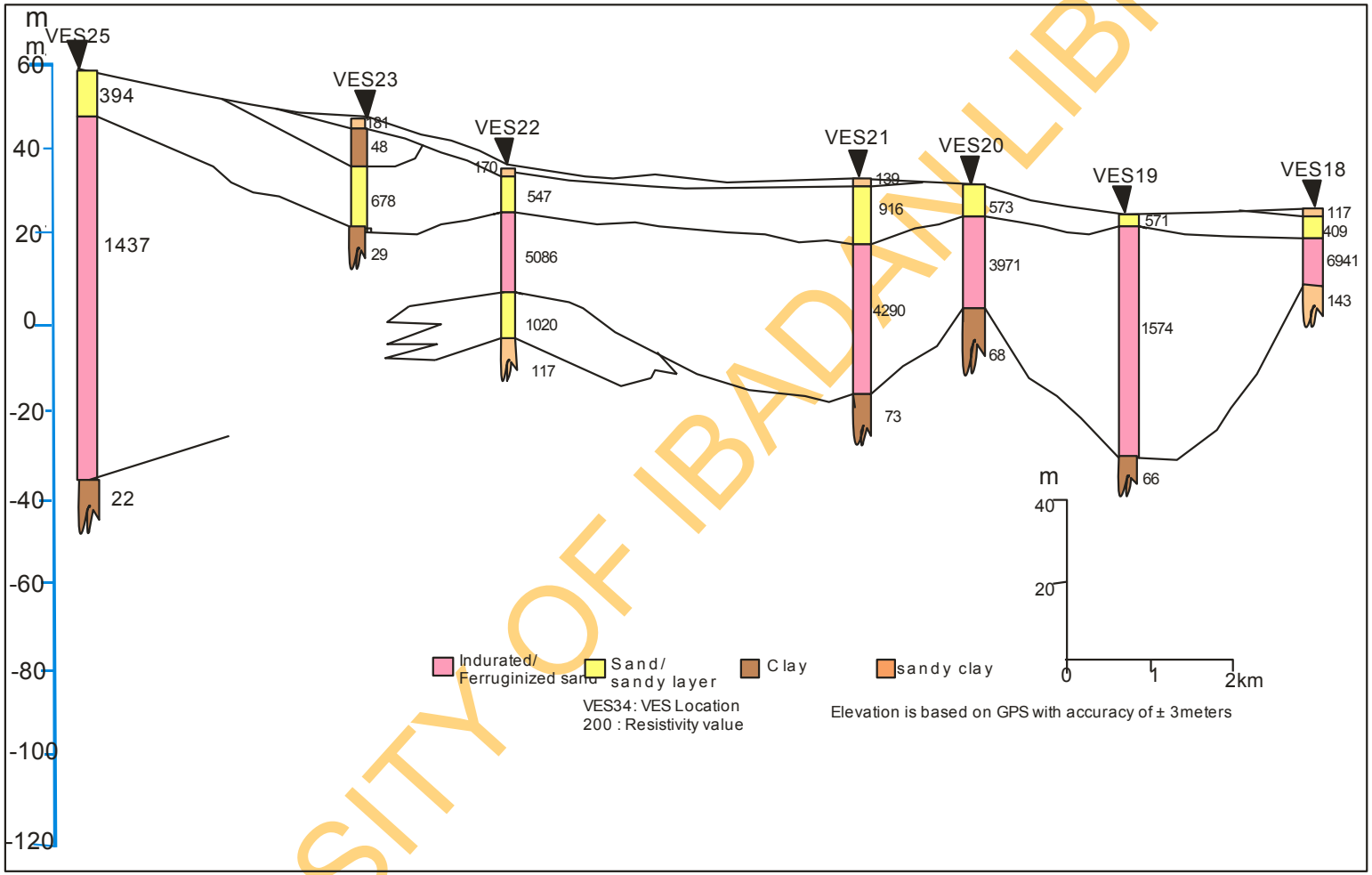

Fig.4.32: Geo-electric section of VES locations along profile 2 in Ikorodu area.

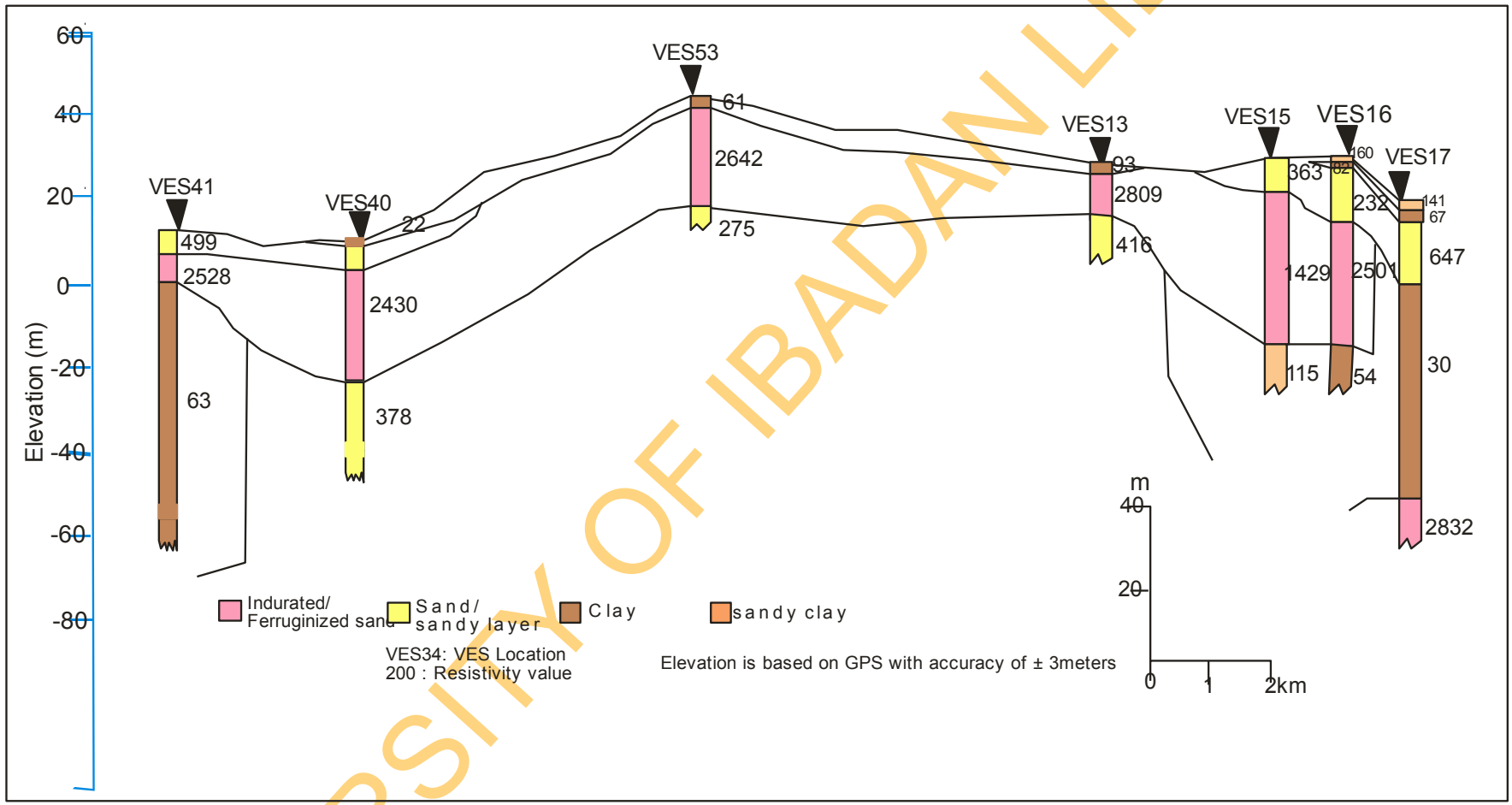

Fig.4.33: Geo-electric section of VES locations along profile 3 in Ikorodu area.

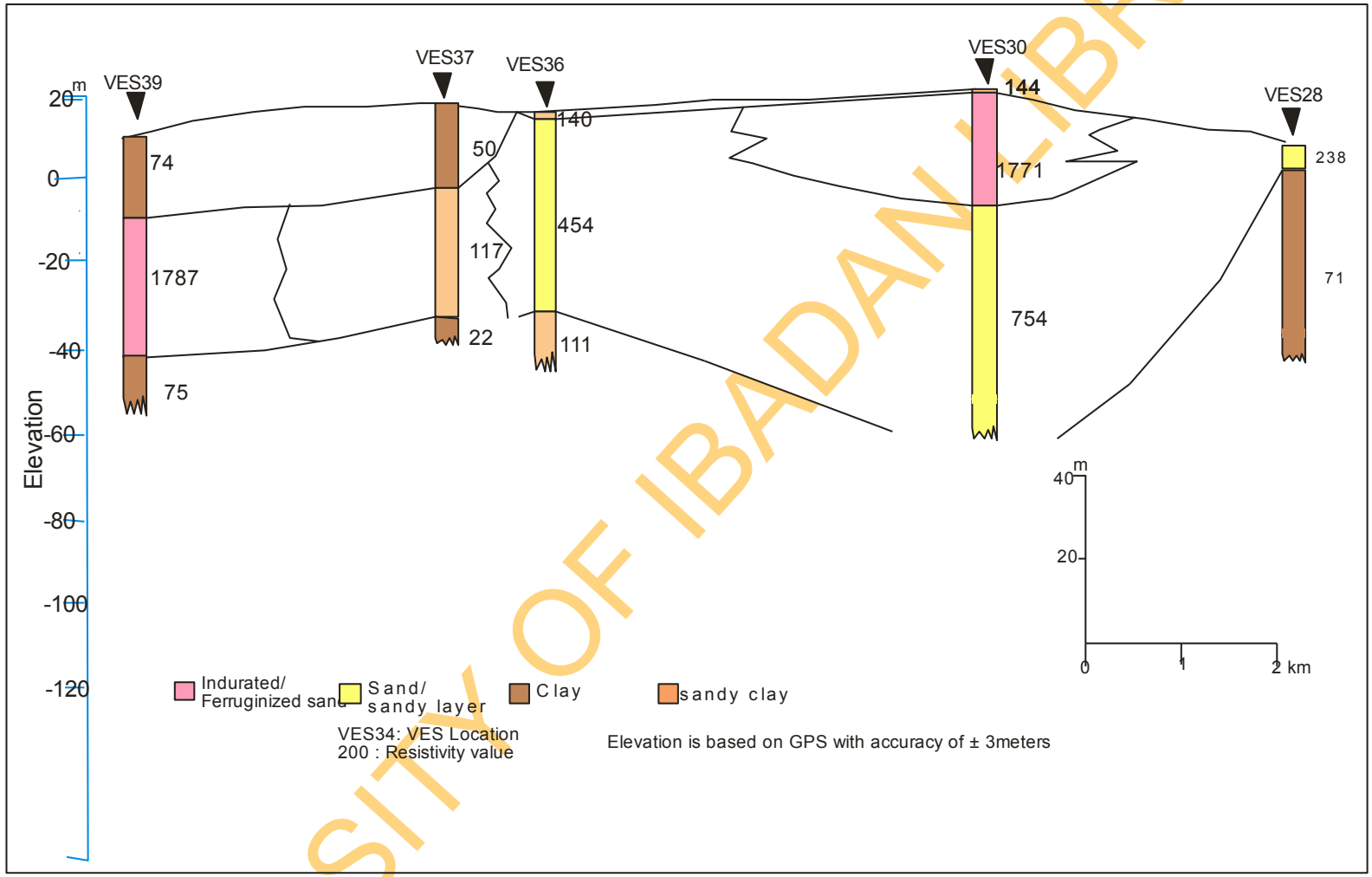

Fig.4.34: Geo-electric section of VES locations along profile 4 in Ikorodu area.

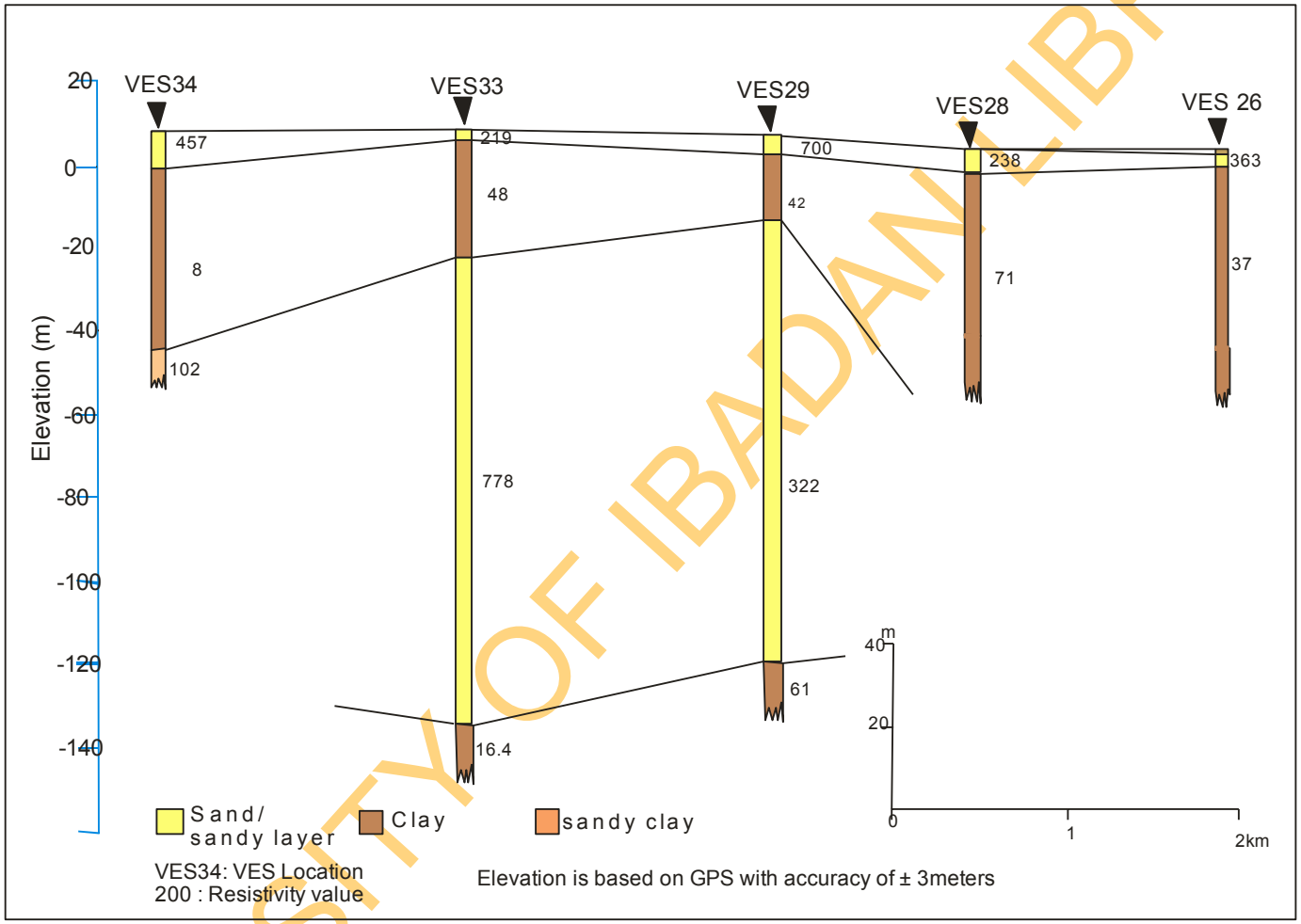

Fig.4.35: Geo-electric section of VES locations adjacent to the Lagos lagoon (profile 5) in Ikorodu area.

4.4.1.6. Profile 6

This profile, shown in Fig. 4.36, consists of VES 18, VES 17 and VES 26 providing a third dimension for profile 2. The topography along the profile is gentle between VES 18 and 17 but steep between 17 and 26. The first layer, overlying the sand described earlier in profile 2, grades between sandy clay (141 ohm-m) and clay (83 ohm-m). The sand (upper sand) has a resistivity of 363-647 ohm-m in the area. Beneath this layer, the highly resistive sands (6941 ohm-m) described in profile 2 as extending from north-eastern part to the southern area, gradually thins out towards VES 17. The sands are underlain by sandy clay that grades abruptly to a thick clay horizon (30-37 ohm-m) towards the lagoon. The highly resistive sand re-appears below the clay to sandy clay horizon around VES 17.

A combination of profiles 1, 3, 4 and 5 reveals that generally in Ikorodu area, the lower, mostly confined sand occurs continuously in the central area of the profiles, revealing that the sand occurs at a shallower elevation in the central area along the NE-SW trend. The flanks of the profiles (Fig 4.31 – 4.36) all have thicker clay horizons and the sand was not encountered in many parts of the flanks of the area, suggesting that the sandy layer occurs at greater depth at the flanks. These situations are partly due to differences in elevation, or could be structural because in most of the profiles the central areas appear like the centre of horst structure, such that the sediments at the centre have been pushed upward relative to the flanks. This is not unlikely as the Dahomey basin has been described by Whiteman (1982) as having the graben and horst structure.

4.4.2 Lithologic, Electrical Resistivity and Gamma Logs

Two lithological logs obtained from Ikorodu area were correlated with the geophysical log of VES 38, sounded about 100 m from the wells. The summary of the lithologies of the two boreholes drilled in the area are presented in the Tables 4.6 a and b. The lithologic log of Well 1 revealed the presence of sandy clay horizon at the top, underlain by a clay layer overlying a sandy horizon between the depths of 10 and 30 m. This sand is separated from lower sand, which occurs between the depths of 32 and 50 m. Beneath the lower sand is a thick clay stratum that overlies a sandy layer that contains clay lens. The second log obtained from another well drilled about 100 metres away from Well 1 reveals similar lithology. However, the upper sand is divided into many units by the presence of clay lenses, which are absent in Well 1. These differences in lithologic logs of the wells sited about 100 m apart; further confirm the rapid

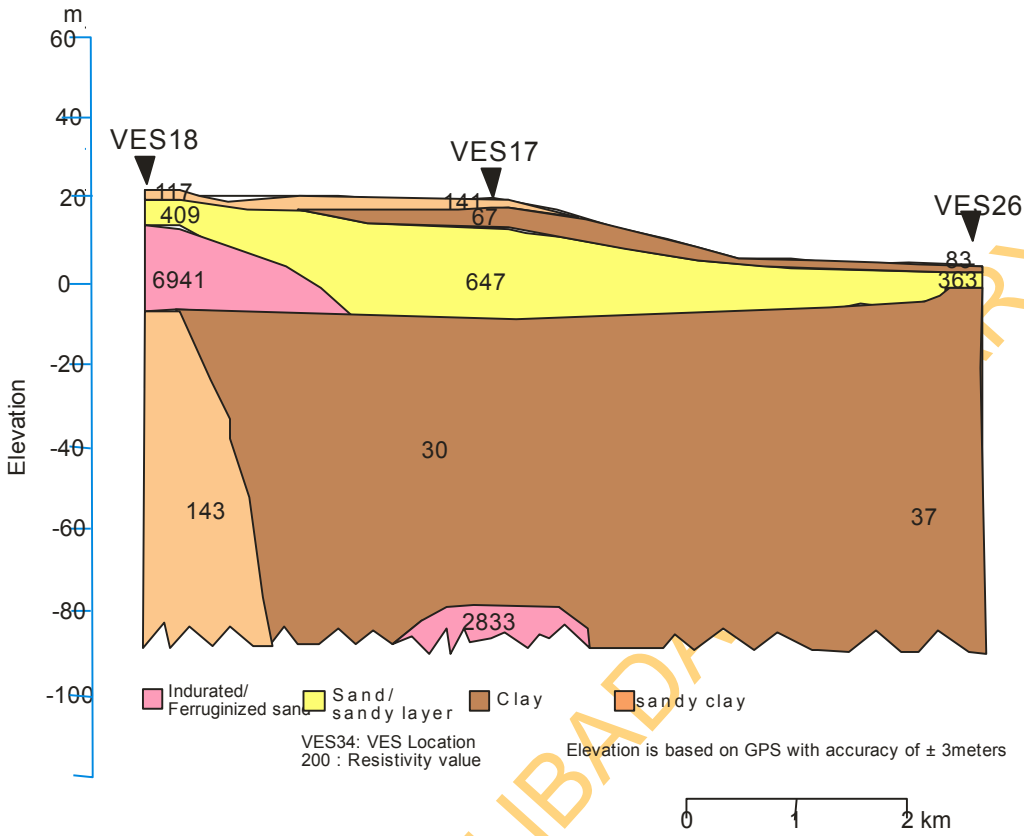

Fig.4.36: Geo-electric section of VES locations along profile 6 in Ikorodu area.

Table 4.6: Lithologic Logs (a) Borehole 1 (b) Borehole 2

(a) Depth (m) From	To	Lithology
0	3	Reddish clayey, medium grained sand
3	15	Pinkish white, sandy, coarse grained, clay
15	33	Grey, medium grained sand
33	36	Grey, clayey, medium grained sand
36	51	Grey, medium grained sand
51	54	Grey, fine grained clay
54	78	Brownish, clayey, fine grained sand
78	90	Grey, clayey, fine grained sand
90	99	Brownish medium grained sand
99	108	Grey coarse grained sand
108	114	Dark brown clayey, medium grained sand
114	117	Dark brown, very coarse grained sand
117	125	Dark brown clayey, medium grained sand

(b)

Depth (m)		Lithology
From	To	
0	3	Reddish, clayey laterite
3	15	Light red, sandy coarse grained, clay
15	21	Light red, fine grained clay
21	27	Pinkish white, medium grained sand
27	30	Light red, clayey, medium-coarse sand
30	33	Grey, coarse grained sand
33	36	Brown, clayey, medium grained sand
36	48	Light brown, medium grained sand
48	51	Brown, clayey, medium grained sand
51	57	Light brown, medium grained sand
57	63	Grey, fine grained clay
63	69	Light brown, fine-medium grained sand
69	72	Grey, fine grained clay
72	76	Grey, coarse grained sand
76	93	Grey clayey, fine grained sand
93	109	Whitish, coarse grained sand
109	120	Whitish, clayey, medium-fine grained sand

change of facies in this area as noticeable in some of the sections of the geophysical profile and as reported by Ako et al (2005).

The geophysical log of VES 38 (Fig.4.37) which is located closest to the boreholes BH 1& BH2 shows a succession of sandy clay, followed by clay, then thick sandy horizon between 12 and 41 m. The sand is underlain by clay layer, which is the last layer delineated in the area. This agrees with the logs described above.

Electrical resistivity and gamma logs of the wells presented in Fig 4.38 further confirm the lithologies described for the area. In addition, the high resistivity values (between 500 and 1000Ωm) of the sands encountered in the area suggest that the sands are fresh water sands; hence the aquifers contain fresh water.

4.4.3 Aquifers in Ikorodu Area

As shown in the preceeding discussions, the aquifer in Ikorodu area can be classified into two, namely:

I. The upper sand (mostly unconfined); and
II. The lower sand (mostly confined).

4.4.3.1The upper sand (mostly unconfined)

The upper sand is exposed to the surface in almost all areas close to the Lagos lagoon and in some of the landward areas, due to elevation differences and effect of erosion that has carved out the area to the present rugged undulating topography. The upper sand shown in Figures 4.31-4.36 is recharged mostly by precipitation in areas where it is exposed to the surface. Although, it is present in virtually all parts of Ikorodu, it has little hydrogeological significance in the landward area due to the relatively high elevation (20-60 m above sea level) in comparison to the elevation in the coastal area (<10 m). In the coastal area, it has very high groundwater potential as water flows from the landward area towards the coast due to the hydraulic gradient between the areas. It supplies water to shallow wells in the coastal area all year round due to the availability of recharge through precipitation and perennial surface water bodies.

4.4.3.2 The lower sand (mostly confined)

The lower sand occurs at greater depth than the upper sand with a depth range of between 20-80 m in the central area. It is shown in Figures 4.31- 4.36. It is generally thicker than the upper sands and mostly sandwiched between two confining layers by clay at the top and clay or

resistive sand (feruginized) in a few places. The sand is in hydraulic continuity throughout the area, especially in the central NE-SW area, where it is encountered in all profiles. The confined aquifer supplies water to the deep-wells and boreholes used mostly for domestic purposes in the study area. The depth of occurrence of the lower sand correlates strongly with the lithological logs (Fig 4.37) and geophysical logs (Fig 4.38) of wells in the area. In addition, it perfectly coincides with the estimated depth of some functional boreholes in the area, based on information supplied by the inhabitants.

4.5 Geochemistry of Groundwater

The summary of the results of the physical parameters of groundwater in Abeokuta and Ikorodu areas are presented in Table 4.7. The minimum, 25th percentile, median, 75th percentile and maximum are presented as box plots for graphical views of the data distribution of the constituents of groundwater in the study areas that are greater than 1 mg/l in most of the groundwater analysed. Cross plots were used to determine and analyse inter-elemental relationships.

In addition, hydrochemical maps (isocones) were produced for all major ions and some heavy metals, as the baseline hydrochemical map for these dissolved ions and elements in the areas. Furthermore, Stiff maps, Gibbs diagrams, Piper trilinear diagrams, Scholler diagrams were all plotted for groundwater characterization. The discussions of the results are divided into physical parameters, chemical parameters and groundwater isotopes of the study areas.

4.5.1 Physical Parameters

The statistical summary of the physical parameters of groundwater in the study areas are presented in Table 4.7. The physical parameters presented include the static water level, total well depth, pH, total dissolved solids, electrical conductivity and hardness in Abeokuta and Ikorodu areas.

4.5.1.1Static water level, total well depth and flow direction in the study areas

The groundwater in all the locations in Abeokuta area was tapped from shallow aquitard/aquifers through traditional hand-dug well. Interaction with inhabitants revealed that yield is generally low to moderate in most of these wells. The static water level in Abeokuta area (Fig.4.39) is mostly between 1.2 and 9.4 m with an average of 4.1± 1.85 m and a coefficient of variation of 45%. The total well depth ranges between 1.5 and 14.0 m and a mean of 6.5± 2.8 m.

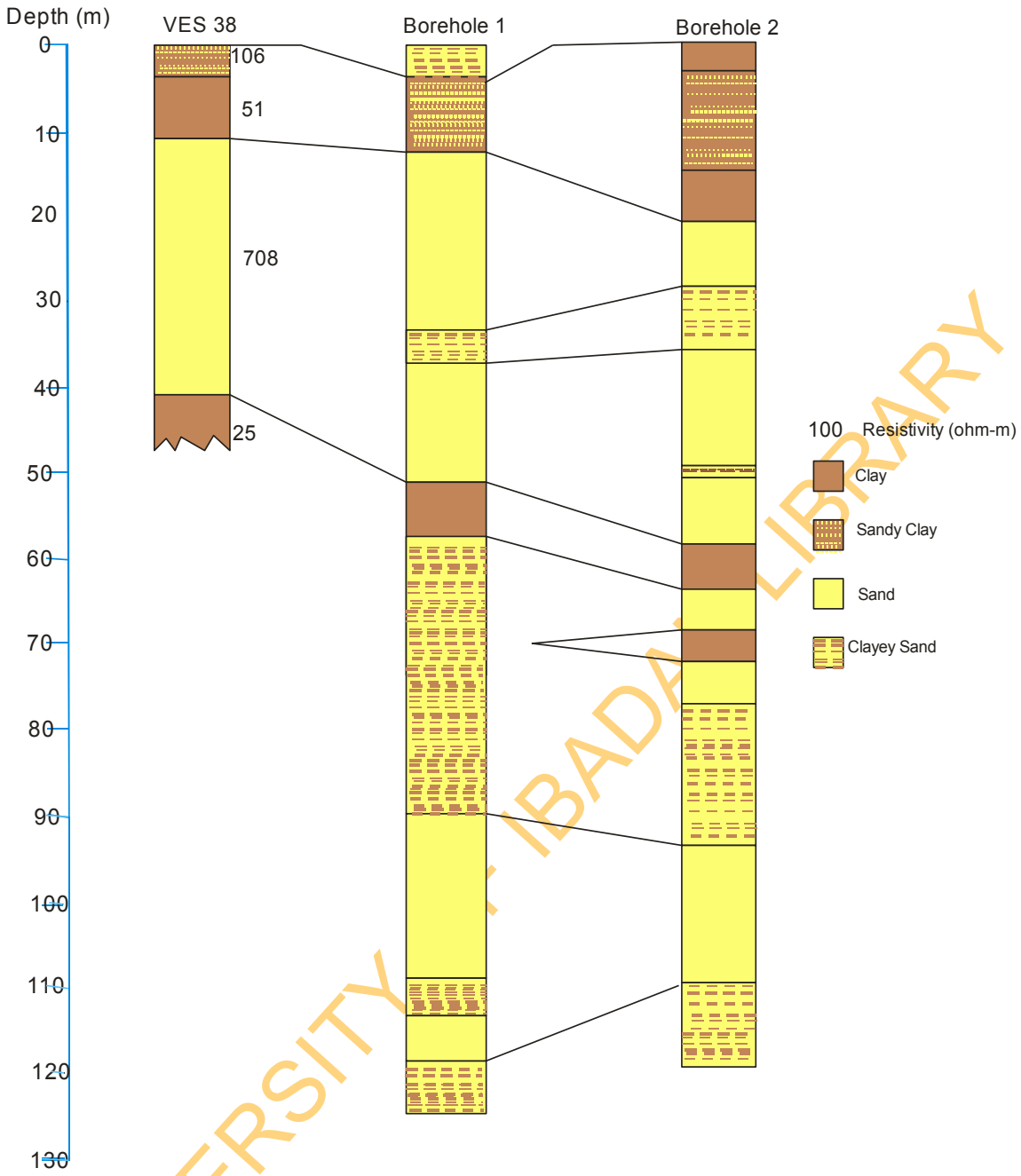

Fig.4.37: Geo-log of VES 38 and lithologic logs of adjacent boreholes.

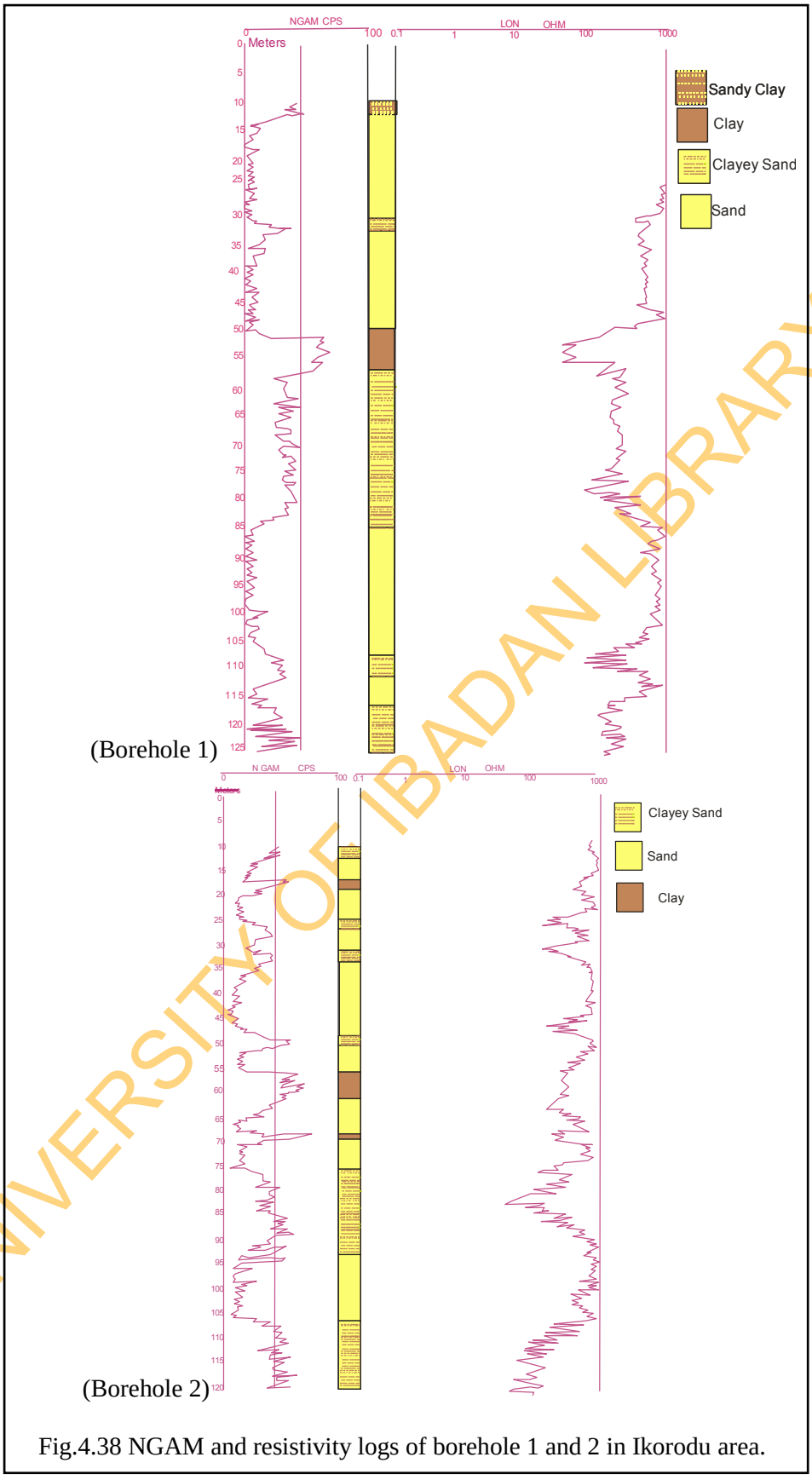

Fig.4.38 NGAM and resistivity logs of borehole 1 and 2 in Ikorodu area.

Table 4.7: Statistical Summary of the physical parameters of groundwater in the study areas

Study Areas	Parameters	Total Well Depth (m)	Static Water Level (m)	pH	TDS (mg/l)	EC	Hardness (mg/l)
Abeokuta	Minimum	1.5	1.2	5.9	78	119	29.0
	Maximum	14.0	9.4	8.6	1504	2331	84.0
	Mean	6.5	4.1	6.9	476	864	59.4
	First quartile	5.0	2.6	6.4	254	421	50.5
	Third quartile	8.0	5.2	7.2	675	1366	69.5
	Standard deviation	2.8	1.9	0.6	322	557	13.3
	Coefficient of variation (%)	42.0	45.0	9.0	68	64	0.2
Ikorodu	Minimum	3.7	1.8	4.2	22	150	1.6
	Maximum	27.0	25.0	8.0	1091	7961	134.0
	Mean	6.8	8.3	6.5	237	1630	30.6
	First quartile	4.5	3.1	5.9	48	310	8.9
	Third quartile	5.3	9.4	7.3	254	1727	37.0
	Standard deviation	6.7	9.2	1.0	275	1924	32.4
	Coefficient of variation (%)	100.0	110.0	20.0	120	120	110.0

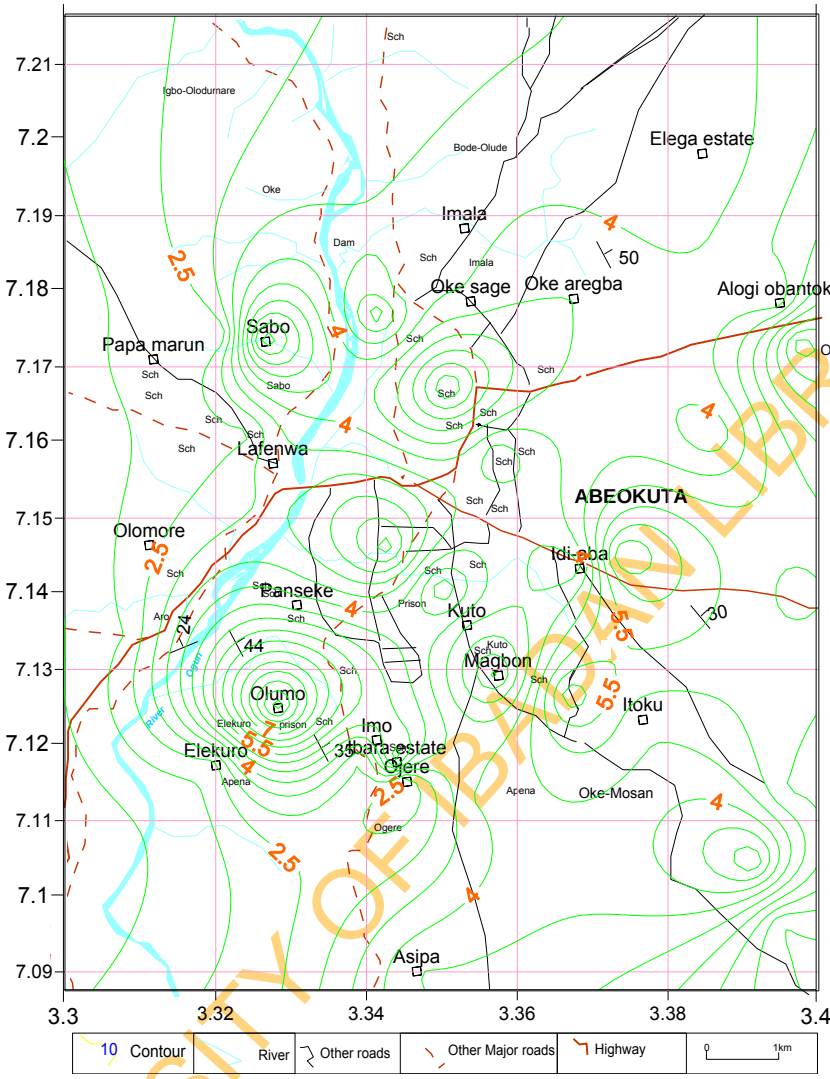

Fig 4.39: Static water levels in Abeokuta area.

In Ikorodu area, groundwater is obtained from deep-wells/boreholes in most areas, especially in places with high elevation (20-50 m) above sea level while at the locations close to the lagoon; most of the inhabitants rely on groundwater from shallow hand-dug wells. In the area around the lagoon where data on static water level and total well depth were measured, the static water level and total well depth vary from 1.8 m to 25.0 m and 3.7 to 27 m respectively. In the landward area with high elevation 20-50 m, the aquifer is confined by thick layer of lateritic soil and clay with depth to water of between 15 and 45 m while in the coastal area where the elevation is between 3 and 15 m (Fig.4.40), the aquifer is unconfined with depth to water of between 1.8 and12 m.

The groundwater flow direction in Abeokuta area (Fig 4.41) indicates that generally groundwater flow towards River Ogun. The groundwater head relief map is largely influenced by the relief of the area as groundwater flow directions are mostly towards R. Ogun from either sides of the river. This finding agrees with those of Xong et al (1999) that noted that the configuration of the water table is similar to the topographic configuration in humid tropical areas. The dominant flow towards R. Ogun suggests that the river is significantly recharged through groundwater base flow. The river and its tributaries similarly recharge the groundwater when the river level rises above the water table. In Ikorodu area, there are insufficient physical parameters to determine the direction of groundwater flow.

The geology of Abeokuta area has partly influenced the static water level, total well depth (TWD) and saturated water column in the area. The area underlain by porphyritic granite and porphyroblastic gneiss have thicker water column than the areas underlain by hornblende-biotite gneiss and granite as shown in Fig 4.42. This agrees with the groundwater potential map of the area (Fig. 4.27) generated from the geophysical and geological parameters. Similarly, static water level and total well depth occur at greater depth in these parts (Fig.4.39 and Fig 4.43) of Abeokuta.

The water column shows a strong correlation (0.74) with total well depth and weak negative correlation with TDS (-0.48). The implication of these relationships displayed in Fig.4.44a and Fig. 4.44b is significant showing that thick water column is dependent on the total depth of the well (in the area) and where the column is thinner, deeper wells may result in thicker water column. The inverse relationship between the TDS and water column suggests that the thickness of the water column has a little influence on the TDS, such that the the thicker the column and invariably the higher the quantity of water in well and the lower is the TDS. The relationships between total well depth and static water level with the major anions were evaluated

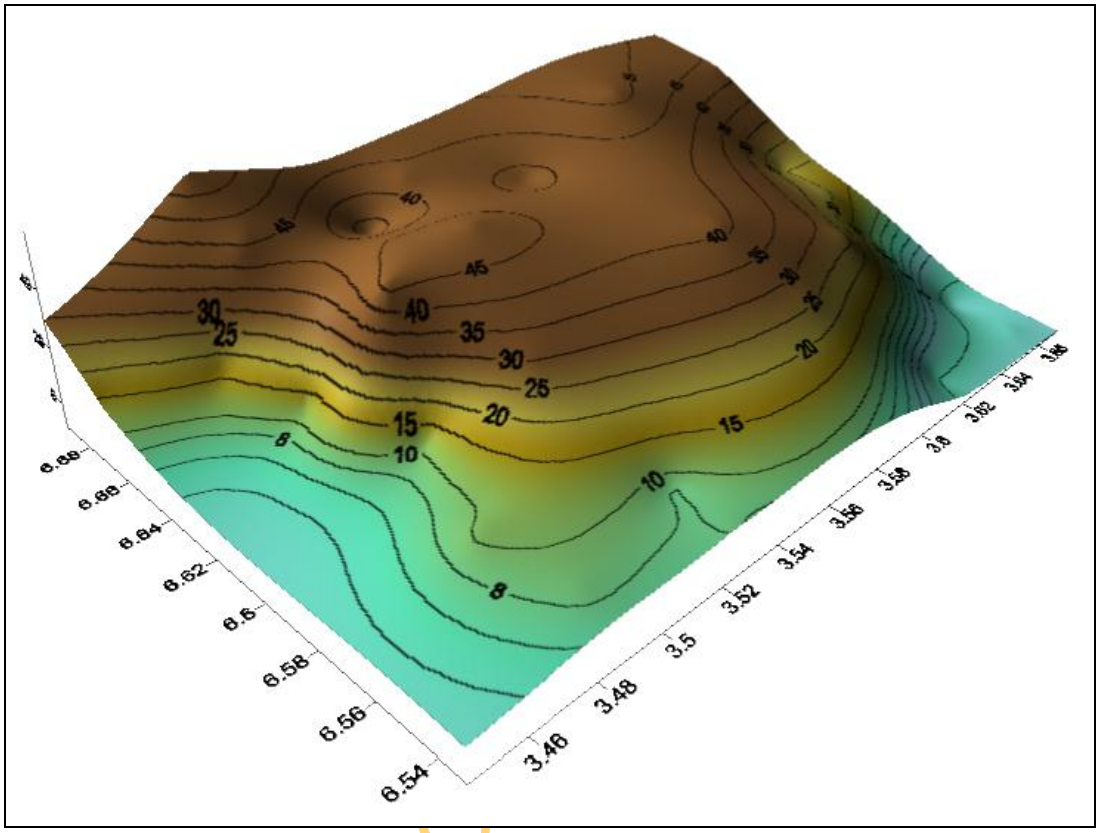

Fig. 4.40 3D elevation map of Ikorodu area

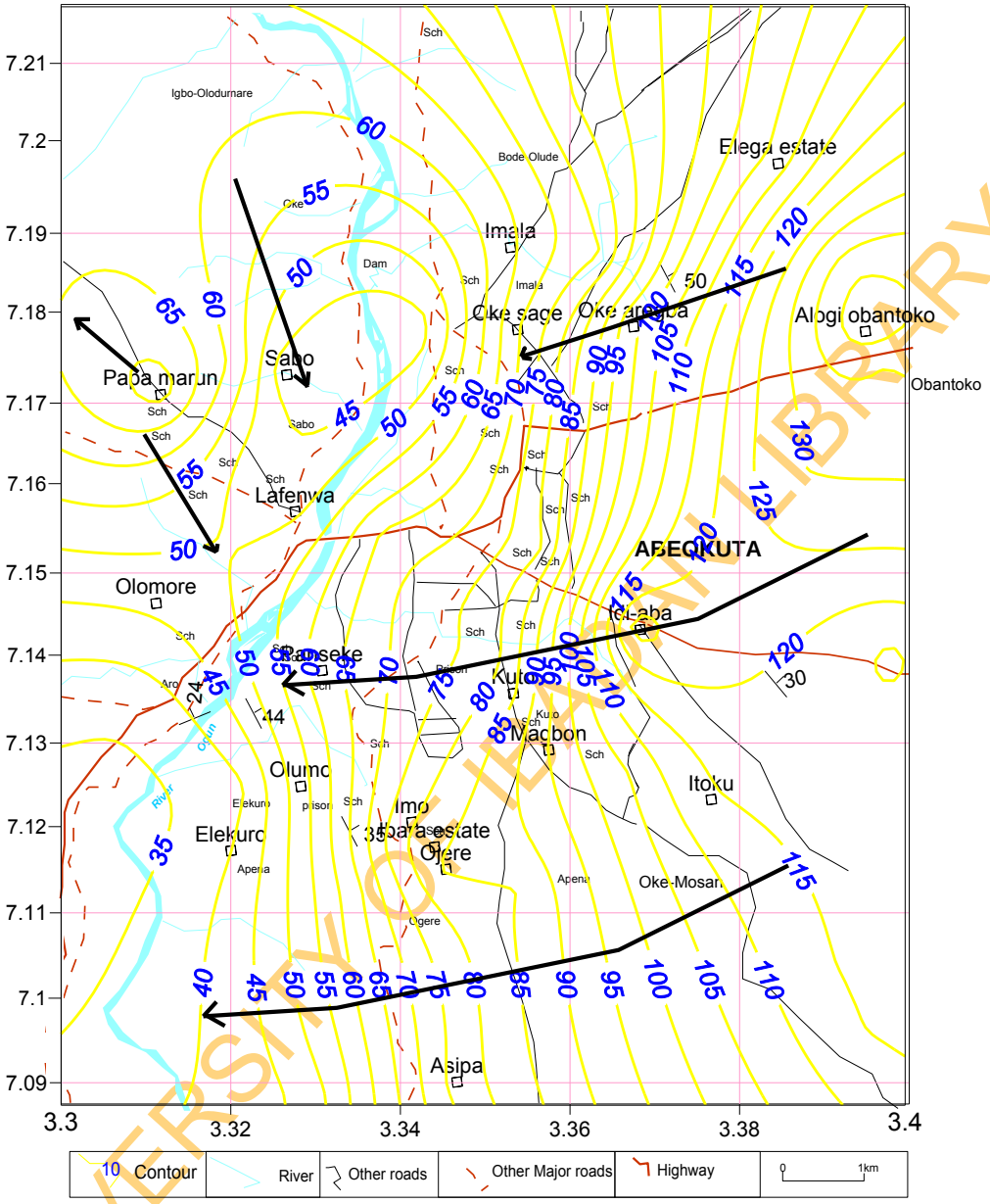

Fig. 4.41: Groundwater flow direction in Abeokuta area.

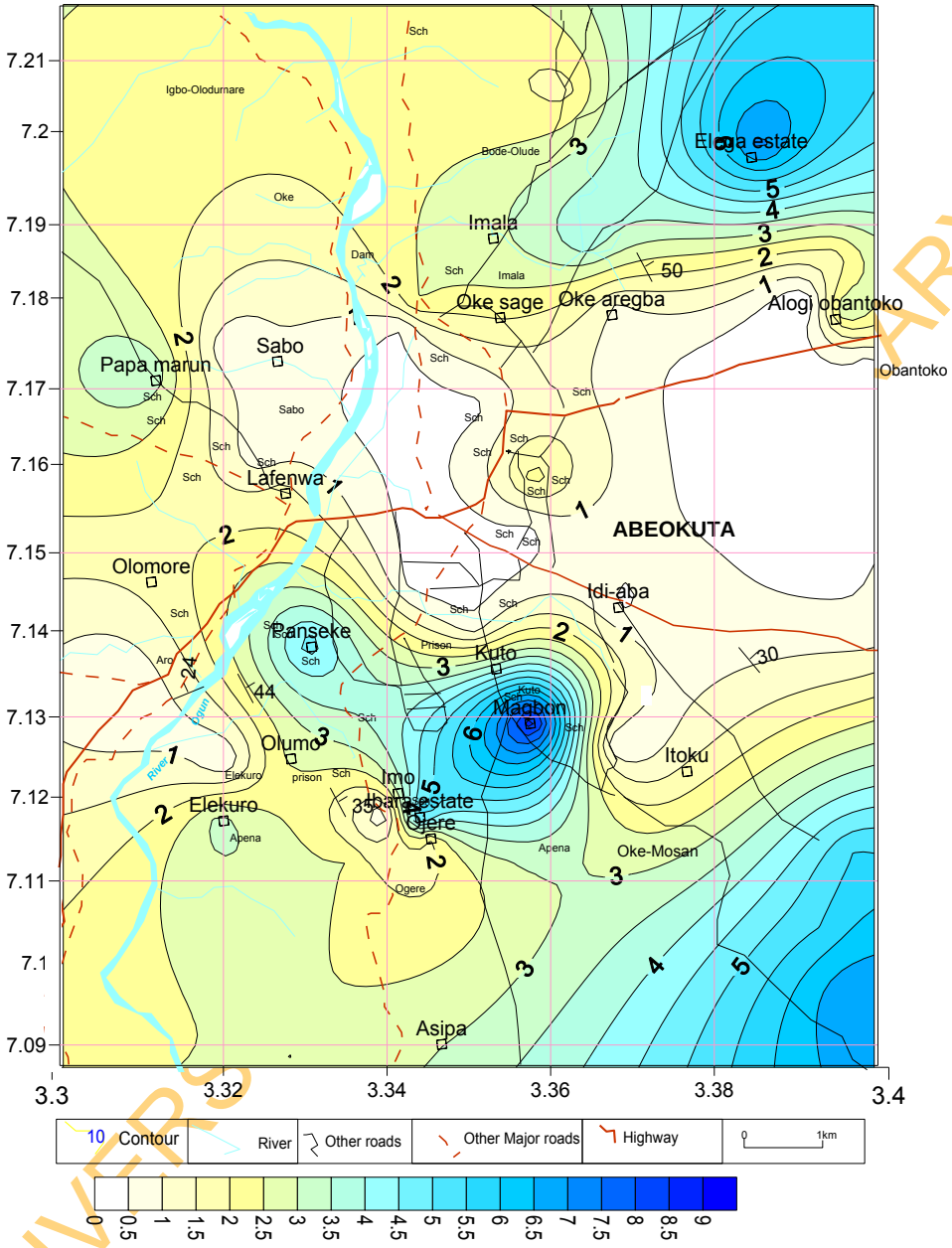

Fig.4.42: Water column in Abeokuta area.

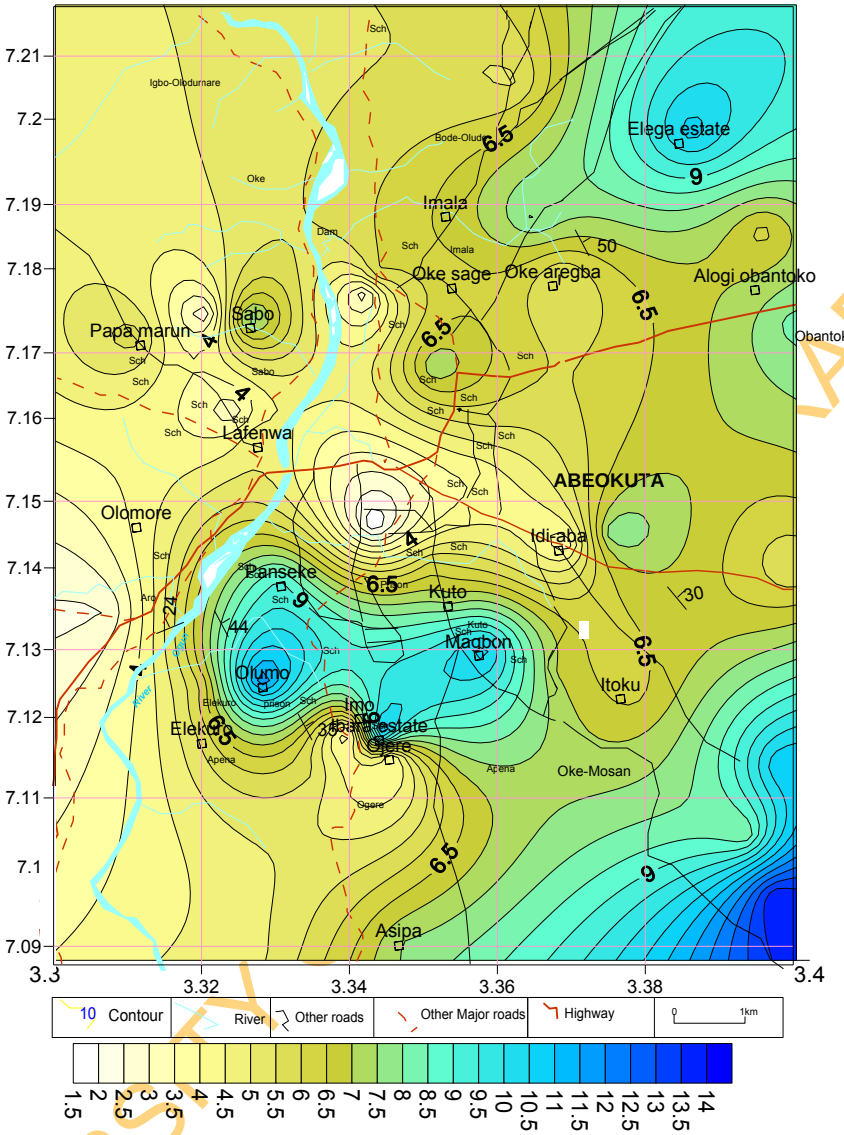

Fig.4.43: Total well depth in Abeokuta area.

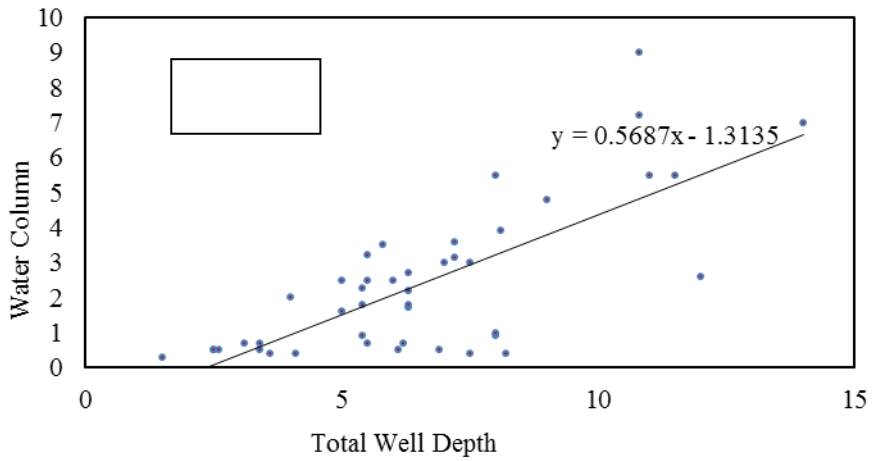

(a)

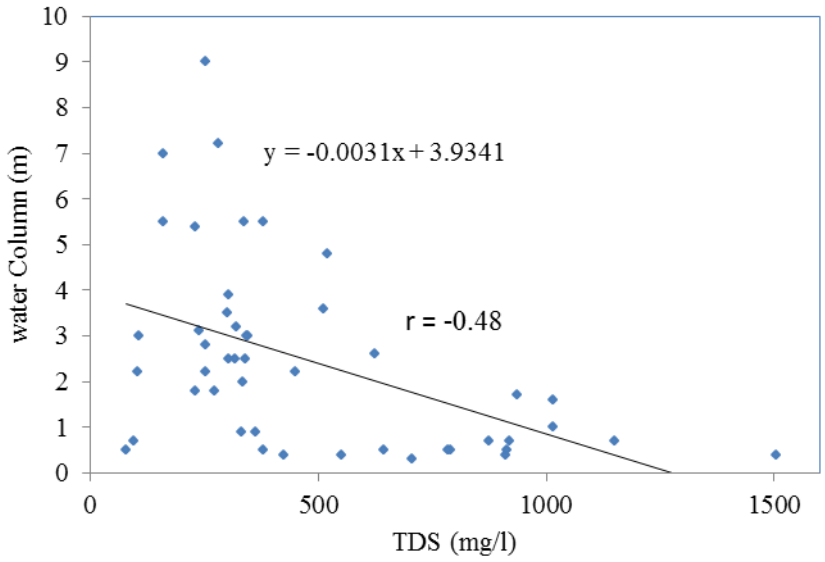

(b)

Fig. 4.44: Cross plot between water column and (a.) Total well depth; (b) TDS in Abeokuta area

to assess the possible contribution of these ions from surface sources.

In Abeokuta area, the total well depth shows weak negative correlation (Fig 4.45 a-d) with bicarbonate (-0.23), nitrate (-0.04), sulphate (-0.19) and chloride (-0.03). This invariably indicates that the contribution of these ions from surface sources especially nitrate may not be related to the well depth but rather due to other factors such as localized occurrences of such surface sources. (such as livestock, agricultural wastes, seepages from drainages and septic tanks).

The water column in Ikorodu area shows weak correlation coefficients of 0.33 with total well depth (TWD) and -0.21 with TDS respectively as shown in Fig. 4.46. The implication of these relationships when compared with weathered aquifer of Abeokuta area is that water column is largely independent of well depth, but rather it is dependent on the aquifer characteristics. The negative relationship between the TDS and water column suggests that the thickness of the water column has no significant influence on the TDS. The total well depth in Ikorodu area has fair negative correlation with nitrate, having coefficients of correlation of -0.58 (Fig. 4.47). This suggests that as depth of wells increases, nitrate concentration reduces. This invariably implies that nitrate concentration is partly related to surface sources specifically in the shallow hand-dug wells.

4.5.1.2 pH of groundwater in the study areas

pH is a very important physical parameter of groundwater as many groundwater reactions are dependent on the pH of the water. In addition, consumption of water having low pH over a long period of time may lead to derangement of the acid-base balance in the body system, which may cause metabolic acidosis and respiration may become deep and rapid in severe cases (Ofoma et al, 2005).

The groundwater in Abeokuta area is generally slightly acidic to alkaline with pH that varies from 5.9 to 8.6 with a low coefficient of variation of 9%. Fifty eight percent of the groundwater sampled in the area falls between the classes of acidic to slightly acidic water, using the classification of Ezeigbo (1989) while forty two percent falls within the class of neutral to slightly alkaline water in the area. Such low pH value of mostly less than 8 is indicative of free CO_2 and dissolved carbonates exist almost entirely in HCO_3^- ion form (Tijani and Abimbola, 2003 citing Freeze and Cherry, 1979). Positive correlation of 0.55 established between HCO_3^- and pH as shown Fig. 4.48, indicates the role of pH in the CO_3^{2-} dissolution process in the groundwater of the weathered aquifer.

The groundwater in Ikorodu area is acidic to alkaline with a pH that varies between 4.2 and 8.0. The coefficient of variation of the pH is 20% while the pH and HCO_3^- show a weak positive correlation of 0.21 for the shallow well Samples. In the deep wells/boreholes, a weak negative correlation coefficient of -0.32 was established between pH and HCO_3^-, which may be indicative of the mildly different roles of pH in the CO_3^{2-} dissolution process in the groundwater from shallow wells and the boreholes.

4.5.1.3 Total dissolved solids and electrical conductance of groundwater

Dissolved constituents of groundwater originate through natural sources (weathering and dissolution), sewage and run-off. The Total Dissolved Solids (TDS) of groundwater is generally higher in Abeokuta area, with a range of 78 to 1504 mg/l and an average TDS of 518.6 ± 322.3 mg/l. The TDS has a relatively high coefficient of variation of 68%, though it is much less than a variation of 120% obtained in Ikorodu area. TDS of water samples in Ikorodu varies from 22-1090.5 mg/l with a mean of 237±275.1 mg/l and a coefficient of variation of 120%. In the area, the TDS averages 122±99.1 mg/l in the borehole samples while the mean TDS in the shallow wells is 392±337.8 mg/l. Except for three locations very close to the lagoon, the TDS is generally less than 1000mg/l, the cut-off value for fresh water (Todd, 1980).

The overall data on groundwater chemistry show that the TDS and the concentrations of the different chemical character of the groundwater samples from the Abeokuta area vary widely. The variation is largely due to anthropogenic contribution from River Ogun and partly to the variation of bedrock lithology. Groundwater in Abeokuta has higher TDS than the groundwater in Ikorodu because in addition to anthropogenic factor, the weathered product of the underlying rocks is rich in soluble silicates minerals unlike in Ikorodu area where the groundwater is flowing through rock rich in silica (quartz) and remnant of feldspars. In addition to the contribution by weathering and dissolution in Abeokuta area, higher TDS in areas on both side of River Ogun and its tributaries is indicative of the impact of the river on the dissolved constituents of the groundwater in the areas close to the river.

The TDS is generally lower in the landward area than around the lagoon. This is largely related to the impact of the lagoon on the groundwater and as noted by Freeze and Cherry (1979), shallow groundwater in the recharge areas has lower TDS than that in discharge areas. The large variation of TDS in the groundwater of Ikorodu is mainly due to the large difference in dissolved constituents of landward areas and those of areas adjacent to

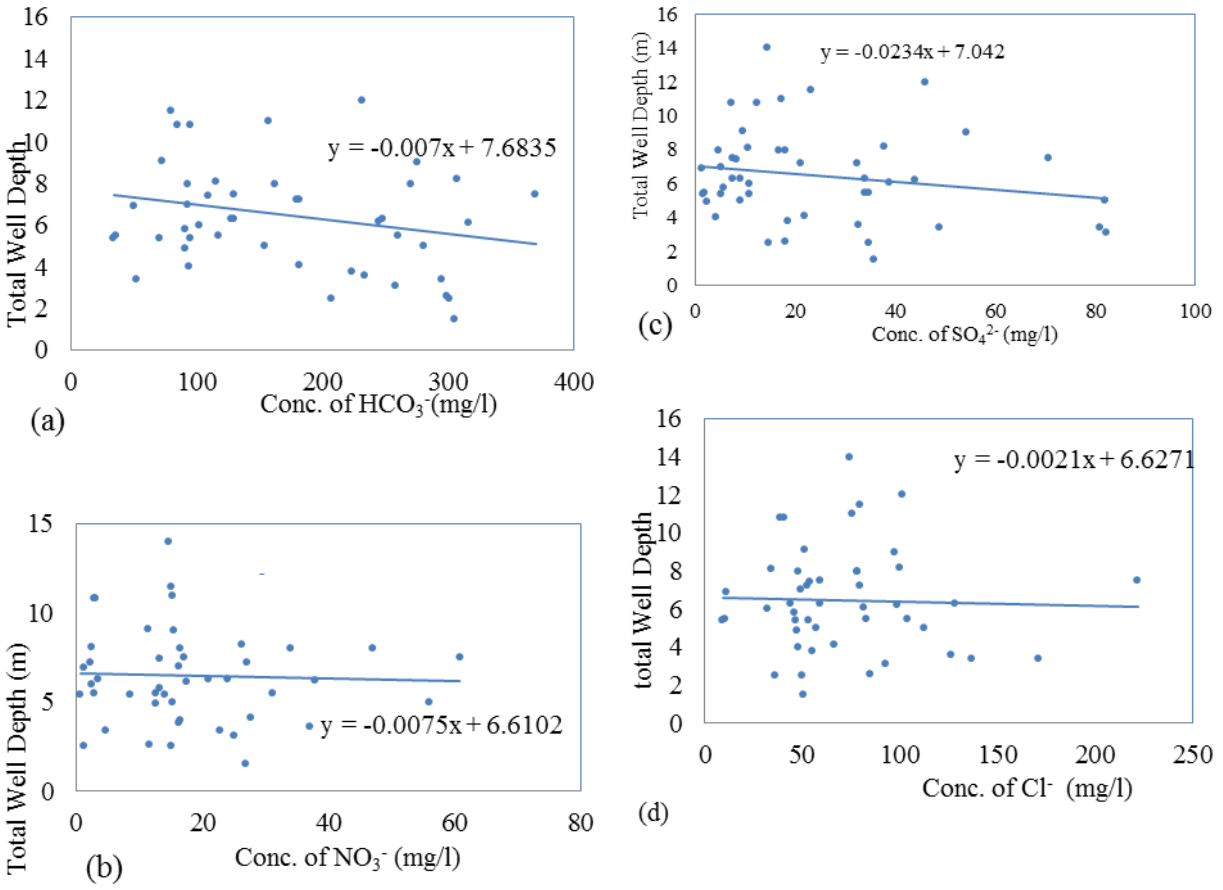

Fig.4.45: Cross plot of total well depths & concentration of HCO_3^- (b) NO_3^- (c) Conc. of SO_4^{2-} and (d) Cl^- in Abeokuta area

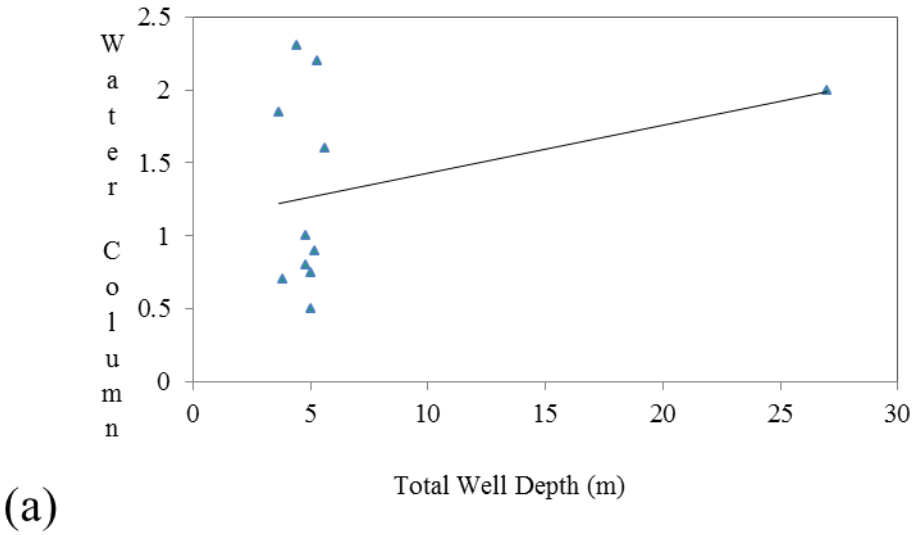

(a)

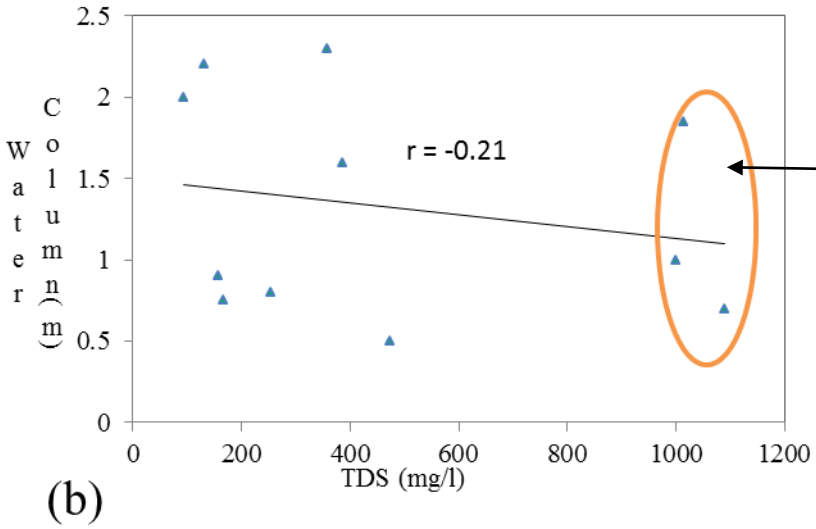

(b)

Fig 4.46: Cross Plot between water column and (a) TWD; (b) TDS in Ikorodu

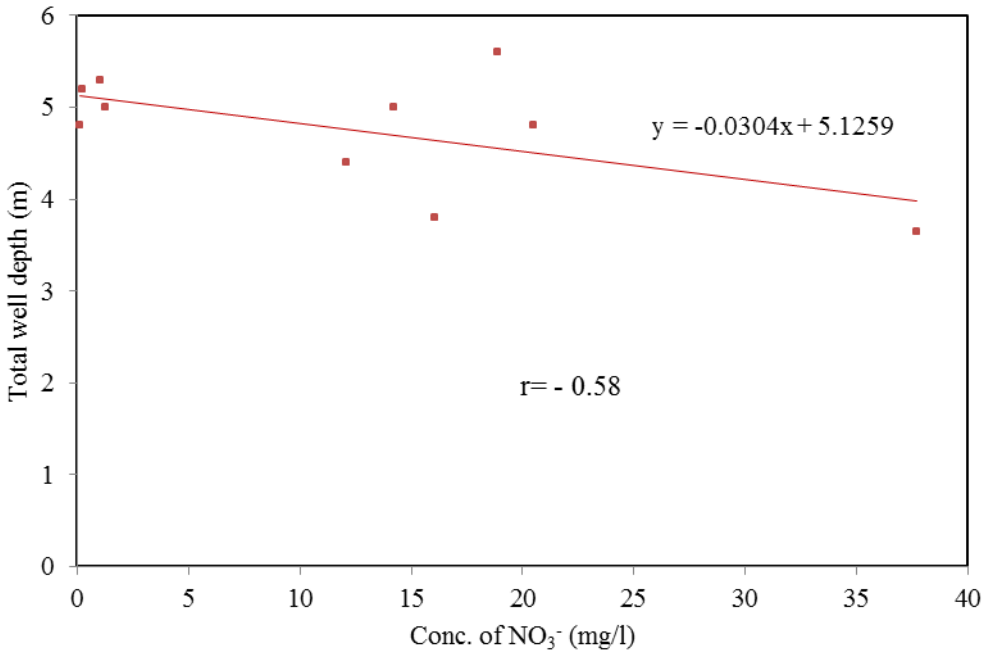

Fig. 4.47: Cross plots of total well depth against conc. of NO_3^- in Ikorodu

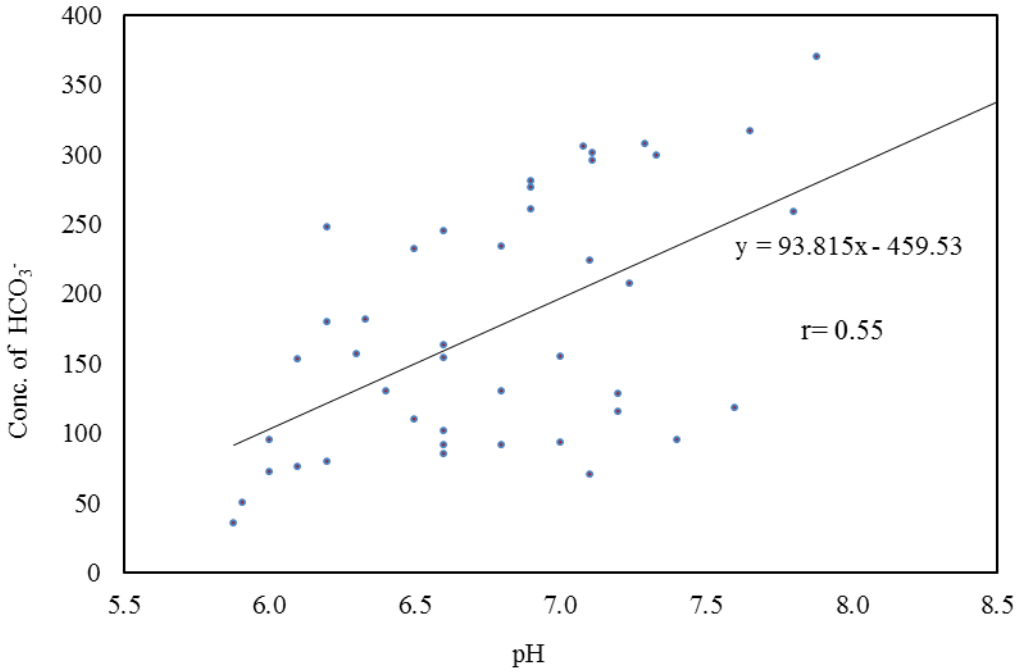

Fig 4.48: Cross plot of concentration HCO_3^- and pH in groundwater of Abeokuta area.

the Lagos lagoon. Health based guidelines for TDS is not available (WHO 2006). However, the presence of high level of TDS (>1000 mg/l) in groundwater may be objectionable for drinking.

The electrical conductance (EC) of the groundwater from Abeokuta area varies from 119-2331 uS/cm with an average of 863.9±557.1 uS/cm and a coefficient of variation of 68%. Very strong correlation coefficients were established between electrical conductivity and Na^+ and Cl^- (Fig 4.49).

The electrical conductance of groundwater samples from Ikorodu area (Table 4.10) varies from 149.6-7960.8 uS/cm with an average conductance of 1629.7±1923.7 uS/cm and a coefficient of variation of 120%. It is largely influenced by the chloride as displayed by the very strong correlation coefficients of 0.93 and 0.95 respectively between EC and Cl and EC & Na (Fig 4.50). It varies from 149.6-2516.9 uS/cm in the boreholes/deep-wells and averages 786.0±629.0 while in the shallow wells, it varies from 220.0-7960.0 uS/cm and has a mean of 2925.6±2356.2 uS/cm. The areas closer to the lagoon have higher conductance relative to the landward areas.

The electrical conductance in Abeokuta based on the Wilcox (1995) classification for irrigation water is doubtful (750-2250 uS/cm) while in Ikorodu area, the borehole groundwater samples fall within the doubtful class whereas the samples around the lagoon area are generally unsuitable (>2250 uS/cm).

4.5.1.4 Hardness

Water hardness is caused primarily by the presence of cations such as calcium and magnesium and anions such as carbonate, bicarbonate, chloride and sulfate in water. Water hardness has no known adverse effects; however, some evidence indicates its role in heart disease (Schroeder, 1960). Hardness in the groundwater of Abeokuta and Ikorodu areas respectively vary from 29 to 84 ppm and 1.6 to 134 ppm. The mean for these areas are 59.4±13.3 ppm and 30.6±32.4 ppm correspondingly for Abeokuta and Ikorodu areas. Based on the classification by Sawyer and McCarty (1967), the groundwater in the study areas is soft (<75 ppm) to moderately hard (75-150 ppm).

4.5.2 Major Ionic Constituents of Groundwater in the Study Areas

The statistical summary of the geochemical parameters as well as isotopic characteristics (deuterium, deuterium excess and oxygen 18) of groundwater in Abeokuta and Ikorodu areas are presented in Tables 4.8 and 4.9 respectively. The summary includes minimum, maximum, mean, 1st quartile, 3rd quartile, standard deviation and coefficient of variation. The statistical distribution of the major cations and anions in the study areas is as shown in Fig. 4.51a and b while the average concentration and the ionic variation of individual samples in meq/l (Schoeller diagram) are presented in Fig 4.52a and b.

In Abeokuta area, sodium is the most abundant cation in groundwater constituting between 3.2 mg/l and 121 mg/l with a mean value of 42.3±27.31 mg/l. The coefficient of variation is relatively high at 65% though this is not unexpected because of the varieties of the underlying bedrock. Sodium constitutes more than 30% of the total cations in over 91% of the analysed water samples, with the lowest percentage being 14.7%. Potassium, on the other hand, varies from 1.20 to 121 mg/l with a mean of 14.73±22.4 mg/l and a very high coefficient of variation of 152%. Similarly, in Ikorodu area, sodium is the most abundant cation with a concentration of between 1.5 mg/l and 138 mg/l and a mean of 21±28.3 mg/l and having a coefficient of variation of 140%. This indicates that there is a wide variation in the occurrence of sodium in the area. It constitutes greater than 30% of the total cations in over 92% of the water samples, with the lowest percentage of sodium being 13%. The range for Na^+ in shallow wells and borehole (Table 4.10) in the area are 3.2-138 mg/l and 1.5-40.9 mg/l respectively. Concentration of sodium in the groundwater from shallow well and borehole in Ikorodu area averages 42.4±40.9 mg/l and 10.6±9.8 mg/l respectively. The higher concentration of Na in the shallow hand dug wells can be attributed to the impact of the Lagos lagoon on the shallow aquifer adjacent to the Lagoon.

Potassium (on the other hand) in the groundwater from Ikorodu area, varies from 0.2 to 72.9 mg/l with a mean value of 8.1±12.6 mg/l with a coefficient of variation of 160%. Potassium has a mean concentration of 16.4±18.7 mg/l for the borehole samples while the average in the shallow wells is 4.1±5.1 mg/l.

Jointly, the alkali metals constitute greater than 50% in more than 70% of the water samples in Abeokuta area with the alkali earths being dominant in about 30% of the groundwater. In Ikorodu area, the alkali metals constitute greater than 50% in more than 92%

Table 4.8: Statistical summary of the hydrochemical parameters of groundwater in Abeokuta area

	Parameters	Min	Max	Mean	1st quartile	3 rd Quartile	SD	CV
Major ions and elements (mg/l)	Ca^{2+} (mg/l)	0.1	83.8	31.57	16.6	42.3	21.6	68
	Mg^{2+} (mg/l)	0.8	19.8	7.46	3.2	11.15	5.27	71
	K^{+} (mg/l)	1.2	126	14.73	3.25	16.85	22.44	152
	Na^{+} (mg/l)	3.2	121	42.26	23.45	52.9	27.31	65
	Cl^{-} (mg/l)	9.1	222	70.52	47	88.75	40.31	57
	HCO_3^{-} (mg/l)	34.3	369.8	169.81	93.4	253.5	91.23	54
	SO_4^{2-} (mg/l)	1.19	82.3	23.94	7.75	34.75	21.91	92
	NO_3 (mg/l)	0.8	60.8	17.14	3.5	24.5	15.66	91
Trace Elements and Heavy Metals	Fe (mg/l)	0.01	4.79	0.64	0.07	0.45	1.26	196
	Si (mg/l)	4.8	46.4	15.6	8.8	17.3	9.92	64
	Al (mg/l)	0.1	4.1	0.69	0.2	0.9	1.01	146
	Mn (mg/l)	0.01	0.77	0.12	0.02	0.1	0.17	148
	S (mg/l)	2	29	8.95	3	14	7.48	84
	Ba (ug/l)	20	2040	191.04	75	205	296.21	155
	Cu (ug/l)	2	78	16.3	6	22	16.68	102
	Sr (ug/l)	30	590	199.38	80	320	146.67	74
	Zn (ug/l)	6	1000	97.5	23	96	162.84	167
	As (ug/l)	30	30	30				
	Bi (ug/l)	40	60	50			14	28
	Cd (ug/l)	3	19	10.1	4	17	6.49	64
	Co (ug/l)	2	10	4.7	3.5	6	2.5	52
	Cu (ug/l)	2	78	16.61	6	22	16.72	101
	Mo (ug/l)	6	10	8.3			2.1	25
	Ni (ug/l)	6	6	6			0	
	P (mg/l)	0.02	1.62	0.23	0.04	0.39	0.32	141
	Pb (ug/l)	10	20	14	10	20	5.5	39
	Sb (ug/l)	10	10	10	10	10	0	
	S (ug/l)	2	29	8.95	3	14	7.48	84
	Se (ug/l)	20	20	20				
	Sn (ug/l)	30	60	45			21	47
	Sr (ug/l)	30	590	199	80	320	147	74
	Te (ug/l)	10	30	20	18	23	7.1	35
	Ti (ug/l)	10	180	50.6	15	55	55.9	110
	Tl (ug/l)	20	100	60			57	94
	U (mg/l)	0.06	0.19	0.12	0.08	0.17	0.05	4
	V (ug/l)	10	20	15			7.1	47
	W (ug/l)	10	20	16	10	20	5.5	34
	Y (ug/l)	10	30	16	10	20	6.5	4
	Zn (ug/l)	6	1000	97.5	23	96	162.8	167
	F	0.1	1.5	0.554	0.195	0.695	0.461	83
	NO_2 (as N)	0.09	0.09	0.09				
	Br	0.04	0.31	0.163	0.1	0.2	0.0817	50

Table 4.8: Statistical summary of the hydrochemical parameters of groundwater in Abeokuta area (contd)

	Parameters	Min	Max	Mean	1st quartile	3 rd Quartile	SD	CV
isotopes	Oxygen 18	-2.61	-2.22	-2.5	-2.58	-2.42	0.13	5
	deut. Excess	9.64	10.42	10	9.78	10.24	0.28	3
	deuterium	-11.08	-7.56	-10	-10.51	-9.76	1.05	10

Table 4:9: Statistical summary of the hydrochemical parameters of groundwater in Ikorodu area

Parameters		Min	Max	Mean	1st quartile	3 rd Quartile	SD	CV
Major Constituents (>1mg/l)	Ca (mg/l)	0.2	34.2	8.3	2.3	11.4	7.9	100
	Mg (mg/l)	0.1	20.9	2.9	0.5	3.7	4.2	140
	K (mg/l)	0.2	72.9	8.1	0.6	11.4	12.6	160
	Na (mg/l)	1.5	138	20.8	3.8	23.7	28.3	140
	Cl (mg/l)	3.2	194	25.3	5.4	30.9	37.5	150
	HCO_3 (mg/l)	2.4	212.1	46.8	14	69.8	48.9	100
	SO_4 (mg/l)	0.1	80.6	9.4	0.7	9	16.9	180
	Mn (mg/l)	0	0.8	0.1	0	0.2	0.2	150
	Fe (mg/l)	0	2.2	0.2	0.1	0.2	0.4	170
	Al (mg/l)	0.1	1.4	0.4	0.2	0.4	0.3	90
	Si (mg/l)	3.1	30.8	8.2	4.7	9.6	6.3	80
	NO_3 (mg/l)	0	45.8	8.1	0.3	15.1	11.3	140
Trace Elements and Heavy Metals	Ba (ug/l)	4.2	1020	181	32.5	117.5	288.5	160
	Be (ug/l)	2	3.2	2.6			0.8	30
	Cd (ug/l)	2	5	4	3	5	1.4	40
	Ce (ug/l)	120	120	120				
	Co (ug/l)	2	62.2	11.7	2.5	20.1	15.9	140
	Cu (ug/l)	2	58	15.7	6	20	15.1	100
	Ni (ug/l)	6	12	9			4.2	50
	P (mg/l)	0	0.1	0	0	0	0	30
	Pb (ug/l)	10	110	60			70.7	120
	Sb (ug/l)	10	10	10				
	S (mg/l)	1	28	8.2	3	11	8.6	100
	Sr (ug/l)	10	350	99	30	165	100	100
	Ti (ug/l)	40	40	40				
	Y (ug/l)	10	60	26.7			28.9	1.1
	Zn (ug/l)	8.2	271.8	66.5	25	85	60.5	0.9
	F (mg/l)		0.1	0	0	0.1	0	0.8
	NO2 (mg/l)		0.1	0	0	0.1	0	0.9
	Br (mg/l)		0.5	0.1	0	0.1	0.1	100
	PO_4 (as P)		0.2	0.1	0	0.1	0.1	90
Isotopes	O18	-3.29	-2.46	-2.86	-3.07	-2.625	0.28	9
	D-Excess	5.64	7.80	6.82	6.37	7.29	0.69	10
	Deuterium	-18.49	-14.01	-16.09	-17.51	-14.54	1.63	10

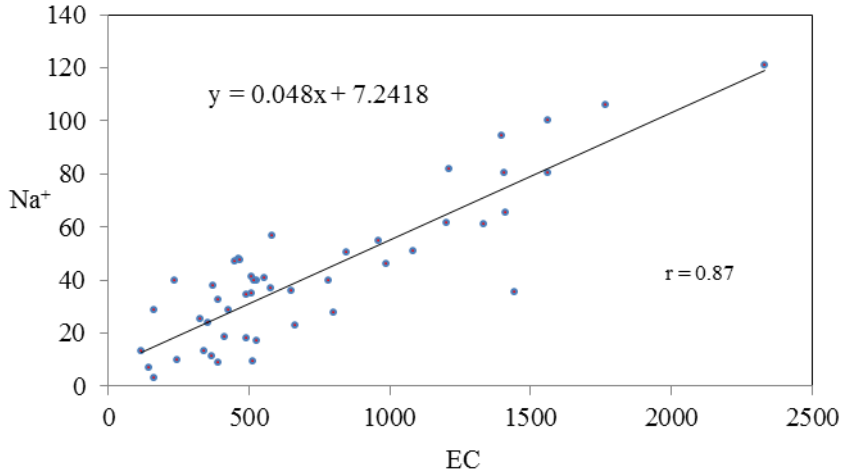

a

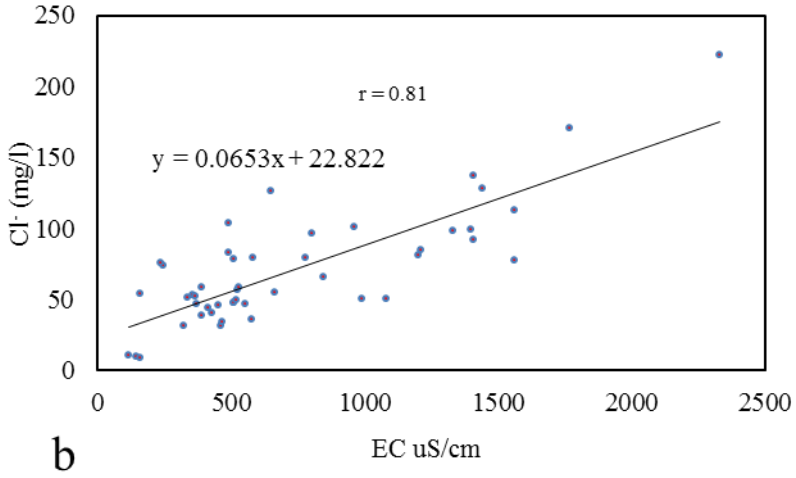

b

Fig. 4.49: Cross Plot of EC and (a) Na^{+}; (b) Cl^{-} in the groundwater of Abeokuta

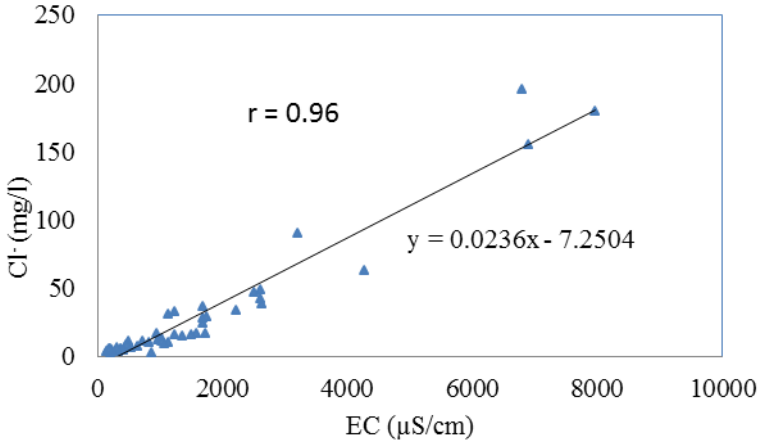

(a)

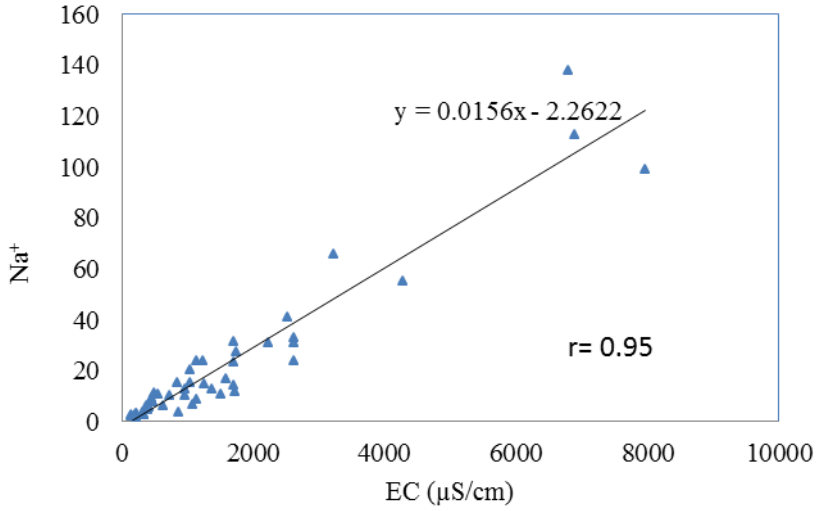

(b)

Fig. 4.50: Cross plot of EC and (a) Na^+; (b) Cl^- in groundwater of Ikorodu

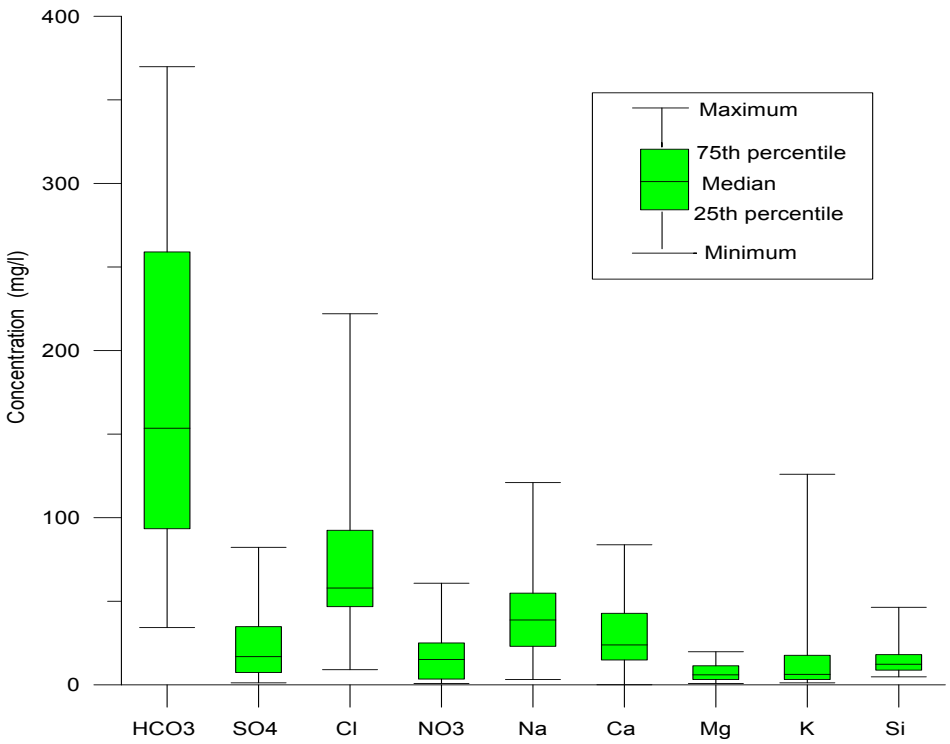

(a)

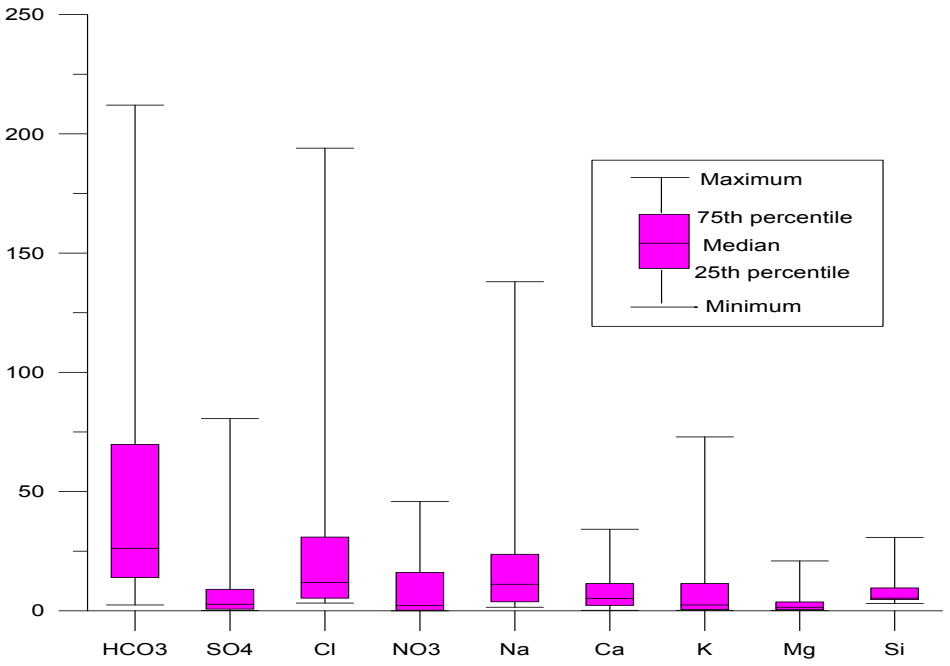

(b)

Fig.4.51: Box-plot of Concentration of selected elements in the groundwater of (a) Abeokuta area. (b) Ikorodu area

Table 4.10: Comparison of the groundwater constituents of borehole and shallow wells samples in Ikorodu area

	Shallow Wells					Borehole				
	Min	Max	Mean	Standard deviation	Coefficient of variation	Min	Max	Mean	Standard deviation	Coefficient of variation
TDS	30.15	1090.52	419.41	337.76	0.81	22.00	405.29	122.50	99.09	0.81
EC	220.07	7960.80	2925.6	2356.20	0.81	149.60	2516.86	786.81	628.99	0.80
Hardness	5.00	134.00	46.02	41.17	0.89	1.60	63.90	19.95	17.90	0.90
pH	4.84	8.03	6.76	1.00	0.15	4.20	7.80	6.51	0.87	0.13
Ca	0.59	34.20	13.47	10.10	0.75	0.20	19.60	5.88	5.27	0.90
Mg	0.25	20.90	5.59	6.35	1.14	0.10	5.40	1.65	1.70	1.03
K	0.55	72.90	16.42	18.69	1.14	0.20	15.31	4.12	5.07	1.23
Na	3.16	138.00	42.35	40.92	0.97	1.50	40.94	10.60	9.75	0.92
Cl	9.90	194.00	55.35	54.51	0.98	3.23	46.40	11.22	9.76	0.87
SO_4	3.00	80.60	23.73	24.32	1.02	0.14	16.40	2.72	3.42	1.26
HCO_3	7.00	212.05	65.33	68.09	1.04	2.44	124.34	38.06	34.67	0.91
NO_3	0.08	45.80	11.80	13.70	1.16	0.02	26.00	5.06	6.98	1.38
Mn	0.01	0.79	0.16	0.21	1.32	0.01	0.63	0.12	0.19	1.60
Ba	20.00	1020.00	267.86	328.36	1.23	20.00	1020.00	153.08	264.18	1.73
Al	0.10	1.40	0.41	0.38	0.94	0.10	1.00	0.27	0.22	0.82
Si	3.10	26.90	10.41	6.26	0.60	3.60	30.80	7.19	5.90	0.82
Co	2.00	62.23	14.59	18.98	1.30	2.00	26.00	7.14	8.65	1.21
Fe	0.05	2.17	0.52	0.59	1.13	0.02	0.36	0.09	0.08	0.88
Cu	3.00	38.00	9.13	11.87	1.30	2.00	58.00	17.05	15.38	0.90
P	0.02	0.05	0.03	0.01	0.33	0.02	0.04	0.03	0.01	0.26
S	1.00	28.00	9.80	9.03	0.92	1.00	6.00	2.55	1.37	0.54
Sr	30.00	310.00	121.33	86.92	0.72	10.00	350.00	71.30	75.09	1.05
Zn	8.00	272.00	55.63	62.63	1.13	12.00	245.00	73.76	54.70	0.74
F	0.01	0.12	0.04	0.04	1.04	0.01	0.06	0.03	0.02	0.53
Br	0.04	0.45	0.12	0.12	0.96	0.03	0.11	0.06	0.02	0.43
			n = 16					n = 34		

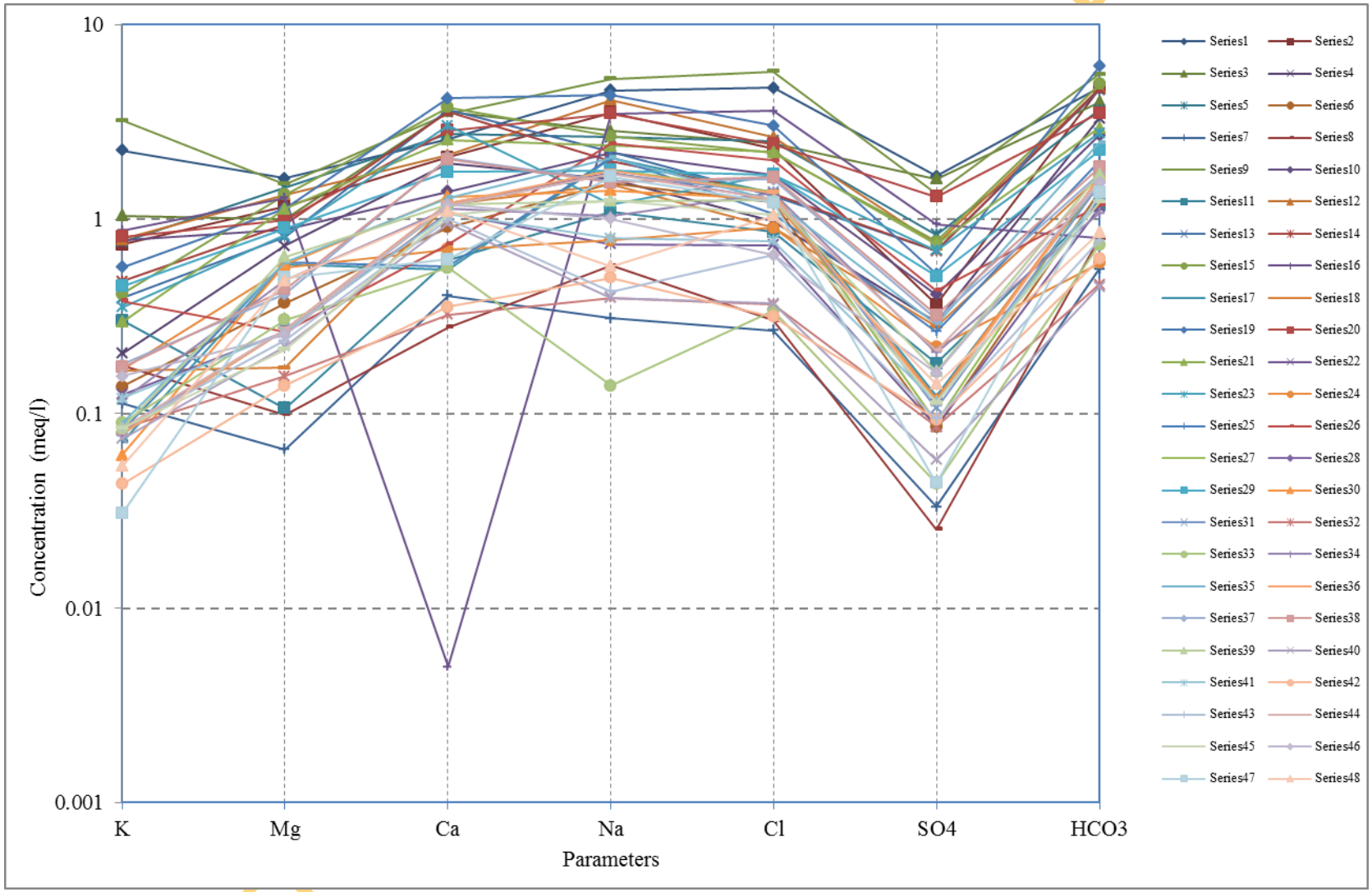

Fig.4.52a: Schoeller diagram of groundwater in Abeokuta area

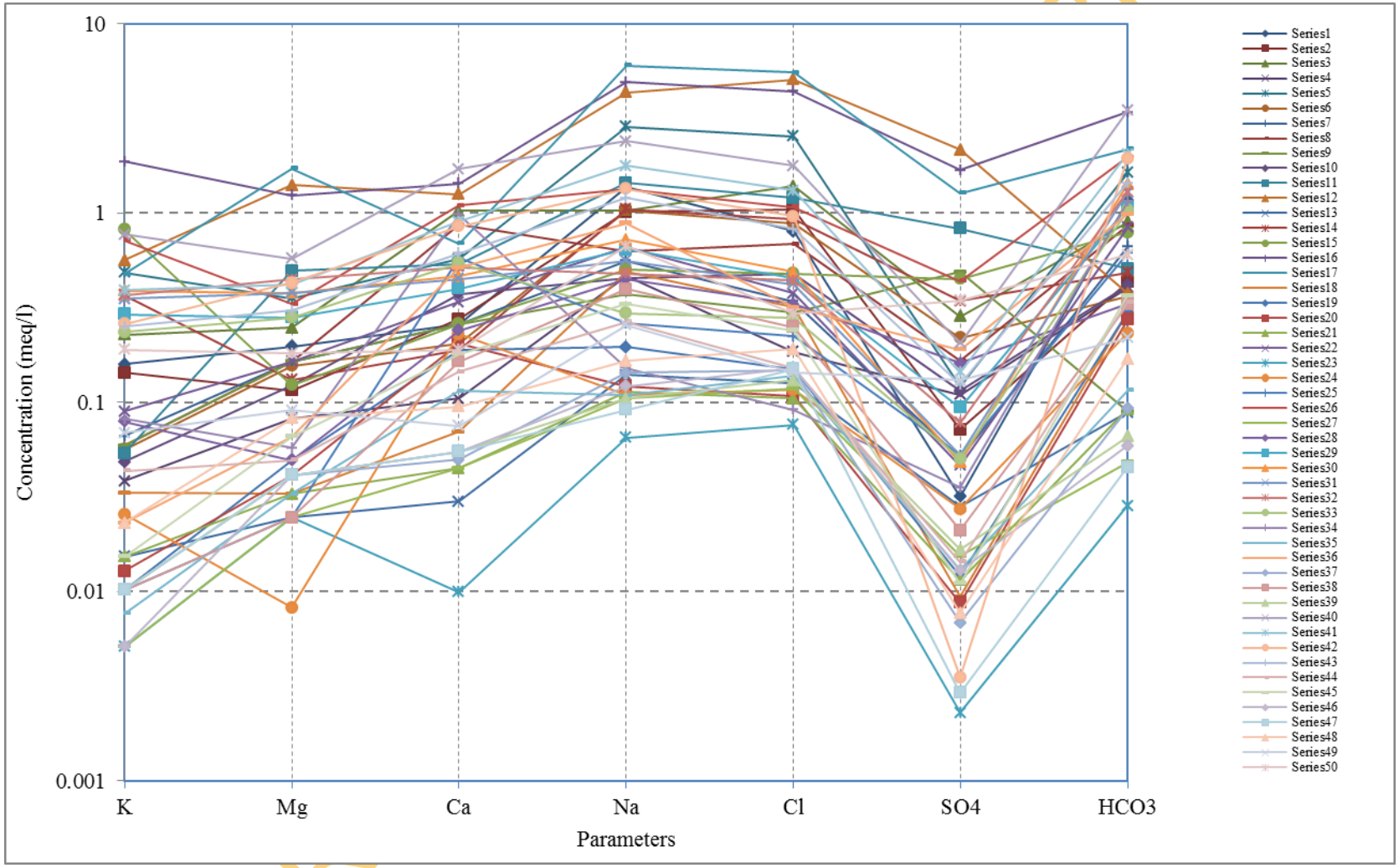

Fig.4.52b: Schoeller diagram of groundwater in Ikorodu area

of the water samples. In Abeokuta area, the alkali earths are important constituents of the minerals (hornblende, feldspar, and biotite) in the underlying rocks unlike Ikorodu area where the aquifer is essentially made of silica and feldspar fragments and as groundwater travels along its flow path from recharge area to discharge area, the chemistry changes gradually and tends towards NaCl water. Furthermore, the lagoon affects groundwater composition due to low elevation of many areas around the lagoon which make them susceptible to flooding during heavy storm.

For the alkali-earth metals in Abeokuta area, the concentration of calcium varies from 0.10 to 83.8 mg/l and averages 31.6±21.6 mg/l while magnesium averages 7.5±5.27 mg/l and varies from 0.8 to 19.8 mg/l. A relatively high coefficient of variation of 68% and 71% were obtained respectively for calcium and magnesium. In Ikorodu area, calcium is the most dominant alkali-earth metals, with a concentration of 0.2 -34.2 mg/l and averages 8.3±7.9mg/l and a coefficient of variation of 100%. It is less than 30% in more than 78% of the samples analysed while magnesium averages 2.9±4.2 mg/l, varies from 0.1 to 20.9 mg/l and coefficient of variation of 140%.

The order of cationic abundance based on the average (Fig 4.51a) and individual (Schoeller, 1959) samples (Fig 4.52a), in Abeokuta area is Na >K >Ca>Mg while in Ikorodu area it is Na >Ca>K >Mg (Fig.4.51b and Fig. 4.52b).

As shown in Table 4.1, sodium oxide is the second most abundant oxide in the rocks underlying Abeokuta area after potassium. The abundance of sodium ion relative to potassium in the groundwater of the area agrees with Milliot (1970) finding that during rock weathering and mineral dissolution, sodium dominates in natural solutions because it is more mobile than potassium. Hence, sodium is dominant over potassium in the groundwater of the area as a result of the higher mobility of Na^+ (2.40) in comparison to that of potassium (1.25). On the other hand, magnesium has a low mobility of 1.30 and constitutes the least oxides in the rocks underlying the study area; therefore, its low concentration in underlying rocks is largely responsible for its low occurrence compared with the other major cations in the groundwater samples.

In Abeokuta area, strong correlation exists among sodium on one hand and potassium, magnesium, chloride, sulphate and bicarbonate on the other hand with correlation coefficients of 0.78, 0.83, 0.69, 0.64 and 0.62 respectively. The cross plots of major cations and TDS (Fig 4.53) in the area show strong correlations between TDS and Na^+ (r=0.87), TDS and K^+ (r= 0.82), TDS and Ca (r=0.82) and lastly TDS and Mg^{2+} (r=0.85). These values of regression

coefficients clearly indicate the magnitude of the contributions of these components to the overall mineralization.

A comparison of the contribution of alkali metals and that of alkali-earth metals to mineralization as shown in the Figs 4.54a & b revealed that the alkali metals jointly have stronger correlation of 0.90 compared with 0.80 for alkali-earth metals. This invariably indicates that the alkali metals are the most important contributor to the total mineralization in Abeokuta area. This may largely be due to concentration of alkali metal relative to alkali-earth metal in the weathering products of the underlying bedrock in the area.

The cross plots of TDS and the major cations of groundwater in Ikorodu area (Fig. 4.55) show strong correlations with Na^{+}, K^{+}, Ca^{2+} and Mg^{2+} with coefficients of regression of 0.96, 0.77, 0.78, and 0.95 respectively. The alkali metals contribution to that of alkali-earth metals as shown in the Fig. 4.56 reveal that the alkali jointly have stronger correlation of 0.97 compared with 0.92 for alkali-earth metals. Similarly, as observed in the groundwater of Abeokuta area, the alkali metals are the most important contributor to the total mineralization in Ikorodu area. This is not unexpected in sedimentary area, especially close to the coast as groundwater gradually assumes the composition of sodium chloride. This is because alkaline earth carbonate type water occurs in the primary stage of evolution, while sodium chloride type occurs in the final stage of groundwater evolution (Tijani, 1994).

Comparatively, individually and on the average, the concentration of cations in groundwater from Abeokuta area is generally higher than that of Ikorodu area, thus the groundwater in Ikorodu is less mineralised compared with the groundwater from the weathered aquifer in Abeokuta area. In addition, there is a higher variation in the major ionic constituents in the groundwater of Ikorodu area than in the groundwater of Abeokuta area. The higher concentration of the cations in Abeokuta area is largely due to the fact that the weathering product of the underlying rocks in Abeokuta area is rich in these ions which are important constituents of the minerals (plagioclase and alkali felsdar, biotite, hornblende) in the rocks.
The variation in the chemistry of groundwater in Abeokuta is lower than that of Ikorodu because the underlying rocks are mineralogically and chemically similar, though texturally different. The large variation in groundwater chemistry in Ikorodu is largely related to the influence of the Lagos lagoon on the groundwater in areas close to the lagoon.

Bicarbonate is the most dominant anion in the groundwater of Abeokuta area, and it varies from 27.4-374.18 mg/l and averages 169.8±91.2 mg/l. There is a high variation of bicarbonate in the area as shown by the coefficient of variation of 54%. Bicarbonate constitutes

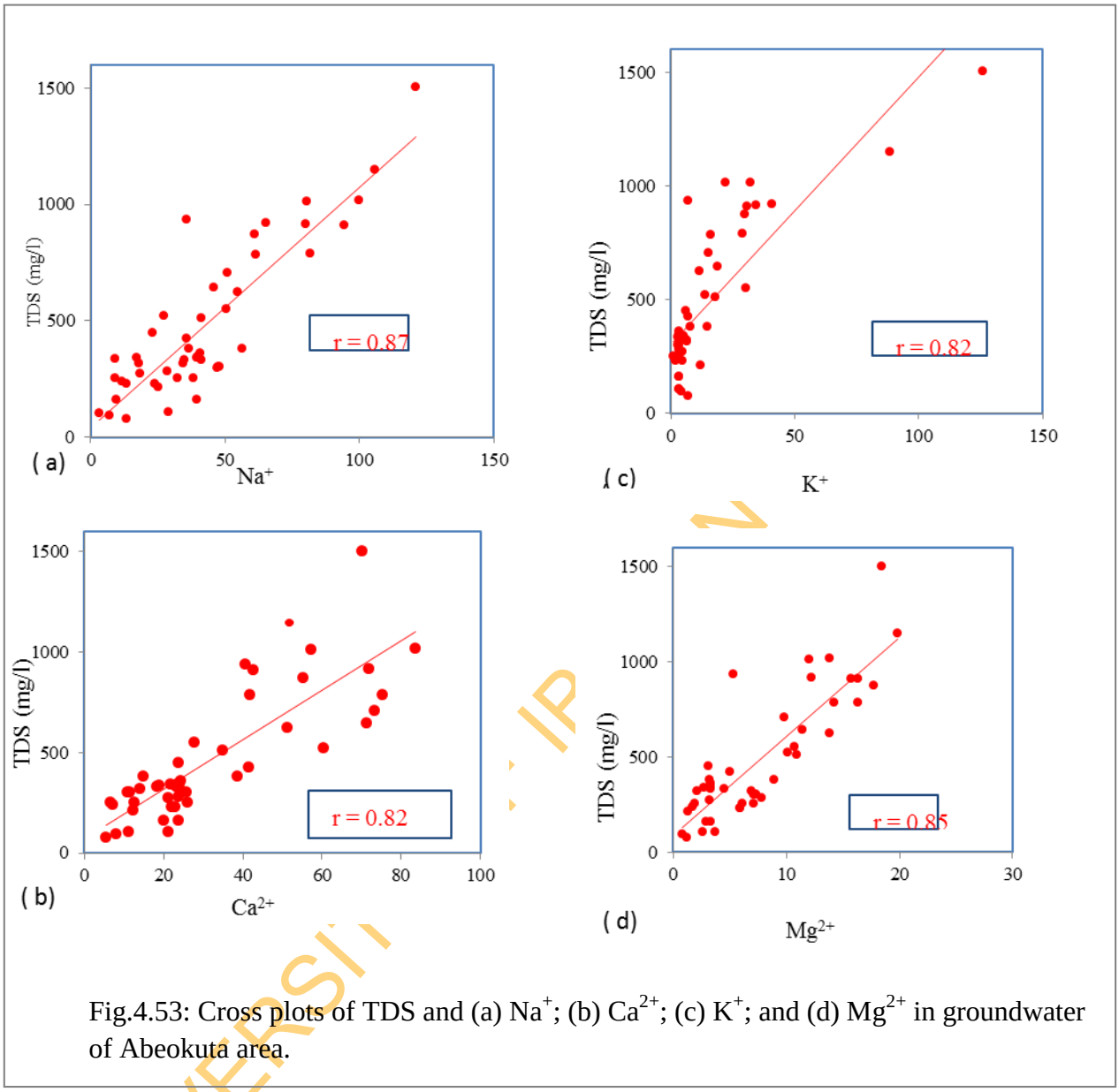

Fig.4.53: Cross plots of TDS and (a) Na^{+}; (b) Ca^{2+}; (c) K^{+}; and (d) Mg^{2+} in groundwater of Abeokuta area.

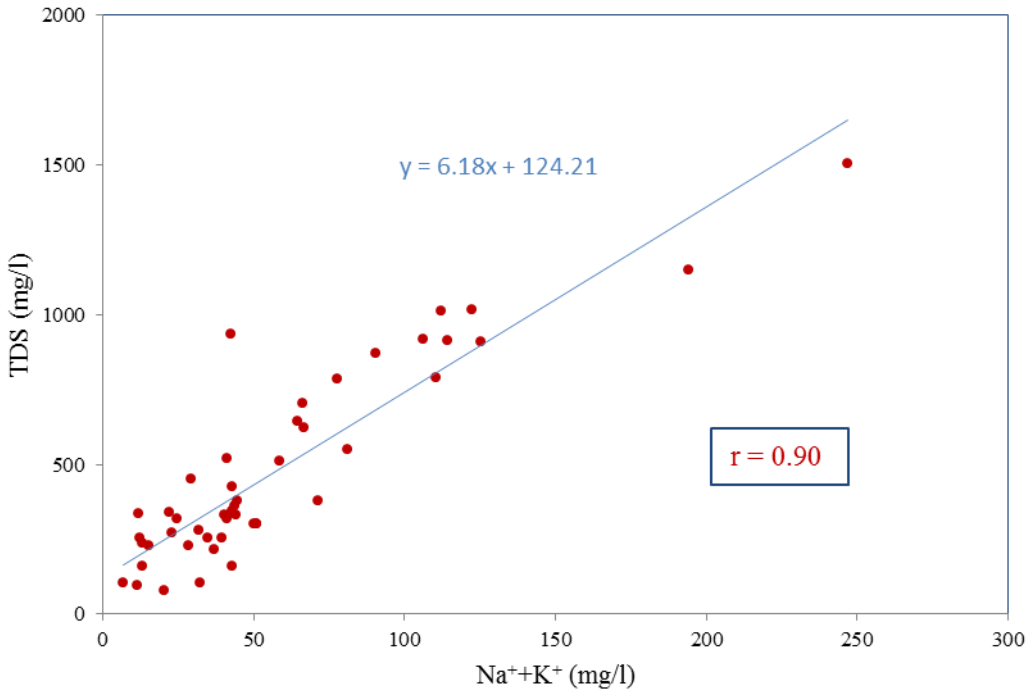

(a)

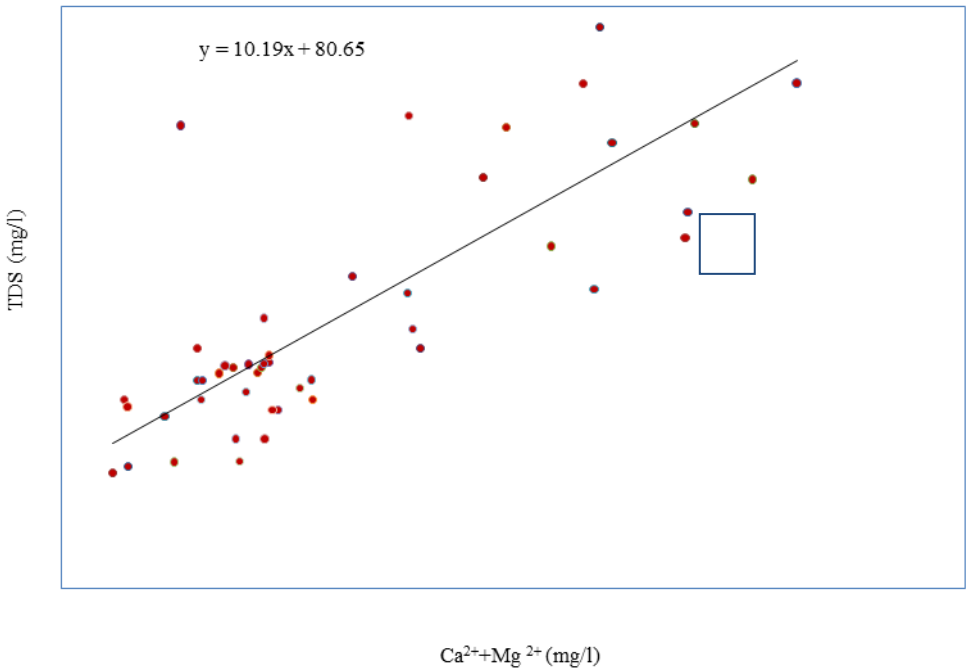

Fig 4.54: Cross plot of TDS against (a) $Na^{+}+K^{+}$ and (b) $Ca^{2+}+Mg^{2+}$ in groundwater of Abeokuta.

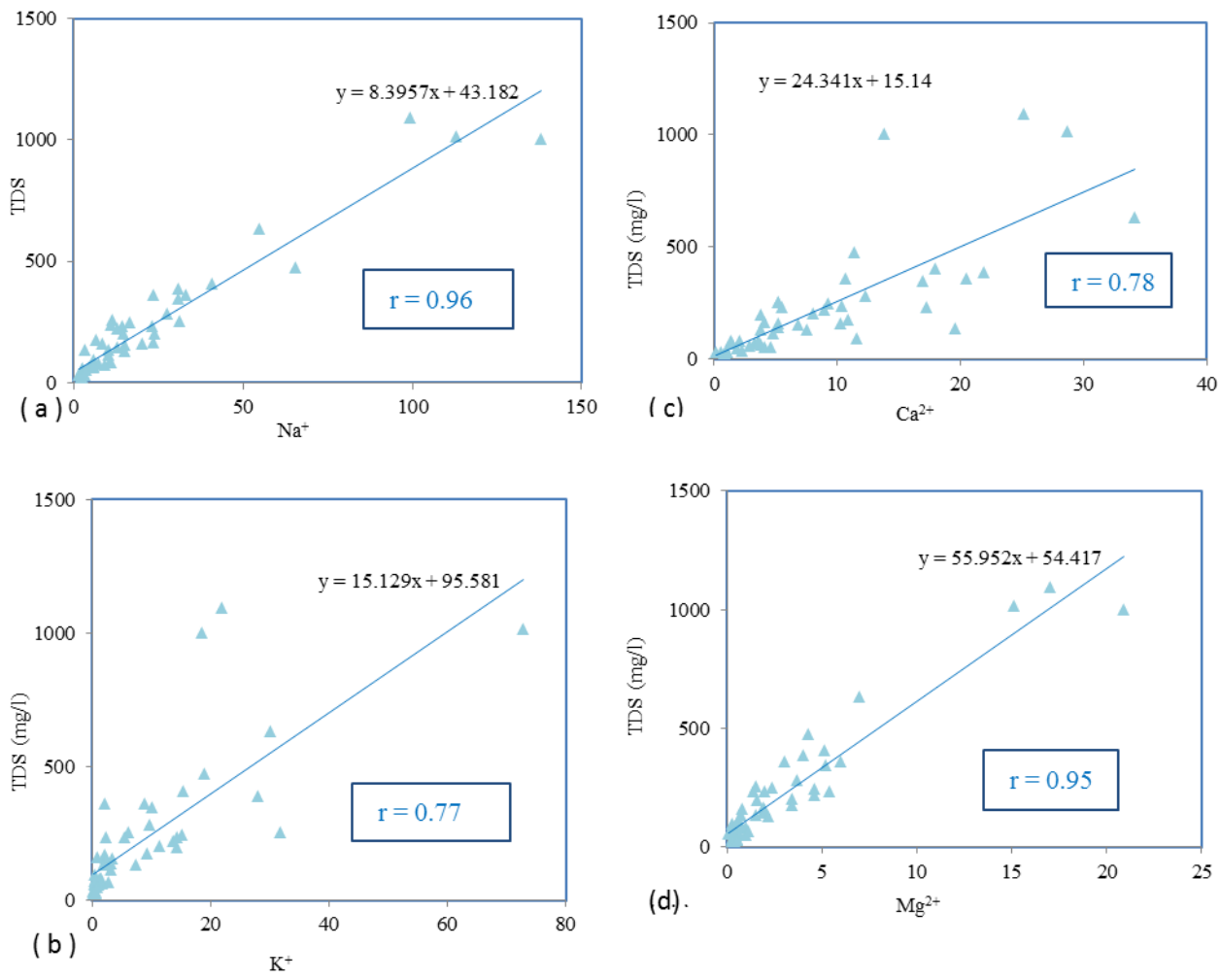

Fig 4.55: Cross plot between TDS and and (a) Na^{+}; (b) K^{+}; (c) Ca^{2+} ; (d) Mg^{2+} in the groundwater of Ikorodu

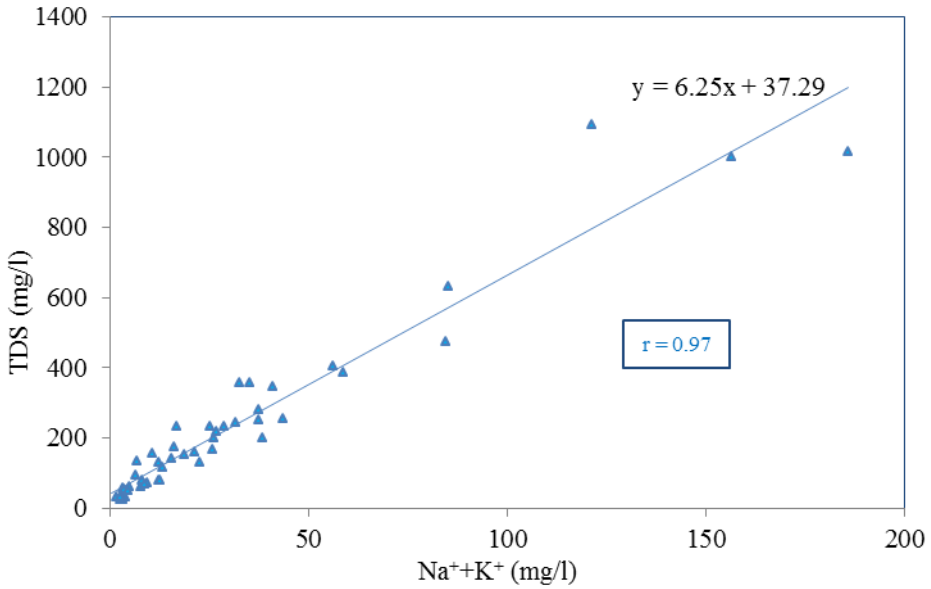

(a)

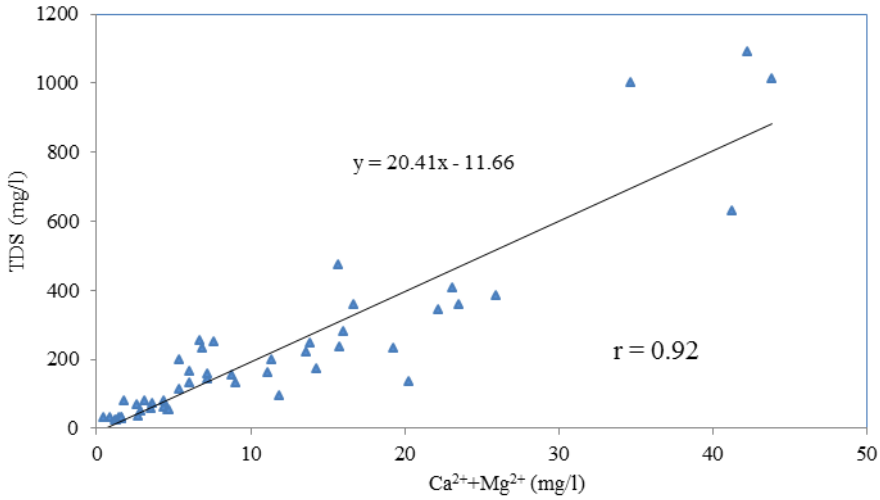

(b)

Fig 4.56: Cross plot between TDS and (a) $Na^{+}+K^{+}$ and (b) $Ca^{2+}+Mg^{2+}$ in groundwater of Ikorodu

more than 40% in over 97% of the water samples, except location 16 where it constitutes about 22%. This location has the least calcium concentration (0.1 mg/l) and high Cl^-. The source of bicarbonate in this type of aquifer without primary carbonate is carbon dioxide gas in atmospheric air and soil vapour as well as low concentration of carbonate minerals present as weathering products (Williams, 1997). In Ikorodu area, bicarbonate, the most dominant anion in the groundwater sampled varies from 1.73-212.1 mg/l and averages 46.8±48.9 mg/l with a coefficient of variation of 100%. Bicarbonate constitutes more than 60% in about 50% of the analysed water samples. These are groundwater samples dominated by HCO_3^- and are mostly found in the landward area from boreholes/deep-wells (with the exception of a few samples). There is a gradual transition from bicarbonate dominated groundwater to chloride dominated groundwater as the water flows towards the coast in the area.

Concentration of chloride in groundwater from Abeokuta area varies from 9.5- 204.2 mg/l with a mean of 70.5±40.3 mg/l and coefficient of variation of 57%. Approximately 44% of the groundwater analysed contain ≥ 30% chloride concentration while the sample with least chloride concentration contains about 12% chloride. Interestingly, the maximum chloride concentration was obtained where the maximum nitrate (60.5 mg/l) was obtained and in most places where nitrate concentration is greater than 30 mg/l concentration of chloride exceeds 100 mg/l. Chloride varies from 2.7 to 195.8 mg/l and the mean concentration is 25.3±37.5 mg/l with a coefficient of variation of 150% in Ikorodu. The variation of Cl in Ikorodu is largely due to the distinct range of chloride for groundwater from shallow wells around the lagoon and those from boreholes. Approximately, 44% of the groundwater samples contain ≥ 30% chloride. The level of chloride in groundwater in Ikorodu area showed a particular variation trend such that relatively small concentration occurs in landward locations while high chloride concentrations were obtained from groundwater sampled in areas adjacent to the lagoon (coast). In Ikorodu area, the concentration of chloride in landward locations range from 3.2 to 15.9 mg/l while the range in the area close to the lagoon is 6.46-194 mg/l (area less than 1 km to the lagoon).

Studies have shown that high concentration of chloride in groundwater, especially in areas contiguous to the sea is usually indicative of seawater encroachment. Lusczynski and Swarzenski (1966) suggested that 50 mg/l of chloride in groundwater in Long Island, USA is indicative of saltwater encroachment. Similarly, Amadi et al (1989) considered chloride contents of greater than 50 mg/l to be indicative of saltwater contamination in the Niger

Delta, Nigeria. On the other hand Trembley et al (1973) stated that chloride concentrations greater than 40 mg/l are indicative of saltwater contamination in Summerside area of Prince Edward Island.

The chloride in the groundwater of most of the locations contiguous to the lagoon is greater than 40mg/l, suggesting seawater encroachment into the groundwater of the coastal areas of Ikorodu. The encroachment of lagoon water in the coastal area is largely due to the low elevation and the proximity of the locations to the Lagos lagoon, as results of the geophysical survey did not indicate that the area is affected by saline water intrusion. Most of the areas around the coast with high chloride are enriched in Mg^{2+} relative to Ca^{2+} when compared with landward areas. Tripathy and Panigrahy (1999) citing Davis and DeWeist (1966) noted that an increase in Mg^{2+} values towards the coast similarly indicates of saltwater encroachment. This is however limited to areas with very low elevation athat are very close to the coast.

Concentration of sulphate in groundwater from Abeokuta area is the least among the major anions, with an average concentration of 23.9±21.9 mg/l and concentration range of 1.2 to 79.8 mg/l. The coefficient of variation of 92% for sulphate suggests that it is the most widely varied of all the major ions in the groundwater of Abeokuta area. This further indicates anthropogenic influence on groundwater chemistry in the area. It is generally less than 10% in 77% of the water samples and the highest occurrence was approximately 20% at the location (16) with the lowest bicarbonate and calcium occurrence. In Ikorodu, sulphate has the least concentration among the major anions; with average concentration of 9.4±16.9 mg/l, concentration range of 0.11 to 103.5 mg/l, with a coefficient of variation of 180%. It is generally less than 20% in 86% of the water samples and the highest occurrence was approximately 59% at the location 50 with the least bicarbonate occurrence. However, when the molar concentration was considered, HCO_3^- and Cl^- have approximately almost equal concentration in order of abundance in Ikorodu area.

Summarily, the order of abundance of the anions in Abeokuta area is HCO_3>Cl>SO_4 (Fig. 4.51a and and Fig 4.52a) while the order is is Cl > HCO_3>SO_4 as shown in Fig. 4.51b and Fig 4.52b in Ikorodu area.

The major anions have strong positive correlation with TDS (Fig. 4.57), having regression coefficients of 0.81, 0.89 and 0.86 respectively for HCO_3^-, Cl^- and SO_4^{2-} in Abeokuta area. Similarly, cross plots of TDS and major anions in Ikorodu area indicate strong positive correlations (Fig. 4.58), having regression coefficients of 0.71, 0.96 and 0.86 respectively for HCO_3^-, Cl^- and SO_4^{2-}.

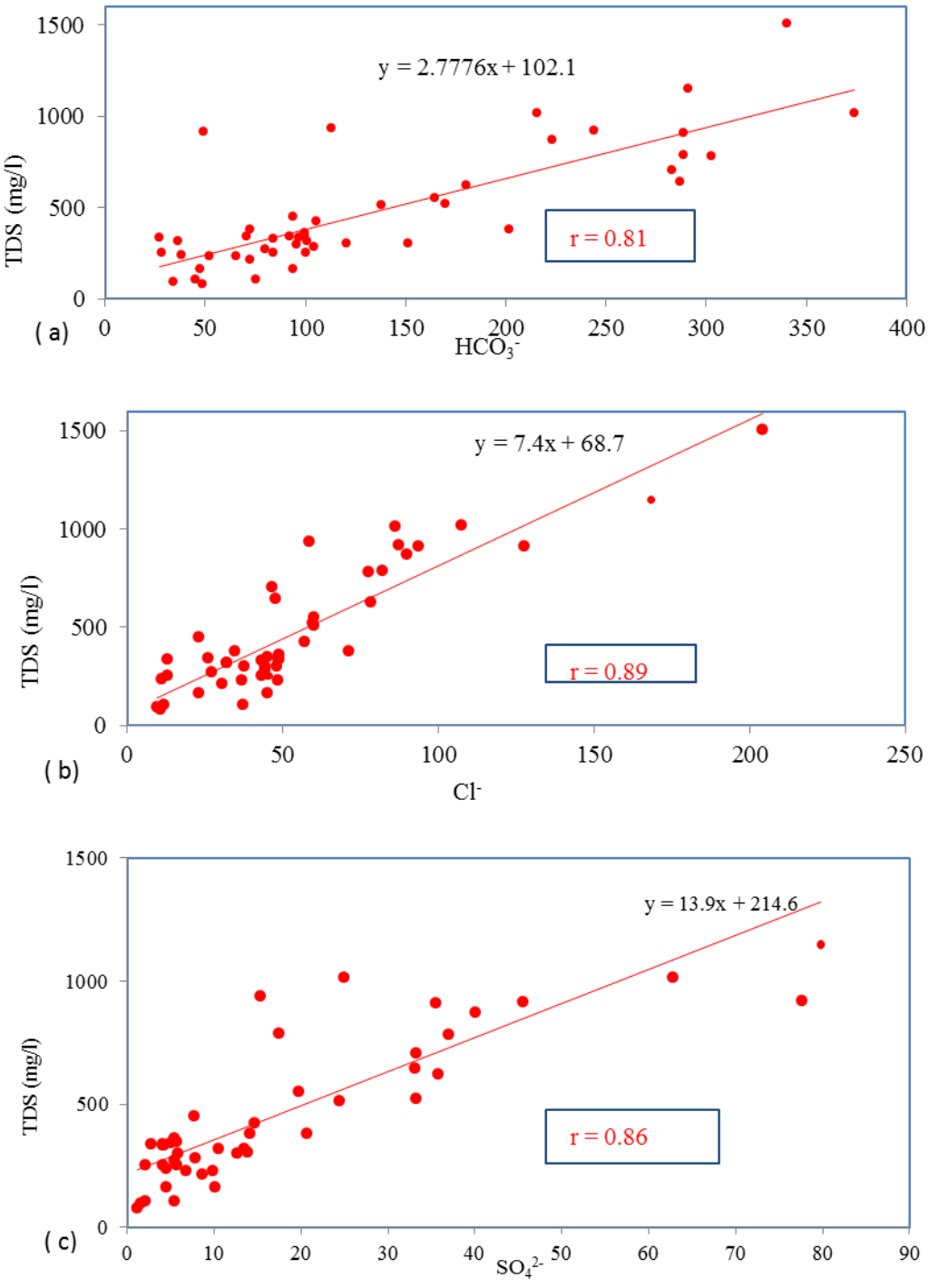

Fig. 4.57: Cross plots of TDS and (a) HCO_3^- (b) Cl^- and (c) SO_4^{2-} in groundwater of Abeokuta

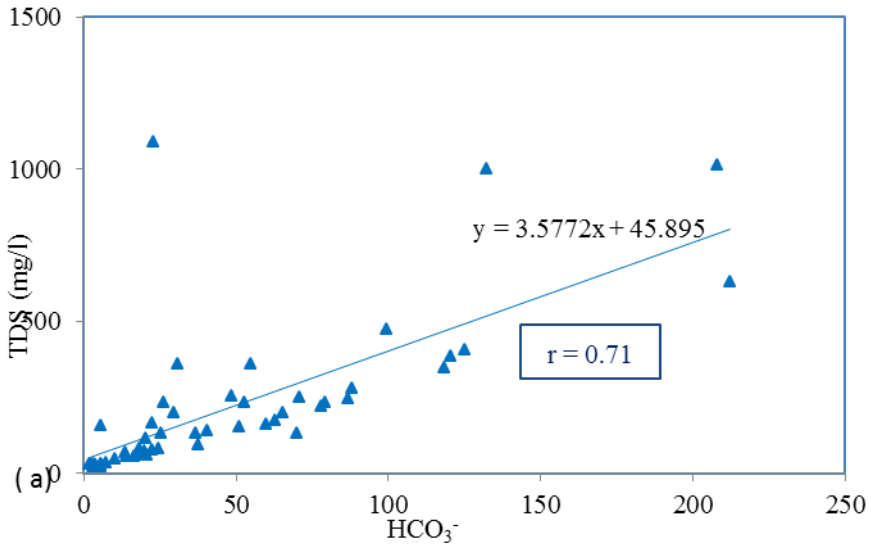

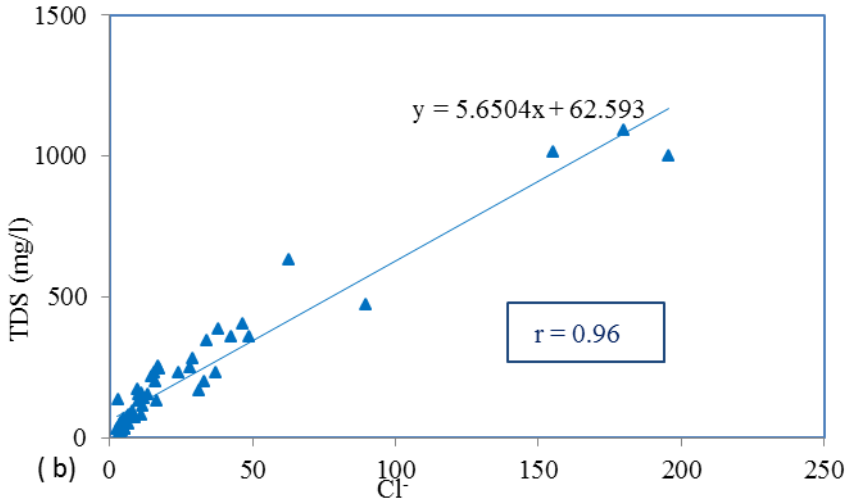

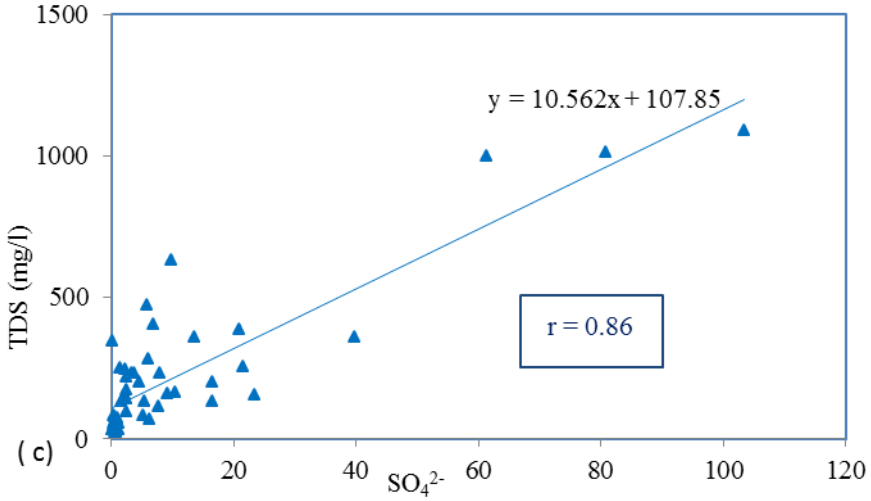

Fig. 4.58: Cross Plot between TDS and (a) HCO_3^-; (b) Cl^- and (c) SO_4^{2-} in Ikorodu area.

Assessment of the impact of the lagoon on groundwater chemistry in area contiguous to the lagoon in Ikorodu area (coastal plain sands and the alluvium) was made using the ionic ratio of the major cations to plot the Schoeller diagrams (Singhal and Guptal, 1999) of groundwater from shallow wells adjacent to the lagoon (Fig. 4.59). This was compared with the ionic ratio of some major ions of average seawater concentration quoted by Tijani et al (2005). Most of the landward samples show distinct ionic ratio from the seawater average ionic ratio, hence the area is not affected by seawater. However, some of the shallow well samples especially those that are very close to the lagoon (e.g locations 11, 12, L17), have similar character with the seawater average, although the ratio of most of the ions in those groundwater samples is greater than that of the seawater, thus indicating little impact of the Lagos lagoon on groundwater samples from some of the shallow wells.

4.5.3 Nitrate in the Groundwater of the Study Areas

The concentration of nitrate in the groundwater of Abeokuta area varies from 0.8 mg/l to 60.8 mg/l. The nitrate concentration averages 17.4 ± 15.7 mg/l and has a high coefficient of variation of 91%. The concentration of nitrate in the groundwater of Ikorodu area varies from 0.1 mg/l to 45.8 mg/l, with a mean of 8.1±11.3 mg/l and has a coefficient variation of 140%. It varies from 0.02 to 26.0 mg/l and 0.08 to 45.8 mg/l respectively in the groundwater from boreholes and shallow-wells in the area. It averages 5.1±7.0 and 11.8±13.7 in the groundwater from boreholes and shallow wells respectively in Ikorodu area.

Tijani and Abimbola (2003) noted that the sources of nitrate in groundwater include natural sources, waste materials, and irrigated agricultural practises (Keeney, 1989 cited in Canter, 1996). Nitrate contributed from natural sources in groundwater is usually less than 10 mg/l and concentration above this value suggests the additional contribution of nitrate through anthropogenic sources (Hernandez-Garcia and Custodio, 2004 citing Custodio and Liamas, 1983). However, evapo-concentration of rainwater may produce up to 30 mg/l+ of nitrate in groundwater (Hernandez-Garcia and Custodio, 2004). The mean concentration of nitrate in the Abeokuta area suggests the contribution of nitrate through anthropogenic sources in some locations. These sources include septic tanks, poor drainages and pit latrines.

Generally, nitrate in the groundwater of Ikorodu is low when compared with the groundwater from the shallow weathered aquifer of Abeokuta area. However, in many places the nitrate is above the concentration of nitrate from natural sources (10 mg/l) in

groundwater as stated by Hernandez-Garcia and Custodio, (2004) citing Custodio and Liamas (1983). This implies the possible influence of anthropogenic contribution in Ikorodu area. Although, evapo-concentration of rainwater may produce up to 30 mg/l of nitrate in groundwater (Hernandez-Garcia and Custodio, 2004), a few locations contain nitrate greater than 30 mg/l, thus confirming anthropogenic influence in a few places (4%). While no relationship exists between nitrate and either static water level or total well depth in Abeokuta area, the strong inverse correlation of -0.58 and -0.55 between nitrate & total well depth and nitates & static water level respectively in Fig. 4.47, indicate that nitrate concentration in the shallow wells is partly related to surface (anthropogenic) sources in Ikorodu area.

Cross plots of nitrate in groundwater from Abeokuta area (Fig. 4.60) show strong positive correlations with TDS, bicarbonate and chloride, with coefficients of correlation of 0.63, 0.53 and 0.68 respectively in the area. Relatively strong correlation coefficients in Abeokuta (Figs 4.61) between Na^+ and NO_3^- (0.49), K^+ and NO_3^- (0.47) Mg^{2+} and NO_3^- (0.46), and SO_4^{2-} and NO_3^- (0.51) implies additional contribution of these other ions through anthropogenic sources in the area. Relating the nitrate concentration with the sanitary level of the environment revealed that high nitrate concentration were obtained mostly in wells sited around tombs, gutters and waste dumps whereas lower nitrate concentration is associated with clean environs. The contribution of nitrate to mineralization in Ikorodu area is highlighted by the strong positive correlation (Fig 4.62) established between nitrate and TDS (0.79). Similarly in Ikorodu area, cross plots between NO_3^- and HCO_3^-, NO_3^- and Cl^-, NO_3^- and SO_4^{2-}, in Ikorodu (Fig 4.62) show very strong correlation coefficients of 0.92, 0.64, and 0.50 respectively. Na^+, Ca^{2+}, Mg^{2+} and K^+ all show strong positive correlation of 0.77, 0.67 and 0.74 respectively with nitrate.

The relatively high regression coefficients between nitrate and other major cations and anions may be largely due to anthropogenic influence on groundwater chemistry in Abeokuta area. As noted by Piskin (1973) and Ritters & Chimside (1984), cited in Tijani et al (2002), correlation coefficient > 0.35 between NO_3^- and Cl^- suggests the effect of municipal waste. Hence, the relatively high correlation between NO_3 and Cl (Fig 4.60b) in Abeokuta area indicates significant anthropogenic influence on groundwater chemistry. This invariably indicates the influence of domestic waste on groundwater in the area. Similarly, correlation coefficient of 0.64 between nitrate and chloride in Ikorodu displayed in Fig 4.62 further indicates the 'additional'' ionic contribution through anthropogenic sources (Tijani et al, 2002). Few locations where NO_3^- is above 10mg/l are mostly associated with relatively

high chloride concentration but are localised and mainly associated with the shallow hand-dug wells close to the lagoon.

Elevated Cl^- concentration in the groundwater sampled in Abeokuta area is frequently associated with higher NO_3^-, thus suggesting a similar or related anthropogenic source. NO_3^- concentration greater than the WHO (2006) guideline of 45mg/l was observed in only three samples, namely locations 9, 19 and 20. Hence, nitrate pollution is a localized event rather than a regional pollution. The mean concentration of NO_3^- is generally above the threshold for natural sources of nitrate in few parts of the study area. This further confirms the anthropogenic contribution of nitrate, which may likely be attributed to infiltration of water contaminated by livestock in close proximity to the wells and other activities within the community. The high correlation between TDS and NO_3^- in Abeokuta indicates significant contribution of dissolved constituents to groundwater chemistry from localized anthropogenic sources (such as agricultural seepages, household contaminants). The relative contribution by anthropogenic and geogenic factors were evaluated using coefficient of variation (Table 4.11). In the groundwater of Abeokuta, SO_4^{2-}, NO_3^-, Cl^- and HCO_3^- have higher coefficient of variations than the cations (except K), indicating stronger anthropogenic influence than geogenic influence. This is because the cations are important constituent of underlying rocks and commonly released into groundwater through mineral dissolution. Whereas high coefficients of variation of NO_3^-, SO_4^{2-} and Cl suggests variations in the anthropogenic contributions of these ions as NO_3^- is largely contributed through decaying of plant and animal material, lifestock wates and leakages from sewage systems.. Additional Cl^- is contributed through sewage and refuse leachates while SO_4^{2-} is additionally contributed to groundwater through decomposition of organic matter. In the groundwater of Ikorodu, the impact of the Lagos lagoon on groundwater chemistry is responsible for the high coefficients of variation of the ions, especially the high CV of SO_4^{2-} and Cl^-, Mg^{2+} and K^+, as these ions are significantly high in groundwater samples in areas contiguous to the Lagos lagoon.

4.5.4 Fluoride in Groundwater of the Study Areas

Fluoride is an important minor constituent of groundwater in many places in the world, but notably in Asia and Africa (Appelo and Postma, 2005). Fluoride is basically brought into groundwater by leaching of minerals in the rocks (Handa, 1975; Jacks et al., 1993; Saxena and Ahmed, 2003). Absence and excessive concentration of fluoride may constitute health hazards causing dental fluorosis (tooth mottling) and more seriously,

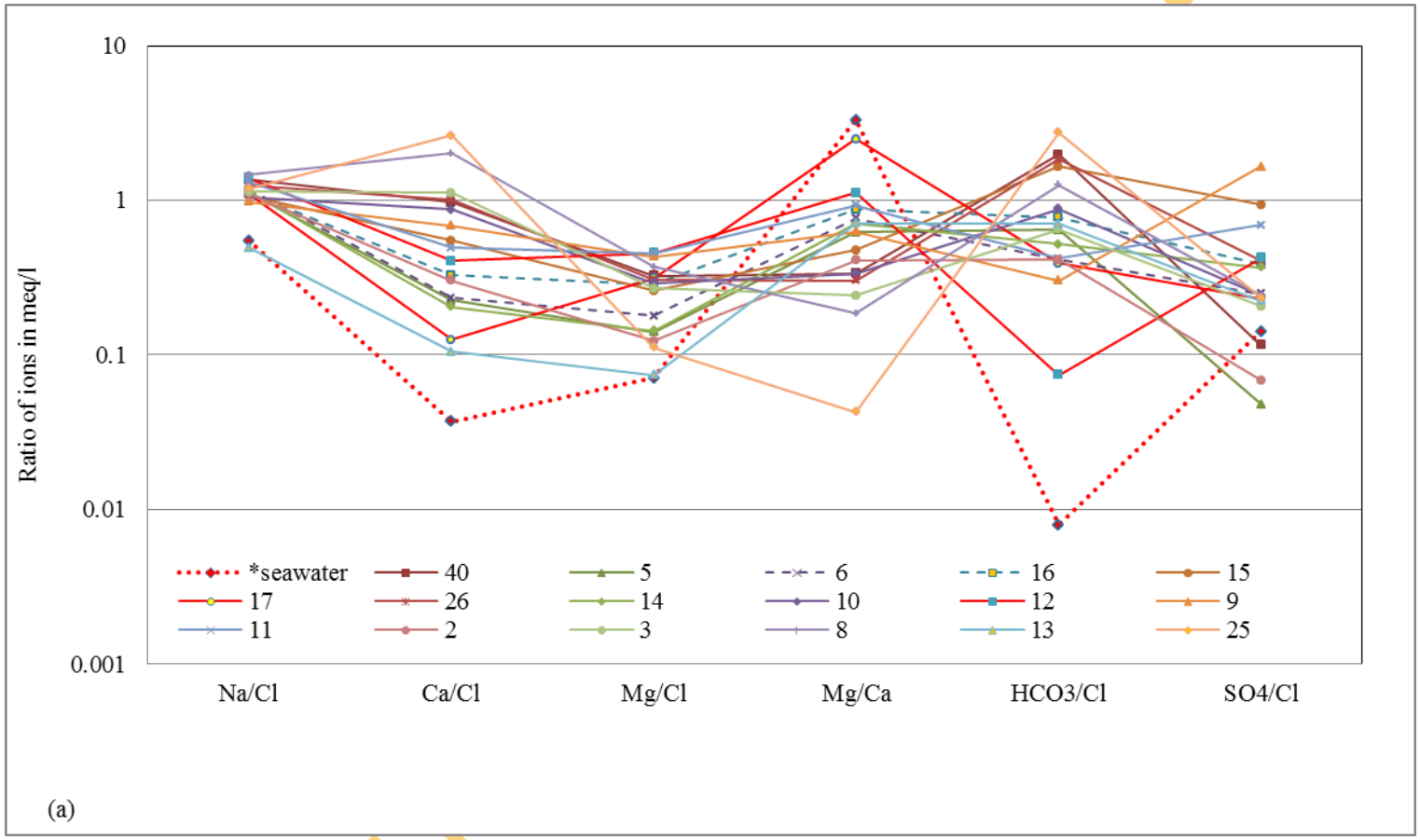

Fig. 4.59a: Schoeller diagram (ionic ratio) of samples from wells in Ikorodu area

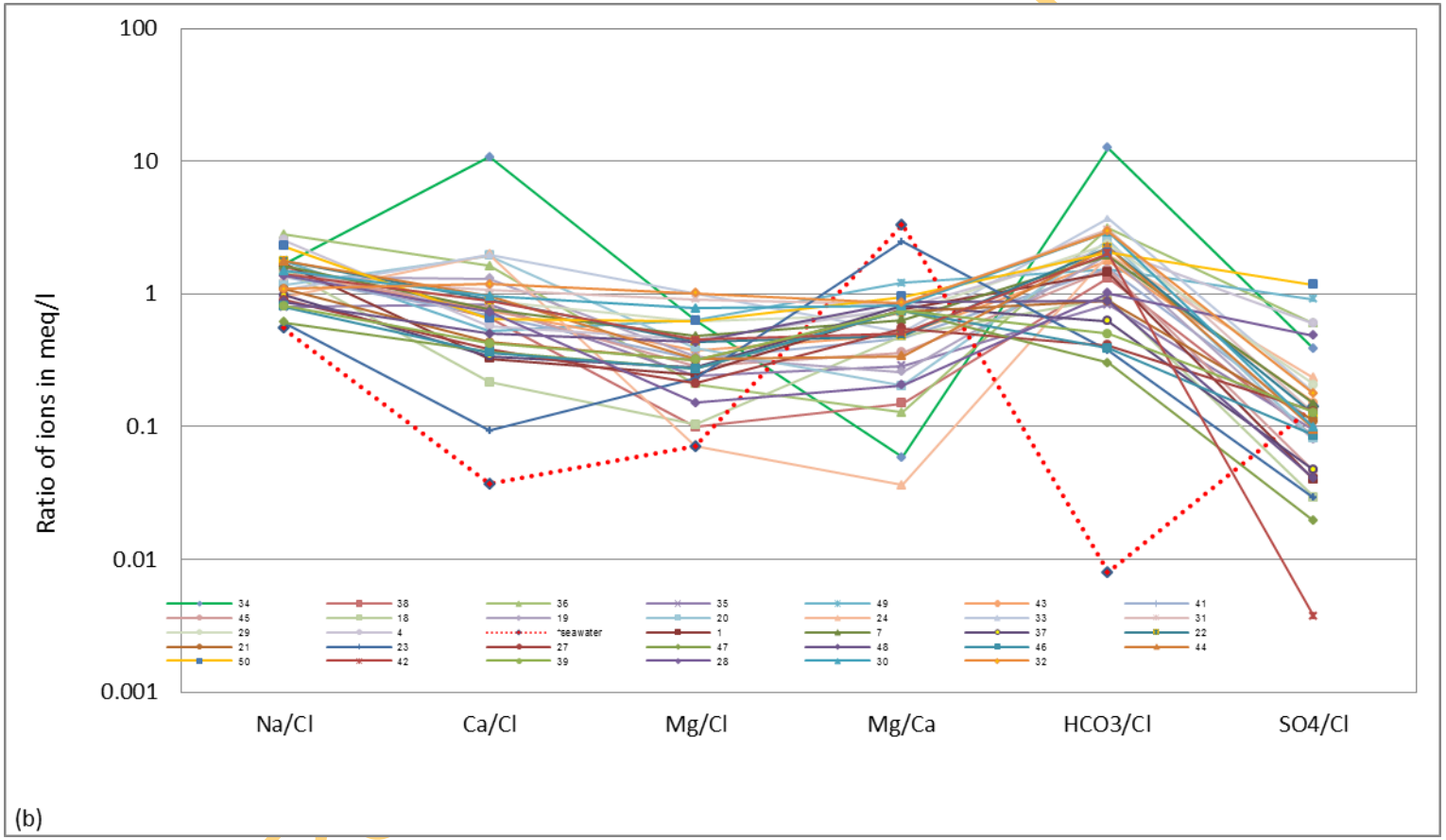

Fig. 4.59b: Schoeller diagram (ionic ratio) of samples from boreholes in Ikorodu area

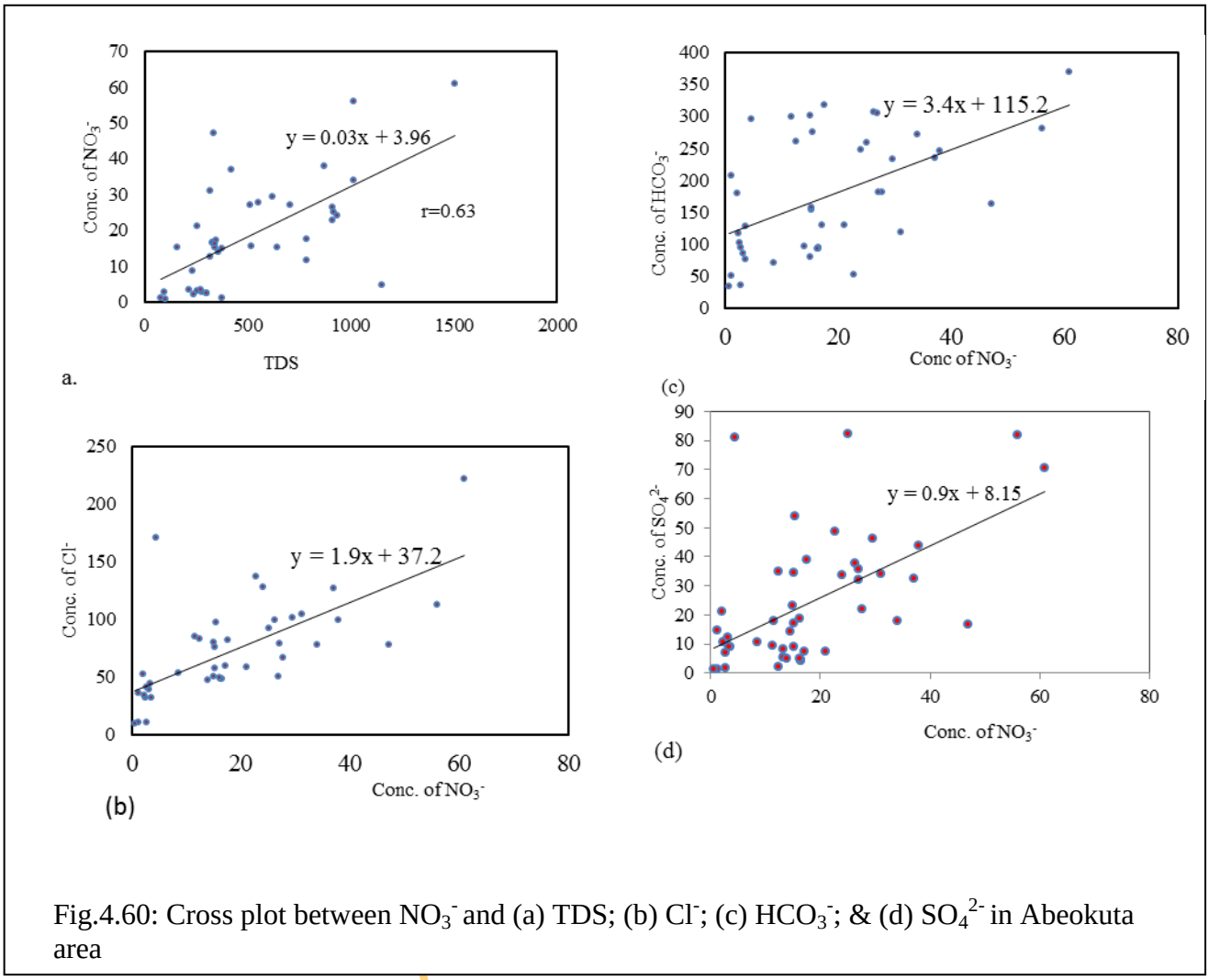

Fig.4.60: Cross plot between NO_3^- and (a) TDS; (b) Cl^-; (c) HCO_3^-; & (d) SO_4^{2-} in Abeokuta area

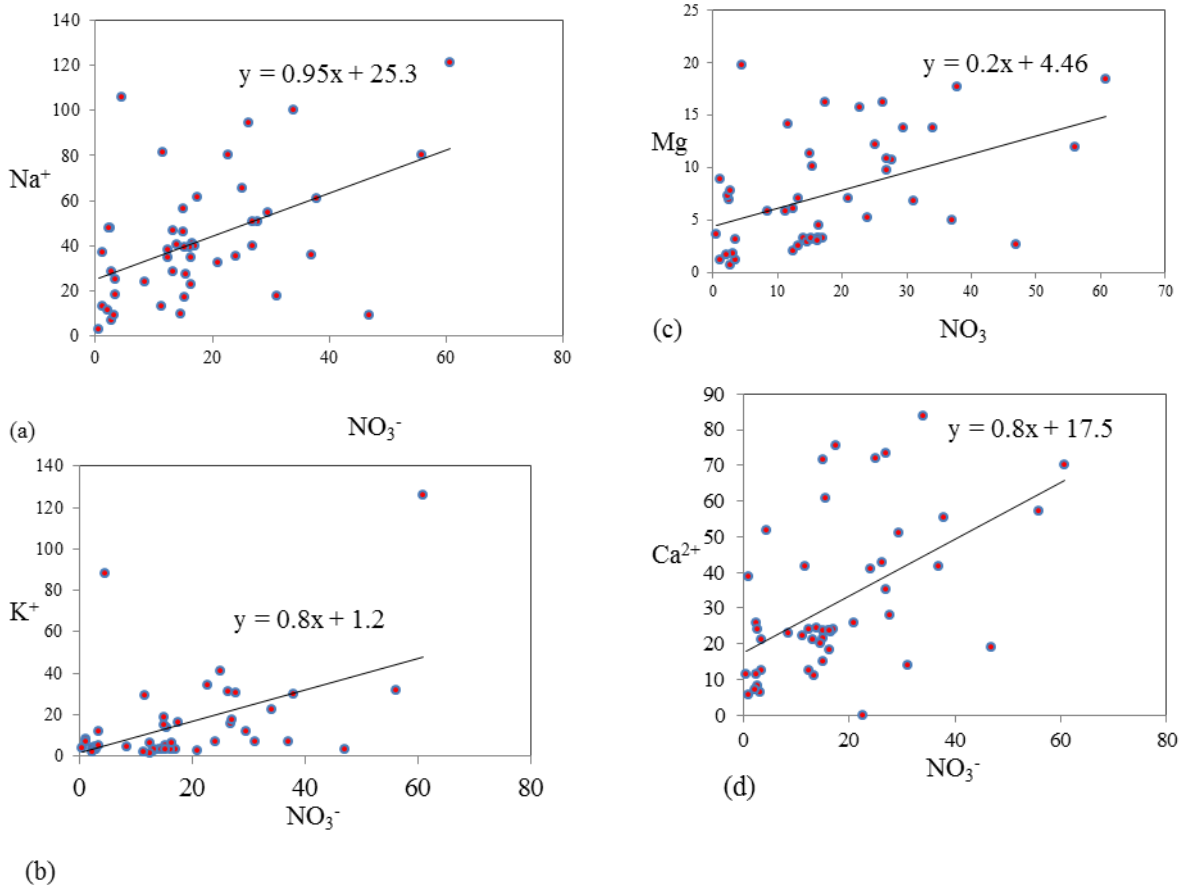

Fig.4.61: Cross plot between NO_3^- and (a) Na^+; (b) K^+ (c) Mg^{2+} and (d) Ca^{2+} in Abeokuta area

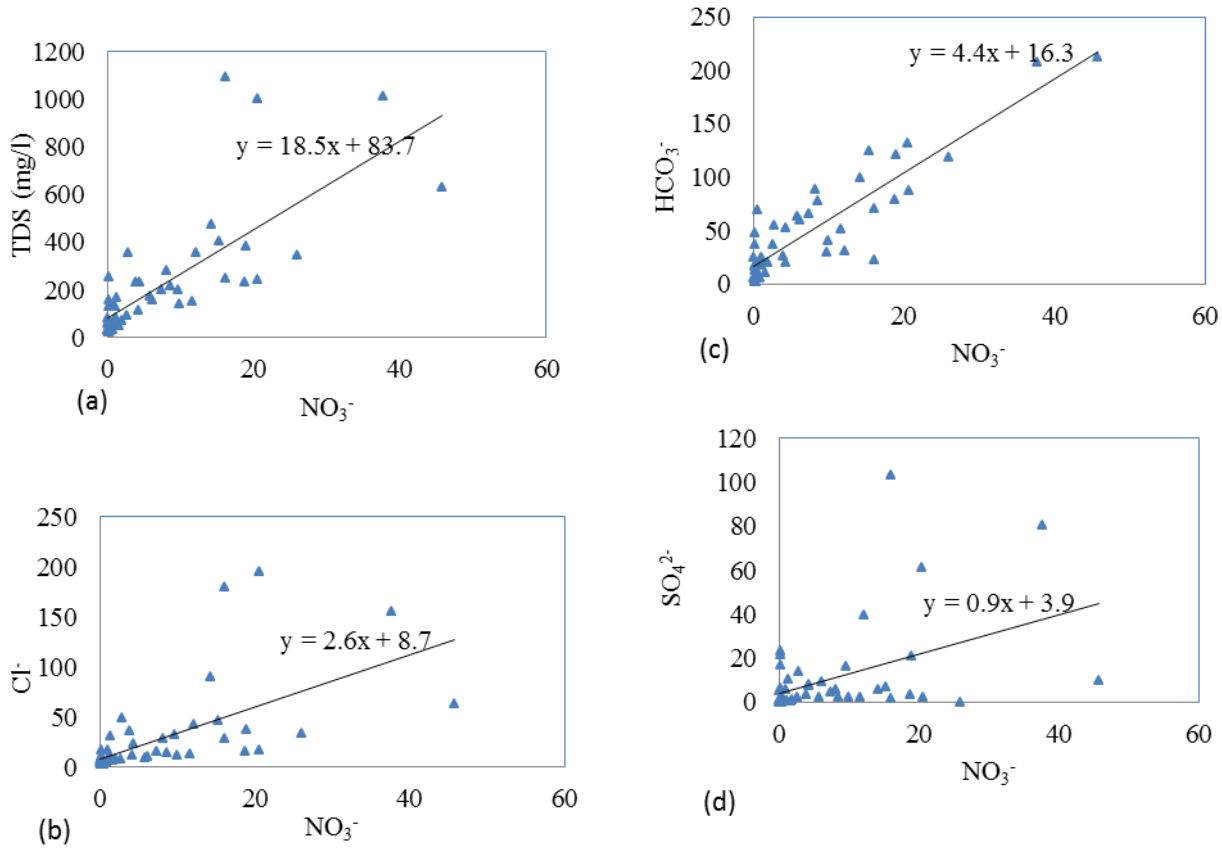

Fig 4.62: Cross plot between NO_3^- and (a) TDS; (b) Cl^-; (c) HCO_3^- & (d) SO_4^{2-} in Ikorodu area.

Table 4.11: Coefficients of the major ions in groundwater of the study area

	Ions	Coefficcient of correlation
Abeokuta	K^+	152.1
	SO_4^{2-}	105.8
	NO_3^-	78.5
	Mg^{2+}	70.6
	Cl^-	70
	HCO_3^-	69.5
	Ca^{2+}	68.4
	Na^+	64.5
Ikorodu	SO_4^{2-}	195
	K^+	155.9
	Cl^-	153.8
	Mg^{2+}	144.3
	NO_3^-	138.8
	Na^+	136.3
	HCO_3^-	102.1
	Ca^{2+}	95.3

Skeletal fluorosis (bone deformation and painful brittle joints in older people (Dissidayanke, 1999; Appelo and Postma, 2005)

Fluoride occurs in the range of between 0.1 and 1.5 mg/l with an average value of 0.55±0.46 mg/l in Abeokuta area, while it varies from 0.01- 0.12 mg/l in Ikorodu area. In the two locations, fluoride occurs below detection limit in large percentage of the groundwater, while in the remaining samples, the groundwater is generally deficient in fluoride. Unlike most other constituents of groundwater which absence in groundwater are not known to have any effect on human health, fluoride is an essential constituent of groundwater which is needed for good health. Excessive concentration of fluoride in groundwater has health implications (Table 4.12).

Although, fluoride concentrations in the two locations are generally within permissible level, there is a general deficiency of fluoride in the groundwater. Deficiency of fluoride in groundwater has serious implication on health, causing limited growth and fertility as well as dental caries (Appelo and Postma, 2005, Dissanayake, 1991).

4.5.5 Heavy Metals and Trace Elements in Groundwater

The heavy metals and trace elements occur in small quantities, mostly less than 1mg/l in the groundwater samples. However, despite their low concentrations in groundwater, studies have shown that regional occurrence of these metals or elements above certain levels may affect groundwater potability and palatability. Deficiencies of some of the heavy metals and trace elements may be harmful to human health e.g. fluoride has been associated with common ailments (Appelo and Postma, 2005, Dissidayanke, 1991).

Heavy metals, non-metals and trace elements constituents in all or some of the analysed groundwater in Abeokuta area include arsenic (As), barium (Ba), bismuth (Bi), cadmium (Cd), copper (Cu) , cobalt (Co), iron (Fe), manganese (Mn), molybdenum (Mo), nickel (Ni), phosphorus (P), lead (Pb), antimony (Sb), sulphur (S), selenium (Se), silicon (Si), tin (Sn), strontium (Sr), tellurium (Te), titanium (Ti), thallium (Tl), uranium (U), vanadium (V), tungsten (W), yttrium (Y) and zinc while beryllium (Be), silver (Ag), cerium (Ce) , chromium (Cr) and lithium (Li) are all below detection limits in the groundwater of Abeokuta Area. In Ikorodu area, heavy metals detected in groundwater include; barium (Ba), cadmium (Cd), copper (Cu), cobalt. (Co), iron (Fe), manganese (Mn), nickel (Ni), phosphorus (P), lead (Pb), antimony (Sb), sulphur (S), silicon (Si), strontium

(Sr), titanium (Ti), yttrium (Y) and zinc. On the other hand, arsenic (As), beryllium (Be), bismuth (Bi), cerium (Ce), chromium (Cr) and lithium (Li), molybdenum (Mo), selenium

Table 4.12: Impact of fluoride in drinking water on health

Concentration of fluoride in (mg/l)	Impact on Health
Nil	limited growth and fertility
0.0-0.5	dental caries
0.5-1.5	promotes dental health
1.5-4.0	dental fluorisis(mottling of teeth)
4.0-10.0	dental and skeletal fluorisis(pain in the back and neck bones)
>10.0	crippling fluorisis

(Dissanayake, 1991 cited in Singhal and Gupta, 1999, p.228)

(Se), silver (Ag), tin (Sn), uranium (U), vanadium (V), tungsten (W), are all below detection limits (Table 5.6b) in the groundwater of the area.

Most of the heavy metals occur in few locations in the groundwater of Abeokuta area (1-15% of the samples) while iron, manganese, silicon, barium, copper, strontium, zinc, cadmium, cobalt, phosphorus, sulphur, titanium and yttrium were found as constituents in between 27 and 100% of groundwater samples. Barium, manganese, silicon, iron, copper, cobalt aluminium, phosphorus, strontium, sulphur and zinc occur in between 36 and 100% of the groundwater samples from Ikorodu area, while the others were detected in less than 10% of the groundwater from the area.

Manganese is distributed mainly as manganese oxides of which pyrolusite (MnO_2) is the most common and occurs as impurities in iron oxides, some silicates as well as carbonates. Mn occurrence in variable oxidation states (usually II and IV but from III to VII) and its ion exchange properties play important roles in trace metals adsorption in soils and aquifers (British geological survey, 2003). Manganese commonly co-exists with Fe in water though usually lower in concentration due to greater crustal abundance of Fe. The upper crust abundance of manganese is about 0.05-0.1% MnO (Taylor and Mclennan, 1985). Mn was found in only 71% of the groundwater samples and it concentration varies between <0.01 to 0.77 mg/l with a mean concentration of 0.12±0.17mg/l and a coefficient of variation of 148% in Abeokuta area. Mn was found at concentrations above the detection limit in about 90% of the analysed water samples from Ikorodu area. In the area, Mn varies between 0.01 to 0.79 mg/l with a mean concentration of 0.12±0.2 mg/l. Mn occurs in both Ikorodu and Abeokuta within similar range and having the same average concentration unlike most other trace constituents of groundwater that are distinctly higher in concentration in Abeokuta than Ikorodu. Unlike Fe, Mn has mean concentrations of 0.12 mg/l in the borehole samples as well as in the shallow wells in Ikorodu area.

In Abeokuta area, Mn shows weak correlations (Table 4.13) though positive with all the major cations and anions with Cl^-, SO_4^{2-}, HCO_3^-, Na^+, K^+, Mg^{2+} and Ca^{2+}. With the exception of Fe (r=0.49). Other trace elements show very weak correlation with Mn. Unlike Abeokuta area, Mn in the groundwater of Ikorodu area shows weak positive correlation (Table 4.14) with the major cations and anions, having correlation coefficients of 0.35, 0.32, 0.35, 0.56, 0.29, 0.21 and 0.50 respectively with Na^+, K^+, Mg^{2+}, Ca^{2+}, Cl^-, SO_4^{2-} and HCO_3^-. It correlated positively though weakly with Si (0.44). However, strong positive correlation (r=0.73) between Mn and Ba (Fig. 4.63a) in Ikorodu area, invariably indicates that Mn has

similar origin with the Ba. This inference is further reinforced by the similarity between the isocone of Mn in Fig. 4.63b and the isocone of Ba in Fig 4.63c, showing distribution of these metals in the area. Similarly, very strong correlation of 0.78 was obtained between Mn and Sr.

Iron (Fe) in groundwater from Abeokuta area is within a range of 0.01 mg/l to 4.79 mg/l and averages 0.64 ± 1.26 mg/l with a coefficient of variation of 196%. In Ikorodu area, Iron (Fe) occurs in the range of 0.02 mg/l to 2.17 mg/l (average; 0.25±0.4 mg/l) and coefficient of variation of 170%. The average concentration of the Fe in the shallow coastal aquifer is 0.54 mg/l compared with 0.08 mg/l in the deep-wells/boreholes.

In Abeokuta area, Fe shows fairly stronger correlation coefficients of 0.51 and 0.66 correspondingly with Na^+ and K^+ compared with 0.13 for Fe^{2+} and Ca^{2+} as well as 0.41 for Fe^{2+} and Mg^{2+} in the area. Poor correlation was obtained between Fe and the major anions, with values of 0.45, 0.33 and 0.27, respectively for Cl^-, sulphate and bicarbonate. In Ikorodu area, it shows fairly strong correlation of 0.65, 0.67, 0.55 and 0.67 respectively with Na^+, Mg^{2+}, SO_4^{2-} and Cl^- while the correlation coefficients of 0.23, 0.16, 0.11 and 0.11 were correspondingly obtained between Fe and Ca^{2+}, K^+, HCO_3^- and NO_3^- respectively. Fe exhibit very weak positive correlation (between 0.08 and 0.20) with Mn, Co, Al, Si and Sr.

Occurrence of Mn and Fe in groundwater is usually closely related because they are both readily available in rock. In addition, the dissolution of both metals is favoured largely by anaerobic condition and acidic to slightly acidic groundwater. Fe and Mn are readily available in the rocks and their weathered products underlying Abeokuta area. Fair positive correlation of 0.49 between Mn and Fe in Abeokuta is an indication of the relationship between the metals in Abeokuta area. However, the occurrences of both iron and manganese in Ikorodu area are not related (r=-0.02). While iron is largely influenced by acidic condition and closeness to the lagoon, Mn concentration in groundwater of Ikorodu area is largely related to a localized source close to the Lagos lagoon (Fig 4.64 and Fig 4.63c). In Ikorodu the acidic to slightly acidic nature of most of the samples from shallow hand-dug wells is largely responsible for higher concentration of Fe at this depth, as the aerobic condition at shallow depth is not favourable to dissolution of Fe and usually higher concentration Fe is expected in deep-wells/ boreholes. However acidic condition can aid Fe dissolution. In addition, as shown in Fig 4.64, the Lagos lagoon has greatly influenced the concentration of iron, especially around the lagoon. In this area, Fe is generally above the threshold of 0.5 mg/l, the maximum level at which groundwater is acceptable for domestic purposes.

Table 4.13: Correlation coefficients of chemical parameters of groundwater in Abeokuta area.

	Na^+	K^+	Ca^{2+}	Mg^{2+}	HCO_3^-	Cl^-	SO_4^{2-}	NO_3^-	Al	Ba	Br	Cd	Co	Cu	F	Fe	Mn	P	Pb	S	Si	Sr	Zn
Na^+	1.00	0.78	0.62	0.83	0.62	0.69	0.64	0.49	0.39	0.11	0.16	0.36	0.31	-0.14	0.42	0.51	0.31	0.69	-0.27	0.75	0.13	0.64	-0.03
K^+	0.78	1.00	0.51	0.72	0.58	0.78	0.72	0.47	0.30	0.08	0.18	0.11	0.12	-0.19	0.17	0.66	0.34	0.78	-0.40	0.78	-0.02	0.57	0.07
Ca^{2+}	0.62	0.51	1.00	0.70	0.86	0.48	0.65	0.51	0.33	0.15	0.04	0.05	0.02	-0.21	0.34	0.13	0.12	0.32	-0.17	0.74	-0.13	0.87	-0.07
Mg^{2+}	0.83	0.72	0.70	1.00	0.67	0.65	0.71	0.46	0.35	0.17	0.05	0.56	0.14	-0.32	0.31	0.41	0.29	0.49	-0.43	0.79	0.16	0.79	-0.10
HCO_3^-	0.62	0.58	0.86	0.67	1.00	0.63	0.72	0.53	0.49	0.13	0.05	0.17	0.24	-0.14	0.48	0.27	0.30	0.53	-0.07	0.72	-0.10	0.81	-0.04
Cl^-	0.69	0.78	0.48	0.65	0.63	1.00	0.80	0.68	0.21	-0.03	0.25	0.31	0.13	-0.01	0.28	0.45	0.19	0.64	-0.46	0.83	-0.15	0.54	-0.06
SO_4^{2-}	0.64	0.72	0.65	0.71	0.72	0.80	1.00	0.57	0.19	0.05	0.13	0.29	0.01	-0.17	0.19	0.33	0.22	0.45	-0.46	0.91	-0.11	0.81	-0.12
NO_3^-	0.49	0.47	0.51	0.46	0.53	0.68	0.57	1.00	0.00	-0.09	0.17	-0.04	0.01	-0.03	0.18	0.07	-0.31	0.48	-0.30	0.50	-0.29	0.44	-0.11
Al	0.39	0.30	0.33	0.35	0.49	0.21	0.19	0.00	1.00	0.61	0.15	0.45	0.93	-0.11	0.40	0.78	0.35	0.32	0.32	0.30	0.32	0.43	0.56
Ba	0.11	0.08	0.15	0.17	0.13	-0.03	0.05	-0.09	0.61	1.00	-0.07	0.40	0.65	-0.14	-0.08	0.47	0.24	-0.08	-0.23	0.04	-0.02	0.26	0.84
Br	0.16	0.18	0.04	0.05	0.05	0.25	0.13	0.17	0.15	-0.07	1.00	0.31	0.13	0.13	0.10	0.06	0.06	0.50	-0.44	0.08	-0.23	-0.01	0.16
Cd	0.36	0.11	0.05	0.56	0.17	0.31	0.29	-0.04	0.45	0.40	0.31	1.00	0.32	0.13	0.16	0.41	0.25	-0.17	-0.04	0.22	0.49	0.23	0.24
Co	0.31	0.12	0.02	0.14	0.24	0.13	0.01	0.01	0.93	0.65	0.13	0.32	1.00	0.62	0.34	0.70	0.36	0.20	0.36	-0.04	0.23	0.11	0.67
Cu	-0.14	-0.19	-0.21	-0.32	-0.14	-0.01	-0.17	-0.03	-0.11	-0.14	0.13	0.13	0.62	1.00	0.15	-0.10	-0.06	-0.08	0.39	-0.19	-0.16	-0.29	0.19
F	0.42	0.17	0.34	0.31	0.48	0.28	0.19	0.18	0.40	-0.08	0.10	0.16	0.34	0.15	1.00	0.15	0.42	0.25	0.55	0.24	0.11	0.24	-0.16
Fe	0.51	0.66	0.13	0.41	0.27	0.45	0.33	0.07	0.78	0.47	0.06	0.41	0.70	-0.10	0.15	1.00	0.49	0.50	0.49	0.39	0.13	0.22	0.47
Mn	0.31	0.34	0.12	0.29	0.30	0.19	0.22	-0.31	0.35	0.24	0.06	0.25	0.36	-0.06	0.42	0.49	1.00	0.28	0.18	0.28	0.01	0.10	0.21
P	0.69	0.78	0.32	0.49	0.53	0.64	0.45	0.48	0.32	-0.08	0.50	-0.17	0.20	-0.08	0.25	0.50	0.28	1.00	-0.24	0.44	0.12	0.30	0.06
Pb	-0.27	-0.40	-0.17	-0.43	-0.07	-0.46	-0.46	-0.30	0.32	-0.23	-0.44	-0.04	0.36	0.39	0.55	0.49	0.18	-0.24	1.00	-0.43	0.78	-0.69	-0.32
S	0.75	0.78	0.74	0.79	0.72	0.83	0.91	0.50	0.30	0.04	0.08	0.22	-0.04	-0.19	0.24	0.39	0.28	0.44	-0.43	1.00	-0.14	0.84	-0.12
Si	0.13	-0.02	-0.13	0.16	-0.10	-0.15	-0.11	-0.29	0.32	-0.02	-0.23	0.49	0.23	-0.16	0.11	0.13	0.01	0.12	0.78	-0.14	1.00	-0.08	-0.12
Sr	0.64	0.57	0.87	0.79	0.81	0.54	0.81	0.44	0.43	0.26	-0.01	0.23	0.11	-0.29	0.24	0.22	0.10	0.30	-0.69	0.84	-0.08	1.00	-0.03
Zn	-0.03	0.07	-0.07	-0.10	-0.04	-0.06	-0.12	-0.11	0.56	0.84	0.16	0.24	0.67	0.19	-0.16	0.47	0.21	0.06	-0.32	-0.12	-0.12	-0.03	1.00

Table.4.14: Correlation coefficients of chemical parameters of groundwater in Ikorodu area.

	Na^+	K^+	Ca^{2+}	Mg^{2+}	HCO_3^-	Cl^-	SO_4^{2-}	Al	Ba	Br	Co	Cu	F	Fe	Mn	NO_3^-	P	S	Si	Sr	Zn
Na^+	1.00	0.70	0.64	0.94	0.65	0.99	0.84	-0.04	0.27	0.97	-0.03	-0.27	0.35	0.63	0.31	0.69	-0.04	0.77	0.21	0.60	-0.06
K^+	0.70	1.00	0.69	0.67	0.79	0.70	0.70	0.24	0.22	0.61	-0.09	-0.27	0.61	0.17	0.25	0.75	0.04	0.57	0.06	0.57	-0.08
Ca^{2+}	0.64	0.69	1.00	0.64	0.79	0.60	0.52	-0.06	0.50	0.41	0.13	-0.37	0.34	0.20	0.49	0.78	0.23	0.43	0.15	0.81	-0.19
Mg^{2+}	0.94	0.67	0.64	1.00	0.61	0.93	0.85	0.02	0.16	0.91	-0.05	-0.24	0.15	0.64	0.30	0.68	-0.02	0.83	0.17	0.59	-0.03
HCO_3^-	0.65	0.79	0.79	0.61	1.00	0.64	0.42	0.05	0.55	0.57	-0.02	-0.18	0.68	0.08	0.47	0.90	-0.04	0.24	0.07	0.80	0.01
Cl^-	0.99	0.70	0.60	0.93	0.64	1.00	0.84	-0.04	0.25	0.98	-0.03	-0.25	0.42	0.65	0.25	0.66	-0.07	0.80	0.18	0.57	-0.07
SO_4^{2-}	0.84	0.70	0.52	0.85	0.42	0.84	1.00	0.14	-0.10	0.81	0.03	-0.32	-0.19	0.56	0.14	0.48	-0.10	0.96	0.23	0.39	-0.15
Al	-0.04	0.24	-0.06	0.02	0.05	-0.04	0.14	1.00	-0.09	-0.10	0.12	0.17	0.29	0.00	0.04	0.05	0.16	0.13	0.11	-0.23	0.25
Ba	0.27	0.22	0.50	0.16	0.55	0.25	-0.10	-0.09	1.00	0.05	0.39	-0.24	0.55	-0.07	0.72	0.50	0.13	-0.29	0.38	0.67	-0.10
Br	0.97	0.61	0.41	0.91	0.57	0.98	0.81	-0.10	0.05	1.00	-0.16	-0.25	0.61	0.61	0.08	0.48	-0.07	0.76	0.01	0.46	-0.12
Co	-0.03	-0.09	0.13	-0.05	-0.02	-0.03	0.03	0.12	0.39	-0.16	1.00	-0.21	0.10	-0.06	0.63	0.03	-0.29	-0.05	0.59	0.20	-0.15
Cu	-0.27	-0.27	-0.37	-0.24	-0.18	-0.25	-0.32	0.17	-0.24	-0.25	-0.21	1.00	-0.07	-0.14	-0.23	-0.11	-0.36	-0.33	-0.29	-0.37	0.20
F	0.35	0.61	0.34	0.15	0.68	0.42	-0.19	0.29	0.55	0.61	0.10	-0.07	1.00	-0.20	0.23	0.55	-0.42	-0.36	0.04	0.33	0.15
Fe	0.63	0.17	0.20	0.64	0.08	0.65	0.56	0.00	-0.07	0.61	-0.06	-0.14	-0.20	1.00	-0.02	0.13	0.07	0.58	0.15	0.16	-0.05
Mn	0.31	0.25	0.49	0.30	0.47	0.25	0.14	0.04	0.72	0.08	0.63	-0.23	0.23	-0.02	1.00	0.50	0.21	0.06	0.46	0.57	-0.15
NO_3^-	0.69	0.75	0.78	0.68	0.90	0.66	0.48	0.05	0.50	0.48	0.03	-0.11	0.55	0.13	0.50	1.00	-0.09	0.42	0.00	0.77	-0.02
P	-0.04	0.04	0.23	-0.02	-0.04	-0.07	-0.10	0.16	0.13	-0.07	-0.29	-0.36	-0.42	0.07	0.21	-0.09	1.00	-0.10	0.10	0.03	-0.28
S	0.77	0.57	0.43	0.83	0.24	0.80	0.96	0.13	-0.29	0.76	-0.05	-0.33	-0.36	0.58	0.06	0.42	-0.10	1.00	0.04	0.40	-0.25
Si	0.21	0.06	0.15	0.17	0.07	0.18	0.23	0.11	0.38	0.01	0.59	-0.29	0.04	0.15	0.46	0.00	0.10	0.04	1.00	0.19	-0.11
Sr	0.60	0.57	0.81	0.59	0.80	0.57	0.39	-0.23	0.67	0.46	0.20	-0.37	0.33	0.16	0.57	0.77	0.03	0.40	0.19	1.00	-0.27
Zn	-0.06	-0.08	-0.19	-0.03	0.01	-0.07	-0.15	0.25	-0.10	-0.12	-0.15	0.20	0.15	-0.05	-0.15	-0.02	-0.28	-0.25	-0.11	-0.27	1.00

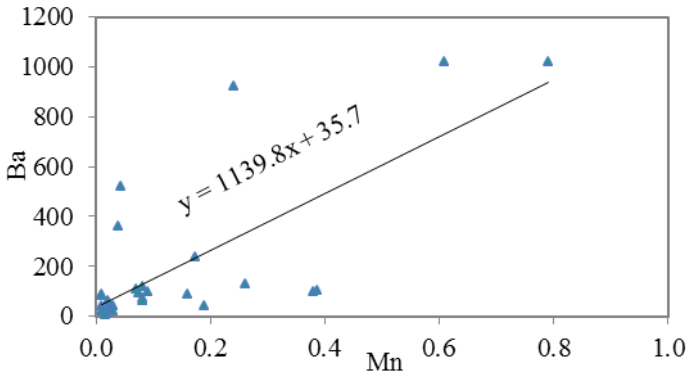

(a)

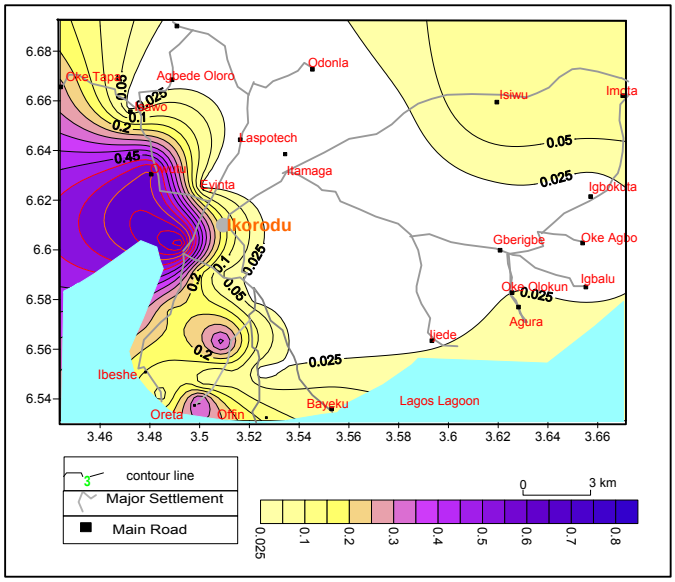

(b)

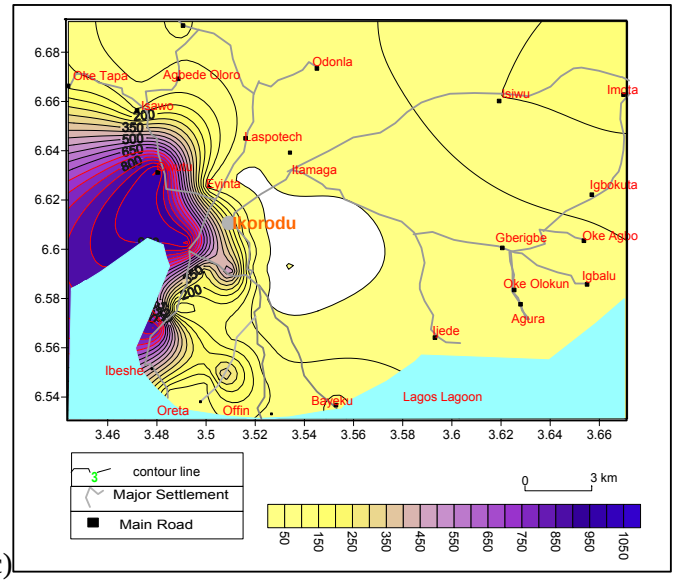

(c)

Fig 4.63: Relationship between Mn and Ba {(a) Ba vs Mn; (b) hydrochemical map of Mn &(c) hydrochemical map of Ba} in Ikorodu.

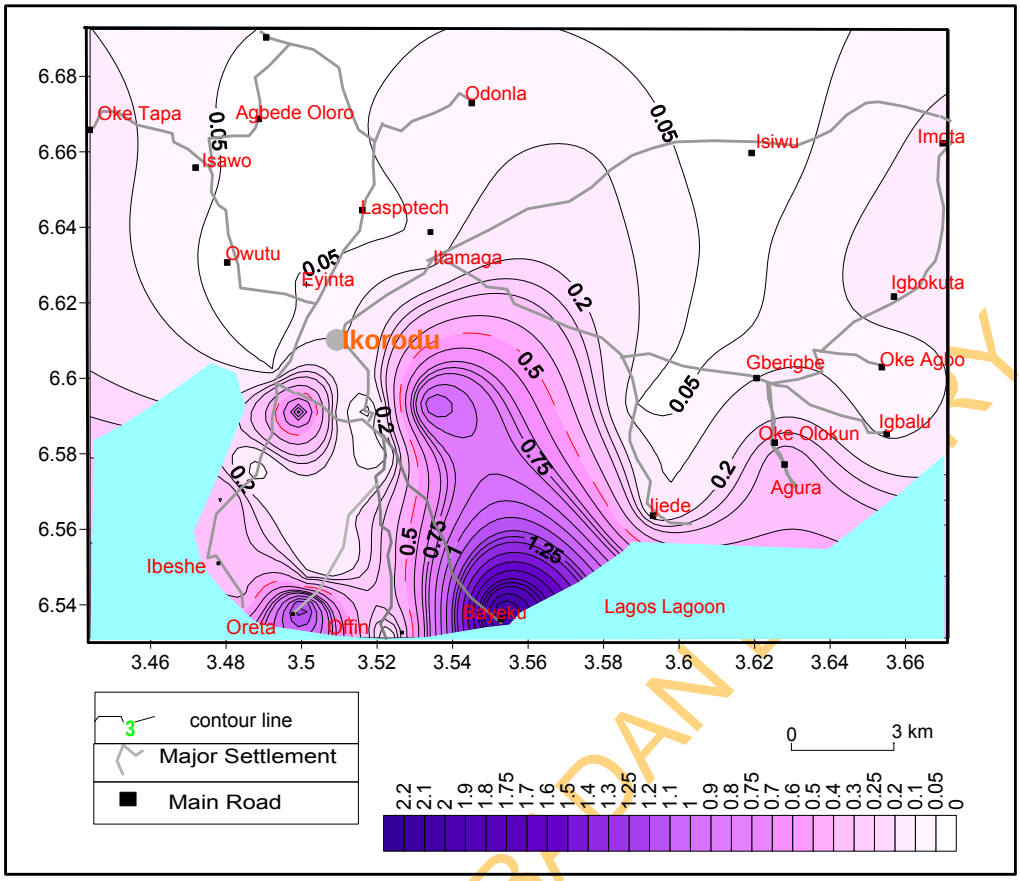

Fig 4.64: Hydrochemical map of Fe in groundwater of Ikorodu area.

Zinc occurs as a natural mineral in many drinking waters and is an essential dietary nutrient and a beneficial element in human metabolism (Vallee, 1957). Zn occurs in all the groundwater samples from Abeokuta area within a range from 6 µg/l to 1 mg/l and average of 97.5±162.8 ug/l. Zn concentration in Ikorodu area averages 58.3 µg/l in the shallow hand-dug wells and 71.3 µg/l in deep-wells. The average for the entire sample in the area is 66.5±60.5 µg/l. As shown by the relatively close mean concentration in deep and shallow wells, as well as the hydrochemical map of Zn in Fig 4.65. Zn concentration in groundwater of Ikorodu area is neither influenced by the closeness to the lagoon nor the well depth as noticed in some of the other heavy metals.

Poor correlation coefficients exist between Zn and all the major cations and anions ($-0.12 \leq r \leq 0.07$) in Abeokuta. However, Ba shows a strong positive correlation of 0.84 with zinc (Table 4.13), indicating a common source for both Zn and Ba in the area. Interestingly, both metals exhibit a fair correlation of 0.47 with Fe, hence further establishing the relationship between the metals. Zn occurrence in groundwater of Ikorodu area is not related to the occurrences of the major cations and anions as Na^+, K, Mg^{2+}, Ca^{2+}, HCO_3^-, Cl^-, SO_4^{2-} and NO_3^- all show very weak inverse correlation with Zn with all of them having correlation coefficients of between -0.02 and -0.21. Similarly, Zn exhibits a very poor negative correlation with most trace metals/elements such as Mn, Ba, Si, Sr, Fe and S in Ikorodu.

Barium is present as a trace element in both igneous and sedimentary rocks. Although, it is not found free in nature (US EPA, 1985a), it occurs in a number of compounds, most commonly barium sulfate (barite) and, to a lesser extent, barium carbonate (witherite). Ba was above detection limits in all the locations in Abeokuta area, with concentration of between 20 µg/l and 2040 µg/l and mean of 191±296.2 µg/l. Ba shows a very weak correlation with the major cations and anions, as well as other constituents with the exception of Zn. In Ikorodu area,Ba was above detection limit in the groundwater analysed in most of the areas with concentration range of 20 -1020 µg/l. The range and the mean as well as coefficient of variation are similar in both the shallow wells and the boreholes in Ikorodu (Table 4.11). The high concentration of Ba is not associated with every area around the lagoon (Fig 4.63b) but rather it is a localised in the western part of Ikorodu adjacent to the Lagos lagoon. Furthermore, Ba and Mn are closely associated in the area as indicated by the high correlation between them (r = 0.73) and the similarity of the isocones of both ions (Figs 4.63b & c) as well as the excessive occurrence of both metals in the same area. As observed with Mn, Sr shows a very strong correlation with Ba suggesting that their

source(s) in the groundwater of the area is/are similar. Weak to fair positive correlation exists between Ba and most of the major ions.

Aluminium is above the detection limit in 54% of the location with concentration of between 0.1 and 4.1 mg/l (av. 0.69±1.01 mg/l) and a high coefficient of variation of 146%. The average concentration of Al in the groundwater samples is similar in the shallow wells (0.39 mg/l) and the deep wells (0.33 mg/l) from Ikorodu, with mean value of 0.36 ± 0.3 mg/l in the entire area. Generally, Al varies from 0.1 to 1.4 mg/l though below the detection limit (0.1 mg/l) in some of the locations. Al exhibits very weak correlation with some of the major ions some positive (K^+, HCO_3^-, SO_4^{2-} and NO_3^-) while others such as Na^+, Ca^{2+} are inverse.

Weak positive correlations were obtained between Al and the major ions in the groundwater of Abeokuta area, Al and HCO_3^- (0.48), Al and Na^+ (0.39), Al and Ca^{2+} (0.32), Al and Mg^{2+} (0.34), Al and K^+ (0.29), Al and SO_4^{2-} (0.18) and Al and Cl^- (0.20). Aluminium shows strong correlations with Fe (0.78), Ba (0.61) and Zn (0.57), whereas, it exhibits weak correlations with Mn (0.37), Sr (0.42), Si (0.41) and Cu (-0.1). The very strong positive relationship between Al and Fe is largely because both are important constituents of residual product of weathering of the Basement Complex rocks underlying the area.

The concentration of copper varies from 2 µg/l to78 µg/l with an average of 16.3 ± 16.7 µg/l and coefficient of variation of 101% in the groundwater in Abeokuta area while in Ikorodu area, Cu varies from 2 µg/l to 58 µg/l and averages 15.7 ± 15.15 µg/l. The mean concentration of Cu in the deep-wells (18.3µg/l) is twice the average in the shallow wells (9.05 µg/l), suggesting that the concentration may be related to the depth to the water table. Cu exhibits weak correlations with all the major cations and anions ($-0.30 \leq r \leq -0.4$) as well as most of the trace elements and heavy metals in groundwater from Ikorodu area. Similarly, in Abeokuta area, Cu exhibits low negative correlations with Na^+, Ca^{2+}, Mg^{2+}, K^+, HCO_3^-, SO_4^{2-}, Fe, Al, Mn, Si, Ba and Sr. Weak positive correlation were observed between Cu and Zn (0.19) and Cu and NO_3^- (0.38) and a fairly strong coefficient of 0.62 between Cu and Co in Abeokuta area.

Phosphorus, a non-metal occurs in about 67% of the groundwater samples from Abeokuta area above the detection limit between 0.02 and 1.62 mg/l, with a mean concentration of 0.23±0.32 mg/l and coefficient of variation of 141%. Whereas in Ikorodu phosphorus occurs in about 58% of the samples above the detection limit between 0.02 and 0.05 mg/l and with a mean concentration of 0.03 mg/l. Phosphorus occurrence is weakly related to the major cations and anions as indicated by the weak correlation coefficients ($-0.09 \leq r \leq 0.32$)

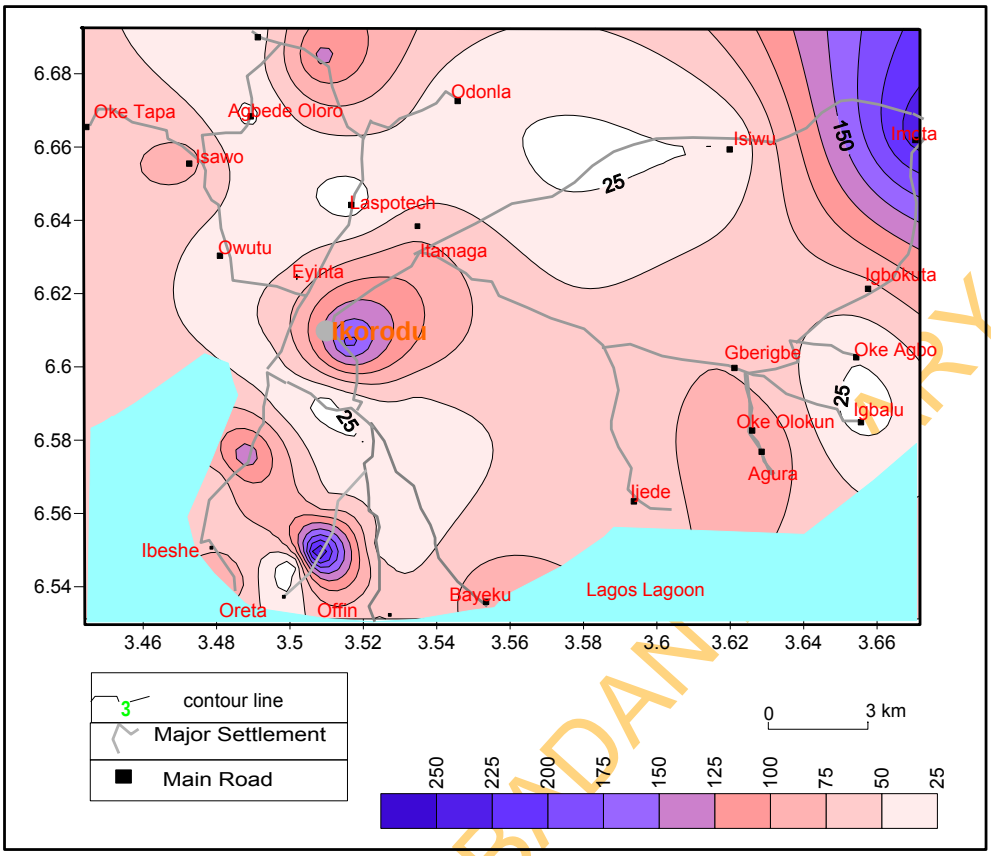

Fig 4.65: Hydrochemical map of Zn in groundwater of Ikorodu area.

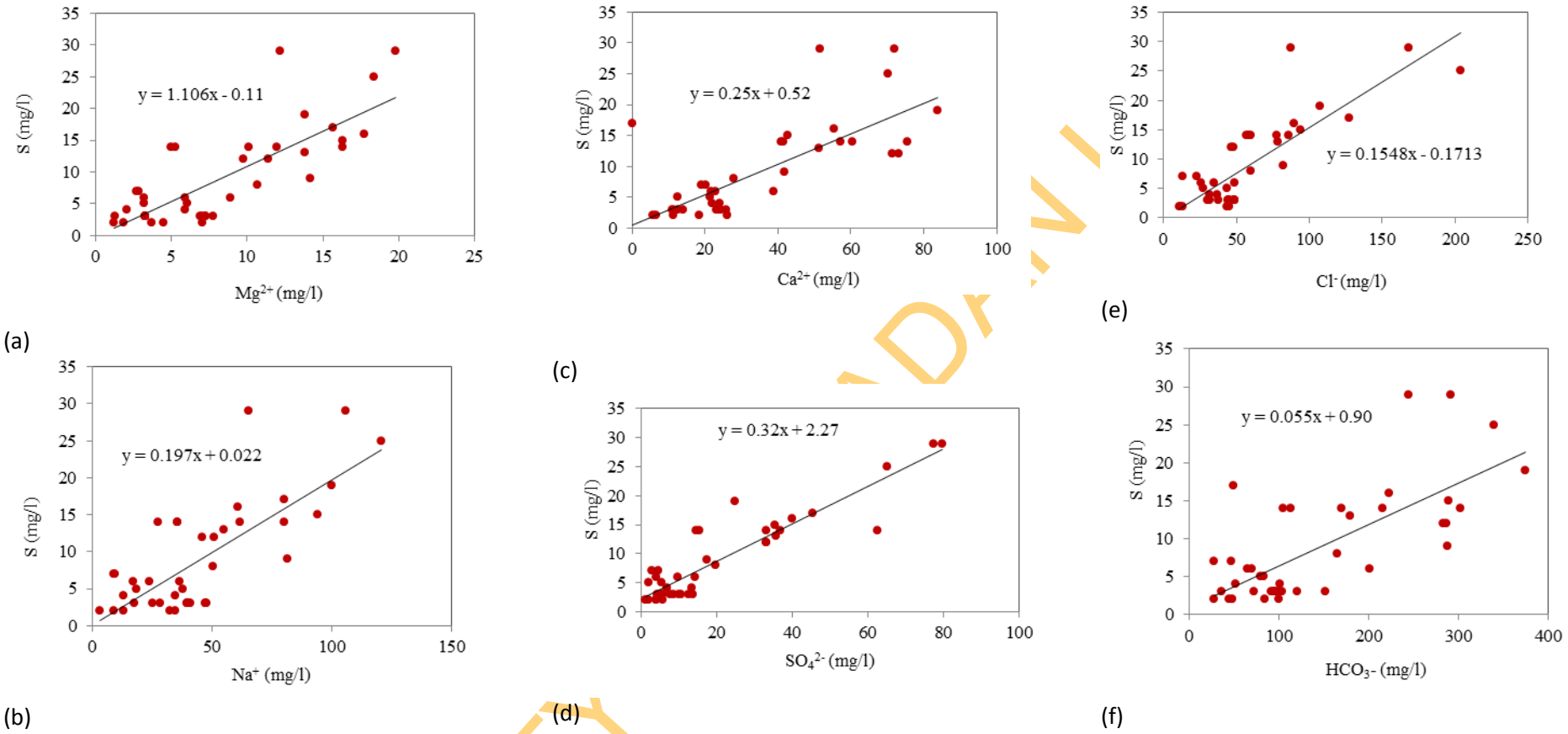

Fig. 4.66: Relationships between some trace elements and other groundwater constituents { (a) S & Na^{+}; (b) S & Mg^{2+}; (c) S & Ca^{2+}; (d) S & SO_4^{2-}; (e) S & Cl^{-}; and (f) S & HCO_3- } in Abeokuta

between phosphorus and all the major ions (Table 4.14.). In Abeokuta area, it exhibits strong to fair positive relationships with Na^+ (0.69), K^+ (0.78), Mg^{2+} (0.49), Fe (0.49), HCO_3^- (0.53), Cl^- (0.64), SO_4^{2-} (0.45) and S (0.44) while, it shows weak relationships with Al, Ca^{2+}, Mn , Sr and Co as shown in Table 4.13. The strong correlations with some of the major ions suggest that phosphorus has similar source(s) to some of the major ions, especially potassium and sodium.

Sulphur is another non-metal that was found in more than 83% of the groundwater samples, having a concentration of between 2 and 29 mg/l and an average of 8.95 ± 7.48 mg/l) in Abeokuta area while it varies between 1 and 28 mg/l (av.8.21 mg/l) in groundwater from Ikorodu area. In both study areas, sulphur shows strong relationships with the major cations and anions. In Abeokuta, the regression coefficients of sulphur and the major cations and anions (Table 4.13 & Fig 4.66) vary from 0.72 to 0.78 while in Ikorodu area (Fig 4.67) r varies from 0.77 to 0.96. Sulphate by far has the strongest influence on the sulphur in the groundwater as indicated by the near perfect correlation between them.

Strontium (Sr) occurs in all igneous rocks mostly as sulphate (celestite- SrSO4), and carbonate (strontianite- $SrCO_3$). Sr is similarly a constituent of sedimentary rock. When Sr in-take is extremely high (thousands of ppm range), it can cause disruption of bone development (Marie et al., 2001). However, Sr level in drinking water is not high enough to be able to cause these effects. In Abeokuta area, Sr is detected in all the groundwater samples at a concentration of between 30 µg/l and 590 µg/l (average = 199.4 ± 147 µg/l). Sr occurrence is closely related to the major ions, especially the alkaline-earth metals; Ca^{2+} (r = 0.87) and Mg^{2+} (0.79) as shown in Fig 4.68. Sr shows a strong correlation with Na^+, K^+, Cl^- and NO_3^- with correlation coefficients of 0.64, 0.57, 0.54 and 0.57 respectively, between Sr and these ions. HCO_3^- and SO_4^{2-} show very strong correlation with Sr in the area, having correlation coefficient of 0.81 for the relationship between Sr and both ions. Sr exhibits a very strong correlation with S with a coefficient of 0.84 as shown in Table 4.13. In Ikorodu area, Sr occurs above the detection limit in about 50% of the water samples at a range of 10 µg/l to 350 µg/l (av.= 99.1 µg/l). The average concentration in the shallow wells is 138 µg/l and 83 µg/l in deep-wells. Its occurrence is closely related to the calcium (r = 0.81) and bicarbonate (r = 0.80) as shown by Fig 4.67e & f. Sr in the groundwater likewise shows strong correlation with Na^+, K^+, Mg^{2+}, Cl^- and SO_4^{2-} with coefficients of 0.58, 0.57, 0.57, 0.55 and 0.40 respectively while HCO_3^- and NO_3^- show very strong correlation with Sr in the area.

Cd is a metal that is chemically similar to Zn and occurs naturally with Zn and Pb in sulfide ores. Cd concentration in unpolluted natural waters is usually below 1 µg/litre

(Friberg et al., 1986). Median concentrations of dissolved cadmium around the world is <1 µg/litre, and maximum value of 100 µg/l in the Rio Rimao in Peru (WHO/UNEP, 1989). Cd was detected in 25% of the groundwater samples in Abeokuta area and the concentration varies between 3 and 19 µg/l (av. =10.1±6.5 µg/l). Cd shows a weak correlation with the major cations and anions (r is between 0.05 and 0.36), with the exception of Mg. The correlation coefficient of 0.56 was obtained between Cd and Mg. Similarly other metals and non- metals exhibit weak correlation with Cd and the regression coefficients range from 0.22 to 0.49. Cd is below detection limit in over 90% of groundwater samples from Ikorodu.

Co occurs within a range of 2.0 to 62.2 ug/l averaging 11.7 µg/l in about 48% in the groundwater samples from Ikorodu area while Co is below detection limit in over 90% of groundwater samples from Abeokuta area. It has weak correlations ($-0.09 \leq r \leq 0.37$) with all the major ions including NO_3^-. Co exhibits poor inverse correlations with all other metals and non-metals except silicon (r = 0.59), Mn (0.63) and Sr (0.65).

High Mn concentration in groundwater is often accompanied by high concentrations of other metals such as Fe, Cu, Zn and As, as well as SO_4^{2-}, which are all derived by oxidation of the sulphide minerals, especially in acidic water as observed in this area. The principal controls on Mn concentration in groundwater are the pH (acidity) and redox (oxidation-reduction) conditions. Mn is mobilised under acidic conditions. Hence concentrations can be relatively high in acidic waters. Under such conditions, dispersion of dissolved Mn away from the site of oxidation is greater than that of Fe (Hem, 1992)

In pH-neutral conditions, the mobility of Mn is determined by ambient redox conditions. Under aerobic conditions typical of many shallow aquifers and surface waters, Mn is stable in its oxidised form, MnO_2, which is highly insoluble. Hence, concentrations of Mn in aerobic water are usually low and commonly below analytical detection limits. This of course is the condition in Abeokuta area. Hence, anaerobic conditions in aquifers are typically demonstrated by the presence of Fe and Mn in the groundwater.

In less than 10% of the groundwater samples, Be, Cd, Ce, Pb, Ni, Ti and Y were found above detection limits. Be averages 2.6 µg/l and is above detection limits in two locations while Cd was found in four locations with a mean value of 4 ug/l. Y on the other hand varies between 10 and 60 µg/l while Pb found in 4% of the location varies from 10 to 110 µg/l and Ti was detected at a concentration of 40 µg/l in one location. Ce was found in one of the groundwater samples (L40) at a concentration of 120 µg/l. interestingly, the sample similarly has the highest concentration of Ba (1020 µg/l), Mn (0.79 mg/l), HCO_3^-

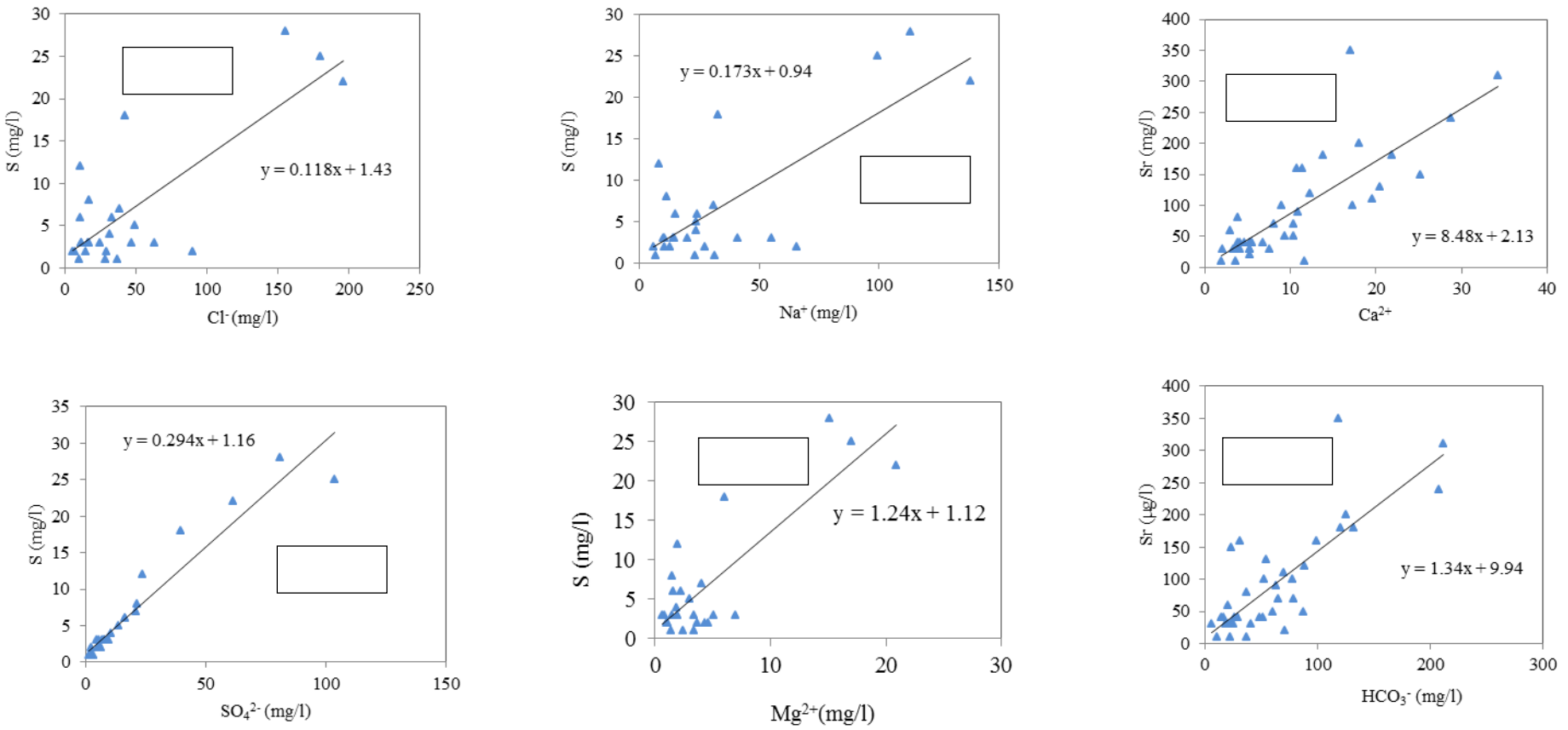

Fig 4.67: Relationships between some trace elements and major ions [(a) S & Cl^-; (b) S & SO_4^{2-}; (c) S & Na^+; (d) S & Ca^{2+}; (e) Sr & Ca^{2+}; and (c) Sr vs HCO_3^-] in groundwater in Ikorodu

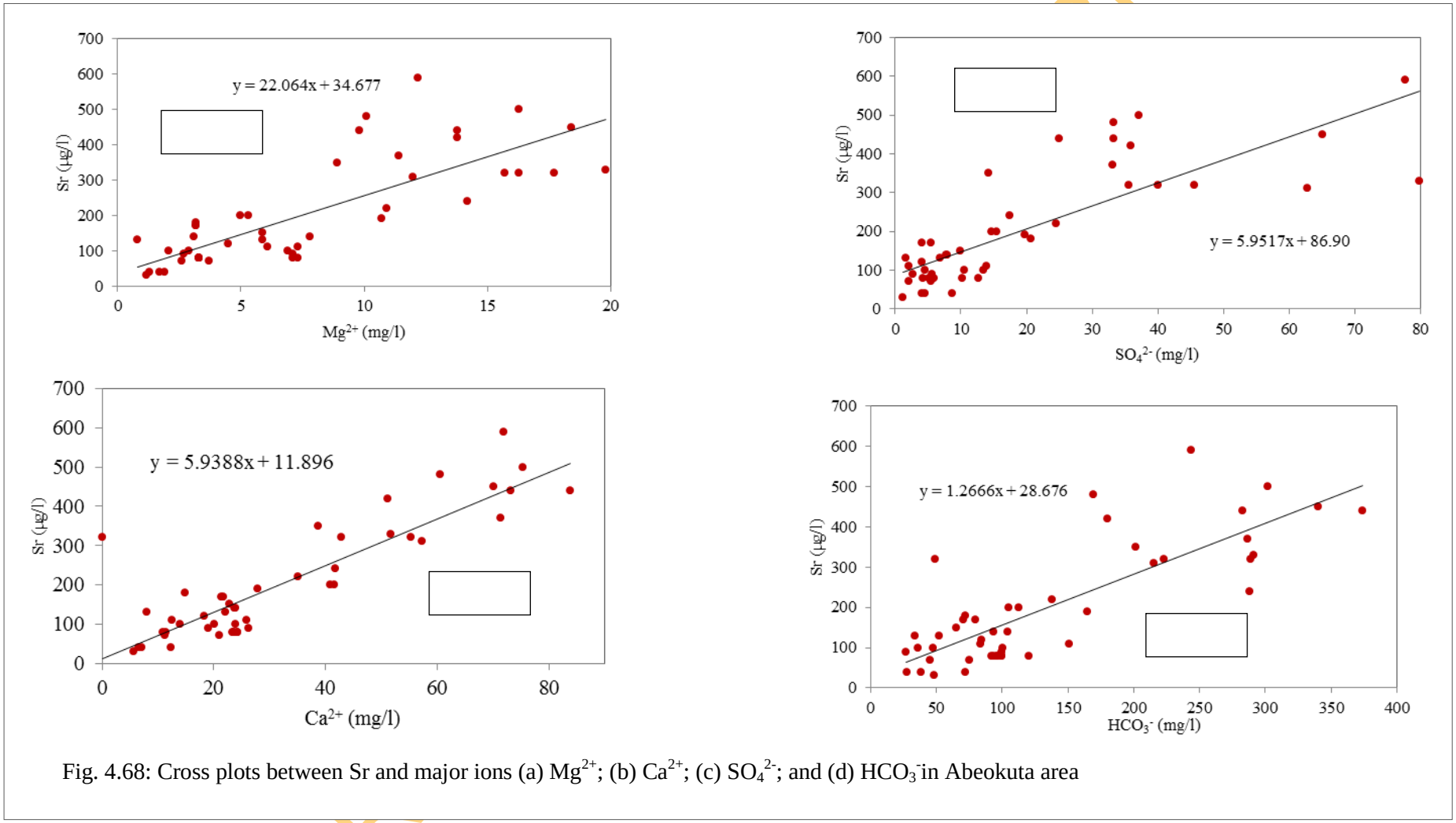

Fig. 4.68: Cross plots between Sr and major ions (a) Mg^{2+}; (b) Ca^{2+}; (c) SO_4^{2-}; and (d) HCO_3^- in Abeokuta area

(212 mg/l), Y (60 µg/l) and relatively very high concentration of Sr (310 µg/l), Co (22 µg/l) and NO_3^- (45.8 mg/l). The location is swampy area adjacent to the Lagos lagoon around Ibeshe. A large textile company (Nichemtex) is located around this vicinity. All areas around this location generally have high concentration of Ba and Mn. The high nitrate concentration is indicative of anthropogenic influence on groundwater chemistry.

4.5.6 Effects of Heavy Metals and Trace Elements on Groundwater Quality

Fluoride occurs in Ikorodu and Abeokuta areas within the recommended guidelines by WHO (2006) and standards by SON (2007). However, there is a general deficiency of F in both locations. F deficiencies have serious implications (Table 4.14) on health causing limited growth and fertility as well as dental caries (Dissanayake 1991 & Appelo and Postma, 2005).

Fe and Mn are both above permissible levels (Table 5.10b) in some of the areas. Mn is an essential trace element for human health with a daily nutritional requirement of 30–50 µg/kg of body weight (WHO, 1993) and readily absorbed in human metabolism. Nonetheless, the degree of absorption depends on dose, chemical form and effects of other metals. There is little evidence to show that toxic effects result from manganese injection. However, a provisional health based guideline of 0.5 mg/l has been set by WHO (2006). Nevertheless, even at a concentration below this value, manganese can affect groundwater acceptability by consumers. The most notable effects of these metals in water are the staining of clothes and household fixtures such as clothes washers, dishwashers, and bathtubs. Iron and manganese can impart a metallic taste to the water. A less obvious effect of Fe and Mn in well water is the accelerated deterioration of pipes, water heaters, and home heating systems (Joseph et al 1999). Therefore, based on groundwater acceptability, the WHO guideline for groundwater is 0.1 mg/l. However, many studies have shown that at excessive concentrations (> 0.5 mg/l), manganese can be detrimental to human health (Takeda, 2003; Foster, 1992; Iwami et al. 1994 and Cawte et al. 1987).

Zn, Cu, Cd, Ni, As and Cr were detected in some samples, all within the permissible level of WHO (2006) in both Ikorodu and Abeokuta areas. However, recent studies indicate that levels of arsenic in drinking water, which are lower than the current drinking-water standard, could be related to an increased risk of cancer (Karagas et.al., 1998). The USEPA has identified arsenic as a "known" human carcinogen based on occupational and drinking-water exposures: "arsenic is the only known carcinogen for which exposure through drinking water has been demonstrated to cause human cancer"

(U.S. Environmental Protection Agency, 1998a). The USEPA has set maximum contaminant levels (MCLs) that must be met to ensure public health and safety. For arsenic, the current MCL is 0.05 mg/L. Arsenic in groundwater in the area can be largely attributed to weathering of rocks, since there is no known application of arsenical pesticides in areas (Joseph et al, 1999), as the areas are essentially residential with few industries.

Al and Ba occur at levels higher than the permissible level (Table 4.15) in groundwater in the areas. There are indications that orally ingested aluminium is acutely toxic to humans despite the widespread occurrence of the element in foods, drinking-water and many antacid preparations. However, it has been hypothesized that Al exposure is a risk factor for the development or acceleration of onset of Alzheimer disease (AD) in Humans (WHO, 2006). In addition to the link of aluminium toxicity to Alzheimer's disease, it has been associated with central nervous system disorders and dialysis dementia (Moskowitz et al., 1986; Monier-Williams, 1935).

Barium is present as a trace element in both igneous and sedimentary rocks, and barium compounds are used in a variety of industrial applications; however, Ba in water in the study areas comes primarily from natural sources. Food is the primary source of intake for the non-occupationally exposed population. However, where Ba levels in water are high, drinking-water may contribute significantly to total intake. There is no evidence that barium is carcinogenic or mutagenic, nonetheless it has been shown to cause nephropathy in laboratory animals, but the toxicological end-point of the greatest concern to humans appears to be its potential to cause hypertension (WHO, 2006). Barium concentrations in water higher than the WHO (2006) value have been associated with symptoms of gastro-intestinal tract, vomiting and diarrhoea, and breakdown of the central nervous system, causing violent tonic and chronic spasms followed in some cases by paralysis (Browning, 1961; Patty, 1962). The concentration of lead (Pb) in groundwater samples is above the WHO (2006) permissible level in very few of the locations in the two areas. These occurrences have great influence on groundwater potability because high lead concentrations result in metabolic poisoning that manifests in symptoms such as tiredness, sluggishness, slight abdominal discomfort, irritation, anaemia and, in the case of children, behavioural changes (WHO, 1980). Interestingly all the major constituents of groundwater that are known to affect groundwater potability are all within permissible levels as many previous studies have noted but as highlighted above many of the trace constituents are present in the groundwater at concentrations that could cause serious health effects.

Table 4.15: Groundwater constituents and drinking water quality standards

Parameter	Range in Ikorodu	Range in Abeokuta	[1]**WHO (2006)**	[2]**SON (NIS, 2007)**	[3]EEC (Lloyd & Heathcote,1985)	[4]ISI (1983)	**Health Impact**
Hardness (as CaCO3) mg/l	1.6-134	29-84		150			None
Conductivity (µS/cm)	28-1348	119-2331		1000	1400		None
pH	4.2-7.8	5.9-8.6	6.5-9.0	6.5-8.5	6.5-8.5		None
TDS-mg/l	21-1011	78-1504	1000	500	1500	500	None
Mg- mg/L	0.1-20.9	0.8-19.8	50		50	30	Consumer acceptability (SON,2007; WHO,2006)
Na- mg/l	15-138	3.2-121		200	150		None
Cl (mg/l)	3.2-194	9.1-222		250	250		None
SO_4 (mg/l)	0.14-80.6	1.19-82.3	400	100	250	150	None
NO_3 (mg/l)	0.02-45.8	0.5-60.8		50	50		Cyanosis and asphyxia (blue-baby syndrome) in infants under 3 months syndrome) in infants under 3 months
Al (mg/l)	<0.1-0.5	0.1-4.1	0.2	0.2			Potential Neuro-degenerative disorders (SON 2007)
As mg/l	<0.03	<0.03-0.03		0.01	0.05		Cancer
Ba- (mg/l)	<0.02-1.02	0.02-2.04	0.7	0.7			Hypertension
Cd (mg/l)	<0.002-0.005	0.003-0.019	0.005	0.003	0.005	0.01	Toxic to the kidney
Ni (mg/l)	<0.002-0.012	<0.002-0.006	0.02	0.02			Possible carcinogenic
Cu (mg/l)	<0.002-0.058	0.002-0.078	2	1	0.05	0.05	Gastrointestinal disorder
F- (mg/l)	<0.01-0.06	0.1-1.5	1.5	1.5	1.5	0.6-1.2	Fluorosis, Skeletal tissue (bones and teeth) morbidity (SON,2007, Dissidayanke, 1991)
Fe- mg/l	0.02-2.17	0.01-4.79		0.3	0.2	0.3	None
Pb- mg/l	<0.01-0.11	<0.01-0.02	0.01	0.01	0.05		Cancer, interference with Vitamin D metabolism, affect mental development in infants, toxic to the central and peripheral nervous systems (SON,2007)
Tl			0.002				None
U (mg/l)		0.06-0.19	0.015				None
Mn (mg/l)	<0.01-0.79	<0.01-0.77	0.05	0.2			Neurological disorder (SON 2007)
Zn (mg/l)	0.011-0.245	0.006-1.000	3	3	5	5	None

[1]WHO- World Health Organization [3]EEC - European Economic Community
[2]SON -Standard Organization of Nigeria [4]-ISI- Indian Standard Institution

4.5.7 Chemical Influence of Hydrologic Units

Groundwater chemistry is determined by ionic inputs from precipitation, chemical weathering and dissolution of minerals within the geologic formation through which water flows (Tijani, 1994). This is obtainable in a comparatively simple and uncomplicated situation, in the case of an aquifer that receives direct recharge from rainfall and from which water is discharged without contacting any other aquifer or other water (Hem, 1985). In nature, such a scenario is rare especially in areas underlain by rocks with diverse mineralogy as well as poor sanitation practices.

Commonly, the situation may become complex by influences such as mixing of different waters, interconnected aquifers of different compositions, chemical reactions such as cation exchange and adsorption of dissolved ions as well as anthropogenic influences. Various sources of chemical inputs are more important in the different parts of the groundwater system (Close, 1987). The unconfined nature of the groundwater system in substantial parts of the study areas suggests an open system where interplay of precipitation (recharge) and the weathering process constitutes an important determinant of the overall chemical character of the groundwater.

In Abeokuta area, a typical Basement Complex terrain, CO_2-charged precipitation makes groundwater mildly acidic as a result of formation of carbonic acid (equation 4.1), which is subsequently dissociated to produce hydrogen and bicarbonate ions (equation 4.2). The generally warm soil (ground) temperature causes marked dissociation of the percolating water, leading to build up of H^+ that is responsible for cation exchange reactions.

Percolating water acts as a carrier of weathered (soluble) products (Malomo, 1983 cited in Tijani, 1994) which usually resulted in the leaching of cations (such as Na^+, K^+, Ca^{2+}, Mg^{2+}) in the silicate minerals, by the hydrogen ions, leaving behind aluminosilicate residues. The residues are commonly clay minerals such as kaolinite, illite and montmorillonite.

$$H_2O + CO_2 \rightleftharpoons H_2CO_3 \quad \text{.....4.1}$$

Water + Carbondioxide ⇌ Carbonic acid

$$4H_2CO_3 \rightleftharpoons H^+ + HCO_3^- \quad \text{.....4.2}$$

Carbonic acid ⇌ Hydrogen ion + Bicarbonate ion

$CaAl_2Si_2O_8 + 2CO_2 + 3H_2O \rightarrow Ca^{2+} + 2HCO_3^- + Al_2Si_2O_5(OH)_4$ 4.3

feldspar + carbondioxide + water → dissolved calcium +bicarbonate ions + clay mineral

The alteration and dissolution processes, are parts of chemical weathering that occurs along a number of complex pathways (such as hydrolysis, oxidation) that controlled the thermodynamic factors (Acworth, 1987).

In sedimentary areas such as alluvial and the coastal plain sands of Ikorodu, the groundwater chemistry can be described in terms of three main zones, which correlate in a general way with depth (Domenico, 1972). These are:

1. The upper zone – characterized by active groundwater flushing through relatively well-leached rocks. Water in this zone has HCO_3^- as the dominant anion and is low in total dissolved solids;

2. The intermediate zone – with less active groundwater circulation and higher total dissolved solids. Sulphate is normally the dominant anion in this zone; and

3. The lower zone – with very sluggish groundwater flow. Highly soluble minerals are commonly present in this zone because very little groundwater flushing has occurred. High Cl^- concentration and high total dissolved solids are characteristic of this zone.

Foster (1993) stated that the groundwater chemistry of an aquifer in the humid tropics is distinguished by the following two processes:

1. Relatively rapid dissolution of minerals, associated with the high rates of circulation of infiltrating meteoric water, leading quite commonly to highly dissolved SiO_2 concentration; and

2. Very large dilution and thus generally low levels of salts concentrated in the soil by transpiration (such as NaCl and $CaSO_4$) as a result of high groundwater recharge rates.

Chebotarev (1955) in a classic paper based on more than 10,000 chemical analyses of groundwater samples from Australia, concluded that groundwater tends to evolve chemically toward the composition of seawater. The study observed that this evolution is normally accompanied by the following regional changes in dominant anion species (Freeze and Cherry 1979):

Travel along flow path]

$HCO_3^- \rightarrow HCO_3^- + SO_4^{2-} \rightarrow SO_4^{2-} + HCO_3^- \rightarrow SO_4^{2-} + Cl^- \rightarrow Cl^- + SO_4^{2-}$

Increasing age →

These changes occur as the water moves from shallow zones of active flushing through intermediate zones into low zones where the flow is very sluggish and the water is old.

4.5.8 Stiff Maps of the Study Areas

The Stiff method (Stiff, 1951) uses four parallel horizontal axes extending on each side of a vertical zero axis. The concentration of cations and anions are plotted to the left and right of the vertical zero axis. The resulting points are connected to give an irregular polygon pattern, which shows differences or similarities in water composition. The width of the pattern is an approximate indication of ionic content.

The Stiff diagrams were prepared for each groundwater sample to show the groundwater character of individual samples. Stiff map on the other hand, provides a vivid spatial visualization of groundwater character and provides an easy identification of regional change in groundwater chemistry. The stiff maps of the study areas are presented in Fig 4.69 and Fig 4.70 for Abeokuta and Ikorodu areas respectively. On the basis of sizes of the polygons the dissolved constituents in the groundwater of Abeokuta area are generally greater than those of Ikorodu area.

The Stiff diagram of Abeokuta area revealed the occurrence of higher dissolved constituents (bigger polygons) of groundwater in areas on both sides of River Ogun and its tributaries than the other areas as shown in Figure 4.69. This indicates the impact of River Ogun on the dissolved constituents of groundwater in areas contiguous to the river.

The shape and the spatial distribution of the polygons show that groundwater in Abeokuta area is generally bicarbonate dominated in almost every part of the area; though chloride dominated water occurs in a few areas like Ibara, Imo and Ogere areas. $Na^{+}+K^{+}$ constitutes the dominant cation over Ca^{2+} around the central area of the map and few places around River Ogun. In other areas, the dominant cation between $Na^{+}+K^{+}$ and Ca^{2+} vary from point to point. Generally, the major cation in the area cannot be clearly distinguished by the geology of the area. This is largely due to the the significant influence of the surface water on groundwater chemistry and the similarities in mineralogy and chemistry of the underlying rock types in the area. All these ions (Na^{+}, K^{+}, Ca^{2+}) are important constituents of the minerals in all the rocks underlying the area.

In Ikorodu area, the Stiff polygons (Fig 4.70) indicate higher groundwater constituents in both boreholes and shallow wells in areas close to the lagoon (based on the size of the polygons) than in those in the landward areas. In addition, areas around the lagoon with relatively high elevation (> 20m above sea level), despite their closeness to the lagoon have low dissolved constituents in borehole and shallow wells groundwater samples.

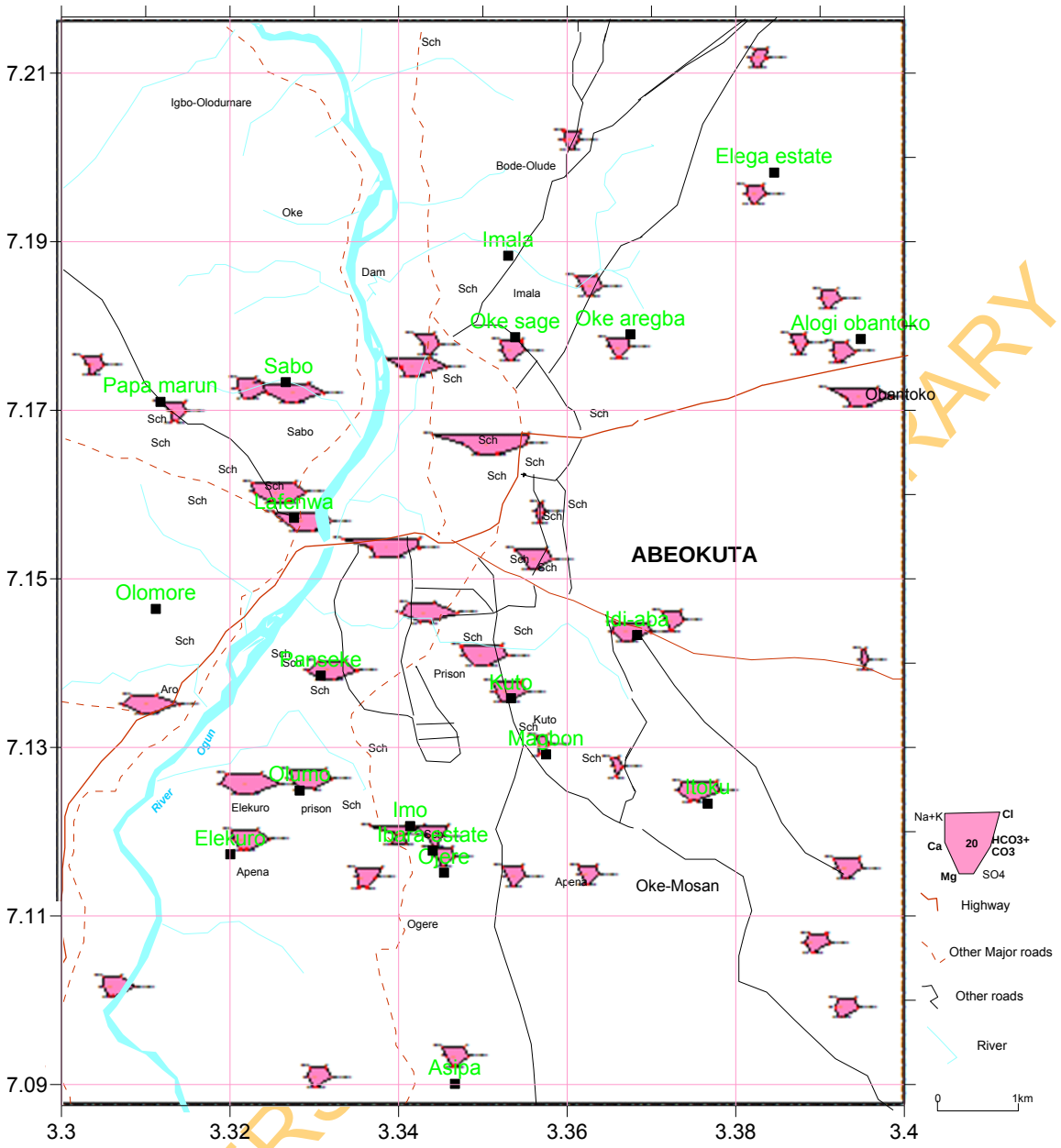

Fig. 4.69: Stiff map of groundwater constituents in Abeokuta area.

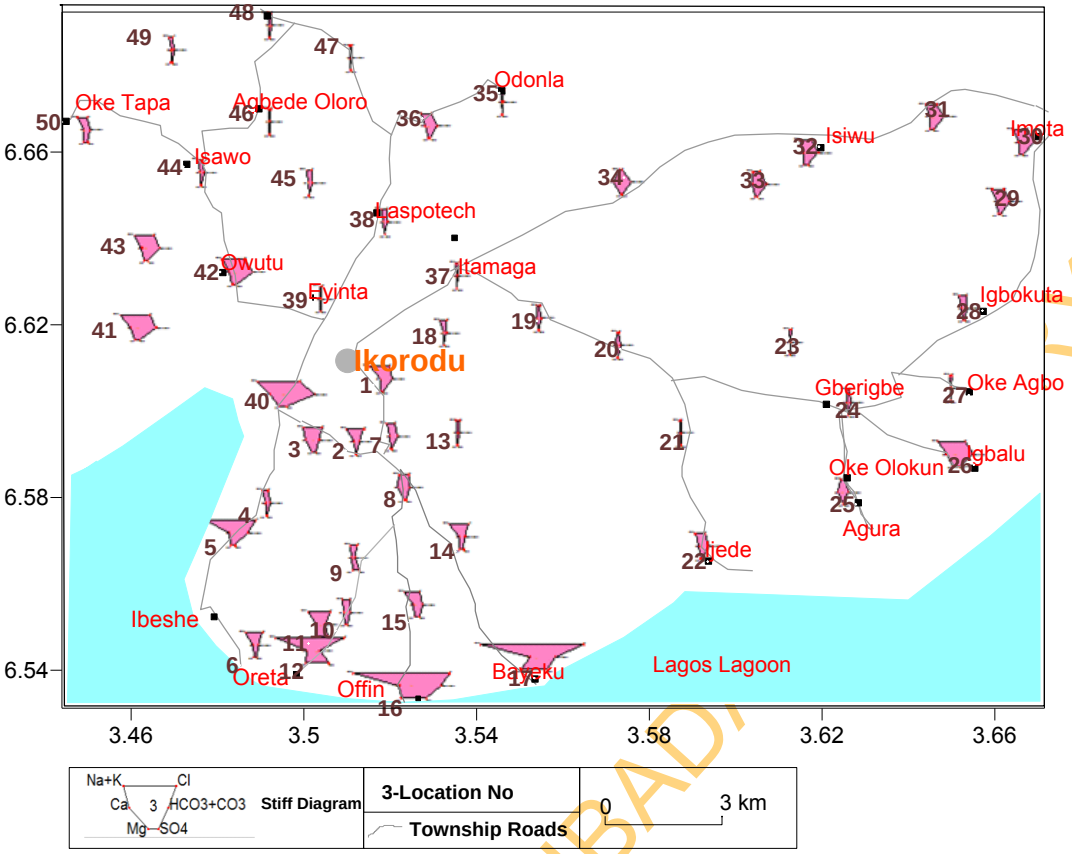

Fig.4.70: Stiff map of groundwater constituents in Ikorodu area.

Furthermore, a comparison of the shape of the polygons across the area revealed a gradual change in the dominant constituents of groundwater from bicarbonate (HCO_3^-) dominated water in the northern part of Ikorodu to chloride (Cl^-) dominated water around the lagoon. This change in water chemistry from bicarbonate water to chloride water agrees with evolution of groundwater along the flow path way as discussed by Chebotarev (1955) and Tijani (1994).

4.5.9 Characterization and Evolution of Groundwater in the Study Areas

The evolution of groundwater types can be explained to a satisfactory extent with the help of the ‘’Theory of encounters’’ proposed by Freeze and Cherry (1979), that states that the order in which groundwater encounters strata of different mineralogical composition can exert important control on the final water chemistry.

As groundwater moves through varying mineralogical strata, the water composition undergoes adjustment of various ionic species, caused by imposition of new mineralogically controlled thermodynamic constraints. Tijani (1994) observed that alkaline earth carbonate- water type occurs in the primary stage of evolution, while sodium chloride type occurs in the final stage. In simple and uncomplicated situation, where an aquifer receives direct recharge from rainfall and from which water is discharged without interacting with any other aquifer or other water, groundwater chemistry is determined by ionic inputs from precipitation, chemical weathering and dissolution of minerals within geologic formation, through which water flows (Tijani, 1994).

In nature, a simple scenario such as this is rare especially in areas underlain by rocks with diverse mineralogy as well as poor sanitation practices. Commonly, the situation may become complex by influences such as mixing of different waters, interconnected aquifers of various compositions, chemical reactions such as cation exchange and adsorption of dissolved ions as well as anthropogenic influences. Different sources of chemical inputs are more important in the different parts of the groundwater system (Close, 1987).

The groundwater in the study areas was characterized using the Piper (1944) trilinear diagram (Fig 4.71). The groundwater samples from Abeokuta area are mostly alkaline earth water types with about 90% of the groundwater falling within the class Ca-Na-HCO_3 and Ca-Na-HCO_3-Cl and other pockets of local variations including $CaHCO_3$, $NaHCO_3Cl$, $NaHCO_3$ and NaCl. In Ikorodu area the water facies in order of abundance are Ca-Na-HCO_3 (30%) and Na-HCO_3-Cl (30%) and together the two water types constitute

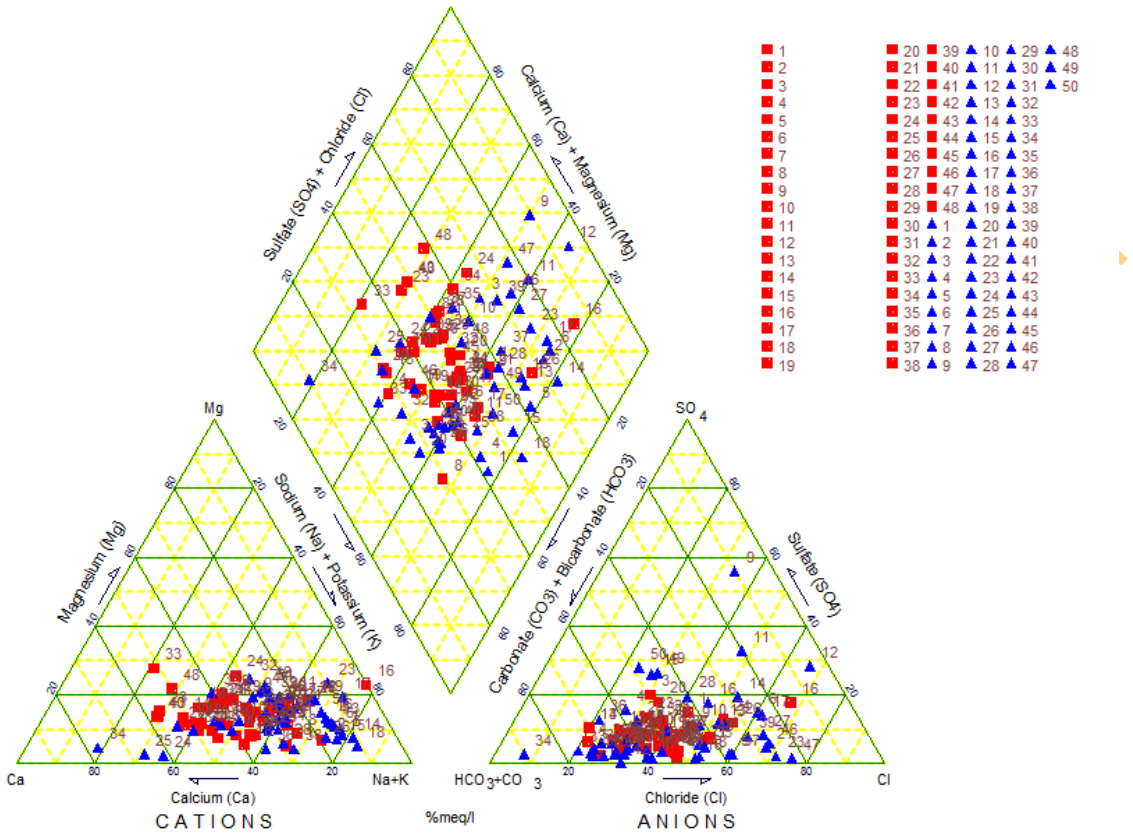

Fig 4.71: Piper diagram of groundwater inAbeokuta (red squares) and Ikorodu (blue triangles) areas

60% of the groundwater analysed. Other water types in the area are NaCl (14%), Ca-Na-HCO_3-Cl (14%), Ca-Na-Cl (8%), Na-HCO_3 (2%) and $CaHCO_3$ (2%).

The common water types in Abeokuta area plotted on the straight line between the position of fresh water and seawater. This indicates water compositions due to conservative mixing of two different waters (Appelo and Postma, 2005). As shown by the Stiff map, River Ogun has significant influence on the groundwater chemistry around the River and its tributaries. Most of the groundwater sampled around River Ogun fall within these classes. These further confirm the influence of the River on the groundwater chemistry.

In Ikorodu area, many of the groundwater samples especially from boreholes and a few shallow well samples plotted in the region between fresh and seawater, representing water from conservative mixing of waters from different sources. While the borehole groundwater samples are farther from seawater composition, many of the well samples are closer to seawater. Most of the borehole samples reflected water from conservative mixing of groundwater in different aquifers as the lithologic logs of Ikorodu has revealed the presence of a number of aquiferous units that are interconnected in the area. The samples around the lagoon as shown in the earlier discussions of the groundwater chemistry are impacted by the Lagos lagoon to support the existence of seawater encroachment into the aquifer(s) in the area.

The characters and evolution of groundwater and the geochemical processes responsible for the groundwater characters in the study areas are discussed in the sub-sections below.

4.5.9.1 Characterization and Evolution of Groundwater in Abeokuta Area

In Abeokuta area diverse water types were identified, mostly Ca-Na-HCO_3 and Ca-Na-HCO_3-Cl (about 85% of the groundwater samples) and other pockets of local variations including $CaHCO_3$, $NaHCO_3Cl$, $NaHCO_3$ and NaCl (all constituting less than 15% of the groundwater samples in the area).

The groundwater in Abeokuta area is mostly alkaline earth water-types with pockets of alkaline water-types (Fig 4.72). The Nigerian Basement Complex areas are typified by alkaline earth water (Tijani, 1994). The $CaHCO_3$ water type dominates in areas with limited mixing trend perhaps reflecting the primary stage in the evolution of its groundwater system (Amadi, 1987). The different water types in Abeokuta area in order of

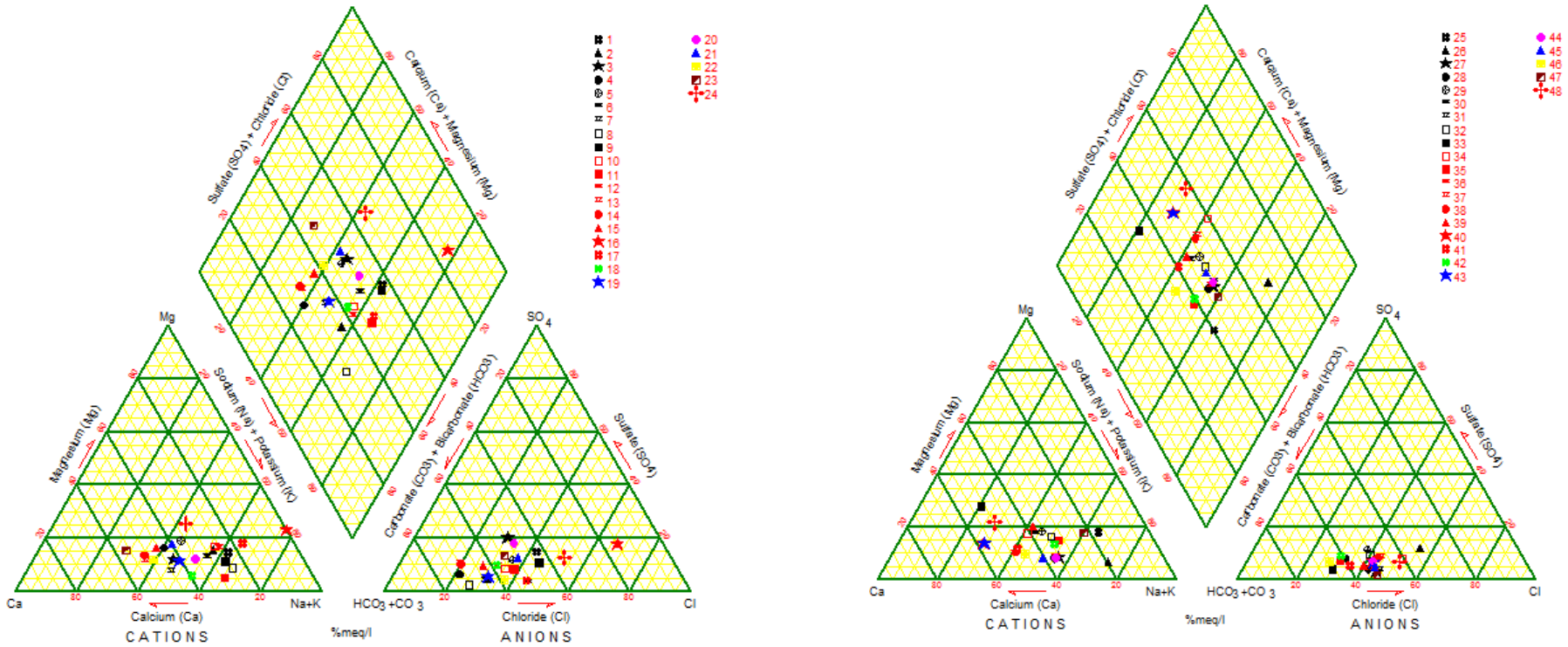

Fig.4.72: Piper trilinear diagram of major groundwater constituent Abeokuta area.

dominance are Ca-Na-HCO_3-Cl (64 %), Ca-Na-HCO_3 (22 %), $NaHCO_3Cl$ (8 %), $NaHCO_3$ (2 %), $CaHCO_3$ (2 %) and NaCl (2 %).

I. Ca -Na-HCO_3 and Ca-Na-HCO_3-Cl

Ca -Na-HCO_3 and Ca-Na-HCO_3-Cl water types jointly constitute 86% of the water types in Abeokuta area (Fig 4.72). Generally, for these water types, the concentration of Na^++K^+ > Cl^- and HCO_3^- > Ca^{2+}+Mg^{2+} (all in meq/l), thereby resulting in excess HCO_3^- and Na^+ (and K^+) ions, thus creating an appreciable amount of $NaHCO_3$. This agrees with the opinion of Lohnert (1970) cited in Tijani (1994) that in exchange water, there is more HCO_3^- ions than alkaline earth metals ions (Ca^{2+} and Mg^{2+}) in equivalent concentration. This indicates cation exchange process and this type of water is referred to as exchange water (Lohnert 1967, 1970, 1970 and 1973 cited in Tijani 1994).

The excess bicarbonate ions then release alkali ions (usually Na^+) into solution by exchange reaction with cation exchanger such as clay minerals and other related minerals that form part of the aquifer materials thus enriching the water with $NaHCO_3$. The process was represented by Tijani (1994) as

$$Ca/Mg\,(CaCO_3)_2 + Na_2E \rightarrow 2NaHCO_3 + Ca/MgE \quad \text{.....4.4}$$

Where E=Exchanger

Apart from the presence of cation exchanger in the form of clay minerals (the weathering product of the underlying rocks), the availability of adequate contact surface area and the long contact time between water and aquifer materials are important for the above reaction to proceed. In Abeokuta area, the weathering profile as shown by the 3D model of the subsurface provide the necessary conditions for the exchange reactions by containing clay minerals and this induced low permeability and allows for long contact time with percolating groundwater.

Appelo and Postma (2005) noted that most of these water types that plot at the centre of this diamond indicates conservative mixture of different waters. Furthermore, as shown in Table 4.16, the Ca-Na-HCO_3-Cl water-type is the dominant water type in all areas underlain by the different rock types. Areas underlain by porphyroblastic gneiss and the hornblende biotite gneiss are mostly dominated by Ca-Na-HCO_3-Cl and Ca-Na-HCO_3 water types. These areas have much higher Ca and Mg in their composition as shown in Table 4.1 relative to other areas. In spite of the dominance of oxides of Na and K relative to oxides of Ca and Mg in area underlain by granites, the groundwater in the areas is still largely dominated by Ca-Na-HCO_3-Cl and Ca-Na-HCO_3 water-types. The higher percentages of $NaHCO_3Cl$, $NaHCO_3$

and NaCl water types in areas underlain by the granites (Table 4.16) indicate some influence of geology on the groundwater samples in the area. The granites as shown by the chemistry of the underlying rocks (Table 4.1) and expectedly in their weathering products are richer in Na and K relative to the gneisses.

II. $CaHCO_3$, $NaHCO_3Cl$, $NaHCO_3$ and NaCl

The $CaHCO_3$, $NaHCO_3Cl$, $NaHCO_3$ and NaCl water types jointly constitute about 15% of the groundwater in the study area. $CaHCO_3$ is alkaline earth water commonly found in Basement Complex of southwestern Nigeria, especially where there is limited mixing (Amadi, 1987) and low or negligible ionic contribution through anthropogenic sources. This water type is only found in few parts of Abeokuta area. This is the primary water type in the study area modified to $CaNaHCO_3Cl$ and $CaNaHCO_3$ largely by ionic contribution through anthropogenic sources (percolation of livestock and domestic wastes, River Ogun). The $NaHCO_3Cl$ and $NaHCO_3$ water types are localised. Geochemical data and mineralogy of the rocks in Abeokuta area (Table 4.1) have both confirmed sodium bearing minerals as important constituents of the underlying rocks in the area. Tijani and Abimbola (2003) have shown that where there are favourable conditions such as the presence of appreciable clay materials (as cation exchanger) in the weathered overburden and apparently low flow velocity, with resultant relatively longer contact or residence time, $NaHCO_3$ water type may emerge in crystalline rock terrains. The NaCl water type is an alkaline water type commonly found in locations close to the coast. However, it occurs in only one location (L16) in Abeokuta area, and it is localized as other nearby locations have different water type (L26 and 27).

The chloride concentration is within the same range for all the alkaline water in Abeokuta area; however concentrations of Ca^{2+} and Mg^{2+} in the area are extremely low relative to Na^+ and K^+ due largely to high concentration of Na^+ and K^+ in the weathered aquifer at the location.

Silicate weathering and other geochemical processes

The unconfined nature of the groundwater system in substantial parts of the study area (Table 4.1) suggests an open system where interplay of precipitation (recharge) and the weathering process constitutes an important determinant of the overall chemical character of the groundwater.

Table 4.16: Percentages of groundwater facies based on underlying rock types/ well type in the study areas

Water types	**Abeokuta (Rock types)**				**Ikorodu**	
	Hornblende Biotite Gneiss	Porphyroblastic Gneiss	Granite	Porphyritic Granite	Borehole	Shallow Wells
$CaHCO_3$				5	3	
$CaHCO_3Cl$		8		15		
$CaNaHCO_3$	27	17	40	10	44	
$CaNaHCO_3Cl$	64	67	40	45	9	25
CaNaCl					6	13
$NaHCO_3$				5	3	0
$NaHCO_3Cl$	9	8	20	15	29	31
NaCl				5	6	31
	100	100	100	100	100	100

The meteoric precipitation, ionic contribution from anthropogenic sources as well as geology of the underlying rocks and their weathering products have contributed significantly to the chemistry of groundwater in Abeokuta area. The concentration of the cations Na^+, Ca^{2+}, K^+, Mg^{2+} correlate considerably with the chemistry of the rocks in the area in terms of the percentages of major oxides as shown in Fig 4.1. Their relative ionic mobility has influenced their relative abundance in the groundwater of the area, hence corroborating the fact that chemical weathering of the silicate minerals partly contributed to groundwater chemistry.

The abundance of sodium to potassium, despite potassium being dominant in the rock, can be attributed to the higher mobility of sodium (2.40) compared to that of K (1.25). This agrees with the claim of Milliot (1970) that during rock weathering and mineral dissolution, sodium dominates in natural solutions because of its higher mobility than potassium.

As shown in the Gibbs (1970) boomerang diagram (Fig 4.73), the scattering of many points away from rock-water interaction suggests the roles of other processes such as ionic input from anthropogenic sources, evaporation, base exchange (ion exchange and reverse ion exchange), and mineral dissolution to the hydrogeochemical characteristics of the groundwater in the area. The chemistry of groundwater samples in Abeokuta is partly influenced by rock-water interaction as some of the groundwater samples plot in the center of the diagram. Mainly, silicate weathering of bedrocks in the area is partly responsible for the higher concentration of Na^+ in groundwater. This is supported by the similarity in the relative abundance of major ions in groundwater and the abundance of the oxides in the rocks underlying the area (Fig 4.51 & Fig 4.1).

Generally, evaporation process would cause an increase in concentrations of all species in water. If the evaporation process is dominant, assuming that no mineral species are precipitated, the Na/Cl ratio would be unchanged (Jankowski and Acworth, 1997). Therefore, the plot of Na/Cl against EC would give a horizontal line, effectively indicating concentration by evaporation or evapotranspiration (Rajmohan and Elango, 2004). The plot of Na/Cl against EC in the area (Fig 4.74a) shows that the ratio of Na/Cl decreases with an increasing EC value. This indicates that evaporation is not the major process controlling groundwater chemistry.

A molar ratio of Na/Cl greater than one is typically interpreted as Na released from a silicate weathering reaction (Mayback 1987). In the present study, the molar ratio of Na/Cl in groundwater samples of the study area generally ranges from 0.18–2.31. The high percentage of groundwater samples (> 50%) in the area that contain Na/Cl ratio greater than one (Fig 4.74a) indicates excess sodium, which might have come from silicate weathering. If silicate weathering is the source of sodium, the water samples will have bicarbonate as the most dominant anion (Rogers 1989). The HCO_3^- is released from the reaction of the feldspar

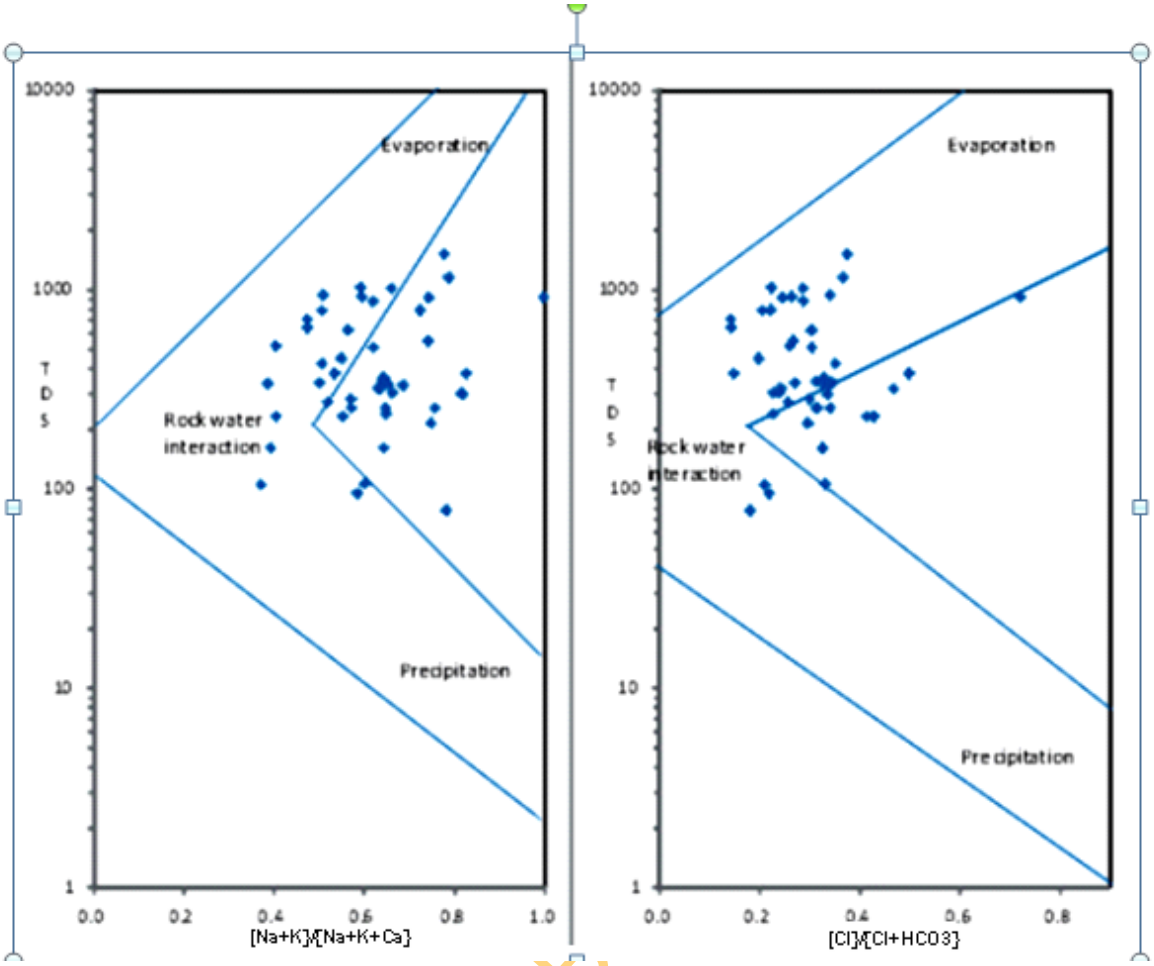

Fig. 4.73: Mechanism controlling groundwater chemistry in Abeokuta (Modified after Gibbs 1970)

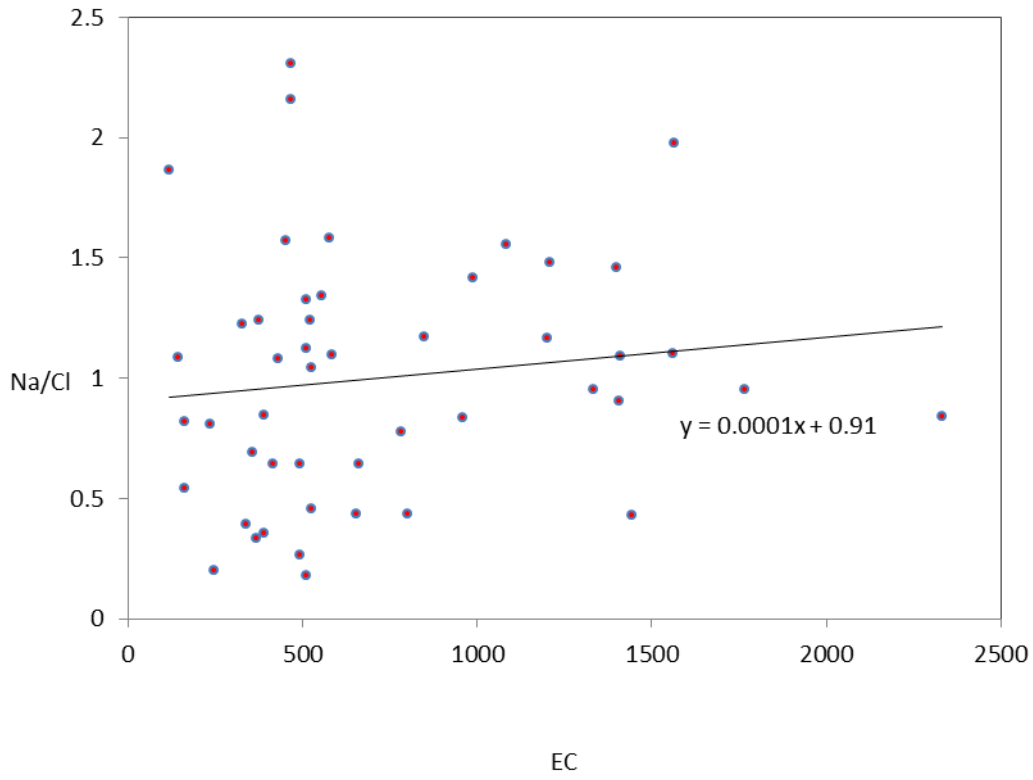

(a)

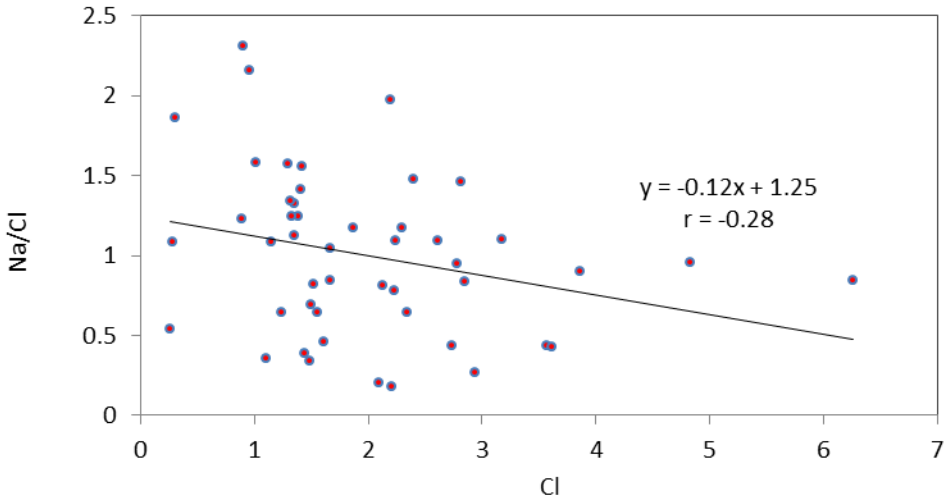

(b)

Fig 4.74: Plots of Na^+/Cl^- against (a) EC and (b) Cl^- in groundwater in Abeokuta area.

minerals (*eq.4.5)* with the carbonic acid in the presence of water (Elango et al 2003). In Fig 4.51a, HCO_3^- is the dominant anion in groundwater of this area. Therefore, silicate weathering contributed to the high sodium concentration in the groundwater of the area.

$$4NaAlSi_3O_8 + 4H_2CO_3 + 2H_2O \rightarrow Al_4Si_4O_{10}(OH)_8 + 4Na^+ + 4HCO_3^- + 8SiO_2 \text{..... } 4.5$$

Feldspar + Carbonic acid + Water → Kaolinite + Dissolved Sodium and Bicarbonate ions + Dissolved silica

The occurrence of samples with Na/Cl ratio around and less than one indicates the roles of some other chemical processes such as ion exchange, mixing of different waters.

Dissolution and mineral deposition

The evaluation of the Ca/Mg (meq/l) ratio suggests some influence of dissolution of silicate minerals on the groundwater chemistry. Katz et al (1998) noted that Ca/Mg ratio greater than 2 is indicates dissolution of silicate minerals; hence Fig. 4.75a suggests that the dissolution of silicate minerals is partly responsible for the contributions of calcium and magnesium to the groundwater chemistry of the area. The plot of $(Ca^{2+}+Mg^{2+})$ against $(SO_4^{2-} + HCO_3^-)$ (Fig 4.75b) reveals that most of the groundwater in Abeokuta area clustered around and below the 1:1 line as a result of excess bicarbonate (Rajmohan and Elango, 2004). If reverse ion exchange is the dominant process in the groundwater system, Rajmohan and Elango (2004) stated that the plot $Ca+Mg-HCO_3-SO_4$ and Na-Cl should form a slope of -1. However, the plot (Fig 4.76) gave a slope of 0.41.

The plot of $m(Ca^{2+}+Mg^{2+})$ against (Cl^-) in Fig 4.75c indicates that $(Ca^{2+}+Mg^{2+})$ increases with increasing salinity while Na/Cl decreases with increasing salinity (Fig 4.75b). Rajmohan and Elango (2004) suggested that these variations with salinity by these cations may be due to ion exchange in the weathered layer. However, the $(mMg^{2+}+mCa^{2+})/mHCO_3^-$ ratio compared with salinity can reveal the sources of Ca^{2+} and Mg^{2+} in groundwater. There is a very slight increase in the ratio with salinity, and as it increases with salinity (Fig 4.76); Mg^{2+} and $Ca^{2+}$are added to the solution at a greater rate than HCO_3^-. If Mg^{2+} and Ca^{2+} originate solely from the weathering of accessory pyroxene or amphibole minerals, this ratio would be about 0.5 (Sami 1992), as the governing weathering equation would be;

For Amphiboles

$$Ca_2Mg_5Si_8O_{22}(OH)_2+14CO_2+22H_2O \rightarrow 2Ca+5Mg+14HCO_3+8Si(OH)_4 \text{.....} 4.6$$

In Fig 4.77, the low (Ca+Mg)/HCO_3 ratio could be the result of either Ca^{2+}+Mg^{2+} depletion by cation exchange or HCO_3^- enrichment. Where the ratio is greater than 0.5, it can be due to depletion of HCO_3 especially under an acidic condition resulting in the formation of carbonic acid (H_2CO_3) as suggested by Spear (1986). In the area, the CO_2-charged precipitation makes groundwater mildly acidic as a result of formation of carbonic acid (eq. 4.7), which is subsequently dissociated to produce hydrogen and bicarbonate ions (eq. 4.8). The generally warm soil (ground) temperature causes marked dissociation of the percolating water, leading to a build up of H^+ that is responsible for cation exchange reactions.

$H_2O + CO_2 \rightarrow H_2CO_3$ 4.7

$H_2CO_3 \rightarrow H^+ + H_2CO_3^-$ 4.8

In order to evaluate the Base Exchange process in the area, the two indices of base exchange (IBE) known as chloro alkaline indices (CAI 1 and CAI 2) were determined with all values in meq/l as suggested by Schoeller (1965), defined as

$$CAI\ 1 = \frac{Cl^- - (Na^+ + K^+)}{Cl^-}$$

$$CAI\ 2 = \frac{Cl^- - (Na^+ + K^+) + HCO_3^- + CO_3^{2-} + NO_3^-}{SO_4^{2-}}$$

If there is an exchange of Na^+ or K^+ in groundwater with Ca^{2+} or Mg^{2+} in an aquifer material, both indices are positive, indicating reverse ion exchange. Where Ca^{2+} or Mg^{2+} in groundwater is exchanged with Na^+ or K^+ in aquifer material both indices will be negative, signifying ion exchange (Rajmohan and Elango 2004). In Abeokuta area, none of the two base exchange processes (Fig 4.78) played dominant role in the groundwater chemistry as in most of the samples, one of the indices is either positive or approximately zero and the other negative or vice versa.

The trace metals in groundwaterv are largely influenced by their concentration in the underlying rocks as all the heavy metals and trace elements are present in the underlying bedrock at varying concentrations.

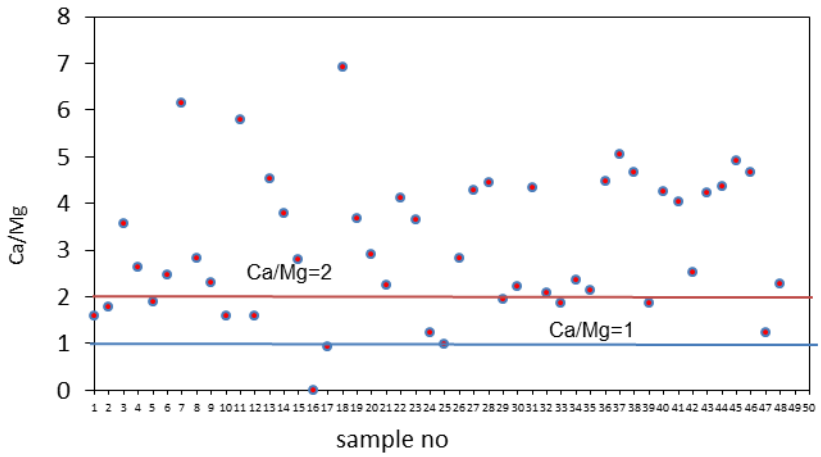

(a)

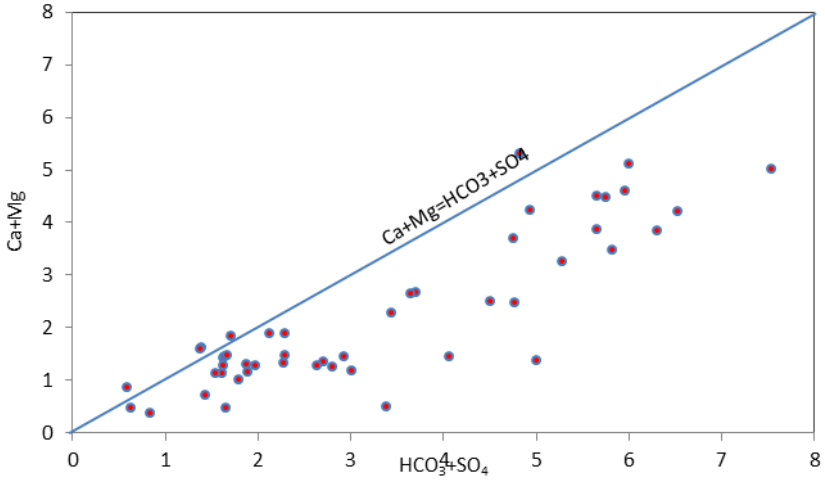

(b)

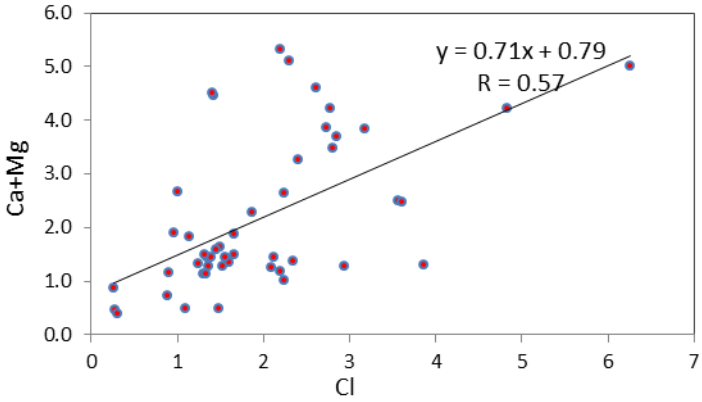

Fig 4.75: Plots of Ca^{2+}/Mg^{2+} and (a) sample no; (b) $HCO_3^{-}+SO_4^{2-}$ and (c) Cl^{-} in Abeokuta area.

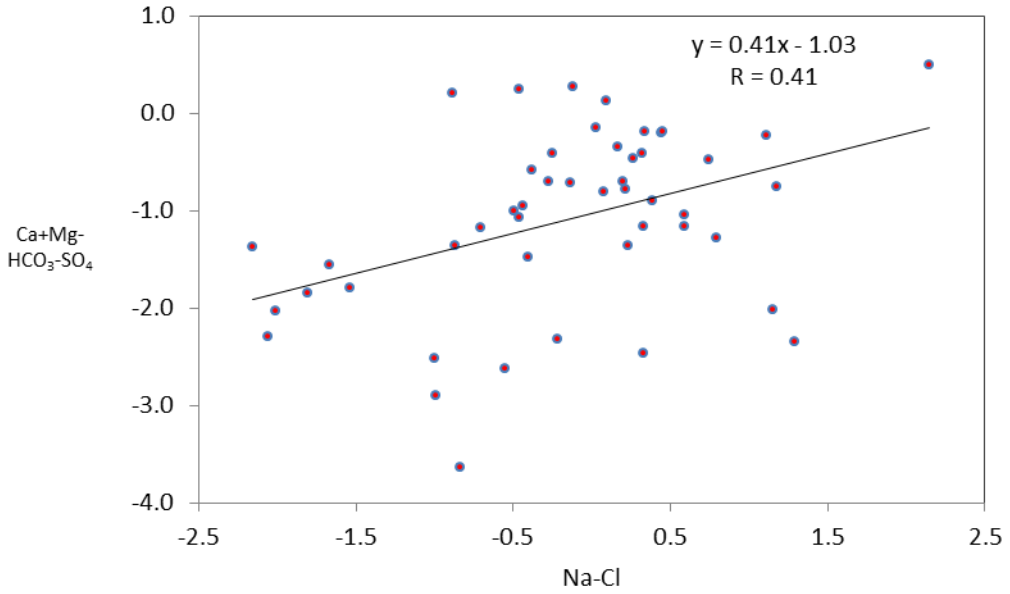

Fig 4.76: The plot of Ca+Mg-HCO_3-SO_4 and Na-Cl in groundwater samples from Abeokuta

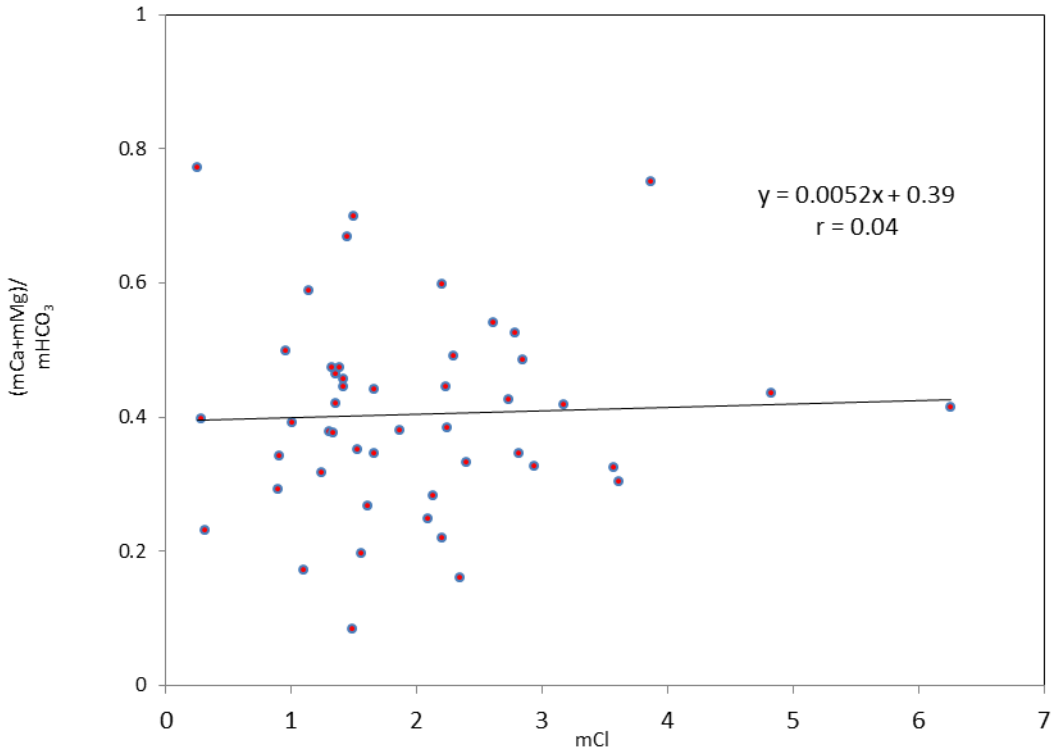

Fig 4.77: The plot of (mCa+mMg)/$mHCO_3$ and mCl in Abeokuta

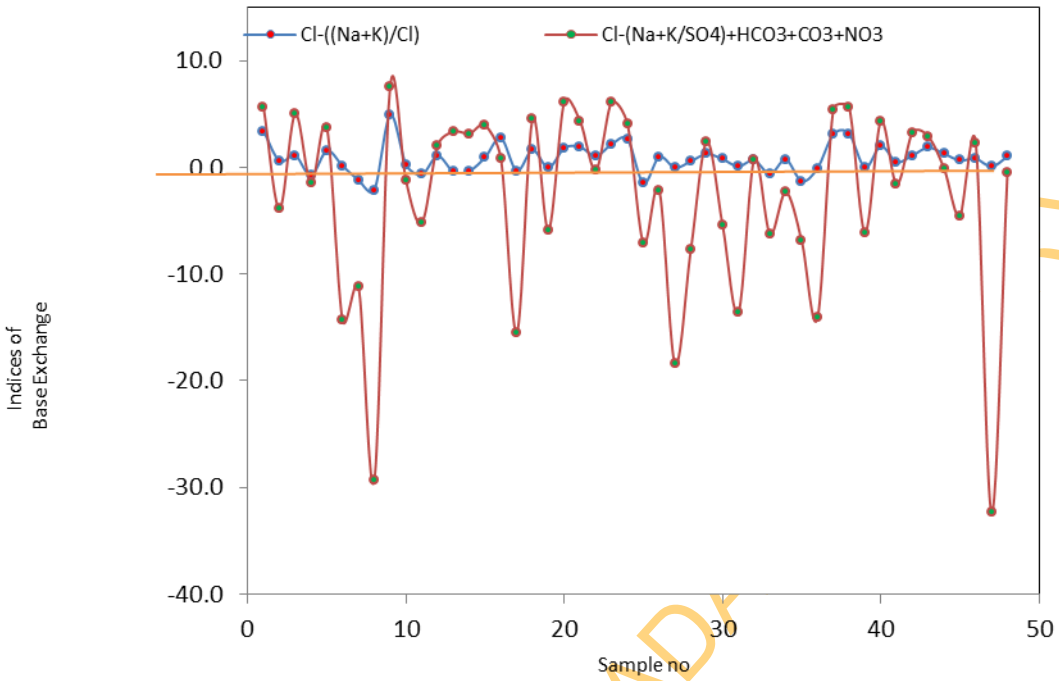

Fig 4.78: The chloro-alkaline indices of the samples in Abeokuta area.

Important influence on groundwater chemistry in the study areas includes diverse rock types, nature of the aquifer, conservative mixing of fresh groundwater and water from River Ogun as well as poor sanitary practices.

4.5.9.2 Characterization and Evolution of Groundwater in Ikorodu Area

The groundwater in these areas is mostly alkaline water in which alkalis exceed alkaline earths (Na+K>Ca+Mg) while in 20% of the groundwater analysed alkaline earths exceed alkalis. In the area, 52% of the groundwater analysed is predominantly chloride water complemented with bicarbonate.

These areas are prone to flooding during heavy storms, hence are impacted by the lagoon water. Groundwater in most of the shallow hand dug wells and boreholes close to the Lagos lagoon in Baiyeku, Offin and other environs around the lagoon are either mostly Na-Cl or Na -HCO_3- Cl water. The chloride in the groundwater is a reflection of its travel in the groundwater flow trajectory while the bicarbonate is mainly from carbon dioxide gas in the atmospheric air and soil vapour (William, 1997).

The groundwater in some of the wells has character such as ionic ratio (Fig 4.59) and the water facie similar to those of sea water. However, the total dissolved solids of most of the groundwater in the wells is not close to the TDS for seawater or brackish water (except one:1091 mg/l), although the values are generally above average and a few are greater than the limit for fresh water.

William (1997) noted that bicarbonate is usually present and can be the dominant anion in groundwater from most aquifer types except for water from oil and gas field region. On the basis of the concept of hydrochemical facies (Back, 1961) using the Piper (1953) diagram as the basis for classification of water into various facies, two major and other minor facies are recognised (Fig 4.79). The major facies, Ca-Na-HCO_3 (30%) and Na-HCO_3-Cl (30%), together constitute 60% of the groundwater samples while the minor facies are NaCl (14%), Ca-Na-Cl (8%), Ca-Na-HCO_3-Cl (14%), Na-HCO_3 (2%) and CaHCO_3 (2%).

I. Na-HCO_3-Cl, Na-Cl and Na-HCO_3

Na-HCO_3-Cl, Na-Cl and Na-HCO_3 water types are alkaline water which are either predominantly chloride with some bicarbonate or predominantly bicarbonate with some

chloride. The Na-Cl water facie is alkaline water that is essentially chloride, and it constitutes 14% in Ikorodu area. It is found mainly in locations adjacent to Lagos lagoon, with low elevation such as Baiyeku, Oreta.

II. Ca-Na-HCO_3, Ca-Na-HCO_3-Cl, and Ca-Na-Cl

Ca-Na-HCO_3, Ca-Na-HCO_3-Cl, and Ca-Na-Cl water types are groundwater facies that are earth alkaline water either mainly bicarbonate or those that are bicarbonate with some chloride and those that are mostly chloride with some bicarbonate. The Ca-Na-HCO3 and Ca-Na-Cl-HCO3 groundwater facies constitute 46% of the water samples in the area and are mostly groundwater from borehole and deep wells in high elevation area from where groundwater flows towards the coast. The Ca-Na -HCO_3-Cl facies is from shallow wells about 2 km from the Lagos lagoon and like most groundwater from hand-dug wells, chloride is the dominant anion, though the amount of alkali earths exceed those of the alkalis.

Silicate weathering and other geochemical processes

The Na^+/Cl^- and EC plot (Fig 4.80a) of this area clearly indicates that the ratio of Na^+/Cl^- slightly increases with an increasing EC value in the groundwater samples. A high sodium chloride ratio is observed at low EC value in many samples (<1300 µS/cm). Hence, sodium in the groundwater might have been derived from some other processes other than evaporation. If halite dissolution is responsible for sodium, the Na^+/Cl^- molar ratio should be approximately equal to one, while a ratio greater than one is typically interpreted as Na^+ released from silicate weathering reaction (Mayback 1987). In this study, the molar ratio of Na^+/Cl^- for groundwater samples of the study area generally varies from 0.49-2.79.

Samples having a Na^+/Cl^- ratio greater than one indicate excess sodium from silicate weathering. The occurrence of HCO_3^- as the most abundant anion in Ikorodu groundwater samples confirms silicate weathering as an important source of sodium (Rogers 1989). The reaction of the feldspar minerals with the carbonic acid in the presence of water releases HCO_3^- (Elango et al 2003). A plot of $Na^+ + K^+/Na^+ + K^+ + Ca^{2+}$ against TDS (Fig.4.81) similarly indicates the importance of rock water interaction in this area (Gibbs 1970). However, samples with a Na/Cl ratio less than one indicate the possibility of some other chemical processes, such as ion exchange processes.

Dissolution and mineral deposition

The study of the Ca^{2+}/Mg^{2+} ratio of groundwater from this area supports the dissolution of calcite and dolomite (Fig. 4.82a). Maya and Loucks (1995) noted that if the ratio $Ca^{2+}/Mg^{2+}=1$, dissolution of dolomite should occur, whereas a higher ratio indicates greater calcite contribution. Higher Ca^{2+}/Mg^{2+} molar ratio (>2) indicates the dissolution of silicate minerals, which contribute calcium and magnesium to groundwater (Katz and et al. 1998). In Fig 4.82a, four percent (4%), points closer and below the line ($Ca^{2+}/Mg^{2+}=1$) indicate the dissolution of dolomite. Most of the samples (64%) having a ratio between 1 and 2 indicate the dissolution of calcite. Those with values greater than 2 indicate the contribution of silicate minerals.

The plot of $(Ca^{2+}+Mg^{2+})$ versus $(SO_4^{2-}+HCO_3^-)$ will be close to the 1:1 line if the dissolutions of calcite, dolomite and gypsum are the dominant reactions in a system. Ion exchange tends to shift the points to the right due to an excess of SO_4+HCO_3 (Cerling et al 1989; Fisher and Mulican 1997). If reverse ion exchange is the process, it will shift the points to the left due to a large excess of $(Ca^{+}+Mg^{+})$ over $(SO_4^{2-}+HCO_3^-)$.

In the plot of $Ca^{2+}+Mg^{2+}$ versus $SO_4^{2-}+HCO_3^-$ (Fig 4.82b) in Ikorodu area (coastal plain sands and alluvium), the samples clustered around and below 1:1 line, indicating excess bicarbonate in many of the groundwater samples in the area. A plot of $Na^{+}–Cl^-$ versus $Ca^{2+}+Mg^{2+}–HCO_3^-–SO_4^{2-}$ should form a line with a slope of 1, if ion exchange is the dominant process in the system, (Rajmohan and Elango, 2004). However, the diagrams show that the points give a line with a slope of -1.41. This indicates that ion exchange process is not a dominant process in the system. However, high correlation coefficient between $Na^{+}–Cl^-$ and $Ca^{2+}+Mg^{2+}–HCO_3^-–SO_4^{2-}$ (Fig. 4.83) indicates some influence of ion exchange process (Rajmohan and Elango, 2004). The plot of $m(Ca^{2+}+Mg^{2+})$ against $m(Cl^-)$ in Fig.4.82c indicates that Ca^{2+} and Mg^{2+} increase with increasing salinity. The plots of $m(Na^{+}/Cl^-)$ and $m(Cl^-)$ in Fig. 5.79b and $m(Ca^{2+}+Mg^{2+})$ and $m(Cl^-)$ (Fig.4.82c) indicate that salinity increases with the decrease in Na^{+}/Cl^- and increase in Ca^{2+}+Mg. The slight decrease in sodium as salinity increases and increase in $Ca^{2+}+Mg^{2+}$ suggests reverse ion exchange in the clay/weathered layer (Rajmohan and Elango, 2004).

As the ratio $(mMg+mCa)/mHCO_3$ decreases mildly with salinity (Fig 4.84), Mg and Ca are exchanged for Na^+ in the aquifer matrix through the ion exchange process. However, the two Base Exchange processes identified based on the chloro alkaline indices in Fig 4.85 are mostly negative, further indicating that where base exchange processes occur in the

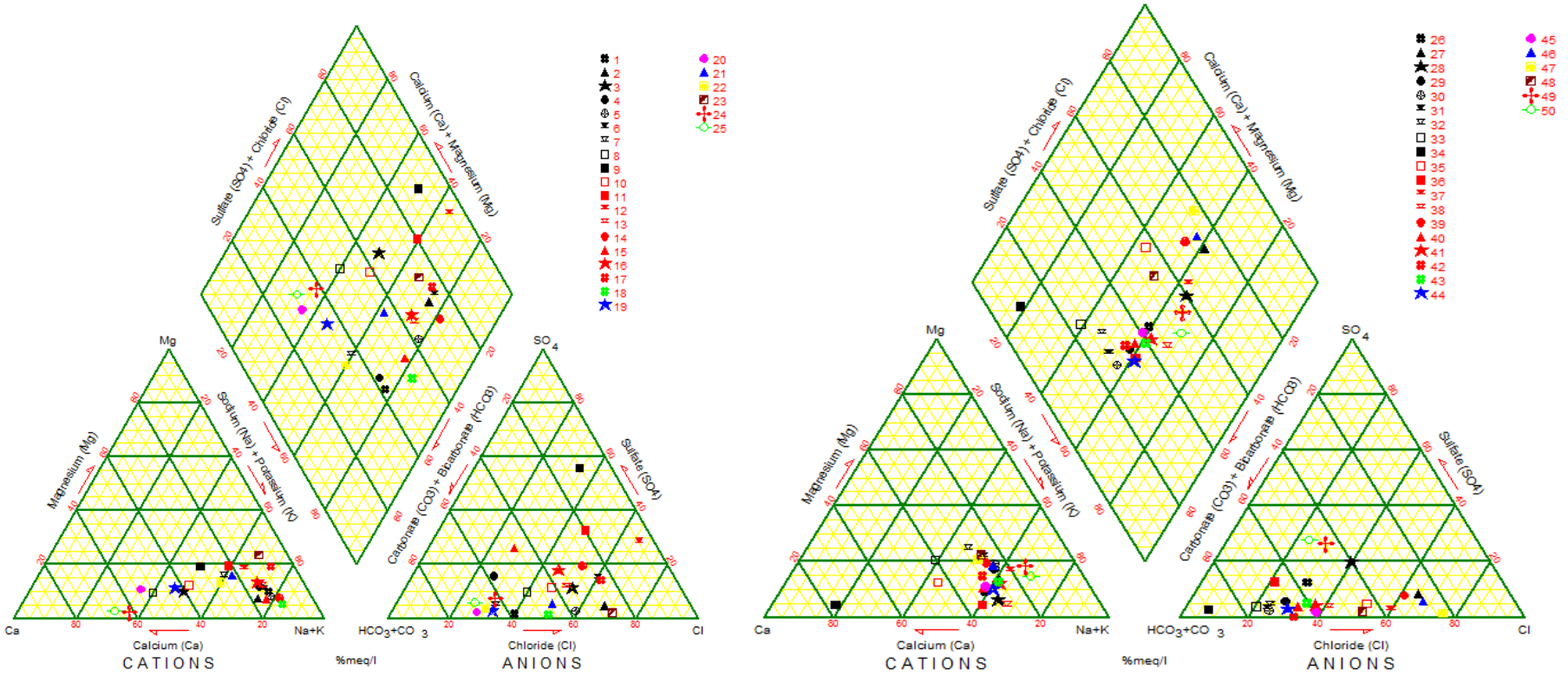

Fig 4.79: Piper trilinear diagram for groundwater samples from Ikorodu area.

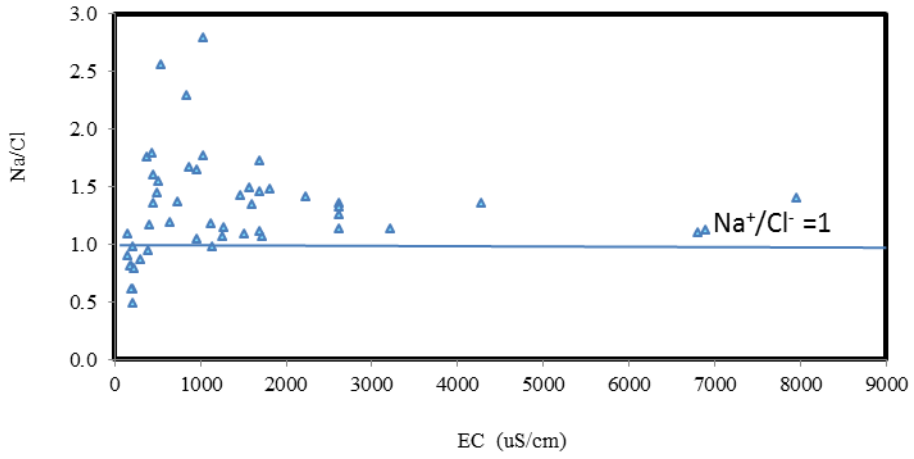

Fig 4.80: Plot of Na/Cl against EC in groundwater samples of Ikorodu area

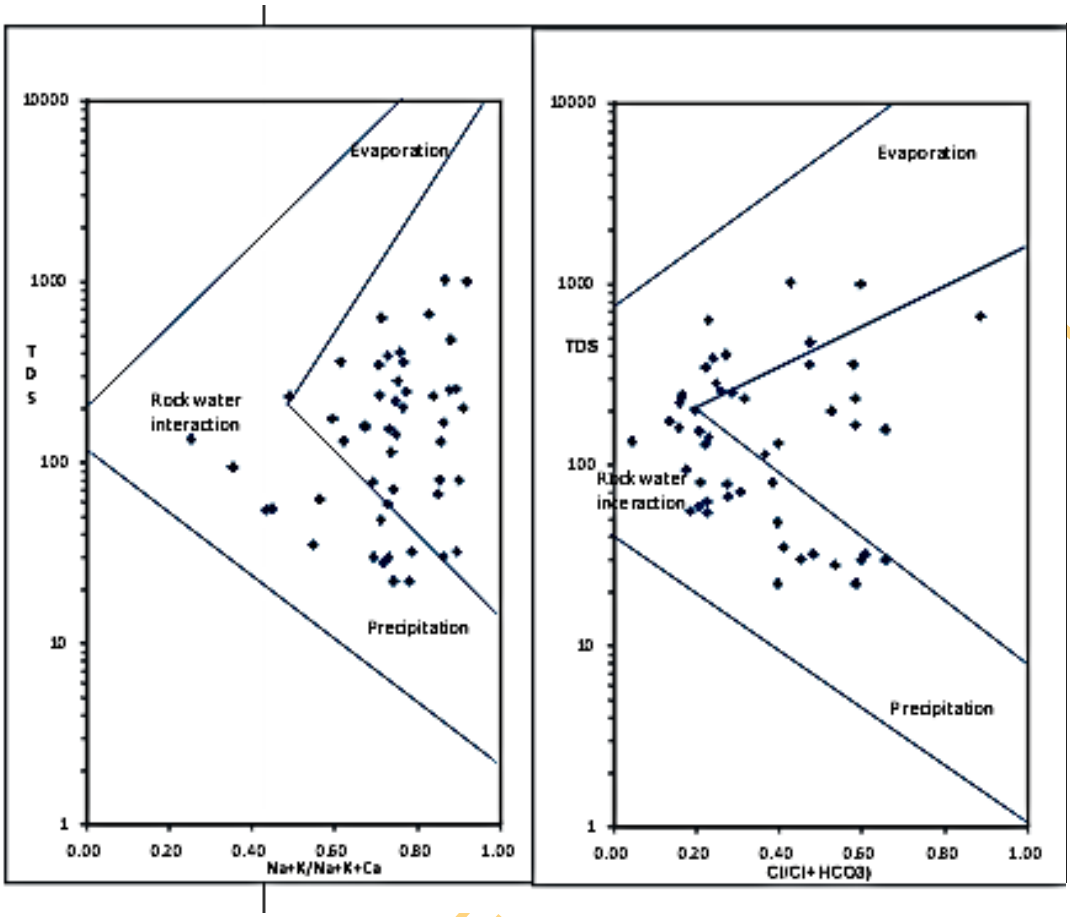

Fig. 4.81: Mechanism Controlling Groundwater Chemistry in Ikorodu (Modified after Gibbs 1970)

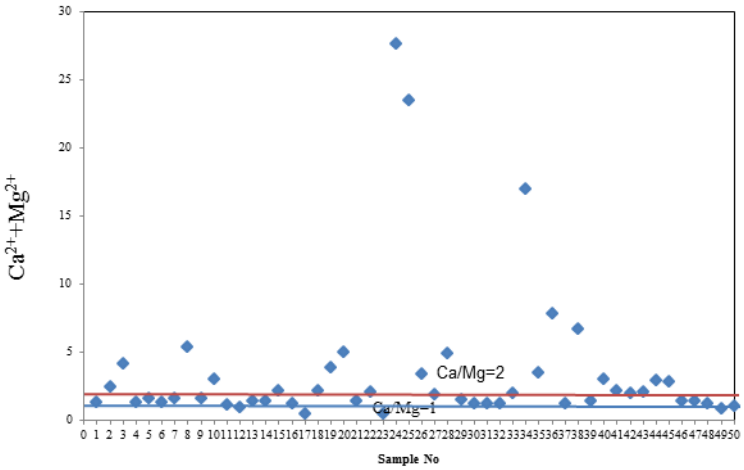

(a)

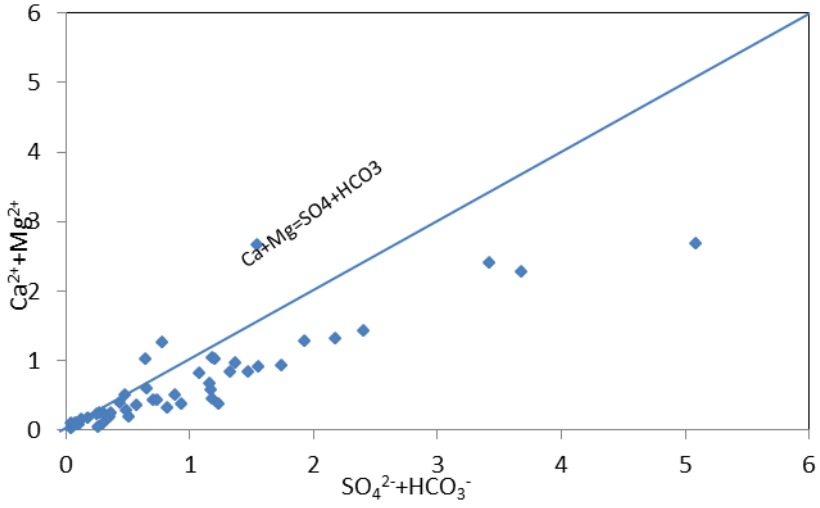

(b)

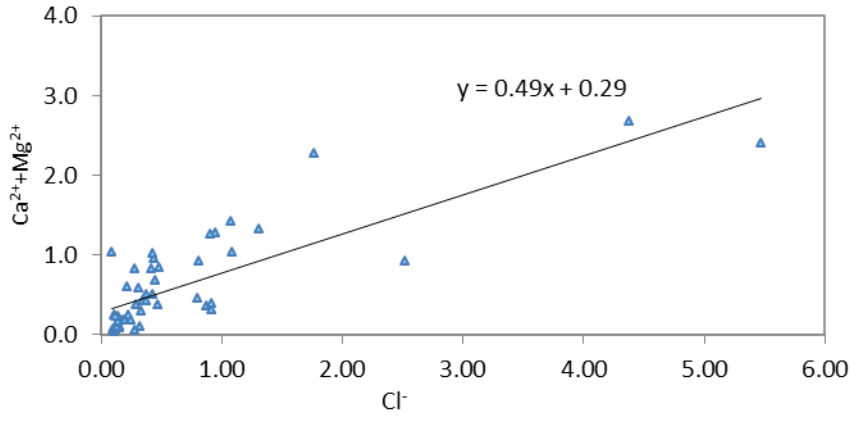

(c)

Fig 4.82: Plot of Ca^{2+}+ Mg^{2+} against (a) Sample no; (b) SO_4^{2-}+HCO_3^- and (c) Cl^- in Ikorodu

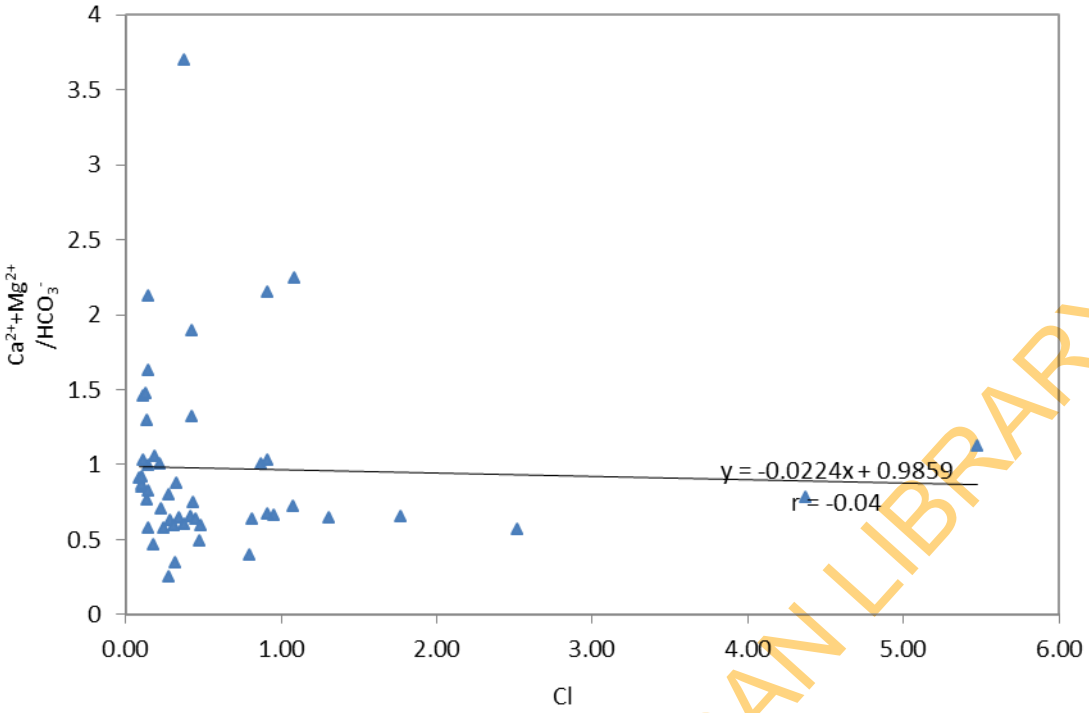

Fig 4.83: Plot of mCa+mMg/mHCO$_3^-$ against mCl$^-$ in Ikorodu

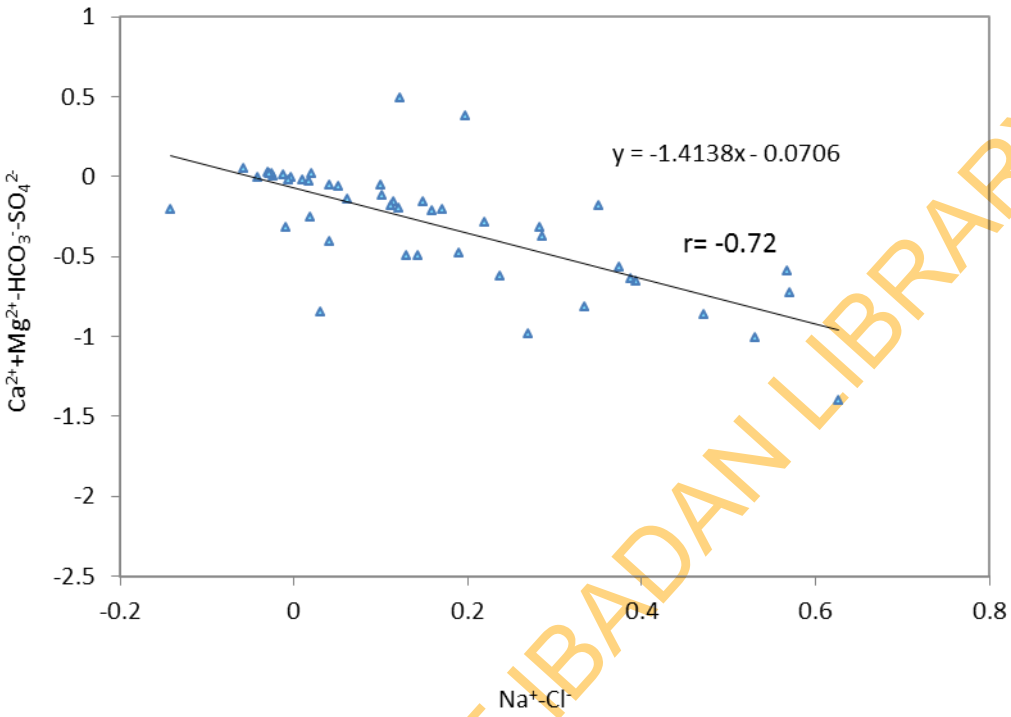

Fig 4.84: Plot of $Ca^{2+}+Mg^{2+}-HCO_3^{-}-SO_4^{2-}$ against $Na^{+}-Cl^{-}$ in Ikorodu area

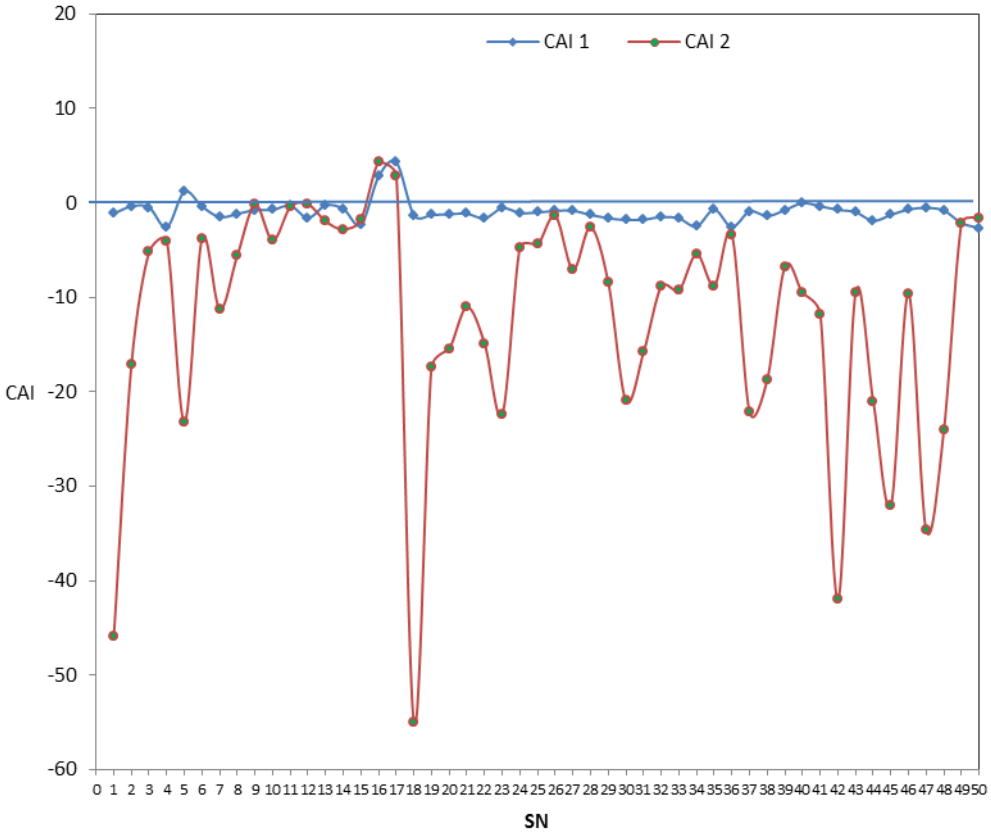

Fig 4.85: Plot of CAI and samples no in Ikorodu area

area, the base exchange is essentially ion exchange.

4.5.10 Hydrochemical Maps of the Study Areas

Hydrochemical maps depict spatial variation in the hydrochemical characteristics of groundwater and constitute a useful aspect of hydrochemical studies (Singhal and Guptal, 1999). The hydrochemical maps of the study areas for the major ions and common heavy metals are attached as appendix IV.

In Abeokuta area, all the major cations (for example, Fig 4.86) have higher concentrations in areas around R. Ogun in the central part of the town. This indicates that the river has significant influence on the character of the groundwater in the area. . Chloride (Fig 4.87), bicarbonate and sulphate show similar trend in the area hence confirming the influence of the river on groundwater chemistry. This further confirms the role of ionic input through anthropogenic sources (River Ogun and its tributaries) on the chemistry of groundwater in Abeokuta area.

Occurrence of high concentrations of the major cations in other areas further indicates some influence of relative abundance of the oxides of these ions in the underlying rocks of the area on the groundwater chemistry. In addition, the concentration of calcium in the groundwater (Fig 4.88) in Abeokuta area is high both around River Ogun and in the areas underlain by hornblende-biotite gneiss. However, River Ogun flows though area underlain by hornblende-biotite gneiss. Therefore, the high concentration of Ca^{2+} in the area can be attributed to the influence of River Ogun as the concentrations of other major ions are high in this area.

As explained in the earlier discussion, the heavy metals occurrence in the groundwater of the area is related to the relative abundance of the metals in the weathered product of the underlying rocks. The isocones of the heavy metals in Abeokuta area that were presents in more than 80% of the studied area are attached as appendix V. Some heavy metals have high concentration in the groundwater from areas underlain by specific rock types. For example, Zinc concentration in the porphyroblastic gneiss (107 ppm), porphyritic granite (73 ppm) and granite (35 ppm) from Abeokuta area is significantly higher than in hornblende biotite gneiss (8 ppm). This is reflected in the groundwater chemistry, as Zn is very low in groundwater from area underlain by hornblende-biotite gneiss while Zn is significantly higher in concentration in groundwater in areas underlain by granite and porphyritic granite. Copper, barium similarly shows the same trend.

There is gradual increase in the Na^{+} (Fig 4.89a) and Cl^{-} (Fig. 4.89b) in Ikorodu area, as the water flows towards the Lagos lagoon from the landward area with generally high concentration of these ions in areas adjacent to the coast. Potassium shows similar trend as

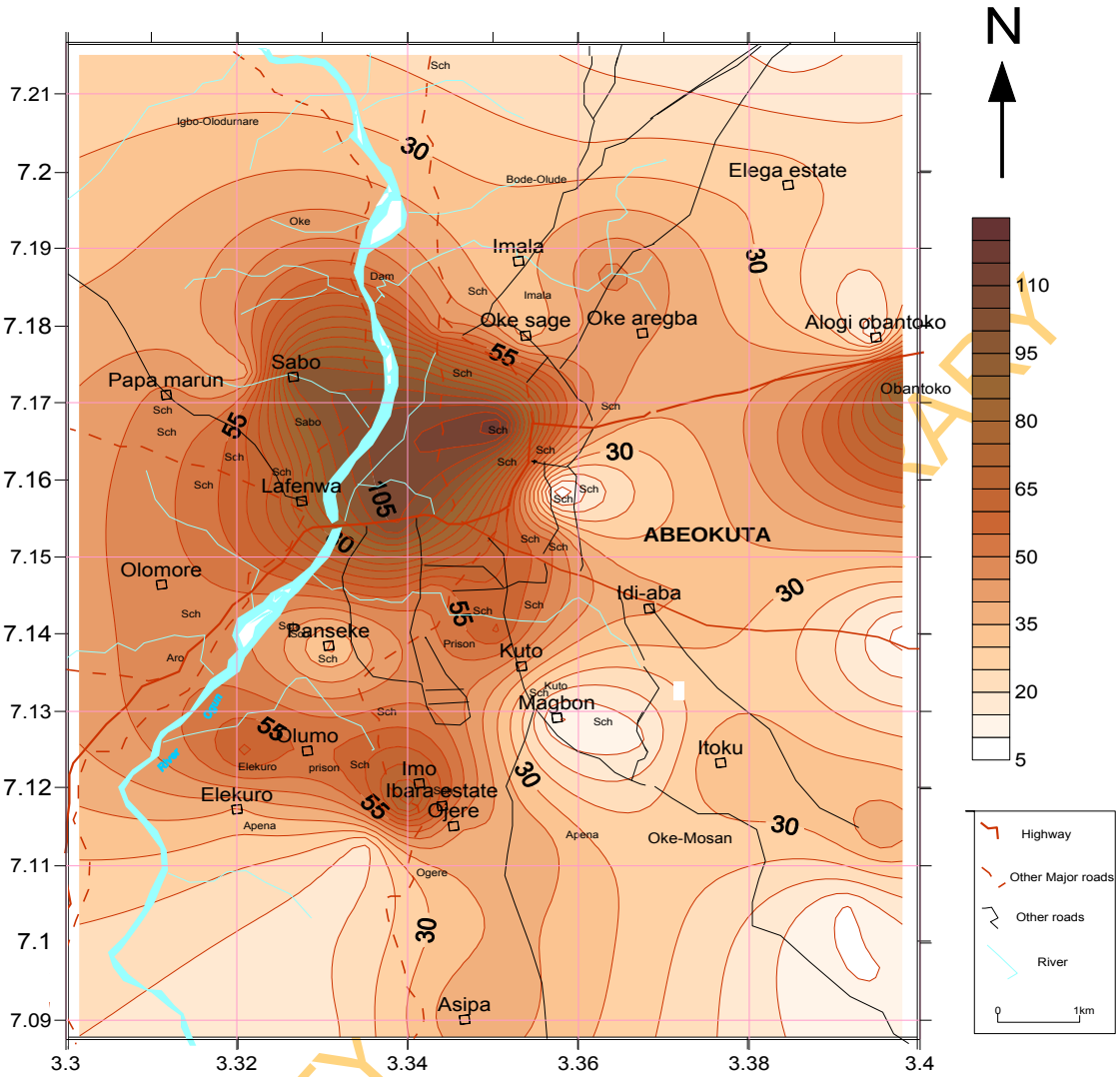

Fig.4.86: Hydrochemical map of sodium in groundwater of Abeokuta area

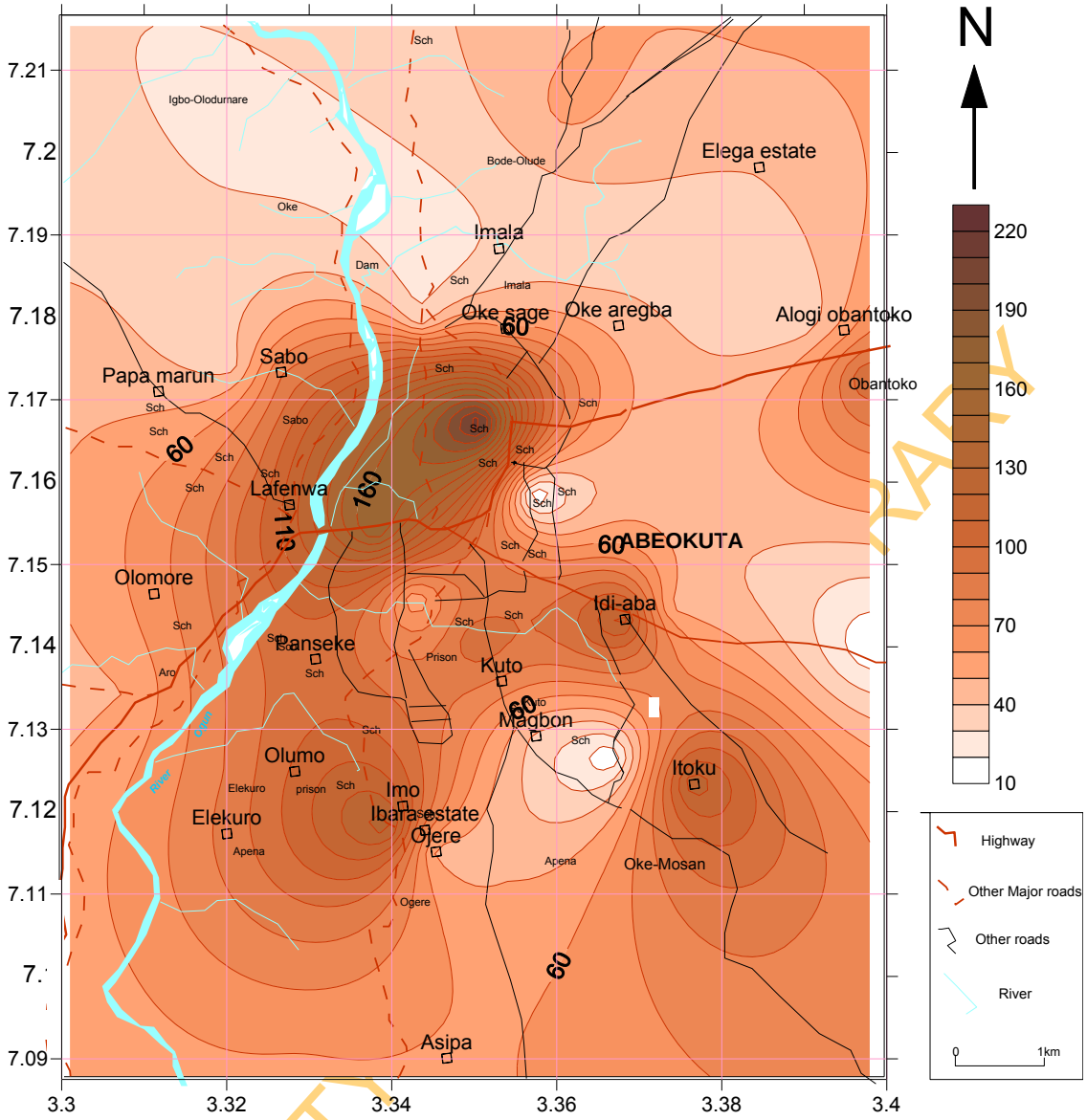

Fig 4.87: Hydrochemical map of chloride in groundwater of Abeokuta area

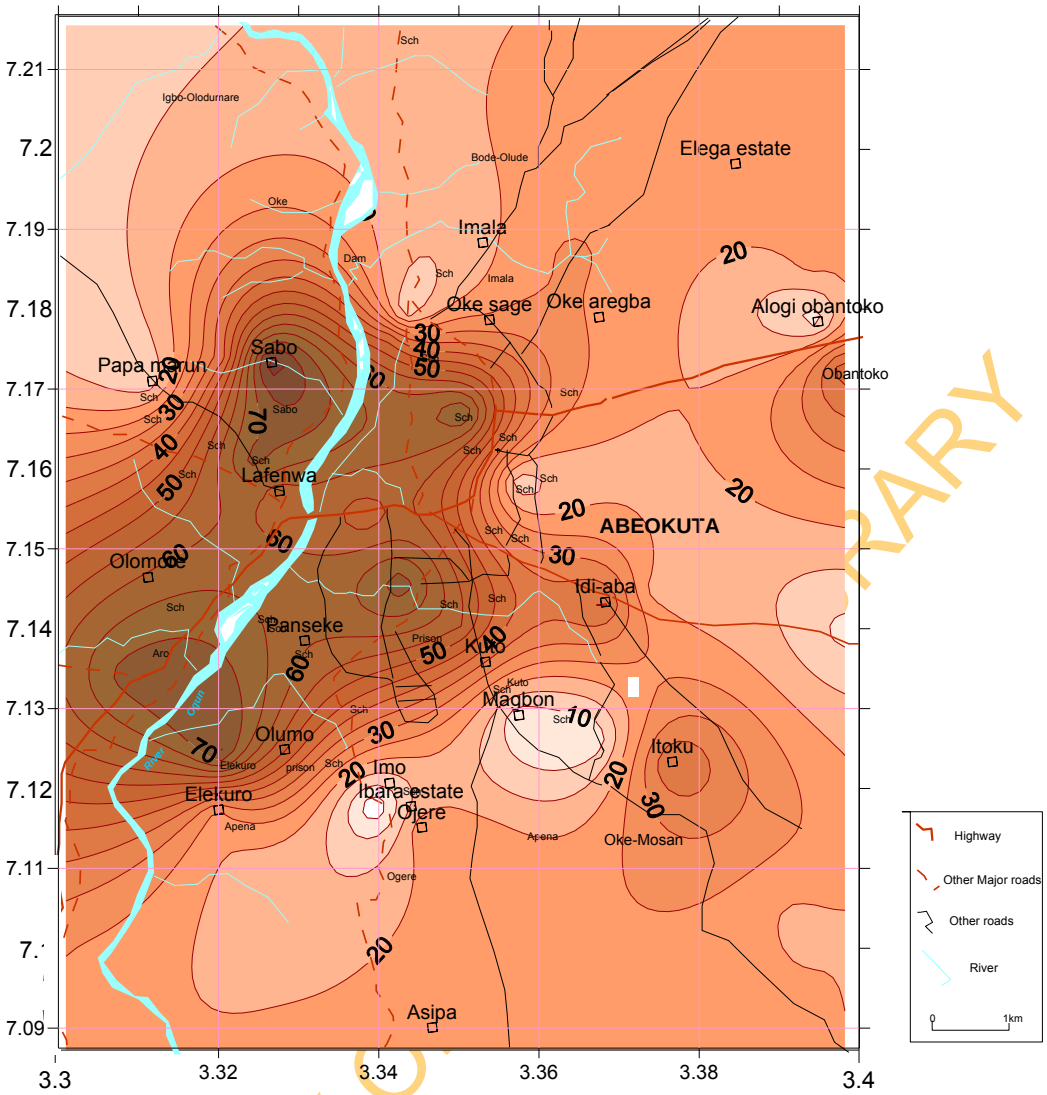

Fig 4.88: Hydrochemical map of calcium in groundwater of Abeokuta area

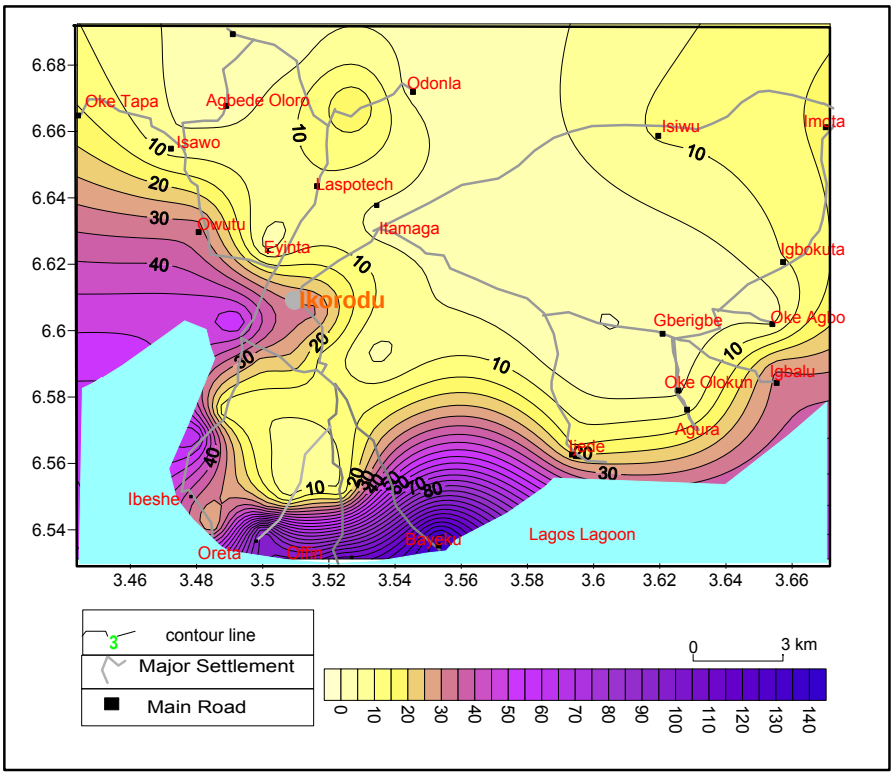

(a)

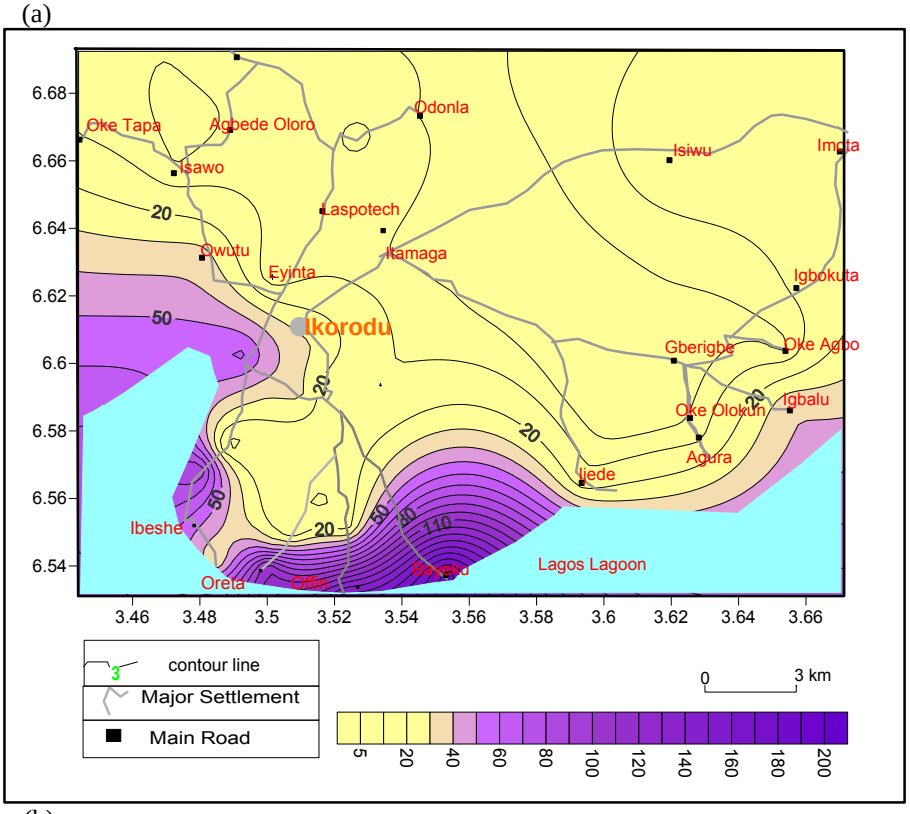

(b)

Fig 4.89: Hydrochemical maps of (a) Na^+ (mg/l) and (b) Cl^-(mg/l) in groundwater of Ikorodu Area

sodium and chloride. Magnesium and sulphate ions exhibit this trend; however the concentration of these ions are generally low in every part of Ikorodu with the exception of Baiyeku and its environs, affected by occasional flooding from Lagos lagoon during heavy storms, as a result of its low elevation above sea level (less than 3 m). The groundwater in these areas is therefore affected by direct percolation of lagoon water. The isocone of total dissolved solids (Fig. 4.90) reveals that only groundwater in these areas (Baiyeku, Offin and part of Oreta) have TDS greater than 1000 mg/l (green contour line) the threshold value for fresh water (Todd, 1980). Calcium and bicarbonate similarly have elevated concentration in some areas adjacent to the lagoon. However, some other landward areas have high concentration of these ions. Manganese and barium are strongly related as indicated by the very high correlation coefficient of 0.73 between the two metals and the very similar isocones of the metals (Fig 90 a & b). In addition, concentrations of the metals occur in excess of WHO (2006) guideline for drinking water for these metals (red contour lines in Fig. 91 a & b).

As noted by Singhal and Gupta (1999), the isochlor map (Fig 4.88b) depicting the distribution of chloride ion is a good indicator of groundwater flow direction as chloride concentration is likely to increase in the flow direction. Furthermore, the direction of groundwater movement and distance of given groundwater sample from its initial recharge area can be determined using HCO_3^-/Cl^- (eq/l) ratio. The ratio of HCO_3^-/Cl^- will decrease in the direction of flow (Fig. 92) due to greater dissolution of Cl^-. The SO_4^{2-} and TDS will increase in the direction of groundwater flow (Singhal and Guptal, 1999; Verma and Jolly, 1992).

The combination of these parameters in the study area reveal that groundwater flow direction in Ikorodu area is NE-SW direction, as chloride, sulphate and TDS increase in this direction while HCO_3^-/Cl^- (eq/l) decreases consistently in the same direction.

4.6 Isotopic Characteristics of Groundwater in the Study Areas

From the ocean to precipitation to recharge the stable isotopes are modified such that each environment has a characteristic isotopic signature. This signature serves as a natural tracer for the provenance of groundwater. Many studies including those by Onugba et al (1989), Xong et al (1999), Tijani and Abimbola (2003), Hernandez-Garcia and Custodio (2004), Porowski (2004) Onugba and Eduvie (2005) and Diop and Tijani (2008) have shown relevance of complementing hydrogeochemical characteristics of groundwater with isotopic data especially in provenance studies. In addition to provenance study, it is used to study recharge processes, subsurface processes, geochemical reactions and reaction rates. The importance of isotopes in the studies of biogeochemical cycles and soil-water- atmosphere processes is increasingly being

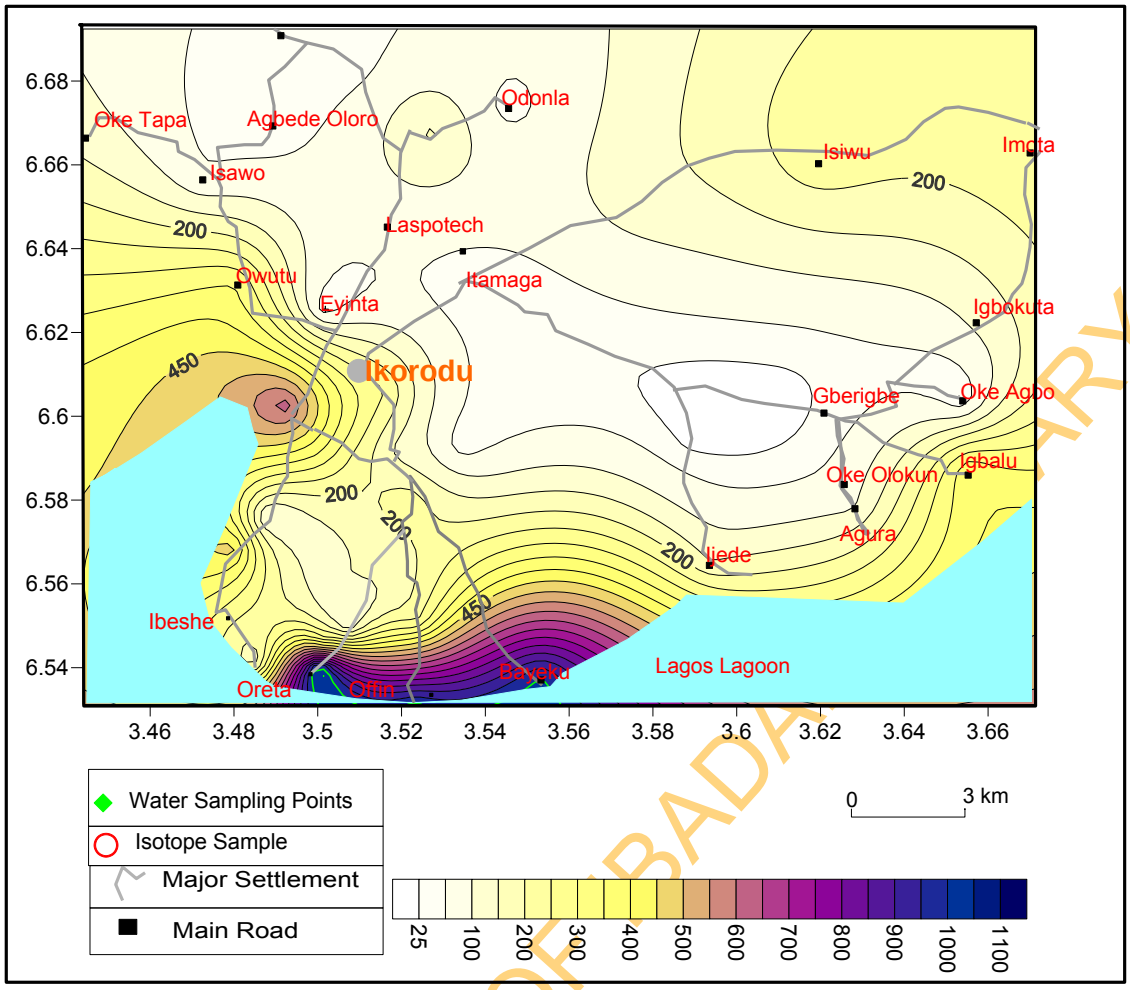

Fig 4.90: Hydrochemical map of TDS (mg/l) in groundwater of Ikorodu area.

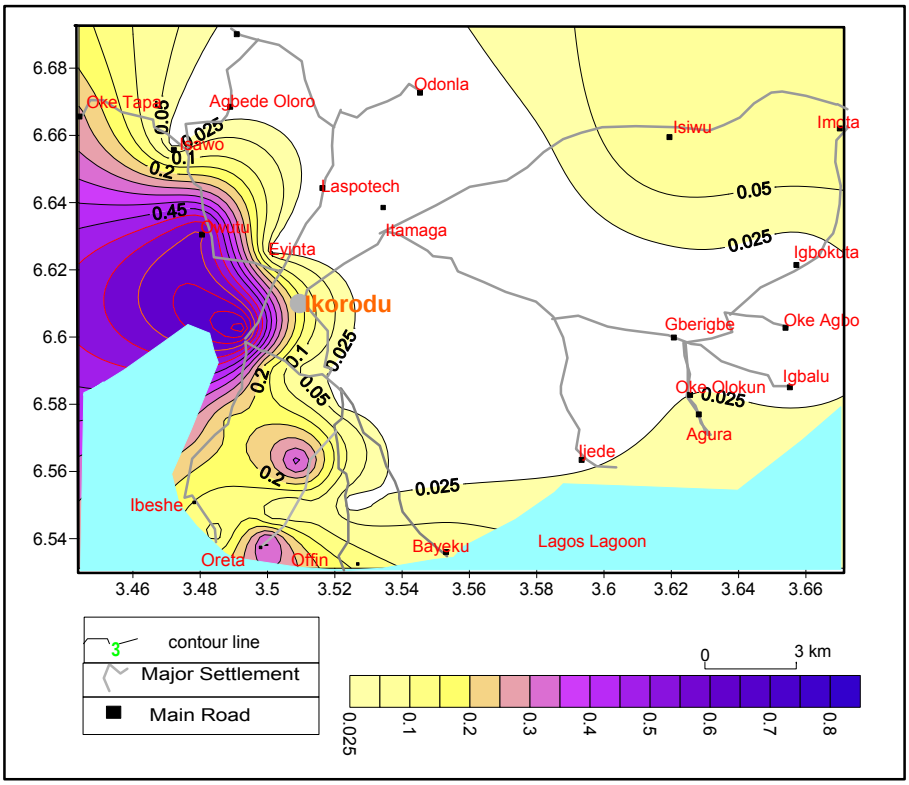

(a)

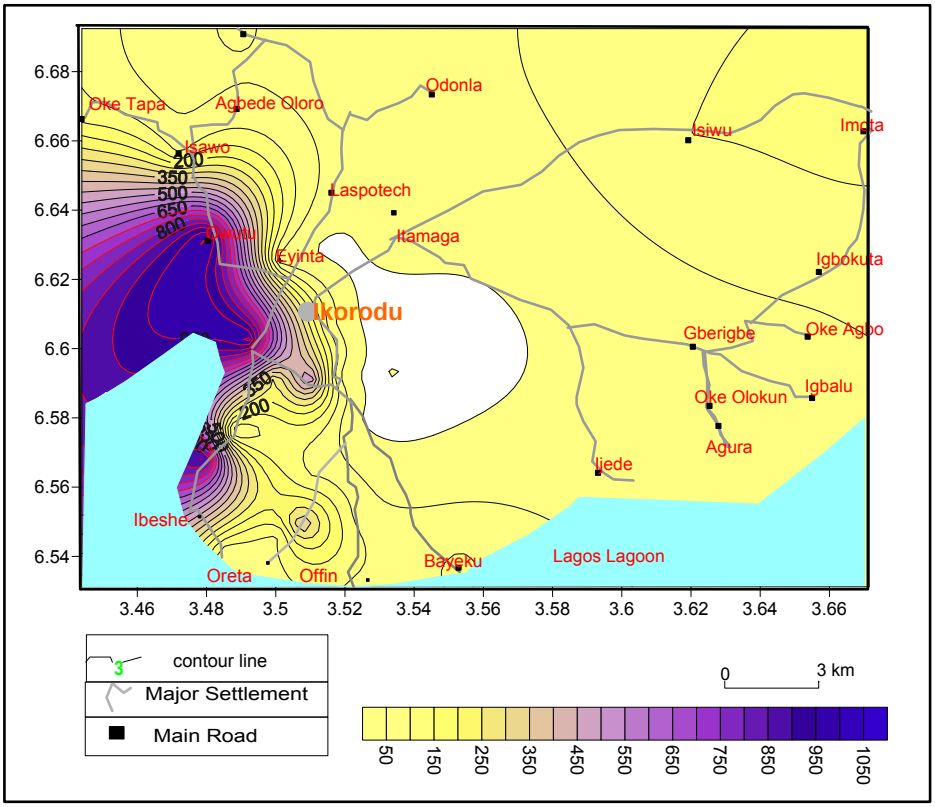

(b)

Fig 4.91: Hydrochemical maps of (a) Manganese in mg/l and (b) Barium ug/l in groundwater of Ikorodu Area

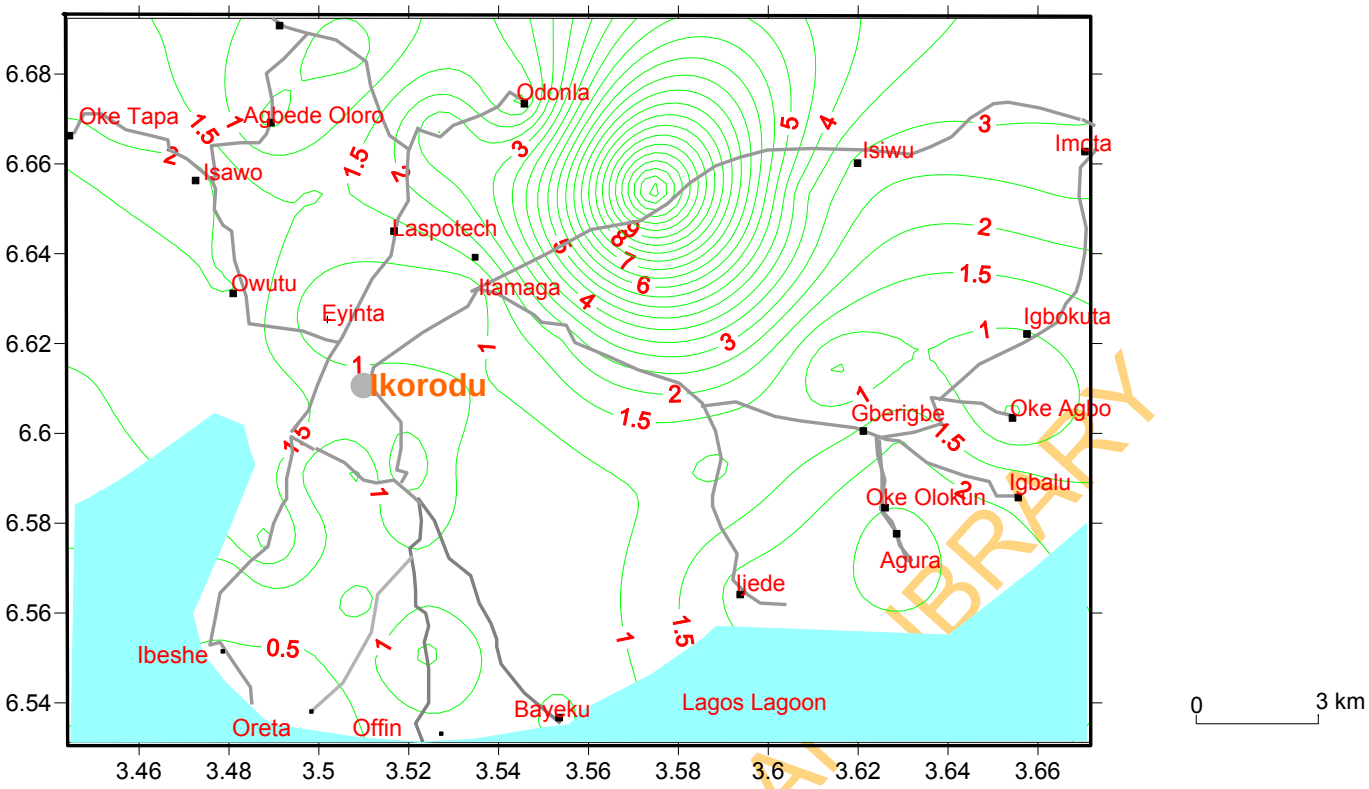

Fig 4.92: Hydrochemical map of HCO_3^-/Cl^- in groundwater of Ikorodu area

recognized, and new applications in contaminant hydrogeology are being made. In this study deuterium and oxygen 18 were employed specifically to study the groundwater provenance. The data on oxygen 18, deuterium and deuterium excess in Abeokuta and Ikorodu areas are presented in Table 4.16. The data on the isotopic composition in the study areas are all reported in per-mille (‰) with reference to the V-SMOW (Vienna Standard Mean Ocean Water), with accuracy of ±0.3 ‰ for deuterium and ± 0.06 ‰ for ^{18}O.

4.6.1 Oxygen 18 and Deuterium in Groundwater of the Study Areas

In Abeokuta area, deuterium (^{2}H) varies from -7.6‰ to -11.1‰ with a mean value of 10.0 ‰ while oxygen 18 (^{18}O) varies from -2.29 ‰ to -2.71 ‰ and averages -2.55‰ (Table 4.17). Groundwater in the coastal plain sands and recent sediments of Ikorodu area, south-western has $\partial^{2}H$ that varies from -14.2 ‰ to -18.5 ‰ with a mean of -16.09 ‰ while $\partial^{18}O$ varies from -2.46 to -3.29 with a mean of -2.86. In Oke-Ogun area of south-western Nigeria, Tijani and Abimbola (2003) obtained $\partial^{2}H$ that varies from -20.8 ‰ to -11.9 ‰ with a mean of -15.4 ‰ and $\partial^{18}O$ of between -3.61 ‰ and -1.96 ‰ with a mean of -2.97 ‰ . The oxygen 18 and deuterium in groundwater of Abeokuta and Ikorodu areas are enriched relative to the oxygen 18 and deuterium in the groundwater of Oke-Ogun area due to latitude effect. The Oke Ogun area is located at higher latitude (between latitude 7.83^{0} and 8.83^{0}) compared with the study area. As highlighted by Appelo and Postma (2005), rain is generally more depleted in higher and colder latitudes.

As a result of stronger kinetic fractionation in ^{18}O than in ^{2}H, the water becomes relative to equilibrium process more depleted in ^{18}O than in ^{2}H (Appelo and Postma, 2005). Therefore, there is greater depletion on ^{18}O than ^{2}H and hence, there is deuterium excess calculated from analyzed value by Appelo and Postma (2005) as

$$d = \partial^{2}H - 8\,\partial^{18}O \qquad \text{.....4.10}$$

The deuterium excess calculated from equation 4.10 in Abeokuta area varies from 9.60 to 11.4 with a mean value of 10.43 while in Ikorodu area the deuterium excess range from 5.6 to 7.8 and it averages 6.82 in the groundwater of the area. The basic relationships between ^{18}O and ^{2}H in groundwater of the study areas are shown in Figs.4.93 a & b. The ^{18}O and ^{2}H of the groundwater samples in the study areas show similar trends (Fig 4.93). This observation is further reinforced by the strong positive correlation of 0.88 and 0.92 obtained between deuterium and oxygen 18 respectively for Abeokuta and Ikorodu areas. The regression line of the groundwater in Abeokuta and Ikorodu areas presented in equations 4.11and 4.12 respectively, fulfil

Table 4.17: Isotopic composition of groundwater in the study areas

Sample no	Abeokuta			Ikorodu		
	d O18	**d D**	**D-Excess**	**δ O18**	**δ D**	**D-Excess**
	‰	‰		‰	‰	
1	-2.71	-11.1	10.6	-2.80	-15.2	7.2
2	-2.29	-7.6	10.8	-2.93	-16.6	6.8
3	-2.59	-10.3	10.4	-3.29	-18.5	7.8
4	-2.57	-10.5	10.0	-3.19	-18.3	7.2
5	-2.58	-10.5	10.2	-3.0	-16.6	7.4
6	-2.62	-10.8	10.2	-2.46	-14.0	5.7
7	-2.50	-10.4	9.6	-2.57	-14.3	6.2
8	-2.52	-9.8	10.4	-2.48	-14.2	5.6
9	-2.46	-8.9	10.8	-3.10	-17.8	7.0
10	-2.70	-10.2	11.4	-2.84	-15.4	7.3
Average	-2.55	-10.1	10.4	-2.86	-16.1	6.8

$$\partial\,^{2}H = 7.59\,\partial^{18}O + 9.30. \ldots\ldots\ldots\ldots\ldots 4.11$$

$$\partial\,^{2}H = 5.84\,\partial^{18}O + 0.81. \ldots\ldots\ldots\ldots\ldots 4.12$$

In Abeokuta area, the Local Meteoric Water Line (LMWL) established is very similar and close to the equation of the global meteoric water line ($\partial\,^{2}H=8\,\partial^{18}O + 10$). This indicates that the origin of groundwater can be related to meteoric source i.e recent precipitation water formed by Rayleigh's under equilibrium conditions, recharging the associated shallow basement aquifer with little or no kinetic evaporation. This agrees with the findings of Xong et al (1999), Tijani and Abimbola (2003), Onugba (2005) and Diop and Tijani (2008). This is a typical equation of groundwater in the basement complex aquifer (Xong et al, 1999; Onugba 2005; Diop and Tijani, 2008). As noted by Tijani and Abimbola (2003), this is reflected in the fact that the average deuterium excess, d-values range from 9.6-11.1 (10±1.1), very close to 10, the d- value of meteoric water. In Abeokuta area, some samples are found above the GMWL, suggesting a recent recharge history but they may have suffered evaporative effects, resulting in some fractionation, thus, leading to an enrichment of the groundwater in the area (Pelig-Ba, 2008).

Samples with similar isotopic composition as the precipitation, as indicated by those plotted on the GMWL, are regarded as recharging directly from local precipitation through preferential flow channels such as cracks or fractured zones (Mathieu & Bariac, 1996).

In this case, rainwater flows through macro pores and preferential flow channels to the water table with little mixing taking place (Clark & Fritz, 1997). As noted by Pelig-Ba (2008) the open crevices and fractures in some selected places in the Basement Complex allow easy heat flow into the water table to cause more evaporation than the relative effect of capillary heat flow into the water table usually observed in sedimentary terrains. This explains the higher isotopic enrichment observed in the Basement Complex area than in the sedimentary area.

In Ikorodu area, the little differences in isotopic characters resulted in the data plotting in a tight group. This indicates groundwater from the sampled region originating from same sources independent of lithologic unit and groundwater mixing between the lithologic units may be ongoing. Onugba and Eduvie (2005) classified groundwater within the Bima sandstone with deuterium and oxygen values in per mille that falls within this range as precipitation during colder climatic conditions that now represent paleo-climatic recharge termed ‘ancient’ water. In the area, as shown in Fig 4.93, the data plot on the right side of GMWL and the (LMWL) slope of 5.84 as well as the deuterium excess deviate considerably from the slope and the deuterium excess of GMWL. These indicate the depletion of Oxygen 18 and deuterium relative to meteoric

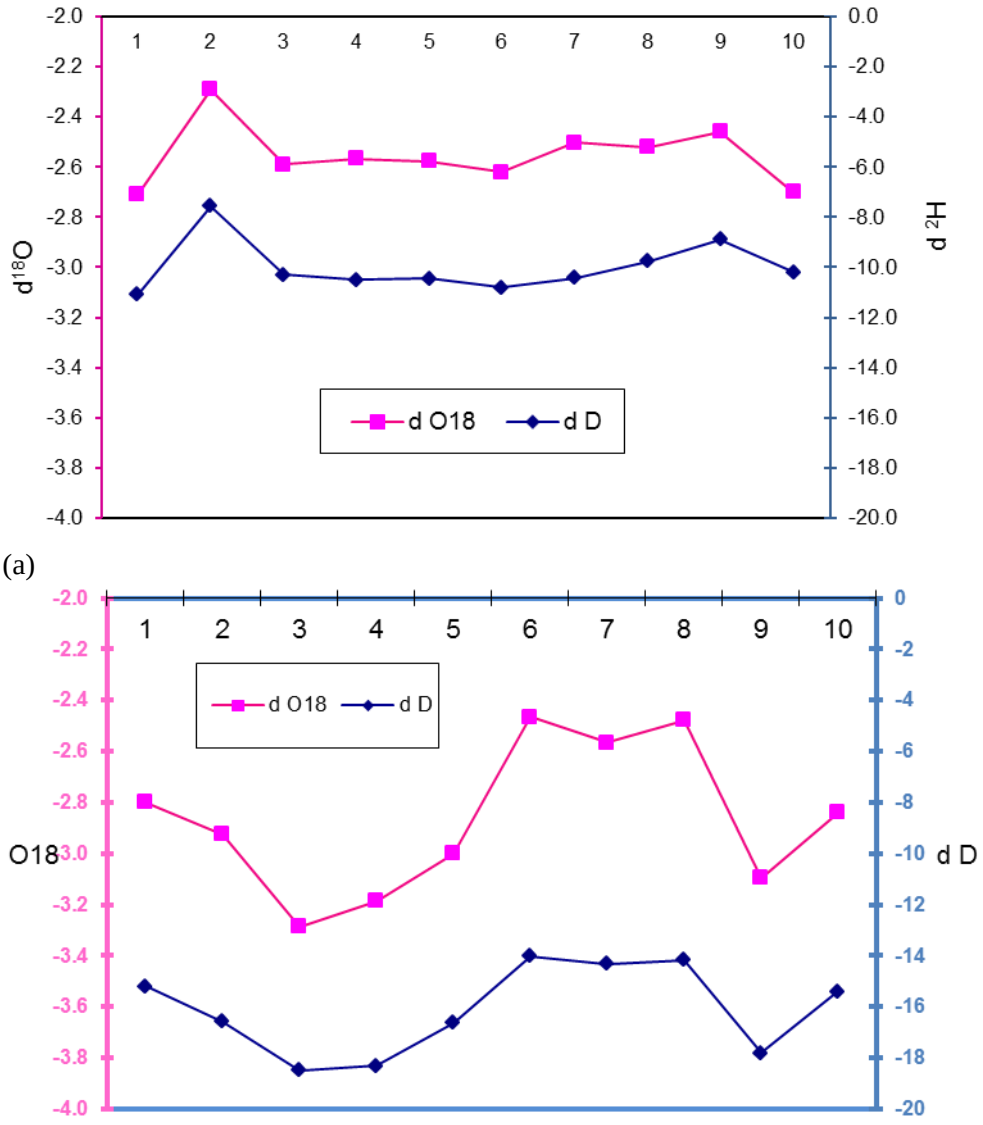

Fig. 4.93: Trend between $d^{2}H$ and $d^{18}O$ in groundwater of (a) Abeokuta & (a) Ikorodu area

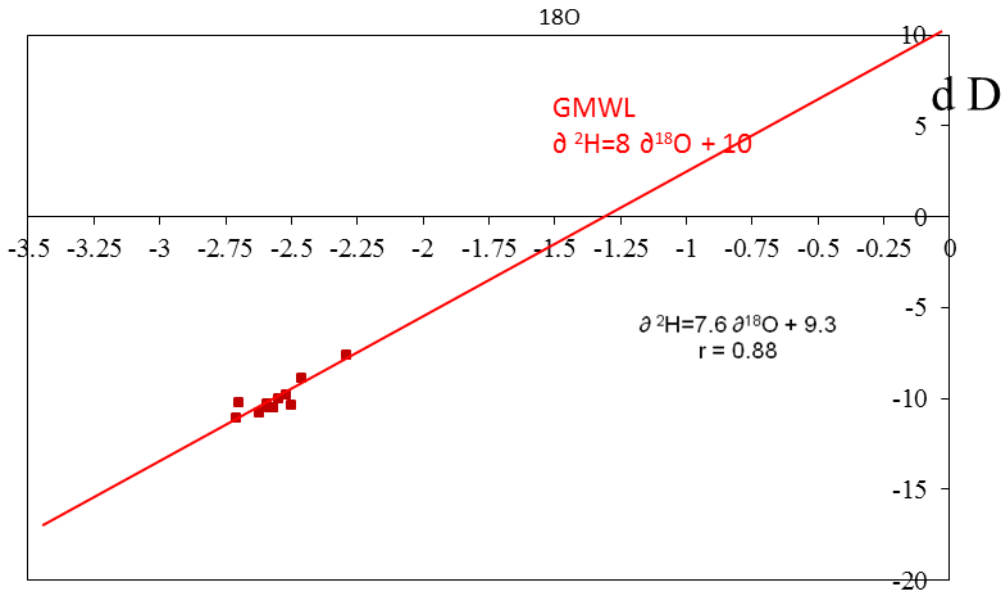

(a)

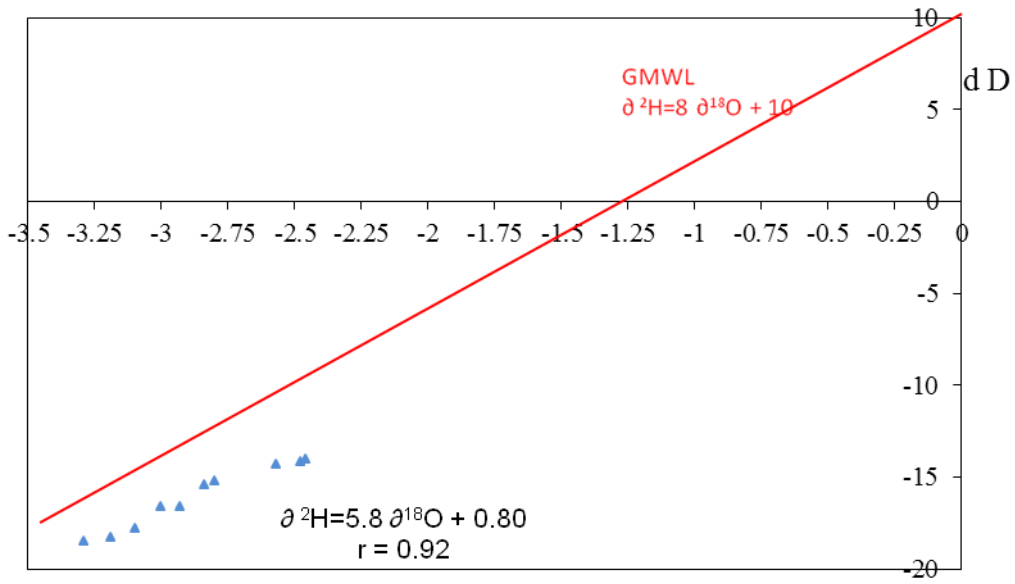

(b)

Fig.4.94: Cross plot of deuterium and oxygen 18 in groundwater of (a) Abeokuta (b) Ikorodu

water. The depletion of Oxygen 18 and deuterium relative to meteoric water, according to Pelig-Ba (2008), can be caused by three factors, namely: (i) Rainfall might have suffered some level of evaporation before reaching the groundwater table; (ii) groundwater might not have been recharged from the local precipitation but from distant sources; and (iii) isotopic exchange between enriched groundwater and aquifer materials, thus, reducing the amount of heavy isotope content in the groundwater as compared to the rainfall. Ikorodu and Abeokuta areas have similar climatic conditions, therefore, as shown by the isotopic character of groundwater in Abeokuta area, groundwater recharge is done with little or no kinetic evaporation, therefore since the climatic conditions in the two areas are similar, evaporation will have little or no influence on the recharge of groundwater in Ikorodu area. As shown in earlier discussions in section (4.3.3), the aquifers in the area are connected and are recharged by local precipitation in the exposed area. The deeper nature of the aquifer in the area suggests the isotopic exchange with aquifer minerals is occurring in the system.

The relationships between deuterium and oxygen-18 as shown in the preceding discussions vary in the two locations (Abeokuta and Ikorodu), both in slope and intercept (d) called d-value of the equation. The variation in d values can be caused by many mechanisms (Eraifej and Abu-Jaber, 1999) that include the source of vapour, type of cloud causing precipitation and the climate where the rain falls (Gat, 1980) .Comparatively the trend of $\partial^{2}H$ and $\partial^{18}O$ in the study areas are similar. However, isotopes (^{18}O and ^{2}H) in groundwater from Abeokuta area are generally heavier than those in the groundwater of Ikorodu area and are similar to meteoric water. On the contrary, groundwater in Ikorodu area has isotopic composition that is depleted relative to meteoric water largely due to isotopic exchange between groundwater and the aquifer materials.

CHAPTER FIVE

CONCLUSIONS AND RECOMMENDATIONS

5.1 Conclusions

Geological, geophysical, geochemical characteristics of rocks and groundwater in parts of Abeokuta and Ikorodu areas of southwestern Nigeria were carried to evaluate the occurrence, quality and geochemistry including the isotopic characteristics of groundwater. The study revealed the following:

Abeokuta and its environs are underlain by hornblende-biotite gneiss, porphyroblastic gneiss, granite, porphyritic granite and pegmatite intrusions. The rocks have distinct textures, mostly acidic and have similar mineralogy and chemistry. The relative abundance of the oxides in the rocks is in the order SiO_2>Al_2O_3>K_2O>Na_2O>CaO>MgO with varying concentrations of heavy and trace metals (such as Pb, Co, Sr). The surficial materials in Ikorodu include clay in the landward area and sand in the coastal area. The two earth materials are parts of the recent alluvium and the coastal plain sands, which underlie most parts of Lagos area.

Geophysical studies reveal the dominance of the AK type-curves in Ikorodu area constituting over 56% while the H type -curves which constitutes more than 72% dominated the curve types in Abeokuta area. The AK curve in Ikorodu typically represents a succession of clay to sandy clay overlying sand, which is underlain by resistive sand (ferruginized) that overlies clay which grades to sandy clay. The H curve, on the other hand, represents topsoil overlying a low resistivity intermediate layer made up of clay to sandy clay overlying the basement. Areas in Abeokuta underlain by porphyroblastic gneiss and porphyritic granite have geo-electric parameters that favour high groundwater occurrence than the areas underlain by either granite or hornblende biotite gneiss. Over 50% of Abeokuta area has poor groundwater potential based on geophysical parameters and geological considerations while less than 25% of the area has high groundwater potential, mainly in parts of Abeokuta underlain by porphyroblastic gneiss and porphyritic granite. In Ikorodu area, domestic water needs are largely supplied by two aquiferous horizons; the upper and the lower sands. While the upper sand supports only shallow hand-dug wells exclusively around the coastal area, the lower sand provides groundwater supply in the landward areas.

The groundwater in the weathered/fractured aquifer in Abeokuta area is generally fresh, slightly acidic to alkaline and has higher TDS in areas close to R. Ogun. On the other hand, groundwater in Ikorodu is mostly fresh, acidic to alkaline with low TDS except in the area close to the Lagos lagoon. The order of abundance of the main constituents of groundwater are Na^+ >K^+ >Ca^{2+}>Mg^{2+} and HCO_3^->Cl^->SO_4^{2-} respectively of the cations and anions in Abeokuta area.

In Ikorodu area, the order of major ionic constituents are $Na^+ > Ca^{2+} > K^+ > Mg^{2+}$ and $HCO_3^- > Cl^- > SO_4^{2-}$ respectively of the cations and anions, with high concentration of chloride (>40 mg/l) in the area around the lagoon. The high concentration of chloride in groundwater indicates the percolation of the lagoon water in area around the lagoon as a result of encroachment of the coastal area by lagoon water through flooding during storms.

Nitrate in most of the groundwater samples (70%) of Ikorodu area is mainly from natural sources while in some places in Abeokuta area nitrate concentration in groundwater is greater than the range expected from natural sources. However, in Ikorodu area, anthropogenic influence on groundwater around the Lagoon area is indicated by relationship between depth and nitrate. In Abeokuta area, the strong correlation coefficient established between nitrate and chloride indicates significant anthropogenic contribution of nitrate to groundwater chemistry. Generally, in both areas, there is fluoride deficiency in groundwater however, the deficiency is more pronounced in groundwater from Ikorodu Area. Abeokuta and some parts of Ikorodu have excess concentration of aluminium, barium, iron and manganese. While iron and manganese affect water taste and acceptability, Lead (Pb) is present in the groundwater in some parts of the study areas above permissible level.

Groundwater in Abeokuta environs is alkaline-earth water having mostly Ca(Mg)-Na-HCO_3 and Ca(Mg)-Na-HCO_3-Cl water-types (90%) and with pockets of other water types (mostly alkaline) that include $CaHCO_3$, $NaHCO_3Cl$, $NaHCO_3$ and NaCl. Groundwater character in Abeokuta area is largely influenced by River Ogun. Furthermore, concentration of most heavy/trace metals is largely influenced by their relative concentration in the underlying rocks. Eighty percent of the groundwater in Ikorodu area is mostly alkaline water. The groundwater character of the area is dominated by Ca-Na-HCO_3 (30%), $NaHCO_3$-Cl (30%) and NaCl (14%). The lagoon area is dominated mainly by Na-HCO_3-Cl and NaCl while the landward area is dominated by Ca-Na-HCO_3 water type. Furthermore, groundwater character is influenced largely by silicate weathering, ion exchange as well as the Lagos lagoon.

The isotopic character of groundwater in Abeokuta is defined by $\partial^2H=7.59\ \partial^{18}O + 9.30$, suggestsing recharge is dominated by precipitation (meteoric source) with little or no influence of evaporation. The character in Ikorodu area is defined by $\partial\ ^2H=5.84\ \partial^{18}O + 0.81$, which indicates isotopic exchange between enriched groundwater and the aquifer materials, thus reducing the amount of heavy isotope content in the groundwater.

In Ikorodu area, the presence of localized resistive sands several meters thick pose a major challenge (in terms of cost) for manually rotated drilling method often used for drilling in many parts of southwestern Nigeria underlain by sedimentary rocks. In addition, abrupt rapid

change in facies common in this area suggests the need for comprehensive pre-drilling groundwater exploration for construction of successful boreholes. In Abeokuta area the low groundwater potential in most parts of the study area suggests the need for detailed groundwater exploration for location and construction of successful boreholes. The groundwater character in Ikorodu is largely influenced by geogenic factors, however character of groundwater in shallow wells in areas with low elevation around the Lagos lagoon is partly influenced by the lagoon.

Groundwater potential in the area underlain by crystalline rocks in Abeokuta is influenced by the rock types and the groundwater chemistry in Abeokuta is significantly influenced by the ionic contributions from anthropogenic sources. The major constituents of groundwater are within the guidelines and standards for potable water but deficiency and excessive concentration of minor/trace constituents of groundwater that affect palatability (acceptability) and potability of groundwater are common in the study areas.

5.2 Recommendations

Similar studies covering groundwater occurrences, characters, quality and provenance should be extended to other areas with limited hydrogeological information. Assessment of groundwater potability and palatability should not be limited to the major cations and anions in groundwater. Studies on groundwater quality should incorporate heavy metals and other trace elements concentrations in groundwater, as these trace constituents in small quantities affect groundwater potability.

More studies on isotopic characteristics of groundwater in other areas should be encouraged in order to generate quality data which can be available for future groundwater monitoring and assessment.

REFERENCES

Abimbola, A. F., Odukoya A.M and Olatunji. A. S. (2002): Influence of bedrock on the hydrogeochemical characteristics of groundwater in northern parts of Ibadan Metropolis. Water Resource-journal of Nigerian Association of Hydrogeologists (NAH) Vol 13 pp1-6

Abimbola, A.F, Tijani, M. N. and Nurudeen, S.I. (1999): Some aspect of groundwater quality in Abeokuta and its environs, southwestern Nigeria. Water Resource-journal of Nigerian Association of Hydrogeologists (NAH) Vol 10 pp. 6-10.

Acworth, R. I. (1987): The development of crystalline Basement aquifer in a tropical environment. Q.J Eng Geo London 20:265-272.

Adebanjo, O. F (2008): Geology and hydrogeochemistry of groundwater in Ago-Iwoye, southwestern Nigeria. Unpublished B.Sc., thesis, Olabisi Onabanjo University, Ago-Iwoye, 79p.

Adegoke, O. S. (1969): Eocene stratigraphy of southwestern Nigeria. Mineral Memoir,69, 23-46

Adegoke O. S. (1970): type section Ewekoro formation (Palaeocene) of western Nigeria, bio-stratigraphy and microfacies .4th African Micropal.Coll Abidjan (1970), 37-39

Adelana S. M. A and Olasehinde, P. I., (2001): Hydrogeological investigation of Sokoto Basin using environmental Isotopes. Water Resources, Journal of Nigeria Association of Hydrogeologists, Vol. 12, pp22-26.

Adeyemi, G.O (1991): Lineament nature and groundwater accumulation in the basement complex of southwestern Nigeria. Nigeria Journal of science, 25, p111-118

Agagu, O.K (1985): A geological guide to bituminous sediments of southwestern Nigeria. Unpublished report of Department of geology, Ibadan: University of Ibadan, 16.

Ajayi C.O. and Hassan, M., (1990): The delineation of the aquifer overlying the basement complex in the western part of the Kubani Basin of Zaria (Nigeria). Journal of Mining and Geology, 26, 117-125.

Akanni, C.O. (1992): Relief, drainage, soil and climate of Ogun state in: Ogun State in maps. Eds. Onakomaiya, S.O, Oyesiku, O.O and Jegede, F.J. Published by Rex Charles publication, pp 6-20.

Ako B. D, Ajayi, T. R., Arubayi, J. B and Enu, E. I (2005): The groundwater and its occurrence in the coastal plains sands and alluvial deposits of parts of Lagos State, Nigeria Water Resources 16;7-17.

Amadi, U. M. P. (1987): Mixing phenomenon in groundwater systems and its relevance in water quality assessment in Nigeria. In: Iwugo,K (Ed) Paper presented at the 2nd annual Symposium/Conference of the Nigerian water & sanitation Association. pp 17.1-17.31

Amadi, P. A.; Ofoegbu, C. O and Morrison, T; (1989): Hydrochemical assessment of groundwater quality in parts of Niger Delta, Nigeria. Environ. Geol. Water Sci., vol. 14, no. 3, p195-202.

Appelo C. A. J and Postma, D., (2005): Geochemistry, Groundwater and Pollution, 2nd Edition, A.A. Balkema Publishers, Leiden, Netherlands,649p.

Back W. (1961): Techniques for mapping hydrochemical facies. US Geol. Survey Prof. Paper 424-D.

Barker, R. D., White, C. C. and Houston, J. F. T. (1992): Borehole siting in an African accelerated drought relief project. Hydrogeology of Crystalline Basement Aquifers in Africa, In: E.P Wright, and W.G. Burgess, Geological Society of London Special Publication No. 66 pp. 183-201

Bayowa, O. G., Olorunfemi M. O. and. Ademilua L.O :(2007) A Comparative Study of the Accuracy of Preliminary Interpretation Techniques in Computer-aided Vertical Electrical Sounding (Ves) Data Interpretation, Journal of Applied Sciences Research, 3(10): 1001-1009.

Berggren, W. A., (1960): Paleocene biostratigraphy and planktonic foraminifera of Nigeria (West Africa). Proc. XX1st. Int. Geol. Congress, Pt. 6.

Bhattacharya, P. K., and Patra, H. P. (1968). Direct Current Geo-electric Sounding. Elsevier Pub. Co., Amsterdam,

Billman, H. G., (1976): Offshore stratigraphy and Paleontology of Dahomey Embayment, West Africa Proc. 7th African Micropaleontology Conference, Ile-Ife

British Geological Survey (2003): Water fact Sheet: Manganese p1-4

Browning E. (1961): Toxicity of industrial metals. Butterworth, London

Burke, K. C. and Dewey, J. F. (1972): Orogeny in Africa. In: Africa Geology (edited by Dessauvagie, T. F.J. and Whiteman, A. J.) Ibadan University Press, p. 583-608.

Buttle, J. M., (1994): Isotope hydrograph separations and rapid delivery of pre event water from drainage basins. Progress in Physical Geography, 18: 16-41.

Canter L. W (1996): Nitrates in groundwater CRC lewis Publ. New York 263p.

Cawte, J., Hams, G. and Kilburn, C., (1987): Manganism in a neurological ethnic complex in northern Australia. The Lancet, 2, 1257.

Cerling T. E., Pederson B. L., Damm K. L. V. (1989): Sodium-calcium ion exchange in the weathering of shales: Implications for global weathering budgets. Geology 17:552–554

Chebotarev I. I. (1955): Metamorphism of natural waters in the crust of weathering. Geochim Cosmochim Acta 8 : 22–48, 137–170,198–212

Chilton, P. J and Smith-Carington, A. K., (1984): Characteristics of weathered basement aquifer in Malawi in relation to rural water supplies. IAH publications, No144,57-72.

Clark, I. and Fritz, P., 1997. Environmental isotopes in hydrogeology. CRC Press, Boca Raton, Fl, 328 p.

Close M. E. (1987): irrigation and groundwater-friend or foe. Soil water. Winter :10-13

Cooray, P. G., (1977): Classification of the charnockitic rocks of Nigeria: Journal of Mining and Geology, v.14, p.1-6.

Coplen, T. B., (1994): Reporting of stable hydrogen, carbon, and oxygen isotopic abundances. Pure Appl. Chem., 66: 273-276.

Coplen, T. B., (1995): Discontinuance of SMOW and PDB. Nature, 375(6529): 285.

Coplen, T. B., (1996): New guidelines for reporting stable hydrogen, carbon and oxygen isotope-ratio data. Geochim. et Cosmochim. Acta, 60: 3359-3360.

Craig, H. (1961): Isotopic variations in meteoric waters. Science 133, 1702-1703.

Custodio E and Liamas, M. R. (1983): Hidrologia subterranean, "2nd edition, Omega, Barcelona

Dan-Hassan, M. A and Adekile, D. A. (1991): Geophysical exploration for groundwater in crystalline basement terrain: A case study of Zabenawan Dansudu, Kano State, Nigeria.

Dansgaard W. (1964): Stable isotopes in precipitation. Tellus 15(4) : 436–468

David L.M., Jr. (1988): Geoelectric study of shallow hydrogeological parameters in the area around Idere, southwestern Nigeria, PhD thesis, University of Ibadan

Davis, S. N. and De Weist, R. J. M., (1966): Hydrogeology, John Wiley , New York, 453pp.

Diop, S. and Tijani M. N (2008): Assessing the basement aquifers of Eastern Senegal. Hydrogeology Journal 16:1349-1369.

Dissanayake, C. B. (1991): The fluoride problem in the groundwater of Sri-Lanka-environmental management and health. Int. Jour. env. Studies, 38, 137-56.

Dobrin M. B. (1976): Introduction to geophysical prospecting (3rd Ed) McGraw Hill. N.T

Domenico P. A. (1972): Concepts and models in groundwater hydrology. McGraw-Hill, New York

Ehinola O. A. (2002): Hydrochemical characteristics of groundwater in parts of the basement complex of southwestern Nigeria. Journal of Mining and Geology. Vol 38(2) pp125-133

Elango L., Kannan R. and Senthil Kumar M. (2003): Major ion chemistryand identification of hydrogeochemical processes of groundwater in a part of Kancheepuram district, Tamil Nadu, India. J Environ Geosci 10(4):157–166

Elueze, A. A, Omidiran, J. O and Nton, M. E (2004): Hydrogeochemical investigation of surface water and groundwater around Ibokun, Ilesha area, southwestern Nigeria. Journal of Mining and Geology.Vol10(1) pp57-64.

Epstein S. and Mayed T. (1953): Variation of O18 content of waters from natural sources Geochim. Cosmochim. Acta 5: 213-224.

Eraifej N and Abu-Jaber (1999): Geochemistry and pollution of shallow aquifers in Mafraq area, north Jordan. Environmental Geology, 37 (1-2): 162-168

Ezeigbo, A. A. (1989): Groundwater Quality Problem in parts of Imo State, Nigeria. Nig., J. of Min. and Geol. Vol. 25, pp. 10-22.

Falconer, J. D. (1911): The geology and geography of northern Nigeria, Macmillan, London. 237p.

Faure G. (1986): Principles of Isotope Geology. 2nd Edition, John Wiley and Sons, New York, 589pp.

Fayose E. A. (1970): Stratigraphical Paleontology of Afowo 1 well SW Nigeria Jour. Min. Geol. Nigeria. Vol 5, no 1.

Fisher R. S and Mulican III W. F. (1997): Hydrochemical evolution of sodium-sulphate and sodium-chloride groundwater beneath the Northern Chihuahuan desert, Trans-Pecos, Texas, USA. Hydrogeol J 5(2):4–16

Foster, H. D. (1992): Health, Disease and the Environment. Belhaven Press, London.

Foster S. S. D (1993): Groundwater conditions and problems characteristic of the humid tropics. In: Hydrology of warm humid regions. IAHS Publ. No. 216, pp 433–449

Freeze R. A. and Cherry J. A (1979): Groundwater, Prentice-Hall Inc., Englewood Cliffs, New Jersey.

Friberg L., Nordberg G. F., Vouk V. B., eds. (1986): *Handbook of the toxicology of metals.* Vol. II.Amsterdam, Elsevier, pp. 130–184.

Gat J. (1980): The isotopes of hydrogen and oxygen in precipitation. In: Fritz J and Fontes J (eds) Handbook of environmental isotope geochemistry. Elsevier, Amsterdam, 1(A), p 21 Gibbs RJ (1970) Mechanisms controlling world water chemistry.Science 17 : 1088–1090

Gat, J. R. and Gonfiantini R. (1981): Stable isotope hydrology, Deuterium and Oxygen-18 in the water cycle. IAEA, Tech. Rept. Series No.210, 337p.

Gibbs R.J (1970): Mechanism of controlling Water chemistry. Science 17:1088-1090.

Gonfiantini, R. (1978): Standards for stable isotope measurements in natural compounds. Nature 271: 534-536.

Gonfiantini R. (1986): Environmental isotopes in lake studies. In Handbook of Environmental Isotope Geochemistry A., Elsevier.Vol. 1 (ed. P. Fritz and J. C. Fontes), pp. 113-168.

Handa, B. K. (1975): Geochemistry and genesis of fluoride-containing groundwater in India. Groundwater 13, 275-281.

Hazell J. R. T, Cratchley, C. R. and Jones, C. R. C., (1992): The hydrogeology of crystalline aquifers in Northern Nigeria and geophysical techniques used in their exploration. In: Wright, E.P. and Burgess, W.G (eds.).The hydrogeology of crystalline basement aquifers in Africa. Geological Society Special Publication No. 66, 155-182.

Hem, J.D. (1985): Study and interpretation of the chemical characteristics of natural water. US Geological Survey. Water supply paper 2254,3rd ed.263p

Hem, J. D. (1992): Study and Interpretation of the Chemical Characteristics of Natural Water. USGS Water-Supply Paper, 2254

Hernandez-Garcia, M. E. and Custodio E. (2004): Natural baseline quality of Madrid Tertiary Detrital Aquifer groundwater (Spain): a basis for aquifer management. Environmental Geology 46:173-188.

IAEA (1998): Analytical quality in the IAEA isotope hydrology laboratory: Some recent improvements. Water and environment news, IAEA, No.3, pp 5-7.

Idowu, O. A, Ajayi, O. and Martins, O. (1999): Occurrence of groundwater in parts of the Dahomey Basin, southwestern Nigeria. Journal of Min. and Geol. Vol. 35 (2) p229-236.

ISI (1983): Characteristics of drinking water IS:10500, Indian Standard Institute., New Delhi, pp6-11.

Iwami, O., Watanabe, T., Moon, C. S., Nakatsuka, H. and Ikeda, M. (1994): Motor neuron disease on the Kii Peninsula of Japan: excess manganese intake from food coupled with low magnesium in drinking water as a risk factor. The Science of the Total Environment, 149, 121-135.

Jacks, G., Rajagopalan, K., Alveteg, T, and Johnson, M., (1993): Genesis of high-F groundwaters. Southern india. Appl. Geochem. Suppl. Issue 2, 241-244.

Jankowski, J. and Acworth R. I. (1997): Impact of depris-flow deposits on hydrogeochemical processes and the development of dryland salinity in the Yass River catchment, New South Wales, Australia. Hydrogeol J 5(4):71–88

Jones, M. J. (1985): The weathered zone aquifers of the basement complex areas of Africa. Quarterly journal of Engineering Geology, 18, 35-46.

Jones, H. A. and Hockey, R. D. (1964): The Geology of some parts of southwestern Nigeria. Geol. Surv. Nigeria Bull. 31, pp. 87-91.

Joseph D. Ayotte, Martha G. Nielsen, Gilpin R. Robinson, Jr. and Richard B. Moore, (1999): Relation of Arsenic, Iron, and Manganese in Ground Water to Aquifer Type, Bedrock Lithogeochemistry, and Land Use in the New England Coastal Basins, U.S.G.S Water Resource Investigation Reports, WRI-99-4162, 61p

Karagas, M .R., Tosteson T .D., Blum J, Morris J S, Baron, J .A. and Klaue B. (1998): Design of an epidemiologic study of drinking water arsenic exposure and skin and bladder cancer risk in a U.S. population. Environ Health PerspectAugust; 106(Suppl 4): 1047–1050.

Katz B. G., Coplen T. B., Bullen T. D. and Davis J. H (1998): Use of chemical and isotopic tracers to characterize the interaction between groundwater and surface water in mantled Karst. Groundwater 35(6):1014–1028

Keeney D. R (1989): Sources of Nitrate in groundwater. In: Follet R.F.(Ed), Nitrogen Management and groundwater Protection. Elsevier, Amsterdam, NL

Kehinde-Phillips, O. O, Odukoya, A. M and Otuyele, A. S (2005): Health effects of arsenic and cadmium concentrations in the well and surface waters of Ago-Iwoye, southwestern Nigeria. Water Resources 16: 25-30

Kendall, C. and Caldwell, E. A. (1998): "Fundamentals of Isotope Geochemistry", In: C. Kendall and J.J. McDonnell (Eds.), Isotope Tracers in Catchment Hydrology. Elsevier Science, Amsterdam, pp. 51-86.

Knauth, L. P., and M. A. Beeunas, (1986): Isotope Geochemistry of Fluid Inclusions in Permian Halite with Implications for the Isotopic History of Ocean Water and the Origin of Saline Formation Waters: *Geochim. Cosmochim. Acta*, v. 50, p. 419-433.

Le Maitre. R. W., Bateman, P., Dudek, A., Keller, J., Lameyre, J.. Le Bas, M.J., Sabine, P. A., Schmid, R., Sorensen, H., Streckeisen, A., Woolley, A. R. & Zanettin, B., (1989): A Classification of Igneous Rocks and Glossary of terms: Recommendations of the International Union of Geological Sciences Subcommission on the Systematics of Igneous Rocks. Blackwell Scientific Publications, Oxford, U.K.

Lloyd J. W and Heathcote J. A., (1985): Natural inorganic hydrochemistry in relation to Ground Water-An Introduction, Clarendon Press, oxford, p.296.

Löhnert E. (1967): Grundwassertypen tieferer stockwerke in Hamburg, Neues Jahrb geol palaeonto Abh 129(2); 113-136

Löhnert E. (1970): Grundwasserchemismus und kationentauch im norddeutschen Flachland.Z Dtsch geol. Ges Sonderh hydrogeol hydrogeochem no November 139-159

Löhnert E. (1973): Austauchwasser. In: Schneider H (Ed). DieGrundwasserschlieBung 2. Auflage, Essen: Vulkan-Verlag. Pp 138-144

Lusczynski N. J and Swarzenski W. V (1966): Saltwater encroachment in southern Nassau and SE Queens counties, Long Island, New York. US Geol Surv Paper 1613-F

Malomo S. (1983): Weathering and Weathering products of Nigerian rocks: engineering Implications. In ola S.A (Ed), Tropical soils of Nigeria in Engineering practice. Balkema, Rotterdam pp 39-58.

Marie P. J, Ammann P., Boivin G. and Rey, C. (2001): Mechanisms of action and therapeutic potential of strontium in bone *Calcif Tissue Int.* Sep;69(3):121-9.

Mariotti, A., Landreau, A. and Simon, B. (1988): ^{15}N Isotope biogeochemistry and natural denitrification process in groundwater. Application to the chalk aquifer of northern France. Geochim. Cosmoch. Acta. V. 52, p549-555.

Mathieu R. and Bariac, T. (1996): An isotopic study (2H and 18O) of water movements in the clayey soils under semi-arid climate. Water Resources. Res. 32: 779-789

Maya A. L. and Loucks, M. D. (1995): Solute and isotopic geochemistry and groundwater flow in the Central Wasatch Range, Utah.J Hydrol 172:31–59

Mayback M. (1987): Global chemical weathering of surficial rocksestimated from river dissolved loads. Am J Sci 287:401–428

McDonnell, J. J. and Kendall, C. (1992): Stable isotopes in catchment hydrology. EOS, Transactions American Geophysical Union, 73(24): 260-261

Milliot G. (1970): Geology of clays. Springer, Paris Berlin Heidelberg

Monier-Williams, G. W. (1935): Aluminium in Food. Ministry of Health, London.

Moser, H. and Rauert, W. (1980): Isotope methods in hydrogeology (In Deutsch). Lehrbuch, Hydrogeologie, 8, Stuttgart, 400 pp.

Moskowitz P. D., Coveney E. A., Hamilton L. D., Kaplan E. and Medeiros W. H. (1986): Identifying human population at risk from acid deposition mobilised materials in drinking water supplies: A preliminary pilot study. Acid precipitation and health –part 1. Wat. Qual. Bull

Ocan, O. O. (2006): Contributions of Professor M.A.O Rahaman to the understanding of Precambrian geology of Nigeria. In: O. Oshin (ed.), The Basement complex of Nigeria and its mineral resources, a tribute to prof. M.A.O. Rahaman. p3-11.

Odumosu T. (1999): Ikorodu Local government In: Balogun, Y., Odumosu T. and Ojo, K. (eds.) Lagos State in Maps pp142-148.

Offodile, M. E. (2002): Groundwater Study and Development in Nigeria, second edition, Mecon Geology and Eng. Services Ltd, 453p

Ofoma, A. E, Omologbe, D. A and Aigbema, P. (2005): physic-chemical quality of groundwater in parts of Port-Harcourt city, eastern Niger Delta. Water Resource 16: 18-24.

Ogbe, F. A. G (1970): Stratigraphy of strata exposed in Ewekoro Quarry Western Nigeria African geology Dessuvagie T F J and A J Whiteman Eds Univ of Ibadan Press, Nigeria p305-324

Ojo, O. (1977): The Climates of West Africa, Heinemann Education Book (Nig.) Ltd.

Okagbue, C. O. (1988): Hydrology and chemical characteristics of surface and groundwater resources of Okigwe area and environs,Imo state, Nigeria. In: C.O Offoegbu (ed.) Groundwater and mineral resources of Nigeria(Earth evolution science seies),Brauschweig, Wisbadan:Fried, Vieweg and son p.3-14.

Oladapo, M. I., Mohammed, M. Z. Adeoye. O. O. and Adetola, B. A. (2004): Geoelectrical investigation of the Ondo State Housing Corporation Estate, Ijapo, Akure, southwestern Nigeria. Journal of Mining Geology, Vol 20, Pp. 412 – 480.

Olarewaju, V. O (1999): Fluid inclusion studies of coarse-grained charnokitic and hybrid rocks in Ukpilla area, southwestern Nigeria. Journal of Mining Geology, 35(1), 1-7.

Olarewaju, V. O (2006): The charnokitic intrussives of Nigeria. In: O. Oshin (ed.). The Basement complex of Nigeria and its mineral resources, a tribute to prof. M.A.O. Rahaman, 45-70.

Olatunji, A. S. (2006): Geochemical Evaluation of the Lagos Lagoon sediments. Unpublished PhD Thesis. Department of Geology, University of Ibadan. 162p.

Olatunji, A. S., Abimbola, A. F., Oloruntola, M. O. and Odewande A. A (2005): Hydrogeochemical evaluation of groundwater resources in shallow coastal aquifers around Ikorodu area, southwestern Nigeria. Water Resource 16: 65-71.

Olatunji, A. S., Tijani, M. N, Abimbola, A. F and Oteri, A.U (2001): Hydrogeochemical evaluation of the water resources of Oke-Agbe Akoko, southwestern Nigeria. Water Resource-journal, Vol 12 pp 81-87

Olayinka, A. I., (1990): Electromagnetic profiling for groundwater in Pre-Cambrian basement complex areas of Nigeria. Nordic Hydrology, Vol. 21, 205-216.

Olayinka, A. I.(1996): Non-uniqueness in the interpretation of bedrock resistivity from sounding curves and its hydrogeological implications, Water Resources, Journal of NAH, Vol. 7, Nos 1 & 2 p49-55.

Olayinka, A.I, Abimbola, A. F. Isibor,R.A and Rafiu, A.R (1999): A geoelectrical-hydrogeochemical investigation of shallow groundwater occurrence in Ibadan, southwestern Nigeria. Environmental geology 37 (1-2),pp.31-39.

Olayinka, A. I. and Olorunfemi, M.O. (1992): Determination of Geo-electrical characteristics in Okenne area and Implication for Borehole sitting. Journal of mining and Geology. Vol. 28 (2) Pp. 403 – 412.

Olorunfemi, M. O., Ojo, J. S. and Akintunde, O. M. (1999): Hydrogeophysical evaluation of the groundwater potentials of Akure metropolis. Southwestern Nigeria. Journal of mining and Geology. Vol.35(2) 207-228.

Olorunfemi, M. O and Oloruniwo, M. A., (1985): Geoelectric parameters and aquifer characteristics of some parts of southwestern Nigeria. Geologia Applicante E Idrogeologia, 20, 99-109.

Omatsola, M. E. and Adegoke, O S. (1981): Tectonic evolution and cretaceous stratigraphy of the Dahomey Basin. Journal of Mining Geology. p 130-137.

Onugba, A., Blavoux, B., Guiraud, R. and De Rooy, C. (1989): Results of preliminary hydrochemical and environmental isotope study of the groundwater in Gongola State (N.E. Nigeria). Water Resources, Vol. 1 no.2. p.147-153.

Onugba A., and Eduvie, O. M., (2005): The hydrochemistry and environmental isotopes of the aquifer system in the upper Benue area, Nigeria Water Resources, Vol. 16. p.80-89.

Oyawoye, M. O. (1964): The Petrology of a Potassic Syenite at Shaki, Western Nigeria. Contrib. Min. Petrol., v. 16, 345-358.

Oyawoye, M. O. (1965): Bauchite: a new variety in the quartz-monzonite series. Nature, 205, 689p.

Oyawoye, M. O. (1972): The Basement complex of Nigeria in Dessauvagie, T. F. J., Whiteman, A. J. (Eds). African Geology. Ibadan University Press, Ibadan, Nigeria. Pp. 41-56.

Patty, F. A. (1962): Industrial hygiene and toxicology, Vol. II. John A. Wiley, New York. pp. 998–1002.

Pelig-Ba, K. B. (2009): Analysis of Stable Isotope Contents of Surface and Underground Water in Two Main Geological Formations in the Northern Region of Ghana) West African Journal of Applied Ecology, vol. 15, p1-8

Piper, A. M. (1944): A graphic procedure in Geochemical Interpretation of water analysis Trans Amer. Geophys. Union 25: 914-928.

Piper, A. M. (1953): A graphic procedure in Geochemical Interpretation of water Us Geol. Surv. Groundwater Notes, 12, 14p

Piskin, R.(1973): Evaluation of Nitrate Content of groundwater in Hall county, Nebraska. Ground water 11(6): 14-113.

Porowski, A. (2004): Isotopic evidence of the origin of mineralized waters from the central Carpathian Synclinorium, SE Poland, Environmental Geology 46:661-669

Raeburn, C. and Jones, D. G (1934): The Chad basin: Geology and Water supply. G.S.N Bull No15.

Rahaman, M. A. (1973): the geology of the district around iseyin Western State, Nigeria, PhD Thesis University of Ibadan 268p

Rahaman, M. A. (1976): Review of the basement geology of southwestern Nigeria. In Kogbe,C. A (ed) Geology of Nigeria. Elizabethan Pub. Co. Lagos 45-58.

Rahaman, M.A. (1981): Recent advances in the study of the basement complex of Nigeria, First symposium on the Precambrian Geology of Nigeria.

Rahaman, M. A. (1988): Recent advances in the study of the basement complex of Nigeria, In Precambrian Geology of Nigeria. Surv. Of Nigeria. Pub. Kaduna. Pp11-43

Rajmohan N. and Elango L. (2004): Identification and evolution of hydrogeochemical processes in the groundwater environment in an area of the Palar and Cheyyar River Basins, Southern India, Environmental Geology (2004) 46:47–61

Reuben K. U. (1970): Geographical Regions of Nigeria. Morrison and Gibb Ltd, London and Edinburgh, 72p

Reyment, R. A (1965): Aspect of geology of Nigeria, University Press. 133 Pp 18.

Ritter, W. F. and Chimside, A. E. M., (1984): Impact of Land use on groundwater quality in southern Delaware Groundwater;22 (9)38-47.

Rogers, R. J. (1989): Geochemical comparison of groundwater in areas of New England, New York, and Pennsylvania. Groundwater 27(5):690–712

Rozanski, K., Araguas-Araguas,I and Gonfiantini, R., (1993): Isotopic patterns in modern global precipitation. In P.K. Swart (ed) Continental isotope indicators of climate, AGU Monogr. 78,1-36.

Russ, W. (1924): The phosphate deposit of Abeokuta province Geol. Surv Nigeria bull. No. 38. 46

Russ, W. (1957): The Geology of parts of Niger, Zaria and Sokoto with special reference to the occurrences of Gold Provinces Geol. Surv. Of Nigeria, Bull. No.27, p. 42.

Sami, K. (1992): Recharge mechanisms and geochemical processesin a semi-arid sedimentary basin, Eastern Cape, South Africa.J Hydrol 139:27–48

Saxena, V. K and Ahmed, S. (2003): Inferring the chemical parameters for the dissolution of fluoride in groundwater. Env. Geol. 43, 731-736.

Sawyer, G. N. and McCarthy, D. L. (1967): Chemistry of sanitary Engineers, *2nd ed, McGraw Hill, New York*, p-518.

Schoeller, H. (1959): Arid zone Hydrogeology: Recent developments, UNESCO, Paris 125 p

Schoeller, H. (1965): Hydrodynamique lans lekarst (ecoulemented emmagusinement). Actes Colloques Doubronik, I, AIHS et UNESCO, pp 3–20

Schroeder. H. A. (1960): Relations between hardness ofwater and death rates from certain chronic and degenerative diseases in the United States, *J. Chrondisease*, *12*:586-591

Singhal, B. B. and Guptal, R. P (1999): Applied Hydrogeology of fractured rocks. Kluwer Academic Publishers,Dordrecht, Netherlands.400p

Sklash, M. G. (1990): Environmental isotope studies of storm and snowmelt runoff generation. In: Process Studies in Hillslope Hydrology, (MG Anderson and TP Burt, ed.), John Wiley and Sons Ltd., Sussex, England, 401-435.

SON, (2007): Nigerian Industrial Standard, Nigerian Standard for drinking Water quality, ICS 13.060.20, SON Standard Organization of Nigeria , 30p

Spears, D. A. (1986): Mineralogical control of the chemical evolution of groundwater. In: Trudgill ST (ed) Solute processes. Wiley, Chichester, UK, p 512

Stiff, H. A. (1951): The Interpretation of Chemical Water Analysis by means of Patterns; Jour. Petroleum Technology, Vol. 3, No. 10, pp. 15-17

Takeda, A. (2003): Manganese action in brain function. Brain Research Reviews, 41, 79-87

Tattam, C. M. (1943): A Review of the Nigerian Stratigraphy. Annual Rept Geol. Survey Nigeria.

Taylor, S. R and McLennan, S. M (1985): The continental crust: its composition and evolution. Blackwell, Oxford

Telford, W. M., Geldart, L. P. and Sheriff, R. E. (1976): Applied Geophysics Cambridge University Press, Cambridge pp. 532-538.

Tijani, M. N. (1994): Hydrogeochemical assessment of groundwater in Moro area, Kwara State, Nigeria. Environ. Geol. 24. p. 194-202

Tijani, M. N. and Ayodeji, O. A., (2001): Hydrogeochemical assessment of surface and groundwater in part of Dahomey basin, southwestern Nigeria. Water Resource 12: 88-93.

Tijani, M. N and Abimbola, A. F (2003): Groundwater chemistry and isotopes studies of weathered basement aquifer: a case study of Oke-ogun area, SW Nigeria, African Geoscience review, Vol 10, No4,p-373-387.

Tijani, M. N., Onibalusi, S.O. and Olatunji A. S. (2002): Hydrochemical and environmental impact assessment of Orita Aperin waste dumpsite, southwestern Nigeria. Water Resource-journal of Nigerian Association of Hydrogeologists (NAH) Vol 13 pp. 78-85

Tijani, M. N., Olatunji A. S., Sangogbade, O. O. and Chuckwurah, B. N. (2005): Hydrochemical evaluation of seawater influence on water quality in metropolitan Lagos, Nigeria. Geoscience Review, Vol. 12(3): 225 – 240.

Todd, D. K. (1980): Groundwater Hydrology. 2nd edition. John Wiley and Sons. New York. 555p

Trembley, J. J., Cruz, D. and Anger, H. (1973): Salt water intrusion in the Summerside Area. Groundwater 11: 4.

Tripathy, J. K. and Panigrahy, R. C. (1999): Hydrochemical assessment of groundwater in parts of south coastal Orissa, India, Journal of Environmental hydrology, Vol 7, paper 3, 1-9

Truswell, F. J., and Cope, R. N. (1963): The geology of Niger and Zaria Provinces. Northern Nigeria. Nigeria Geological Survey Bull. pp 29- 52.

Turner, D. C (1983): Upper Proterozoic schist belts in the Nigeria sector of the Pan-African ages of two charnockite-granite associations from Southwestern Nigeria. Contrib. Miner. Petrol pp 88, 188-195.

Urey, H. C. (1947): Thermodynamic properties of isotopic substances. J. Chem. Soc.: 562-581.

US EPA (1985a): *Health advisory — barium.* Washington, DC, US Environmental Protection Agency, Office of Drinking Water.

Vallee B. L. (1957): Zinc and its biological significance. Arch. Industrial. Health 16: 147.

Vaughn, B. H., White, J. W. C., Delmotte, M., Trolier, M., Cattani, O. and Stievenard, M., (1998): An automated system for hydrogen isotope analysis of water. Chemical Geology, volume 152, number 3-4, Nov 1998.

Verma, M. N. and Jolly, P. B. (1992): Groundwater occurrence in fractured rocks in Darwin rural area, N.T., in AWRC Conference on Groundwater in Fractured rocks, series No. 5, 229-39

White, C. C., Houston, J. F. T. and Barker, R. D., (1988): The Victoria Province Drought Relief Project,I, Geophysical sitting of boreholes. Ground water, 26, 309-316.

Whiteman, A. J., (1982): Nigeria-Its Geology, Resources and potential, Vol 2, Grahan and Trontman, London.

Wilcox, L. V. (1995): Classification and use of irrigationwaters, US Department of Agriculture, *Washington Dc*, p-19

William J. Deutch, (1997): Groundwater Geochemistry. Fundamentals and Application to Contamination, Lewis publisher, 221p

WHO (1980): Recommended health-based limits in occupational exposure to trace metals. Technical Report Series, No. 647. Vienna, Austria

WHO (1993): Guidelines for drinking water quality.Revision of the 1984 guidelines.

WHO (2006): Guidelines for drinking-water quality [electronic resource] : incorporating first addendum. Vol. 1, Recommendations – 3rd ed., Electronic version for the Web.595p

WHO/UNEP (1989) *GEMS — Global fresh water quality*. Published on behalf of the World Health Organization/United Nations Environment Programme. Oxford, Blackwell Reference.

Xong X., Kayane, I., Tanaka, T.., and Shimada J. (1999): Conceptual model of the evolution of groundwater quality at the wet zone in Sri Lanka. Environmental Geology 39 (2):149-164

Zohdy A. A. R., Eaton, G. P and Mabey, D. R. (1974): Application of surface geophysics to groundwater investigations. Techniques of Water Resources Investigations of the U.S. Geological survey, Book 2, Chapter D1

APPENDIX I

Geophysical Data

Table 5.1: Vertical Electrical Sounding Field Data of Abeokuta area

Location NO		VES 1	VES 2	VES 3	VES 4	VES 5	VES 6	VES 7	VES 8	VES 9	VES 10
Easting		3.36893	3.39970	3.38887	3.36003	3.37520	3.35423	3.37403	3.39413	3.39573	3.39573
Northing		7.14552	7.14008	7.14207	7.12832	7.12022	7.13900	7.16197	7.16153	7.15690	7.17803
Elevation (m)		138.4	121.3	101	100.2	118.2	84.8	139.1	135.7	136.6	148.4
$^{AB}/_{2}$	$^{MN}/_{2}$	(Ohm-m)	(Ohm-m)	(Ohm-m)	(Ohm-m)	(Ohm-m)	(Ohm-m)	(Ohm-m)	(Ohm-m)	(Ohm-m)	(Ohm-m)
1	0.3	1304.0	436.4	256.0	527.5	206.6	187.1	525.4	152.0	382.0	38.2
2	0.3	636.1	458.9	284.3	671.0	194.8	92.8	465.0	72.6	410.5	44.7
3	0.3	445.4	450.5	254.3	669.3	165.3	49.2	384.3	53.2	367.0	70.0
4	0.3	281.8	486.0	197.5	616.8	167.8	30.7	270.7	44.7	299.5	52.3
6	0.3	496.6	492.0	120.4	306.2	183.6	44.8	154.2	37.6	274.7	59.0
6	0.5	251.8	480.0	124.1	380.0	183.4	49.6	135.1	37.1	282.9	65.6
9	0.5	191.9	588.0	105.3	257.9	288.2	27.0	87.9	32.5	275.6	84.8
12	0.5	162.1	644.7	82.7	280.2	436.2	30.2	82.5	30.5	298.3	96.6
15	0.5	231.3	728.8	98.1	339.0	545.1	36.5	80.9	28.6	318.3	96.6
15	1	104.0	716.8	89.5	295.5	494.2	37.3	72.9	28.2	307.5	87.0
20	1	508.3	839.6	42.8	399.3	556.2	48.5	108.4	28.1	314.1	92.4
25	1	510.4	963.6	89.6	480.8	382.5	62.1	132.3	32.4	220.9	85.6
32	1	1008.1	1102.6	63.9	515.4	678.4	80.3	195.2	41.9	279.0	75.8
40	1	311.0	1243.0	88.3	608.2	764.1	102.4	197.6	46.6	275.0	70.9
40	2.5	220.8	1086.4	129.7	625.0	830.9	102.7	181.4	45.7	441.0	72.7
50	2.5	297.4		150.6	710.7	809.2	120.3	222.3	43.7	606.0	53.4
65	2.5	428.2	919.1	187.6	823.8	951.1	160.4	217.0	61.5	435.0	65.2
80	2.5	499.2	831.8	174.9	830.1	1073.0	208.3	187.3	170.3	248.1	85.9
100	2.5	697.0	712.9	143.4	934.0	1812.4	301.3	499.9	516.7	266.7	85.1
100	5	1042.0	723.5	242.5	868.5	1054.0	310.2	566.0	181.0	559.0	99.7

Table 5.1: Vertical Electrical Sounding Field Data of Abeokuta area (continuation)

Location NO		VES 11	VES 12	VES 13	VES 14	VES 15	VES 16	VES 17	VES 18	VES 19	VES 20
Easting		3.3775	3.3674	3.3554	3.3574	3.3100	3.3100	3.3194	3.3196	3.3269	3.3095
Northing		7.1718	7.1781	7.1753	7.1599	7.1476	7.1560	7.1630	7.1758	7.1766	7.1699
Elevation (m)		145.5	106.1	76.4	85.8	45.5	47.9	44.8	65.2	48.5	77.6
$^{AB}/_{2}$	$^{MN}/_{2}$	(Ohm-m)	(Ohm-m)	(Ohm-m)	(Ohm-m)	(Ohm-m)	(Ohm-m)	(Ohm-m)	(Ohm-m)	(Ohm-m)	(Ohm-m)
1.0	0.3	115.1	17.6	134.7	134.7	354.8	15.4	547.9	288.5	4420.0	1491.0
2.0	0.3	117.1	32.1	76.8	76.8	126.8	9.7	237.4	265.1	8905.0	1246.0
3.0	0.3	100.8	26.5	46.0	46.0	74.0	81.0	111.9	196.0	2795.0	863.7
4.0	0.3	80.4	23.7	30.7	30.7	50.2	11.9	65.2	119.8	1847.0	555.8
6.0	0.3	44.0	35.0	18.0	18.0	45.7	15.3	45.1	74.3	775.0	225.9
6.0	0.5	46.6	34.6	27.9	27.9	49.9	17.5	51.0	77.6	706.0	223.9
9.0	0.5	26.0	38.6	29.5	29.5	62.2	23.4	54.4	79.9	538.0	88.1
12.0	0.5	22.1	33.7	37.6	37.6	98.4	48.5	57.0	96.2	1331.0	72.6
15.0	0.5	23.5	48.6	49.0	49.0	158.2	37.9	75.4	116.9	942.0	74.8
15.0	1.0	23.0	55.6	54.5	54.5	115.1	27.0	57.9	111.7	535.7	72.5
20.0	1.0	27.1	96.2	97.4	97.4	355.8	28.7	59.9	143.8	582.0	82.8
25.0	1.0	30.3	116.3	128.9	128.9	96.0	34.5	87.1	181.3	850.3	77.8
32.0	1.0	30.6	121.6	88.0	88.0	139.6	42.1	114.4	236.4	944.7	120.8
40.0	1.0	40.2	84.8	104.2	104.2	187.6	36.9	115.3	291.6	1980.0	118.4
40.0	2.5	40.6	73.6	116.3	116.3	160.3	44.6	116.5	296.9	634.0	132.9
50.0	2.5	48.3	90.1	145.6	145.6	195.6	51.9	142.5	326.2	338.8	147.9
65.0	2.5	66.9	128.2	191.7	199.7	58.0	67.9	199.7	411.8	113.2	335.2
80.0	2.5	66.8	60.9	235.2	203.0	309.0	73.1	232.8	661.4	889.0	260.6
100.0	2.5	144.8	65.9	235.2	235.2	365.2	100.5	307.1	591.2	902.0	389.2
100.0	5.0	109.5	101.4	196.0	196.0	362.0	157.3	322.8	553.0	1395.0	355.6

Table 5.1: Vertical Electrical Sounding Field Data of Abeokuta area (continuation)

Location NO		VES 21	VES 22	VES 23	VES 24	VES 25	VES 26	VES 27	VES 28	VES 29	VES 30
Easting		3.3347	3.3434	3.3461	3.3413	3.3320	3.3339	3.3284	3.3447	3.3397	3.3401
Northing		7.1560	7.1794	7.1541	7.1451	7.1372	7.1235	7.1153	7.1177	7.1143	7.0906
Elevation (m)		62.1	47.8	86.3	71.6	69.7	76.1	60.6	91.2	76.9	75.8
$^{AB}/_{2}$	$^{MN}/_{2}$	(Ohm-m)	(Ohm-m)	(Ohm-m)	(Ohm-m)	(Ohm-m)	(Ohm-m)	(Ohm-m)	(Ohm-m)	(Ohm-m)	(Ohm-m)
1.0	0.3	258.0	176.4	97.7	167.0	526.3	170.6	383.6	120.8	461.8	248.9
2.0	0.3	127.6	141.9	73.3	182.0	392.4	162.9	131.2	97.1		291.8
3.0	0.3	78.1	102.2	63.2	212.2	360.0	173.6	281.8	78.9	99.5	168.8
4.0	0.3	57.0	77.4	60.6	206.4	304.6	180.4	222.7	80.6	100.8	102.7
6.0	0.3	43.0	82.7	67.8	153.6	214.4	181.0	154.7	88.7	280.2	63.8
6.0	0.5	30.2	85.6	70.3	166.7	196.5	158.6	160.5	99.7	165.6	35.8
9.0	0.5	25.6	95.6	77.8	135.0	139.5	135.5	145.1	124.9	155.2	26.3
12.0	0.5	40.4	113.0	200.6	165.9	127.3	117.0	163.3	143.3	174.1	42.5
15.0	0.5	47.0	115.9	214.7	135.7	132.6	978.0	181.4	151.3	236.1	99.8
15.0	1.0	48.6	112.0	119.2	78.8	127.1	99.8	214.1	150.5	151.8	13.3
20.0	1.0	41.4	137.7	106.0	78.6	143.0	99.7	245.4	141.1	173.0	203.0
25.0	1.0	114.9	171.0	96.0	105.7	139.8	110.3	413.3	144.1	163.6	122.5
32.0	1.0	164.7	222.0	123.0	100.7	181.2	86.7	324.7	136.0	148.6	144.9
40.0	1.0	220.9	265.0	275.5	136.6	147.8	139.7	514.2	129.5	199.8	164.9
40.0	2.5	53.0	257.7	142.0	162.7	370.0	248.0	348.2	123.8	634.2	163.8
50.0	2.5	391.0	290.0	173.4	158.6	253.7	298.9	358.2	120.7	592.4	404.6
65.0	2.5	446.0	348.2	349.0	310.0	287.5	374.1	200.6	119.5	631.5	297.4
80.0	2.5	499.0	382.3	192.0	266.2	335.3	467.0	362.2	105.4	307.6	522.7
100.0	2.5	716.0	479.5	499.0	815.3	390.6	507.8	423.6	115.0	446.5	1039.1
100.0	5.0	533.0	470.9	293.1	230.0	419.0	560.6	435.6	111.2	174.6	1870.5

Table 5.1 Vertical Electrical Sounding Field Data of Abeokuta area (continuation)

Location NO		VES 31	VES 32	VES 33	VES 34	VES 35	VES 36	VES 37	VES 38	VES 39	VES 40
Easting		3.3252	3.3371	3.3213	3.3132	3.3064	3.3081	3.4000	3.3929	3.3950	3.3873
Northing		7.0897	7.1069	7.1256	7.1136	7.0912	7.1030	7.0883	7.1046	7.0990	7.1123
Elevation (m)		38.9	60.6	44.5	29.7	37.6	23.9	112.1	115.2	125.8	128.8
$AB/2$	$MN/2$	(Ohm-m)	(Ohm-m)	(Ohm-m)	(Ohm-m)	(Ohm-m)	(Ohm-m)	(Ohm-m)	(Ohm-m)	(Ohm-m)	(Ohm-m)
1.0	0.3	783.6	260.5	121.8	195.8	112.7	1368.9	383.6	850.0	210.0	783.6
2.0	0.3	425.6	167.8	59.7	172.1	46.3	656.1	330.0	450.0	210.0	425.6
3.0	0.3	303.3	87.1	46.4	137.8	23.4	562.2	281.8	320.0	160.0	310.0
4.0	0.3	282.8	53.5	46.4	121.3	15.8	597.5	230.2	270.0	110.0	270.0
6.0	0.3	250.2	30.3	49.9	121.3	12.2	773.7	170.1	210.0	52.5	210.0
6.0	0.5	209.9	29.7	50.0	133.9	11.7	788.1	174.2	221.4	63.6	218.9
9.0	0.5	180.2	23.6	61.8	157.1	13.0	1057.5	145.1	155.0	35.7	170.0
12.0	0.5	170.9	24.1	77.6	169.1	15.6	1349.0	163.3	160.0	39.1	148.0
15.0	0.5	229.9	25.5	93.1	192.2	18.6	1640.0	180.0	170.0	46.6	130.0
15.0	1.0	126.7	21.6	93.2	192.7	17.4	1647.0	189.0	175.6	51.3	136.8
20.0	1.0	117.6	24.2	93.2	250.4	23.4	2177.0	230.0	190.0	62.5	130.0
25.0	1.0	119.6	26.2	93.2	289.3	28.8	2658.0	280.0	210.0	82.5	140.0
32.0	1.0	261.3	26.2	93.2	339.8	38.4		324.7	240.0	110.0	160.0
40.0	1.0	565.5	25.7	93.2	366.9	45.0	3670.5	380.0	280.0	140.0	200.0
40.0	2.5	89.7	27.3	93.2	342.4	55.2	3147.0	392.3	284.2	133.5	198.8
50.0	2.5	228.7	34.0	93.2	351.5	67.0		430.0	320.0	170.0	250.0
65.0	2.5	316.4	46.5	93.2	329.8	90.4	3637.0	500.0	400.0	210.0	316.4
80.0	2.5	780.0	68.8	93.2	366.6	98.3	3572.6	550.0	480.0	260.0	480.0
100.0	2.5	960.1	88.0	93.2	677.5	153.7	3031.0	630.0	600.0	300.0	600.0
100.0	5.0	972.3	72.0	93.2	546.0	67.0	2940.0	631.0	621.0	315.0	611.0

Table 5.1: Vertical Electrical Sounding Field Data of Abeokuta area (continuation)

Location NO		VES 41	VES 42	VES 43	VES 44	VES 45	VES 46	VES 47	VES 48	VES 49	VES 50
Easting		3.3596	3.3701	3.3507	3.3626	3.3670	3.3615	3.3764	3.3899	3.3695	3.3888
Northing		7.1149	7.1157	7.1884	7.1869	7.2077	7.2033	7.2159	7.2103	7.1849	7.1847
Elevation (m)		90.9	121.2	81.6	77.9	113.1	105.3	98.7	111.2	79.1	149.1
$^{AB}/_{2}$	$^{MN}/_{2}$	(Ohm-m)	(Ohm-m)	(Ohm-m)	(Ohm-m)	(Ohm-m)	(Ohm-m)	(Ohm-m)	(Ohm-m)	(Ohm-m)	(Ohm-m)
1.0	0.3	260.5	195.8	792.0	134.5	1630.5	1553.0	4811.0	2247.5	2736.0	148.1
2.0	0.3	167.8	172.1	369.8	234.7	501.0	1582.9	4614.0	546.0	787.6	110.7
3.0	0.3	87.1	137.8	261.5	238.8	169.1	1533.0	2672.3	182.5	362.0	73.1
4.0	0.3	53.5	121.3	249.3	355.4	128.0	1134.0	1547.0	126.0	260.0	70.6
6.0	0.3	29.0	125.0	313.4	935.6	88.8	633.7	723.0	110.0	229.5	71.2
6.0	0.5		133.2	320.8	544.8	76.3	645.9	466.4	80.0	218.5	77.2
9.0	0.5	23.6	150.0	489.6	558.6	162.0	234.0	106.0	75.0	248.9	79.5
12.0	0.5	24.1	169.1	644.9	841.9	513.7	172.9	67.0	103.5	434.5	84.8
15.0	0.5	24.0	192.5	719.1	943.9	345.4	192.6	108.0	310.6	436.3	90.2
15.0	1.0	28.2	187.5	923.7	990.6	119.5	120.8	729.0	150.0	411.1	93.4
20.0	1.0	24.2	250.4	1033.0	1423.4	255.8	172.2	114.6	161.0	524.0	109.9
25.0	1.0	25.0	289.3	798.4	1844.5	306.8	203.7		193.6	585.0	132.0
32.0	1.0	25.2	339.8	858.2	2997.6	536.2	230.0	320.0	246.9	533.9	172.5
40.0	1.0	26.0	366.0	1051.0	4532.2	1105.0	325.7	726.8	342.0	877.0	206.1
40.0	2.5	28.2	372,1	1118.5	4765.0	1372.0	280.7	83.3	530.0	488.6	182.6
50.0	2.5	34.0	440.0	1332.4		1907.3	286.3		995.0	411.7	196.1
65.0	2.5	46.5	520.0	1530.5	5142.2	1090.0	327.4	1680.0	1700.0	773.0	239.8
80.0	2.5	68.8	600.0	1883.9		1838.0	326.6	1031.0	4094.0	1173.0	297.9
100.0	2.5	88.0	677.5	2550.0		3034.0	393.4	2141.0	1715.0	1755.0	299.0
100.0	5.0	91.2	679.2	2964.0		2856.9	379.6	1052.0	1105.0	1890.0	378.6

Table 5.1: Vertical Electrical Sounding Field Data of Abeokuta area (continuation)

Location NO		VES 51	VES 52	VES 53	VES 54	VES 55	VES 56	VES 57	VES 58	VES 59	VES 60
Easting		3.3415	3.3407	3.3394	3.3288	3.3051	3.3102	3.3007	3.3075	3.3131	3.3115
Northing		7.1869	7.1972	7.2106	7.2148	7.2067	7.2100	7.2037	7.1869	7.1986	7.1923
Elevation (m)		53.6	57.1	66	63.6	47.3	54.4	59.5	96.8	94.2	95.7
AB/2	MN/2	(Ohm-m)	(Ohm-m)	(Ohm-m)	(Ohm-m)	(Ohm-m)	(Ohm-m)	(Ohm-m)	(Ohm-m)	(Ohm-m)	(Ohm-m)
1	0.25	114.2	251.6	292.2	936.1	1176.5	3711.5	3328.6	1161.8	2733.5	2433.1
2	0.25	53.7	184.8	222.4	300.1	707.7	3404.7	3078.1	1301.5	2209.6	1737.0
3	0.25	36.4	88.2	155.6	86.5	516.7	2634.1	2667.8	943.5	1454.6	921.1
4	0.25	26.2	60.3	92.9	42.2	328.5	2143.2	2203.3	651.0	644.0	347.5
6	0.25	14.0	52.8	40.4	33.9	125.6	1095.3	1081.7	393.6	316.4	152.4
6	0.5	18.1	47.2	40.5	33.0	198.1	1297.4	1169.3	469.5	320.1	121.3
9	0.5	20.3	78.9	26.6	36.8	111.1	558.2	313.8	423.2	251.7	120.0
12	0.5	26.8	110.7	31.2	58.7	83.0	323.4	120.1	481.0	290.2	148.1
15	0.5	35.3	140.4	34.6	69.9	143.4	240.8	115.1	543.0	311.4	161.0
15	1	38.4	151,.23	31.3	67.2	70.1	823.5	110.5	533.8	345.2	188.6
20	1	42.6	180.2	45.1	92.1	62.1	1184.7	111.6	485.8	483.9	186.2
25	1	51.3	217.8	53.0	141.4	69.9		144.2			199.7
32	1	64.0	261.2	62.0	209.7	88.9		187.7	689.1	652.6	221.3
40	2.5	71.5	321.5	88.8	247.4	148.4	644.4	248.6	943.8	748.5	296.8
40	2.5	83.2	354.2	90.2	268.5	123.8	654.3	219.4	731.1	767.9	276.9
50	2.5	97.2	456.8	112.9	370.4	165.4		274.1	841.1		318.9
60	2.5	125.0	518.7	131.2	429.3	194.2	219.1	295.8	989.1	975.6	
80	2.5	160.0	527.5	149.4	513.0	270.8	365.6	442.0	1209.0	1179.0	392.6
100	5	188.0	532.8	168.6	702.0	331.1	427.0	509.5	1415.2	1308.3	444.1
100	5	192.3	496.8	181.2	698.6	349.7	369.8	543.5	1567.5	1459.1	452.3

Table 5.1: Vertical Electrical Sounding Field Data of Abeokuta area (continuation)

Location NO		VES 61	VES 62	VES 63	VES 64	VES 65	VES 66	VES 67	VES 68	VES 69	VES 70
Easting		3.3231	3.3399	3.3110	3.3122	3.3881	3.3837	3.3664	3.3908	3.3958	3.3993
Northing		7.1919	7.1735	7.1765	7.1825	7.1703	7.1662	7.1525	7.1992	7.2084	7.2137
Elevation (m)		72.8	40.9	81.9	89.9	124.9	135.9	68.2	113.5	111.2	110.6
AB/2	MN/2	(Ohm-m)	(Ohm-m)	(Ohm-m)	(Ohm-m)	(Ohm-m)	(Ohm-m)	(Ohm-m)	(Ohm-m)	(Ohm-m)	(Ohm-m)
1	0.25	6115.1	120.2	220.3	2645.2	154.4	90.1	72.3	229.2	1355.0	2450.8
2	0.25	5097.1	137.6	246.9	2103.2	162.3	112.8	52.2	238.0	1360.9	1635.5
3	0.25	3959.5	109.7	237.6	1381.6	182.5	110.9	32.0	195.4	836.8	790.8
4	0.25	2523.8	74.8	247.4	927.4	178.1	118.5	24.0	162.7	593.9	345.5
6	0.25	874.0	37.3	241.2	472.0	171.0	109.1	22.8	90.3	376.0	113.8
6	0.5	914.3	31.7	212.9	432.5	189.8	117.3	16.8	84.2	390.9	111.8
9	0.5	227.3	23.8	172.8	180.1	169.5	101.2	28.2	56.6	324.8	71.3
12	0.5	124.7	21.2	150.4	161.0	158.1	96.2	37.0	61.0	324.7	71.4
15	0.5	100.2	24.7	137.0	154.2	141.2	99.8	50.0	64.3	360.9	74.9
15	1	101.7	25.0	130.6	173.5	147.1	110.5	59.0	72.5	348.0	101.4
20	1	102.2	32.0	129.8	141.0	123.9	111.1	71.5	86.2	465.7	90.9
32	1	123.1	53.4	155.0	212.4	124.2	121.9	114.6	121.4	632.7	94.6
40	2.5	146.2	59.6	173.8	296.8	146.3	154.2	190.0	141.4	565.8	118.0
40	2.5	139.6	67.6	181.3	276.4	139.8	141.7	161.7	135.6	544.0	138.0
60	2.5	187.4	81.7	225.8	361.3	175.9	188.3	226.5	240.3	519.4	130.1
80	2.5	249.6	128.6	285.3		227.8	244.3	260.0	221.8	558.5	156.7
100	5	232.4	182.4	282.6	540.1	263.1	286.2	301.1	248.7	605.3	251.2
100	5	313.4	192.0	291.5	529.5	252.7	291.3	299.9	272.7	583.0	198.2

Table 5.1: Vertical Electrical Sounding Field Data of Abeokuta area (continuation)

Location NO		VES 71	VES 72	VES 73	VES 74	VES 75
Easting		3.3825	3.3908	3.3040	3.3116	3.3369
Northing		7.1937	7.1986	7.1357	7.1397	7.1029
Elevation (m)		114.4	98.4	36.5	45	58.7
AB/2	MN/2	(Ohm-m)	(Ohm-m)	(Ohm-m)	(Ohm-m)	(Ohm-m)
1	0.25	2056.05	336.39	225.63	119.00	170.26
2	0.25	1524.18	272.42	230.36	67.30	183.59
3	0.25	775.61	247.12	174.11	34.77	117.38
4	0.25	429.65	190.49	146.82	20.83	74.11
6	0.25	149.05	116.53	88.75	16.03	33.87
6	0.5	125.16	116.48	80.99	13.37	27.18
9	0.5	99.79	70.03	47.95	20.55	25.12
12	0.5	92.14	61.88	2.26	28.91	32.58
15	0.5	94.63	58.61	38.84	34.60	40.25
15	1	83.75	60.18	28.63	32.38	38.71
20	1	95.28	80.86	43.88	42.07	50.15
32	1	119.52	163.00	56.49	54.42	73.01
40	2.5	142.08	227.39	68.50	60.73	101.49
40	2.5	166.87	247.00	71.87	71.12	124.34
60	2.5	176.15	398.99	95.58	85.82	135.50
80	2.5	219.03	549.03	120.54	144.64	
100	5	249.12		212.96	175.84	231.09
100	5	267.33		242.22	137.90	211.81
120	5	271.00				
150	5	289.53				

Table 5.2: Vertical Electrical sounding survey Field data of Ikorodu area

Location No		VES IKD 1	VES IKD 2	VES IKD 3	VES IKD 4	VES IKD 5	VES IKD 6	VES IKD 7	VES IKD 8	VES IKD 9	VES IKD 10
Easting		3.64435	3.627383	3.598167	3.59225	3.545883	3.566283	3.550067	3.5887	3.598867	3.6028
Northing		6.670167	6.663417	6.663417	6.673483	6.627583	6.61655	6.6412	6.596517	6.611883	6.61375
Elevation (m)		23	28	28	26	33	38	41	33.5	29	37
AB/2	MN/2	Resistivity (Ohm-m)	Resistivity (Ohm-m)	Resistivity (Ohm-m)	Resistivity (Ohm-m)	Resistivity (Ohm-m)	Resistivity (Ohm-m)	Resistivity (Ohm-m)	Resistivity (Ohm-m)	Resistivity (Ohm-m)	Resistivity (Ohm-m)
1	0.25	165.5	175.0	145.5	117.8	46.2	73.6	83.7	53.7	160.2	77.1
2	0.25	238.8	256.3	269.0	80.4	66.1	115.6	112.8	93.1	178.9	137.1
3	0.25	254.4	310.0	379.1	81.4	100.4	158.9	133.1	119	204.4	246.6
4	0.25	280.4	328.5	475.7	88.2	126.0	197.2	180.8	142	233.4	238.4
6	0.25	302.2	433.4	582.6	95.5	192.0	248.0	261.5	197.3	303.1	319.6
6	0.5	322.4	444.8	598.7	84.2	187.4	239.3	289.8	201	337.0	370.7
9	0.5	388.9	512.5	718.0	86.5	265.6	287.0	438.7	287	475.7	472.4
12	0.5	479.7	688.8	766.5	85.1	332.9	312.1	579.9	354	618.3	556.9
15	0.5	544.5	874.2	815.6	85.5	396.2	351.7	735.8	476	790.2	650.4
15	1	523.3	872.7	812.9	80.9	393.4	345.6	746.0	420	739.0	600.0
20	1	609.3	1097.6	923.9	85.1	484.5	412.5	860.0	504	995.4	731.5
25	1	625.4	1237.1	988.1	98.7	467.6	468.6	991.1	602	1186.2	839.1
32	1	676.6	1388.6	949.8	100.4	536.8	528.7	1113.7	687.2	1374.1	946.6
40	1	776.2	1336.4	874.2	139.2	680.8	590.3	1215.8	778	1652.9	1012.3
40	2.5	757.1	1398.1	837.3	119.5	578.9	564.9	1424.2	711	1567.4	984.5
50	2.5	811.7	1291.3	755.3	100.1	586.1	614.3	1451.1	739	1715.9	1009.2
65	2.5	694.6	1047.2	607.1	126.5	514.8	729.0	1442.2	659	1656.9	840.4
80	2.5	584.6	847.8	496.2	150.7	412.6	729.6	1342.0	603	1775.9	707.9
100	2.5	497.4	636.8	416.4	159.5	383.1	790.0	1126.0	547	1475.8	563.3
100	5	511.5	680.1	431.3	131.9	391.8	771.0	944.1	558.8	1429.2	542.2
120	5	424.1	509.5	397.0	171.6	339.2	763.3	887.4	467	1210.5	433.6
		VES	VES	VES	VES	VES IKD	VES IKD	VES IKD	VES IKD	VES IKD	VES IKD

Location No		IKD 1	IKD 2	IKD 3	IKD 4	5	6	7	8	9	10
Easting		3.64435	3.627383	3.598167	3.59225	3.545883	3.566283	3.550067	3.5887	3.598867	3.6028
Northing		6.670167	6.663417	6.663417	6.673483	6.627583	6.61655	6.6412	6.596517	6.611883	6.61375
Elevation (m)		23	28	28	26	33	38	41	33.5	29	37
AB/2	MN/2	Resistivity (Ohm-m)	Resistivity (Ohm-m)	Resistivity (Ohm-m)	Resistivity (Ohm-m)	Resistivity (Ohm-m)	Resistivity (Ohm-m)	Resistivity (Ohm-m)	Resistivity (Ohm-m)	Resistivity (Ohm-m)	Resistivity (Ohm-m)
160	5	310.2	272.4	345.5	157.5	270.8	675.0	488.7	345	903.2	297.3
200	5	207.2	234.9	202.2	91.7	271.3	602.9	425.0	275	550.1	213.5
200	20	210.8	333.8	190.8	95.4	261.9	583.2	410.9	234	583.6	263.3
250	20	96.8	157.0	150.4	51.0	282.5	497.0	526.3		330.4	156.8
300	20	98.0	94.2	92.3	52.8	244.9	376.8	665.8		209.0	113.0
300	30							901.0		195.0	126.7
350	30	23.1	102.6	46.2	212.9	174.4	307.8			146.7	0.0
350	30	109.6	134.6	48.1		167.3	282.7				
400	30		37.6	36.8		100.3	178.3	232.4		102.8	87.8
500	30						108.1	125.5		59.5	

Table 5.2: Vertical Electrical Sounding survey Field data of Ikorodu area (Continuation)

Location No		VES IKD 11	VES IKD 12	VES IKD 13	VES IKD 14	VES IKD 15	VES IKD 16	VES IKD 17	VES IKD 18	VES IKD 19	VES IKD 20
Easting		3.595	3.59	3.5614	3.59	3.583	3.592	3.6	3.6284	3.6397	3.6482
Northing		6.595	6.591	6.5899	6.58	6.575	6.57	6.564	6.5777	6.5933	6.6073
Elevation (m)		31	38.7	24	30	27.4	26.8	19	22	20	29
AB/2	MN/2	Resistivity (Ohm-m)	Resistivity (Ohm-m)	Resistivity (Ohm-m)	Resistivity (Ohm-m)	Resistivity (Ohm-m)	Resistivity (Ohm-m)	Resistivity (Ohm-m)	Resistivity (Ohm-m)	Resistivity (Ohm-m)	Resistivity (Ohm-m)
1	0.25	156.1	609.7	167.3	93.2	527.6	141.3	121.4	141.4	555.5	426.5
2	0.25	243.7	1001	319.4	139.3	696.8	132.9	88.1	229.6	628.5	509.7
3	0.25	300.5	1104	452.7	184.2	817.9	118.3	83.0	260.0	618.4	562.2
4	0.25	327.5	1119	568.9	234.4	749.4	131.5	91.0	301.5	657.0	549.8
6	0.25	365.8	1179	709.1	318.2	823.3	167.8	119.0	389.8	709.1	652.7
6	0.5	356.1	1223	691.9	316.8	845	147	102.2	407.7	722.3	686.3
9	0.5	348.9	1249	1278.7	430.3	897	176	134.7	510.0	847.4	718.0
12	0.5	426.8	1267	2583.5	509.0	947	187	163.5	577.2	1029.8	828.8
15	0.5	526.1	1240	3290.7	588.2	978	213	189.3	664.5	1206.1	962.5
15	1	518.0	1345	2174.8	640.8	994.8	193.2	187.6	721.4	1171.8	939.6
20	1	705.8	1289	3898.9	846.8	1098	234	230.7	929.0	1372.8	1174.1
25	1	862.7	1295	4146.7	1013.6	1124	267	258.8	1130.3	1465.6	1337.1
32	1	1030.2	1225	7425.0	1179.6	1107	328	268.4	1335.5	1526.8	1547.7
40	1	1107.8	1178	6154.5	1359.0	1079	398	258.5	1622.8	1489.6	1700.6
40	2.5	1131.7	1210	2423.7	1361.1	1096	367	292.4	1664.5	1450.2	1739.6
50	2.5	1162.8	1068	6899.1	1571.8	1056	456	285.2	1563.9	1535.7	1773.9
65	2.5	1203.6	912.4	7234.1		1015	574.9	229.5	1590.6	1110.8	1680.8
80	2.5	1072.8	687		1775.9	814	634	180.8	1550.9	1096.9	1498.7
100	2.5	910.6	555	9690.2	1739.6	661.5	657	175.4	1281.1	808.9	1187.6
100	5	890.1	509	5121.2	1698.7	614	727.3	196.6	1216.0	846.2	1156.5
120	5	764.7	347	5871.6	1368.5	487	645	100.1	944.0	677.9	849.6

Location No		VES IKD 11	VES IKD 12	VES IKD 13	VES IKD 14	VES IKD 15	VES IKD 16	VES IKD 17	VES IKD 18	VES IKD 19	VES IKD 20
Easting		3.595	3.59	3.5614	3.59	3.583	3.592	3.6	3.6284	3.6397	3.6482
Northing		6.595	6.591	6.5899	6.58	6.575	6.57	6.564	6.5777	6.5933	6.6073
Elevation (m)		31	38.7	24	30	27.4	26.8	19	22	20	29
AB/2	MN/2	Resistivity (Ohm-m)	Resistivity (Ohm-m)	Resistivity (Ohm-m)	Resistivity (Ohm-m)	Resistivity (Ohm-m)	Resistivity (Ohm-m)	Resistivity (Ohm-m)	Resistivity (Ohm-m)	Resistivity (Ohm-m)	Resistivity (Ohm-m)
160	5	523.1	267	4050.0	851.0	307	527	85.4	607.5	458.8	432.3
200	5	501.1	198		567.7	237	405	102.1	390.6	319.0	2574.8
200	20	391.9	214.1		551.6	205.1	398.2	93.4	444.8	342.8	269.4
250	20	263.4			421.5	157.6		130.2	311.2	243.9	155.1
300	20	161.9			240.1			165.1	115.4	154.1	90.8
300	30	168.0			232.3			169.0	108.7	155.8	83.1
350	30				173.6						
350											
400	30	125.0			129.1				159.1	171.6	68.3
500	30									56.1	

Table 5.2: Vertical Electrical Sounding survey Field data of Ikorodu area (Continuation)

Location No		VES IKD 21	VES IKD 22	VES IKD 23	VES IKD 24	VES IKD 25	VES IKD 26	VES IKD 27	VES IKD 28	VES IKD 29	VES IKD 30
Easting		3.651917	3.6695	3.6768	3.664167	3.691083	3.566333	3.551667	3.552517	3.5425	3.534633
Northing		6.618317	6.6505	6.663633	6.669167	6.691083	6.542233	6.5383	6.542733	6.547	6.565617
Elevation (m)		30	38	48	23	64	4	4	4	7	18
AB/2	MN/2	Resistivity (Ohm-m)	Resistivity (Ohm-m)	Resistivity (Ohm-m)	Resistivity (Ohm-m)	Resistivity (Ohm-m)	Resistivity (Ohm-m)	Resistivity (Ohm-m)	Resistivity (Ohm-m)	Resistivity (Ohm-m)	Resistivity (Ohm-m)
1	0.25	220.3	210	186	109.2	379.6	95.7	148	542	182.6	182.6
2	0.25	361.7	300	128	48.2	401.3	138	112.6	465	319.2	346.4
3	0.25	503.2	356	105	34.4	358.8	154	96	342	358.9	496.5
4	0.25	612.9	396.3	87	25.3	339.8	150.4	73	265	369.6	600.9
6	0.25	663.9	487.5	69.75	18.2	311.8	119	59	154	345.7	747.5
6	0.5	686.3	454.2	66.78	22.2	305.0	110	61	167	429.1	744.7
9	0.5	794.1	570.2	57.89	14.8	323.8	78	40.5	90.2	297.9	844.9
12	0.5	843.7	640	59.372	12.4	357.6	44	30	47	207.8	912.4
15	0.5	858.0	750	67.452	12.1	403.3	27.3	24.2	26	147.6	998.5
15	1	879.8	759.62	73.21	11.9	425.0	32	25.1	29.5	136.5	974.8
20	1	950.9	880	83	14.1	494.5	21	16.5	19	82.7	1179.7
25	1	1104.8	997.23	98.307	16.5	535.8	18.2	13	16	63.9	1310.7
32	1	1378.9	1147.4	115.627	19.1	563.1	17.8	9.8	14	65.1	1491.4
40	1	1582.6	1314.6	165.821	25.1	639.6	18.7	9.5	13.7	75.9	2019.7
40	2.5	1462.2	1209.8	154.204	23.5	624.0	16.2	8.9	12	97.4	1345.0
50	2.5	1587.4	1475.8	174.324	29.5	679.9	16.5	8	12.7	99.5	1253.7
65	2.5	1500.5	1773.2	178.865	42.3	793.0	16.7	7.9	12.8	116.9	848.3
80	2.5	1888.4	1800	180.17	58.6	796.4	17.4	7.6	16.5	133.0	1028.6
100	2.5	1928.0	1680	164.271	86.7	799.3	19.1	7	21	162.0	867.9
100	5	1717.5	1680.5	157.321	83.3	926.2	20.6	7.7	24	144.6	853.9
120	5	1716.3	1540.2	144.721	100.6	1040.0	20.4	7.6	26	160.9	752.6
160	5	1751.8	975.9	120	146.0	962.4	22.6	9.2	29.2	170.7	509.6

Location No		VES IKD 21	VES IKD 22	VES IKD 23	VES IKD 24	VES IKD 25	VES IKD 26	VES IKD 27	VES IKD 28	VES IKD 29	VES IKD 30
Easting		3.651917	3.6695	3.6768	3.664167	3.691083	3.566333	3.551667	3.552517	3.5425	3.534633
Northing		6.618317	6.6505	6.663633	6.669167	6.691083	6.542233	6.5383	6.542733	6.547	6.565617
Elevation (m)		30	38	48	23	64	4	4	4	7	18
AB/2	MN/2	Resistivity (Ohm-m)	Resistivity (Ohm-m)	Resistivity (Ohm-m)	Resistivity (Ohm-m)	Resistivity (Ohm-m)	Resistivity (Ohm-m)	Resistivity (Ohm-m)	Resistivity (Ohm-m)	Resistivity (Ohm-m)	Resistivity (Ohm-m)
200	5	1155.5	705.4	98.721	179.9	903.0	26	13.4	31	171.8	386.8
200	20	1116.7	694.8	104.3	193.1	933.7	23	12.5	34	179.8	331.3
250	20	623.9				753.7				181.0	207.3
300	20	447.6				410.6				187.9	195.0
300	30	441.4								168.4	191.3
350	30					132.9					
350						137.5					
400	30	215.8				108.7				120.8	233.3
500	30	117.4				95.4					

Table 5.2: Vertical Electrical Sounding survey Field data of Ikorodu area (Continuation)

Location No		VES IKD 31	VES IKD 32	VES IKD 33	VES IKD 34	VES IKD 35	VES IKD 36	VES IKD 37	VES IKD 38	VES IKD 39	VES IKD 40
Easting		3.5252	3.521133	3.523967	3.5075	3.483783	3.5042	3.493783	3.4959	3.472817	3.470467
Northing		6.58145	6.56715	6.5462	6.551467	6.571783	6.595367	6.600383	6.6236	6.6198	6.661267
Elevation (m)		18	12	8	8	6	13	15		5	10
AB/2	MN/2	Resistivity (Ohm-m)	Resistivity (Ohm-m)	Resistivity (Ohm-m)	Resistivity (Ohm-m)	Resistivity (Ohm-m)	Resistivity (Ohm-m)	Resistivity (Ohm-m)	Resistivity (Ohm-m)	Resistivity (Ohm-m)	Resistivity (Ohm-m)
1	0.25	62.2	556.7	149.0	406.5	132.0	144.3	44.4	114.2	18.1	22.7
2	0.25	113.1	1942.3	172.2	328.3	116.8	158.6	16.3	95.1	27.2	39.0
3	0.25	157.3	4105.5	150.5	293.2	110.5	185.9	8.9	96.6	34.3	51.6
4	0.25	189.3	6399.7	104.3	273.4	130.6	204.3	6.0	92.5	40.2	66.5
6	0.25	239.8	15311.4	101.6	240.1	140.5	247.3	5.0	89.3	38.6	90.6
6	0.5	292.0	4122.4	99.9	273.0	136.8	244.9	5.1	91.2	32.6	97.4
9	0.5	369.4	7966.7	56.1	227.6	140.1	297.9	3.8	70.0	33.5	129.1
12	0.5	397.0	12736.9	52.8	182.9	169.4	343.7	3.4	78.1	37.9	182.9
15	0.5	444.9	18784.0	44.5	141.0	199.1	362.3	3.4	75.2	47.9	210.4
15	1	428.3	9888.5	40.9	142.2	198.5	339.6	3.4	75.0	52.1	224.2
20	1	482.0	22127.1	42.7	89.2	214.4	354.2	5.6	79.1	36.8	282.1
25	1	526.4	29507.2	32.7	51.9	205.9	369.6	4.0	87.7	43.4	339.2
32	1	633.2	53356.8	24.3	22.8	242.7	408.2	4.7	110.0	47.2	360.0
40	1	708.4	38233.1	26.6	17.3	211.0	387.9	11.8	158.3	78.1	378.1
40	2.5	669.0	7110.7	27.0	12.6	220.3	364.6	13.2	162.5	50.0	397.6
50	2.5	750.6	23647.1	25.1	9.6	208.4	336.9	19.1	198.7	56.3	281.9
65	2.5	821.8	40799.9	29.2	14.1	164.4	337.2	13.5	306.6	73.4	290.6
80	2.5	867.9	53758.6	24.1	8.8	120.5	352.8	45.8	240.0	110.5	466.9
100	2.5	952.1	51496.6	37.7	8.2	81.6	284.5	18.2	216.4	150.7	1149.3
100	5	790.1	1250.5	42.6	11.4	75.2	238.2		221.4	157.0	1200.4
120	5	736.9	1860.1	43.1	15.3	67.7	194.2		201.8	201.2	1626.0
160	5	408.6	2708.1	76.1	46.5	112.5	160.7	10.4	171.7	298.6	3150.0

Location No		VES IKD 31	VES IKD 32	VES IKD 33	VES IKD 34	VES IKD 35	VES IKD 36	VES IKD 37	VES IKD 38	VES IKD 39	VES IKD 40
Easting		3.5252	3.521133	3.523967	3.5075	3.483783	3.5042	3.493783	3.4959	3.472817	3.470467
Northing		6.58145	6.56715	6.5462	6.551467	6.571783	6.595367	6.600383	6.6236	6.6198	6.661267
Elevation (m)		18	12	8	8	6	13	15		5	10
AB/2	MN/2	Resistivity (Ohm-m)	Resistivity (Ohm-m)	Resistivity (Ohm-m)	Resistivity (Ohm-m)	Resistivity (Ohm-m)	Resistivity (Ohm-m)	Resistivity (Ohm-m)	Resistivity (Ohm-m)	Resistivity (Ohm-m)	Resistivity (Ohm-m)
200	5	319.7	4130.8	104.7	15.7	87.9	150.7	21.4	121.1	301.4	4220.2
200	20	457.3	502.4	124.1	21.5	111.7	142.8	15.6	119.8	314.2	8087.5
250	20	327.3	79.0	126.8	42.4	115.1	117.6	19.5	101.2	253.4	
300	20	134.4	38.0	70.4	33.8	136.5	120.4			199.2	
300	30	230.5		60.7	35.0	56.0	122.2			186.6	
350	30										
350											
400	30	339.1		66.7	40.8	191.6					
500	30	105.7			40.4						

Table 5.2: Vertical Electrical Sounding survey Field data of Ikorodu area (Continuation)

Location No		VES IKD 41	VES IKD 42	VES IKD 43	VES IKD 44	VES IKD 45	VES IKD 48	VES IKD 49	VES IKD 50	VES IKD 51	VES IKD 52	VES IKD 53
Easting		3.44575	3.488433	3.487695	3.504867	3.5218	3.527367	3.538183	3.51955	3.513117	3.5203	3.510367
Northing		6.675883	6.67515	6.683234	6.686983	6.667933	6.671467	6.671883	6.654067	6.636967	6.630483	6.628817
Elevation (m)		14	44	48	54	40	33	40	50	52	27	42
AB/2	MN/2	Resistivity (Ohm-m)	Resistivity (Ohm-m)	Resistivity (Ohm-m)	Resistivity (Ohm-m)	Resistivity (Ohm-m)	Resistivity (Ohm-m)	Resistivity (Ohm-m)	Resistivity (Ohm-m)	Resistivity (Ohm-m)	Resistivity (Ohm-m)	Resistivity (Ohm-m)
1	0.25	229.2	109.7	595.0	199.9	128.5	32.5	22.8	38.9	34.9	41.9	22.9
2	0.25	251.1	193.0	601.5	208.8	118.6	38.1	25.1	58.1	38.4	66.6	31.4
3	0.25	292.0	257.8	775.2	209.0	113.0	45.1	25.9	74.6	48.2	108.7	38.5
4	0.25	329.5	316.5	872.7	207.5	121.2	58.4	26.7	94.8	57.6	149.9	38.3
6	0.25	372.4	445.1	962.2	233.8	84.8	90.9	29.9	164.6	74.3	212.7	42.2
6	0.5	394.3	469.5	979.6	251.3	94.3	89.5	29.8	148.6	73.3	202.0	50.9
9	0.5	505.1	649.5	999.4	319.3	67.7	146.6	22.5	197.1	140.1	307.5	90.6
12	0.5	584.0	736.7	995.3	380.4	57.6	203.6	35.1	314.8	177.1	414.6	137.3
15	0.5	702.6	788.8	1011.3	410.4	48.6	239.3	38.5	373.6	218.2	533.2	178.7
15	1	612.0	735.5	900.6	426.6	48.5	228.1	39.9	332.5	228.7	535.9	244.2
20	1	771.6	828.7	940.1	497.4	43.4	265.4	47.9	376.7	304.6	606.8	347.9
25	1	791.1	903.8	1018.3	559.2	48.4	287.7	55.9	408.8	359.8	710.7	374.5
32	1	670.2	1022.1	1166.3	637.5	62.5	314.7	64.1	422.7	448.4	747.3	422.7
40	1	459.7	1120.4	1130.7	719.9	85.8	310.2	75.2	532.6	482.8	761.1	585.3
40	2.5	473.7	1258.9	1075.1	769.8	75.4	263.2	43.2	567.9	481.7	722.1	493.7
50	2.5	268.4	1064.0	859.1	921.7	96.5	254.0	95.2	528.1	777.3	763.2	482.7
65	2.5	128.6	1399.8	632.7	1062.5	122.0	227.6	120.6	475.9	654.8	779.4	617.7
80	2.5	69.5	847.8	462.4	1090.9	123.1	176.4	139.2	440.8	570.1	577.0	598.7
100	2.5	49.6	1369.1	485.5	1110.2	109.6	126.7	170.2	373.7	612.9	459.7	590.3
100	5	50.5	1112.6	535.2	1119.2		123.2	172.5	446.4	686.4	421.5	679.7
120	5	37.9	912.4	609.7	1163.5	150.5	84.2	191.7	505.5	599.4	301.0	736.9
160	5	51.4	1194.1		1052.8	196.0	51.8	210.8	638.6	554.5	312.5	1089.6

Location No		VES IKD 41	VES IKD 42	VES IKD 43	VES IKD 44	VES IKD 45	VES IKD 48	VES IKD 49	VES IKD 50	VES IKD 51	VES IKD 52	VES IKD 53
Easting		3.44575	3.488433	3.487695	3.504867	3.5218	3.527367	3.538183	3.51955	3.513117	3.5203	3.510367
Northing		6.675883	6.67515	6.683234	6.686983	6.667933	6.671467	6.671883	6.654067	6.636967	6.630483	6.628817
Elevation (m)		14	44	48	54	40	33	40	50	52	27	42
AB/2	MN/2	Resistivity (Ohm-m)	Resistivity (Ohm-m)	Resistivity (Ohm-m)	Resistivity (Ohm-m)	Resistivity (Ohm-m)	Resistivity (Ohm-m)	Resistivity (Ohm-m)	Resistivity (Ohm-m)	Resistivity (Ohm-m)	Resistivity (Ohm-m)	Resistivity (Ohm-m)
200	5	54.0	346.7		886.4	204.1	66.0	185.6	507.7	417.0	282.1	0.0
200	20	29.6	381.4		809.3	216.1	68.0	188.6	531.9	466.6	280.0	566.1
250	20	45.4	255.1		562.0	192.7	79.8	127.8	550.7	318.0	811.7	463.4
300	20	37.3	182.3		402.6	93.8	99.1	85.9	416.7	425.1	1101.5	429.3
300	30	46.7	217.9				103.4		0.0	0.0	1241.1	434.9
350	30				268.5	113.0	126.5	67.8				
350					253.3	111.8		70.1				
400	30	158.3	109.1		192.2	210.6		33.8		395.7	261.6	703.2
500	30	53.5	82.2		88.5	32.5		11.4			397.9	

Table 5.3:Geo-electrical parameters in Abeokuta area

VES NO	layers no	Resistivity (Ohm-m)	Thickness (m)	Depth (m)	Reflection coefficient (K)	Elevation (m)	Rock type	curve types	Inferred Lithology
1	1	1232.7	1.1	1.1	0.907	138.4	PG	H	**gravelly topsoil**
	2	170.7	23.5	24.6					**sandy clay**
	3	3486.6							**Bedrock**
2	1	444.9	1	1	0.548	121.3	PBG	A	**sandy topsoil**
	2	518.6	5.9	6.9					**sandy horizon**
	3	1777.9							**Bedrock**
3	1	271.9	1	1	0.805	101	PBG	KH	**sandy topsoil**
	2	351.3	1.1	2.1					**sandy horizon**
	3	63.4	15.9	18					**clayey horizon**
	4	586.4		0					**Bedrock**
4	1	511.6	0.7	0.7	0.754	100.2	PG	KH	**sandy topsoil**
	2	1610.9	0.7	1.4					**resistive sandy horizon**
	3	172.3	6.6	8					**sandy horizon**
	4	1229.8		0					**Bedrock**
5	1	228.9	0.9	0.9	0.802	118.2	PG	H	**sandy topsoil**
	2	133.1	2.8	3.7					**sandy horizon**
	3	1212.5							**Bedrock**
6	1	215.6	0.9	0.9	0.962	84.8	PG	H	**sandy topsoil**
	2	21.5	8	8.9					**clayey horizon**
	3	1102							**Bedrock**
7	1	545.2	1.9	1.9	0.961	139.1	PBG	H	**sandy topsoil**
	2	52.7	10.5	12.4					**clayey horizon**
	3	2623.8							**Bedrock**
8	1	159.9	1	1	0.948	135.7	PBG	H	**sandy topsoil**
	2	28.2	24.1	25.1					**clayey horizon**
	3	1064							**Bedrock**
9	1	419.1	1.8	1.8	0.641	136.6	PBG	H	**sandy topsoil**
	2	193.7	6.9	8.7					**sandy horizon**
	3	886.4		8.7					**Bedrock**
10	1	33.7	1.1	1.1	0.829	148.4	PBG	KH	**clayey topsoil**
	2	102.5	11.5	12.6					**sandy horizon**
	3	55.2	41.1	53.7					**clayey horizon**
	4	589.1		0					**Bedrock**
11	1	121.1	1	1	0.787	145.5	PBG	KH	**topsoil**
	2	169.1	1	2					**sandy topsoil**
	3	15	10.1	12.1					**clayey horizon**
	4	126.1		0					**Bedrock**
12	1	97.1	0.7	0.7	0.887		PBG	HK	**clayey topsoil**
	2	14.8	2.3	3					**clayey horizon**
	3	246.4							**Bedrock**
13	1	151	1	1	0.941	76.4	PBG	H	**sandy topsoil**
	2	15.6	4.4	5.4					**clayey horizon**
	3	510.5		5.4					**Bedrock**
14	1	803.6	0.7	0.7	0.86	85.8	PG	H	**sandy topsoil**
	2	75.8	8.9	9.6					**clayey horizon**
	3	1007.1		9.6					**Bedrock**
15	1	458.6	0.7	0.7	0.938	45.5	HB	HA	**sandy topsoil**
	2	33.1	3.2	3.9					**clayey horizon**

VES NO	layers no	Resistivity (Ohm-m)	Thickness (m)	Depth (m)	Reflection coefficient (K)	Elevation (m)	Rock type	curve types	Inferred Lithology
	3	212.4	35.9	39.8					**sandy horizon**
	4	6654.5		0					**Bedrock**
16	1	24.2	0.5	0.5	0.64	47.9	HB	HA	**clayey topsoil**
	2	7	1.7	2.2					**clayey horizon**
	3	37	14.4	16.6					**clayey horizon**
		168.6		0					**Bedrock**
17	1	675.1	0.8		0.832	44.8	G	H	**sandy topsoil**
	2	44.2	9.3						**clayey horizon**
	3	480.8		0					**Bedrock**
18	1	319	1.4	1.4	0.942	65.2	G	H	**sandy topsoil**
	2	46.7	5.6	7					**clayey horizon**
	3	1560		0					**Bedrock**
19	1	340.3	1.3	1.3	0.943	48.5	G	H	**sandy topsoil**
	2	61	7.8	9.1					**clayey horizon**
	3	2085.4		0					**Bedrock**
20	1	1521.8	1.8	1.8	0.94	77.6	HB	H	**resistive topsoil**
	2	59.9	16.6	18.4					**clayey horizon**
	3	1923.1		0					**Bedrock**
21	1	264.9	1.1	1.1	0.996	62.1	PG	H	**sandy topsoil**
	2	24.9	5	6.1					**clayey horizon**
	3	11563.1		0					**Bedrock**
22	1	179.3	1.2	1.2	0.821	47.8	PG	H	**sandy topsoil**
	2	58.7	5.3	6.5					**clayey horizon**
	3	598.9		0					**Bedrock**
23	1	119	0.6	0.6	0.756	86.3	PG	HKH	**sandy topsoil**
	2	52.2	2.2	2.8					**clayey horizon**
	3	111.5	19.3	22.1					**sandy horizon**
	4	92.6	3.4	25.5					**clayey horizon**
	5	667.2							**Bedrock**
24	1	82.1	0.7	0.7	0.926	71.6	PG	KH	**clayey topsoil**
	2	846.4	0.8	1.5					**sandy horizon**
	3	45.9	12.3	13.8					**clayey horizon**
	4	1195.4		0					**Bedrock**
25	1	505.3	1.8	1.8	0.69	69.7	PG	H	**sandy topsoil**
	2	104.2	12.7	14.5					**sandy horizon**
	3	567.8		0					**Bedrock**
26	1	161	1.2	1.2	0.985	76.1	HB	KH	**sandy topsoil**
	2	228.5	2.7	3.9					**sandy horizon**
	3	42.5	6.6	10.5					**clayey horizon**
	4	5443.9		0					**Bedrock**
27	1	360	1.7	1.7	0.75	60.6	HB	H	**sandy topsoil**
	2	120	7.3	10					**sandy horizon**
	3	840							**Bedrock**
28	1	124.2	0.9	0.9	0.72	91.2	PG		**sandy topsoil**
	2	55.2	2.1	3.0					**clayey horizon**
	3	276.0	8.4	11.4					**sandy horizon**
	4	65.1	35.1	46.6					**clayey horizon**
	5	400.2							**Bedrock**
29	1	752.3	0.9	0.9	0.852	76.9	HB	H	**sandy topsoil**
	2	158.1	20.7	21.6					**sandy horizon**

VES NO	layers no	Resistivity (Ohm-m)	Thickness (m)	Depth (m)	Reflection coefficient (K)	Elevation (m)	Rock type	curve types	Inferred Lithology
	3	1973.4		0					**Bedrock**
30	1	240.5	1.8	1.8	0.988	75.8	HB	H	**sandy topsoil**
	2	19.6	5.7	7.5					**clayey horizon**
	3	3290		0					**Bedrock**
31	1	690.9	1.3	1.3	0.97	38.9	HB	H	**sandy topsoil**
	2	132.8	24.9	26.2					**sandy horizon**
	3	8816.3		0					**Bedrock**
32	1	283.5	1.1	1.1	0.957	60.6	HB	H	**sandy topsoil**
	2	22	28.2	29.3					**clayey horizon**
	3	990.3		0					**Bedrock**
33	1	116.7	1.2	1.2	0.988	44.5	HB	H	**sandy topsoil**
	2	7.4	1	2.2					**clayey horizon**
	3	1242.7		0					**Bedrock**
34	1	221.3	1	1	0.799	29.7	HB	H	**sandy topsoil**
	2	105.4	6.5	7.5					**sandy horizon**
	3	945.7		0					**Bedrock**
35	1	146.4	0.8	0.8	0.939	37.6	HB	H	**sandy topsoil**
	2	11.9	9.3	10.1					**clayey horizon**
	3	375.6		0					**Bedrock**
36	1	2035.3	0.6	0.6	0.846	23.9	HB	H	**resistive topsoil**
	2	329	1.9	2.5					**sandy horizon**
	3	3936.1		0					**Bedrock**
37	1	221.7	1.1	1.1	0.729	112.1	PG	H	**sandy topsoil**
	2	1584.3	30	31.1					**sandy horizon**
	3	514.8		0					**Bedrock**
38	1	519.5	1.9	1.9	0.857	115.2	PG	H	**sandy topsoil**
	2	360.5	2.1	4					**sandy horizon**
	3	4675.4		0					**Bedrock**
39	1	255.4	1.7	1.7	0.418	125.8	PG	A	**sandy topsoil**
	2	731.5	11.9	13.6					**sandy horizon**
	3	1780.8		0					**Bedrock**
40	1	370.8	1.5	1.5	0.669	128.8	PG	HKH	**sandy topsoil**
	2	48.5		1.5					**clayey horizon**
	3	291.2	8.4	9.9					**sandy horizon**
	4	248.9	4.1	12.5					**sandy horizon**
	5	1257		0					**Bedrock**
41	1	455.3	0.4	0.4	0.677	90.9	PG	KH	**sandy topsoil**
	2	1799.4	5.2	5.6					**resistive sandy horizon**
	3	554	4.7	10.3					**sandy horizon**
		2874.8		0					**Bedrock**
42	1	361.6	1.3	1.3	0.99	121.2	PG	H	**sandy topsoil**
	2	44.5	9.7	11					**clayey horizon**
	3	8575		0					**Bedrock**
43	1	1504.8	0.5	0.5	0.872	81.6	PBG	H	**resistive topsoil**
	2	241.2	6	6.5					**sandy horizon**
	3	3526.7		0					**Bedrock**
44	1	126	1.3	1.3	0.894	77.9	PBG	A	**sandy topsoil**
	2	2250	0.6	1.9					**Gravelly**
	3	2700		0					**Bedrock**

VES NO	layers no	Resistivity (Ohm-m)	Thickness (m)	Depth (m)	Reflection coefficient (K)	Elevation (m)	Rock type	curve types	Inferred Lithology
45	1	1814.6	0.7	0.7	0.929	113.1	PBG	H	**resistive topsoil**
	2	123.9	6.6	7.3					**sandy horizon**
	3	3366.3		0					**Bedrock**
46	1	1763.3	2.3	2.3	0.844	105.3	PBG	H	**resistive topsoil**
	2	123	15.5	17.8					**sandy horizon**
	3	1452.6		0					**Bedrock**
47	1	1604.7	2.1	2.1	0.962	98.7	PBG	H	**resistive topsoil**
	2	110.1	10.7	12.8					**sandy horizon**
	3	5648.1		0					**Bedrock**
48	1	2024.6	0.8	0.8	0.978	111.2	PBG	H	**resistive topsoil**
	2	86.8	10.6	11.4					**clayey horizon**
	3	7964.4		0					**Bedrock**
49	1	4095	0.7	0.7	0.942	79.1	PBG	HKH	**resistive topsoil**
	2	195.7	4.9	4.9					**sandy horizon**
	3	1498.3	3.5	8.4					**resistive topsoil**
	4	272.6	12.3	20.7					**sandy horizon**
	5	9095.3							**Bedrock**
50	1	155.6	0.9	0.9	0.785	149.1	PBG	H	**sandy topsoil**
	2	65.2	10.2	11.1					**clayey horizon**
	3	541.1							**Bedrock**
51	1	125.7	0.9	0.9	0.983	53.6	PG	H	**sandy topsoil**
	2	15.2	6.7	7.7					**clayey horizon**
	3	1796.3							**Bedrock**
52	1	310.8	1	1	0.962	57.1	G	H	**sandy topsoil**
	2	24.9	2.4	3.4					**clayey horizon**
	3	1296.7							**Bedrock**
53	1	313.9	1.5	1.5	0.882	66	G	H	**sandy topsoil**
	2	22.2	8.8	10.2					**clayey horizon**
	3	355.4							**Bedrock**
54	1	1383.7	0.7	0.7	0.995	63.6	G	H	**resistive topsoil**
	2	22.4	4.1	4.8					**clayey horizon**
	3	8318.9							**Bedrock**
55	1	941.7	1.8	1.8	0.967	47.3	G	H	**resistive topsoil**
	2	63.7	19.8	21.6					**clayey horizon**
	3	3790.2							**Bedrock**
57	1	3493.2	2.5	2.5	0.954	59.5	G	H	**resistive topsoil**
	2	59.2	10	12.5					**clayey horizon**
	3	2516.6	1.5						**Bedrock**
58	1	1379.1		1.5	0.635	96.8	G	H	**resistive topsoil**
	2	368.2	9.4	10.9					**sandy horizon**
	3	1648.5							**Bedrock**
59	1	3171.5	1.4	1.4	0.861	94.2	G	H	**resistive topsoil**
	2	151.5	5.4	6.8					**sandy horizon**
	3	2034							**Bedrock**
60	1	2919.1	1.2	1.2	0.701	95.7	G	H	**resistive topsoil**
	2	93.9	7.1	8.3					**clayey horizon**
	3	533.9							**Bedrock**
61	1	6428.3	1.8	1.8	0.92	72.8	G	H	**resistive topsoil**
	2	97.9	29.3	31.2					**clayey horizon**
	3	3790.2							**Bedrock**

VES NO	layers no	Resistivity (Ohm-m)	Thickness (m)	Depth (m)	Reflection coefficient (K)	Elevation (m)	Rock type	curve types	Inferred Lithology
62	1	95.1	0.5	0.5	0.978	40.9	PG	KH	**sandy topsoil**
	2	262.1	0.9	1.4					**sandy horizon**
	3	13.4	7.9	9.3					**clayey horizon**
	4	1474.9							**Bedrock**
63	1	221.5	0.9	0.9	0.718	81.9	HB	KH	**sandy topsoil**
	2	272.9	2.8	3.7					**sandy horizon**
	3	102.6	17.8	21.5					**sandy horizon**
	4	625							**Bedrock**
64	1	2579.7	1.7	1.7	0.86	89.9	G	H	**resistive topsoil**
	2	129.8	17.9	19.6					**sandy horizon**
	3	1725.5							**Bedrock**
65	1	143.3	1.1	1.1	0.91	124.9	PBG	KH	**sandy topsoil**
	2	225.5	3.7	4.8					**sandy horizon**
	3	92.2	25.8	30.5					**clayey horizon**
	4	1959.2							**Bedrock**
66	1	92.3	1	1	0.649	135.9	PBG	KH	**clayey topsoil**
	2	142.1	1.7	2.7					**sandy horizon**
	3	86.9	13.7	16.4					**clayey horizon**
	4	408.9							**Bedrock**
67	1	86.2	1.1	1.1	0.993	68.2	PG	H	**clayey topsoil**
	2	9.1	2.5	3.6					**clayey horizon**
	3	2660.4							**Bedrock**
68	1	253.6	2.2	2.2	0.892	113.5	PBG	H	**sandy topsoil**
	2	34.2	7	9.2					**clayey horizon**
	3	597.6							**Bedrock**
69	1	1533	1.5	1.5	0.63	111.2	PBG	HKH	**resistive topsoil**
	2	220.8	5.5	7					**sandy horizon**
	3	925.6	15.1	22.1					**sandy horizon**
	4	355.5	33.3	55.4					**sandy horizon**
	5	1564.5							**Bedrock**
70	1	2798.6	1.2	1.2	0.563	110.6	PBG	H	**resistive topsoil**
	2	64.8	13.8	14.9					**clayey horizon**
	3	232.1							**Bedrock**
71	1	2161.3	1.3	1.3	0.657	114.4	PBG	H	**resistive topsoil**
	2	86.6	18.8	20.1					**clayey horizon**
	3	418.2							**Basement**
72	1	326.5	2.2	2.2	0.991	98.4	PBG	H	**sandy topsoil**
	2	29.2	5.3	7.5					**clayey horizon**
	3	6646.9							**Bedrock**
73	1	238.5	2.2	2.2	0.972	36.5	HB	H	**sandy topsoil**
	2	30.5	16	18.2					**clayey horizon**
	3	2178.4							**Bedrock**
74	1	142.1	0.9	0.9	0.932	45	HB	H	**sandy topsoil**
	2	12.3	5.3	6.3					**clayey horizon**
	3	347.2							**Bedrock**
75	1	204.1	1.6	1.6	0.974	58.7	HB	H	**sandy topsoil**
	2	13	4.9	6.5					**clayey horizon**
	3	994.8							**Bedrock**

Table 5.4: Geo-electrical parameters in Ikorodu area

VES NO	layers no	Resistivity (Ohm-m)	Thickness (m)	Depth (m)	Elevation (m)	curve types	Inferred Lithology
VES IKD 1	1	150.7	0.7	0.7	23	AK	sandy-clay topsoil
	2	309.8	3.7	4.4			sandy layer
	3	926.3	49.8	54.2			sandy layer
	4	55.9					clayey layer
VES 1KD 2	1	163.1	0.8	0.8	28	AK	sandy clay topsoil
	2	396.6	3.3	4.1			sandy layer
	2	3787.7	14.9	19.0			resistive sand
	3	119.8					sandy clay topsoil
VES IKD 3	1	104.4	0.7	0.7	28	KQ	Sandy-clay topsoil
	2	1925.0	7.3	8.1			resistive sand
	3	521.5	68.3	76.4			sandy layer
	4	62.6					clayey layer
VES IKD 4	1	138.5	0.6	0.6	26	HKHK	sandy clay topsoil
	2	52.5	0.9	1.5			clayey layer
	3	116.0	4.2	5.7			Sandy Clay
	4	40.1	6.6	12.3			clayey layer
	5	322.8	51.0	63.3			sandy layer
	6	9.8					clayey layer
VES IKD 5	1	38.4	1.1	1.1	33	KQQ	Clayey tosoil
	2	1454.4	10.1	11.2			resistive sand
	3	327.7	13.4	24.5			sandy layer
	4	294.0	154.1	178.6			sandy layer
	5	27.8					clayey layer
VES IKD 6	1	71.2	1.0	1.0	38	AK	Clayey tosoil
	2	425.2	11.4	12.4			sandy layer
	3	1020.6	101.9	114.4			sandy layer
	4	27.5					Clayey layer
VES IKD 7	1	76.7	1.4	1.4	41	AKH	clayey topsoil
	2	429.9	0.8	2.2			sandy layer
	3	7789.4	10.3	12.5			resistive sand
	4	142.8	64.0	76.5			Sandy Clay
	5	5785.1					resistive sand
VES IKD 8	1	46.9	1.0	1.0	34	AK	Clayey Topsoil
	2	585.7	4.9	5.9			sandy layer
	3	1961.7	16.2	22.1			resistive sand
	4	194.4					Sandy Clay
VES IKD 9	1	154.7	1.6	1.6	29	AK	sandy clay topsoil
	2	274.9	1.8	3.4			sandy layer
	3	5169.2	26.8	30.2			resistive sand
	4	49.6					Clayey layer

VES NO	layers no	Resistivity (Ohm-m)	Thickness (m)	Depth (m)	Elevation (m)	curve types	Inferred Lithology
VES IKD 10	1	56.7	0.8	0.8	37	K	Clayey topsoil
	2	1222.3	45.0	45.7			resistive sand
	3	71.0					Clayey layer
VES IKD 11	1	118.7	0.5	0.5	31	AK	sandy clay topsoil
	2	358.5	6.7	7.2			sandy layer
	3	3056.8	23.4	30.6			resistive sand
	4	161.4					Sandy Clay
VES IKD 12	1	576.2	0.7	0.7	39	K	sandy topsoil
	2	1368.9	38.5	39.2			resistive sand
	3	155.0					Sandy Clay
VES IKD 13	1	93.9	0.5	0.5	24	AK	Clayey topsoil
	2	2809.0	1.0	1.5			resistive sand
	3	44725.0	12.7	14.2			resistive sand
	4	416.7					sandy layer
VES IKD 14	1	80.4	1.0	1.0	30	AK	clayey topsoil
	2	608.8	4.8	5.8			sandy layer
	3	5573.5	23.6	29.4			resistive sand
	4	78.2					Clayey layer
VES IKD 15	1	389.5	0.6	0.6	27	KHK	sandy topsoil
	2	1053.7	2.4	3.0			sandy layer
	3	363.9	1.5	4.5			sandy layer
	4	1428.8	38.8	43.3			resistive sand
	5	115.4					Sandy Clay
VES IKD 16	1	160.4	0.8	0.8	27	HAK	sandy Clay topsoil
	2	82.1	1.0	1.8			Clayey layer
	3	231.9	13.9	15.7			sandy layer
	4	2500.9	27.2	43.0			resistive sand
	5	54.3					Clayey layer
VES IKD 17	1	141.4	0.6	0.6	19	HKH	sandy Clay topsoil
	2	67.3	3.3	4.0			Clayey layer
	3	646.5	16.3	20.2			sandy layer
	4	30.3	55.8	76.0			Clayey layer
	5	2832.9					resistive sand
VES IKD 18	1	117.2	0.7	0.7	22	AK	sandy Clay topsoil
	2	409.0	4.4	5.1			sandy layer
	3	6941.0	14.6	19.7			resistive sand
	4	143.0					Sandy Clay
VES IKD 19	1	571.1	3.1	3.1	20	K	sandy topsoil
	2	1573.5	60.1	63.2			resistive sand
	3	66.0					Clayey layer
VES IKD 20	1	438.3	0.9	0.9	29	AK	sandy topsoil
	2	573.1	5.6	6.5			sandy layer
	3	3971.3	23.7	30.2			resistive sand

VES NO	layers no	Resistivity (Ohm-m)	Thickness (m)	Depth (m)	Elevation (m)	curve types	Inferred Lithology
	4	68.4					Clayey layer
VES IKD 21	1	139.4	0.5	0.5	30	AK	
	2	915.7	14.0	14.4			sandy layer
	3	4289.8	42.3	56.8			resistive sand
	4	72.8					Clayey layer
VES IKD 22	1	169.9	0.7	0.7	38	AKQ	sandy Clay topsoil
	2	547.3	7.8	8.5			sandy layer
	3	5086.0	21.9	30.4			resistive sand
	4	1020.2	15.0	45.4			sandy layer
	5	116.7					Sandy Clay
VES IKD 23	1	181.3	1.3	1.3	48	HK	sandy Clay topsoil
	2	47.8	9.1	10.5			Clayey layer
	3	678.2	20.1	30.6			sandy layer
	4	28.8					Clayey layer
VES IKD 24	1	134.9	0.9	0.9	23	HA	sandy Clay topsoil
	2	18.4	19.7	20.5			Clayey layer
	3	250.6	15.9	36.4			sandy layer
	4	3592.1					resistive sand
VES IKD 25	1	393.5	1.6	1.6	59	HK	sandy topsoil
	2	293.5	9.5	11.1			sandy layer
	3	1437.2	86.2	97.3			resistive sand
	4	22.4					Clayey layer
VES IKD 26	1	83.0	0.8	0.8	4	KH	clayey topsoil
	2	363.0	1.4	2.2			sandy layer
	3	16.0	50.8	53.0			Clayey layer
	4	37.0					Clayey layer
VES IKD 27	1	144.1	1.3	1.3	4	QH	sandy Clay
	2	51.3	5.9	7.3			Clayey layer
	3	7.4	85.8	93.1			Clayey layer
	4	21.7					Clayey layer
VES IKD 28	1	588.8	1.2	1.2	4	QQH	sandy topsoil
	2	238.0	2.2	3.3			sandy layer
	3	71.5	2.9	6.2			Clayey layer
	4	11.3	43.9	50.1			Clayey layer
	5	70.5					Clayey layer
VES IKD 29	1	155.5	0.7	0.7	7	KHK	sandy Clay topsoil
	2	700.4	2.7	3.4			sandy layer
	3	41.6	16.8	20.2			Clayey layer
	4	322.1	106.2	126.4			sandy layer
	5	61.2					Clayey layer
VES IKD 30	1	144.4	0.7	0.7	18	AKQ	sandy clay
	2	1345.0	7.5	8.2			resistive sand
	3	1771.4	18.9	27.1			resistive sand

VES NO	layers no	Resistivity (Ohm-m)	Thickness (m)	Depth (m)	Elevation (m)	curve types	Inferred Lithology
	4	754.2	45.0	72.1			sandy layer
	5	209.0					sandy layer
VES IKD 31	1	41.5	0.6	0.6	18	AK	Clayey topsoil
	2	610.8	12.5	13.1			sandy layer
	3	1347.1	48.6	61.7			resistive sand
	4	96.6					Clayey layer
VES IKD 33	1	130.3	0.5	0.5	8	KQHK	sandy clay topsoil
	2	219.9	1.4	1.9			sandy layer
	3	48.4	11.3	13.2			Clayey layer
	4	10.0	18.5	31.7			Clayey layer
	5	778.4	112.4	144.1			sandy layer
	6	16.4					Clayey layer
VES IKD 34	1	457.0	0.6	0.6	8	QH	sandy topsoil
	2	267.8	7.8	8.5			sandy layer
	3	8.0	55.1	63.6			Clayey layer
	4	102.6					Sandy Clay
VES IKD 35	1	128.4	1.4	1.4	6	HKHA	sandy clay topsoil
	2	96.4	3.3	4.6			Clayey layer
	3	439.0	15.9	20.6			sandy layer
	4	27.0	39.9	60.4			Clayey layer
	5	224.0	47.1	107.5			sandy layer
	6	822.9					sandy layer
VES IKD 36	1	140.0	1.7	1.7	13	AK	sandy clay topsoil
	2	394.1	7.3	9.0			sandy layer
	3	454.0	34.0	43.0			sandy layer
	4	111.2					Sandy Clay
VES IKD 37	1	49.7	0.9	0.9	15	HK	Clayey topsoil
	2	3.3	18.8	19.7			Clayey layer
	3	116.9	30.9	50.6			Sandy Clay
	4	22.1					Clayey layer
VES IKD 38	1	105.5	2.9	2.9		HK	sandy Clay
	2	51.0	11.9	11.9			Clayey layer
	3	707.7	29.0	40.9			sandy layer
	4	25.3					Clayey layer
VES IKD 39	1	11.2	0.5	0.5	5	KHAK	Clayey Topsoil
	2	52.2	2.1	2.6			Clayey layer
	3	23.9	9.0	11.6			Clayey layer
	4	73.6	7.6	19.2			Clayey layer
	5	1786.8	35.5	54.7			resistive sand
	6	75.9					Clayey layer
VES IKD 40	1	22.2	1.2	1.2	10	AK	Clayey Topsoil
	2	340.5	6.9	8 .1			sandy layer
	3	2430.2	20.9	29			resistive sand

VES NO	layers no	Resistivity (Ohm-m)	Thickness (m)	Depth (m)	Elevation (m)	curve types	Inferred Lithology
	4	750.3	15.3	44.4			sandy layer
VES IKD 41	1	226.7	2.0	2.0	14	AKH	sandy topsoil
	2	499.3	1.3	3.3			sandy layer
	3	2528.0	5.4	8.7			resistive sand
	4	23.6	62.6	71.4			Clayey layer
	5	63.4					Clayey layer
VES IKD 42	1	74.8	0.7	0.7	44	AK	Clayey topsoil
	2	1139.6	15.8	16.5			sandy layer
	3	3137.8	24.6	41.1			resistive sand
	4	81.2					Clayey layer
VES IKD 43	1	545.3	1.0	1.0	48	AKH	sandy topsoil
	2	1038.4	11.4	12.4			sandy layer
	3	2437.2	7.3	19.7			resistive sand
	4	200.3	34.1	53.8			sandy layer
	5	2643.9					resistive sand
VES IKD 44	1	403.5	1.1	1.1	54	HK	sandy topsoil
	2	311.9	11.1	12.3			sandy layer
	3	1526.3	81.3	93.6			resistive sand
	4	21.6					Clayey layer
VES IKD 45	1	124.2	4.4	4.4	40	HK	Sandy clay
	2	17.4	7.1	11.5			Clayey layer
	3	694.8	47.3	58.8			sandy layer
	4	7.0					Clayey layer
VES IKD 48	1	29.1	1.4	1.4	33	AKH	Clayey topsoil
	2	131.0	0.8	2.2			Sandy Clay
	3	1802.5	6.2	8.4			resistive sand
	4	21.4	64.0	72.4			Clayey layer
	5	2046.9					resistive sand
VES IKD 49	1	22.4	0.9	0.9	40	AK	Clayey topsoil
	2	28.6	10.3	11.2			Clayey layer
	3	765.7	31.6	42.8			sandy layer
	4	5.7					Clayey layer
VES IKD 50	1	35.2	1.3	1.3	50	KHK	Clayey topsoil
	2	1147.4	12.7	14.0			sandy layer
	3	278.5	31.8	45.8			sandy layer
	4	1650.2	37.6	83.4			resistive sand
	5	207.8					sandy layer
VES IKD 51	1	32.3	1.7	1.7	52	AKH	Clayey topsoil
	2	111.8	1.0	2.8			Sandy Clay
	3	3218.1	13.2	15.9			resistive sand
	4	301.0	47.4	63.3			sandy layer
	5	348.8					sandy layer

VES NO	layers no	Resistivity (Ohm-m)	Thickness (m)	Depth (m)	Elevation (m)	curve types	Inferred Lithology
VES IKD 52	1	27.1	0.7	0.7	27	KQH	Clayey topsoil
	2	3765.0	7.6	8.3			resistive sand
	3	424.7	10.0	18.3			sandy layer
	4	134.8	41.5	59.8			Sandy Clay
	5	284.4					sandy layer
VES IKD 53	1	22.4	1.4	1.4	42	AK	Clayey Topsoil
	2	61.0	1.2	2.7			Clayey layer
	3	2642.1	21.5	24.2			resistive sand
	4	274.5					sandy layer

APPENDIX II

Geochemical Data

Table 5.5: Results of analysis of the rock samples in Abeokuta area

Analyte	Unit	MDL	Pegmatite	Porphyritic granite	Hornblende-Biotite Gneiss	Granite	Porphyroblastic Gneiss
Wgt	KG	0.01	<0.01	<0.01	0.01	<0.01	0.01
SiO_2	%	0.01	74.36	72.35	54.51	73.08	66.17
Al_2O_3	%	0.01	14.12	14.29	17.05	12.83	13.79
Fe_2O_3	%	0.04	0.24	1.58	8.86	4.02	5.22
MgO	%	0.01	0.03	0.22	2.47	0.67	1.07
CaO	%	0.01	0.10	1.07	12.55	2.90	2.32
Na_2O	%	0.01	1.39	3.00	0.95	3.10	2.70
K_2O	%	0.01	9.33	6.67	0.20	1.52	4.26
TiO_2	%	0.01	<0.01	0.12	2.17	0.75	1.11
P_2O_5	%	0.01	0.01	0.12	0.47	0.25	0.45
LOI	%	-5.1	0.40	0.40	0.40	0.70	2.60
Sum	%	0.01	99.96	99.83	99.69	99.82	99.70
Ba	PPM	1	486.00	422.00	43.00	169.00	771.00
Be	PPM	1	<1	4.00	<1	<1	2.00
Co	PPM	0.2	0.40	1.30	15.30	6.50	10.10
Cs	PPM	0.1	0.60	3.60	<0.1	0.40	1.40
Ga	PPM	0.5	13.50	21.10	21.10	24.50	24.50
Hf	PPM	0.1	0.40	4.20	6.00	10.70	14.40
Nb	PPM	0.1	2.00	13.00	13.30	14.90	19.70
Rb	PPM	0.1	306.30	290.40	3.80	120.90	245.40
Ni	PPM	20	<20	<20	29.00	<20	<20
Sc	PPM	1	<1	3.00	42.00	5.00	7.00
Ta	PPM	0.1	0.10	1.40	0.80	0.80	1.00
Th	PPM	0.2	3.70	48.00	1.30	77.70	84.50
U	PPM	0.1	0.30	4.70	0.50	2.50	3.90
V	PPM	8	<8	<8	314.00	25.00	40.00
W	PPM	0.5	<0.5	<0.5	<0.5	<0.5	0.80
Zr	PPM	0.1	7.20	111.20	241.10	387.60	532.60
Y	PPM	0.1	0.90	14.50	34.00	18.80	27.70
La	PPM	0.1	3.90	43.00	43.60	96.00	113.10
Ce	PPM	0.1	7.20	94.10	96.30	216.40	269.20
Pr	PPM	0.02	0.83	11.79	13.58	28.04	35.15
Nd	PPM	0.3	2.80	42.30	58.60	106.50	138.00
Sm	PPM	0.05	0.54	8.45	10.31	15.40	18.12
Eu	PPM	0.02	0.40	0.47	2.30	0.95	1.25
Gd	PPM	0.05	0.37	5.89	8.38	8.26	9.65
Tb	PPM	0.01	0.05	0.80	1.22	0.97	1.23
Dy	PPM	0.05	0.21	3.05	6.53	3.98	5.42
Ho	PPM	0.02	0.04	0.50	1.25	0.52	0.94
Er	PPM	0.03	0.06	1.00	3.12	1.32	2.53
Tm	PPM	0.01	<0.01	0.13	0.41	0.15	0.35

Table 5.5: Results of analysis of the rock samples in Abeokuta area

Analyte	Unit	MDL	Pegmatite	Porphyritic granite	Hornblende-Biotite Gneiss	Granite	Porphyroblastic Gneiss
Yb	PPM	0.05	<0.05	0.83	2.66	1.12	2.12
Lu	PPM	0.01	0.01	0.12	0.39	0.14	0.31
TOT/C	%	0.02	0.06	0.19	0.03	0.16	0.09
Mo	PPM	0.1	<0.1	0.40	<0.1	0.40	0.30
Cu	PPM	0.1	1.90	4.90	1.50	11.00	13.20
Pb	PPM	0.1	1.80	9.30	1.10	4.10	4.20
Zn	PPM	1	2.00	35.00	8.00	73.00	107.00
Ni	PPM	0.1	0.60	1.50	3.30	4.20	5.40
As	PPM	0.5	<0.5	1.50	1.00	<0.5	<0.5
Sb	PPM	0.1	<0.1	0.20	<0.1	0.10	<0.1
Au	PPB	0.5	1.20	1.30	0.60	1.70	0.90
Tl	PPM	0.1	<0.1	0.40	<0.1	0.50	0.70

Table 5.6 Physical parameters in Abeokuta area

sample No	Easting	Northing	Total Well Depth	Static Water Level	pH	Total Dissolved Solids (mg/l)	Electrical Conductance (uS/cm)	Hardness mg/l $CaCO_3$
1	3.3384	7.1539	3.4	2.7	7.1	1149	1766	89.2
2	3.3418	7.1766	2.6	2.1	7.3	789	1210	76.5
3	3.3246	7.1610	3.1	2.4	7.8	919	1409	106.2
4	3.3210	7.1739	2.5	2.0	7.2	379	578	61.7
5	3.3504	7.1403	6.2	5.5	6.6	873	1333	91.3
6	3.3742	7.1447	8.0	7.1	7.0	331	509	28.9
7	3.3983	7.1399	5.5	4.8	5.9	95	144	9.2
8	3.3671	7.1264	6.9	6.4	5.9	78	119	7.3
9	3.3510	7.1669	7.5	7.1	7.9	1504	2331	118
10	3.3568	7.1525	4.1	3.7	6.3	552	847	53.6
11	3.3900	7.1795	ND	ND	6.1	214	326	15.2
12	3.3977	7.1728	8.2	7.8	7.3	910	1398	82.8
13	3.3430	7.1458	1.5	1.2	7.1	706	1082	102.4
14	3.3081	7.1343	2.5	2.0	7.1	644	989	103.8
15	3.3206	7.1243	6.1	5.6	7.7	784	1201	119.3
16	3.3398	7.1179	3.4	2.9	7.6	914	1408	33.6
17	3.3118	7.1710	5.8	2.3	6.6	300	452	26.6
18	3.3200	7.1173	5.5	2.3	6.9	319	491	53.3
19	3.3266	7.1733	8.0	7.0	7.1	1016	1563	123.1
20	3.3276	7.1572	5.0	3.4	6.9	1014	1560	89.4
21	3.3283	7.1249	12.0	9.4	6.5	624	960	52.5
22	3.3292	7.0875	5.0	2.5	6.6	340	527	29.8
23	3.3308	7.1385	9.0	4.2	6.9	521	802	70.5
24	3.3352	7.1125	5.5	3.0	7.6	318	493	72.8
25	3.3435	7.1795	6.0	3.5	6.6	302	465	26.8
26	3.3441	7.1178	11.5	6.0	6.2	379	583	79.9
27	3.3454	7.1151	4.0	2.0	6.5	333	509	54.8
28	3.3467	7.0901	7.5	4.5	6.4	345	528	67.2
29	3.3533	7.1358	7.2	3.6	7.1	511	782	62.1
30	3.3538	7.1787	6.3	4.1	6.8	254	391	69.1
31	3.3542	7.1127	7.0	4.0	8.6	342	520	58.2
32	3.3575	7.1292	10.8	1.8	6.6	254	391	9.9
33	3.3575	7.1583	5.4	3.2	7.0	105	162	19.3
34	3.3615	7.2051	5.4	3.6	6.7	231	356	37.2
35	3.3638	7.1868	8.1	4.2	6.6	303	467	43.7
36	3.3675	7.1790	5.4	4.5	6.3	361	555	33
37	3.3683	7.1433	3.6	3.2	6.8	424	652	43
38	3.3767	7.1233	6.3	4.6	6.2	937	1442	46
39	3.3846	7.1982	10.8	3.6	6.5	282	429	42.6
40	3.3917	7.1043	8.0	2.5	8.3	337	512	25.7
41	3.3938	7.1851	6.3	4.5	7.3	273	415	29.4
42	3.3948	7.1785	7.2	4.1	6.2	238	366	10.1
43	3.3953	7.0962	14.0	7.0	6.1	161	246	27.5

Table 5.6 Physical parameters in Abeokuta area

sample No	Easting	Northing	Total Well Depth	Static Water Level	pH	Total Dissolved Solids (mg/l)	Electrical Conductance (uS/cm)	Hardness mg/l $CaCO_3$
44	3.3958	7.1137	11.0	5.5	6.3	161	237	56
45	3.3634	7.1129	7.4	4.4	6.5	106	163	29.4
46	3.3035	7.0989	3.8	1.6	7.1	451	663	31.7
47	3.3013	7.1768	4.9	2.1	6.8	254	373	26.2
48	3.3850	7.2153	9.1	3.7	7.1	231	340	36.3

Table 5.7 Physical parameters in Ikorodu area

S /No	Easting	Northing	Medium	Static Water Level	Total Well Depth	Total Dissolved Solids (mg/l)	Electrical Conductance (uS/cm)	Hardness mg/l $CaCO_3$	pH
1	3.516	6.606	Borehole			250	1700	23	4.2
2	3.510	6.591	Shallow well			232	1694	18	7.8
3	3.500	6.591	Shallow well			358	2616	37	8.0
4	3.488	6.576	bh (Deep)			80	544	9.1	7.5
5	3.480	6.569	Shallow well	4.5	5	473	3216.4	46.3	7.2
6	3.485	6.541	Shallow well	4.3	5	166	1128.8	17.9	7.2
7	3.518	6.592	Borehole	24		142	965.6	21.2	4.5
8	3.522	6.580	Shallow well			232	1694	35	8.0
9	3.509	6.562	Shallow well	4.3	5.2	156	1142	21	4.8
10	3.507	6.549	Shallow well	3.1	5.3	131	957	21	6.3
11	3.501	6.546	Shallow well	2.1	4.4	358	2616	30	6.2
12	3.500	6.540	Shallow well	3.1	3.8	1091	7961	35	5.9
13	3.534	6.593	Shallow well			30	220	5	5.3
14	3.535	6.568	Shallow well			198	1232.0	12.2	7.2
15	3.524	6.551	Shallow well	4	4.8	254	1727.2	19	7.5
16	3.523	6.531	Shallow well	1.8	3.65	1014	6895.2	134	6.4
17	3.553	6.538	Shallow well	3.8	4.8	1000	6800	120	7.3
18	3.531	6.617	Borehole			80	494.4	1.7	6.6
19	3.554	6.621	Borehole			62	387.1	7.8	7.4
20	3.573	6.614	Borehole			55	344.4	7.9	6.5
21	3.588	6.593	Borehole			22	149.6	3.7	6.3
22	3.594	6.565	Borehole			153	1040.4	25.1	5.8
23	3.615	6.615	Borehole			32	217.6	1.6	6.6
24	3.629	6.600	Borehole			54	337.2	7.2	6.3
25	3.628	6.578	Deep well	25	27	94	639.2	30.2	7.5
26	3.655	6.588	Shallow well	4	5.6	386	2624.8	70.9	7.4
27	3.654	6.604	Borehole			22	149.6	3.6	5.6
28	3.657	6.623	Borehole			114	735.3	14.3	6.3
29	3.666	6.649	Borehole			200	1244.6	29.4	7.1
30	3.671	6.664	Borehole			245	1580.25	42.4	4.9
31	3.650	6.670	Borehole			219	1361.7	37	6.9
32	3.619	6.661	Borehole			234	1509.3	48.2	4.7
33	3.607	6.654	Borehole			173	1076.1	35.6	6.8
34	3.574	6.654	Borehole			134	864.3	51.8	7.8
35	3.545	6.674	Borehole			35	225.75	7.3	6.9
36	3.527	6.668	Borehole			160	1032	29	7.4
37	3.534	6.631	Borehole			32	217.6	4.6	6.5
38	3.517	6.644	Borehole			71	457.95	9.3	6.7
39	3.501	6.626	Borehole			28	180.6	4.6	6.8
40	3.492	6.602	Shallow well			630	4284	114	5.5

Table 5.7 Physical parameters in Ikorodu area (contd)

S /No	Easting	Northing	Medium	Static Water Level	Total Well Depth	Total Dissolved Solids (mg/l)	Electrical Conductance (uS/cm)	Hardness mg/l $CaCO_3$	pH
41	3.457	6.619	Borehole			405	2516.9	58.5	7.2
42	3.481	6.632	Borehole			345	2225.25	63.9	6.3
43	3.459	6.638	Borehole			281	1742.8	39.9	7.1
44	3.472	6.657	Borehole			59	380.55	9.7	7.3
45	3.498	6.654	Borehole			78	482.5	8.3	6.7
46	3.489	6.669	Borehole			30	193.5	4.9	6.4
47	3.508	6.684	Borehole			30	193.5	4.9	6.0
48	3.489	6.692	Borehole			48	309.6	8.9	6.7
49	3.465	6.687	Borehole			67	414.0	5.1	6.7
50	3.444	6.667	Borehole			130	838.5	18.7	7.2

Table 5.8: Major chemical constituents of groundwater in Abeokuta area

Analyte Symbol	Na	K	Mg	Ca	Cl	SO4	HCO_3	NO3 (as N)	S	P	F	NO2 (as N)	Br	PO4 (as P)
Unit Symbol	mg/L	mg/L	mg/L	mg/L	mg/L	mg/L	mg/L	mg/L	mg/L	mg/L	mg/L	mg/L	mg/L	mg/L
Detection Limit	0.1	0.1	0.1	0.1	0.03	0.03		0.01	1	0.02	0.01	0.01	0.03	0.02
1	106	88.3	19.8	51.7	168.49	79.79	291.15	4.55	29	0.46	0.49	<0.01	0.34	<0.08
2	81.6	29	14.2	41.8	82.01	17.52	288.42	11.6	9	0.71	1.3	<0.02	0.18	<0.04
3	65.4	40.8	12.2	71.9	87.20	77.61	244.13	25.1	29	0.24	0.1	<0.04	0.19	<0.06
4	36.8	8	8.9	38.8	34.83	14.21	201.72	1.15	6	0.02	0.18	<0.01	0.08	<0.03
5	60.9	29.8	17.7	55.4	89.90	40.06	223.40	37.9	16	0.06	0.57	0.05	0.2	<0.05
6	35	5.4	4.5	18.3	43.31	4.10	84.12	16.4	2	0.04	0.27	<0.02	0.11	<0.02
7	7.1	4.4	0.8	8.1	9.50	1.60	33.91	2.77	< 1	< 0.02	0.14	<0.01	0.03	<0.02
8	13.3	6.9	1.2	5.6	10.72	1.22	48.62	1.15	2	0.07	0.17	<0.01	0.04	<0.02
9	121	126	18.4	70.1	204.21	65.11	340.20	60.8	25	1.62	0.4	0.09	0.44	<0.08
10	50.5	30.5	10.7	27.9	60.02	19.73	164.80	27.7	8	0.38	0.21	<0.04	0.14	<0.03
11	25.2	11.8	1.3	12.4	30.44	8.72	72.40	3.51	3	0.1	0.19	<0.01	0.08	<0.02
12	94.4	30.8	16.3	42.8	93.72	35.52	288.71	26.3	15	0.47	1.3	<0.04	0.21	<0.05
13	50.9	15.3	9.8	73.3	46.70	33.22	283.04	26.9	12	0.02	0.75	<0.04	0.11	<0.04
14	46	18.7	11.4	71.4	47.74	33.12	286.90	15.1	12	0.05	0.25	<0.02	0.11	<0.04
15	61.7	16.1	16.3	75.4	77.76	37.05	302.38	17.5	14	< 0.02	0.6	<0.02	0.17	<0.04
16	80.2	34.3	15.7	0.1	127.67	45.51	49.11	22.7	17	0.1	0.2	<0.03	0.28	<0.06
17	47.2	2.8	7.1	11	48.32	5.90	95.81	13.3	3	0.48	0.25	<0.02	0.1	<0.02
18	34.6	6.5	2.1	24	32.10	13.50	100.80	12.5	4	0.53	0.76	<0.02	0.17	<0.04
19	100.1	22.2	13.8	83.8	107.59	25.04	374.11	34.2	19	0.32	0.83	0.05	0.16	<0.04
20	80.5	31.9	12	57.3	86.21	62.79	215.36	56	14	0.4	0.89	0.08	0.23	<0.07
21	54.9	11.6	13.8	51.2	78.44	35.82	180.02	29.5	13	0.03	0.25	<0.04	0.21	<0.05
22	17.1	4.9	3.2	21.7	26.12	4.12	70.41	15.2	6	0.08	0.6	<0.02	0.12	<0.03
23	27.5	13.8	10.1	60.6	59.78	33.30	169.82	15.5	14	< 0.02	0.2	<0.02	0.2	<0.05
24	17.9	6.6	6.9	14	32.12	10.55	36.42	31.1	3	< 0.02	0.14	<0.04	0.21	<0.05
25	47.9	3.2	7.3	11.4	37.82	12.70	120.81	2.5	3	0.48	0.25	<0.01	0.08	<0.02
26	56.5	14.9	3.2	14.9	71.43	20.71	72.21	15	< 1	< 0.02	0.6	<0.02	0.17	<0.04
27	41.2	3.1	3.3	23.3	49.03	4.32	96.60	16.5	3	0.03	0.2	<0.02	0.17	<0.02
28	39.8	3.1	3.3	24.2	45.21	5.70	99.59	17.1	3	0.02	0.14	<0.02	0.4	<0.03

Table 5.8: Major chemical constituents of groundwater in Abeokuta area (Contd)

Analyte Symbol	Na	K	Mg	Ca	Cl	SO4	HCO_3	NO3 (as N)	S	P	F	NO2 (as N)	Br	PO4 (as P)
Unit Symbol	**mg/L**	**mg/L**	**mg/L**	**mg/L**	**mg/L**	**mg/L**	**mg/L**	**mg/L**	**mg/L**	**mg/L**	**mg/L**	**mg/L**	**mg/L**	**mg/L**
Detection Limit	**0.1**	**0.1**	**0.1**	**0.1**	**0.03**	**0.03**		**0.01**	**1**	**0.02**	**0.01**	**0.01**	**0.03**	**0.02**
29	41.1	17.7	10.9	35.1	60.12	24.50	137.72	27.1	< 1	< 0.02	0.17	<0.04	0.21	<0.04
30	32.4	2.4	7.1	26.2	45.32	5.71	100.10	21.3	2	0.06	0.25	<0.03	0.19	<0.03
31	39.6	3.2	3.3	23.6	48.59	5.11	92.20	16.2	3	< 0.02	0.6	<0.02	1.3	<0.02
32	9.1	3.3	1.9	6.5	12.89	4.11	28.09	3.1	2	< 0.02	0.2	<0.01	0.75	<0.03
33	3.2	3.5	3.7	11.3	12.02	2.10	45.10	0.6	2	< 0.02	0.14	<0.01	0.03	<0.02
34	23.8	4.6	5.9	22.9	48.60	9.90	65.70	8.5	6	0.04	0.17	<0.01	0.12	<0.03
35	47.6	3.5	7.3	25.9	44.40	13.90	151.32	2.4	3	0.1	0.4	<0.01	0.08	<0.02
36	40.7	3.1	3.3	24.3	48.82	5.41	99.69	14	3	0.12	0.21	<0.02	0.1	<0.02
37	35.9	7	5	41.6	56.94	14.69	105.18	36.9	14	< 0.02	0.19	0.05	0.26	<0.05
38	35.6	6.8	5.3	40.8	58.44	15.42	113.19	24	14	0.04	1.3	<0.03	0.26	<0.05
39	28.5	3.3	7.8	23.9	44.39	7.91	104.33	2.8	3	0.08	0.67	<0.01	0.09	<0.02
40	9.1	2.9	2.7	19.0	13.11	2.79	27.41	47.2	7	< 0.02	0.2	0.07	0.16	<0.03
41	18.4	4.7	3.2	21.3	27.40	5.51	79.71	3.5	5	0.08	0.75	<0.01	0.1	<0.02
42	11.5	1.7	1.7	7.1	11.20	4.49	38.22	2.2	< 1	< 0.02	0.25	<0.01	0.12	<0.03
43	9.8	3.3	2.9	20.2	23.16	4.53	47.67	14.6	7	0.03	0.6	<0.02	0.16	<0.03
44	39.6	3.3	3.3	23.7	45.10	10.20	94.05	15.2	3	0.03	0.2	<0.02	0.16	<0.03
45	28.8	3.3	2.6	21.1	37.21	5.50	75.04	13.2	< 1	0.08	0.14	<0.02	0.12	<0.03
46	23.1	6.1	3.1	23.8	23.14	7.80	93.58	16.3	<1	< 0.02	0.17	<0.02	0.12	<0.03
47	38.1	1.2	6.1	12.5	43.32	2.12	83.79	12.5	5	0.03	0.4	<0.02	0.11	<0.02
48	13.2	2.1	5.9	22.1	36.91	6.81	52.11	11.3	4	0.03	0.21	<0.02	0.11	<0.03

Table 5.9: Major chemical constituents of groundwater in Ikorodu area

Analyte Symbol	Na	K	Mg	Ca	Cl	SO4	HCO_3	NO3 (as N)	S	P	F	NO2 (as N)	Br	PO4 (as P)
Unit Symbol	mg/L	mg/L	mg/L	mg/L	mg/L	mg/L	mg/L	mg/L	mg/L	mg/L	mg/L	mg/L	mg/L	mg/L
Detection Limit	0.1	0.1	0.1	0.1	0.03	0.03		0.01	1	0.02	0.01	0.01	0.03	0.02
1	31.4	6.2	2.4	5.2	28.30	1.53	70.67	16.10	1	< 0.02	0.04	< 0.01	0.06	0.11
2	23.2	5.6	1.4	5.5	37.03	3.44	26.37	3.87	1	0.03	0.02	< 0.01	0.08	< 0.02
3	23.7	8.9	3.0	20.5	49.01	13.67	54.68	2.83	5	0.05	0.02	< 0.02	0.08	< 0.02
4	10.7	1.5	1.0	2.1	6.54	5.28	24.68	0.02	2	< 0.02	< 0.01	< 0.01	< 0.03	< 0.02
5	65.6	18.9	4.3	11.4	89.79	5.84	99.36	14.20	2	< 0.02	0.12	0.05	0.18	< 0.02
6	23.7	2.2	1.9	4.1	31.27	10.52	22.22	1.26	4	0.02	< 0.01	< 0.01	0.08	< 0.02
7	12.9	2.6	2.0	5.2	12.12	2.43	40.34	9.92	< 1	< 0.02	0.04	< 0.01	< 0.03	< 0.02
8	14.4	2.3	2.0	17.3	24.26	7.95	52.49	4.35	3	0.03	< 0.01	< 0.01	0.05	< 0.02
9	8.5	2.3	2.0	5.2	10.52	23.47	5.48	0.21	12	0.02	0.02	< 0.01	0.04	0.05
10	10.4	1.9	1.5	7.5	16.80	5.51	25.36	1.04	3	0.03	< 0.01	< 0.01	0.05	< 0.02
11	33.1	2.1	6.0	10.7	42.60	39.78	30.94	12.10	18	0.03	< 0.01	0.03	0.1	< 0.02
12	99.3	22.0	17.0	25.2	179.62	103.46	22.99	16.09	25	0.04	0.01	< 0.01	< 0.03	< 0.02
13	3.2	0.6	0.3	0.6	4.45	1.35	5.39	0.08	<1	0.02	0.02	< 0.02	0.04	< 0.02
14	24.1	14.4	1.6	3.8	32.96	16.48	29.58	9.66	6	< 0.02	0.02	< 0.01	0.08	0.02
15	11.6	31.9	1.5	5.2	16.93	21.47	48.34	0.15	8	0.05	< 0.01	< 0.01	0.1	0.02
16	113.0	72.9	15.1	28.7	155.15	80.68	207.92	37.70	28	0.02	< 0.02	< 0.02	0.35	< 0.05
17	138.0	18.6	20.9	13.8	195.75	61.25	132.41	20.50	22	0.03	< 0.02	< 0.02	0.45	< 0.05
18	11.3	1.3	0.4	1.4	11.30	0.45	18.09	1.10	< 1	< 0.02	< 0.01	0.02	0.04	0.05
19	4.5	0.4	0.6	3.8	5.30	0.58	18.16	0.13	< 1	< 0.02	0.01	< 0.01	< 0.03	< 0.02
20	2.8	0.5	0.5	4.1	3.80	0.42	16.63	0.26	< 1	< 0.02	< 0.01	< 0.01	< 0.03	< 0.02
21	2.6	0.6	0.4	0.9	3.70	0.55	5.62	0.21	< 1	< 0.02	< 0.01	< 0.01	< 0.03	0.07
22	15.2	3.5	2.0	6.8	13.35	2.22	51.02	11.60	< 1	< 0.02	0.02	< 0.01	0.04	0.17
23	1.5	0.2	0.3	0.2	2.70	0.11	1.73	0.13	< 1	< 0.02	< 0.01	< 0.01	< 0.03	< 0.02
24	2.5	1.0	0.1	4.6	4.13	1.31	14.13	0.31	< 1	0.03	< 0.01	< 0.01	< 0.03	0
25	6.0	0.4	0.3	11.6	7.93	2.52	37.37	2.60	< 1	0.04	< 0.01	< 0.01	< 0.03	< 0.02
26	30.9	28.0	4.0	21.9	38.13	20.92	120.44	18.90	7	0.04	< 0.01	0.11	0.08	< 0.02
27	2.4	0.2	0.3	0.9	4.17	0.74	2.94	0.27	< 1	< 0.02	< 0.01	< 0.01	< 0.03	< 0.02
28	10.3	3.1	0.6	4.8	11.69	7.72	20.26	4.23	3	0.02	< 0.01	< 0.01	< 0.03	< 0.02
29	14.7	11.4	3.4	8.0	15.99	4.51	65.40	7.34	3	0.02	0.03	0.02	0.05	< 0.02

Table 5.9: Major chemical constituents of groundwater in Ikorodu area (contd)

Analyte Symbol	Na	K	Mg	Ca	Cl	SO4	HCO_3	NO3 (as N)	S	P	F	NO2 (as N)	Br	PO4 (as P)
Unit Symbol	mg/L	mg/L	mg/L	mg/L	mg/L	mg/L	mg/L	mg/L	mg/L	mg/L	mg/L	mg/L	mg/L	mg/L
Detection Limit	0.1	0.1	0.1	0.1	0.03	0.03		0.01	1	0.02	0.01	0.01	0.03	0.02
30	16.6	15.2	4.6	9.3	17.26	2.31	86.98	20.60	< 1	< 0.02	0.06	< 0.01	0.03	< 0.02
31	12.9	13.8	4.6	9.0	14.85	2.52	77.96	8.55	2	< 0.02	0.03	< 0.01	0.05	< 0.02
32	11.0	14.3	5.4	10.4	15.53	3.74	79.05	18.70	< 1	< 0.02	0.04	< 0.01	0.04	< 0.02
33	6.8	9.2	3.4	10.9	9.86	2.43	62.85	5.82	1	< 0.02	0.05	< 0.01	0.04	< 0.02
34	3.5	3.2	0.7	19.6	3.24	1.70	70.02	0.57	< 1	0.03	0.03	0.01	< 0.03	< 0.02
35	2.5	0.3	0.4	2.3	4.91	0.63	7.04	0.29	< 1	< 0.02	< 0.01	< 0.01	< 0.03	< 0.02
36	20.3	0.9	0.8	10.3	11.23	9.10	59.99	6.16	3	< 0.02	0.01	< 0.01	0.05	< 0.02
37	3.3	0.4	0.5	1.0	5.26	0.33	5.66	0.81	< 1	< 0.02	< 0.01	< 0.01	< 0.03	< 0.02
38	9.1	0.4	0.3	3.3	8.81	1.01	19.99	1.97	< 1	< 0.02	< 0.01	< 0.01	0.07	< 0.02
39	2.4	0.4	0.5	1.1	4.63	0.80	4.02	0.27	< 1	< 0.02	< 0.01	< 0.01	< 0.03	< 0.02
40	55.0	30.1	7.0	34.2	62.95	9.83	212.05	45.80	3	< 0.02	0.1	< 0.01	0.1	< 0.03
41	40.9	15.3	5.1	18.0	46.72	6.94	125.21	15.30	3	0.04	< 0.01	< 0.01	0.11	< 0.02
42	30.9	10.1	5.2	17.0	33.97	0.17	118.37	26.00	< 1	< 0.02	0.01	0.02	0.1	< 0.02
43	27.6	9.8	3.7	12.3	29.04	5.97	88.06	8.12	2	< 0.02	< 0.01	< 0.01	0.08	< 0.02
44	6.1	1.7	0.6	2.9	5.38	0.69	20.72	0.86	< 1	< 0.02	< 0.01	< 0.01	< 0.03	< 0.02
45	7.6	0.6	0.8	3.6	8.49	0.53	22.38	1.20	< 1	0.04	0.02	< 0.01	< 0.03	< 0.02
46	2.8	0.2	0.5	1.1	5.38	0.62	3.60	0.26	< 1	< 0.02	< 0.01	< 0.01	< 0.03	< 0.02
47	2.1	0.4	0.5	1.1	5.32	0.14	2.77	0.33	< 1	< 0.02	< 0.01	< 0.01	< 0.03	< 0.02
48	3.8	0.9	1.0	1.9	6.77	0.37	10.33	1.61	< 1	< 0.02	< 0.01	< 0.01	< 0.03	< 0.02
49	5.9	2.7	1.1	1.5	5.11	6.28	13.37	0.23	2	0.04	< 0.01	< 0.01	< 0.03	< 0.02
50	15.3	7.4	2.2	3.8	10.42	16.59	36.63	0.18	6	0.03	0.02	< 0.01	0.04	0.03

Table 5.10: Trace Elements in groundwater of Abeokuta Area

Analyte Symbol	Al	Ba	Cd	Co	Cu	Fe	Mn	Ni	Pb	Si	Sr	Ti	U	Y	Zn
Unit Symbol	mg/L	ug/L	ug/L	ug/L	ug/L	mg/L	mg/L	ug/L	ug/L	mg/L	ug/L	ug/L	mg/L	ug/L	ug/L
Detection Limit	0.1	20	2	2	2	0.01	0.01	5	10	0.1	10	10	0.05	10	5
1	0.9	200.00	19	4	5.00	4.40	0.77	< 5	< 10	19.80	330.00	60	< 0.05	20	33.00
2	< 0.1	110.00	4	6	15.00	0.68	0.57	< 5	< 10	15.00	240.00	< 10	< 0.05	10	29.00
3	< 0.1	150.00	3	4	5.00	0.07	0.02	< 5	< 10	12.50	590.00	10	< 0.05	10	9.00
4	3.3	2040.00	18	10	8.00	3.06	0.35	< 5	10	13.80	350.00	170	< 0.05	20	1000.00
5	0.2	290.00	16	2	11.00	0.23	0.02	< 5	< 10	10.70	320.00	20	< 0.05	< 10	31.00
6	0.2	140.00	3	4	4.00	0.24	0.02	< 5	< 10	10.00	120.00	10	< 0.05	10	19.00
7	0.2	50.00	4	2	2.00	0.15	0.03	< 5	< 10	9.60	130.00	< 10	< 0.05	20	10.00
8	0.1	60.00	3	2	5.00	0.17	0.02	< 5	< 10	15.10	30.00	< 10	< 0.05	10	20.00
9	1.9	260.00	5	6	14.00	4.79	0.07	< 5	10	13.50	450.00	180	< 0.05	20	362.00
10	0.1	140.00	10	4	2.00	0.12	0.01	< 5	< 10	20.30	190.00	< 10	< 0.05	10	19.00
11	1.4	740.00	9	7	9.00	4.12	0.19	< 5	20	18.30	40.00	50	0.18	20	431.00
12	4.1	300.00	18	10	16.00	4.49	0.18	6	20	29.60	320.00	120	< 0.05	30	53.00
13	< 0.1	180.00	5	< 2	5.00	0.07	0.21	< 5	< 10	13.60	440.00	< 10	< 0.05	10	6.00
14	< 0.1	150.00	10	4	7.00	0.03	0.02	< 5	< 10	12.40	370.00	< 10	0.11	< 10	14.00
15	< 0.1	280.00	16	2	2.00	0.06	0.02	< 5	< 10	15.60	500.00	< 10	0.13	< 10	7.00
16	0.5	220.00	19	5	7.00	1.53	0.01	< 5	10	16.50	320.00	20	< 0.05	20	45.00
17	< 0.1	20	< 2	< 2	2	0.18	0.1	< 5	< 10	36.6	80	< 10	< 0.05	< 10	14
18	< 0.1	70	< 2	< 2	16	0.03	< 0.01	< 5	< 10	24.5	100	< 10	0.19	< 10	28
19	< 0.1	210	< 2	< 2	6	0.06	< 0.01	< 5	< 10	10.5	440	< 10	< 0.05	< 10	11
20	0.1	190	< 2	< 2	8	0.13	< 0.01	< 5	< 10	10.9	310	< 10	< 0.05	< 10	32
21	0.2	260	< 2	< 2	6	0.16	0.02	< 5	< 10	14.5	420	< 10	< 0.05	< 10	21
22	< 0.1	80	< 2	< 2	6	0.09	< 0.01	< 5	< 10	11.2	170	< 10	< 0.05	< 10	8
23	< 0.1	240	< 2	< 2	22	0.04	< 0.01	< 5	< 10	12.9	480	< 10	< 0.05	< 10	25
24	0.1	220	< 2	4	6	0.15	0.05	6	< 10	8.8	100	< 10	0.13	< 10	27

Analyte Symbol	Al	Ba	Cd	Co	Cu	Fe	Mn	Ni	Pb	Si	Sr	Ti	U	Y	Zn
Unit Symbol	**mg/L**	**ug/L**	**ug/L**	**ug/L**	**ug/L**	**mg/L**	**mg/L**	**ug/L**	**ug/L**	**mg/L**	**ug/L**	**ug/L**	**mg/L**	**ug/L**	**ug/L**
Detection Limit	**0.1**	**20**	**2**	**2**	**2**	**0.01**	**0.01**	**5**	**10**	**0.1**	**10**	**10**	**0.05**	**10**	**5**
25	0.1	30	< 2	< 2	45	0.19	0.1	< 5	< 10	36.4	80	< 10	< 0.05	< 10	73
26	< 0.1	180	< 2	< 2	50.9	0.7	< 0.01	< 5	< 10	10.9	180	< 10	< 0.05	< 10	145
27	0.2	150	< 2	< 2	78	0.26	0.02	< 5	< 10	8.3	80	10	< 0.05	< 10	225
28	0.3	150	< 2	< 2	6	0.32	0.02	< 5	< 10	8.4	80	20	< 0.05	< 10	57
29	< 0.1	190	< 2	< 2	12.7	0.15	0.1	< 5	< 10	9.8	220	< 10	< 0.05	< 10	113
30	0.9	100	< 2	< 2	8	0.5	0.03	< 5	< 10	15.2	90	30	< 0.05	< 10	47
31	< 0.1	140	< 2	< 2	33	0.01	< 0.01	< 5	< 10	8.2	80	< 10	0.07	< 10	252
32	< 0.1	60	< 2	< 2	16	0.01	0.1	< 5	< 10	8.3	40	< 10	< 0.05	< 10	245
33	0.1	50	< 2	< 2	6	0.57	0.38	< 5	< 10	5.7	70	< 10	0.06	< 10	33
34	0.2	130	< 2	< 2	12	0.19	0.03	< 5	< 10	11.9	150	< 10	< 0.05	< 10	40
35	< 0.1	50	< 2	< 2	22	0.08	< 0.01	< 5	< 10	37.6	110	< 10	< 0.05	< 10	59
36	0.3	150	< 2	< 2	2	0.32	0.02	< 5	< 10	8.3	80	20	< 0.05	< 10	65
37	< 0.1	70	< 2	< 2	4	0.01	< 0.01	< 5	< 10	7.3	200	< 10	< 0.05	< 10	25
38	0.7	80	< 2	< 2	49	0.39	< 0.01	< 5	< 10	8.1	200	40	< 0.05	< 10	33
39	< 0.1	110	< 2	4	8	0.23	0.05	< 5	< 10	46.4	140	< 10	< 0.05	< 10	46
40	0.2	40	< 2	< 2	49	0.11	< 0.01	< 5	< 10	4.8	90	< 10	< 0.05	< 10	153
41	< 0.1	90	< 2	< 2	29	0.06	< 0.01	< 5	< 10	11.2	170	< 10	< 0.05	< 10	79
42	1.3	40	< 2	< 2	24	0.63	0.21	< 5	< 10	12.3	40	40	< 0.05	< 10	78
43	0.2	40	< 2	< 2	43	0.11	< 0.01	< 5	< 10	6.1	100	< 10	< 0.05	< 10	226
44	0.2	150	< 2	< 2	37	0.24	0.02	< 5	< 10	8.4	80	10	< 0.05	< 10	123
45	0.2	100	< 2	< 2	30.8	0.01	< 0.01	< 5	< 10	8.8	70	< 10	< 0.05	< 10	175
46	< 0.1	80	< 2	< 2	7.7	0.01	0.04	< 5	< 10	18.1	140	< 10	< 0.05	< 10	29
47	0.4	280	< 2	< 2	8.9	0.5	0.1	< 5	< 10	34.2	110	< 10	< 0.05	< 10	70
48	< 0.1	110	< 2	< 2	11.6	0.13	0.02	< 5	< 10	38	130	40	< 0.05	< 10	35

Table5.10: Trace Elements in groundwater of Abeokuta Area (Contd)

Analyte Symbol	Ag	As	Be	Bi	Ce	Cr	Li	Mo	Sb	Se	Sn	Te	Tl	V	W
Unit Symbol	**ug/L**	**ug/L**	**ug/L**	**ug/L**	**ug/L**	**ug/L**	**mg/L**	**ug/L**	**ug/L**	**ug/L**	**ug/L**	**ug/L**	**ug/L**	**ug/L**	**ug/L**
Detection Limit	**5**	**30**	**2**	**20**	**30**	**20**	**0.05**	**5**	**10**	**20**	**10**	**10**	**10**	**10**	**10**
1	< 5	< 30	< 2	< 20	< 30	< 20	< 0.05	6	< 10	< 20	30	< 10	< 10	< 10	10
2	< 5	< 30	< 2	< 20	< 30	< 20	< 0.05	10	< 10	< 20	< 10	< 10	< 10	< 10	< 10
3	< 5	< 30	< 2	< 20	< 30	< 20	< 0.05	< 5	< 10	< 20	< 10	< 10	< 10	< 10	< 10
4	< 5	< 30	< 2	< 20	< 30	< 20	< 0.05	< 5	< 10	< 20	< 10	< 10	< 10	< 10	20
5	< 5	< 30	< 2	< 20	< 30	< 20	< 0.05	< 5	< 10	< 20	< 10	< 10	< 10	< 10	< 10
6	< 5	< 30	< 2	< 20	< 30	< 20	< 0.05	< 5	< 10	< 20	< 10	< 10	< 10	< 10	< 10
7	< 5	< 30	< 2	< 20	< 30	< 20	< 0.05	< 5	< 10	< 20	< 10	< 10	< 10	< 10	< 10
8	< 5	< 30	< 2	< 20	< 30	< 20	< 0.05	< 5	< 10	< 20	< 10	< 10	< 10	< 10	< 10
9	< 5	< 30	< 2	< 20	< 30	< 20	< 0.05	< 5	< 10	< 20	< 10	< 10	< 10	10	< 10
10	< 5	30	< 2	< 20	< 30	< 20	< 0.05	9	< 10	< 20	< 10	< 10	< 10	< 10	< 10
11	< 5	< 30	< 2	< 20	< 30	< 20	< 0.05	< 5	< 10	< 20	< 10	< 10	< 10	< 10	20
12	< 5	< 30	< 2	< 20	< 30	< 20	< 0.05	< 5	< 10	< 20	60	< 10	< 10	20	< 10
13	< 5	< 30	< 2	< 20	< 30	< 20	< 0.05	< 5	< 10	< 20	< 10	< 10	< 10	< 10	< 10
14	< 5	< 30	< 2	< 20	< 30	< 20	< 0.05	< 5	< 10	< 20	< 10	< 10	< 10	< 10	< 10
15	< 5	< 30	< 2	< 20	< 30	< 20	< 0.05	< 5	< 10	< 20	< 10	< 10	< 10	< 10	< 10
16	< 5	< 30	< 2	< 20	< 30	< 20	< 0.05	< 5	< 10	< 20	< 10	10	< 10	< 10	< 10
17	< 5	< 30	< 2	< 20	< 30	< 20	< 0.05	< 5	< 10	< 20	< 10	< 10	< 10	< 10	< 10
18	< 5	< 30	< 2	< 20	< 30	< 20	< 0.05	< 5	< 10	< 20	< 10	< 10	< 10	< 10	< 10
19	< 5	< 30	< 2	< 20	< 30	< 20	< 0.05	< 5	< 10	< 20	< 10	< 10	< 10	< 10	< 10
20	< 5	< 30	< 2	< 20	< 30	< 20	< 0.05	< 5	< 10	< 20	< 10	< 10	< 10	< 10	< 10
21	< 5	< 30	< 2	< 20	< 30	< 20	< 0.05	< 5	< 10	< 20	< 10	< 10	< 10	< 10	< 10
22	< 5	< 30	< 2	< 20	< 30	< 20	< 0.05	< 5	< 10	< 20	< 10	< 10	< 10	< 10	< 10
23	< 5	< 30	< 2	< 20	< 30	< 20	< 0.05	< 5	< 10	< 20	< 10	< 10	< 10	< 10	< 10
24	< 5	< 30	< 2	< 20	< 30	< 20	< 0.05	< 5	< 10	< 20	< 10	< 10	< 10	< 10	< 10

Table5.10: Trace Elements in groundwater of Abeokuta Area (contd)

Analyte Symbol	Ag	As	Be	Bi	Ce	Cr	Li	Mo	Sb	Se	Sn	Te	Tl	V	W
Unit Symbol	**ug/L**	**ug/L**	**ug/L**	**ug/L**	**ug/L**	**ug/L**	**mg/L**	**ug/L**	**ug/L**	**ug/L**	**ug/L**	**ug/L**	**ug/L**	**ug/L**	**ug/L**
Detection Limit	**5**	**30**	**2**	**20**	**30**	**20**	**0.05**	**5**	**10**	**20**	**10**	**10**	**10**	**10**	**10**
25	< 5	< 30	< 2	< 20	< 30	< 20	< 0.05	< 5	< 10	< 20	< 10	< 10	< 10	< 10	< 10
26	< 5	< 30	< 2	< 20	< 30	< 20	< 0.05	< 5	< 10	< 20	< 10	< 10	< 10	< 10	< 10
27	< 5	< 30	< 2	< 20	< 30	< 20	< 0.05	< 5	10	< 20	< 10	< 10	< 10	< 10	< 10
28	< 5	< 30	< 2	< 20	< 30	< 20	< 0.05	< 5	< 10	< 20	< 10	< 10	< 10	< 10	< 10
29	< 5	< 30	< 2	< 20	< 30	< 20	< 0.05	< 5	< 10	< 20	< 10	< 10	< 10	< 10	< 10
30	< 5	< 30	< 2	< 20	< 30	< 20	< 0.05	< 5	< 10	< 20	< 10	< 10	< 10	< 10	< 10
31	< 5	< 30	< 2	< 20	< 30	< 20	< 0.05	< 5	< 10	< 20	< 10	< 10	< 10	< 10	< 10
32	< 5	< 30	< 2	< 20	< 30	< 20	< 0.05	< 5	< 10	< 20	< 10	20	< 10	< 10	20
33	< 5	< 30	< 2	< 20	< 30	< 20	< 0.05	< 5	< 10	< 20	< 10	< 10	< 10	< 10	< 10
34	< 5	< 30	< 2	60	< 30	< 20	< 0.05	< 5	< 10	< 20	< 10	20	< 10	< 10	< 10
35	< 5	< 30	< 2	40	< 30	< 20	< 0.05	< 5	< 10	< 20	< 10	< 10	100	< 10	< 10
36	< 5	< 30	< 2	< 20	< 30	< 20	< 0.05	< 5	10	< 20	< 10	< 10	< 10	< 10	< 10
37	< 5	< 30	< 2	< 20	< 30	< 20	< 0.05	< 5	10	< 20	< 10	< 10	< 10	< 10	< 10
38	< 5	< 30	< 2	< 20	< 30	< 20	< 0.05	< 5	< 10	< 20	< 10	30	< 10	< 10	< 10
39	< 5	< 30	< 2	< 20	< 30	< 20	< 0.05	< 5	< 10	20	< 10	20	20	< 10	< 10
40	< 5	< 30	< 2	< 20	< 30	< 20	< 0.05	< 5	10	< 20	< 10	< 10	< 10	< 10	< 10
41	< 5	< 30	< 2	< 20	< 30	< 20	< 0.05	< 5	< 10	< 20	< 10	< 10	< 10	< 10	< 10
42	< 5	< 30	< 2	< 20	< 30	< 20	< 0.05	< 5	< 10	< 20	< 10	< 10	< 10	< 10	10
43	< 5	< 30	< 2	< 20	< 30	< 20	< 0.05	< 5	< 10	< 20	< 10	< 10	< 10	< 10	< 10
44	< 5	< 30	< 2	< 20	< 30	< 20	< 0.05	< 5	< 10	< 20	< 10	< 10	< 10	< 10	< 10
45	< 5	< 30	< 2	< 20	< 30	< 20	< 0.05	< 5	< 10	< 20	< 10	20	20	< 10	< 10
46	< 5	< 30	< 2	< 20	< 30	< 20	< 0.05	< 5	< 10	< 20	< 10	< 10	< 10	< 10	< 10
47	< 5	< 30	< 2	< 20	< 30	< 20	< 0.05	< 5	< 10	< 20	< 10	< 10	< 10	< 10	< 10
48	< 5	< 30	< 2	< 20	< 30	< 20	< 0.05	< 5	< 10	< 20	< 10	< 10	< 10	< 10	10

Table5.11: Trace elements in groundwater of Ikorodu area

Analyte Symbol	Al	Ba	Be	Cd	Co	Cu	Fe	Mn	Ni	Pb	Si	Sr	Ti	Y	Zn
Unit Symbol	mg/L	ug/L	ug/L	ug/L	ug/L	ug/L	mg/L	mg/L	ug/L	ug/L	mg/L	ug/L	ug/L	ug/L	ug/L
Detection Limit	0.1	20	2	2	2	2	0.01	0.01	5	10	0.1	10	10	10	5
1	0.50	70.00	< 2	< 2	2.00	44.00	0.11	0.08	< 5	< 10	4.40	20.00	< 10	< 10	190.00
2	0.20	520.00	< 2	< 2	2.90	< 2	0.15	0.04	< 5	< 10	10.50	40.00	<10	< 10	18.00
3	0.10	240.00	< 2	< 2	6.79	3.00	0.84	0.17	< 5	< 10	17.00	130.00	<10	< 10	30.00
4	< 0.1	40.00	< 2	< 2	< 2	< 2	0.03	0.19	< 5	< 10	6.20	30.00	< 10	< 10	148.00
5	0.30	920.00	< 2	< 2	33.00	3.00	0.41	0.24	12.00	< 10	19.50	160.00	< 10	< 10	55.00
6	0.10	60.00	< 2	< 2	4.00	< 2	0.40	0.08	< 5	< 10	9.50	30.00	< 10	< 10	90.00
7	0.30	40.00	< 2	< 2	< 2	9.00	0.03	0.03	< 5	< 10	3.90	30.00	< 10	< 10	46.00
8	< 0.1	< 20	< 2	< 2	< 2	< 2	0.05	0.02	< 5	< 10	6.00	100.00	<10	< 10	25.00
9	0.90	110.00	3.16	< 2	62.23	9.00	0.20	0.39	< 5	< 10	26.90	30.00	<10	10.00	56.00
10	< 0.1	360.00	< 2	< 2	< 2	< 2	0.11	0.04	< 5	< 10	9.60	30.00	< 10	< 10	272.00
11	0.40	90.00	< 2	< 2	2.46	3.00	0.30	0.07	< 5	< 10	10.00	160.00	<10	< 10	8.00
12	0.30	100.00	< 2	< 2	20.12	4.00	1.33	0.38	< 5	< 10	14.10	150.00	<10	< 10	22.00
13	< 0.1	< 20	< 2	< 2	< 2	38.00	1.12	0.01	< 5	< 10	3.60	< 10	<10	< 10	52.00
14	< 0.1	20.00	< 2	< 2		< 2	0.65	0.03	< 5	< 10	7.20	40.00	< 10	< 10	36.00
15	1.40	80.00	< 2	< 2	2.00	7.00	0.37	0.01	< 5	< 10	7.10	40.00	40.00	< 10	38.00
16	0.30	90.00	< 2	< 2	3.00	< 2	0.10	0.16	< 5	< 10	5.20	240.00	< 10	< 10	48.00
17	0.30	110.00	< 2	< 2	2.00	6.00	2.17	0.07	< 5	< 10	9.10	180.00	< 10	< 10	92.00
18	0.10	<20	< 2	< 2		4.00	0.03	0.01	< 5	< 10	4.10	< 10	< 10	< 10	112.00
19	0.20	20.00	< 2	< 2		< 2	0.33	0.01	< 5	< 10	4.40	30.00	< 10	< 10	68.00
20	< 0.1	20.00	< 2	< 2		< 2	0.25	<0.01	< 5	< 10	4.30	40.00	< 10	< 10	54.00
21	< 0.1	< 20	< 2	< 2	< 2	12.00	0.05	< 0.01	< 5	< 10	4.00	< 10	< 10	< 10	60.00
22	0.30	< 20	< 2	< 2	< 2	12.00	0.10	0.02	< 5	< 10	3.60	40.00	< 10	< 10	60.00
23	< 0.1	< 20	< 2	< 2	< 2	44.00	0.04	0.01	< 5	< 10	3.80	< 10	< 10	< 10	74.00
24	0.30	30.00	< 2	< 2		< 2	0.12	0.01	< 5	< 10	4.20	40.00	< 10	< 10	66.00
25	0.20	20.00	< 2	4.00	< 2	< 2	0.36	0.03	< 5	< 10	5.00	10.00	< 10	< 10	101.00

Table5.11: Trace elements in groundwater of Ikorodu area (contd)

Analyte Symbol	Al	Ba	Be	Cd	Co	Cu	Fe	Mn	Ni	Pb	Si	Sr	Ti	Y	Zn
Unit Symbol	mg/L	ug/L	ug/L	ug/L	ug/L	ug/L	mg/L	mg/L	ug/L	ug/L	mg/L	ug/L	ug/L	ug/L	ug/L
Detection Limit	0.1	20	2	2	2	2	0.01	0.01	5	10	0.1	10	10	10	5
26	0.10	30.00	< 2	< 2	< 2	< 2	0.06	0.02	< 5	< 10	3.10	180.00	< 10	< 10	11.00
27	< 0.1	40.00	< 2	< 2	< 2	8.00	0.05	0.01	< 5	< 10	4.30	< 10	< 10	< 10	27.00
28	0.20	< 20	< 2	< 2	< 2	4.00	0.16	0.01	< 5	< 10	3.90	< 10	< 10	< 10	72.00
29	0.20	100.00	< 2	< 2		5.00	0.13	0.06	< 5	< 10	4.40	70.00	< 10	< 10	173.00
30	1.00	120.00	< 2	< 2	4.00	16.00	0.12	0.08	< 5	110.00	4.70	50.00	< 10	10.00	245.00
31	< 0.1	120.00	< 2	5.00		< 2	0.08	0.08	< 5	< 10	4.90	100.00	< 10	< 10	153.00
32	0.30	100.00	< 2	< 2	3.00	24.00	0.02	0.09	< 5	< 10	5.30	70.00	< 10	< 10	25.00
33	< 0.1	110.00	< 2	< 2		< 2	0.04	0.05	< 5	< 10	5.30	90.00	< 10	< 10	27.00
34	< 0.1	< 20	< 2	< 2	< 2	11.00	0.12	0.01	< 5	10.00	6.40	110.00	< 10	< 10	19.00
35	0.10	40.00	< 2	< 2	< 2	7.00	0.08	< 0.01	< 5	< 10	5.10	< 10	< 10	< 10	31.00
36	0.20	20.00	< 2	5.00	< 2	< 2	0.08	0.02	< 5	< 10	5.40	50.00	< 10	< 10	55.00
37	< 0.1	30.00	< 2	< 2	< 2	6.00	0.07	0.02	< 5	< 10	5.20	< 10	< 10	< 10	85.00
38	< 0.1	< 20	< 2	< 2	2.00	2.00	0.04	0.01	< 5	< 10	4.90	30.00	< 10	< 10	12.00
39	< 0.1	20.00	< 2	< 2	< 2	58.00	0.06	0.01	< 5	< 10	5.60	< 10	< 10	< 10	54.00
40	0.50	1020.00	< 2	< 2	22.00	< 2	0.05	0.79	< 5	< 10	8.20	310.00	< 10	60.00	37.00
41	0.20	880.00	< 2	< 2		< 2	0.11	0.56	< 5	< 10	17.70	200.00	< 10	< 10	56.00
42	0.10	1020.00	2.00	< 2	26.00	11.00	0.03	0.61	< 5	< 10	10.90	350.00	< 10	< 10	38.00
43	< 0.1	640.00	< 2	< 2		< 2	0.09	0.42	< 5	< 10	19.30	120.00	< 10	< 10	48.00
44	< 0.1	90.00	< 2	< 2	4.00	15.00	0.07	0.01	< 5	< 10	15.10	60.00	< 10	< 10	86.00
45	< 0.1	150.00	< 2	< 2		< 2	0.03	0.63	< 5	< 10	6.10	10.00	< 10	< 10	33.00
46	< 0.1	< 20	< 2	< 2	< 2	10.00	0.02	< 0.01	< 5	< 10	5.30	< 10	< 10	< 10	18.00
47	< 0.1	30.00	< 2	< 2	< 2	29.00	0.02	< 0.01	< 5	< 10	4.70	< 10	< 10	< 10	135.00
48	< 0.1	60.00	< 2	2.00	< 2	35.00	0.05	0.02	< 5	< 10	5.00	10.00	< 10	< 10	25.00
49	0.10	40.00	< 2	< 2		< 2	0.08	0.08	< 5	< 10	16.20	< 10	< 10	< 10	45.00
50	< 0.1	130.00	< 2	< 2	9.00	9.00	0.13	0.26	6.00	< 10	30.80	80.00	< 10	< 10	67.00

Table5.11: Trace elements in groundwater of Ikorodu area (contd)

Analyte Symbol	Ag	As	Bi	Ce	Cr	Li	Mo	Se	Sb	Sn	Te	Tl	U	V	W
Unit Symbol	**ug/L**	**ug/L**	**ug/L**	**ug/L**	**ug/L**	**mg/L**	**ug/L**	**ug/L**	**ug/L**	**ug/L**	**ug/L**	**ug/L**	**mg/L**	**ug/L**	**ug/L**
Detection Limit	**5**	**30**	**20**	**30**	**20**	**0.05**	**5**	**20**	**10**	**10**	**10**	**10**	**0.05**	**10**	**10**
1	< 5	< 30	< 20	< 30	< 20	< 0.05	< 5	< 20	< 10	< 10	< 10	< 10	< 0.05	< 10	< 10
2	< 5	< 30	< 20	< 30	< 20	< 0.05	< 5	< 20	< 10	< 10	< 10	< 10	< 0.05	< 10	< 10
3	< 5	< 30	< 20	120	< 20	< 0.05	< 5	< 20	< 10	< 10	< 10	< 10	< 0.05	< 10	< 10
4	< 5	< 30	< 20	< 30	< 20	< 0.05	< 5	< 20	< 10	< 10	< 10	< 10	< 0.05	< 10	< 10
5	< 5	< 30	< 20	< 30	< 20	< 0.05	< 5	< 20	< 10	< 10	< 10	< 10	< 0.05	< 10	< 10
6	< 5	< 30	< 20	< 30	< 20	< 0.05	< 5	< 20	< 10	< 10	< 10	< 10	< 0.05	< 10	< 10
7	< 5	< 30	< 20	< 30	< 20	< 0.05	< 5	< 20	< 10	< 10	< 10	< 10	< 0.05	< 10	< 10
8	< 5	< 30	< 20	< 30	< 20	< 0.05	< 5	< 20	< 10	< 10	< 10	< 10	< 0.05	< 10	< 10
9	< 5	< 30	< 20	< 30	< 20	< 0.05	< 5	< 20	< 10	< 10	< 10	< 10	< 0.05	< 10	< 10
10	< 5	< 30	< 20	< 30	< 20	< 0.05	< 5	< 20	< 10	< 10	< 10	< 10	< 0.05	< 10	< 10
11	< 5	< 30	< 20	< 30	< 20	< 0.05	< 5	< 20	< 10	< 10	< 10	< 10	< 0.05	< 10	< 10
12	< 5	< 30	< 20	< 30	< 20	< 0.05	< 5	< 20	< 10	< 10	< 10	< 10	< 0.05	< 10	< 10
13	< 5	< 30	< 20	< 30	< 20	< 0.05	< 5	< 20	< 10	< 10	< 10	< 10	< 0.05	< 10	< 10
14	< 5	< 30	< 20	< 30	< 20	< 0.05	< 5	< 20	< 10	< 10	< 10	< 10	< 0.05	< 10	< 10
15	< 5	< 30	< 20	< 30	< 20	< 0.05	< 5	< 20	< 10	< 10	< 10	< 10	< 0.05	< 10	< 10
16	< 5	< 30	< 20	< 30	< 20	< 0.05	< 5	< 20	< 10	< 10	< 10	< 10	< 0.05	< 10	< 10
17	< 5	< 30	< 20	< 30	< 20	< 0.05	< 5	< 20	< 10	< 10	< 10	< 10	< 0.05	< 10	< 10
18	< 5	< 30	< 20	< 30	< 20	< 0.05	< 5	< 20	< 10	< 10	< 10	< 10	< 0.05	< 10	< 10
19	< 5	< 30	< 20	< 30	< 20	< 0.05	< 5	< 20	< 10	< 10	< 10	< 10	< 0.05	< 10	< 10
20	< 5	< 30	< 20	< 30	< 20	< 0.05	< 5	< 20	< 10	< 10	< 10	< 10	< 0.05	< 10	< 10
21	< 5	< 30	< 20	< 30	< 20	< 0.05	< 5	< 20	< 10	< 10	< 10	< 10	< 0.05	< 10	< 10
22	< 5	< 30	< 20	< 30	< 20	< 0.05	< 5	< 20	< 10	< 10	< 10	< 10	< 0.05	< 10	< 10
23	< 5	< 30	< 20	< 30	< 20	< 0.05	< 5	< 20	< 10	< 10	< 10	< 10	< 0.05	< 10	< 10
24	< 5	< 30	< 20	< 30	< 20	< 0.05	< 5	< 20	< 10	< 10	< 10	< 10	< 0.05	< 10	< 10
25	< 5	< 30	< 20	< 30	< 20	< 0.05	< 5	< 20	< 10	< 10	< 10	< 10	< 0.05	< 10	< 10

Table5.11: Trace elements in groundwater of Ikorodu area (contd)

Analyte Symbol	Ag	As	Bi	Ce	Cr	Li	Mo	Se	Sb	Sn	Te	Tl	U	V	W
Unit Symbol	**ug/L**	**ug/L**	**ug/L**	**ug/L**	**ug/L**	**mg/L**	**ug/L**	**ug/L**	**ug/L**	**ug/L**	**ug/L**	**ug/L**	**mg/L**	**ug/L**	**ug/L**
Detection Limit	**5**	**30**	**20**	**30**	**20**	**0.05**	**5**	**20**	**10**	**10**	**10**	**10**	**0.05**	**10**	**10**
26	< 5	< 30	< 20	< 30	< 20	< 0.05	< 5	< 20	< 10	< 10	< 10	< 10	< 0.05	< 10	< 10
27	< 5	< 30	< 20	< 30	< 20	< 0.05	< 5	< 20	< 10	< 10	< 10	< 10	< 0.05	< 10	< 10
28	< 5	< 30	< 20	< 30	< 20	< 0.05	< 5	< 20	< 10	< 10	< 10	< 10	< 0.05	< 10	< 10
29	< 5	< 30	< 20	< 30	< 20	< 0.05	< 5	< 20	< 10	< 10	< 10	< 10	< 0.05	< 10	< 10
30	< 5	< 30	< 20	< 30	< 20	< 0.05	< 5	< 20	< 10	< 10	< 10	< 10	< 0.05	< 10	< 10
31	< 5	< 30	< 20	< 30	< 20	< 0.05	< 5	< 20	< 10	< 10	< 10	< 10	< 0.05	< 10	< 10
32	< 5	< 30	< 20	< 30	< 20	< 0.05	< 5	< 20	< 10	< 10	< 10	< 10	< 0.05	< 10	< 10
33	< 5	< 30	< 20	< 30	< 20	< 0.05	< 5	< 20	< 10	< 10	< 10	< 10	< 0.05	< 10	< 10
34	< 5	< 30	< 20	< 30	< 20	< 0.05	< 5	< 20	10.00	< 10	< 10	< 10	< 0.05	< 10	< 10
35	< 5	< 30	< 20	< 30	< 20	< 0.05	< 5	< 20	< 10	< 10	< 10	< 10	< 0.05	< 10	< 10
36	< 5	< 30	< 20	< 30	< 20	< 0.05	< 5	< 20	< 10	< 10	< 10	< 10	< 0.05	< 10	< 10
37	< 5	< 30	< 20	< 30	< 20	< 0.05	< 5	< 20	< 10	< 10	< 10	< 10	< 0.05	< 10	< 10
38	< 5	< 30	< 20	< 30	< 20	< 0.05	< 5	< 20	< 10	< 10	< 10	< 10	< 0.05	< 10	< 10
39	< 5	< 30	< 20	< 30	< 20	< 0.05	< 5	< 20	< 10	< 10	< 10	< 10	< 0.05	< 10	< 10
40	< 5	< 30	< 20	< 30	< 20	< 0.05	< 5	< 20	< 10	< 10	< 10	< 10	< 0.05	< 10	< 10
41	< 5	< 30	< 20	< 30	< 20	< 0.05	< 5	< 20	< 10	< 10	< 10	< 10	< 0.05	< 10	< 10
42	< 5	< 30	< 20	< 30	< 20	< 0.05	< 5	< 20	< 10	< 10	< 10	< 10	< 0.05	< 10	< 10
43	< 5	< 30	< 20	< 30	< 20	< 0.05	< 5	< 20	< 10	< 10	< 10	< 10	< 0.05	< 10	< 10
44	< 5	< 30	< 20	< 30	< 20	< 0.05	< 5	< 20	< 10	< 10	< 10	< 10	< 0.05	< 10	< 10
45	< 5	< 30	< 20	< 30	< 20	< 0.05	< 5	< 20	< 10	< 10	< 10	< 10	< 0.05	< 10	< 10
46	< 5	< 30	< 20	< 30	< 20	< 0.05	< 5	< 20	< 10	< 10	< 10	< 10	< 0.05	< 10	< 10
47	< 5	< 30	< 20	< 30	< 20	< 0.05	< 5	< 20	< 10	< 10	< 10	< 10	< 0.05	< 10	< 10
48	< 5	< 30	< 20	< 30	< 20	< 0.05	< 5	< 20	< 10	< 10	< 10	< 10	< 0.05	< 10	< 10
49	< 5	< 30	< 20	< 30	< 20	< 0.05	< 5	< 20	< 10	< 10	< 10	< 10	< 0.05	< 10	< 10
50	< 5	< 30	< 20	< 30	< 20	< 0.05	< 5	< 20	< 10	< 10	< 10	< 10	< 0.05	< 10	< 10

APPENDIX III

Vertical Electrical Sounding Curves

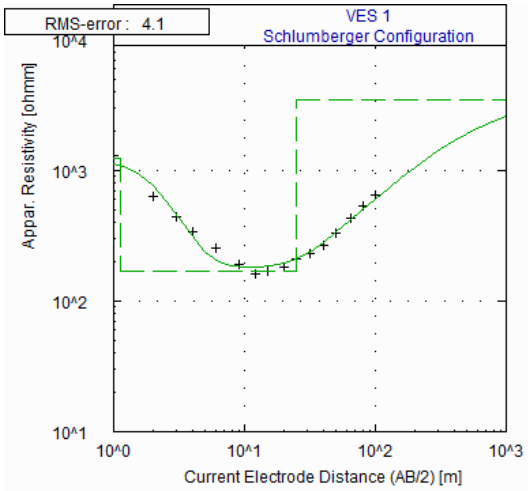

No	Res	Thick	Depth
1	1232.7	1.1	1.1
2	170.7	23.5	24.6
3	3486.6	-.-	-.-

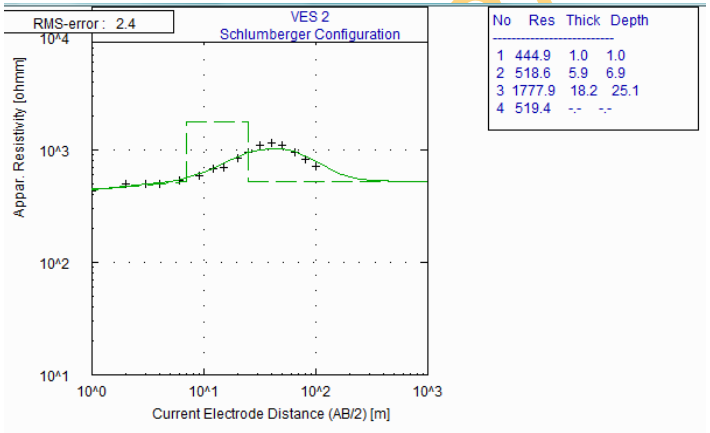

No	Res	Thick	Depth
1	444.9	1.0	1.0
2	518.6	5.9	6.9
3	1777.9	18.2	25.1
4	519.4	-.-	-.-

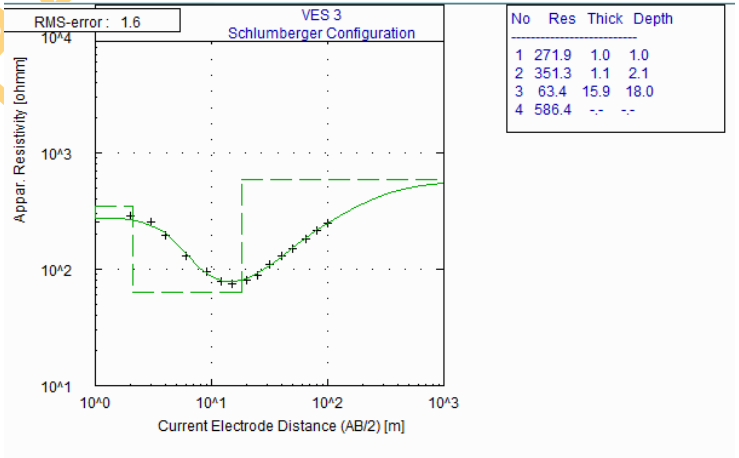

No	Res	Thick	Depth
1	271.9	1.0	1.0
2	351.3	1.1	2.1
3	63.4	15.9	18.0
4	586.4	-.-	-.-

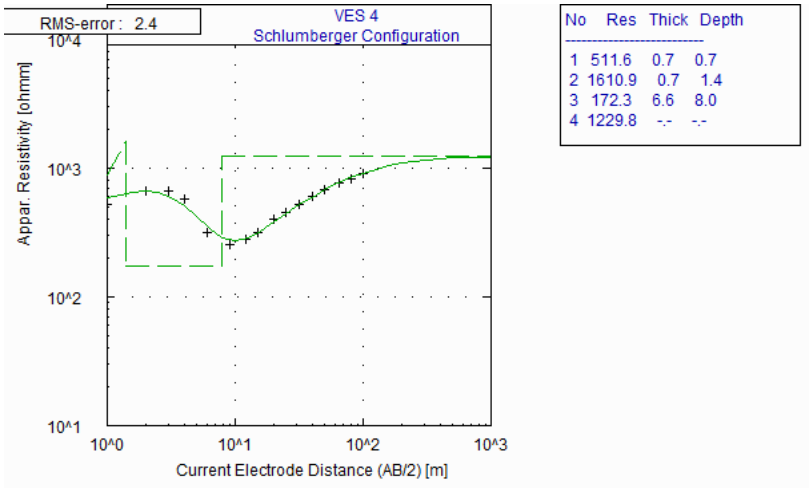

No	Res	Thick	Depth
1	511.6	0.7	0.7
2	1610.9	0.7	1.4
3	172.3	6.6	8.0
4	1229.8	-.-	-.-

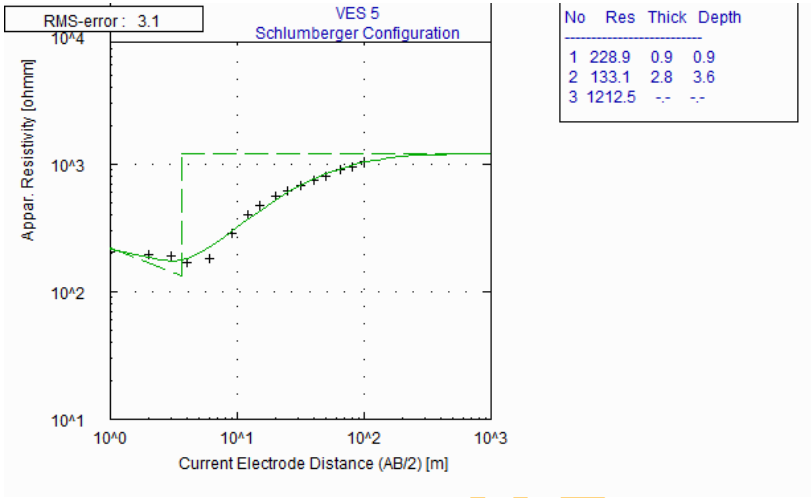

No	Res	Thick	Depth
1	228.9	0.9	0.9
2	133.1	2.8	3.6
3	1212.5	-.-	-.-

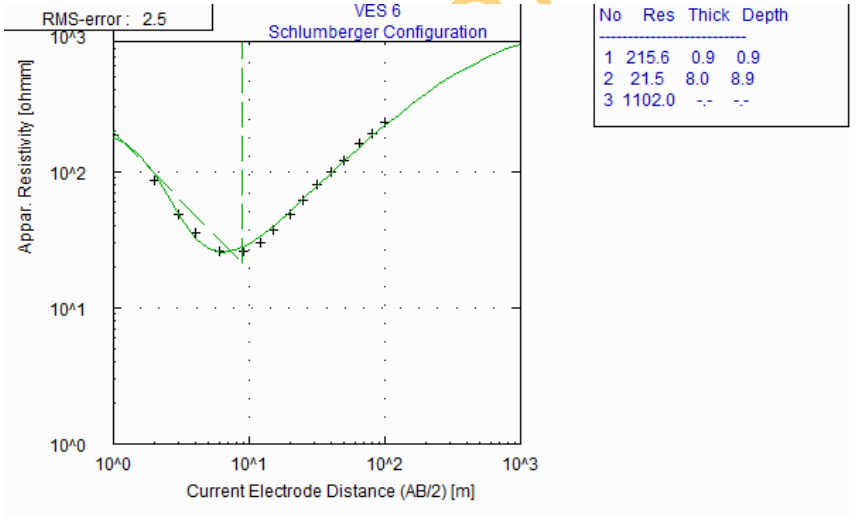

No	Res	Thick	Depth
1	215.6	0.9	0.9
2	21.5	8.0	8.9
3	1102.0	-.-	-.-

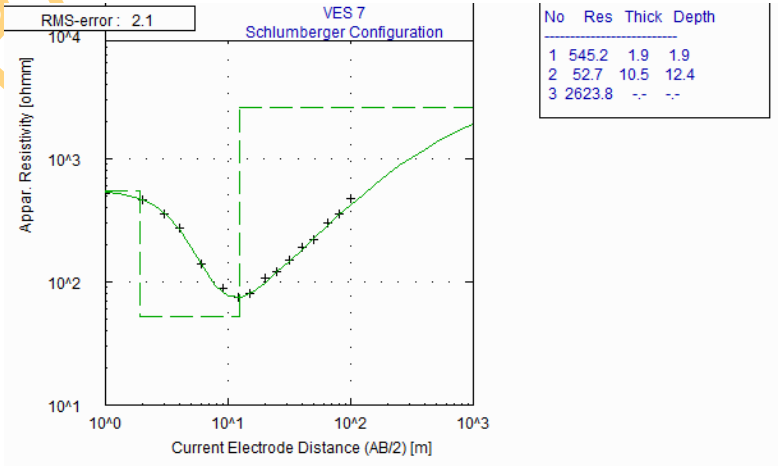

No	Res	Thick	Depth
1	545.2	1.9	1.9
2	52.7	10.5	12.4
3	2623.8	-.-	-.-

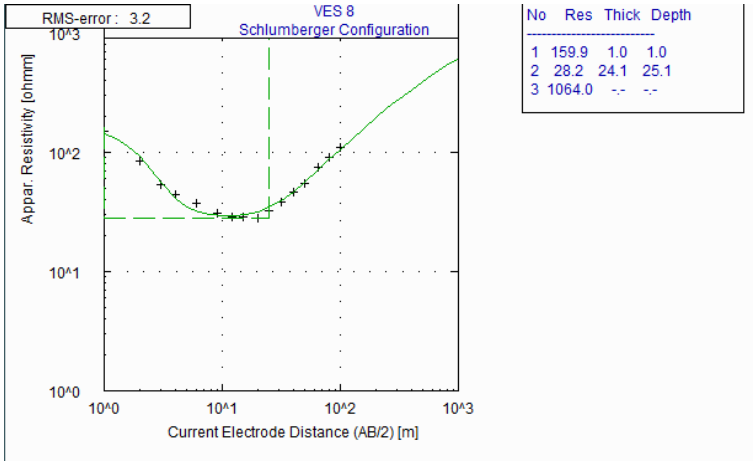

No	Res	Thick	Depth
1	159.9	1.0	1.0
2	28.2	24.1	25.1
3	1064.0	-.-	-.-

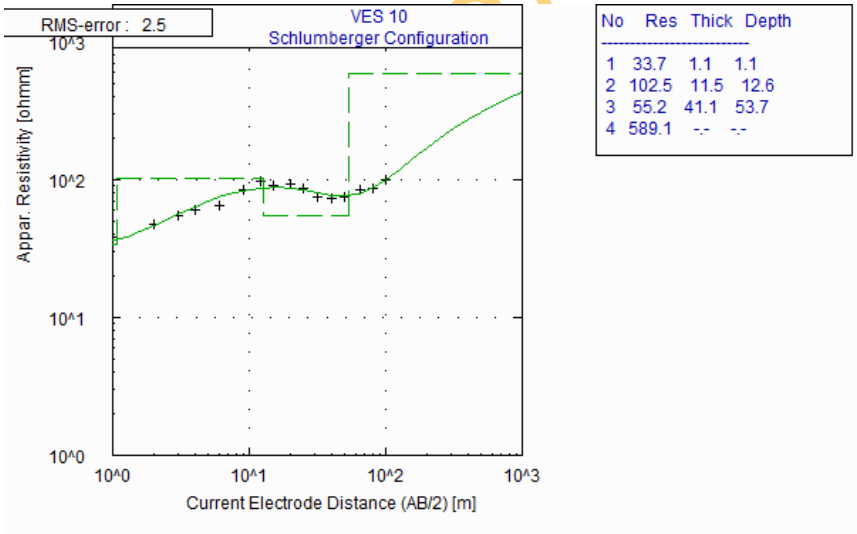

No	Res	Thick	Depth
1	33.7	1.1	1.1
2	102.5	11.5	12.6
3	55.2	41.1	53.7
4	589.1	-.-	-.-

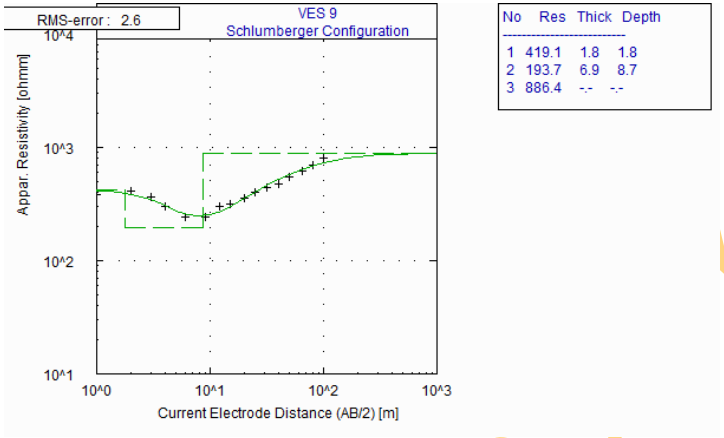

No	Res	Thick	Depth
1	419.1	1.8	1.8
2	193.7	6.9	8.7
3	886.4	-.-	-.-

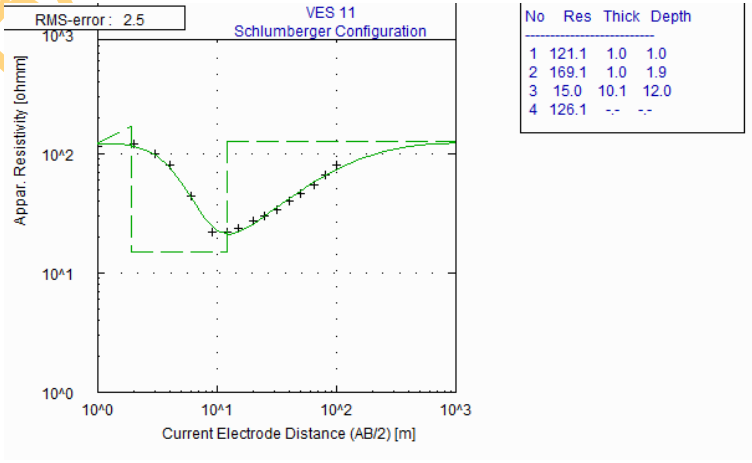

No	Res	Thick	Depth
1	121.1	1.0	1.0
2	169.1	1.0	1.9
3	15.0	10.1	12.0
4	126.1	-.-	-.-

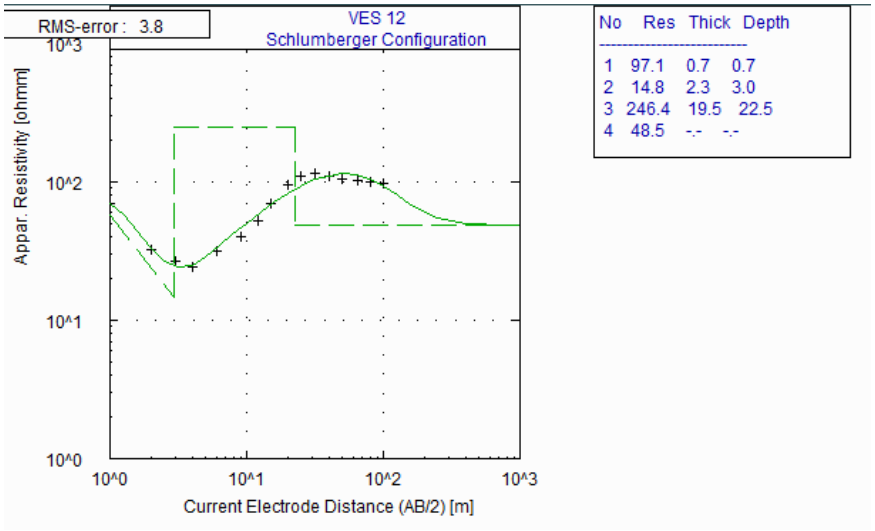
RMS-error : 3.8
VES 12
Schlumberger Configuration
Appar. Resistivity [ohmm]
10^3
10^2
10^1
10^0
10^0
10^1
10^2
10^3
Current Electrode Distance (AB/2) [m]
No Res Thick Depth
1 97.1 0.7 0.7
2 14.8 2.3 3.0
3 246.4 19.5 22.5
4 48.5 -.- -.-

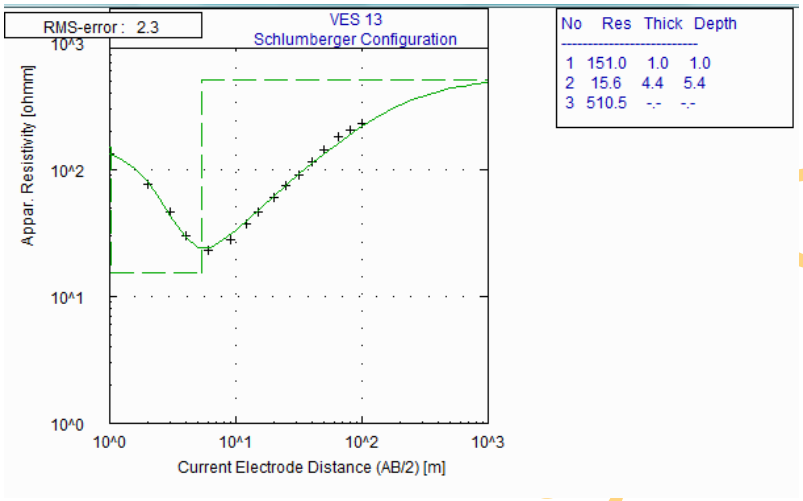
RMS-error : 2.3
VES 13
Schlumberger Configuration
Appar. Resistivity [ohmm]
10^3
10^2
10^1
10^0
10^0
10^1
10^2
10^3
Current Electrode Distance (AB/2) [m]
No Res Thick Depth
1 151.0 1.0 1.0
2 15.6 4.4 5.4
3 510.5 -.- -.-

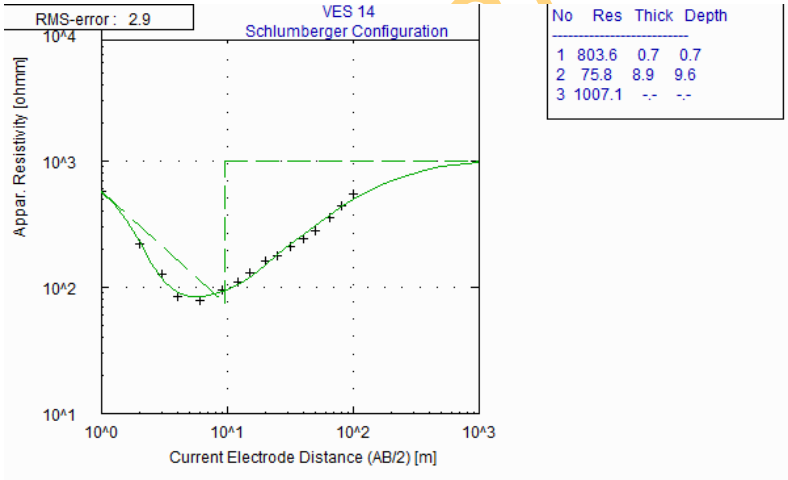
RMS-error : 2.9
VES 14
Schlumberger Configuration
Appar. Resistivity [ohmm]
10^4
10^3
10^2
10^1
10^0
10^1
10^2
10^3
Current Electrode Distance (AB/2) [m]
No Res Thick Depth
1 803.6 0.7 0.7
2 75.8 8.9 9.6
3 1007.1 -.- -.-

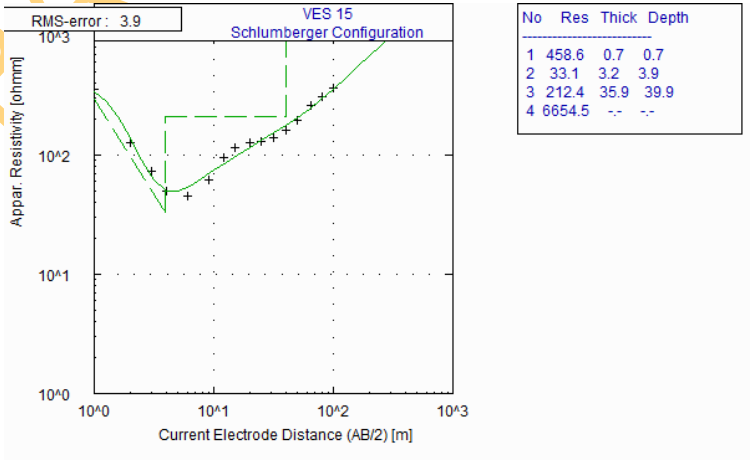
RMS-error : 3.9
VES 15
Schlumberger Configuration
Appar. Resistivity [ohmm]
10^3
10^2
10^1
10^0
10^0
10^1
10^2
10^3
Current Electrode Distance (AB/2) [m]
No Res Thick Depth
1 458.6 0.7 0.7
2 33.1 3.2 3.9
3 212.4 35.9 39.9
4 6654.5 -.- -.-

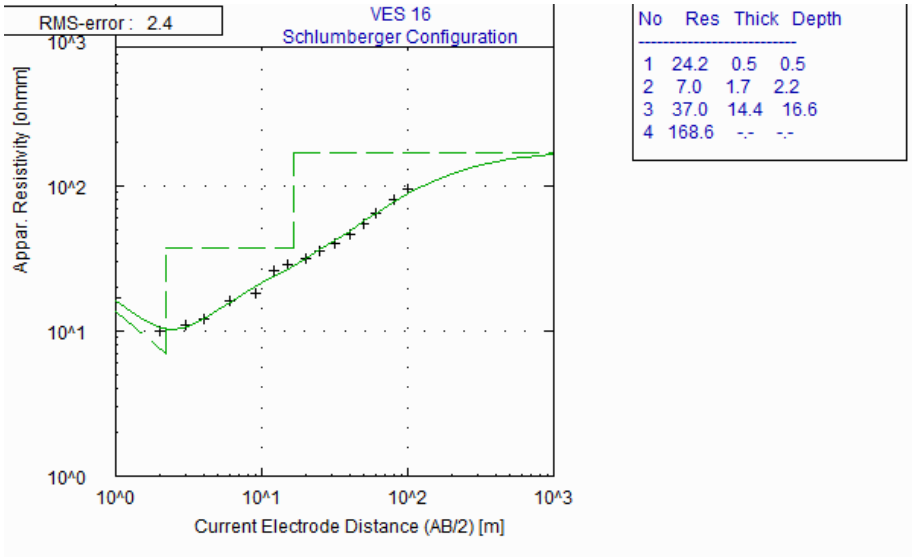

No	Res	Thick	Depth
1	24.2	0.5	0.5
2	7.0	1.7	2.2
3	37.0	14.4	16.6
4	168.6	-.-	-.-

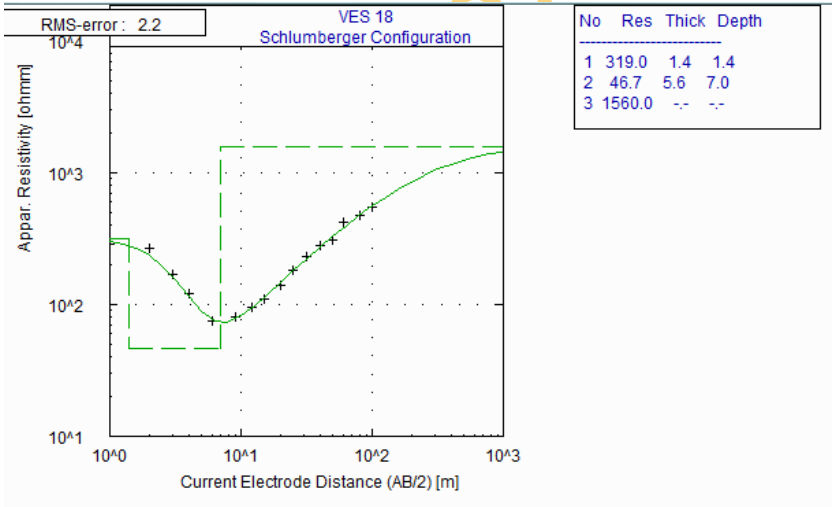

No	Res	Thick	Depth
1	319.0	1.4	1.4
2	46.7	5.6	7.0
3	1560.0	-.-	-.-

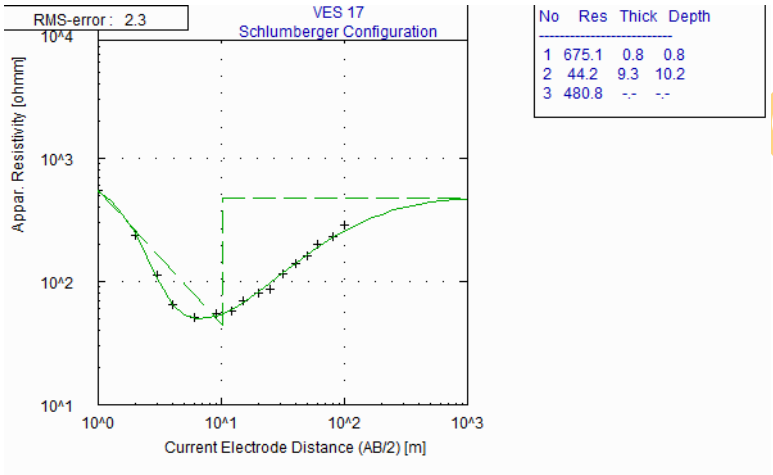

No	Res	Thick	Depth
1	675.1	0.8	0.8
2	44.2	9.3	10.2
3	480.8	-.-	-.-

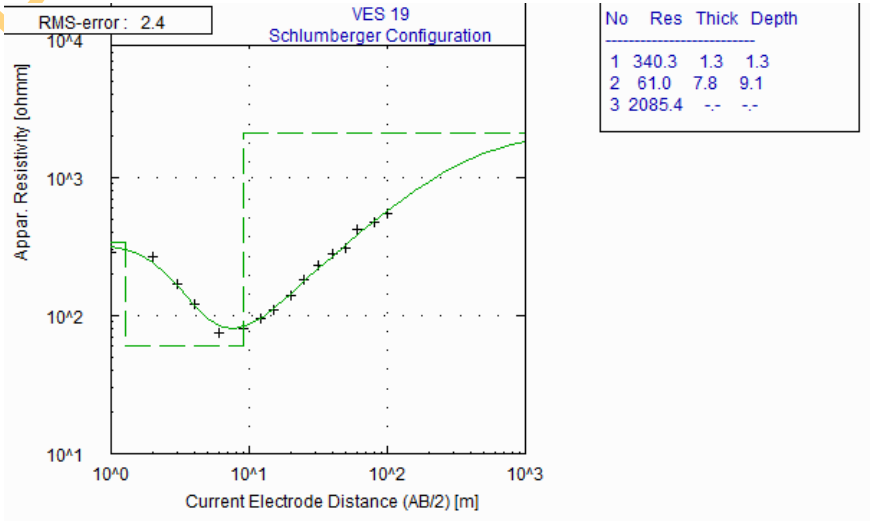

No	Res	Thick	Depth
1	340.3	1.3	1.3
2	61.0	7.8	9.1
3	2085.4	-.-	-.-

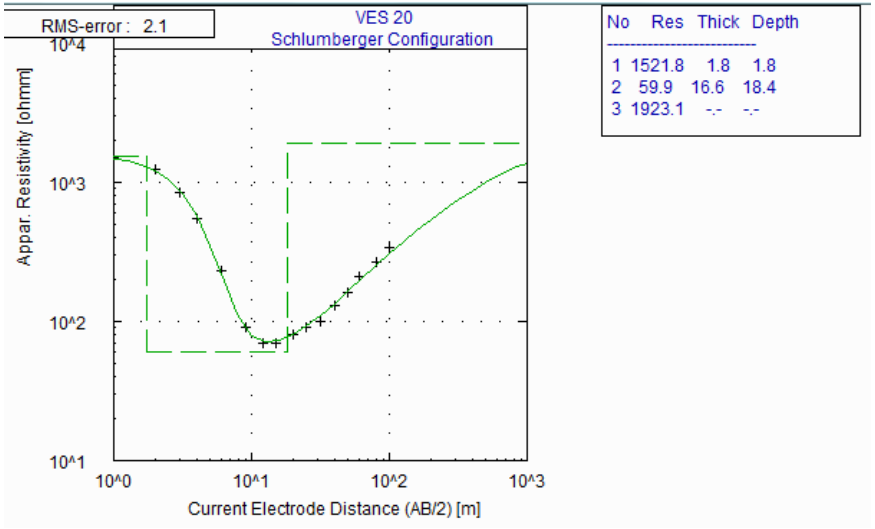
RMS-error : 2.1
VES 20
Schlumberger Configuration
Appar. Resistivity [ohmm]
10^4
10^3
10^2
10^1
10^0
10^1
10^2
10^3
Current Electrode Distance (AB/2) [m]
No Res Thick Depth
1 1521.8 1.8 1.8
2 59.9 16.6 18.4
3 1923.1 -.- -.-

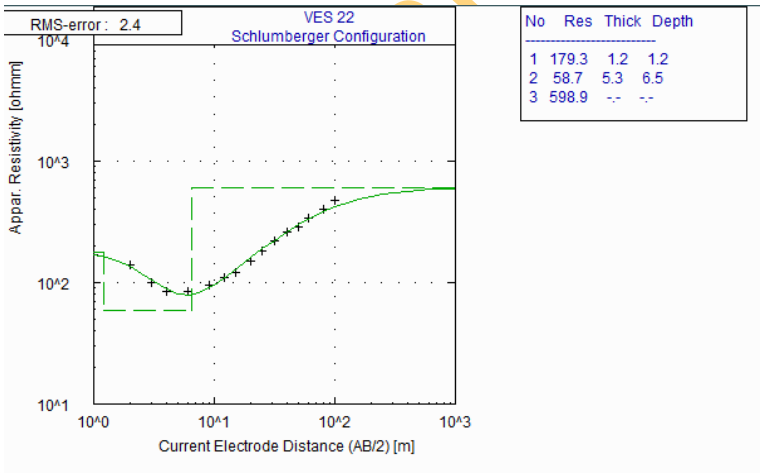
RMS-error : 2.4
VES 22
Schlumberger Configuration
Appar. Resistivity [ohmm]
10^4
10^3
10^2
10^1
10^0
10^1
10^2
10^3
Current Electrode Distance (AB/2) [m]
No Res Thick Depth
1 179.3 1.2 1.2
2 58.7 5.3 6.5
3 598.9 -.- -.-

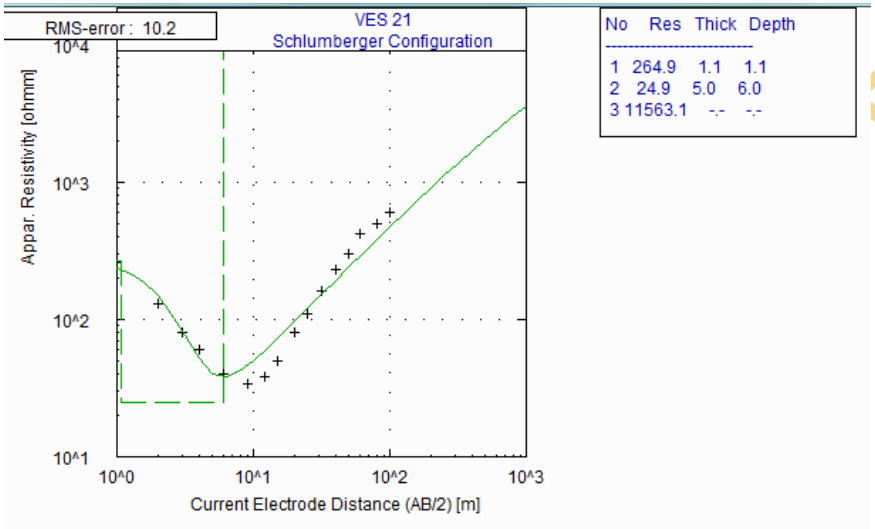
RMS-error : 10.2
VES 21
Schlumberger Configuration
Appar. Resistivity [ohmm]
10^4
10^3
10^2
10^1
10^0
10^1
10^2
10^3
Current Electrode Distance (AB/2) [m]
No Res Thick Depth
1 264.9 1.1 1.1
2 24.9 5.0 6.0
3 11563.1 -.- -.-

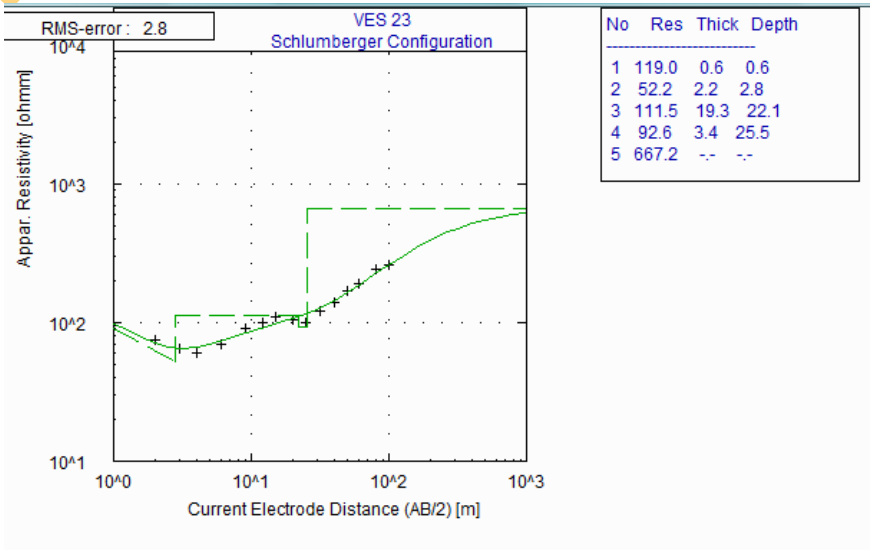
RMS-error : 2.8
VES 23
Schlumberger Configuration
Appar. Resistivity [ohmm]
10^4
10^3
10^2
10^1
10^0
10^1
10^2
10^3
Current Electrode Distance (AB/2) [m]
No Res Thick Depth
1 119.0 0.6 0.6
2 52.2 2.2 2.8
3 111.5 19.3 22.1
4 92.6 3.4 25.5
5 667.2 -.- -.-

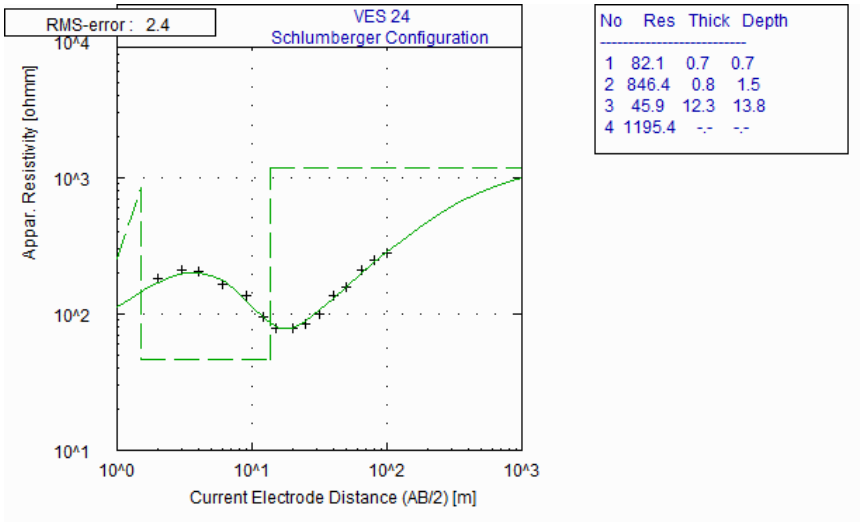

No	Res	Thick	Depth
1	82.1	0.7	0.7
2	846.4	0.8	1.5
3	45.9	12.3	13.8
4	1195.4	-.-	-.-

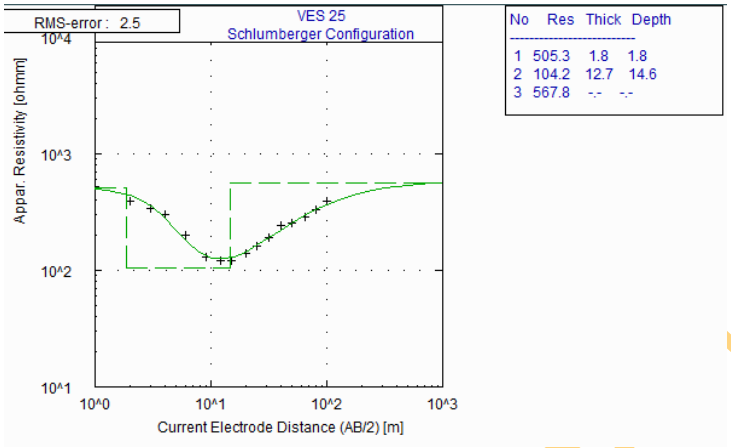

No	Res	Thick	Depth
1	505.3	1.8	1.8
2	104.2	12.7	14.6
3	567.8	-.-	-.-

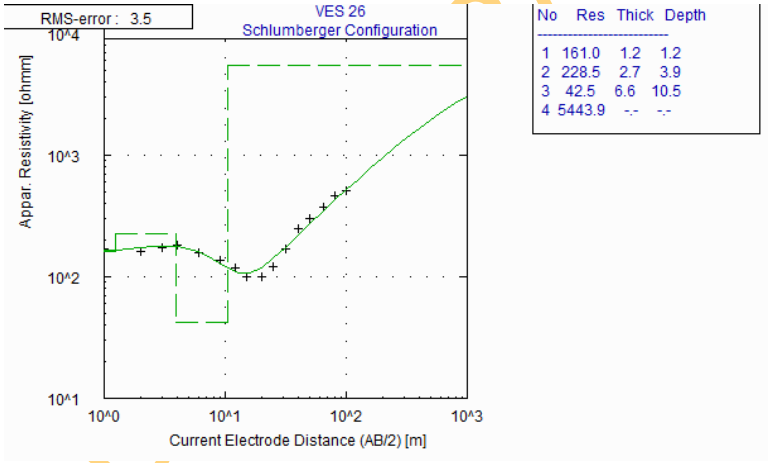

No	Res	Thick	Depth
1	161.0	1.2	1.2
2	228.5	2.7	3.9
3	42.5	6.6	10.5
4	5443.9	-.-	-.-

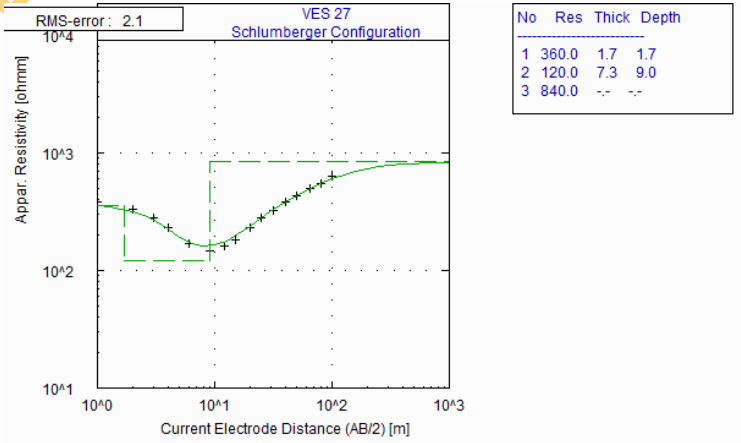

No	Res	Thick	Depth
1	360.0	1.7	1.7
2	120.0	7.3	9.0
3	840.0	-.-	-.-

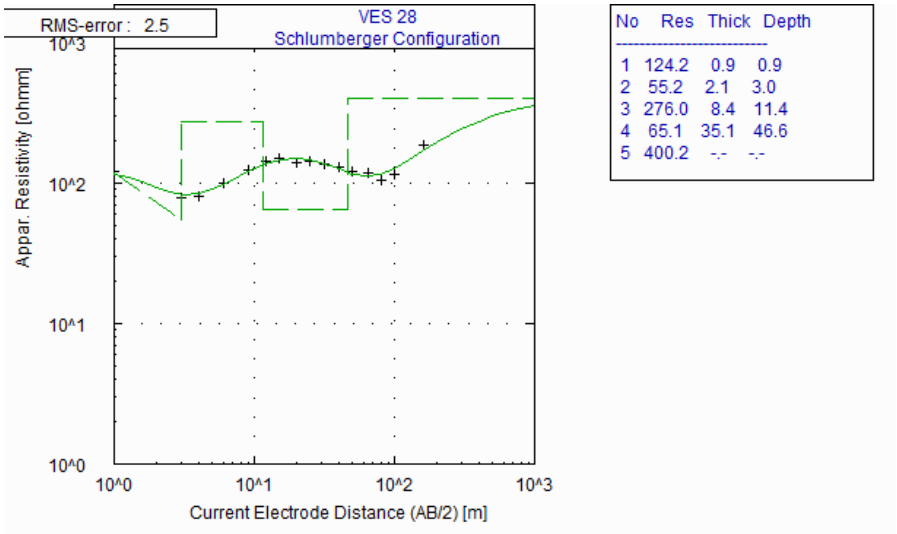

No	Res	Thick	Depth
1	124.2	0.9	0.9
2	55.2	2.1	3.0
3	276.0	8.4	11.4
4	65.1	35.1	46.6
5	400.2	-.-	-.-

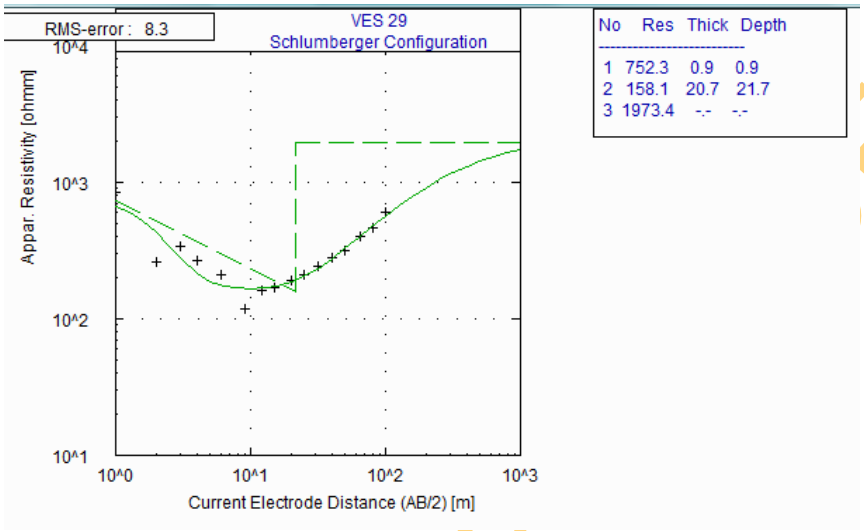

No	Res	Thick	Depth
1	752.3	0.9	0.9
2	158.1	20.7	21.7
3	1973.4	-.-	-.-

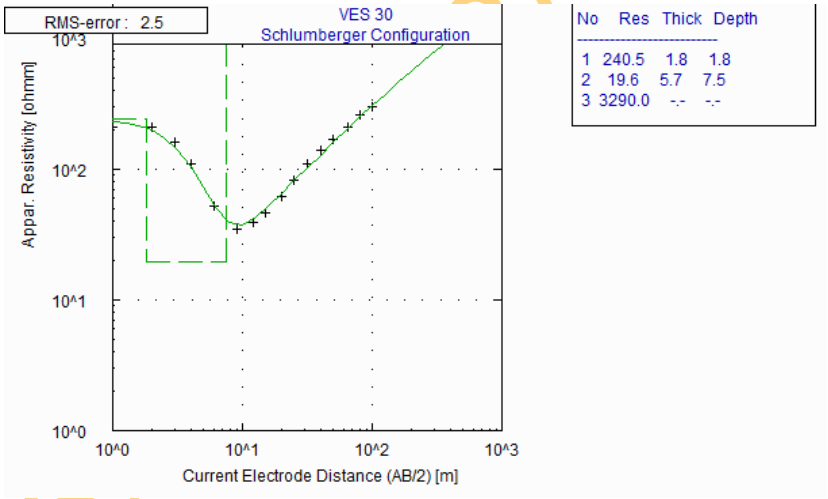

No	Res	Thick	Depth
1	240.5	1.8	1.8
2	19.6	5.7	7.5
3	3290.0	-.-	-.-

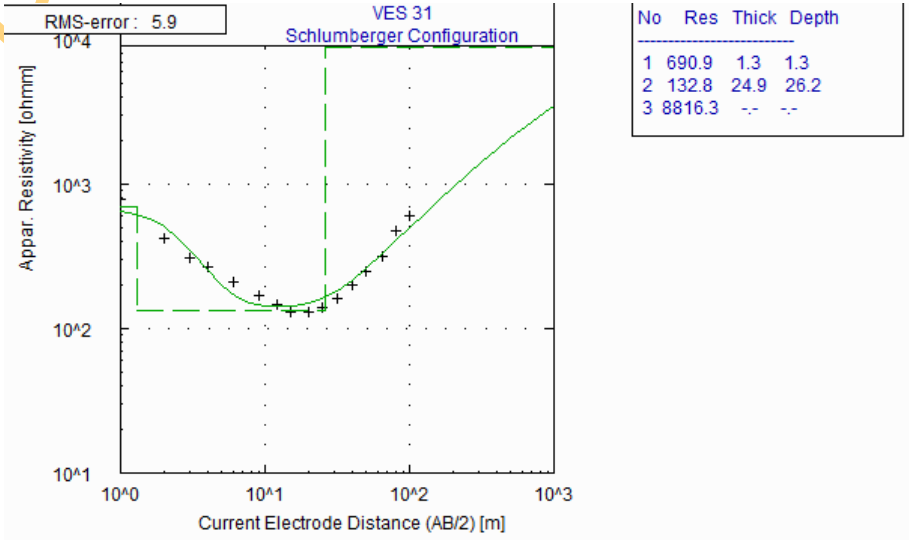

No	Res	Thick	Depth
1	690.9	1.3	1.3
2	132.8	24.9	26.2
3	8816.3	-.-	-.-

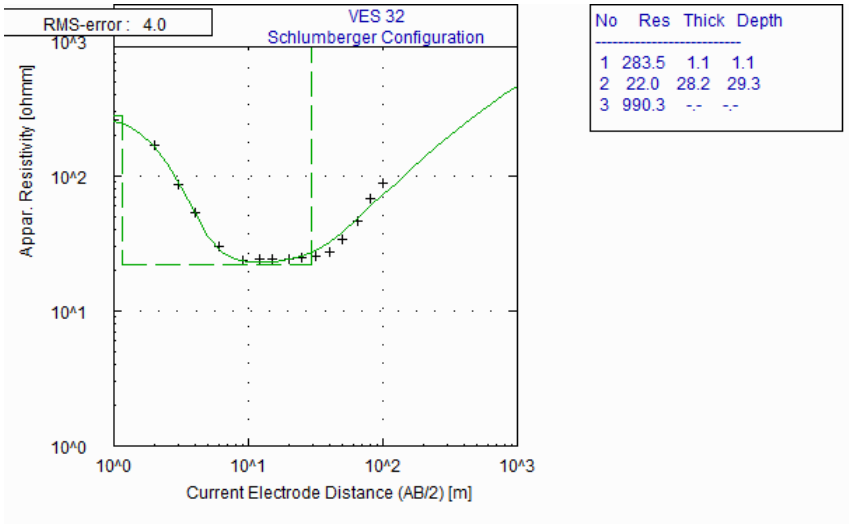

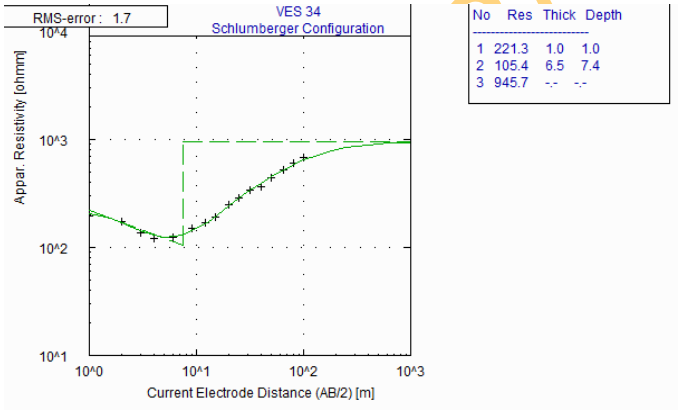

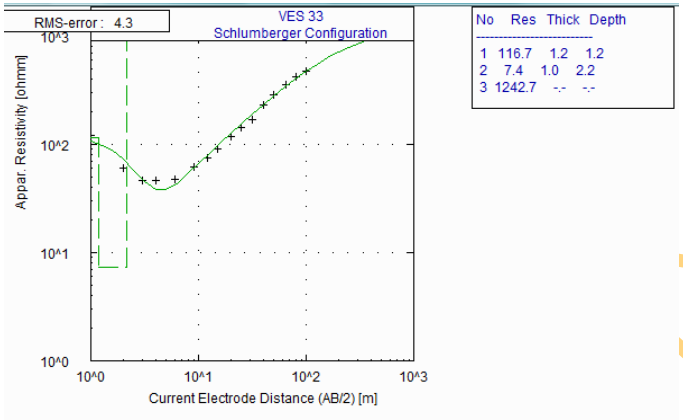

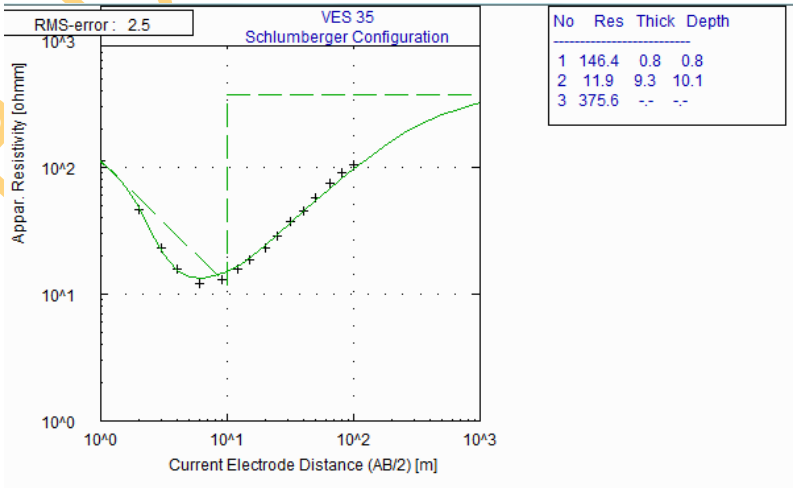

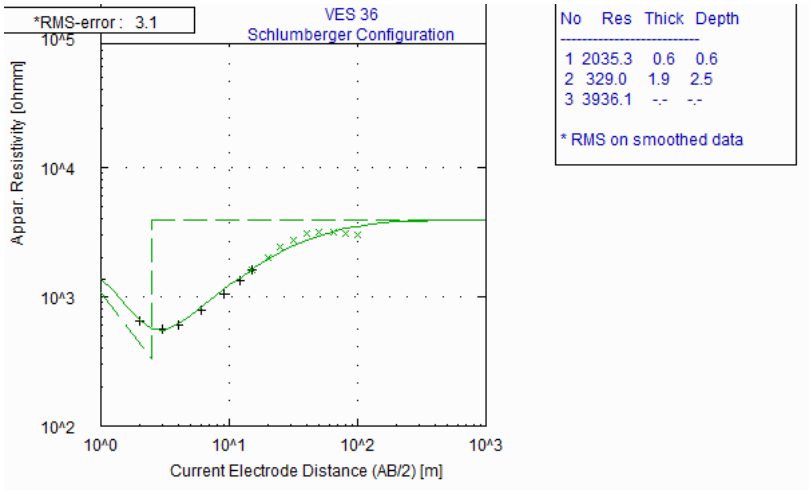
*RMS-error : 3.1
VES 36
Schlumberger Configuration
Appar. Resistivity [ohmm]
10^5
10^4
10^3
10^2
10^0
10^1
10^2
10^3
Current Electrode Distance (AB/2) [m]
No Res Thick Depth
1 2035.3 0.6 0.6
2 329.0 1.9 2.5
3 3936.1 -.- -.-
* RMS on smoothed data

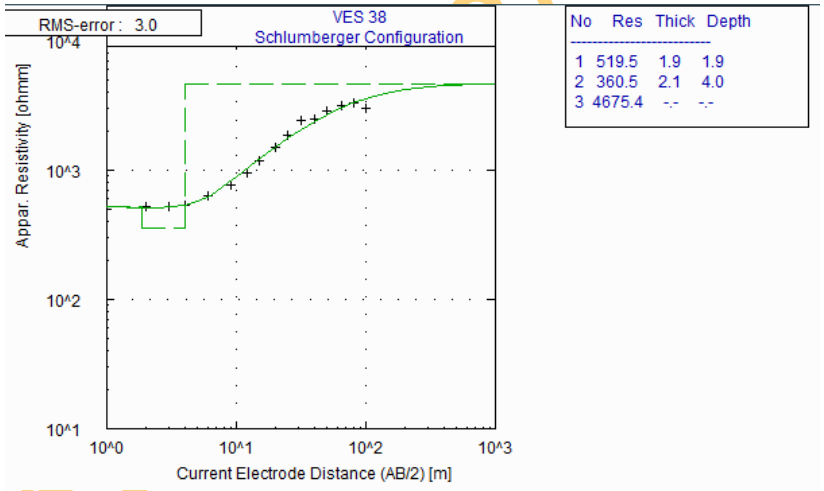
RMS-error : 3.0
VES 38
Schlumberger Configuration
Appar. Resistivity [ohmm]
10^4
10^3
10^2
10^1
10^0
10^1
10^2
10^3
Current Electrode Distance (AB/2) [m]
No Res Thick Depth
1 519.5 1.9 1.9
2 360.5 2.1 4.0
3 4675.4 -.- -.-

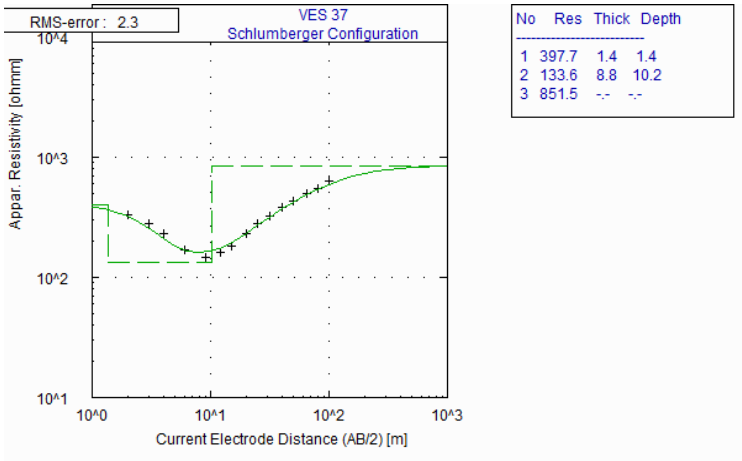
RMS-error : 2.3
VES 37
Schlumberger Configuration
Appar. Resistivity [ohmm]
10^4
10^3
10^2
10^1
10^0
10^1
10^2
10^3
Current Electrode Distance (AB/2) [m]
No Res Thick Depth
1 397.7 1.4 1.4
2 133.6 8.8 10.2
3 851.5 -.- -.-

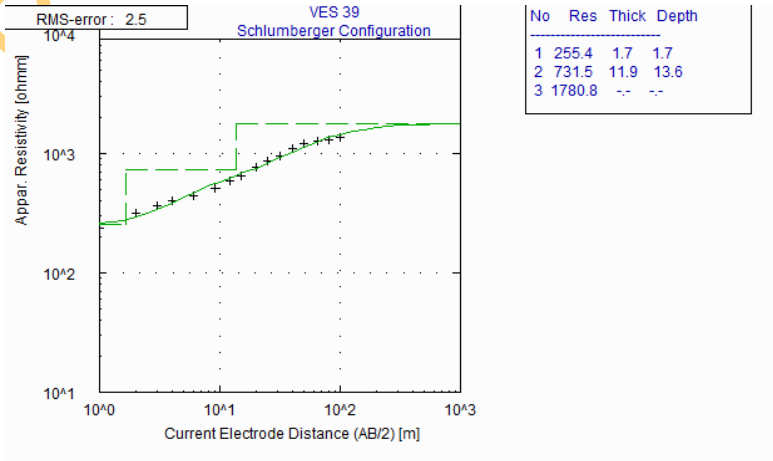
RMS-error : 2.5
VES 39
Schlumberger Configuration
Appar. Resistivity [ohmm]
10^4
10^3
10^2
10^1
10^0
10^1
10^2
10^3
Current Electrode Distance (AB/2) [m]
No Res Thick Depth
1 255.4 1.7 1.7
2 731.5 11.9 13.6
3 1780.8 -.- -.-

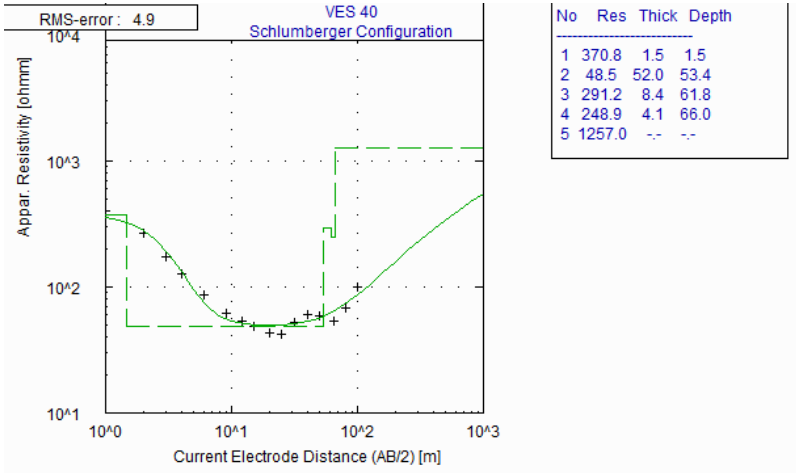
RMS-error : 4.9
VES 40
Schlumberger Configuration
Appar. Resistivity [ohmm]
10^4
10^3
10^2
10^1
10^0
10^1
10^2
10^3
Current Electrode Distance (AB/2) [m]
No Res Thick Depth
1 370.8 1.5 1.5
2 48.5 52.0 53.4
3 291.2 8.4 61.8
4 248.9 4.1 66.0
5 1257.0 -.- -.-

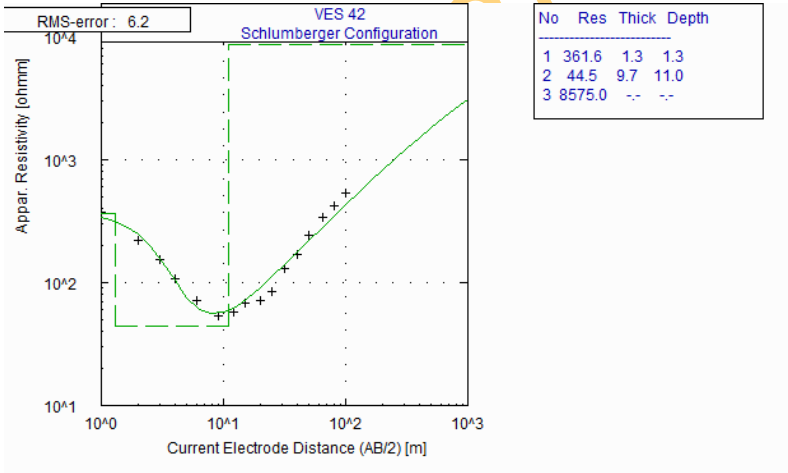
RMS-error : 6.2
VES 42
Schlumberger Configuration
Appar. Resistivity [ohmm]
10^4
10^3
10^2
10^1
10^0
10^1
10^2
10^3
Current Electrode Distance (AB/2) [m]
No Res Thick Depth
1 361.6 1.3 1.3
2 44.5 9.7 11.0
3 8575.0 -.- -.-

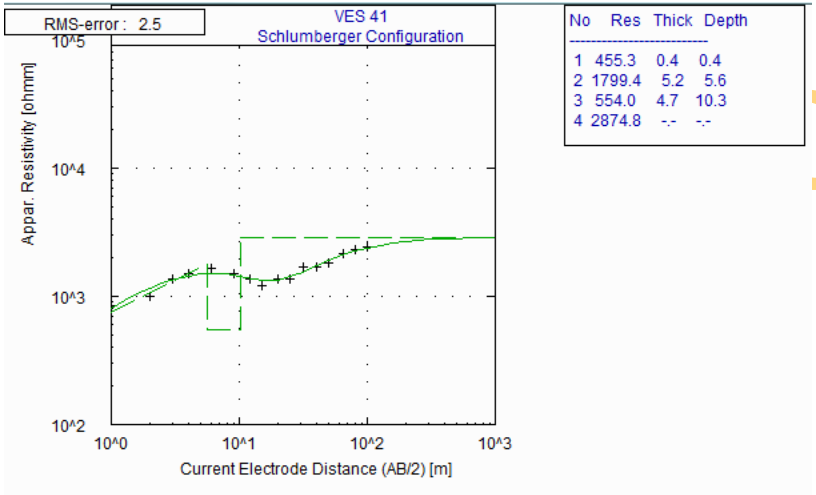
RMS-error : 2.5
VES 41
Schlumberger Configuration
Appar. Resistivity [ohmm]
10^5
10^4
10^3
10^2
10^0
10^1
10^2
10^3
Current Electrode Distance (AB/2) [m]
No Res Thick Depth
1 455.3 0.4 0.4
2 1799.4 5.2 5.6
3 554.0 4.7 10.3
4 2874.8 -.- -.-

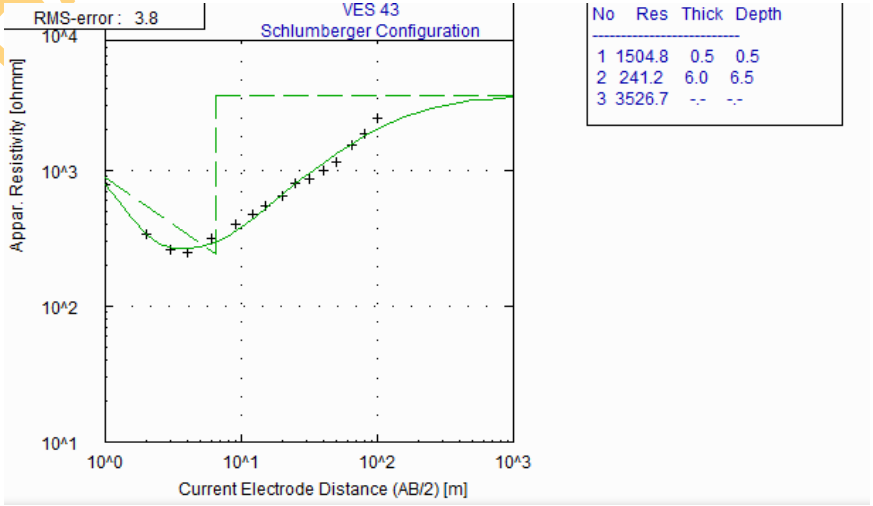
RMS-error : 3.8
VES 43
Schlumberger Configuration
Appar. Resistivity [ohmm]
10^4
10^3
10^2
10^1
10^0
10^1
10^2
10^3
Current Electrode Distance (AB/2) [m]
No Res Thick Depth
1 1504.8 0.5 0.5
2 241.2 6.0 6.5
3 3526.7 -.- -.-

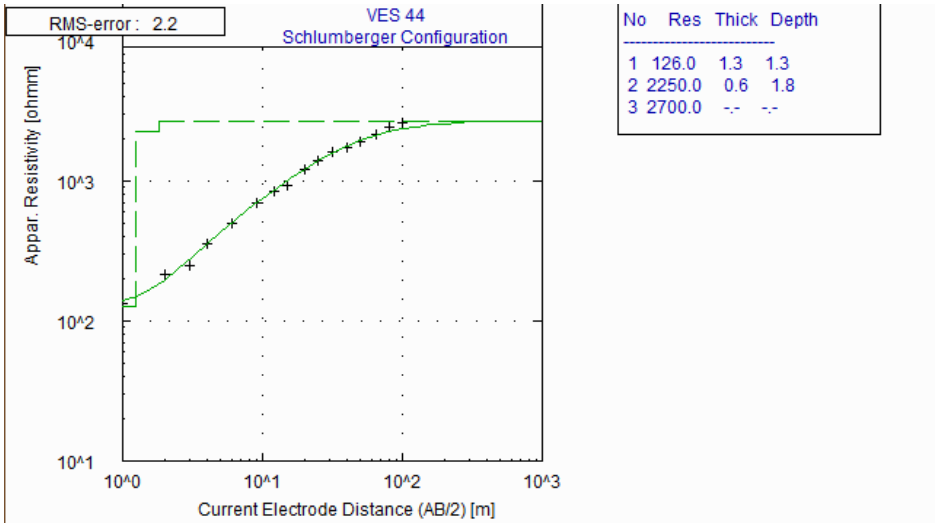

No	Res	Thick	Depth
1	126.0	1.3	1.3
2	2250.0	0.6	1.8
3	2700.0	-.-	-.-

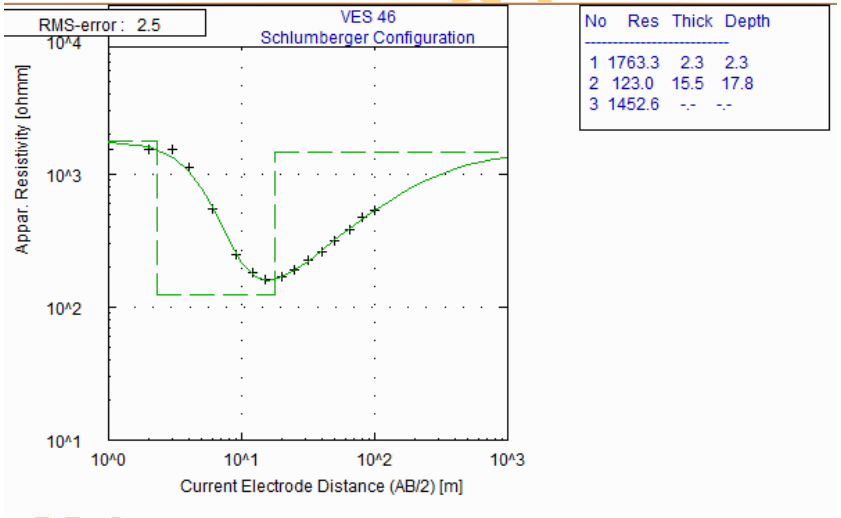

No	Res	Thick	Depth
1	1763.3	2.3	2.3
2	123.0	15.5	17.8
3	1452.6	-.-	-.-

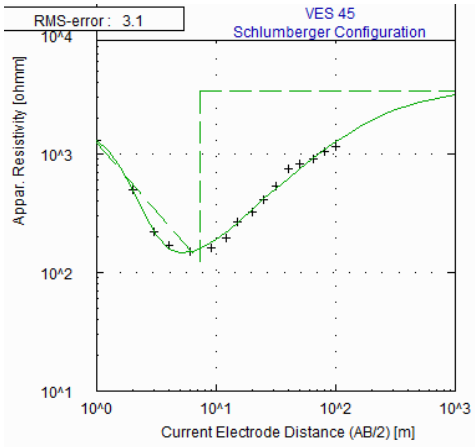

No	Res	Thick	Depth
1	1814.6	0.7	0.7
2	123.9	6.6	7.3
3	3366.3	-.-	-.-

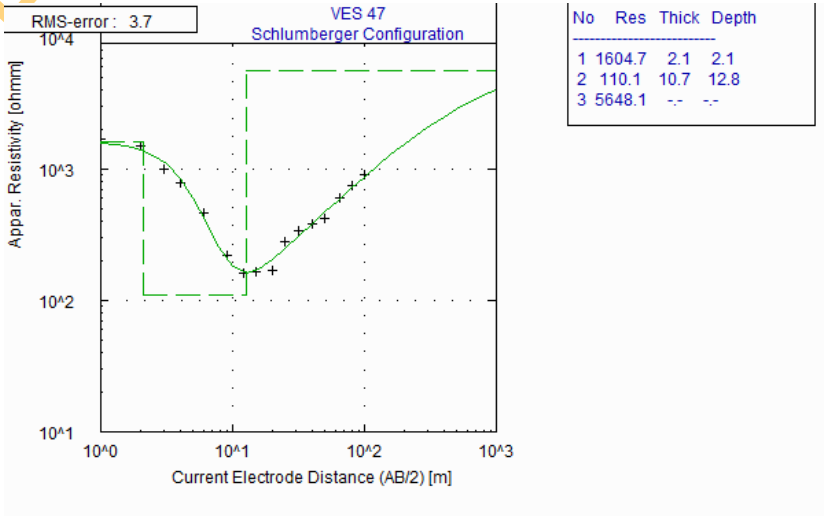

No	Res	Thick	Depth
1	1604.7	2.1	2.1
2	110.1	10.7	12.8
3	5648.1	-.-	-.-

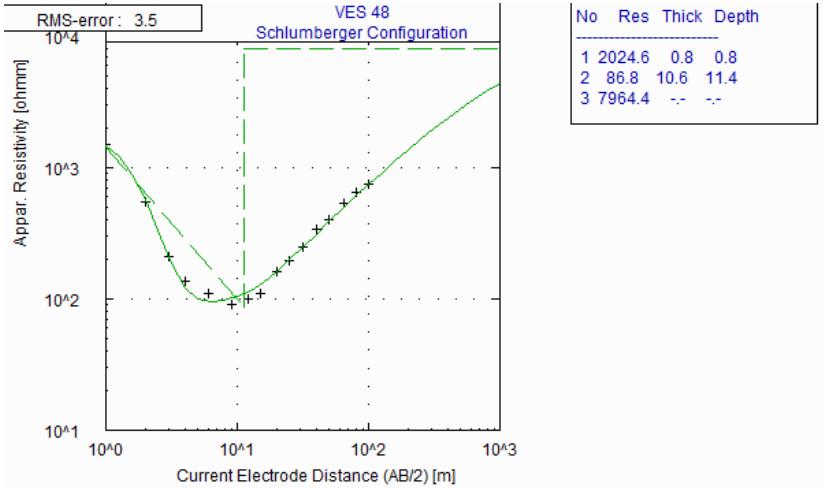

No	Res	Thick	Depth
1	2024.6	0.8	0.8
2	86.8	10.6	11.4
3	7964.4	-.-	-.-

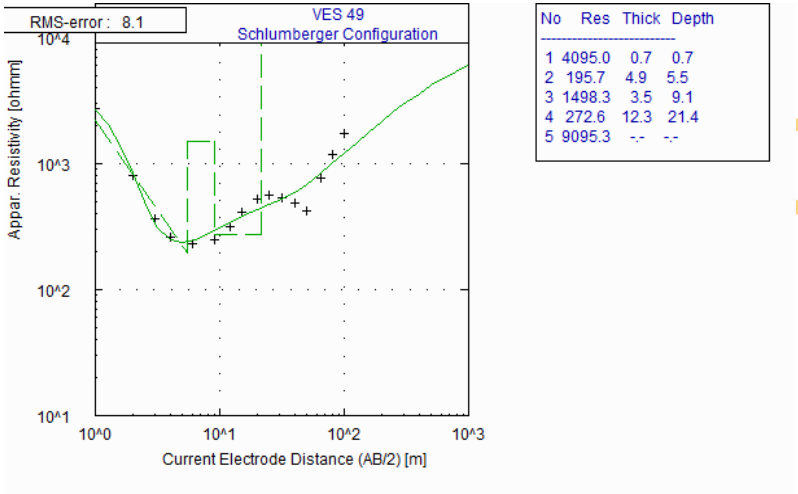

No	Res	Thick	Depth
1	4095.0	0.7	0.7
2	195.7	4.9	5.5
3	1498.3	3.5	9.1
4	272.6	12.3	21.4
5	9095.3	-.-	-.-

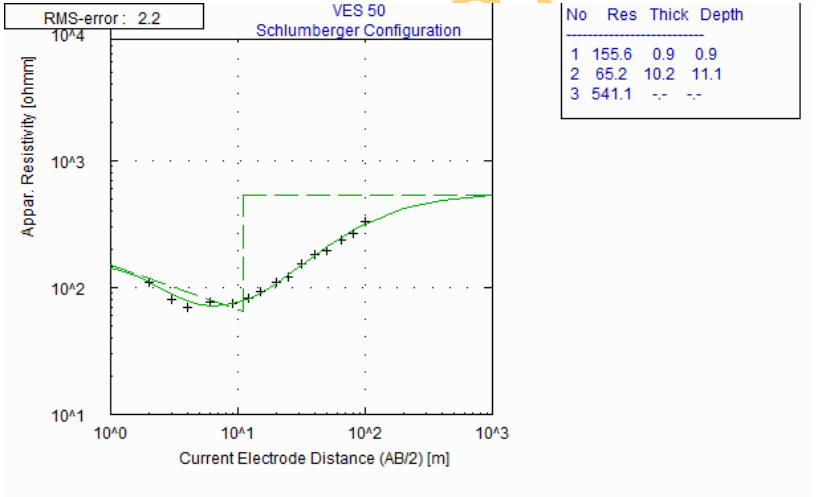

No	Res	Thick	Depth
1	155.6	0.9	0.9
2	65.2	10.2	11.1
3	541.1	-.-	-.-

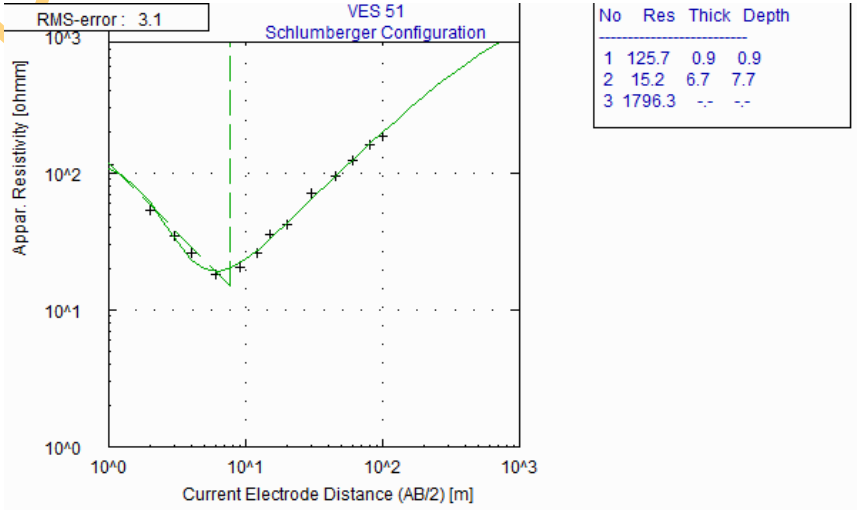

No	Res	Thick	Depth
1	125.7	0.9	0.9
2	15.2	6.7	7.7
3	1796.3	-.-	-.-

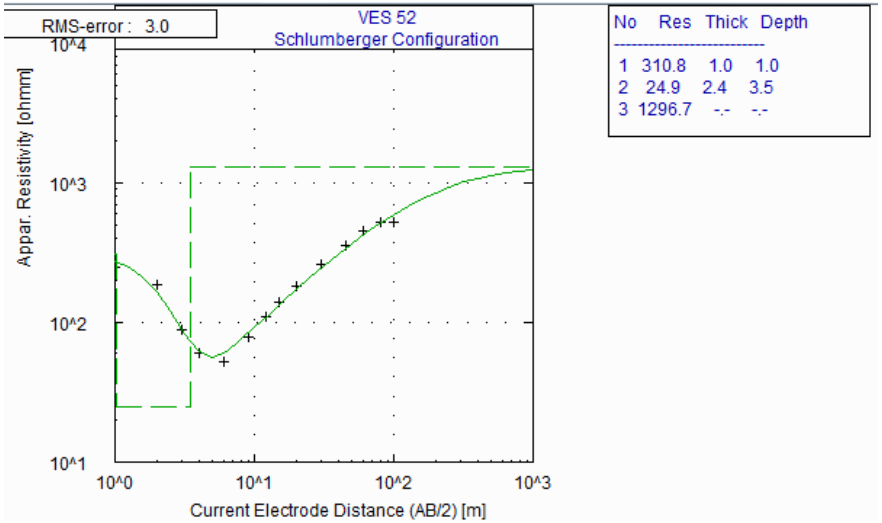
RMS-error : 3.0
VES 52
Schlumberger Configuration
No Res Thick Depth
1 310.8 1.0 1.0
2 24.9 2.4 3.5
3 1296.7 -.- -.-
Appar. Resistivity [ohmm]
Current Electrode Distance (AB/2) [m]

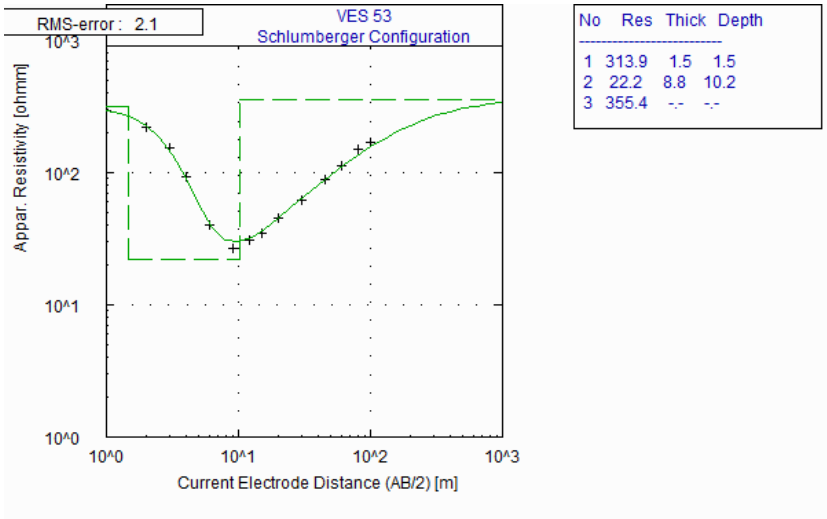
RMS-error : 2.1
VES 53
Schlumberger Configuration
No Res Thick Depth
1 313.9 1.5 1.5
2 22.2 8.8 10.2
3 355.4 -.- -.-
Appar. Resistivity [ohmm]
Current Electrode Distance (AB/2) [m]

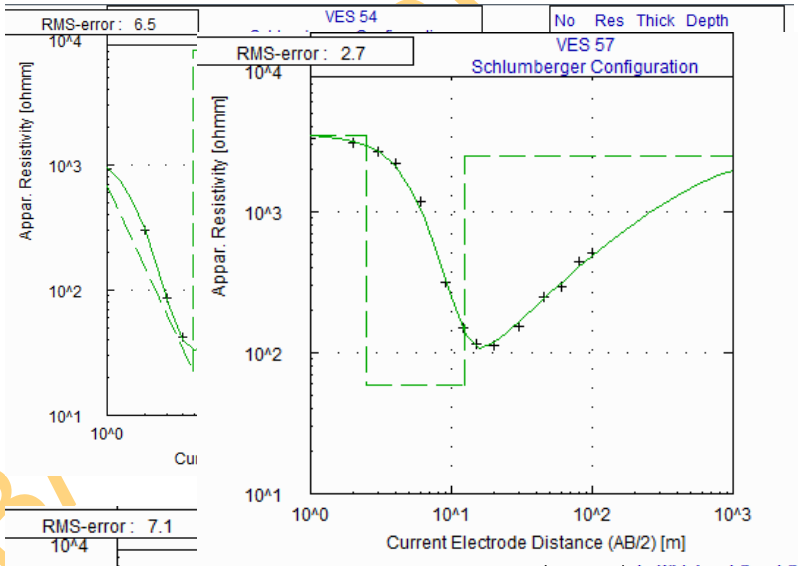
RMS-error : 6.5
VES 54
RMS-error : 2.7
VES 57
Schlumberger Configuration
No Res Thick Depth
1 3493.2 2.5 2.5
2 59.2 10.0 12.5
3 2516.6 -.- -.-
Appar. Resistivity [ohmm]
Current Electrode Distance (AB/2) [m]

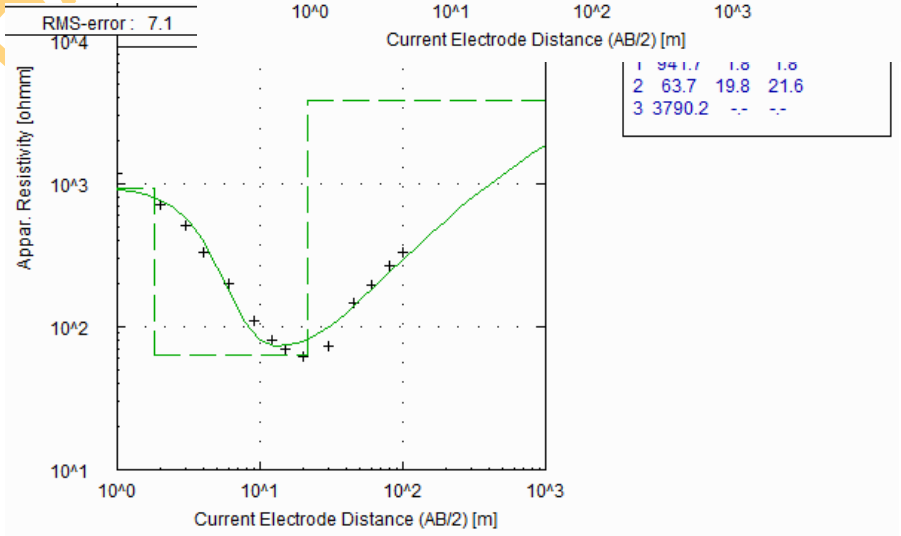
RMS-error : 7.1
2 63.7 19.8 21.6
3 3790.2 -.- -.-
Appar. Resistivity [ohmm]
Current Electrode Distance (AB/2) [m]

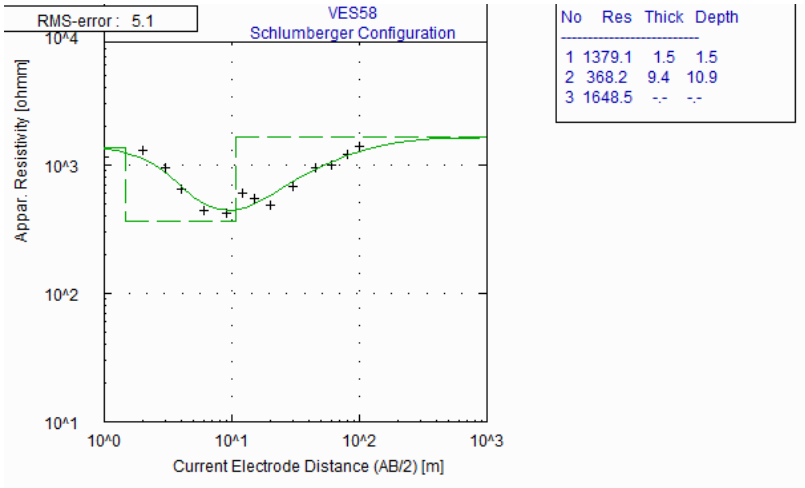

No	Res	Thick	Depth
1	1379.1	1.5	1.5
2	368.2	9.4	10.9
3	1648.5	-.-	-.-

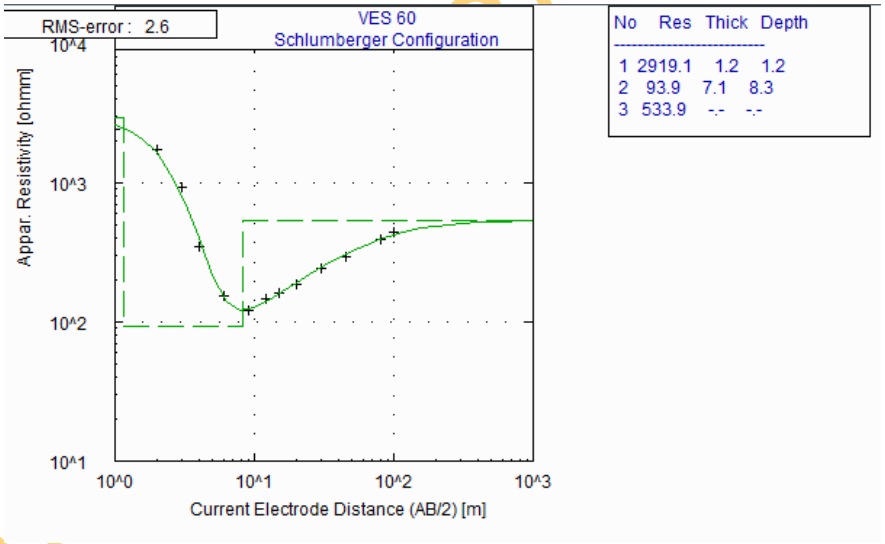

No	Res	Thick	Depth
1	2919.1	1.2	1.2
2	93.9	7.1	8.3
3	533.9	-.-	-.-

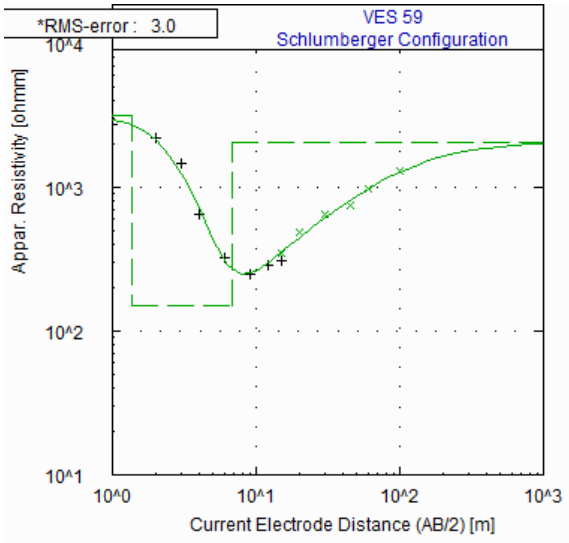

No	Res	Thick	Depth
1	3171.5	1.4	1.4
2	151.5	5.4	6.8
3	2034.2	-.-	-.-

* RMS on smoothed data

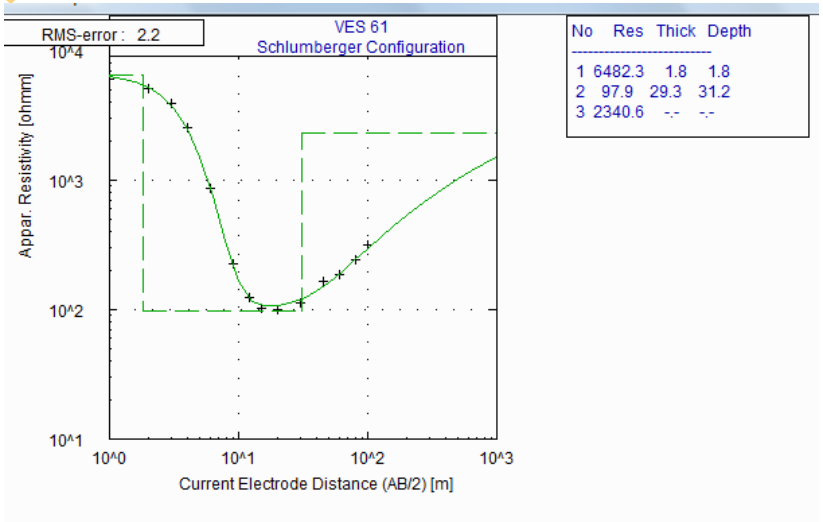

No	Res	Thick	Depth
1	6482.3	1.8	1.8
2	97.9	29.3	31.2
3	2340.6	-.-	-.-

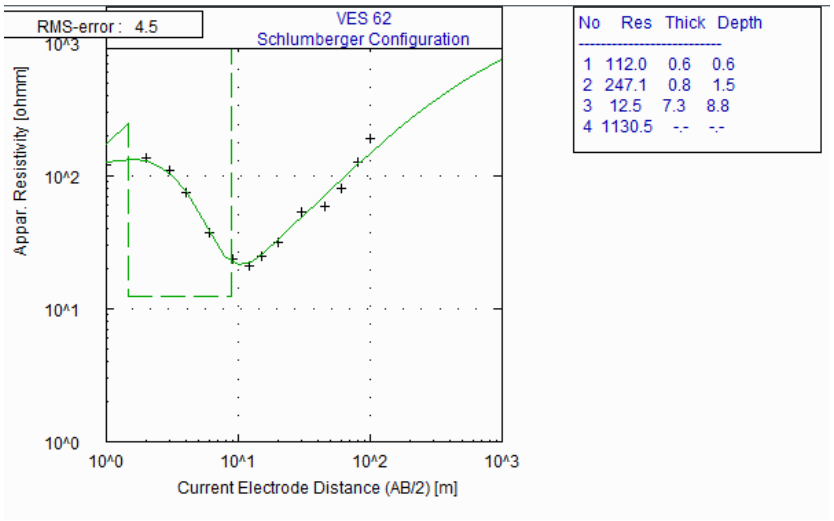

No	Res	Thick	Depth
1	112.0	0.6	0.6
2	247.1	0.8	1.5
3	12.5	7.3	8.8
4	1130.5	-.-	-.-

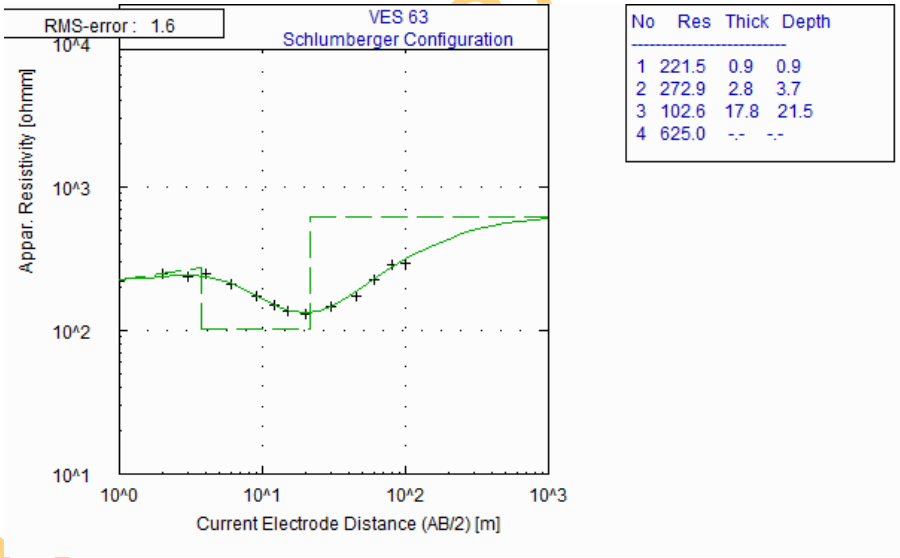

No	Res	Thick	Depth
1	221.5	0.9	0.9
2	272.9	2.8	3.7
3	102.6	17.8	21.5
4	625.0	-.-	-.-

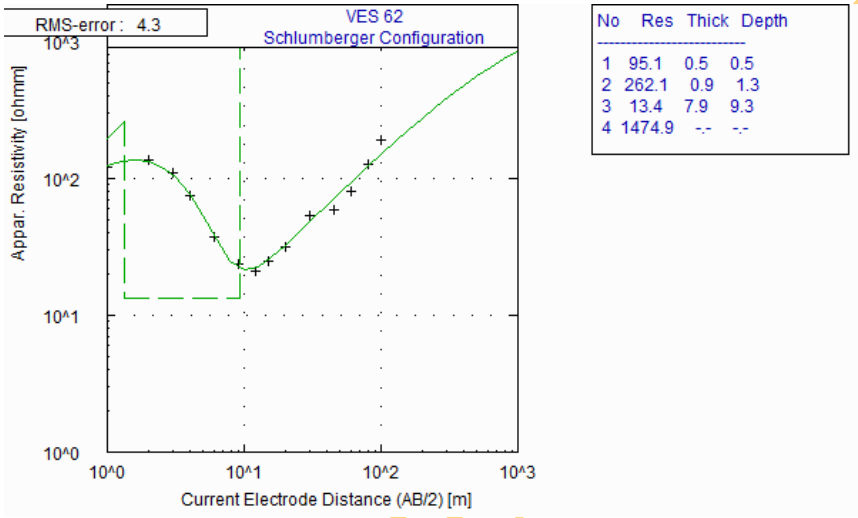

No	Res	Thick	Depth
1	95.1	0.5	0.5
2	262.1	0.9	1.3
3	13.4	7.9	9.3
4	1474.9	-.-	-.-

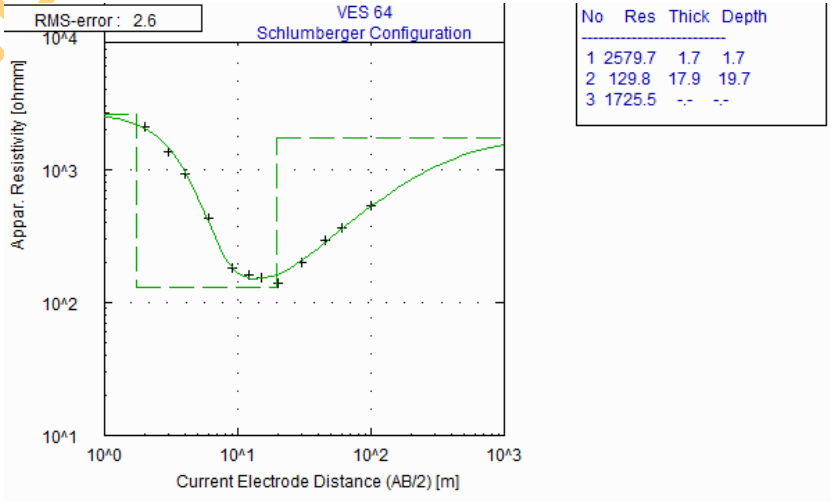

No	Res	Thick	Depth
1	2579.7	1.7	1.7
2	129.8	17.9	19.7
3	1725.5	-.-	-.-

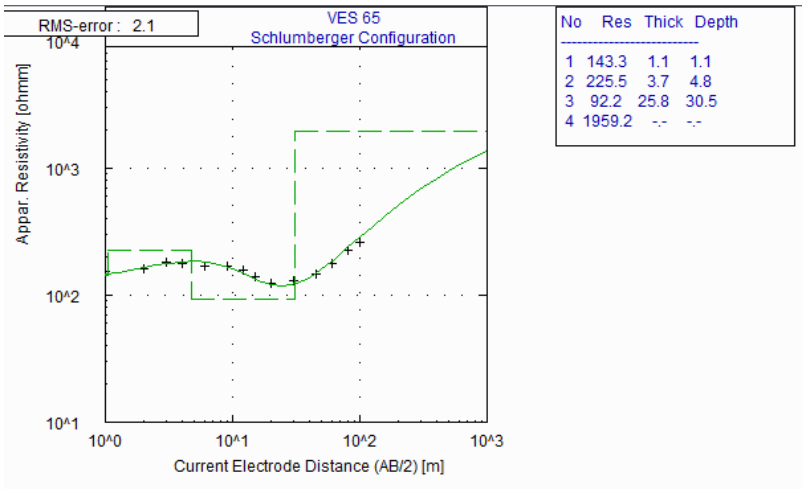
RMS-error : 2.1
VES 65
Schlumberger Configuration
Appar. Resistivity [ohmm]
Current Electrode Distance (AB/2) [m]
No Res Thick Depth
1 143.3 1.1 1.1
2 225.5 3.7 4.8
3 92.2 25.8 30.5
4 1959.2 -.- -.-

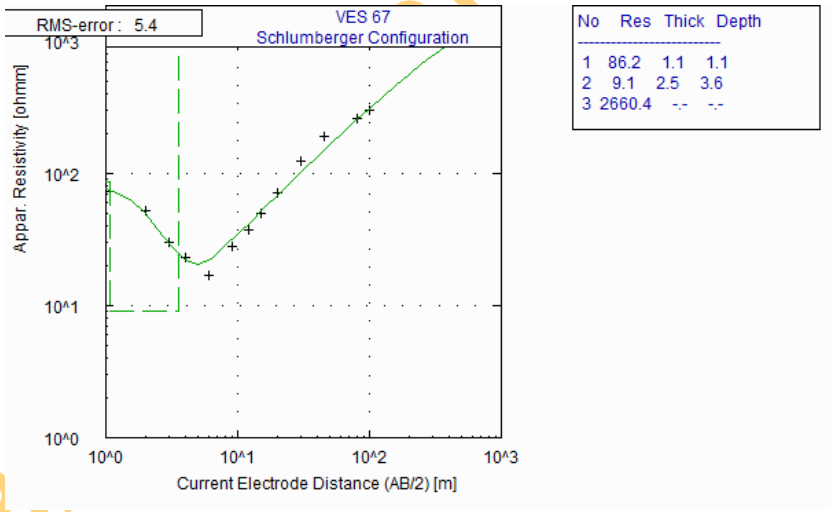
RMS-error : 5.4
VES 67
Schlumberger Configuration
Appar. Resistivity [ohmm]
Current Electrode Distance (AB/2) [m]
No Res Thick Depth
1 86.2 1.1 1.1
2 9.1 2.5 3.6
3 2660.4 -.- -.-

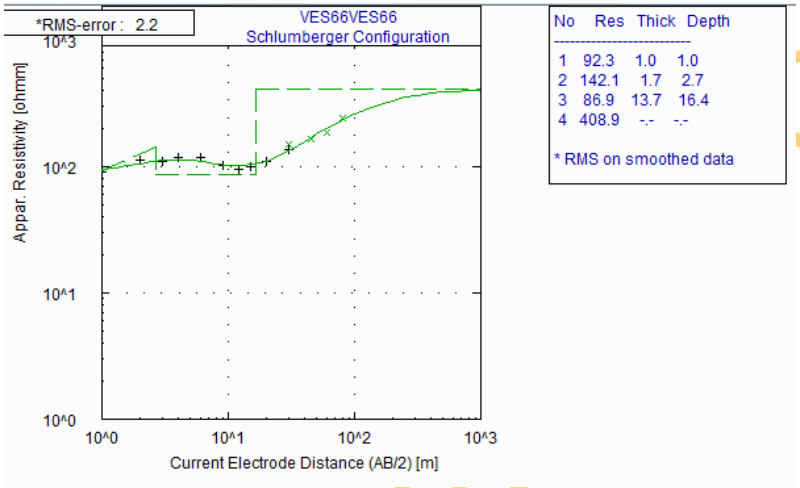
*RMS-error : 2.2
VES66VES66
Schlumberger Configuration
Appar. Resistivity [ohmm]
Current Electrode Distance (AB/2) [m]
No Res Thick Depth
1 92.3 1.0 1.0
2 142.1 1.7 2.7
3 86.9 13.7 16.4
4 408.9 -.- -.-
* RMS on smoothed data

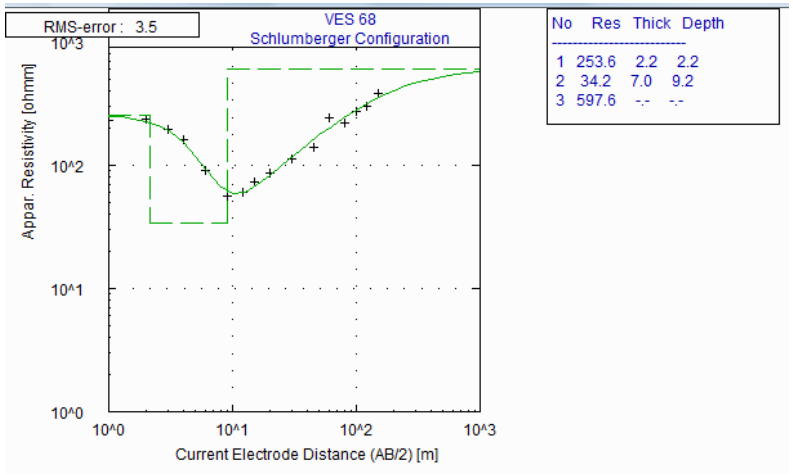
RMS-error : 3.5
VES 68
Schlumberger Configuration
Appar. Resistivity [ohmm]
Current Electrode Distance (AB/2) [m]
No Res Thick Depth
1 253.6 2.2 2.2
2 34.2 7.0 9.2
3 597.6 -.- -.-

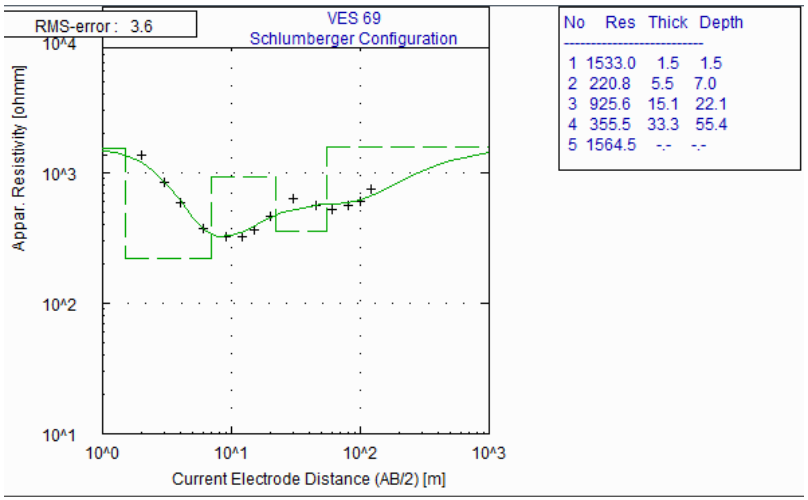
RMS-error : 3.6
VES 69
Schlumberger Configuration
No Res Thick Depth
1 1533.0 1.5 1.5
2 220.8 5.5 7.0
3 925.6 15.1 22.1
4 355.5 33.3 55.4
5 1564.5 -.- -.-
Appar. Resistivity [ohmm]
10^4
10^3
10^2
10^1
10^0
10^1
10^2
10^3
Current Electrode Distance (AB/2) [m]

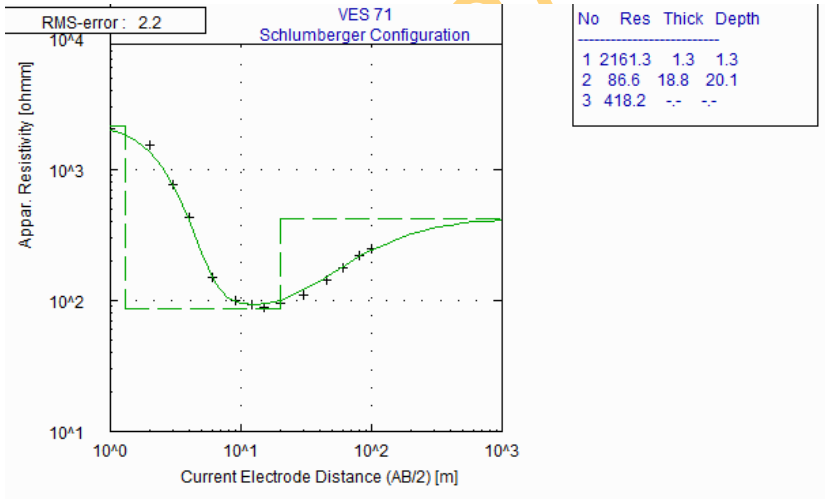
RMS-error : 2.2
VES 71
Schlumberger Configuration
No Res Thick Depth
1 2161.3 1.3 1.3
2 86.6 18.8 20.1
3 418.2 -.- -.-
Appar. Resistivity [ohmm]
10^4
10^3
10^2
10^1
10^0
10^1
10^2
10^3
Current Electrode Distance (AB/2) [m]

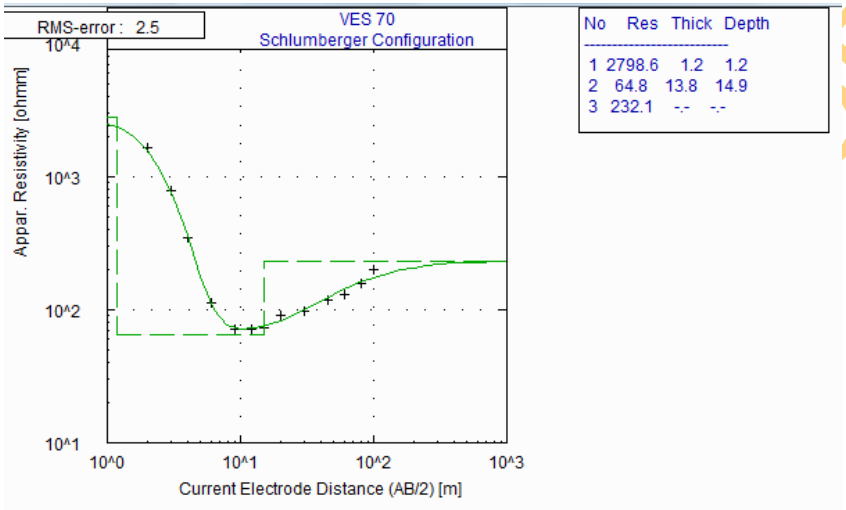
RMS-error : 2.5
VES 70
Schlumberger Configuration
No Res Thick Depth
1 2798.6 1.2 1.2
2 64.8 13.8 14.9
3 232.1 -.- -.-
Appar. Resistivity [ohmm]
10^4
10^3
10^2
10^1
10^0
10^1
10^2
10^3
Current Electrode Distance (AB/2) [m]

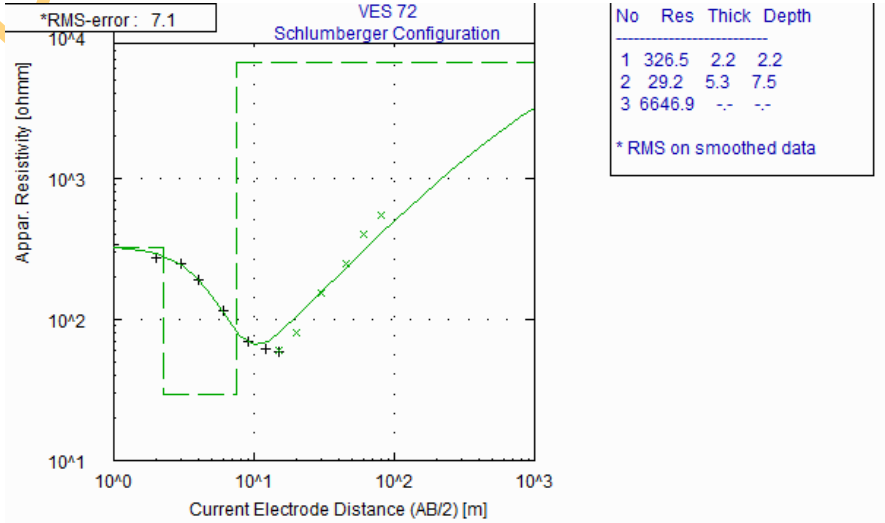
*RMS-error : 7.1
VES 72
Schlumberger Configuration
No Res Thick Depth
1 326.5 2.2 2.2
2 29.2 5.3 7.5
3 6646.9 -.- -.-
* RMS on smoothed data
Appar. Resistivity [ohmm]
10^4
10^3
10^2
10^1
10^0
10^1
10^2
10^3
Current Electrode Distance (AB/2) [m]

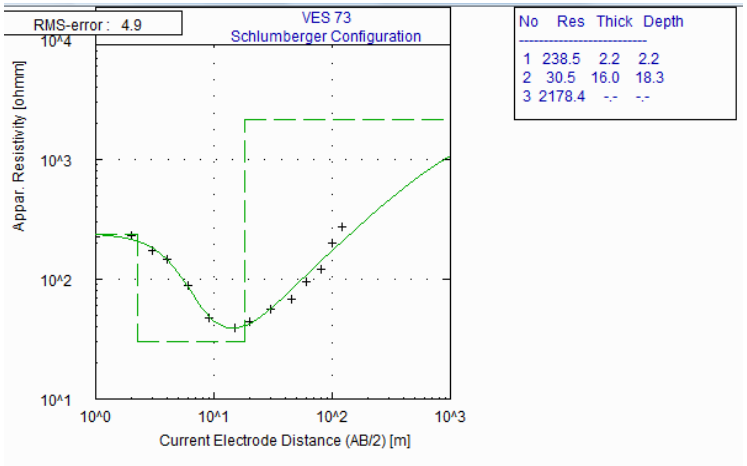

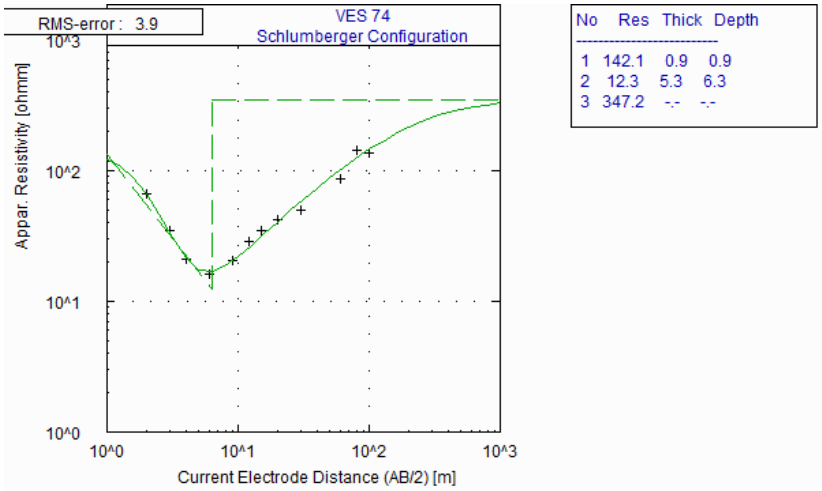

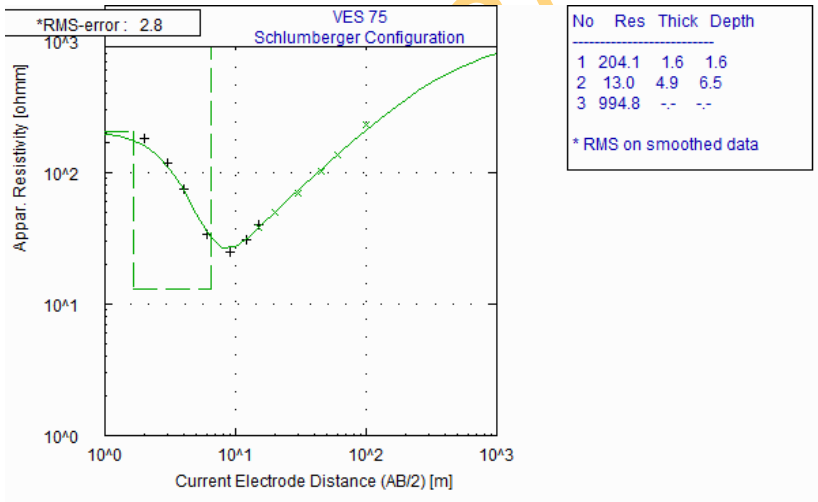

Fig 5.1: VES Curves of Abeokuta area (VES1-VES75)

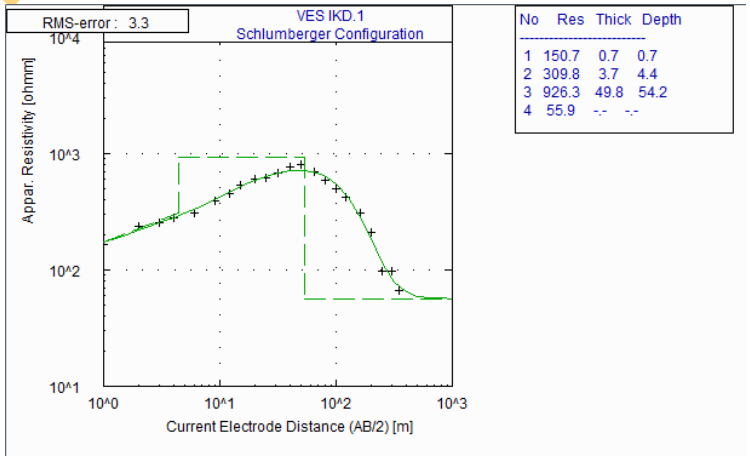

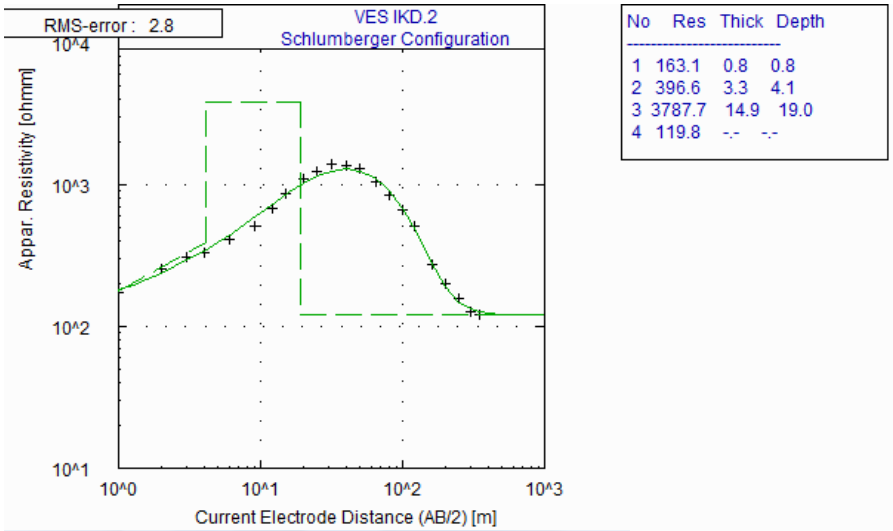

No	Res	Thick	Depth
1	163.1	0.8	0.8
2	396.6	3.3	4.1
3	3787.7	14.9	19.0
4	119.8	-.-	-.-

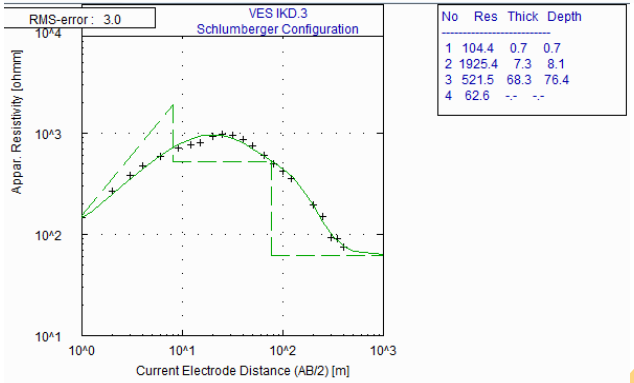

No	Res	Thick	Depth
1	104.4	0.7	0.7
2	1925.4	7.3	8.1
3	521.5	68.3	76.4
4	62.6	-.-	-.-

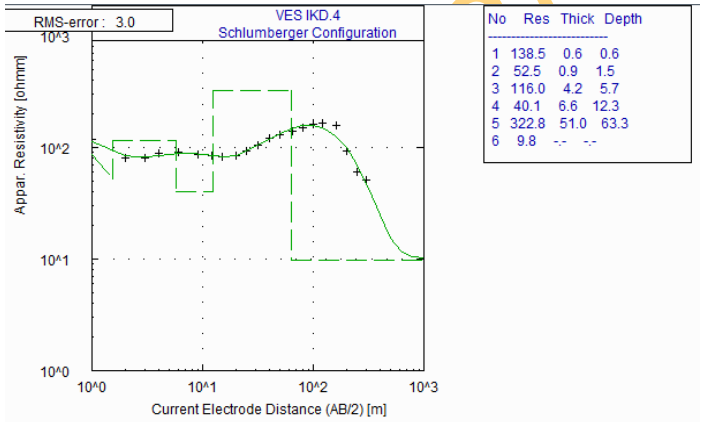

No	Res	Thick	Depth
1	138.5	0.6	0.6
2	52.5	0.9	1.5
3	116.0	4.2	5.7
4	40.1	6.6	12.3
5	322.8	51.0	63.3
6	9.8	-.-	-.-

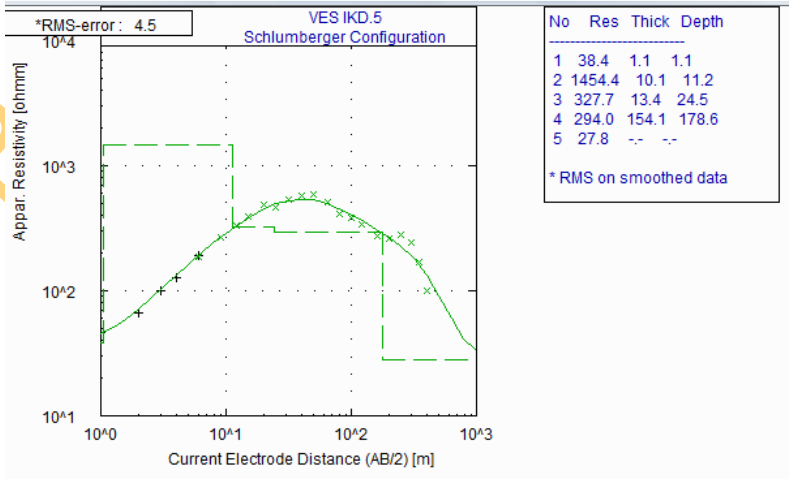

No	Res	Thick	Depth
1	38.4	1.1	1.1
2	1454.4	10.1	11.2
3	327.7	13.4	24.5
4	294.0	154.1	178.6
5	27.8	-.-	-.-

* RMS on smoothed data

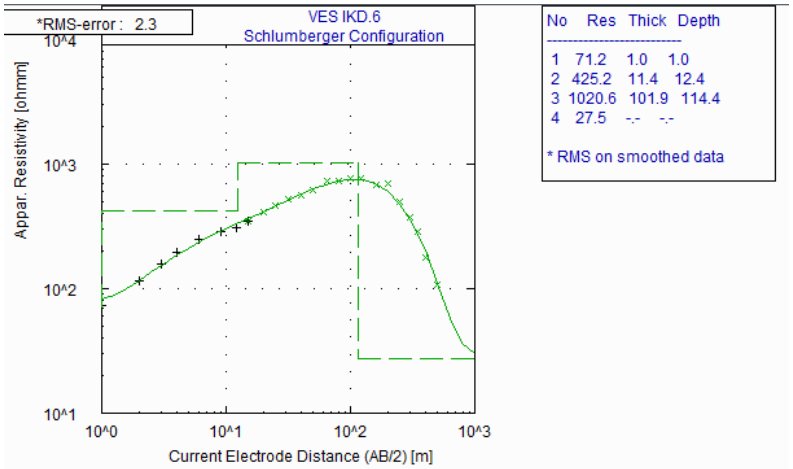

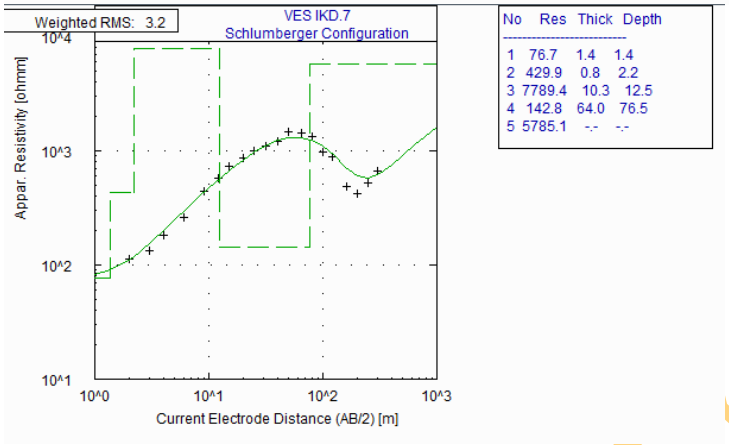

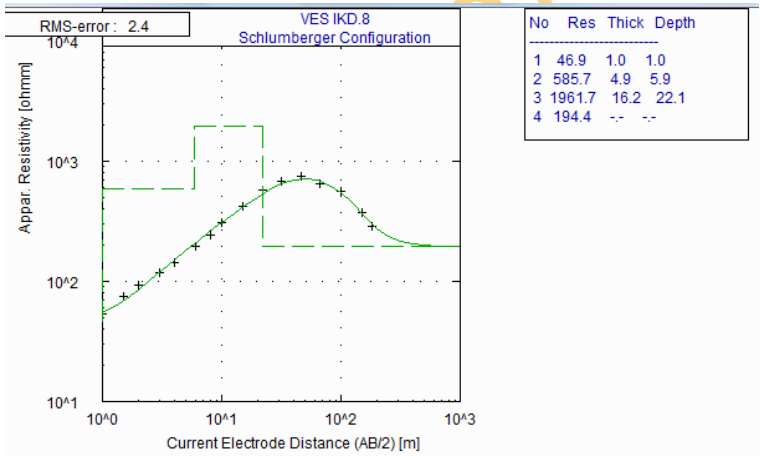

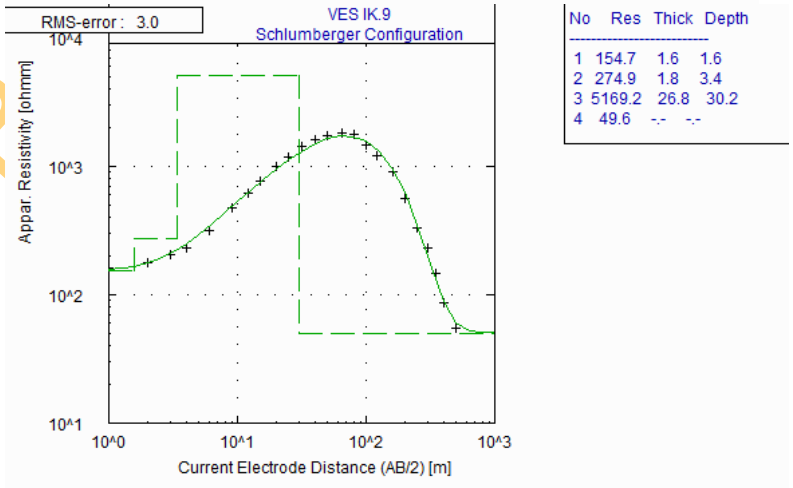

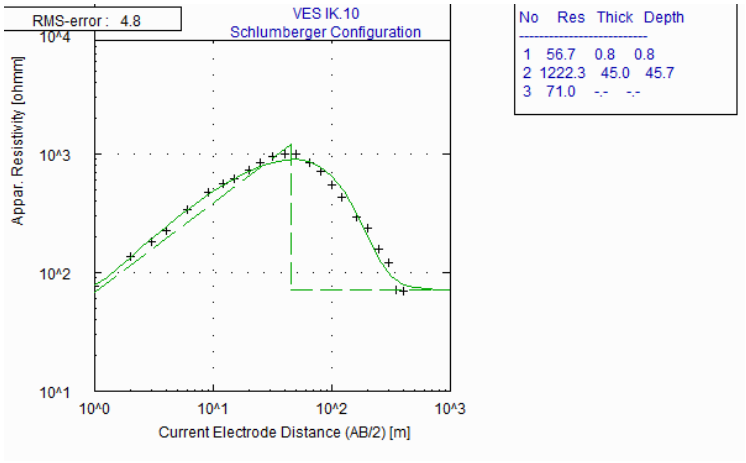

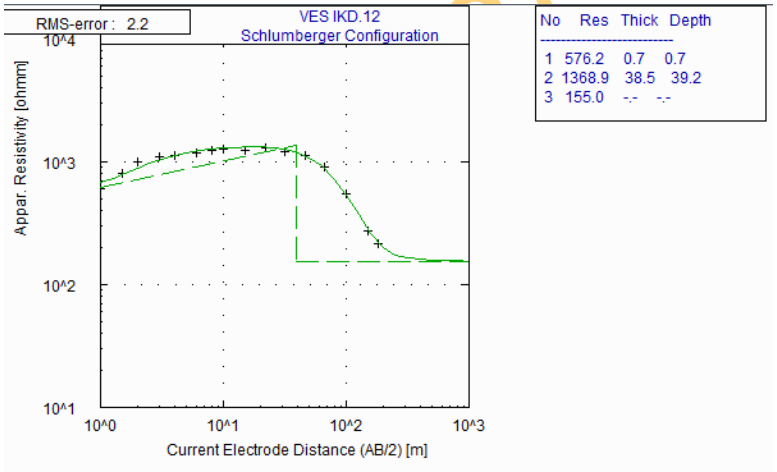

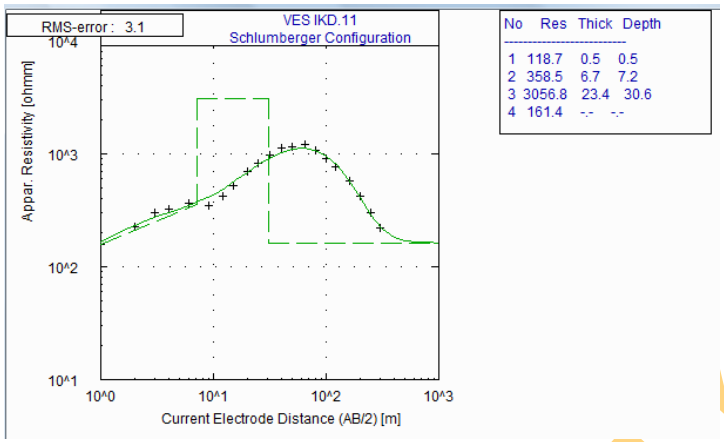

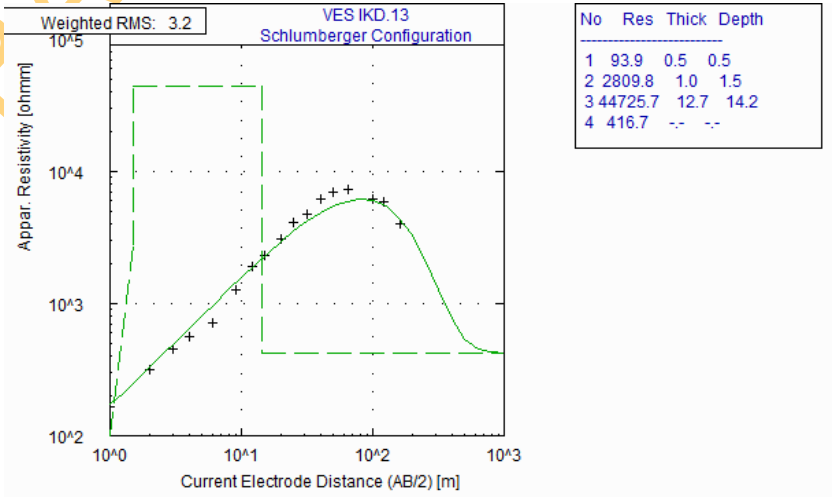

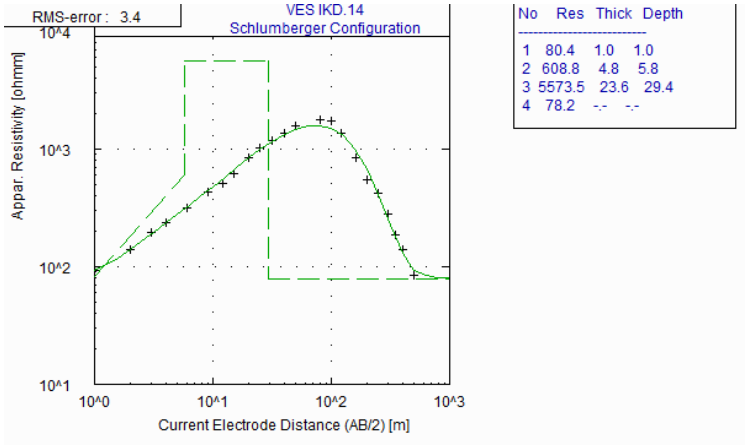

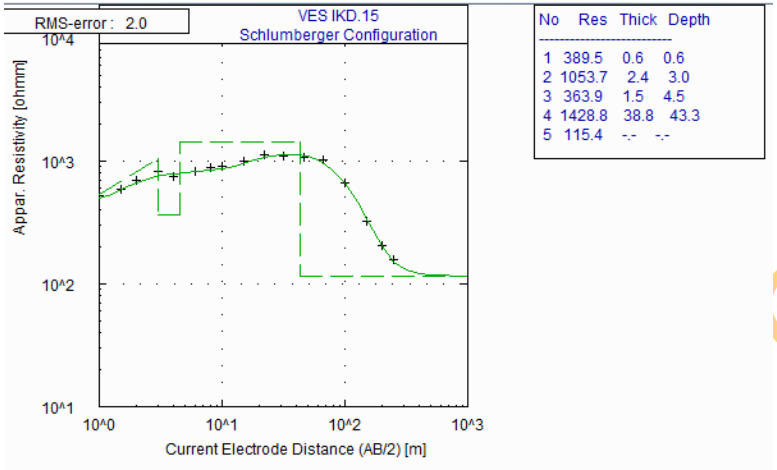

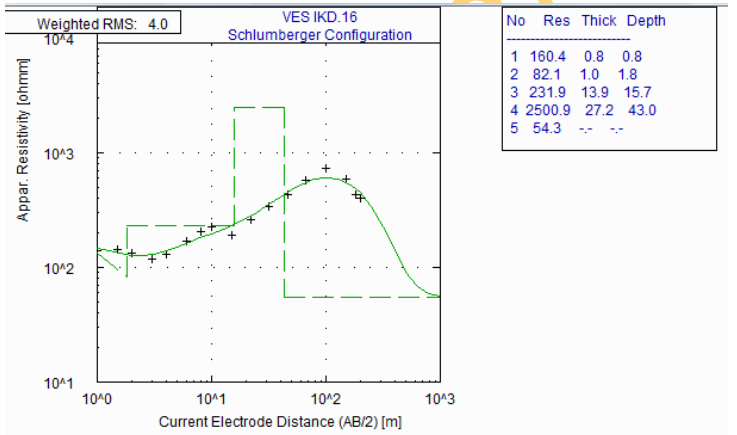

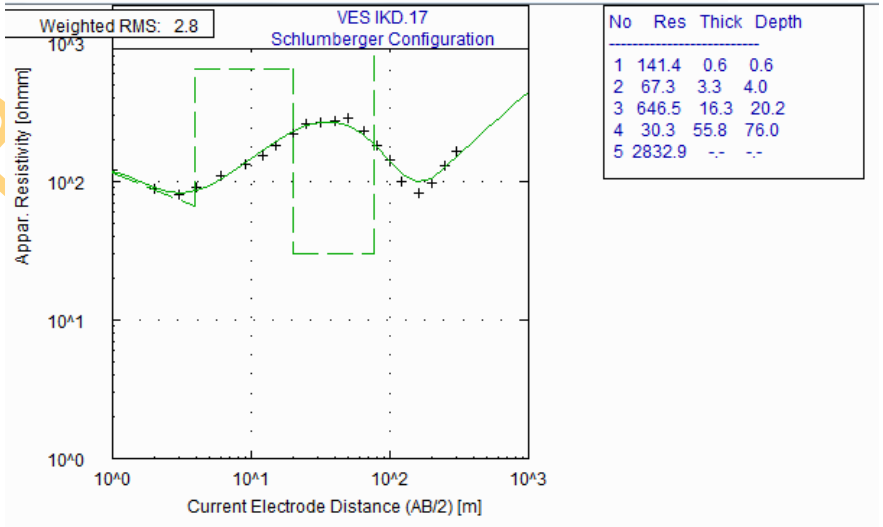

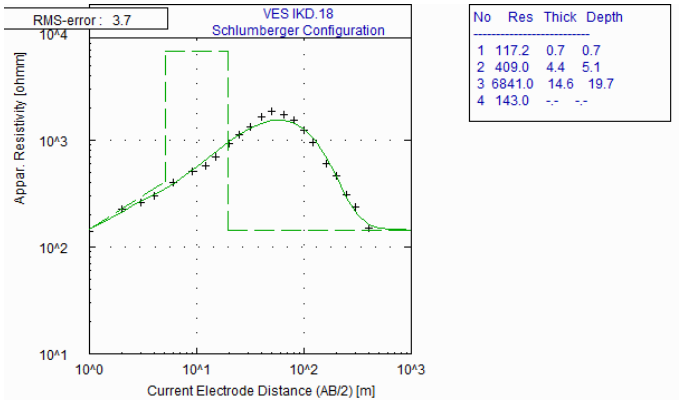

No	Res	Thick	Depth
1	117.2	0.7	0.7
2	409.0	4.4	5.1
3	6841.0	14.6	19.7
4	143.0	-.-	-.-

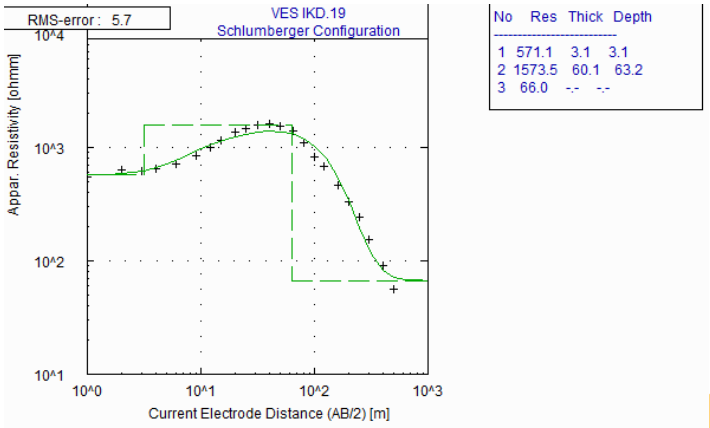

No	Res	Thick	Depth
1	571.1	3.1	3.1
2	1573.5	60.1	63.2
3	66.0	-.-	-.-

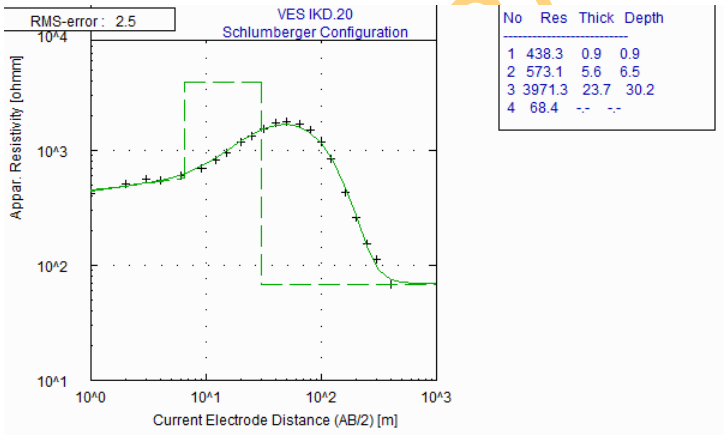

No	Res	Thick	Depth
1	438.3	0.9	0.9
2	573.1	5.6	6.5
3	3971.3	23.7	30.2
4	68.4	-.-	-.-

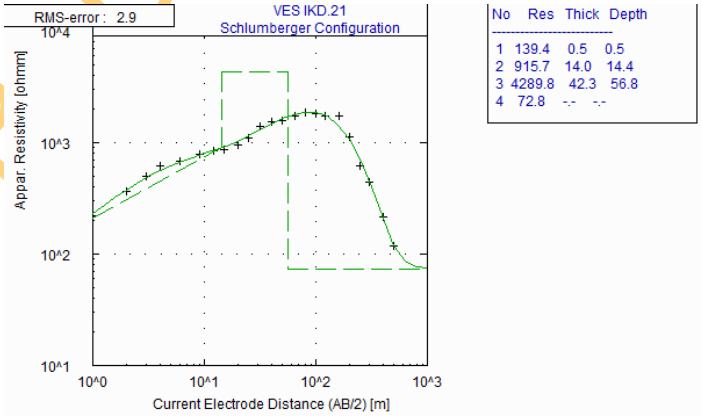

No	Res	Thick	Depth
1	139.4	0.5	0.5
2	915.7	14.0	14.4
3	4289.8	42.3	56.8
4	72.8	-.-	-.-

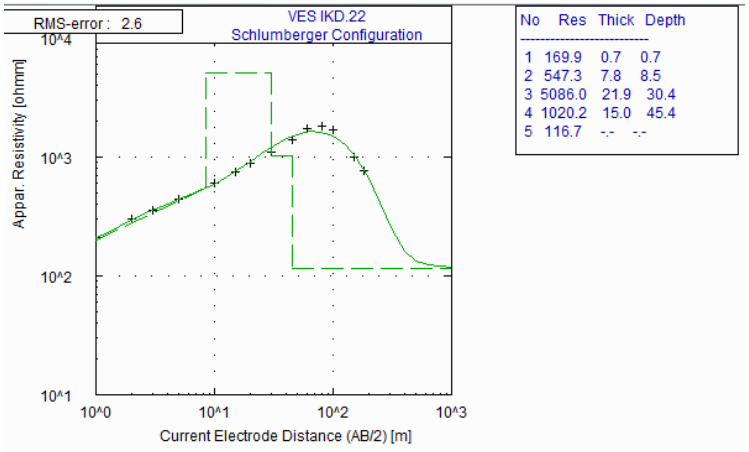

No	Res	Thick	Depth
1	169.9	0.7	0.7
2	547.3	7.8	8.5
3	5086.0	21.9	30.4
4	1020.2	15.0	45.4
5	116.7	-.-	-.-

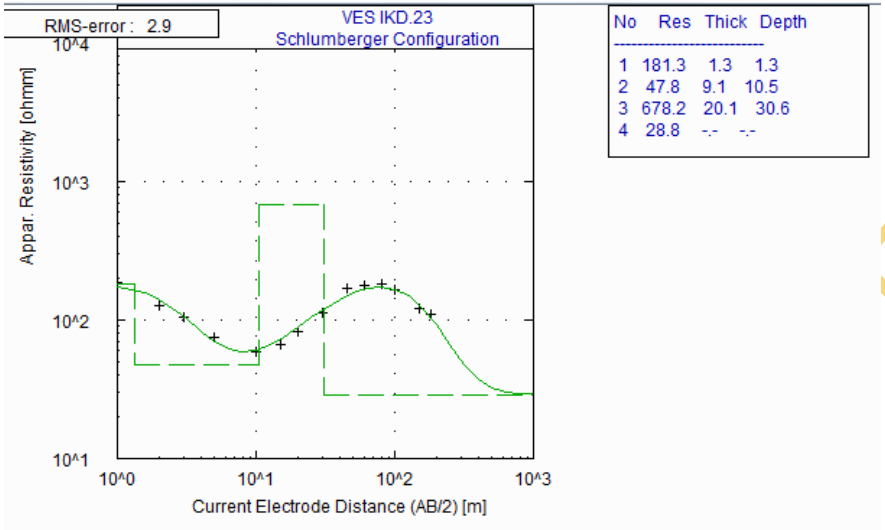

No	Res	Thick	Depth
1	181.3	1.3	1.3
2	47.8	9.1	10.5
3	678.2	20.1	30.6
4	28.8	-.-	-.-

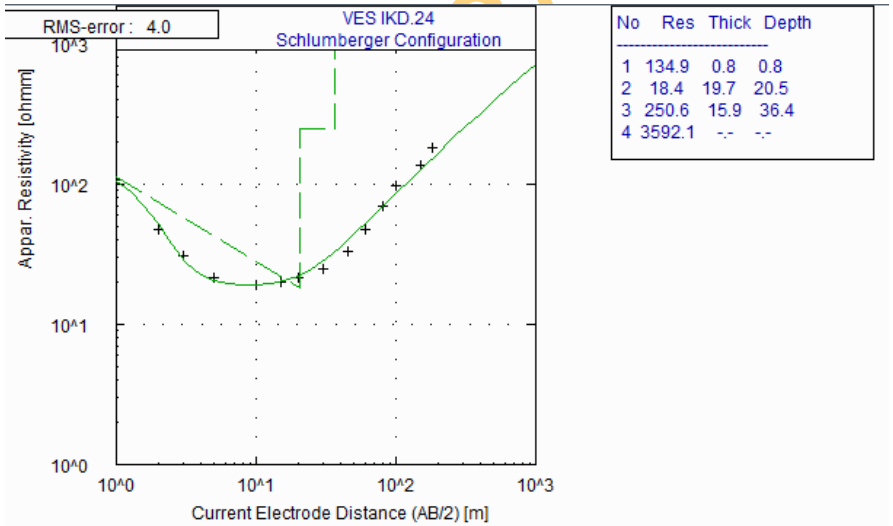

No	Res	Thick	Depth
1	134.9	0.8	0.8
2	18.4	19.7	20.5
3	250.6	15.9	36.4
4	3592.1	-.-	-.-

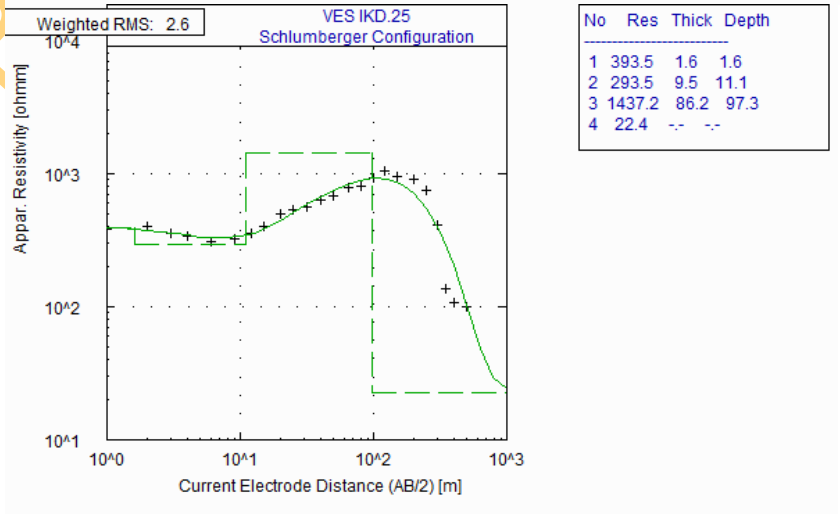

No	Res	Thick	Depth
1	393.5	1.6	1.6
2	293.5	9.5	11.1
3	1437.2	86.2	97.3
4	22.4	-.-	-.-

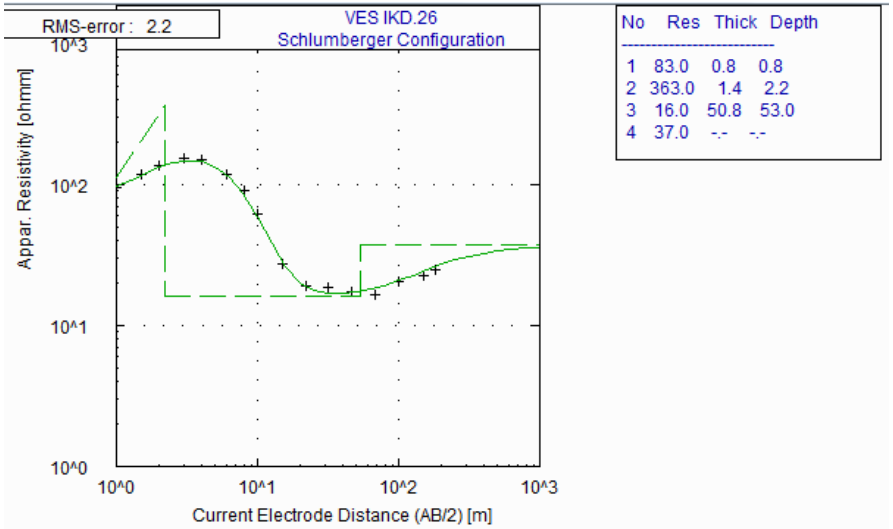
RMS-error : 2.2
VES IKD.26
Schlumberger Configuration
No Res Thick Depth
1 83.0 0.8 0.8
2 363.0 1.4 2.2
3 16.0 50.8 53.0
4 37.0 -.- -.-
Appar. Resistivity [ohmm]
Current Electrode Distance (AB/2) [m]

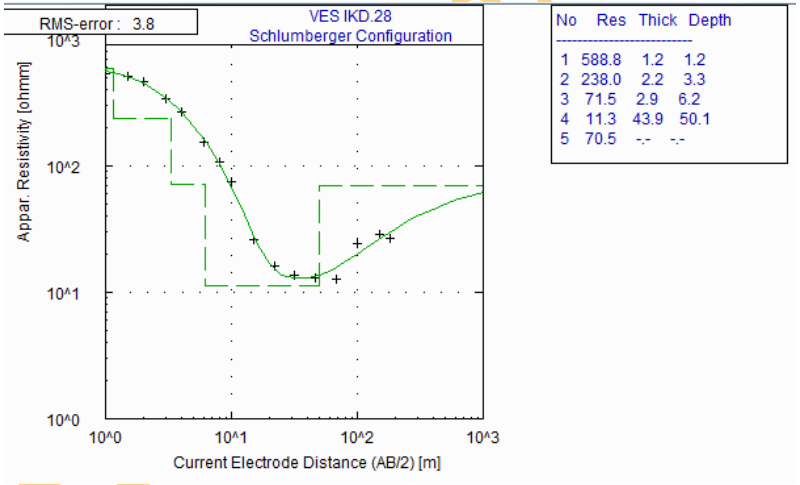
RMS-error : 3.8
VES IKD.28
Schlumberger Configuration
No Res Thick Depth
1 588.8 1.2 1.2
2 238.0 2.2 3.3
3 71.5 2.9 6.2
4 11.3 43.9 50.1
5 70.5 -.- -.-
Appar. Resistivity [ohmm]
Current Electrode Distance (AB/2) [m]

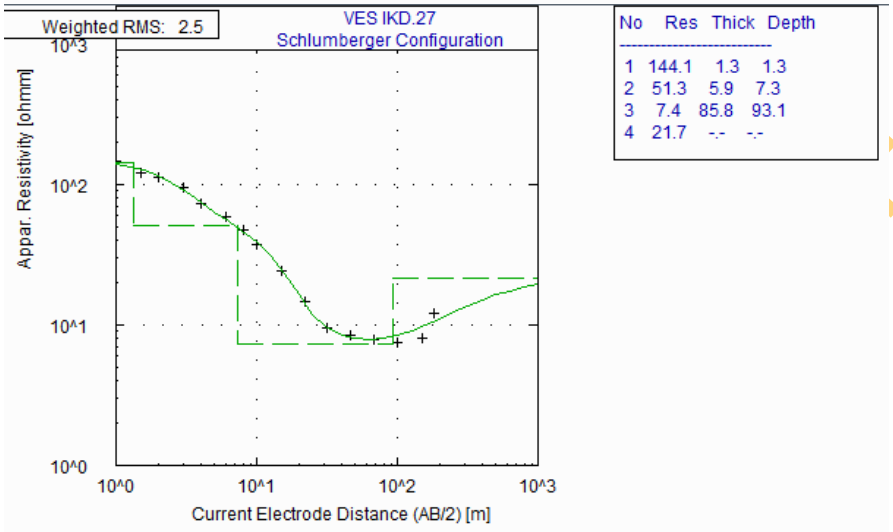
Weighted RMS: 2.5
VES IKD.27
Schlumberger Configuration
No Res Thick Depth
1 144.1 1.3 1.3
2 51.3 5.9 7.3
3 7.4 85.8 93.1
4 21.7 -.- -.-
Appar. Resistivity [ohmm]
Current Electrode Distance (AB/2) [m]

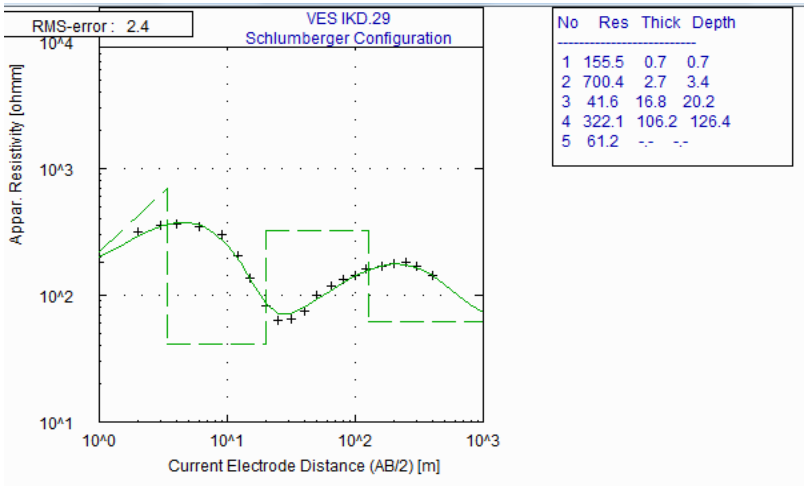
RMS-error : 2.4
VES IKD.29
Schlumberger Configuration
Appar. Resistivity [ohmm]
10^4
10^3
10^2
10^1
10^0
10^1
10^2
10^3
Current Electrode Distance (AB/2) [m]
No Res Thick Depth
1 155.5 0.7 0.7
2 700.4 2.7 3.4
3 41.6 16.8 20.2
4 322.1 106.2 126.4
5 61.2 -.- -.-

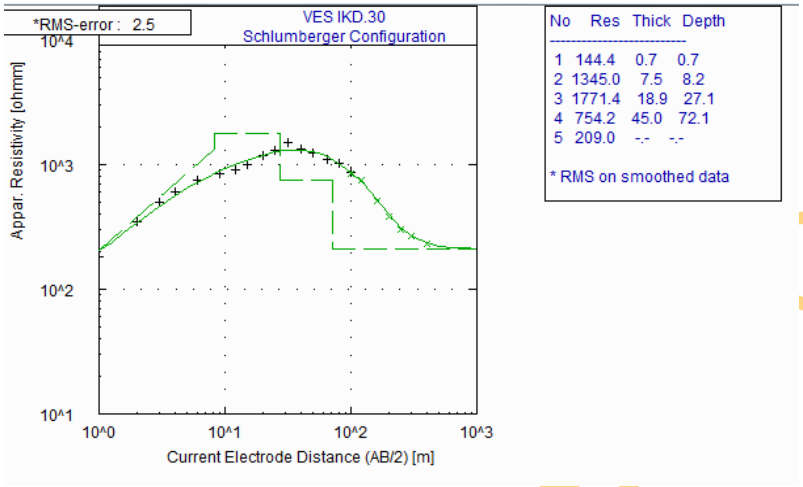
*RMS-error : 2.5
VES IKD.30
Schlumberger Configuration
Appar. Resistivity [ohmm]
10^4
10^3
10^2
10^1
10^0
10^1
10^2
10^3
Current Electrode Distance (AB/2) [m]
No Res Thick Depth
1 144.4 0.7 0.7
2 1345.0 7.5 8.2
3 1771.4 18.9 27.1
4 754.2 45.0 72.1
5 209.0 -.- -.-
* RMS on smoothed data

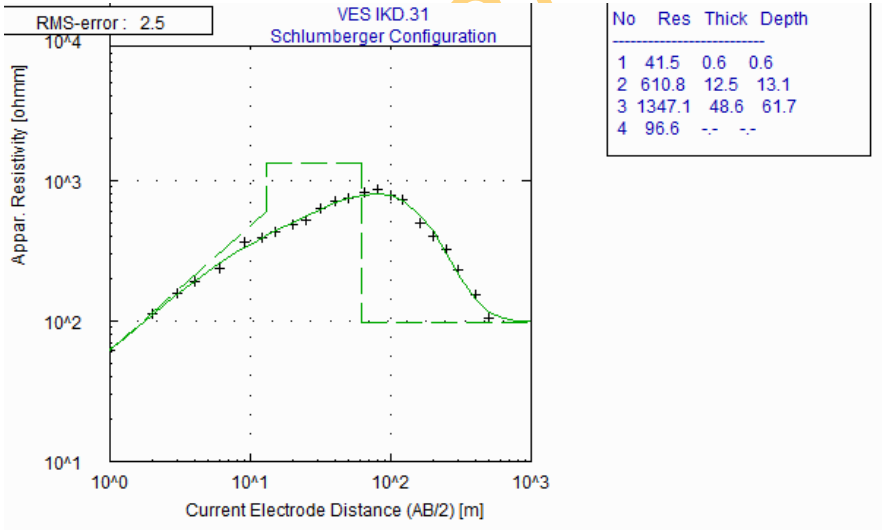
RMS-error : 2.5
VES IKD.31
Schlumberger Configuration
Appar. Resistivity [ohmm]
10^4
10^3
10^2
10^1
10^0
10^1
10^2
10^3
Current Electrode Distance (AB/2) [m]
No Res Thick Depth
1 41.5 0.6 0.6
2 610.8 12.5 13.1
3 1347.1 48.6 61.7
4 96.6 -.- -.-

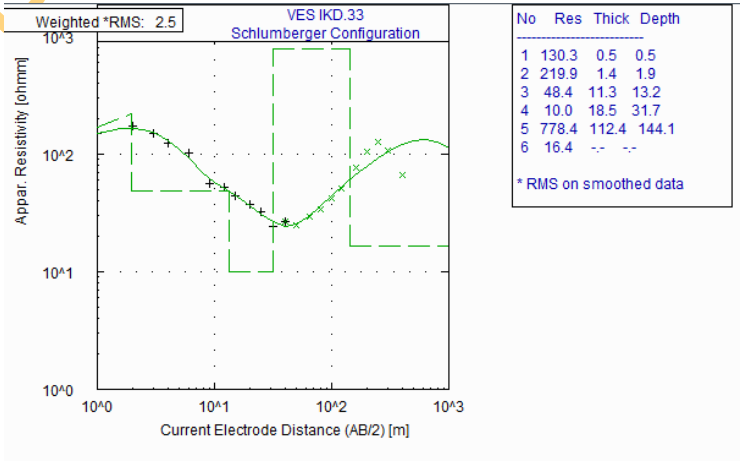
Weighted *RMS: 2.5
VES IKD.33
Schlumberger Configuration
Appar. Resistivity [ohmm]
10^3
10^2
10^1
10^0
10^1
10^2
10^3
Current Electrode Distance (AB/2) [m]
No Res Thick Depth
1 130.3 0.5 0.5
2 219.9 1.4 1.9
3 48.4 11.3 13.2
4 10.0 18.5 31.7
5 778.4 112.4 144.1
6 16.4 -.- -.-
* RMS on smoothed data

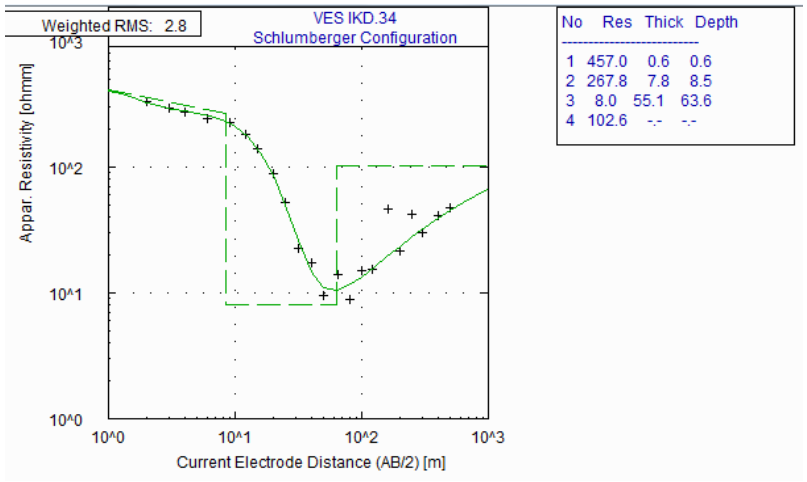

No	Res	Thick	Depth
1	457.0	0.6	0.6
2	267.8	7.8	8.5
3	8.0	55.1	63.6
4	102.6	-.-	-.-

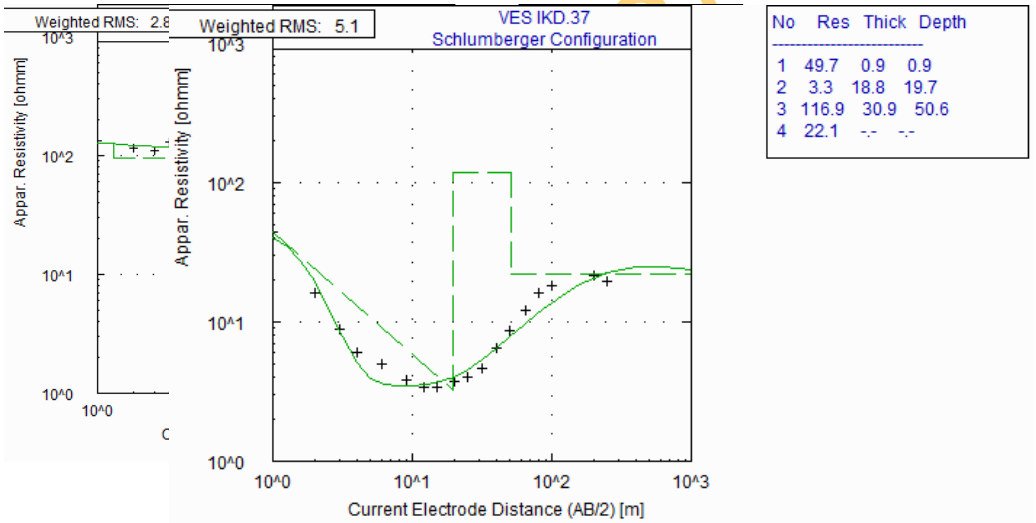

No	Res	Thick	Depth
1	49.7	0.9	0.9
2	3.3	18.8	19.7
3	116.9	30.9	50.6
4	22.1	-.-	-.-

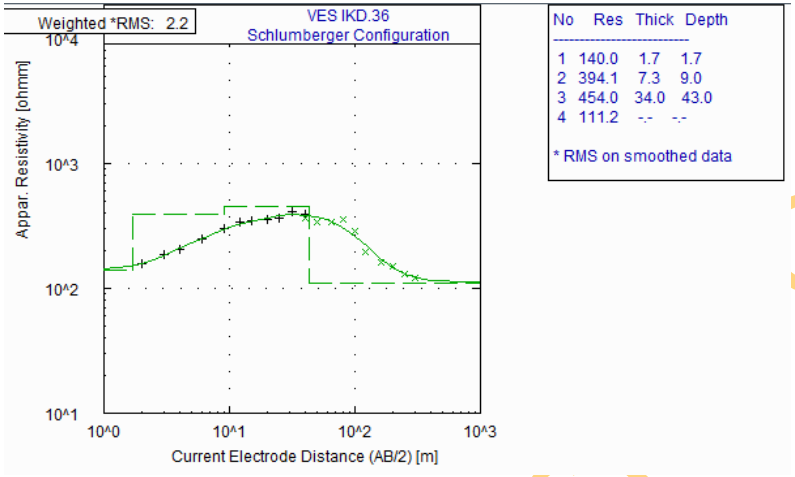

No	Res	Thick	Depth
1	140.0	1.7	1.7
2	394.1	7.3	9.0
3	454.0	34.0	43.0
4	111.2	-.-	-.-

* RMS on smoothed data

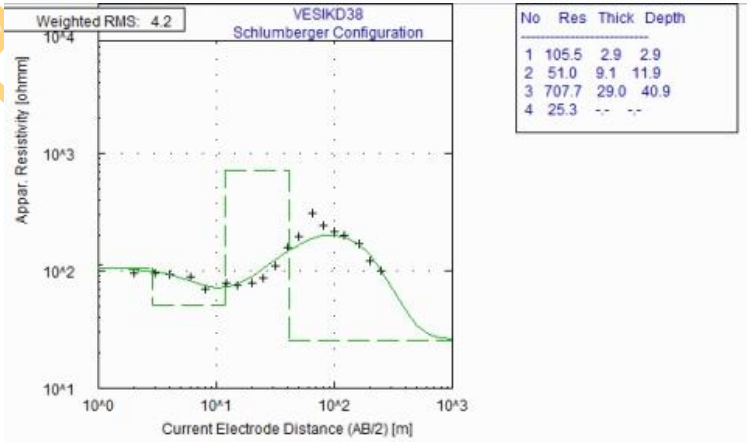

No	Res	Thick	Depth
1	105.5	2.9	2.9
2	51.0	9.1	11.9
3	707.7	29.0	40.9
4	25.3	-.-	-.-

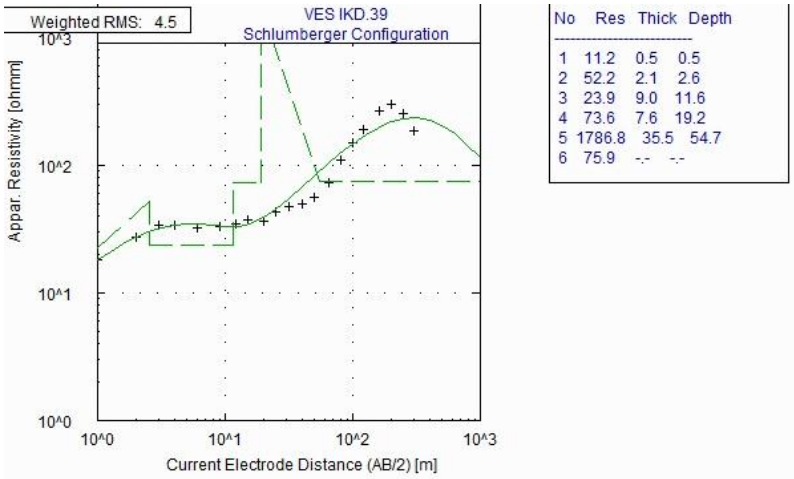

No	Res	Thick	Depth
1	11.2	0.5	0.5
2	52.2	2.1	2.6
3	23.9	9.0	11.6
4	73.6	7.6	19.2
5	1786.8	35.5	54.7
6	75.9	-.-	-.-

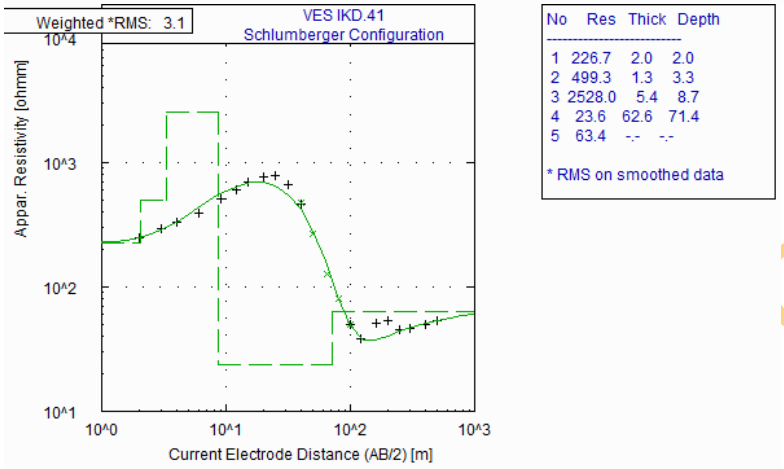

No	Res	Thick	Depth
1	226.7	2.0	2.0
2	499.3	1.3	3.3
3	2528.0	5.4	8.7
4	23.6	62.6	71.4
5	63.4	-.-	-.-

* RMS on smoothed data

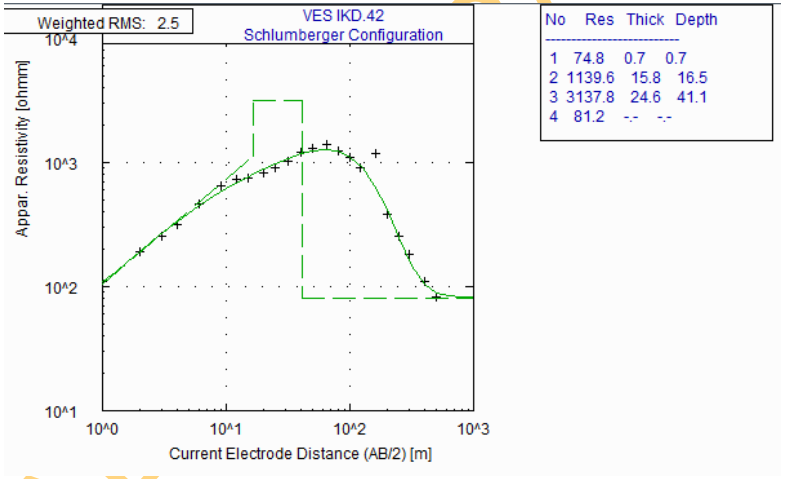

No	Res	Thick	Depth
1	74.8	0.7	0.7
2	1139.6	15.8	16.5
3	3137.8	24.6	41.1
4	81.2	-.-	-.-

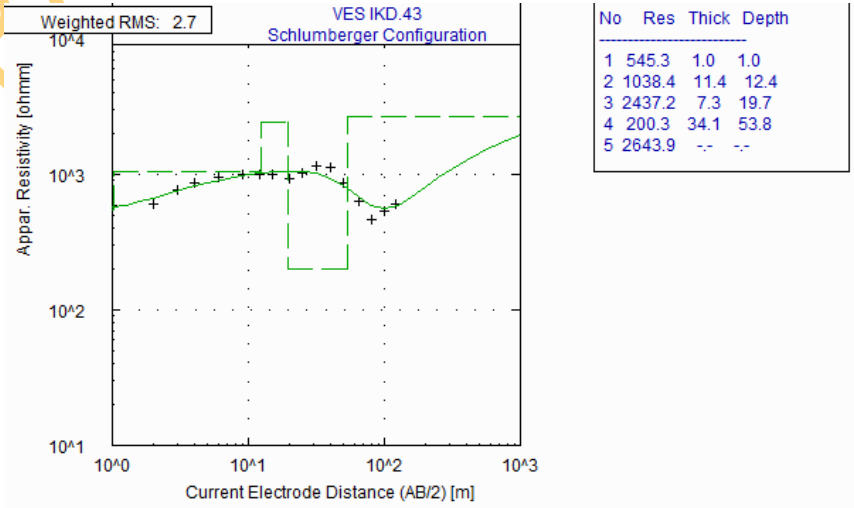

No	Res	Thick	Depth
1	545.3	1.0	1.0
2	1038.4	11.4	12.4
3	2437.2	7.3	19.7
4	200.3	34.1	53.8
5	2643.9	-.-	-.-

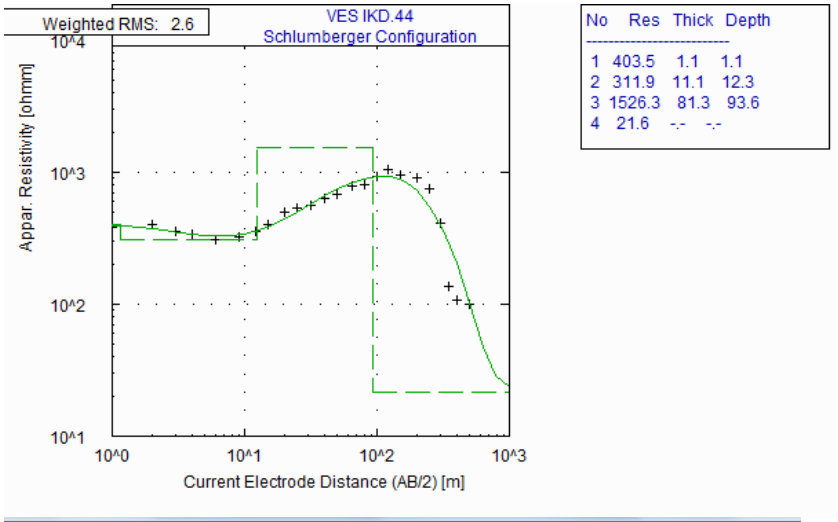

No	Res	Thick	Depth
1	403.5	1.1	1.1
2	311.9	11.1	12.3
3	1526.3	81.3	93.6
4	21.6	-.-	-.-

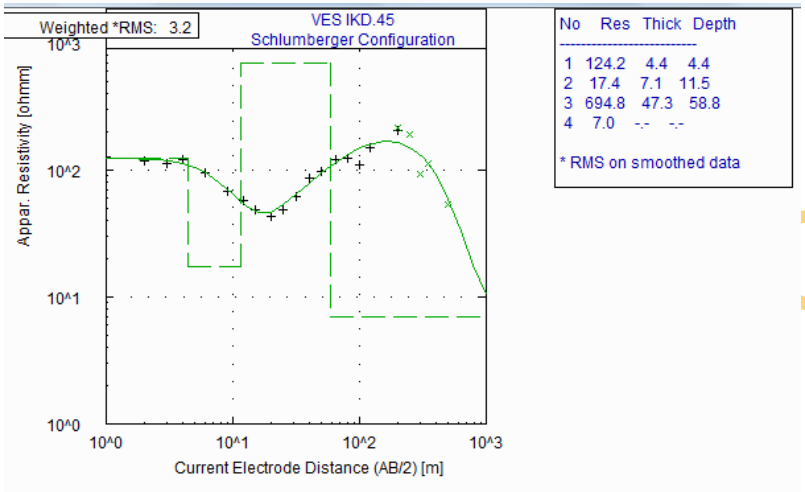

No	Res	Thick	Depth
1	124.2	4.4	4.4
2	17.4	7.1	11.5
3	694.8	47.3	58.8
4	7.0	-.-	-.-

* RMS on smoothed data

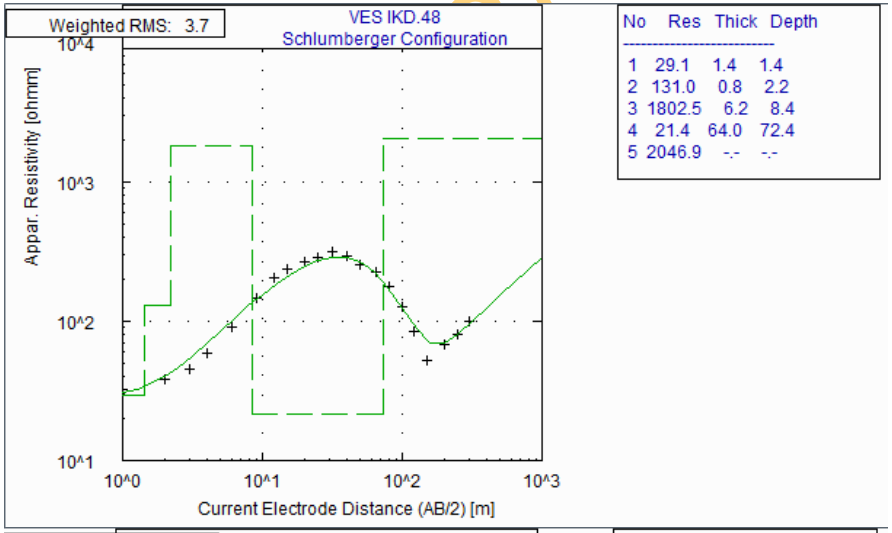

No	Res	Thick	Depth
1	29.1	1.4	1.4
2	131.0	0.8	2.2
3	1802.5	6.2	8.4
4	21.4	64.0	72.4
5	2046.9	-.-	-.-

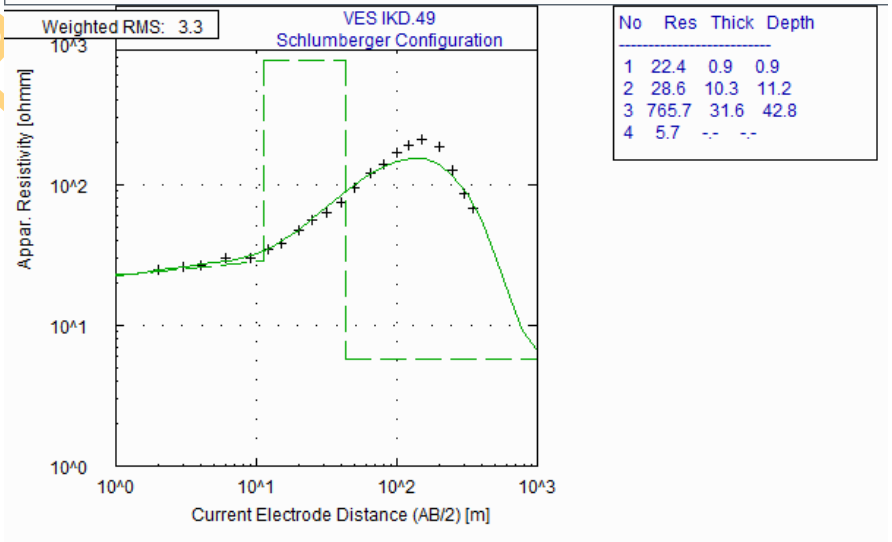

No	Res	Thick	Depth
1	22.4	0.9	0.9
2	28.6	10.3	11.2
3	765.7	31.6	42.8
4	5.7	-.-	-.-

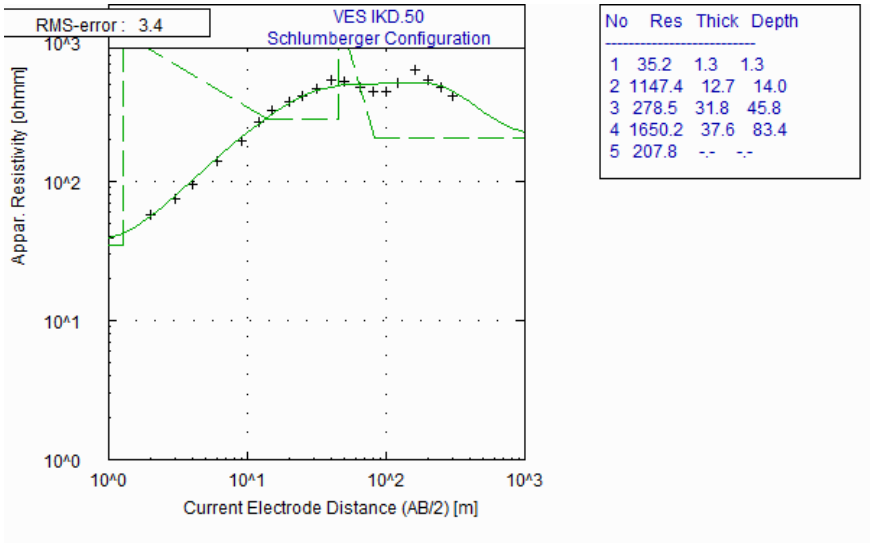

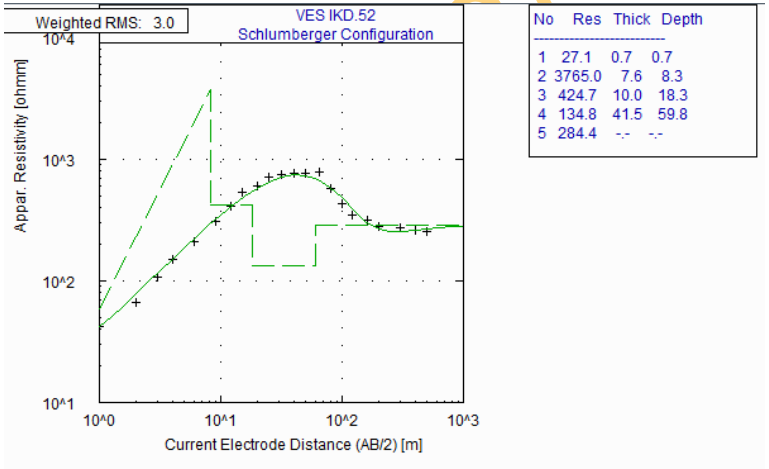

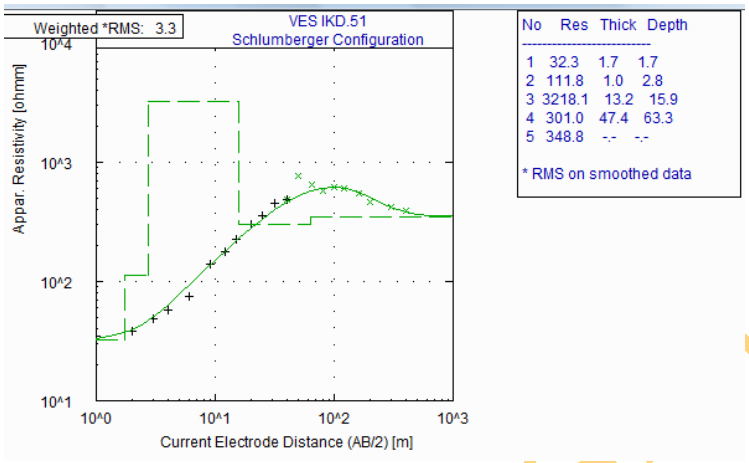

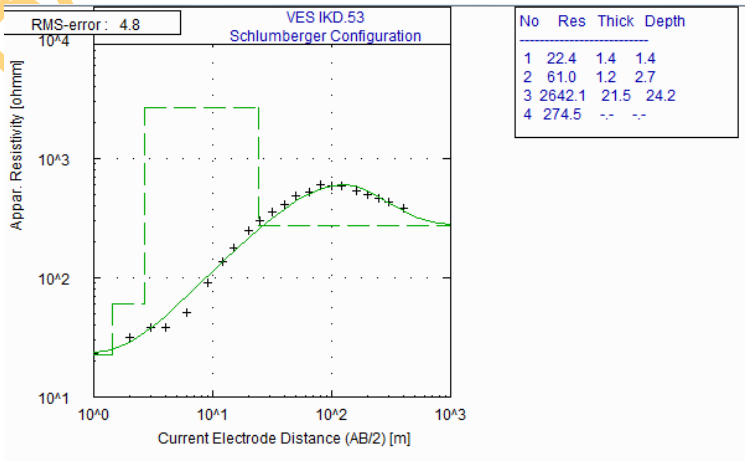

Fig 5.2:VES Curves of Ikorodu area (VES IKD1- VES IKD53)

APPENDIX IV

HYDROCHEMICAL MAPS

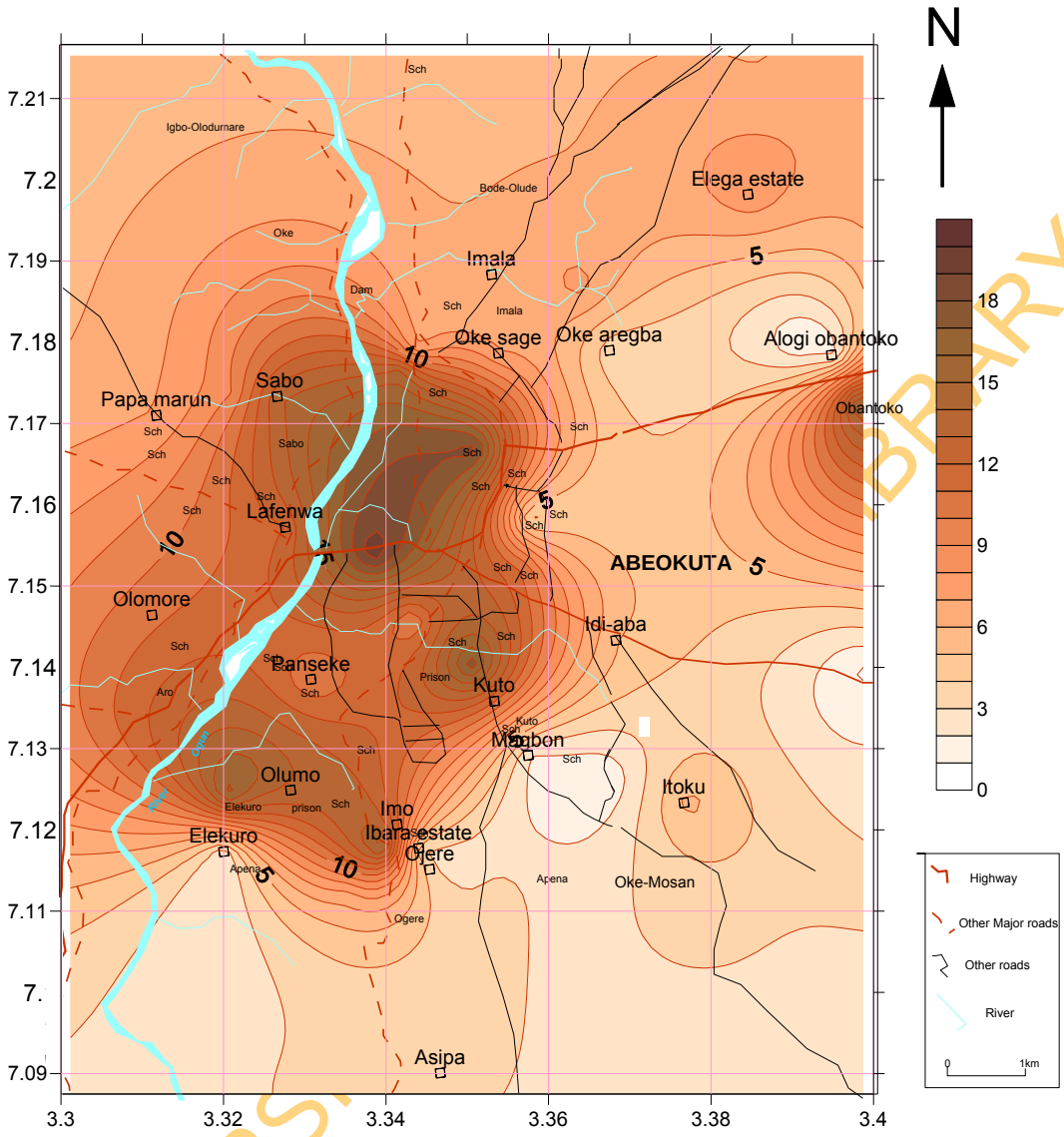

Fig 5.3: Hydrochemical map of Magnesium in groundwater in Abeokuta

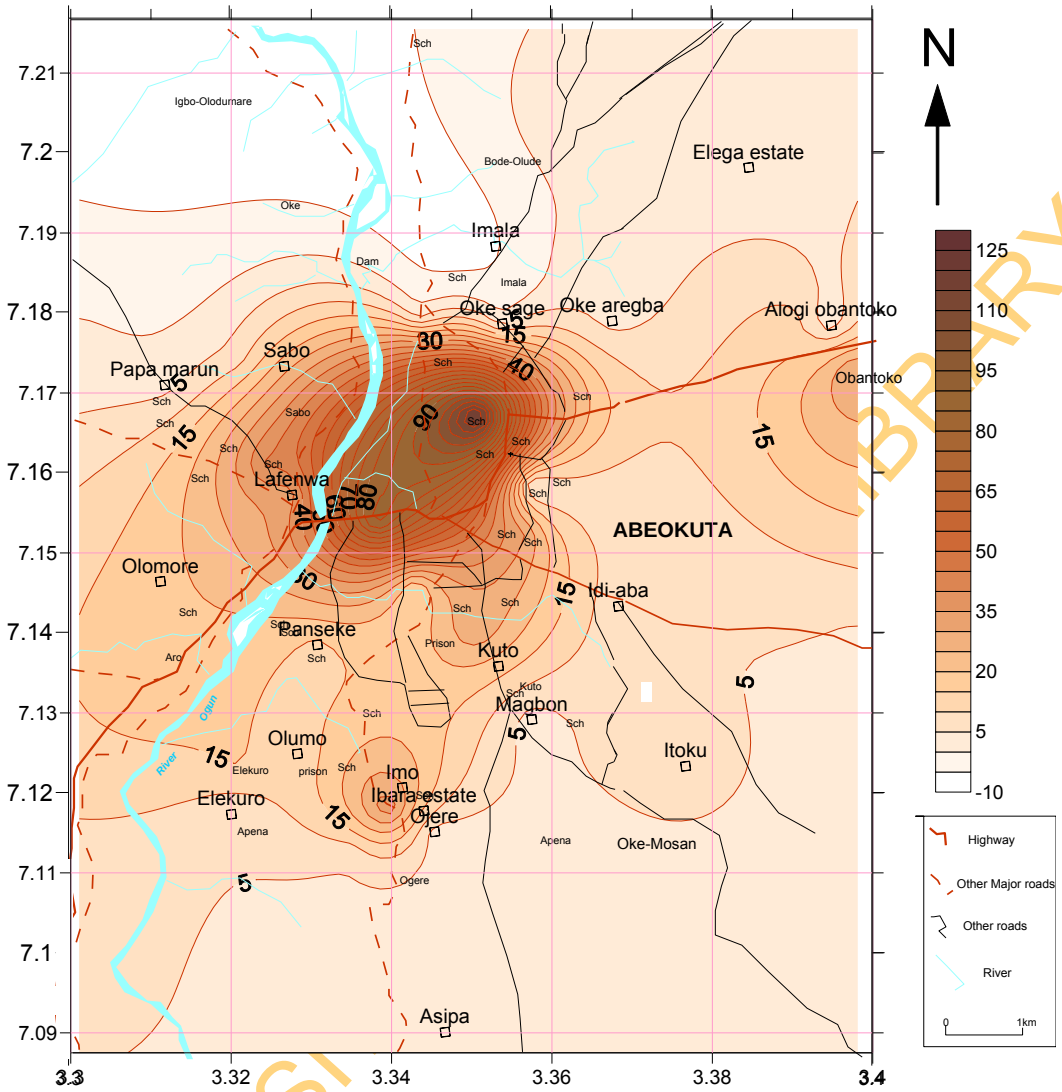

Fig.5.4: Isocone of Potassium in in groundwater in Abeokuta

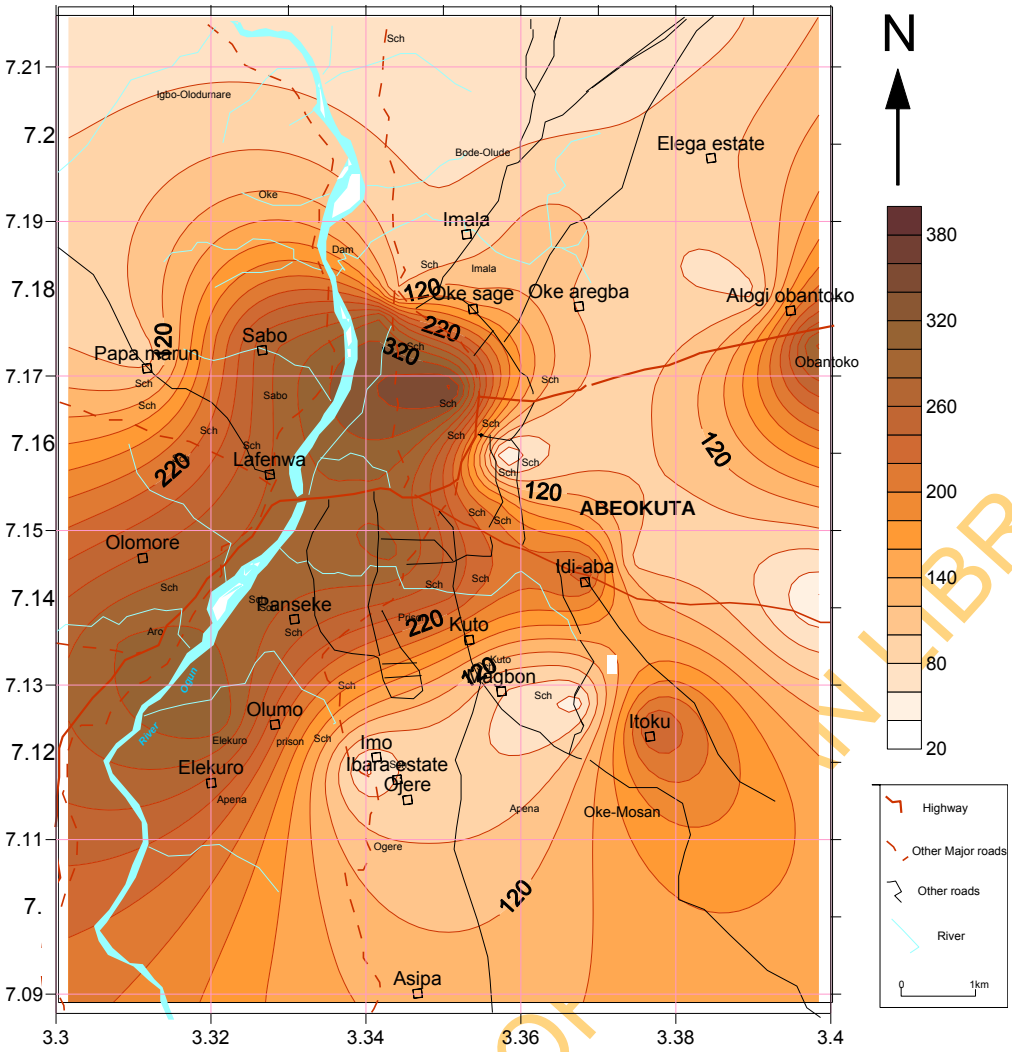

Fig 5.5: Hydrochemical map of bicarbonate in in groundwater in Abeokuta

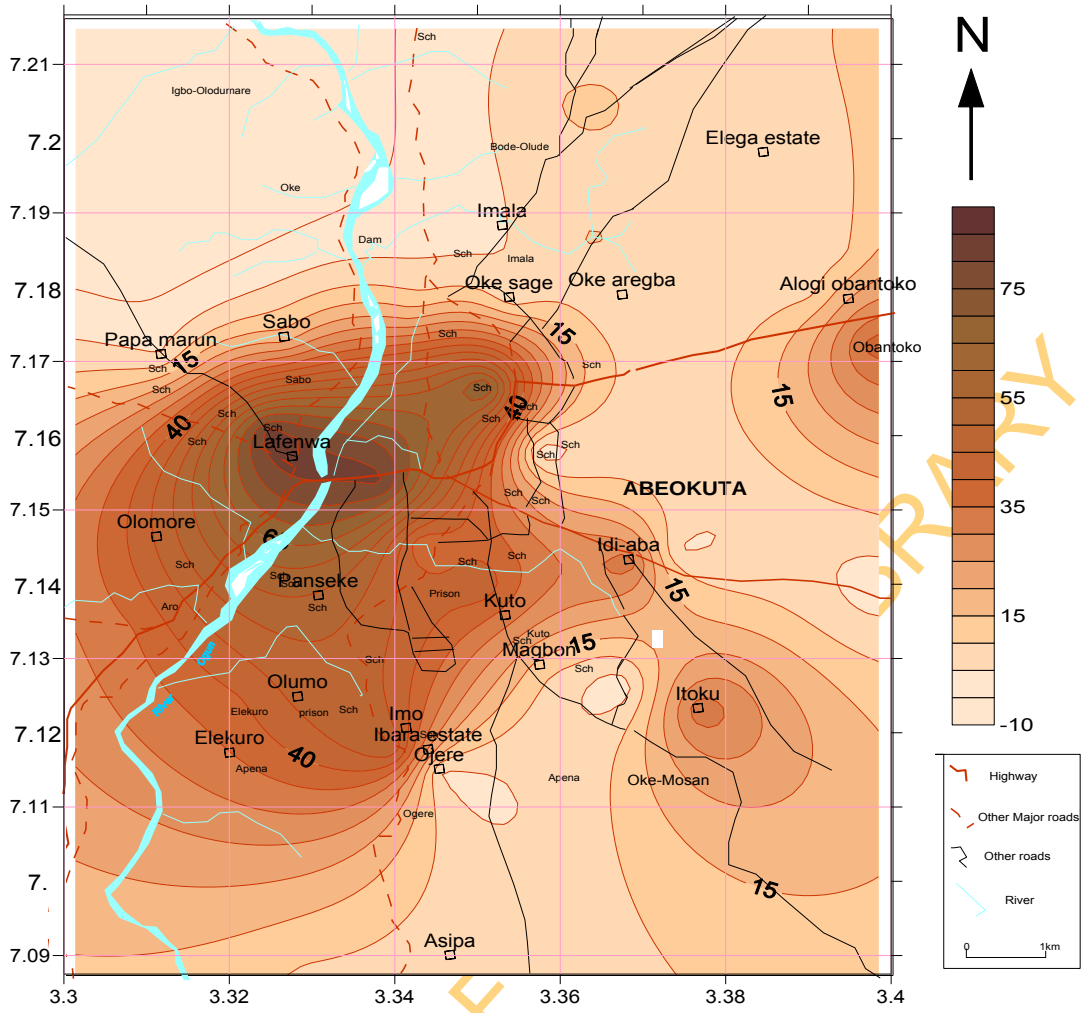

Fig 5.6: Hydrochemical map of Sulphate in in groundwater in Abeokuta

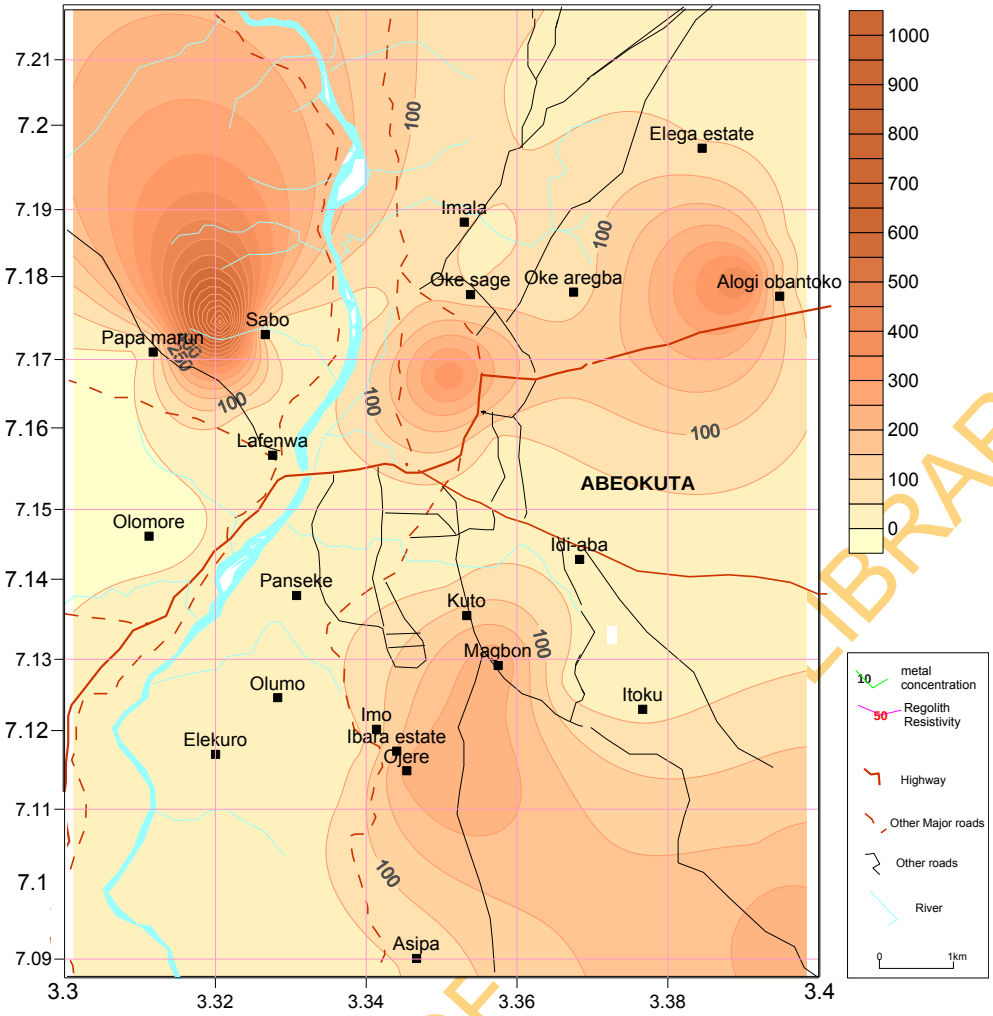

Fig 5.7: Hydrochemical map of Zinc (ug/l) in groundwater in Abeokuta

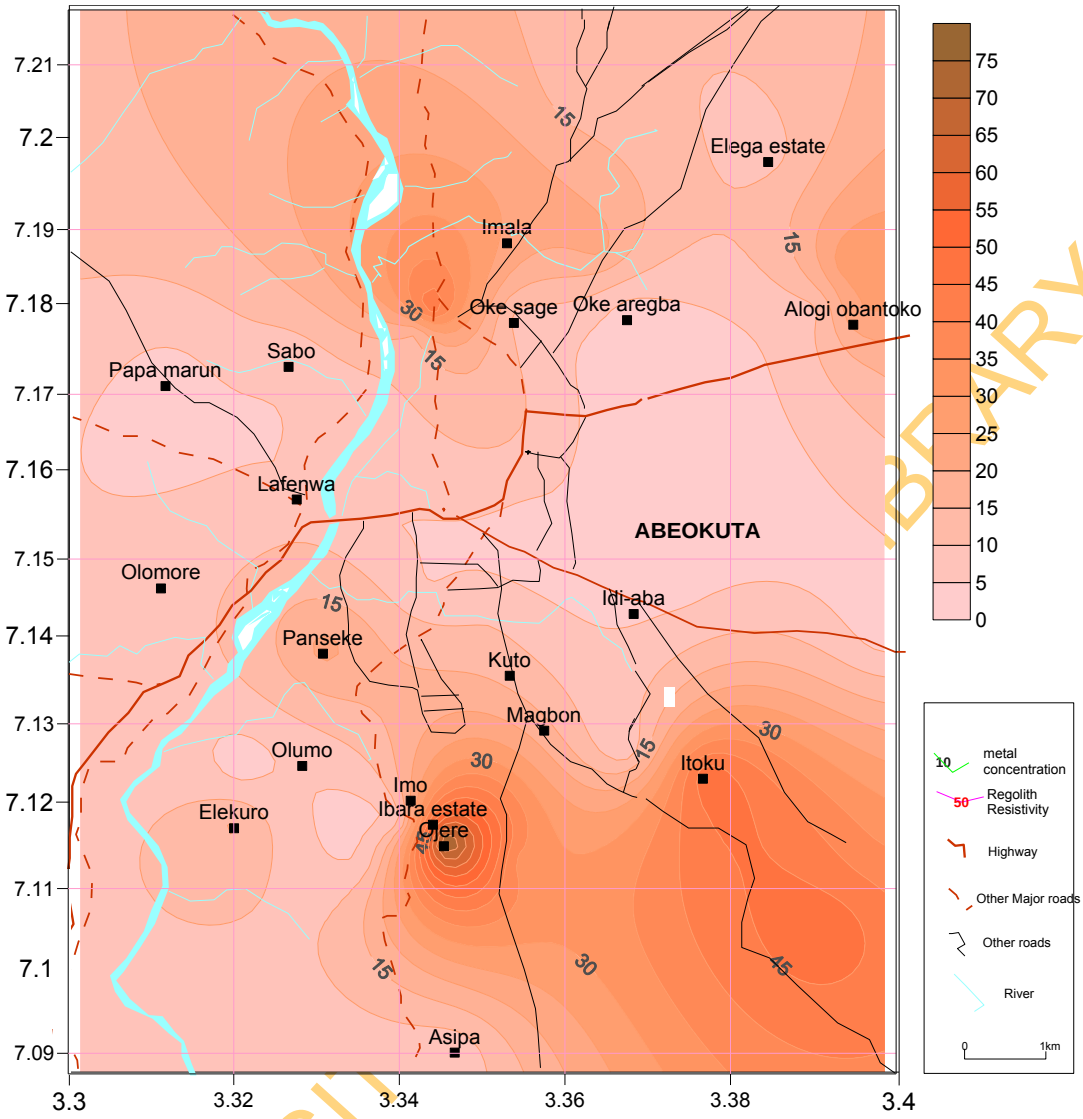

Fig 5.8: Hydrochemical map of Copper (ug/l) in groundwater in Abeokuta .

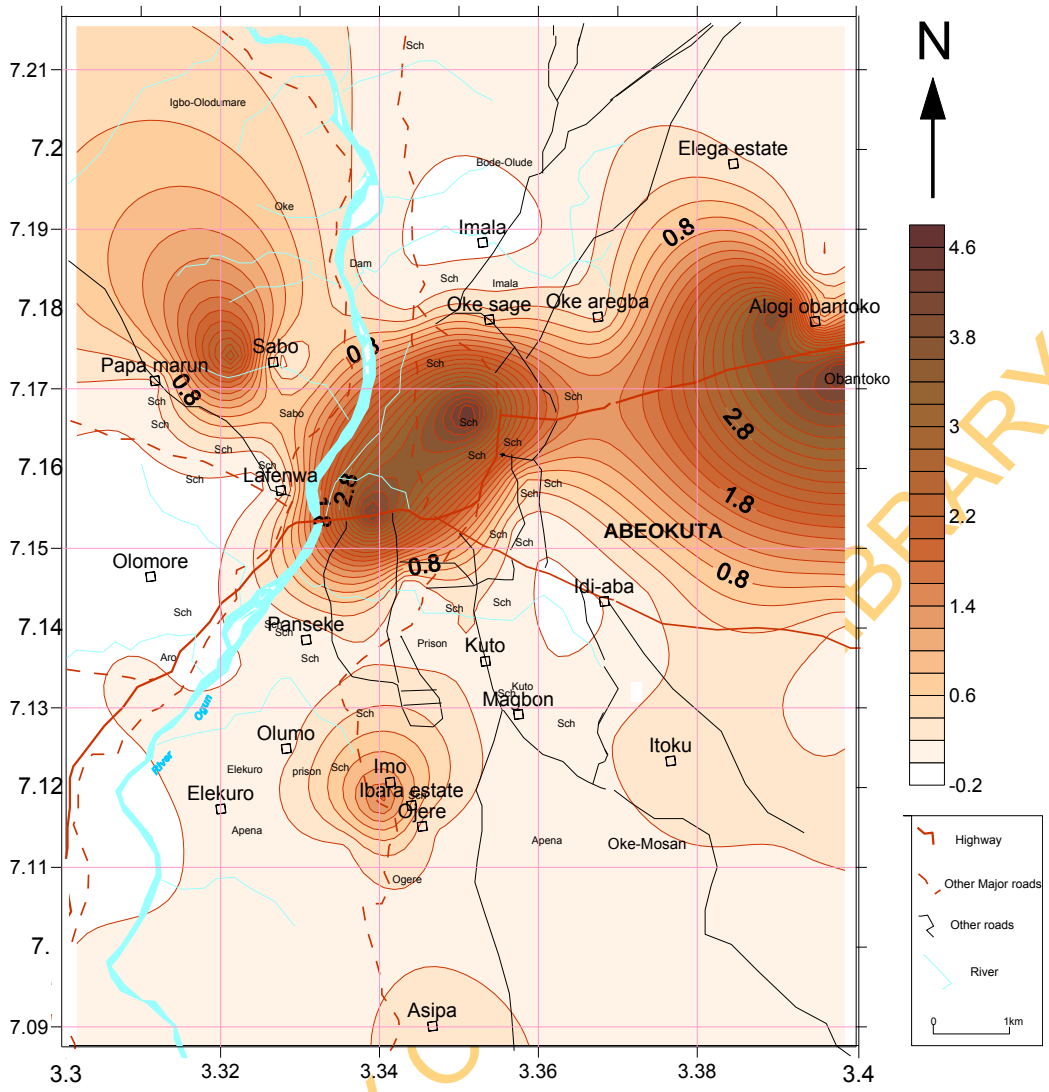

Fig.5.9: Hydrochemical map of Fe (mg/l) in groundwater in Abeokuta.

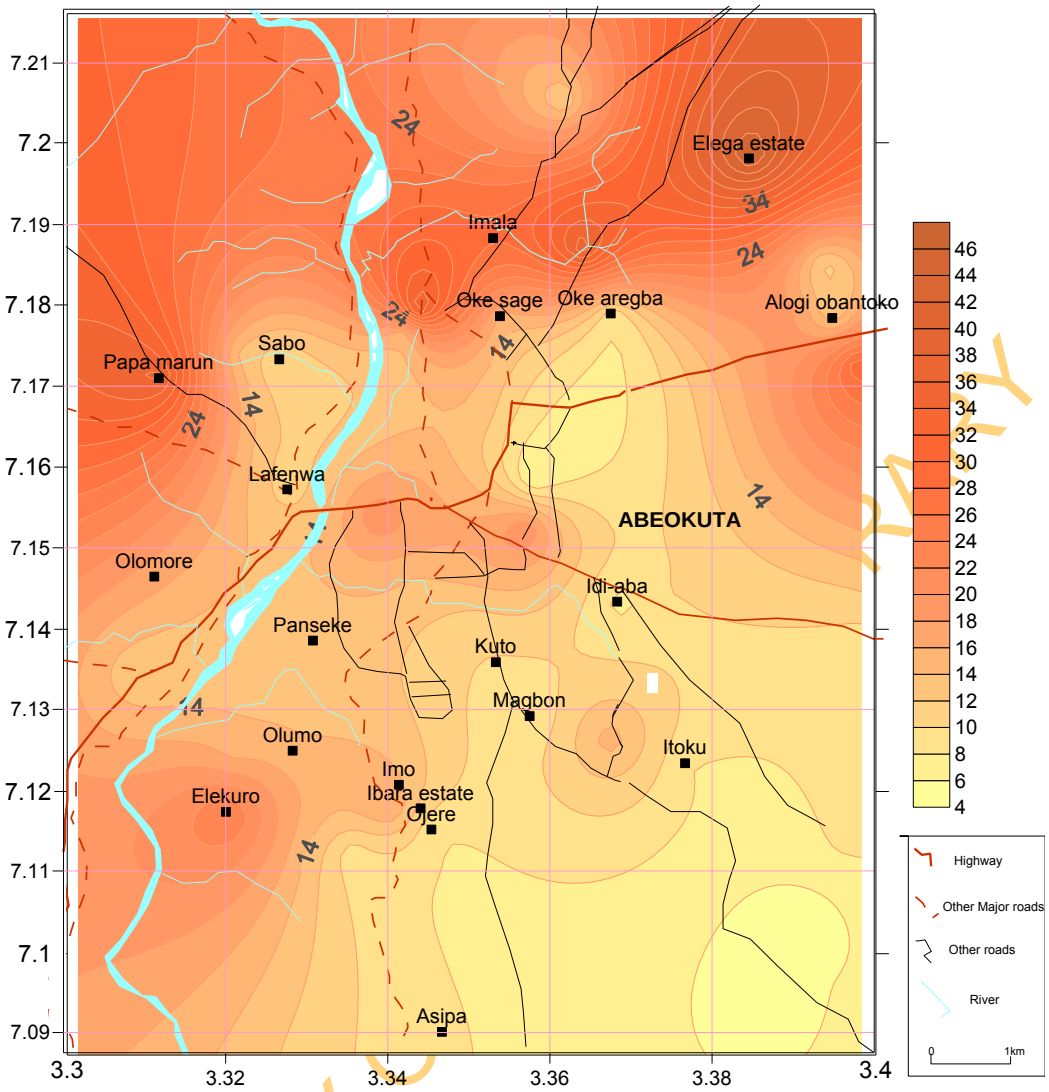

Fig 5.10: Hydrochemical map of Si (mg/l) in groundwater in Abeokuta.

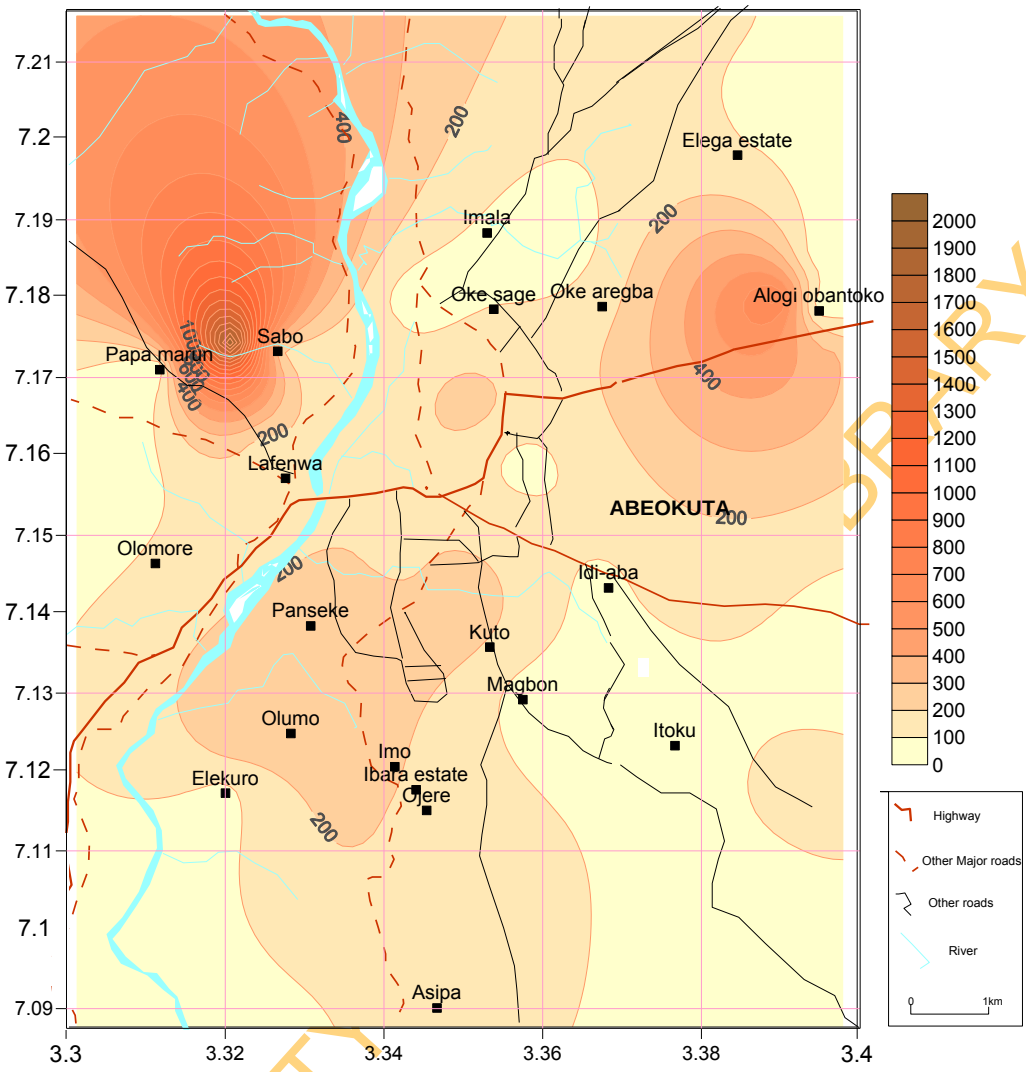

Fig 5.11: Hydrochemical map of Barium (ug/l) in groundwater in Abeokuta .

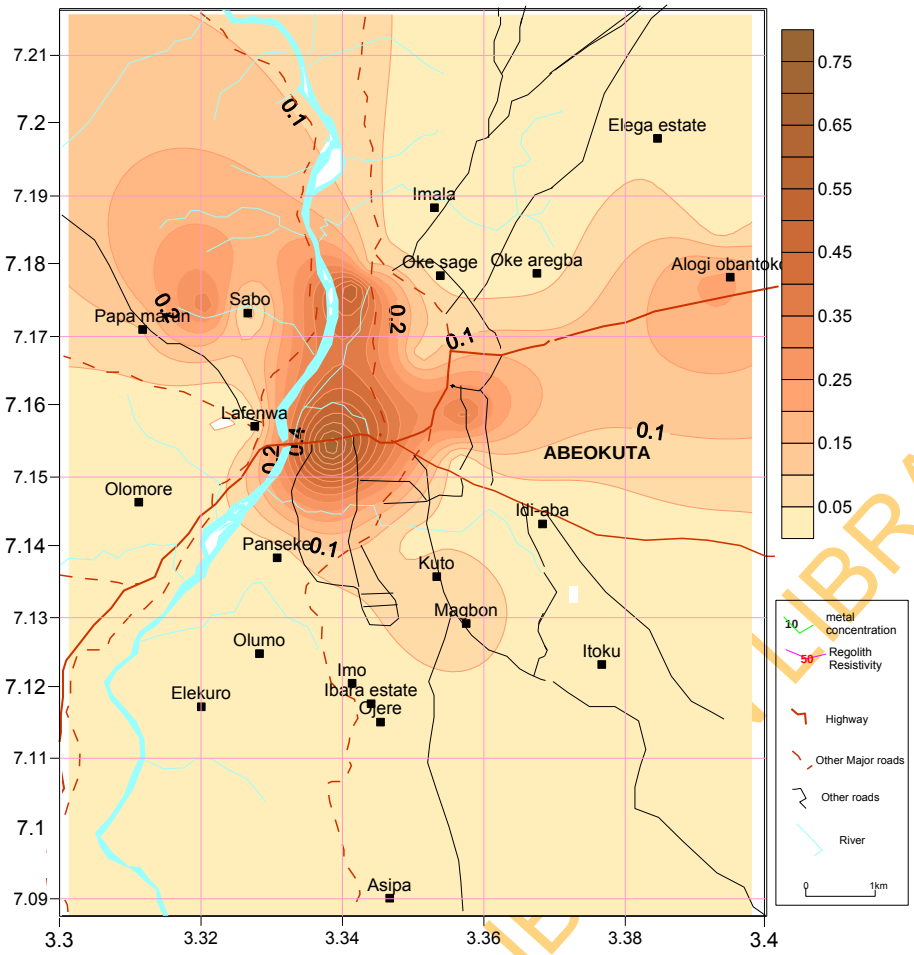

Fig 5.12: Hydrochemical map of Manganese (mg/l in groundwater in Abeokuta.

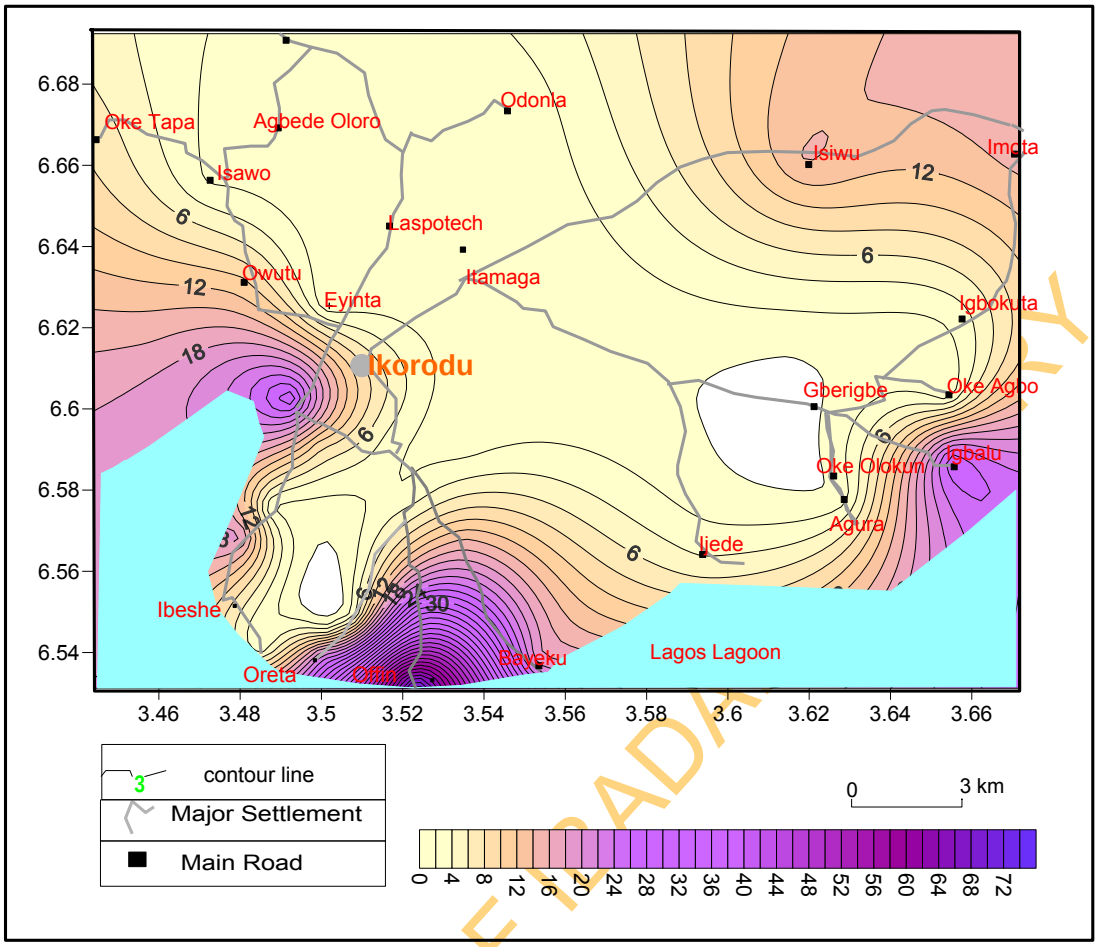

Fig 5.13: Hydrochemical map of Potassium (mg/l) in groundwater in Ikorodu

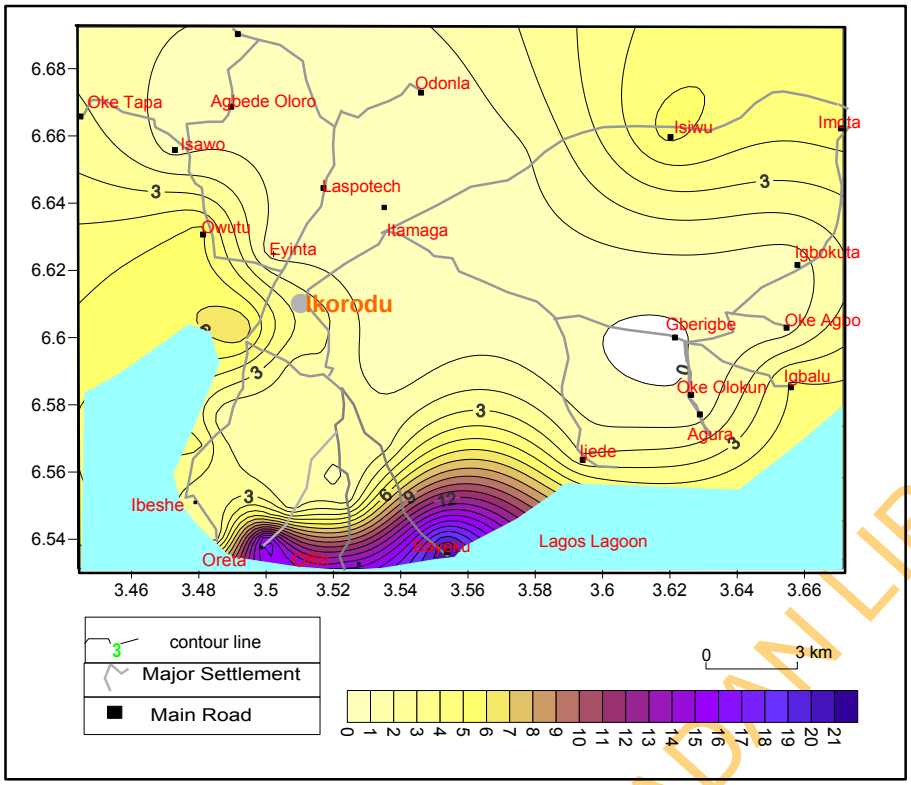

(a)

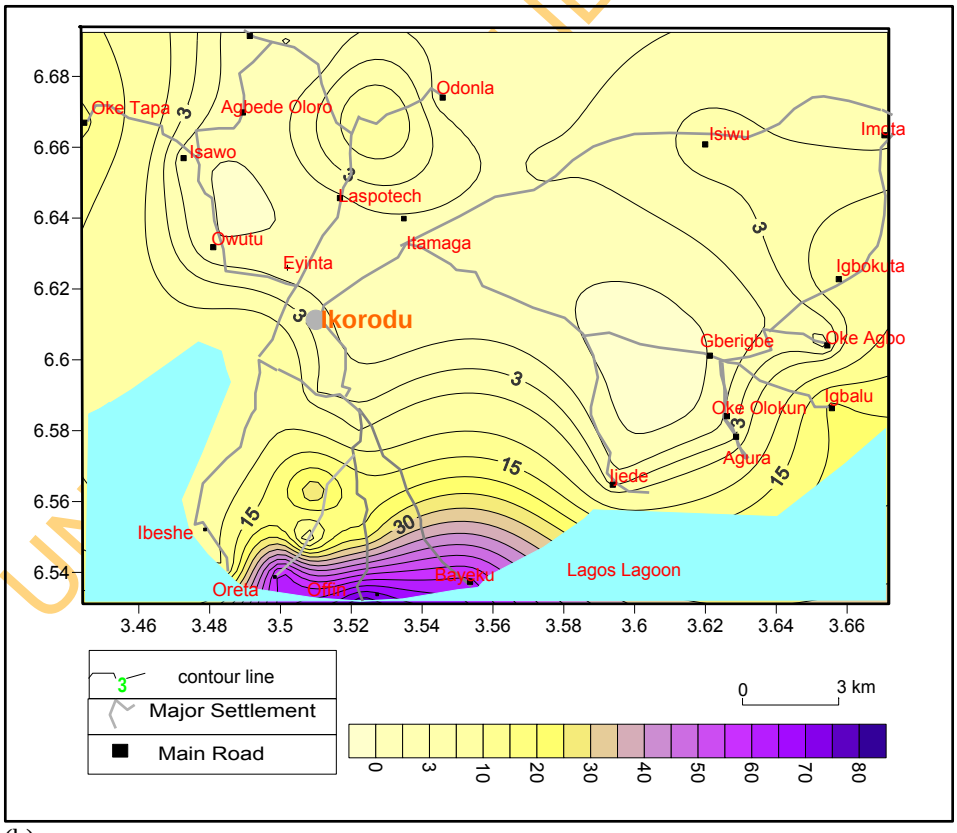

(b)

Fig 5.14: Hydrochemical maps of (a) Magnesium and (b) Sulphate (mg/l) in groundwater in Ikorodu

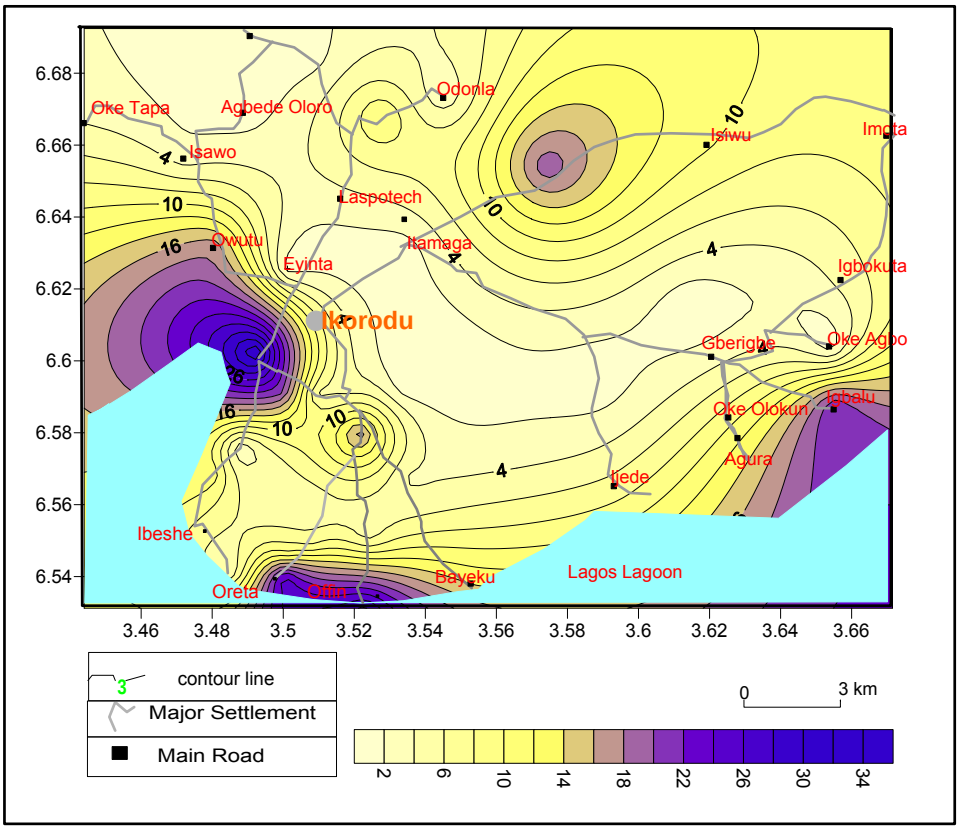

(a)

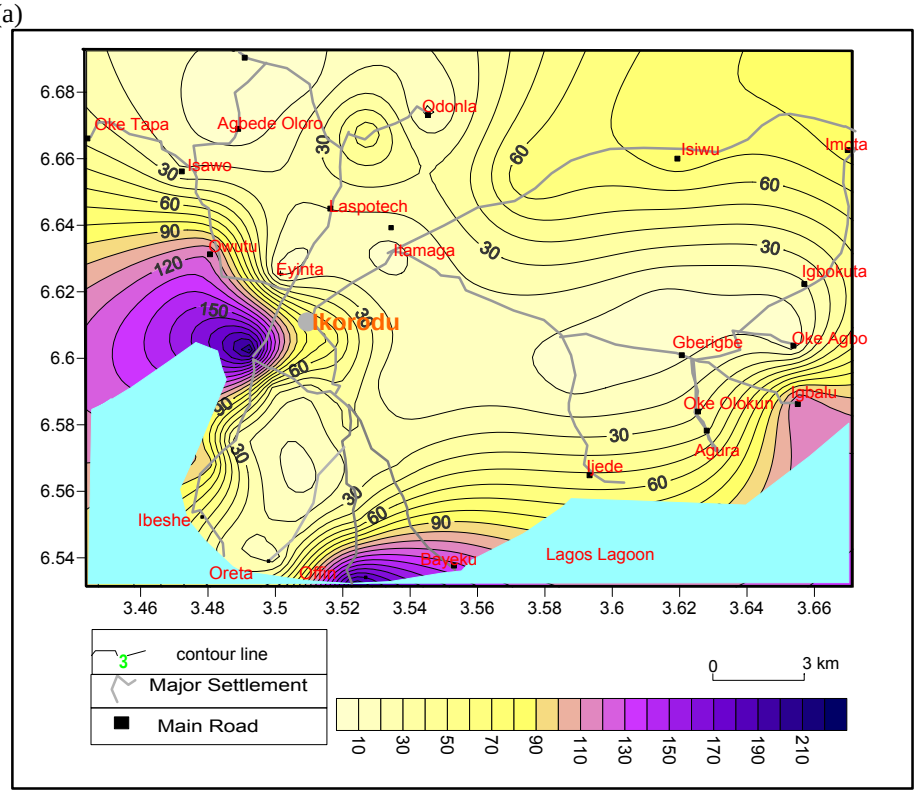

(b)

Fig 5.15a: Hydrochemical maps of (a) Calcium and (b) Bicarbonate (mg/l) in groundwater in Ikorodu